LEABHARLANN CHOLÁISTE NA TRÍONÓIDE, BAILE ÁTHA CLIATH | TRINITY COLLEGE LIBRARY DUBLIN
Ollscoil Átha Cliath | The University of Dublin

Terms and Conditions of Use of Digitised Theses from Trinity College Library Dublin

Copyright statement

All material supplied by Trinity College Library is protected by copyright (under the Copyright and Related Rights Act, 2000 as amended) and other relevant Intellectual Property Rights. By accessing and using a Digitised Thesis from Trinity College Library you acknowledge that all Intellectual Property Rights in any Works supplied are the sole and exclusive property of the copyright and/or other IPR holder. Specific copyright holders may not be explicitly identified. Use of materials from other sources within a thesis should not be construed as a claim over them.

A non-exclusive, non-transferable licence is hereby granted to those using or reproducing, in whole or in part, the material for valid purposes, providing the copyright owners are acknowledged using the normal conventions. Where specific permission to use material is required, this is identified and such permission must be sought from the copyright holder or agency cited.

Liability statement

By using a Digitised Thesis, I accept that Trinity College Dublin bears no legal responsibility for the accuracy, legality or comprehensiveness of materials contained within the thesis, and that Trinity College Dublin accepts no liability for indirect, consequential, or incidental, damages or losses arising from use of the thesis for whatever reason. Information located in a thesis may be subject to specific use constraints, details of which may not be explicitly described. It is the responsibility of potential and actual users to be aware of such constraints and to abide by them. By making use of material from a digitised thesis, you accept these copyright and disclaimer provisions. Where it is brought to the attention of Trinity College Library that there may be a breach of copyright or other restraint, it is the policy to withdraw or take down access to a thesis while the issue is being resolved.

Access Agreement

By using a Digitised Thesis from Trinity College Library you are bound by the following Terms & Conditions. Please read them carefully.

I have read and I understand the following statement: All material supplied via a Digitised Thesis from Trinity College Library is protected by copyright and other intellectual property rights, and duplication or sale of all or part of any of a thesis is not permitted, except that material may be duplicated by you for your research use or for educational purposes in electronic or print form providing the copyright owners are acknowledged using the normal conventions. You must obtain permission for any other use. Electronic or print copies may not be offered, whether for sale or otherwise to anyone. This copy has been supplied on the understanding that it is copyright material and that no quotation from the thesis may be published without proper acknowledgement.

Cancer Cell – Platelet Interactions in Ovarian Cancer Metastasis

A thesis submitted for the degree of

Doctor of Philosophy

By

Darragh Crowley, Dip.Sc, B.Sc. (Hons)

Trinity College

University of Dublin

Michaelmas Term

2012

Supervisors:

Professor Orla Sheils, MA (Dub), MA Med Law and Ethics (Lond), PhD, FAMLS, FRCPath, FTCD

Professor John O'Leary, MD, PhD, MSc, MA, FRCPath, FFPathRCPI, FTCD

TRINITY COLLEGE
2 4 MAY 2013
LIBRARY DUBLIN

Thesis 9965

Declaration

I declare that, except where otherwise acknowledged, this thesis is entirely my own work and has not been submitted previously for a Ph.D. degree at this or any other university.

I agree to deposit this thesis in the University's open access institutional repository or allow the library to do so on my behalf, subject to Irish Copyright Legislation and Trinity College Library conditions of use and acknowledgement.

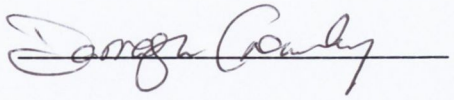

Darragh Crowley

For my parents Tomás & Jennifer

"Science... is made up of mistakes, but they are mistakes which it is useful to make, because they lead little by little to the truth."

– Jules Verne, Journey to the Centre of the Earth (1864)

Table of Contents

Acknowledgements I

List of Abbreviations III

Publications IX

Summary XI

Chapter One

1 General Introduction 2

1.1 Anatomy and Function of the Ovary 2

1.2 Ovarian Cancer 5

1.2.1 Epidemiology of Ovarian Cancer 6

1.2.2 Classification of Ovarian Cancer 10

1.2.3 Serous Ovarian Epithelial Carcinoma 14

1.2.3.1 Confounding Factors in Ovarian Cancer 15

1.2.3.2 Tumour Classification 18

1.2.3.3 Symptoms 22

1.2.3.4 Risk Factors in Ovarian Cancer 22

1.2.4 Diagnosis & Screening of Ovarian Cancer 25

1.2.4.1 Biomarker Investigation 25

1.2.4.2 Ultrasound 26

1.2.4.3 Laparoscopy 27

1.2.4.4 Advanced Imaging Studies 27

1.2.4.5 Biopsy 28

1.2.5 Management of Ovarian Cancer 29

1.3 Platelets 33

1.3.1 Platelet Physiology and Function 33

1.3.1.1 Platelet alpha and dense granules 35

1.3.2 Thrombus/Clot Formation 37

1.3.3 Cancer Cell-Platelet Interaction 39

1.3.3.1 Tumour Cell Induced Platelet Activation 42

1.4 Aims 45

CHAPTER TWO

2	**MATERIALS AND METHODOLOGY**	**47**
2.1	ARCHIVAL TISSUE COLLECTION	47
2.1.1	FORMALIN FIXED PARAFFIN EMBEDDED TISSUE	47
2.1.2	FFPE SAMPLE PREPARATION	47
2.2	NUCLEIC ACID EXTRACTION	49
2.2.1	RNA EXTRACTION FROM FFPE TISSUES	49
2.2.1.1	AMBION® RECOVERALL™ TOTAL NUCLEIC ACID ISOLATION KIT	49
2.2.2	RNA EXTRACTION FROM CELL LINES	50
2.2.2.1	QIAGEN® RNEASY® MINI KIT	50
2.2.2.2	AMBION® MIRVANA™ MIRNA ISOLATION KIT	50
2.3	NUCLEIC ACID QUANTITATION AND ASSESSMENT	51
2.3.1	NANO-DROP™ 2000 SPECTROPHOTOMETER	51
2.3.1.1	LOADING SAMPLES	51
2.3.1.2	BLANK MEASUREMENT	52
2.3.1.3	SAMPLE MEASUREMENT	53
2.3.2	AGILENT BIOANALYSER	54
2.3.2.1	STOCK REAGENT PREPARATION	54
2.3.2.2	CHIP PRIMING STATION SETUP	54
2.3.2.3	ELECTRODE DECONTAMINATION	55
2.3.2.4	GEL PREPARATION	55
2.3.2.5	GEL-DYE MIX PREPARATION	56
2.3.2.6	GEL DYE MIX LOADING	56
2.3.2.7	RNA NANO MARKER LOADING	57
2.3.2.8	LADDER AND SAMPLE LOADING	58
2.3.2.9	BIOANALYSER 2100 SOFTWARE OPERATION	58
2.4	GENE EXPRESSION ANALYSIS	61
2.4.1	TAQMAN® PCR	61
2.4.1.1	TAQMAN® RT-PCR PRIMERS AND PROBES	64
2.4.1.2	CUSTOM TAQMAN® GENE EXPRESSION ASSAY PREPARATION	64
2.4.1.3	REAL-TIME QUANTITATIVE TAQMAN® RT-PCR	65
2.4.1.4	RELATIVE GENE EXPRESSION	66
2.4.1.5	CDNA SYNTHESIS	68
2.4.1.6	PRE-AMPLIFICATION OF CDNA	69
2.4.1.7	TAQMAN® RT-PCR PROTOCOL	71

2.4.2 Fluidigm® High Throughput Real-Time PCR 73
2.4.2.1 Fluidigm® 48.48 Dynamic Array™ 73
2.4.2.2 cDNA Synthesis 74
2.4.2.3 Pre-amplification of cDNA 74
2.4.2.4 Fluidigm® Real-Time PCR Protocol 75
2.4.3 Affymetrix® GeneChip® Human Exon 1.0 ST Array Analysis 77
2.4.3.1 Affymetrix® GeneChip® Human Exon 1.0 ST Array Technology 77
2.4.3.2 Day 1 Workflow 82
2.4.3.3 Day 2 Workflow 83
2.4.3.4 Day 3 Workflow 85
2.4.3.5 Day 4 Workflow 86
2.4.3.6 In Silico Analysis 86
2.5 Cell Culture 93
2.5.1 Cell lines 93
2.5.2 Cell Culture Media and Other Solution Formulation 94
2.5.2.1 Cisplatin Solution Preparation 95
2.5.2.2 Cryopreservation Media 96
2.5.2.3 Trypsin Neutralising Solution 96
2.5.3 Adherent Cell Line Passage 97
2.5.4 Non-Enzymatic Cell Detachment 98
2.5.5 Cell Counting 99
2.5.6 Freezing Cells Stocks 100
2.5.7 Thawing Cells from Frozen Stocks 100
2.5.8 Mycoplasma Testing 101
2.5.9 Thyrocyte γ-Irradiation 102
2.6 Platelet and Platelet Releasate Isolation 103
2.6.1 Washed Platelet Preparation 103
2.6.1.1 Stock Buffer Preparation 103
2.6.1.2 Washed Platelet Preparation From Whole Blood 104
2.6.2 Gel Filtered Platelet Isolation 104
2.6.2.1 Sepharose Column Preparation 104
2.6.2.2 Gel Filtration of Washed Platelets 105
2.6.3 Platelet Releasate Preparation 105
2.6.4 Platelet Releasate Protein Quantitation 106
2.6.4.1 Bradford Protein Assay 106
2.7 Cell-Platelet Interaction Assays 106

2.7.1	In Vitro Platelet Adhesion Assay	106
2.7.1.1	Cell Line Preparation	106
2.7.1.2	Platelet Preparation	107
2.7.1.3	Cancer Cell – Platelet Adhesion Assay	107
2.7.2	Aggregometry Assay	108
2.7.3	Cell line-Platelet Releasate/Washed Platelet Exposure	109
2.8	Detection of Platelet Markers	110
2.8.1	Flow Cytometry	110
2.8.1.1	Antibodies	111
2.8.1.2	Flow Cytometry Assay of $\alpha_{IIb}\beta_3$/p-selectin	111
2.8.2	Fluorescent Microscopy of Cell Surface Markers	112
2.8.2.1	Antibodies	112
2.8.2.2	Staining and Visualisation	112
2.9	Cell Growth and Proliferation Assays	113
2.9.1	Roche Cell Proliferation Assay 1 (MTT)	113
2.10	Apoptosis Assay	114

CHAPTER THREE

3	**THROMBOCYTOSIS AND PLATELET RELATED GENE EXPRESSION IN OVARIAN CANCER**	**116**
3.1	BACKGROUND	116
3.1.1	PLATELET DERIVED GROWTH FACTOR (PDGF) AND PLATELET DERIVED GROWTH FACTOR RECEPTORS (PDGFR)	118
3.1.2	VASCULAR ENDOTHELIAL GROWTH FACTOR (VEGF)	122
3.1.3	CA125	124
3.1.4	THROMBOPOIETIN (TPO)	125
3.1.5	AIM	126
3.2	MATERIALS AND METHODS	127
3.2.1	TISSUE SAMPLE SELECTION	127
3.2.2	FFPE SAMPLE PREPARATION	128
3.2.3	NUCLEIC ACID EXTRACTION	128
3.2.4	TAQMAN® GENE EXPRESSION ANALYSIS	131
3.2.5	DATA ANALYSIS	132
3.3	RESULTS	133
3.3.1	CLINICO-PATHOLOGICAL CHARACTERISTICS OF SAMPLE COHORTS	133
3.3.1.1	PATIENT AGE	133
3.3.1.2	PREOPERATIVE PLATELET COUNT	135
3.3.1.3	COHORT SURVIVAL	137
3.3.1.4	PROGRESSION FREE SURVIVAL (PFS)	139
3.3.1.5	PFS VS THROMBOCYTOTIC STATUS (STRATIFIED BY TUMOUR GRADE)	141
3.3.1.6	OVERALL SURVIVAL (OS)	143
3.3.1.7	OS VS THROMBOCYTOTIC STATUS (STRATIFIED BY TUMOUR GRADE)	145
3.3.2	LONG TERM SURVIVAL ANALYSIS	148
3.3.2.1	2 YEAR SURVIVAL RATE	148
3.3.2.2	5 YEAR SURVIVAL RATE	151
3.3.3	RNA ANALYSIS	156
3.3.4	REAL-TIME PCR DATA QUALITY CONTROL AND ANALYSIS	156
3.3.4.1	QUALITY CONTROL	156
3.3.4.2	NORMALISATION	157
3.3.4.3	SIGNAL CORRELATION	160
3.3.5	GENE EXPRESSION ANALYSIS – RELATIVE QUANTITATION	163
3.3.5.1	TRENDS IN GENE EXPRESSION	166
3.3.5.2	TRENDS IN GENE EXPRESSION - SURVIVAL	174

3.3.5.3 Gene Expression Correlation 183
3.4 Discussion 187
3.5 Conclusion 196

Chapter Three Appendix 198

Chapter Four

4	**Platelet Adhesion to Ovarian Cell Lines**	**201**
4.1	Background	201
4.2	Methodology	202
4.2.1	Stock Solution Preparation	202
4.2.1.1	BSA	202
4.2.1.2	TWEEN 20	202
4.2.1.3	FBS	203
4.2.2	Washed Platelet Preparation	203
4.2.3	Gel Filtered Platelet Preparation	203
4.2.4	Platelet Releasate Preparation	203
4.2.5	Cell Culture	203
4.2.5.1	Thyrocyte Irradiation	204
4.2.6	RNA Extraction	204
4.2.7	TaqMan® Realtime PCR	204
4.2.7.1	Primers	206
4.2.8	Platelet Adhesion Assay	206
4.2.9	Aggregometry Assay	206
4.2.10	Flow Cytometry Assay	206
4.3	Results	207
4.3.1	In Vitro Adhesion Assay Optimisation	207
4.3.1.1	Assay Blocking Strategies	208
4.3.1.2	In Vitro Platelet Adhesion Assay	213
4.3.1.3	Adhesion Assay: Preliminary Testing	213
4.3.1.4	In Vitro Platelet Adhesion Assay: Ovarian Cell Lines	219
4.3.2	Aggregometry Analysis of TCIPA	224
4.3.3	Flow Cytometry Analysis of Cell Line Induced Platelet Activation	229
4.3.3.1	P-selectin	230
4.3.3.2	$A_{2B}B_3$	235
4.4	Discussion & Conclusion	239

Chapter Four Appendix 243

Chapter Five

5	**Tumour Cell Induced Platelet Aggregation Associated Alteration of Gene Expression in Ovarian Cancer**	**246**
5.1	Background	246
5.2	Materials & Methods	247
5.2.1	Gel Filtered Platelet and Platelet Releasate Preparation	247
5.2.2	Pierce® BCA (Bradford) Protein Assay	247
5.2.3	Fluorescent Microscopy of Cell Surface Markers	247
5.2.4	Roche In Situ Cell Death Detection (TUNEL) Assay	247
5.2.5	Roche Cell Proliferation Assay 1 (MTT)	248
5.2.6	BD Pharmigen™ ApoDirect™ Flow Cytometry TUNEL Assay	248
5.2.7	Nucleic Acid Extraction	248
5.2.8	RNA Quantitation & Analysis	248
5.2.9	Affymetrix® GeneChip® Human Exon 1.0 ST Array	248
5.2.10	Fluidigm® Dynamic Array™	248
5.3	Results	249
5.3.1	Platelet Releasate Optimisation	249
5.3.1.1	Bradford Colorimetric Protein Assay	250
5.3.1.2	Roche In Situ Cell Death Detection (TUNEL) Assay	251
5.3.1.3	Roche Cell Proliferation Assay 1 (MTT Assay)	257
5.3.1.4	Apoptosis detection by Flow Cytometry TUNEL Assay	267
5.3.2	Mycoplasma Test	269
5.3.3	RNA Extraction	271
5.3.3.1	Comparison of Extraction Methods	271
5.3.3.2	RNA Quantitation and Integrity Assessment	272
5.3.4	Affymetrix® GeneChip® Human Exon 1.0 ST Array	278
5.3.4.1	Human Exon 1.0 ST Assay Quality Control	278
5.3.4.2	Affymetrix Whole Transcriptome Investigation of Gene Expression	282
5.3.4.3	HIOE-80	285
5.3.4.4	59M	291
5.3.4.5	SK-OV 3	300
5.3.4.6	A2780	310
5.3.4.7	A2780cis	311
5.3.5	Affymetrix® Result Validation – Fluidigm® Dynamic Array™ qPCR	324
5.3.5.1	HIOE-80	326

5.3.5.2 59M 327
5.3.5.3 SK-OV 3 329
5.3.5.4 A2780cis 330
5.4 Discussion 331

Chapter Five Appendix 336

Chapter Six

6 Discussion and Conclusion 339

6.1 Background 339
6.2 Aims of the Thesis 341
6.3 Overview of Results & Conclusions 342
6.3.1 Chapter 3 342
6.3.2 Chapter 4 344
6.3.3 Chapter 5 345
6.4 Future Work 350
6.4.1 Ovarian Cancer Archival Studies 350
6.4.2 In vitro TCIPA Studies 350
6.4.3 TCIPA Induced Alteration of Cancer Cell Gene Expression 352
6.5 Translational Benefits of TCIPA Research 353
6.6 Ovarian Cancer and CTC Studies in the Societal Context 355
6.7 Conclusions 356

Bibliography 357

Appendix

7	**Appendix**	**433**
7.1	Ambion® RecoverAll™ Total Nucleic Acid Isolation Kit Protocol	434
7.2	QIAGEN® RNeasy® Mini Kit Protocol	437
7.3	Ambion® mirVana™ miRNA Isolation Kit Protocol	440
7.4	Affymetrix® GeneChip® Human Exon 1.0 ST Array Technology	443
7.4.1	Day 1 Workflow Protocol	443
7.4.1.1	First Strand cDNA Synthesis	445
7.4.1.2	Second Strand cDNA Synthesis	447
7.4.1.3	cRNA Synthesis	448
7.4.2	Day 2 Workflow Protocol	450
7.4.2.1	cRNA Purification	450
7.4.2.2	cRNA Yield and Size Assessment	452
7.4.2.3	Second Cycle cDNA Synthesis	452
7.4.2.4	cDNA Hydrolysis	455
7.4.2.5	Second Cycle cDNA Purification	455
7.4.2.6	cDNA Yield and Size Assessment	457
7.4.2.7	cDNA Fragmentation	458
7.4.3	Day 3 Work Flow Protocol	460
7.4.3.1	Labelling of Fragmented ssDNA	460
7.4.3.2	GeneChip® Human Exon 1.0 ST Array Hybridisation	461
7.4.4	Day 4 Work Flow Protocol	464
7.4.4.1	Entering Experiment Information	464
7.4.4.2	GeneChip® Wash/Stain	465
7.4.4.3	GeneChip® Scanning	470
7.4.5	Roche Mycoplasma Detection Kit Protocol	472
7.4.5.1	Preparation of Reagents	472
7.4.5.2	Mycoplasma ELISA Protocol	472
7.5	Washed Platelet Preparation Stock Buffer Preparation	476
7.5.1	JNL Buffer Preparation	476
7.5.2	Acid Citrate Dextrose Solution Preparation	477
7.6	Bradford Protein Assay Protocol	477
7.6.1	Preparation of Standards and Working Reagents	477
7.6.2	Preparation of the BCA Working Reagent	478
7.6.3	Microplate Procedure	479

7.7 Roche Cell Proliferation Assay 1 Protocol 479
7.7.1 Stock Solution Preparation 479
7.7.2 MTT Assay Procedure 480
7.8 Roche In Situ Cell Death Detection Kit, TMR red Assay Protocol 480
7.8.1.1 Calculation of Apoptotic Cell Population 483
7.9 BD Pharmigen™ ApoDirect™ Kit Protocol 483

Table of Figures

Figure 1-1: Schematic representation of the ovary. 3

Figure 1-2: H&E Staining Photomicrograph of a malignant Serous Ovarian Carcinoma with stromal micro-invasion. 15

Figure 1-3: Proposed delineation of Type 1 and Type 2 Ovarian Serous Carcinomas based on genomic characteristics and tumourigenesis. 18

Figure 1-4: Schematic representation of unactivated platelet structure. 34

Figure 2-1: NanoDrop™ Spectrophotometer Sample Loading. 52

Figure 2-2: Bioanalyser 2100 Chip Station Setup. 57

Figure 2-3: Bioanalyser 2100 Instrument Indicator Icons. 59

Figure 2-4: Agilent 2100 Bioanalyser Exemplar Electropherograms 60

Figure 2-5: Graphical Illustration of Applied Biosystems TaqMan® RT-PCR 63

Figure 2-6: Typical TaqMan® Gene Expression Assay Amplification Plot. 66

Figure 2-7: Detection capacity of Whole Transcript (WT) versus 3' assay technologies. 78

Figure 2-8: Affymetrix® GeneChip® Human Exon 1.0 ST Array Day 1 Workflow 83

Figure 2-9: Affymetrix® GeneChip® Human Exon 1.0 ST Array Day 2 Workflow 85

Figure 2-10: Graphical illustration of a haemocytometer counting chamber. 100

Figure 2-11: Graphical illustration of ELISA based mycoplasma detection. 102

Figure 2-12: Flow Cytometry Dot plot indicating side scatter (SSC-H) and forward scatter (FSC-H) axes*. 111

Figure 3-1: PDGF Signalling mediated by PDGF Receptors 119

Figure 3-2: Flow chart describing progression from initial Total Sample Cohort to final Analysis Cohort 128

Figure 3-3: Patient Age Vs Histological Grade 134

Figure 3-4: Preoperative platelet count vs Ovarian Tissue Type 136

Figure 3-5: Outlier Analysis – Progression Free Survival 138

Figure 3-6: Outlier Analysis – Overall Survival. 139

Figure 3-7: Kaplan-Meier PFS Curves for ovarian cancer patients classified as either FIGO tumour grade 2 or 3. 140

Figure 3-8: Kaplan-Meier PFS Curves for ovarian cancer patients classified as either thrombocytotic or non-thrombocytotic based on pre-operative platelet count and FIGO tumour grade 2. 142

Figure 3-9: Kaplan-Meier PFS Curves for ovarian cancer patients classified as either thrombocytotic or non thrombocytotic based on pre-surgery platelet count and FIGO tumour grade 3. 143

Figure 3-10: Kaplan-Meier OS Curves for ovarian cancer patients classified as either FIGO tumour grade 2 or 3. 144

Figure 3-11: Kaplan-Meier OS Curves for ovarian cancer patients classified as either thrombocytotic or non thrombocytotic based on pre-surgery platelet count and FIGO tumour grade 2. 146

Figure 3-12: Kaplan-Meier OS Curves for ovarian cancer patients classified as either thrombocytotic or non-thrombocytotic based on pre-operative platelet count and FIGO tumour grade 3. 147

Figure 3-13: Two year survival rate in ovarian cancer stratified by FIGO disease grade. 148

FIGURE 3-14: TWO YEAR SURVIVAL RATE IN GRADE 2 OVARIAN CANCER STRATIFIED BY THROMBOCYTOTIC STATUS..... 149
FIGURE 3-15: TWO YEAR SURVIVAL RATE IN GRADE 3 OVARIAN CANCER STRATIFIED BY THROMBOCYTOTIC STATUS..... 150
FIGURE 3-16: FIVE YEAR SURVIVAL RATE IN OVARIAN CANCER GRADE 2 AND 3..... 151
FIGURE 3-17: FIVE YEAR SURVIVAL RATE IN GRADE 2 OVARIAN CANCER STRATIFIED BY THROMBOCYTOTIC STATUS. 152
FIGURE 3-18: FIVE YEAR SURVIVAL RATE IN GRADE 3 OVARIAN CANCER STRATIFIED BY THROMBOCYTOTIC STATUS. 153
FIGURE 3-19: SPOTFIRE® REALTIME STATMINER™ FAILED SUMMARY..... 157
FIGURE 3-20: ENDOGENOUS CONTROL GENE STABILITY OF EXPRESSION ASSESSMENT..... 158
FIGURE 3-21: LINE GRAPH ILLUSTRATING CANDIDATE ENDOGENOUS CONTROL GENE C_T VALUES BY SAMPLE..... 159
FIGURE 3-22: BOX-AND-WHISKER PLOT DISPLAYING THE OVERALL RANGE OF CT DISTRIBUTION FOR EACH SAMPLE FROM ALL GENES IN THE EXPERIMENT..... 161
FIGURE 3-23: PEARSONS' CORRELATION PLOT (HEAT MAP) OF SAMPLE SIGNAL (C_T) VALUES (OVARIAN CANCER GRADE 3)..... 162
FIGURE 3-24: RELATIVE QUANTITATION PLOT. TARGET GENE EXPRESSION IN OVARIAN CANCER (FIGO GRADES, 2, 2/3, 3) COMPARED TO NORMAL OVARY..... 163
FIGURE 3-25: PDGFA (A) AND PDGFB (B) EXPRESSION CATEGORISED HIGH TO LOW IN NORMAL OVARY AND FIGO GRADE 2 AND 3 OVARIAN CANCERS..... 167
FIGURE 3-26: PDGFRA (A) AND PDGFRB (B) EXPRESSION CATEGORISED HIGH TO LOW IN NORMAL OVARY AND FIGO GRADE 2 AND 3 OVARIAN CANCERS. 169
FIGURE 3-27: VEGFA (A) AND CA125 (B) EXPRESSION CATEGORISED HIGH TO LOW IN NORMAL OVARY AND FIGO GRADE 2 AND 3 OVARIAN CANCERS..... 171
FIGURE 3-28: THPO EXPRESSION CATEGORISED HIGH TO LOW IN NORMAL OVARY AND FIGO GRADE 2 AND 3 OVARIAN CANCERS. 173
FIGURE 4-1: ADHESION OF CALCEIN AM LOADED PLATELETS TO POSITIVE CONTROL (FIBRINOGEN) COATED AND UNCOATED ASSAY WELLS AND JNL (VEHICLE) NEGATIVE CONTROL. 208
FIGURE 4-2: BLOCKING STRATEGY FOR NON-SPECIFIC PLATELET ADHESION – BSA..... 210
FIGURE 4-3: BLOCKING STRATEGY FOR NON-SPECIFIC PLATELET ADHESION – TWEEN..... 211
FIGURE 4-4: BLOCKING STRATEGY FOR NON-SPECIFIC PLATELET ADHESION – FBS. 212
FIGURE 4-5: PLATELET ADHESION TO A PANEL OF CELL LINES OF EPITHELIAL ORIGIN..... 215
FIGURE 4-6: TAQMAN RET/PTC-3 ASSAY IN Γ-IRRADIATED THYROCYTES. 218
FIGURE 4-7: PLATELET ADHESION TO OVARIAN CELL LINES..... 220
FIGURE 4-8: 40X BRIGHTFIELD PHOTOMICROGRAPH OF PLATELET ADHESION TO HIOE-80 AND 59M CELLS..... 222
FIGURE 4-9: 40X BRIGHTFIELD PHOTOMICROGRAPH OF PLATELET ADHESION TO A2780 AND A2780CIS CELLS..... 223
FIGURE 4-10: AGGREGOMETRY – 59M OVARIAN CARCINOMA INDUCED WASHED PLATELET AGGREGATION. 226
FIGURE 4-11: AGGREGOMETRY – OVARIAN CELL LINE INDUCED WASHED PLATELET AGGREGATION..... 227
FIGURE 4-12: AGGREGOMETRY – OVARIAN CELL LINE INDUCED PLATELET RICH PLASMA (PRP) AGGREGATION. 228
FIGURE 4-13: FLOW CYTOMETRY HISTOGRAMS P-SELECTIN FLUORESCENCE VS HIOE-80 AND A2780 CELL COUNT..... 231
FIGURE 4-14: FLOW CYTOMETRY HISTOGRAMS P-SELECTIN FLUORESCENCE VS A2780CIS AND SK-OV-3 CELL COUNT..... 232
FIGURE 4-15: FLOW CYTOMETRY HISTOGRAMS P-SELECTIN FLUORESCENCE VS 59M CELL COUNT AND A PANEL OF CANCER CELL LINES AT $1.5x10^6$ CELLS/ML..... 233
FIGURE 4-16: FLOW CYTOMETRY ANALYSIS OF TCIPA VIA ACTIVATED PLATELET P-SELECTIN: % CELLS P-SELECTIN POSITIVE. ... 234

FIGURE 4-17: FLOW CYTOMETRY ANALYSIS OF TCIPA VIA ACTIVATED PLATELET P-SELECTIN: % CELLS $A_{2B}B_3$ POSITIVE..... 237
FIGURE 5-1: FLUORESCENT PHOTOMICROGRAPHS OF AVB3 (A) AND AV (B) STAINING IN 59M CELLS. 250
FIGURE 5-2: FLUORESCENT PHOTOMICROGRAPHS OF HOECHST STAINED AND TUNEL LABELLED 59M CELLS. 252
FIGURE 5-3: PERCENTAGE OF CELLS UNDERGOING APOPTOSIS IN RESPONSE TO PLATELET RELEASATE EXPOSURE. 254
FIGURE 5-4: TUNEL ASSAY - NORMALISED CELL COUNT PER FIELD OF VIEW FOLLOWING CULTURE IN THE PRESENCE OF PLATELET RELEASATE..... 256
FIGURE 5-5: MTT ASSAY – EFFECT OF PLATELET RELEASATE (PLRL) ON CELL METABOLISM AT DILUTION FACTORS OF 1:1 TO 1:6 IN FULL GROWTH MEDIA (FM) 259
FIGURE 5-6: MTT ASSAY OF CELL GROWTH & PROLIFERATION IN OVARIAN CELL IN RESPONSE TO CULTURE IN THE PRESENCE OF PLATELET RELEASATE AUGMENTED FULL GROWTH MEDIA..... 262
FIGURE 5-7: MTT ASSAY OF CELL GROWTH & PROLIFERATION IN OVARIAN CELL IN RESPONSE TO CULTURE IN THE PRESENCE OF PLATELET RELEASATE AUGMENTED FULL GROWTH MEDIA..... 264
FIGURE 5-8: MTT ASSAY OF CELL GROWTH & PROLIFERATION IN OVARIAN CELL IN RESPONSE TO CULTURE IN THE PRESENCE OF JNL BUFFER AUGMENTED SERUM FREE GROWTH MEDIA..... 266
FIGURE 5-9: FLOW CYTOMETRY TUNEL ASSAY – CELL LINE APOPTOSIS IN FULL GROWTH MEDIA 1:1000 DILUTION PLRL... 268
FIGURE 5-10: PRE-AFFYMETRIX® GENECHIP® ASSAY CELL LINE MYCOPLASMA ASSAY. 270
FIGURE 5-11: BIOANALYZER ELECTROPHEROGRAM OF SAMPLE TRNA. 276
FIGURE 5-12: BIOANALYZER DIGITAL GEL IMAGE OF A RANGE OF TRNA SAMPLES..... 276
FIGURE 5-13: AFFYMETRIX QUALITY CONTROL - HYBRIDISATION CONTROL ASSESSMENT. 280
FIGURE 5-14: AFFYMETRIX QUALITY CONTROL - LABELLING CONTROL ASSESSMENT..... 281
FIGURE 5-15: FLUIDIGM HIGH THROUGHPUT QPCR VALIDATION OF GENES UNDERGOING ALTERED EXPRESSION IN HIOE-80 CELLS IN RESPONSE TO WASHED PLATELET AND PLATELET RELEASATE EXPOSURE..... 326
FIGURE 5-16: FLUIDIGM HIGH THROUGHPUT QPCR VALIDATION OF GENES UNDERGOING ALTERED EXPRESSION IN 59 CELLS IN RESPONSE TO WASHED PLATELET (A) AND PLATELET RELEASATE (B) EXPOSURE. 328
FIGURE 5-17: FLUIDIGM HIGH THROUGHPUT QPCR VALIDATION OF GENES UNDERGOING ALTERED EXPRESSION IN SK-OV 3 CELLS IN RESPONSE TO WASHED PLATELET AND PLATELET RELEASATE EXPOSURE..... 329
FIGURE 5-18: FLUIDIGM HIGH THROUGHPUT QPCR VALIDATION OF GENES UNDERGOING ALTERED EXPRESSION IN A2780CIS CELLS IN RESPONSE TO WASHED PLATELET EXPOSURE. 330
FIGURE 5-19: SUMMARISATION OF GENE EXPRESSION CHANGES OBSERVED IN OVARIAN CELL LINES IN RESPONSE TO WASHED PLATELET/PLATELET RELEASATE EXPOSURE. 334
FIGURE 6-1: NUMBER OF PUBLICATIONS BY YEAR BETWEEN 1981 AND 2011 EXAMINING TCIPA, CTC'S OR PLATELETS & CANCER. 340
FIGURE 6-2: HANAHAN & WEINBERG'S HALLMARKS OF CANCER..... 347
FIGURE 7-1: AFFYMETRIX® GENECHIP® HUMAN EXON 1.0 ST ARRAY. 463

Table of Tables

Table 1-1: Ovarian Cancer Statistics – A Global, Regional, European and Irish Overview. 7

Table 1-2: TNM & FIGO Staging Classification of Ovarian Cancers. 20

Table 2-1: 2X Reverse Transcriptase Master Mix 69

Table 2-2: TaqMan® PreAmp Reaction Preparation 71

Table 2-3: TaqMan® Real-time PCR Setup for a 20ml Reaction Volume 72

Table 2-4: Fluidigm® Sample cDNA Pre-Amplification Reaction Preparation. 74

Table 2-5: Reagent Volumes required for Fluidigm® Real-time PCR. 75

Table 2-6: Serial Dilution Schema of non-enzymatically detached cells for Aggregometry Assay use. 108

Table 3-1: Plate layout for TaqMan® RT-PCR. 130

Table 3-2: Applied Biosystems TaqMan® Assays for real-time PCR and relative quantitation of target genes in ovarian cancer. 131

Table 3-3: T-test values for differences in patient age between cohorts. 135

Table 3-4: T-test values for differences in preoperative platelet count between cohorts. 137

Table 3-5: Spearman's Correlation between patient clinicopathological metrics. 155

Table 3-6: Target Gene Expression in Grade 2, 2/3 borderline and grade 3 Ovarian Cancer – relative quantitation and significance compared to expression in normal ovary. 164

Table 3-7: PDGFA: Gene Expression Level (Low, Normal, High) Vs Survival. 175

Table 3-8: PDGFB: Gene Expression Level (Low, Normal, High) Vs Survival. 176

Table 3-9: PDGFRA: Gene Expression Level (Low, Normal, High) Vs Survival. 177

Table 3-10: PDGFRB: Gene Expression Level (Low, Normal, High) Vs Survival. 179

Table 3-11: CA125: Gene Expression Level (Low, Normal, High) Vs Survival. 180

Table 3-12: VEGFA: Gene Expression Level (Low, Normal, High) Vs Survival. 181

Table 3-13: THPO: Gene Expression Level (Low, Normal, High) Vs Survival. 183

Table 3-14: Spearmans' Correlation - Target Gene Expression (RQ values) Vs Patient Cohort and Survival Metrics. 184

Table 3-15: Spearmans' Correlation - Target Gene Expression (RQ values). 186

Table 3-16: Survival – influence of accepted value for thrombocytosis on % survival at T= 24 and 60 months. 189

Table 3-17: Concentration and A260/280 of RNA extracted from FFPE normal ovarian samples. 198

Table 3-18: Concentration and A260/280 of RNA extracted from FFPE grade 2 and 2/3 ovarian tumour samples. 198

Table 3-19: Concentration and A260/280 of RNA extracted from FFPE grade 3 ovarian tumour samples. 199

Table 4-1: BSA Solution Preparation. 202

Table 4-2: TWEEN 20 Solution Preparation. 202

Table 4-3: FBS Solution Preparation. 203

Table 4-4: ret/PTC-3 TaqMan® RT-PCR Assay Plate Layout. 205

Table 4-5: ret/PTC-3 TaqMan™ Primer-probeset. 206

Table 4-6: T-test Comparison of Platelet Adhesion to Cell Lines. 216
Table 4-7: Nanodrop assessment of cell line tRNA for ret/PTC-3 detection. 217
Table 5-1: Percentage of TUNEL positive cells in response to Platelet Releasate (PLRL) exposure. 255
Table 5-2: TUNEL Assay - Normalised Cell Count Per Field of View (±SEM). 257
Table 5-3: Cell Line Growth (mean ± SEM) in Response to Dilutions of Platelet Releasate. 260
Table 5-4: MTT Assay of cell growth & proliferation in Ovarian Cell in response to culture in the presence of platelet releasate augmented full growth media. 261
Table 5-5: Comparision of total RNA extraction methods. 271
Table 5-6: Quantitation of Sample tRNA prior to Affymetrix® GeneChip® Array Assay 273
Table 5-7: Quantitation of Total RNA of Platelet Origin. 274
Table 5-8: Integrity Assessment of Sample Total RNA prior to Affymetrix® GeneChip® Array Assay. 277
Table 5-9: Genes Undergoing Significantly Altered Expression in Response to Washed Platelet Exposure in HIOE-80 Cells. 285
Table 5-10: Genes Undergoing Significantly Altered Expression in Response to Platelet Releasate Exposure in HIOE-80 Cells. 288
Table 5-11: Genes Undergoing Significantly Altered Expression in Response to Washed Platelet Exposure in 59M Cells. 291
Table 5-12: Genes Undergoing Significantly Altered Expression in Response to Platelet Releasate Exposure in 59M Cells. 295
Table 5-13: Genes Undergoing Significantly Altered Expression in Response to Washed Platelet Exposure in SK-OV 3 Cells. 300
Table 5-14: Genes Undergoing Significantly Altered Expression in Response to Platelet Releasate Exposure in SK-OV 3 Cells. 302
Table 5-15: Genes Undergoing Significantly Altered Expression in Response to Washed Platelet Exposure in A2780cis Cells. 312
Table 5-16: Studies of Kallikrein gene expression in ovarian cancer (2001-2011). 314
Table 5-17: Table of Genes Selected for Fluidigm technical validation of Affymetrix® GeneChip Human Exon 1.0 ST array results. 325
Table 7-1: Poly-A RNA Control Serial Dilution. 444
Table 7-2: First Strand cDNA Synthesis Master Mix Components and Volumes. 446
Table 7-3: Second Strand cDNA Synthesis Master Mix Components and Volumes. 447
Table 7-4: IVT cRNA Synthesis Master Mix Components and Volumes. 448
Table 7-5: cRNA Binding Mix Components and Volumes. 450
Table 7-6: Second Cycle Master Mix Components and Volumes. 454
Table 7-7: cDNA Binding Mix Components and Volumes. 456
Table 7-8: Fragmentation Master Mix Components and Volumes. 458
Table 7-9: Labelling Reaction Master Mix Components and Volumes. 460
Table 7-10: Hybridisation Cocktail Components and Volumes. 462
Table 7-11: Fluidics Protocol for Washing/Staining GeneChip® Human Exon 1.0 ST Arrays. 467

TABLE 7-12: PIPETTING SCHEME FOR MYCOPLASMA DETECTION KIT COATING ANTIBODIES. 473
TABLE 7-13: PIPETTING SCHEME FOR MYCOPLASMA DETECTION KIT SAMPLES AND POSITIVE CONTROLS. 474
TABLE 7-14: PIPETTING SCHEME FOR MYCOPLASMA DETECTION ANTIBODIES. 475
TABLE 7-15: BSA SERIAL DILUTIONS FOR PROTEIN ASSAY (BROAD RANGE). 477
TABLE 7-16: BSA SERIAL DILUTIONS FOR PROTEIN ASSAY (NARROW RANGE). 478
TABLE 7-17: APODIRECT™ DNA LABELLING SOLUTION. 485

Acknowledgements

Firstly I must express my heartfelt thanks to my supervisors Professors John O'Leary and Orla Sheils who made me feel so welcome on joining the department and the lab. John, your encouragement, positivity and enthusiasm for the project helped to keep the motivation high and progress rolling on. Orla, I will always be grateful for your seemingly endless patience, impeccable guidance, unfailing encouragement, excellent advice and support – not to mention some of the best and most interesting lab meetings a student could have had. Unlike some of the horror stories of nerve shattering lab meetings that sometimes travel in scientific circles, the memories I'll take away will include many of laughter. Without the support of such great supervision I'm reluctant to think what my Ph.D. experience could have been like or where time would have taken me by now.

I would also like to thank the HRB for giving me the opportunity to take on this course of study, Drs. Ross Mc Manus and Mike Freeley for guiding the programme and my mentor Dr. Derek Morris for keeping a close eye on my progress over the years.

Huge thanks are due to Paul Smyth. To some he's Dr. Smyth, to others he's Tall Paul or Big Money – for me he's King of The Lab with masses of experience and a huge generosity of time, always willing to help anyone finding themselves hung up on a problem or question and in need of a hand. I'm not sure how I'll be able to repay you for all your support and help but when I can I'll happily pay it times over.

My time in the lab would not have been the same without the friendship of my fellow students on the HRB scholars programme, now friends; Sinéad, whose sense of fun and humour even when in her final few stress filled months in the lab made it a happy place to start work in, and along with Cathy, Therese, and Christine blazed a bright trail to follow. Thanks also to Muriel, Fiona, Jenny and Emma with whom I have shared the highs and lows of the Ph.D. roller coaster ride – you are real friends. To Christine R., Alice, Russell and Chris who followed us into the Ph.D. programme it's been a pleasure to have met and got to know you along the way.

Meeting Sinead was just the beginning of my good fortune, as I was later joined in the lab by Lisa, Emma, Gary and Lynda. Guys, I can honestly say I couldn't have hoped for better lab mates. I owe you my sanity for the lunch and coffee breaks with topics of conversation best described as eclectic, frequently hilarious and better than any form of therapy known to man, for the Monday morning NFL clips, for the tales of a certain mischievous pet rabbit, the excellent Christmas parties, the lot. I know you're going to do great in your studies so keep it up, I'm looking forward to congratulating Drs. Keogh, Dorris, Sommerville and McEvoy in the near future.

Thanks to Conor, Paul, Vivienne, Karen, Shane and Elliott of Lab Rats tag rugby fame, to all the gang past and present of the basement in the IMM including Cormac, Ciaran, Gosia, Annmarie, Jen, Graham, Caoimhe, Denise, Danijela, Ramon, Stephanie, Eugene, Darragh, and Peter and everyone else who's helped me throughout my studies including Sharon O'Toole in the Dept. of Obs & Gynae and Karl Egan and Eimear Dunne in the Royal College of Surgeons.

Thanks to my friends. I know it's like I've been away on a mission to Mars and my appearances and communications have been brief and infrequent, but thanks for not forgetting I was out there when there was the distraction of fun and sessions to be had.

Thanks also to my friends in the Chain Gang Cycling Club and Tralee Mountaineering Club – you've constantly reminded me there's a life and a world beyond the door of the lab, frequently kept me out of breath and made sure the last few years saw more than just my brain get trained. You're a great bunch and I'm looking forward to seeing more high and steep stuff on bike and on foot in future.

To my parents, Tomás and Jennifer, thank you for believing in me, for your encouragement, for your endless support, for everything. Thank you.

Ruth, if I'm strong it's because you support me, if I have motivation it's because you drive me and if I have ambition it's because you inspire me. I don't know what our next adventure will be but I'll walk into it bravely with you.

List of Abbreviations

AC	Analysis Cohort
ACD	Acid Citrate Dextrose
ACS	American Chemical Society
ADP	Adenosine diphosphate
AFP	α-fetoprotein
AGCC	Affymetrix® GeneChip® Command Console™
AJCC	American Joint Committee on Cancer
AMP	Adenosine MonoPhosphate
ANOVA	Analysis Of Variance
APE1	Apurinic/apyrimidinic endonuclease 1
ATP	Adenosine triphosphate
AUC	Area Under the Curve
Bac	Bacterial
BAT	Biotin Allonamide Triphosphate
BCA	Bicinchoninic Acid
β-HCG	Human Chorionic Gonadatrophin
BLAT	BLAST-like alignment tool
Bp	Base Pair
BRdU	5-Bromo-2'-deoxy-uridine
BSA	Bovine Serum Albumen
CA125	Cancer Antigen 125
CDKN1B	Cyclin-dependent kinase inhibitor 1B
cDNA	Complementary DNA
CDS	Coding Sequence
CFU	Colony Forming Units
CFU-MKs	Colony Forming Unit Megakaryocytes
CI	Confidence Interval
CIN	Cervical Intraepithelial Neoplasia
CL	Cardiolipin
CMV	Cytomegalovirus

cRNA	Complementary RNA
CSC	Core Sample Cohort
C_T	Threshold Cycle
CT	Computed Tomography
CTCs	Circulating Tumour Cells
CTD	C-terminal domain
ddH_2O	Double distilled water
DMSO	Dimethyl Sulfoxide
DNA	Deoxyribonucleic Acid
dscDNA	Double Stranded cDNA
dUTP	Deoxyuracil triphosphate
DVT	Deep Vein Thrombosis
EC	Expression Console™
ECS	Endothelial Cells
EDTA	Ethylenediaminetetraacetic acid
EGF	Epidermal Growth Factor
EGFR	Epidermal Growth Factor Receptor
ELISA	Enzyme-Linked Immunosorbent Assay
EMT	Epithelial Mesenchymal Transition
eNOS	Endothelial Nitric Oxide Synthase
EOC	Epithelial Ovarian Cancer
EpCAM	Epithelial Cell Adhesion Molecule
EU	European Union
FBS	Foetal Bovine Serum
FC	Fold Change
FFPE	Formalin Fixed Paraffin Embedded
FGF	Fibroblast Growth Factor
FIGO	The International Federation of Gynaecologists and Obsetricians
FM	Full Growth Media
FRET	Fluorescence Resonance Energy Transfer
FSH	Follicle Stimulating Hormone
F_v	Final Volume

FXI	Factor XI
GDP	Guanine Diphosphate
GIT	Gastro-Intestinal Tract
GnRH	Gonadotrophin-Releasing Hormone
GP	Glycoprotein
GTD	Gestational Trophoblastic Diseases
GTP	Guanine Triphosphate
H&E	Haematoxylin & Eosin
HNSCC	Head and Neck Squamous Cell Carcinoma
HO-1	Heme Oxygenase-1
HRT	Hormone Replacement Therapy
IFC	Integrated Fluidics Circuits
IFN-γ	Interferon Gamma
IL-1β	Interleukin 1-Beta
IP	Intraperitoneal
IQR	Interquartile Range
IVT	*In Vitro* Transcription
LDH	Lactate Dehydrogenase
LH	Luteinizing Hormone
LMP	Low Malignant Potential
LPS	Lipopolysaccharide
MGB	Minor Groove Binder
miRNA	Micro RNA
MKs	Megakaryoctes
MMP	Matrix Metalloproteinase
MRI	Magnetic Resonance Imaging
mRNA	Messenger RNA
mtDNA	Mitochondrial DNA
MTT	3-(4,5-Dimethylthiazol-2-yl)-2,5-diphenyltetrazolium bromide
N	Number
NDP	Nucleotide Diphosphate
NFQ	non-fluorescent quencher

NK	Natural Killer
NSCLC	Non-Small Cell Lung Cancer
nt	nucleotide(s)
NTP	Nucleotide Triphosphate
OC	Ovarian Cancer
OS	Overall Survival
PBP	Platelet Basic Protein
PBS	Phosphate Buffered Saline
PCR	Polymerase Chain Reaction
PDGF	Platelet Derived Growth Factor
PET	Positron Emission Tomography
PF4	Platelet Factor 4
PFA	Paraformaldehyde
PFS	Progression Free Survival
PGC	Poised Gene Cassette
PLD	Phospholipase D
PLRL	Platelet Releasate
PM	Perfect Match
PPC	Primary Peritoneal Cancer
PPV	Positive Predictive Value
PRP	Platelet Rich Plasma
QC	Quality Control
qPCR	Quantitative PCR
RIN	RNA Integrity Number
RLE	Relative Log Expression
RNA	Ribonucleic Acid
RNAP2	RNA Polymerase II
ROS	Reactive Oxygen Species
RPM	Revolutions Per Minute
RQ	Relative Quantitation
rRNA	ribosomal RNA
RSR	Relative Survival Rate

RTK	Receptor Tyrosine Kinase
RT-PCR	Real Time-Polymerase Chain Reaction
SAPE	Streptavidin Phycoreythrin
SEM	Standard Error of Mean
snRNA	Small Nuclear RNA
sscDNA	single stranded cDNA
(S)TIC/L	(Serous) Tubal Intraepithelial Carcinomas or Lesions
Std.	Standard
SV40	Simian Virus 40
TCIPA	Tumour Cell Induced Platelet Aggregation
TdT	Terminal Deoxynucleotidyl Transferase
TE	Tris EDTA
TE	Thromboembolism
TF	Tissue Factor
TGF	Transforming Growth Factor
TLR	Toll-like Receptor
TMR	Tetra-Methyl-rhodamine
TNFR	Tissue Necrosis Factor Receptor
TNF-α	Tumour Necrosis Factor Alpha
TNS	Trypsin Neutralising Solution
TPO	Thrombopoietin (protein)
THPO	Thrombopoietin (gene)
TRAP	Thrombin Receptor Activating Protein
tRNA	Total RNA
TSG	Tumour Supressor Gene
TSC	Total Sample Cohort
TSP	Thrombospondin
TUNEL	TdT-mediated dUTP-X Nick End Labelling
TVU	Trans-Vaginal Ultrasound
UDG	Uracil DNA Glycosylase
UKCTOCS	UK Collaborative Trial of Ovarian Cancer Screening
v/v	Volume by Volume

VEGF	Vascular Endothelial Growth Factor
VSM	Vascular Smooth Muscle
VWF	von Willebrand Factor
WBCs	White Blood Cells
Δ	Delta
X^2	Chi Squared
5-HT	5-hydroxytryptamine/Serotonin

Publications

EGAN, K., CROWLEY, D., SMYTH, P., O'TOOLE, S., SPILLANE, C., MARTIN, C., GALLAGHER, M., CANNEY, A., NORRIS, L., CONLON, N., MCEVOY, L., FFRENCH, B., STORDAL, B., KEEGAN, H., FINN, S., MCENEANEY, V., LAIOS, A., DUCREE, J., DUNNE, E., SMITH, L., BERNDT, M. C., SHEILS, O., KENNY, D. & O'LEARY, J. J., 2011. Platelet adhesion and degranulation induce pro-survival and pro-angiogenic signalling in ovarian cancer cells. *PLoS ONE*. 6(10): e26125. doi:10.1371/journal.pone.0026125

Summary

Ovarian cancer is the leading cause of death from gynaecological malignancy worldwide with an estimated global incidence of 225,900 and mortality of 140,200 per year. In Ireland ovarian cancer is the second most common form of gynaecological cancer, the greatest cause of death from gynaecological malignancy and the fifth greatest cause of all cancer deaths in Irish women. Ovarian cancer has an associated mortality rate of ~75% and a long term survival rate of up to 20%, reflecting the severity of the disease and frequent diagnosis at late stage due to non-specific symptoms and a lack of effective screening tools. Treatment primarily involves debulking surgery and chemotherapy but despite initially high responsiveness, chemo-resistant recurrent disease is common.

Platelets are blood borne, anucleate, discoid, cell fragments containing numerous cytoplasmic granules whose primary role is to maintain haemostasis through their involvement in clotting (thrombosis) in response to blood vessel damage and injury. The normal platelet range is between 150 X 10^9 and 450 X 10^9 platelets per litre varying with between different laboratories, with a count of greater than 450 X 10^9/L clinically considered high and referred to as thrombocytosis.

Numerous observations have confirmed an increased incidence of thrombocytosis and thrombosis in various malignancies, including ovarian cancer, and they are associated with increased metastasis and poor prognosis. This is hypothesised to be associated with a phenomenon known as tumour cell induced platelet aggregation (TCIPA), where circulating tumour cells (CTCs) in the vasculature may induce platelet aggregation to their surface and so become 'cloaked' in platelets. TCIPA is hypothesised to provide several advantages to the CTC. It may play a crucial role in overcoming physical challenges of haematogenous dissemination by assisting in CTC embolisation in the vasculature, enhancing evasion of immune-mediated tumour cell destruction and abrogating the effects of chemotheraputic agents. Thus TCIPA may enhance CTCs' capability for metastasis and contribute significantly to the metastatic load in malignancy.

A majority of studies examining TCIPA have focused on determining the pro-thrombotic initiators and physical mediators underpinning the phenomenon. However, exceptionally little is known about the molecular basis for the improved metastatic potential of cancer cells that become coated in platelets during their time in the circulatory system. Prior to completion of this study, the molecular changes occurring in the cancer cell(s) at the core of the CTC-platelet aggregate was limited to a solitary gene, MMP9, described to be transcriptionally up-regulated in cancer cells as a result of TCIPA.

A retrospective study using archival ovarian samples was performed to examine the association of preoperative thrombocytosis with tumour grade, patient outcome and the expression of selected target genes in an Irish ovarian cancer population. Variations in gene expression included a trend for reduced PDGFRα/β and increased PDGFβ expression. Additionally, thrombocytosis was observed to correlate with increasing tumour grade. It is proposed that ovarian tumour cells signal to encourage neovascularisation while remaining resistant to PDGF growth stimuli, facilitating the development of a microenvironment conducive to sustaining tumour growth.

The relationship between ovarian cancer and TCIPA was investigated using a novel fluorescent *in vitro* adhesion assay. The assay was capable of investigating the varying ability of different cell lines (representing normal ovarian tissue and ovarian cancers) to adhere platelets to their surface. Cancer cells demonstrated a trend for increased capacity to adhere platelets with increasing malignancy/metastatic potential. Flow cytometric assessment of markers of platelet activation revealed dose-dependent platelet activation by cancer cells.

The molecular basis for TCIPA enhancement of ovarian cancer metastatic potential was investigated through unbiased whole transcriptome analysis of ovarian cell line responses to exposure to washed platelets or platelet releasate. Relative changes in gene expression in exposure groups compared to controls indicated significant changes in expression of genes involved in pro-angiogenic, proliferative and anti-apoptotic signalling, as well as regulation of translation, cell cycle and metabolism.

These changes are proposed to indicate TCIPA-related platelet-induced cancer cell priming, mediated through both mechanical platelet-cancer cell signalling and via the content of platelet granules released during the platelet-cancer cell interaction.

CHAPTER ONE

INTRODUCTION

1 General Introduction

1.1 Anatomy and Function of the Ovary

The ovaries (ovaria) are the pair of female pelvic reproductive organs that house the ova and are responsible for the production of the hormones oestrogen and progesterone.

Each ovary is a solid, almond shaped body measuring approximately 3-4cm X 2cm X 1cm and weighing 3-5g in the adult. Their size and weight may vary as during pregnancy they can become enlarged and involute/atrophy following menopause.

The location of the ovary is subject to some variation as during pregnancy the ovary is frequently pulled into the abdominal cavity by the enlarging uterus with the ovary subsequently returning to a variable position after parturition arising from a more lax broad ligament. As such the description here applies to the ovary of the nulliparous woman. The ovaries are located in the broad ligament in shallow depressions, called ovarian fossae in the lateral walls of the pelvic cavity on either side of the uterus. Several paired ligaments support the ovaries and hold them loosely in place:

- The ovary is anchored to the posterior aspect of the broad ligament of the uterus by a peritoneal fold, the mesovary/mesovarium, thus making the ovary an interperitoneal organ.

- The (proper) ovarian ligament connects the uterus and ovary at the ovary's (lower) medial or uterine pole.

- The suspensory ligament of the ovary (infundibular pelvic ligament) attaches the ovary to the pelvic sidewall at the ovary's (upper) lateral or tubular pole. This larger structure also contains the primary ovarian arterial, venous and lymphatic supply as well as nerve supply to the ovary.

The ovary is surrounded by the tunica albuginea, a thin fibrous capsule itself covered by a single layer of cuboidal cells called the germinal epithelium. The body of the ovary is primarily composed of spindle shaped cells, predominantly fibroblasts but also includes smooth muscle cells, fine collagen fibres and ground substance which cumulatively comprise ovarian stroma. The ovary can be further divided into two distinct basic sections (Figure 1-1):

- An outer cortex: This is dense and granular in nature due to the presence of ovarian follicles at various stages of oocyte, female germ cell, development (oogenesis) and atresia. This part of the ovary is responsible for production of steroid hormones oestrogen and progesterone responsible for development of secondary sexual characteristics in puberty, regulation of the menstrual cycle and ovulation, maintenance of the uterine lining during pregnancy and lactation.

- An inner medulla: This comprises of looser stromal connective tissue with abundant blood and lymph vessels and nerves.

Figure 1-1

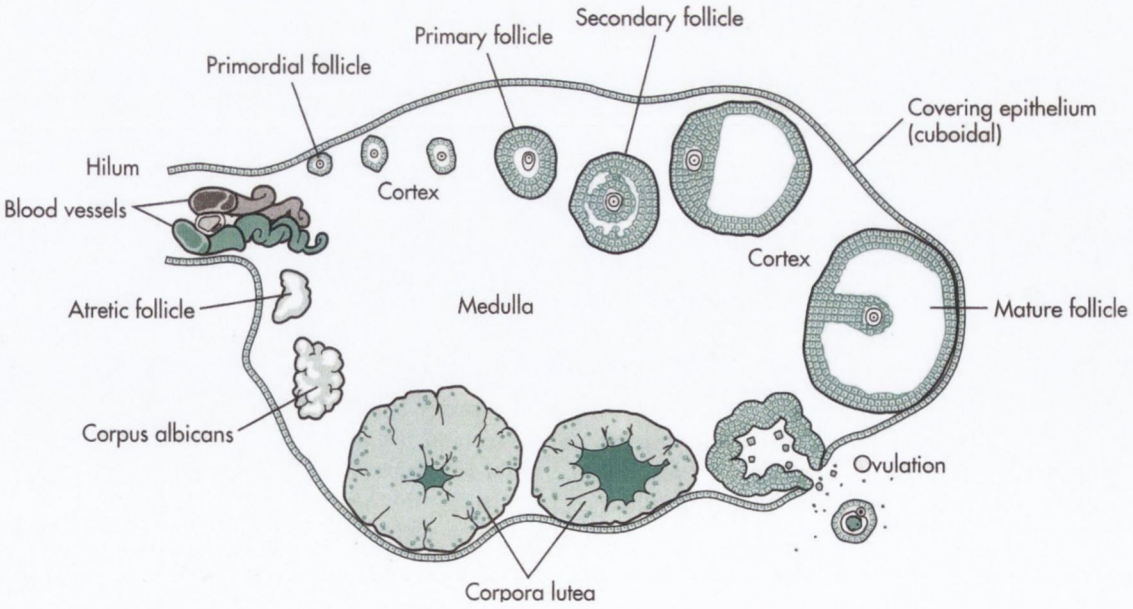

Figure 1-1: Schematic representation of the ovary.

From Berne (2004).

The ovarian blood supply is provided by the ovarian artery. Both right and left arteries, serving the right and left ovary respectively originate from the descending aorta at L1. Additional circulation is also received from the uterine artery which anastamose with the ovarian artery at the fallopian tubes.

Both the ovarian artery and vein enter and exit the ovary at the hilum with the left ovarian vein draining into the left renal vein and the right ovarian vein directly into the inferior vena cava. Lymphatic drainage of the ovary is primarily to the lateral para-aortic nodes.

Nerve supply to the ovaries runs into the ovary at the hilum along with the vasculature. Sympathetic innervation arises from T10 and nerves derived from the hypogastric (or pelvic) plexus, and from the ovarian plexus. Parasympathetic supply comes from the Vagus nerve. (Agur and Dalley, 2009, Drake et al., 2005).

1.2 Ovarian Cancer

From the moment of fertilisation of the ovum until physical maturity is reached the cells of the body undergo controlled growth, proliferation, and where appropriate also destruction, under the direction of the genes encoded within the DNA of the nucleus of the cells as the human body develops from an embryo to infant, through childhood into adolescence and finally into adulthood. From physical maturity onwards the proliferative function of most cells is largely reduced with cellular growth or proliferation occurring to replace worn out cells or being increased in response to injury requiring repair.

Cancer is a patho-physiological condition where as a result of either genetic damage acquired as a result of internal or external factors (such as chemicals introduced through as a result of diet or lifestyle, free-radicals and other metabolic by-products, radiation and infectious organisms) or genes that have inhered damage from a parental source, cells fail to die in response to the damaged DNA as a normal cell would, but instead acquire the capability to continue growing and proliferate. These cells develop a set of characteristics described as 'the hallmarks of cancer' which include the following:

- Self sufficiency of growth signals
- Insensitivity to antigrowth signals
- The capability to invade tissues and metastasise
- Evade senescence
- Drive sustained angiogenesis
- Evasion of apoptosis
- Deregulation of cellular energetics
- Evasion of immune destruction

These characteristics are proposed to be further supported by cancer enabling characteristics, genomic instability and mutation and tumour promoting inflammation (Hanahan and Weinberg, 2011, 2000).

As with other all other body tissues, the ovary is subject to risk of developing cancer arising from cells that make up its structure.

Should ovarian cells acquire the necessary hallmark characteristics to allow them grow and spread in an unregulated manner, they present a significant threat to the health and survival of the affected individual.

Once the primary cancer spreads beyond its site of origin and successfully metastasises, subsequent growth at these secondary sites results in mechanical obstruction, reduced function and ultimately the failure of the organ(s) and death.

1.2.1 Epidemiology of Ovarian Cancer

Globally 12.7 million cancer cases and 7.6 million cancer deaths are estimated to occur annually (Jemal et al., 2011). The predicted cancer mortality for Europe for 2011 is 1,281,466 cancer deaths, 721,252 men and 560,184 women, in the European Union (EU) in 2011 (Malvezzi et al., 2011).

Ovarian cancer is the leading cause of death from gynaecological malignancy worldwide. It has an estimated incidence of 225,900 new cases per year and 140,200 deaths per year globally (Jemal et al., 2011). In the developed world it is estimated to have an incidence of 100,300 and mortality of 64,500 cases, with the developing world estimated to have slightly higher figures of 125,200 and 75,700 cases, respectively. This is attributed to reduced access to healthcare for timely and effective treatment and reduced screening leading to later stage cancer diagnosis in developing countries.

Globally, ovarian cancer represents a significant cost to health care systems and providers and a great loss of life and is the fourth most common cause of death from all female cancers worldwide (Ferlay et al., 2007, Parkin et al., 2005, Laios et al., 2008).

Ovarian cancer is the fifth most common form of women's cancers in Europe with an incidence of 69,565 cases and 44,280 deaths per year (Ferlay J et al., 2010). In the USA ovarian cancer has a predicted incidence of ~22,000 (21,990) and mortality of ~15,500 (15,460) cases for 2011, where it is the ninth most common of cancer and fifth greatest cause of all cancer deaths in females and greatest cause of death arising from gynaecological cancers (American Cancer Society, 2011).

When considered from a global perspective and progressing to a regional and European scale the annual ratio of diagnoses to deaths is broadly similar (Table 1-1). Ireland reports a higher diagnosis:death ratio for ovarian cancer than is calculated for Europe as a whole, but the percentages of the female population diagnosed with and succumbing to ovarian malignancy per year is lower than is calculated for Europe. These figures may be a reflection of both the high frequency and aggressive nature of late stage diagnosis of ovarian cancers, and also of the lower lifetime risk of developing ovarian cancer in Ireland compared to some other industrialised nations.

Table 1-1

	Global	Developed Countries*	Developing Countries*	Europe	Ireland
Cases	225,900	100,300	125,200	69,565	315
Deaths	140,200	64,500	75,700	44,280	269
Ratio	0.621	0.643	0.605	0.637	0.854
Female Population (FP) (estimate)**	3,470,500,744	633,431,085	2,863,194,617	380,686,199	2,310,298
% FP Diagnosed p/a	0.0065	0.0158	0.0044	0.0183	0.0136
% FP Dying p/a	0.0040	0.0102	0.0026	0.0116	0.0116

Table 1-1: Ovarian Cancer Statistics – A Global, Regional, European and Irish Overview.

* As defined by the UN Statistics Division. Developed countries = North America, Europe, Japan, New Zealand & Australia. Developing countries = South & Central Americas, Asia & Middle East (excl. Japan), Africa and Oceania (excl. New Zealand & Australia).

** Determined using total population estimates and the sex ratio for each region (United Nations Department of Economic and Social Affairs, 2011). Irish figures based on 2011 Irish census data (Central Statistics Office (Ireland), 2012).

Ovarian cancer has an associated mortality rate of ~75% and a long term (5 year) survival rate of ~20% (Chan et al., 2006). This is a reflection of the severity of the disease and the unfortunate fact that patients frequently present with stage III or stage IV disease, with associated local or disseminated extra-abdominal metastases (Benedet et al., 2006).

The latest figures for cancer incidence and mortality in Ireland show ovarian cancer represents 3.8% of all female cancer cases and 7% of female cancer deaths (NCRI, 2011a).

The incidence of ovarian cancer (OC) is 315 cases per year in Ireland, making it the second most common form of gynaecological cancer (after uterine cancer) and sixth most common form of solid cancer in females and is associated with a lifetime risk (to 75 years) of developing OC of 1.2%. The average age at diagnosis is 63 years and the greatest proportion of cases is diagnosed in individuals between 50 and 64 years of age.

Annually ovarian cancer is associated with 269 deaths in Ireland, making it the greatest cause of death from gynaecological malignancy and the fifth greatest cause of all cancer deaths in women. It is attributed with the sixth lowest 5 year survival rate of all cancers in Ireland at 36.1%, a lifetime (to 75 years) risk of death of 1.1% and a mean estimated loss of 18.3 years of life in those diagnosed (NCRI, 2011a, 2011b).

While variation in the reported values exists between various studies investigating ovarian cancer survival, this 5 year survival figure for Ireland is comparable to the rates reported for the UK of 38-41% (Easton et al., 2011, Cooper et al., 2008). This is lower than the European average of 41.6-44.1%, itself comparable to the US at 43%-46% (American Cancer Society, 2011), though falls significantly short of survival rates for ovarian cancer in other European countries such as Austria which report a 5 year survival rate of 63.6% (Moller et al., 2009, Karim-Kos et al., 2008). The lifetime risk of developing ovarian cancer in Ireland is slightly better than that normally associated with industrialised countries 1.5%-2% (Ferlay J et al., 2010).

Recent examination of the composition of diagnosed ovarian cancer cases in Ireland determined:

- 47.5% were mucinous or serous carcinomas
- 28.4% were adenocarcinoma
- 5.1% specialised gonadal neoplasms
- 5.7% were other types of neoplasms
- 13.2% of cases were not specified.

Of specific interest with regard to patient survival prognoses, just 11.9% of Irish ovarian cancers were diagnosed at a stage 1/borderline classification. Almost 55% of ovarian cancers were diagnosed at stage 3 (27.4%) or stage 4 (26.9%).

If diagnosed at stage 1/borderline the 5 year survival rate in ovarian cancer may be as high as 94%. By comparison the 5 year survival rate associated with ovarian cancer excluding cases diagnosed at stage 1/borderline is significantly lower (Donnelly et al., 2009, NCRI, 2009).

1.2.2 Classification of Ovarian Cancer

Currently, pelvic carcinoma is classified according to the location of the bulk of the tumour as being ovarian, peritoneal, or fallopian tube in origin. Furthermore, ovarian tumours are classified according to the type of cell from which they arise and whether or not it is benign or malignant in nature. The three primary types of ovarian cancer are:

1. **Ovarian Germ Cell Tumours:** arising from the cells that produce the ova in the cortex of the ovary. These types of tumour are relatively rare, making up ~1.5% of ovarian cancers, and are associated with a very good curative rate, with close to 100% of early stage disease detected and ~75% of advanced germ cell cancers responsive to treatment (Pectasides et al., 2008, Gershenson, 2007). This form of ovarian cancer includes:

   Teratomas: which may contain tissue types reflecting the three germ layers; the mesoderm, ectoderm and endoderm, such as cartilage or adipose, thyroid and lung tissues respectively and may include tissues such as hair or teeth (Choudhary et al., 2009, Saba et al., 2009, Outwater et al., 2001). These forms of cancer make up 0.8% of ovarian cancers and arising from their responsiveness to chemotherapeutic intervention, even if identified at an advance stage, the 5 year RSR for teratoma is 89.1%.

   Dysgerminomas: a common form of ovarian germ cell tumour making up 0.5% of ovarian cancer cases. This form of cancer primarily affects women in their teenage years to early twenties. It is slow in both growth and spreading, and is responsive to chemotherapeutic treatment resulting in high survival rates (Tangjitgamol et al., 2010, Vicus et al., 2010).

   Endodermal sinus tumours: are very rare ovarian neoplasms that typically affect girls and young women. These tumours frequently produce α-fetoprotein (AFP) detectable in the peripheral circulation and are highly malignant, radiotherapy resistant but chemotherapy sensitive.

Embryonal carcinoma: a rare form of ovarian cancer it represents just 1-3% of ovarian germ cell neoplasms. Embryonal carcinoma primarily affects young women with a mean age at diagnosis of 14-16 years and is associated with mean survival rates at 5 years of ~90%

Choriocarcinoma: a very rare malignant germ cell tumour arising from the cells in the chorion layer of the placenta, typically affecting girls and young women between 15 and 19 years of age. Despite the aggressive nature of this cancer, prognosis is usually positive as they tend to be sensitive to chemotherapeutic intervention.

While comparatively rare compared with epithelial ovarian cancers, germ cell tumours are of significant research and clinical interest and importance as they primarily affect younger women and women during their reproductive years.

2. **Ovarian Stromal Cell Tumours**: arising from the cells that provide structure to the ovary. Ovarian cancers of stromal cell origin are rare, making up 1.1% of ovarian cancers. This form of ovarian cancer tends to affect older women, with <50% of stromal tumours diagnosed in patients over 50 years of age. This type of tumour can frequently be hormone producing (female and/or male hormones) and includes benign fibromas and thecomas and low grade malignant granulosa, granulosa-theca and Sertoli-Leydig tumours (Shanbhogue et al., 2010, Lee et al., 2009). Cancerous stromal tumours are often found at an early stage and have a good outlook, with more than 75% of patients surviving long-term.

3. **Ovarian Epithelial Cell Tumours:** arising from the columnar epithelial cells on the outer surface of the ovary. This type of ovarian tumour makes up ~90% of ovarian cancer diagnoses and includes:

Benign ovarian epithelial tumours: account for 15.9% of ovarian epithelial tumours. They do not spread or lead to serious illness and are associated with a 5 year relative survival rate (RSR) of 98.2%.

Serous borderline ovarian tumours (SBT)/low malignant potential (LMP) tumours: these tumours tend to not invade into the stroma of the ovary, or into the lining of the abdomen if they spread to the abdominal lining. These forms of tumour are rarely life threatening and have a long term survival rate of >99% (Seidman and Kurman, 2000).

Epithelial ovarian carcinoma (EOC): the most common form of ovarian cancer making up 89.7% of all ovarian cancer diagnoses. EOC may itself sub-divided into several subcategories including:

- **Serous Ovarian Epithelial Carcinoma:** accounting for more than one quarter of all EOC diagnoses. This form of epithelial ovarian cancer is of primary interest to this study and is discussed in section 1.2.3 of this chapter.

- **Undifferentiated Epithelial Carcinoma:** This form of cancer displays an absence of structures and cell morphologies associated with other forms of epithelial ovarian cancers and is observed as a sheet-like growth of small, uniform tumour cells often bordering abruptly with a better differentiated other form of ovarian epithelial cancer. In cases where undifferentiated ovarian cancer is present, even as a minority focus of a larger other tumour type, it is associated with a poor prognosis (Przybycin and Soslow, 2011, Tafe et al., 2010).

- **Mucinous Carcinoma:** make up 3.4% of ovarian carcinomas and have an associated 5 year RSR of 49.1%. Mucinous carcinomas affect women under the age of 50 more frequently than serous ovarian carcinoma and may frequently be large cystic tumours containing a gelatinous, glycoprotein rich fluid up to 25kg in weight. Though early stage disease is associated with a positive prognosis, mucinous carcinomas are less sensitive to treatment using platinating agents such as carboplatin and paclitaxel and advanced stage mucinous carcinoma is associated with worse outcome than serous ovarian carcinoma at the same stage (Schiavone et al., 2011, Shimada et al., 2009, Hess et al., 2004).

- **Clear cell carcinoma:** These tumours are characterised histologically by large epithelial cells with a clear cytoplasm and represent 4% of epithelial ovarian cancers. This type of cancer tends to be quite aggressive, though a majority of cases present unilaterally and up to 25% of cases are identified at FIGO grades 1 or 2 resulting in positive patient prognosis and a 5 year RSR of 61.5%. (Przybycin and Soslow, 2011, Chan et al., 2008, Hoei-Hansen et al., 2007)

- **Endometrioid carcinoma:** represents 8.9% of ovarian cancers and is associated with a 5 year RSR of 70.9%. It is characterised by its resemblance to endometrial cells normally lining the uterus and is considered to be histologically indistinguishable from endometrial carcinoma. Most cases of this form of cancer present as unilateral disease and are frequently associated with concurrent endometriosis or endometrial neoplasms, however it has a better prognosis than typical serous carcinomas of the ovary. This is suggested to be significantly attributable to a high proportion of cases presenting in early stage disease (Przybycin and Soslow, 2011, Storey et al., 2008, Kosary, 2007).

1.2.3 Serous Ovarian Epithelial Carcinoma

Serous ovarian carcinoma is the most common form of ovarian cancer, making up 26.4% of ovarian cancer cases where it has a 5 year relative survival rate (RSR) of ~21%. It is also a form of ovarian cancer which frequently presents at high grades at diagnosis (>90%) and is the form of ovarian cancer most commonly associated with BRCA and P53 tumour suppressor gene (TSG) mutations. Serous carcinomas may range in size from a few millimetres to greater than 20cm in diameter and present bilaterally twice as frequently as unilateral disease (Przybycin and Soslow, 2011, Kosary, 2007).

Gross tumour appearance varies with the level of tumour differentiation. Well differentiated ovarian serous carcinoma is associated with solid and cystic regions with papillae in the cystic spaces or on the surface and with a minority of cases with disease confined to the surface of the ovary. Conversely, poorly differentiated disease may have solid, friable (loosely held together) and multi-nodular components with small papillary clusters and frequently contains necrotic and/or haemorrhagic areas.

Histologically serous carcinoma is associated with tumours displaying a papillary structures consisting of fibrovascular cores covered in epithelial cells, the presence of calciferous Psammoma bodies, stromal invasion and elements of necrosis. Tumour cells display a high level of nuclear atypia with large multi nucleate nuclei with abnormal mitotic figures and high mitotic activity (American Cancer Society, 2010, Kosary, 2007).

Unlike other gynaecological cancers that result in a significant disease burden and loss of life, such as cervical cancer where the transit time from a precursor lesion to invasive carcinoma is close to 10 years, it appears that high grade ovarian carcinoma spreads to sites beyond the ovary early in disease development.

Significantly, this reduces the time available for detecting ovarian cancer before it has spread, increasing the importance of determining early disease biomarkers and developing effective anti-metastatic regimens.

Arising from the high contribution of serous ovarian epithelial carcinomas to the overall ovarian cancer burden, and the high morbidity and mortality associated with the disease, this form of ovarian cancer is of primary interest in this thesis.

Figure 1-2

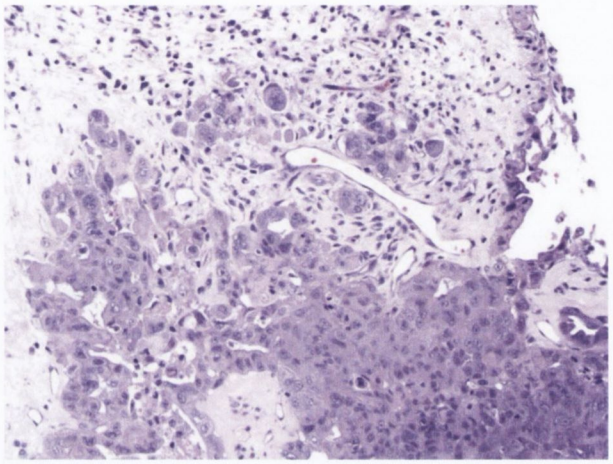

Figure 1-2: H&E Staining Photomicrograph of a malignant Serous Ovarian Carcinoma with stromal micro-invasion.

Note the invasion of strongly stained epithelial (papillary serous) carcinoma cells on right of image into the underlying stromal cells on left (WebPathology.com, 2011).

1.2.3.1 Confounding Factors in Ovarian Cancer

In addition to the non-specific symptoms associated with ovarian cancer (detailed in Section 1.2.3.3), the morphological characteristics of other pelvic/gynaecologic cancers can make the correct diagnosis difficult. In spite of this, the understanding of ovarian cancer is continually evolving and as time has progressed and closer and more detailed gross, histological and molecular investigations have taken place, more cancers that would otherwise have been described in error as ovarian carcinoma have been correctly identified, allowing better, more accurate and appropriate treatment of pelvic/gynaecological cancers.

1.2.3.1.1 Primary Peritoneal Cancer

Primary peritoneal cancer (PPC) has a very similar presentation to epithelial serous carcinoma. It has similar symptoms and biomarker presentation, similar genes have been observed to be altered (p53 and BRCA1), and the staging, treatment and prognosis are alike, but it arises in cells arising from the lining of the abdomen (the peritoneum) and is characterised by diffuse involvement of the peritoneum by papillary carcinoma with an absence of an obvious primary site. Historically, between 10% and 28% (Jaaback et al., 2006, Seidman et al., 2004, Halperin et al., 2001) of ovarian cancers are estimated to have been diagnosed as PPC.

Criteria now employed for the diagnosis of PPC have been described which set out several characteristics to eliminate ovarian disease as the primary neoplasm. These include observing that the ovaries are of a normal size (or enlarged arising from a benign process), that the disease involvement in the peritoneum is greater than that of the ovaries and that tumour presence on the ovaries must either be non-existent or confined to the surface epithelium, with an absence of stromal invasion or stromal involvement and limited to $25mm^2$ area (Schorge et al., 2000). Survival is poor for patients with primary peritoneal carcinoma, with high reported mortality; the median survival reported is 12-25 months, even with extensive surgery and chemotherapy.

1.2.3.1.2 Fallopian Tube Cancers

Cancer arising from the distal fallopian tube/fimbral region is frequently difficult to determine as different to cancer arising from the ovary (Salvador et al., 2008, Piek et al., 2008).

It has been suggested that many ovarian epithelial cancers may in fact be metastases/implants of fallopian tube derived cancers. (Al-Agha and Blake Gilks, 2011, Diniz et al., 2011, Seidman et al., 2011, Przybycin et al., 2010, Roh et al., 2009, Gross et al., 2010, Salvador et al., 2008)

This theory is supported by the observation that fallopian tube lesions (variously termed (serous) tubal intra epithelial carcinomas or lesions (S)TIC/L) have been identified on the fimbriae of the fallopian tube during prophylactic oopherecomy in women predisposed to developing ovarian cancer (BRCA1/BRCA2 mutation carriers).

These (S)TIC/L derived cancers are also suggested to have a higher frequency of P53 mutation and are less genomically stable, resulting in more aggressive cancer types such as high grade serous carcinoma (Kurman and Shih, 2011, 2010, Przybycin et al., 2010, Shaw et al., 2009, Crum et al., 2007, Kindelberger et al., 2007, Piek et al., 2001).

It has been suggested that the varying genetic background arising from the different hypothesised origins of different forms of ovarian cancer may be utilised to amend the classification of ovarian serous cancers to reflect the varying nature of the tumourigenesis of high and low grade cancers:

- Type 1 - non-TIC derived low grade cancers, arising from definable precursor lesions and more commonly associated with KRAS, BRAF, PI3KCA or ERBB2 mutations, greater chromosomal stability and reduced aggressiveness including low grade serous carcinoma, mucinous carcinomas, endometrioid carcinomas, malignant Brenner tumours and clear cell carcinomas (Figure 1-3).

- Type 2 - TIC derived high grade aggressive cancers, presenting with greatest frequency at advanced stages and associated with BRCA and P53 gene mutations including high grade serous carcinoma, malignant mixed mesodermal tumours (carcinosarcoma) and undifferentiated carcinomas (Figure 1-3) (Kurman and Shih, 2011, Przybycin and Soslow, 2011, Vang et al., 2009, Chan et al., 2007).

Figure 1-3

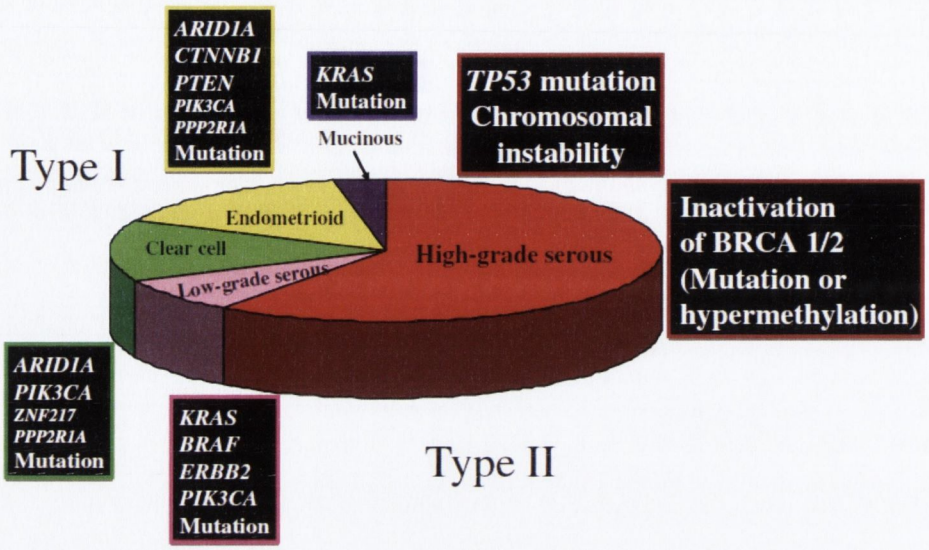

Figure 1-3: Proposed delineation of Type 1 and Type 2 Ovarian Serous Carcinomas based on genomic characteristics and tumourigenesis.

(Image from Kurman and Shih (2011))

1.2.3.2 Tumour Classification

Ovarian cancer, as well as any other type of solid cancer, is described by not only the tumour type but also the tumour gradation and stage.

1.2.3.2.1 Staging and Gradation

Ovarian cancer is both graded and staged. The histologic grade of a tumour is a measurement of the tumour that measures and describes how abnormal or malignant its cells look under the microscope in comparison to normal tissues. Considerations taken when establishing tumour grade include cell appearance/abnormality, alterations in rate of growth and degree of invasiveness. There are four grades indicating the likelihood of the cancer to spread and the higher the grade, the more likely this is to occur (Edge and American Joint Committee on Cancer., 2010).

- Grade 0 is used to describe non-invasive tumours. Grade 0 cancers are also referred to as borderline tumours.

- Grade 1 tumours have cells that are well differentiated (look very similar to the normal tissue) and are the ones with the best prognosis.

- Grade 2 tumours are also called moderately well differentiated and they are made up of cells that resemble the normal tissue.

- Grade 3 tumours have the least favourable prognosis and their cells are abnormal, referred to as poorly differentiated.

Cancer staging is a categorisation of the extent of the primary cancer and the nature of its spread. Two different but similar systems exist that may be employed to describe the stage of ovarian cancers. These systems are the American Joint Committee on Cancer (AJCC) TNM system and the International Federation of Gynaecological Oncologists (FIGO) classification (Table 1-2).

Both systems use a numerical categorisation to describe the tumour's characteristics, with the TNM classification further appending the tumour designation with N and M categorisation values of 0 or 1 to indicate the presence of metastatic spread of the primary tumour to nearby (regional) lymph nodes and whether or not the cancer has spread to distant organs, such as the lungs, liver or other organs respectively. Should either of these be indeterminate or unperformed the value appended is 'X'.

Table 1-2

TNM	FIGO	Tumour Characteristic
Tx	/	No description of the tumour's extent is possible because of incomplete information.
T1	Stage I	Limited to one or both ovaries.
T1a	IA	Involves one ovary; capsule intact; no tumour on ovarian surface; no malignant cells in ascites or peritoneal washings.
T1b	IB	Involves both ovaries; capsule intact; no tumour on ovarian surface; negative washings.
T1c	IC	Tumour limited to ovaries with any of the following: capsule ruptured, tumour on ovarian surface, positive washings.
T2	Stage II	Pelvic extension or implants.
T2a	IIA	Extension or implants onto uterus or fallopian tube; negative washings.
T2b	IIB	Extension or implants onto other pelvic structures; negative washings.
T2c	IIC	Pelvic extension or implants with positive peritoneal washings.
T3	Stage III	Microscopic peritoneal implants outside of the pelvis; or limited to the pelvis with extension to the small bowel or omentum.
T3a	IIIA	Microscopic peritoneal metastases beyond pelvis.
T3b	IIIB	Macroscopic peritoneal metastases beyond pelvis less than 2 cm in size.
T3c	IIIC	Peritoneal metastases beyond pelvis > 2 cm or lymph node metastases.
Any T Any N M1	Stage IV	Distant metastases to the liver or outside the peritoneal cavity.

Table 1-2: TNM & FIGO Staging Classification of Ovarian Cancers.

In the context of ovarian cancer the pattern of progression commonly observed with the spread of the disease may be summarised as follows:

- Stage 1 is associated with the presence of an irregular pelvic mass.

- Stage 2 is associated with the presence of pelvic nodules outside of the ovary.

- Stage 3 is associated with the presence of disease in the omentum, identified by the presence of a mass mid-abdomen superior to the pelvic mass.

- Finally, stage 4 is associated with peripheral metastasis arising from lymphatic and/or haematogenous spread, resulting in shed circulating tumour cells (CTCs) derived from the tumour mass(es) travelling to and becoming established in the lungs and distant organs. At this point, advanced intra-abdominal disease may cause obstructions of the gastro-intestinal tract (GIT) resulting in nausea, vomiting and abdominal pain.

While lymphatic dissemination has been historically seen as the primary route of tumour metastasis in many malignancies, haematogenous spread is gaining increasing acceptance as a significant means of spread, as witnessed by increased identification of and focus on CTCs in malignant disease.

Recent scientific focus on CTCs has observed associations between tumour cells in the circulation and reduced survival, later stage disease and/or worse prognosis in breast, prostate, non-small cell lung, colorectal, gastrointestinal, pancreatic, melanoma and ovarian cancers (Aktas et al., 2011, Hartkopf et al., 2011, Iinuma et al., 2011, Krebs et al., 2011, Poveda et al., 2011, Fan et al., 2009, Liu et al., 2009, Scher et al., 2009, Cohen et al., 2008, de Bono et al., 2008, He et al., 2008b, Hoffmann et al., 2007, Visus et al., 2007, Budd et al., 2006, Fehm et al., 2006, Hayes et al., 2006, Soeth et al., 2005, Cristofanilli et al., 2004, Taubert et al., 2004, Judson et al., 2003).

1.2.3.3 Symptoms

Ovarian cancer associated symptoms include:

- Pelvic or abdominal pain
- Feelings of bloating
- Loss of appetite and difficulty eating (typically due to indigestion or vomiting)
- Weight loss
- Weight gain
- Frequent urination
- Menstrual irregularities

Due to the non-specific nature of these symptoms, individuals with developing ovarian cancer may frequently not respond to look for medical help and risk being misdiagnosed as suffering from other conditions or diseases should medial help be sought, both of which have potential to have significant impact on patient outcome.

1.2.3.4 Risk Factors in Ovarian Cancer

Several risk factors have been identified that modify an individual's risk of developing ovarian cancer.

- Age – based on the age at which ovarian cancer diagnoses are most frequently made, females over 60 years of age have an increased risk of developing ovarian disease.

- Obesity – has been observed to increase risk of developing, with a BMI of greater than 30 associated with an increased risk of up to 50% (Leitzmann et al., 2009, Olsen et al., 2007b).

- Diet – low fat diets have been observed to convey a reduced risk of developing ovarian cancer (Prentice et al., 2007).

- Lifestyle behaviours – smoking and alcohol consumption have not been shown to result in an increased risk of developing most forms of ovarian cancer, though there is evidence that these lifestyle behaviours may convey a slightly increased risk of developing mucinous ovarian cancer (Gram et al., 2011, Modugno et al., 2003). Physical activity is associated with a reduced risk of ovarian cancer development (Olsen et al., 2007a).

- Reproductive history – informs of altered risk of developing ovarian cancer. Nulliparous females are observed to have an increased risk of developing ovarian cancer over that of women who do have children (Modan et al., 2001, Adami et al., 1994).

- Surgery – hysterectomy is associated with a ~1/3 reduced risk of developing ovarian cancer and tubal ligation is associated with ~1/3 reduction of risk (Cibula et al., 2011a).

- Hormone replacement therapy (HRT) – associated with an ~20% increased risk of developing ovarian cancer (Cibula et al., 2010, Beral, 2007). It has been shown that oestrogen-only HRT conveys a greater risk than that of oestrogen and progestin HRT (Pearce et al., 2009, Hildebrand et al., 2010, Tsilidis et al., 2011).

- Oral Contraceptives – the use of oral contraceptives, while associated with a small increase in risk for the development of breast cancer, is associated with up to a 50% reduction in the risk of developing ovarian cancer (Beral et al., 2008).

- Family history – a family history of ovarian cancer is the single largest epidemiological risk factor for the development of ovarian cancer. The familial risk is modified by the number of primary and secondary relatives that have developed ovarian or breast cancer and their age at diagnosis, with a relative risk of seven-

fold higher if an individual has a history indicating a maternal and sibling (two primary relatives) affected (Gardiner, 2007).

In 10-15% of ovarian cancer cases a heritable genetic component is present in its development. These cases frequently involve mutations in the BRCA1 and BRCA2 tumour suppressor genes (TSGs). These are associated with the greatest increases of OC development amongst all other risk factors. The normal lifetime risk of developing ovarian cancer is ~1.6%, but in individuals with a BRCA1 or BRCA2 mutations the risk is significantly higher at 40-50% and ~20% respectively, marking these individuals as part of a high risk population requiring closer monitoring using biomarker and ultrasound screening/diagnostic modalities (Hemminki et al., 2011, van der Kolk et al., 2010, Russo et al., 2009, Boyle et al., 2008, Campeau et al., 2008, Smirnova et al., 2007, Reynolds and Moller, 2006, Antoniou et al., 2003, Modugno, 2003).

The aetiology of the increased risk of developing ovarian cancer associated with BRCA gene mutations is proposed to be related to the significant role their gene products play in maintaining genomic stability by repairing double stranded DNA breaks as part of the Fanconi Anaemia DNA repair pathway (Garcia and Benitez, 2008, D'Andrea and Grompe, 2003).

- Personal history – individuals with a prior history of breast cancer have an increased risk of developing ovarian cancer. This may be related to the presence of heritable BRCA gene mutations. In these individuals, prophylactic oopherectomy would be advised as the most effective strategy for reducing ovarian cancer risk, though the use of oral contraceptives has been suggested as an alternative, if limited, means of reducing risk in this population should oopherectomy be undesirable (Cibula et al., 2011b).

1.2.4 Diagnosis & Screening of Ovarian Cancer

One of the greatest challenges to the effective treatment and cure of ovarian cancers is the lack of an effective early detection system for identifying the cancer in its early development. No definitive precursor lesions that are later attributable to OC have been described and the symptoms associated with the disease are non-specific (Bell, 2005).

As a result, screening and diagnosis of ovarian cancers relies on a small number of methodologies to determine if ovarian neoplasms are present in an individual and whether these neoplasms are malignant and require intervention to protect the health of the individual. These include the investigation of tumour biomarkers, ultrasound examination, laparoscopy, imaging studies and biopsy.

1.2.4.1 Biomarker Investigation

The most commonly employed and studied biomarker for ovarian cancer is a protein called CA125. CA125 is a glycoprotein not normally produced by normal ovarian epithelium, but is over-expressed by serous and mucinous papillary tumours.

About 80% of ovarian cancers present with a CA125 blood concentration of >35 U/ml. When stratified by disease stage it was observed that elevated levels were present in 90% of advanced stage disease, but in only 50% of stage 1 disease, and correlated more strongly with serous than mucinous ovarian cancers. Additionally, in serum samples from 5 years pre-diagnosis, elevated CA125 levels were detected in only 25% of those that subsequently developed disease (Nossov et al., 2008, Reynolds and Moller, 2006).

CA125 levels have also been observed to be increased in benign conditions such as endometriosis, pelvic inflammatory disease, fibroids, benign cysts and menstruation (Whitehouse and Solomon, 2003, Aggarwal and Kehoe, 2010).

Given the inability to effectively predict future ovarian cancer development and the potential to fail to be expressed in ~20% of ovarian cancers, CA125 lacks the resolution and specificity to directly guide treatment. Instead it is used as a supportive marker in the primary assessment and diagnosis of ovarian cancer in addition to other methodologies, and repeat testing informs of the progression or regression of disease or recurrence following chemotherapy (Bast et al., 2005).

Other biomarkers have been identified that may improve the specificity and resolution of biomarker based ovarian cancer screening and diagnosis. These include the studied, but as yet clinically unapproved, B7-H4, HE4, Spondin-2, DcR3, members of the human kallikrein family including KLK6 & KLK10, osteopontin, VEGF, claudin 3, OVX1 and DF3, identified as potential biomarkers for use where CA125 expression is absent or low or in conjunction with CA125 to enhance detection of early stage disease and disease recurrence (Rosen et al., 2005, Simon et al., 2007, Huhtinen et al., 2009, Aggarwal and Kehoe, 2010, Husseinzadeh, 2011, Moore et al., 2010)

Germ cell cancers can cause elevated blood levels of the tumour markers reflective of their different nature to epithelial ovarian cancers. These include human chorionic gonadotropin (βHCG), alpha-fetoprotein (αFP) and lactate dehydrogenase (LDH). Stromal tumours such as ovarian granulosas may present with increased inhibin expression which holds potential as a biomarker for this form of cancer.

1.2.4.2 Ultrasound

In symptomatic or at-risk individuals a trans-abdominal or trans-vaginal ultrasound (TVU) may be performed to determine the presence, size, extent and morphological changes that may indicate a developing malignancy.

Arising from a risk of the potential for false positive diagnoses, ultrasound examinations have been supported with the use of CA125 biomarker detection, which has been shown to return a high specificity (99.9%) and a positive predictive value (PPV) (26.8%) for the correct diagnosis of ovarian cancer (Nossov et al., 2008).

The combination use of CA125 levels and ultrasound examination has been proposed as a potential screening modality for ovarian cancer. One of the largest multi-centre studies ovarian cancer screening studies devised, the UK Collaborative Trial of Ovarian Cancer Screening (UKCTOCS), has been established to conclude in 2014 with the aim of determining if an annual multimodal CA125 with TVU assessment can provide an effective screening methodology to allow better and earlier detection of ovarian cancers (Menon et al., 2009).

1.2.4.3 Laparoscopy

Laparoscopy is a minor surgical operation performed under general anaesthetic that allows visual assessment of a pelvic mass by insertion of a narrow illuminated camera through a small incision in the abdomen. This allows assessment of the ovaries and other pelvic organs and tissues in the area, as well as the capture of samples for biopsy and is useful in confirming the disease stage and so inform what subsequent surgical or other treatments are necessary.

1.2.4.4 Advanced Imaging Studies

In addition to ultrasound imaging, more advanced imaging methods like computed tomography (CT) scans, magnetic resonance imaging (MRI) or positron emission tomography (PET) scans can determine whether a pelvic mass is present. As with ultrasound technologies, studies using these technologies cannot confirm that a mass, if present, is malignant but can direct further investigation and can provide valuable monitoring information about the spread of ovarian malignancy to other tissues and organs.

CT examination collates multiple X-ray images to generate a three dimensional image capable of accurately informing about the size, location and spread of malignancy. As ovarian cancer presents at a late stage in ~70% of diagnoses this form of technology is capable of determining the extent of tumour spread beyond the abdomen, which is not possible by laparoscopy. To improve contrast, oral or intravenous contrast agents may be

required to help clearly outline structures in the body that x-ray technology is normally unable to clearly image.

MRI examination similarly allows the generation of three dimensional imagery for the characterising the physical size and spread of a tumour. This technology uses radiowaves to create images of the different scanned tissues. As each tissue type responds differently to the MRI scan the technology can clearly differentiate different tissue types and has been accepted as providing clearer tumour resolution than CT.

PET examination uses short lived radioactive tracer molecules such as fludeoxyglucose to specifically image malignant tissues due to their greater uptake of the tracer than normal tissues, arising from their increased metabolism and proliferation. This test has can be employed in conjunction with CT and MRI technologies and can help accurately detect primary and metastatic ovarian disease (Iyer and Lee, 2010, Risum et al., 2007, Murakami et al., 2006, Risum et al., 2009).

1.2.4.5 Biopsy

The gold standard and only means of definitively determining if a growth is malignant is through removal of and subsequent histological examination of a sample. The procedure for removing a sample is called a biopsy, and is most commonly performed for ovarian cancer during debulking surgery, though it can also be performed as part of a laparoscopy procedure.

Where patients have tumour associated ascites, a collection of fluid inside the abdomen, samples of this fluid can be extracted in a procedure called paracentesis, and used to assist in cancer diagnosis.

1.2.5 Management of Ovarian Cancer

Management of ovarian cancer currently involves a limited number of interventions aimed at reducing tumour load/burden, reducing tumour growth and spread. This primarily involves surgery and chemotherapy.

The nature and extent of surgical intervention required in the treatment of ovarian cancer varies with the extent of disease and the health of the individual, though commonly involves two aims: staging and debulking (or cytoreductive) surgery.

In ovarian cancer staging usually involves performing a hysterectomy and a bilateral salphingoopherectomy – the removal of the uterus, fallopian tubes and ovaries to determine the extent of spread of the disease. The latter is frequently recommended in individuals known to carry BRCA1/BRCA2 gene mutations that put them at increased risk of developing ovarian cancer (Aletti et al., 2007). Additionally an omentectomy, the removal of the omentum (the adiopose rich tissue covering the abdominal contents) may be performed, as it is frequently affected by ovarian metastases. Local lymph nodes may also be removed for investigation and saline washings may be performed and the fluid sent to be analysed for the presence of cancer cells.

For women with some kinds of ovarian cancers, and cancers in early stage development the performance of these significant surgeries may not be necessary and treatment may instead involve unilateral oopherectomy or fertility saving resection/debulking.

Debulking refers to the other goal of surgery, which is to remove the maximum amount of disease. In ovarian cancer this is important in instances where the tumour has spread throughout the abdomen and conventionally aims to removal all tumours larger than 1 cm. Successful debulking is associated with a much improved prognosis (Hoskins et al., 1992).

Currently platinating agents and taxanes form the mainstay of the chemotherapeutic agents used in the treatment of ovarian cancer.

A combination of these drugs is commonly used in the treatment of the majority of ovarian cancers (EOC). In this combination the platinating agents such as cisplatin or carboplatin affect the proliferating tumour cells by creating DNA adducts and cross links while taxanes such as paclitaxel (Taxol®) or docetaxel (Taxotere®) work to inhibit cell division by inhibiting the normal function of microtubules resulting in impaired chromosomal segregation with both treatments mediating their anti-cancer effect by preventing mitosis from occurring and inducing cancer cell apoptosis (Bharadwaj and Yu, 2004, Fuertes et al., 2003).

Chemotherapeutic treatment is conventionally employed following staging and debulking surgeries with at least 6 cycles of chemotherapy recommended in optimally debulked patients. Neoadjuvant chemotherapy (pre-surgery) has been investigated, though optimal regimen, context of use and advantages over conventional post-surgical chemotherapy remain to be clearly determined (Yildirim et al., 2011, Onda and Yoshikawa, 2011, du Bois et al., 2011).

In most instances chemotherapy is delivered orally or intravenously to ensure systemic delivery of treatment efficacious for the treatment of metastatic disease. In some cases of ovarian cancer, chemotherapy may also be injected through a catheter directly into the abdominal cavity, referred to as intraperitoneal (IP) chemotherapy. Typically this involves IV delivery of paclitaxel treatment with IP delivery of cisplatin and paclitaxel and has the advantage of delivering the greatest concentration of treatment to cells in the abdominal cavity where primary and secondary disease may be focussed. It is associated with better outcome in advanced ovarian cancer over IV chemotherapy alone but is associated with more severe side effects.

Approximately 1/3 of those with primary disease and the majority of those with recurrent disease will develop resistance to one or more chemotherapeutic agents, most frequently platinating agents such as cisplatin, associated with poor prognosis (Vasey, 2003, Stewart et al., 2006).

In Ireland in the period between 2004 and 2008 ovarian cancer was treated as follows:

- Surgical intervention – 62.7% of cases
- Chemotherapeutic intervention – 57.5% of cases
- Radiotherapy – 2.4% of cases
- No treatment – 22.5% of cases

(NCRI, 2011a)

The observation that approximately one fifth of patients presenting with ovarian cancer received no treatment may be a reflection of the high frequency at which ovarian cancer is diagnosed at an advanced stage of disease, with significant morbidity and thus beyond the capacity for beneficial clinical intervention.

In recurrent and platinating agent resistant disease other drugs may be employed, such as doxorubicin, gemcitabine and etoposide. Agents specifically targeting other molecules, including those involved in angiogenic and proliferative signalling, have been investigated for use in recurrent disease or in support of conventional therapies in treating primary disease. Those that have shown efficacy in reducing disease or clinical benefit in terms of improved stable disease time, progression free or overall survival include:

- BIBF-1120/Bevacizumab/Avastin® – an anti-VEGF monoclonal antibody inhibitor of VEGFR signalling (Markman, 2011, Cannistra et al., 2007).

- Volasertib – a small molecule inhibitor of the PLK1 (polo-like kinase 1) designed to induce mitotic (polo) arrest as proliferating cells go through prometaphase, resulting their apoptosis (Rudolph et al., 2009).

- Aflibercept/VEGF Trap – a fusion protein that incorporates portions of human VEGFR1 and VEGFR2 fused to the constant region of human IgG1 that functions as a soluble VEGFR (Moroney et al., 2009, Tew et al., 2007).

- Sorafenib/Nexavar® – an oral tyrosine kinase inhibitor that targets Raf, VEGFR, PDGFR, FLT3 and c-Kit (Matei et al., 2011, Welch et al., 2010).

- Sunitinib/Sutent® – a receptor tyrosine kinase inhibitor with activity against a VEGFR and PDGFR activity through VEGFR inhibition (Biagi et al., 2011).

- Cediranib/Recentin – a selective oral tyrosine kinase inhibitor of VEGFR1, VEGFR2, VEGFR3 and c-Kit (Raja et al., 2011, Matulonis et al., 2009).

- Pazopanib/Votrient – an oral angiogenesis inhibitor targeting VEGFR, PDGFR, and c-Kit (Friedlander et al., 2010, Hashimoto et al., 2010).

All these molecules have shown potential to be effective anti-cancer agents, a number of which are already approved for clinical use in the context of other cancers but require further study to determine their suitability and efficacy in enhancing the treatment of primary and secondary metastatic or recurrent ovarian disease, the greatest causes of mortality in ovarian cancer (Jelovac and Armstrong, 2011, Burger, 2011, Mantia-Smaldone et al., 2011).

1.3 Platelets

Platelets are the smallest circulating blood cells and number approximately 100 times the number of circulating white blood cells (WBCs). Platelets are very small, measuring approximately 2μM in diameter, anucleate, discoid, cell fragments containing numerous cytoplasmic granules, produced by megakaryote cells in the bone marrow and involved in a variety of processes including haemostasis, thrombosis, atherosclerosis and inflammation (García and Senis, 2011, Patel et al., 2005, Italiano and Shivdasani, 2003, White, 1988).

1.3.1 Platelet Physiology and Function

Morphologically, platelets have an invaginated membrane (suited to maximally absorb coagulation proteins and allow efficient expulsion of platelet granule contents) covered in a variety of glycoproteins with integrin activity. As is found in all cells, the platelet cell structure is supported by actin filaments which permit regulation of their shape by means of actin polymerisation/depolymerisation (Nash et al., 2002).

Platelets are derived from the fragmentation of megakaryoctes (MKs), the end point differentiation of Colony Forming Unit Megakaryocytes (CFU-MKs). MKs are formed when cells from this heterogeneous collection of megakaryocyte precursors stop proliferating and undergo endomitosis, becoming polyploid and developing a multilobar nucleus.

Megakaryocytopoiesis and platelet production is driven by a primary mitogen, thrombopoietin (though other IL family cytokines are also known to be involved). This affects these processes via a simple feedback mechanism via the cMPL (CD110) receptor found on both megakaryocytes and, in lesser amounts, on platelets (Cazzola, 2008, Schafer, 2004, Italiano and Shivdasani, 2003).

Figure 1-4

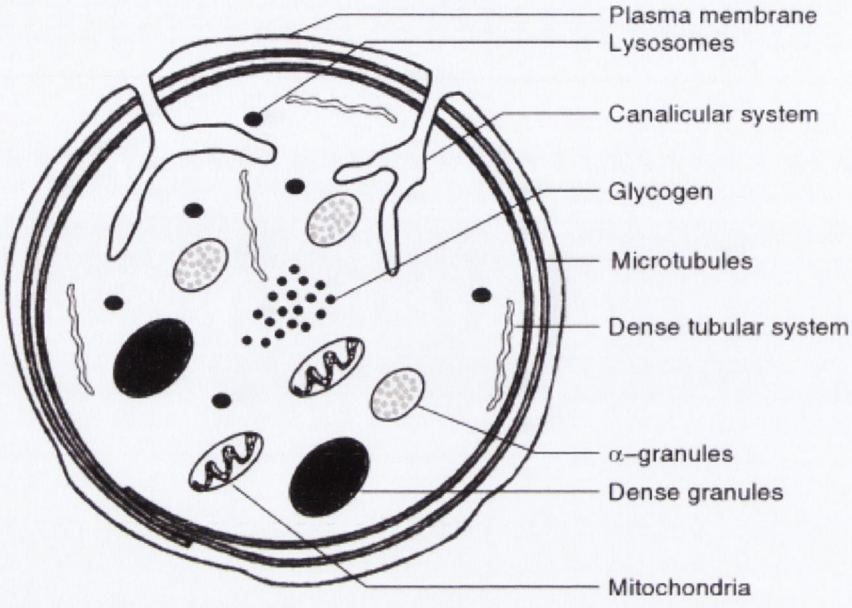

Figure 1-4: Schematic representation of unactivated platelet structure.

(From Garcia & Senis (2011)

The physiologic reference range of platelet counts is 150-400 x 10^9/L (Daly, 2011, McGhee, 2008). The upper limit of the normal platelet count is generally considered to be between 350 and 450 x 10^9/L, varying in different laboratories (Kaushansky and Williams, 2010). A titre in excess of the laboratory-accepted upper threshold is considered to be beyond the clinical normal range of platelet concentration and referred to as thrombocytosis. There are three main forms of thrombocytosis;

- Hereditary thrombocytosis: arising from mutations in JAK2 and MPL genes resulting in increased THP signal transduction or in THPO gene itself resulting in gain of function (increased expression) activity.

- Myleoproliferative/myleodysplastic thrombocytosis: arising from clonal expansion of cells with defects in JAK-2, MPL and/or other genes leading to inappropriately governed platelet production.

- Secondary/Reactive thrombocytosis: arising from malignancy related cytokine driven platelet production, iron deficiency, blood loss and other factors (Cazzola, 2008).

1.3.1.1 Platelet alpha and dense granules

The platelet α- and dense granules contain agents whose release and function are crucial to platelet reactions.

α-granules are the are the largest type of platelet storage granule and contain several types of proteins which are redistributed to the platelet membrane during platelet activation as a result of α-granule fusion to the platelet membrane, where they function to increasing receptor number and amplify the platelet response. Proteins contained in the α-granules include

- Platelet-specific proteins, p-selectin, platelet basic protein (PBP) and platelet factor 4 (PF4).

- Endocytosed proteins scavenged from the plasma and taken in to the platelet by endocytosis such as VWF, fibrinogen and albumin.

- Glycoproteins such as integrins $\alpha_{IIb}\beta_3$, p-selectin/CD62, GPIV and thrombospondin (TSP)

- Growth factors such as platelet derived growth factor (PDGF), transforming growth factor (TGF) and epidermal growth factor (EGF) which drive signalling in endothelial cells (ECs), smooth muscle cells and fibroblasts, and encourage wound healing.

Recent studies have returned data suggesting that in response to different stimuli platelets may release granule contents with specific pro- or anti-angiogenic contents, (Battinelli et al., 2011, Chatterjee et al., 2011, Italiano et al., 2008).

Dense granules are far fewer in number than α-granules (~7 per platelet) and gain their nomenclature arising from their comparatively greater opacity. Dense granules do not contain secretable proteins as α-granules do, but instead contain calcium ions and small molecule activators of platelet aggregation and/or vasoconstriction which are exocytosed or released through transporter during platelet activation.

These include;

- Adenosine diphosphate (ADP) which plays a role in the second wave of platelet activation after initial activation has taken place and also plays a role in phospholipase D (PLD) activation via a P2Y purinergic ADP receptor. ADP has also been shown to be is essential for thromboxane A2-induced platelet aggregation.

- Adenosine triphosphate (ATP), guanine triphosphate (GTP) and guanine diphosphate (GDP).

- Serotonin (5-hydroxytryptamine/5-HT).

(Rendu and Brohard-Bohn, 2001)

1.3.2 Thrombus/Clot Formation

In their normal homeostatic role, platelets are invaluable in maintaining haemostasis through their involvement in clotting (thrombosis) following vessel damage and injury (Jurasz et al, 2002).

The formation of a clot is a multistage process;

- The shear stress and laminar flow forces in the circulatory system ensure platelets remain close to the endothelium. The biological signal for initiation of platelet activation is delivered by the exposure of adhesive components of the sub-endothelium that are normally concealed from the blood by the endothelium. Platelets interact with adhesive proteins through adhesion receptors.

- The circulating platelet is decelerated through interaction of surface GP1b-IX-V integrin complex with exposed von Willebrand Factor (VWF) on the sub-endothelial surface, tethering the platelets in close proximity despite the shear forces at work in the circulatory system. *In vivo*, under conditions of shear stress, binding of VWF to its receptors (predominantly glycoprotein (GP) Ib) on platelet and the vessel wall anchors platelets to the sub-endothelium (Ginsberg et al., 1988, Ginsberg et al., 1993). Following initial contact phase, platelets change shape and spread on the sub-endothelium. The biological role of aggregation is to reinforce platelet adhesion monolayer with a structure based on web-like interactions between the adjacent platelets. The aggregate, thus formed, is firm enough to withstand disintegrating stimuli brought about by blood flow and shear forces.

- The tethered platelets then make closer interactions with collagen in the extracellular matrix via $\alpha_2\beta_1$ and GPVI integrins, allowing firm adherence to the surface and activation. The collagen receptors $\alpha_2\beta_1$ and GPVI are key in collagen induced aggregation and thrombus formation, as blockade of either results in the

abolition of platelet aggregation and thrombus formation, respectively (Chen and Lopez, 2005).

- Platelet-collagen interaction results in activation of the platelets and secretion of platelet granules (α-granules containing glycoproteins, coagulation factors & pro-(thrombospondin, VEGF, PDGF), anti-angiogenic factors and dense granules containing Ca^{2+}, 5-HT, ATP and ADP.

  These factors trigger a biochemical cascade of events that ultimately leads to the activation of the platelet integrin receptor, GPIIb/IIIa ($\alpha_{IIb}\beta_3$), and this allows binding of fibrinogen to the receptors of adjacent platelets. The binding of fibrinogen results in further reinforcement of the existing platelet plug (Radomski and Moncada, 1993) (Jurk and Kehrel, 2005).

1.3.3 Cancer Cell-Platelet Interaction

The earliest documented relationship between cancer and the formation of thrombi or clots comes from Prof. Trousseau in 1865, who made the clinical observation that individuals with cancer suffered an increased risk of thrombosis/embolisms (Trousseau, 1865). It was later observed that individuals suffering from thrombosis frequently had undiagnosed or asymptomatic tumours.

Four years later the first observation of what would later become known as circulating tumour cells (CTCs) was made in Australia by the physician Thomas Ashworth in an individual with metastatic cancer (Ashworth, 1869).

In the same year as Trousseau made his seminal observation, a German scientist, Max Schultze, first described but failed to recognise the nature and significance of the small *'spherules'* which he observed to be present in blood occurring singly but frequently *'bound together loosely in groups'* (Brewer, 2006, Schultze, 1865). It would be another seventeen years before platelets were characterised in 1882 with Giulio Bizzozero's detailed description of platelets as,

> *'discoid corpuscles without a nucleus, consisting of a membrane and a matrix in which there were a few dispersed granules... constant blood particle (s) differing from red and white blood cells',*

along with their role in clotting and thrombosis, as the active partners in clot and thrombus formation (Ribatti and Crivellato, 2007).

While thrombosis and cancer continued to be noted in the intervening period, primarily in the context of clinical observation, it wasn't until the 1960's that the relationship and association of thrombocytosis and malignancy in humans began to be reinvestigated.

During this period the association came under renewed focus, with Levin and Conley putting the topic under the spotlight on the centenary of Trousseau's observation and subsequent works by Gasic and colleagues confirming the importance of platelets in the

metastatic process, with the reduced platelet count observed to result in the reduced formation of secondary tumours in a mouse model of metastatic disease (Levin and Conley, 1964, Gasic et al., 1968). This observation was further supported by work later performed by Pearlstein and colleagues which revealed the capacity to reduce metastatic disease in mouse models of melanoma, lung and colon carcinoma metastasis utilising anti-platelet agents (Pearlstein et al., 1984).

In the following 27 years up to 2011, a renewed interest in the malignancy associated hypercoagulation state, thrombocytosis and thrombosis, and the interaction between cancer cells and platelets has resulted in the generation of a significant body of experimental and clinical data which has been reviewed extensively in the last number of years (Bambace and Holmes, 2011, Gay and Felding-Habermann, 2011, Bergqvist et al., 2007, Caine et al., 2003, Levine and Lee, 2001, Lee and Levine, 2003, Lee et al., 2003, Rickles et al., 2003a, 2001, Rickles and Falanga, 2001, Kakkar, 2003a, 2003b, Sutherland et al., 2003, White, 2003, Nash et al., 2002, Zacharski, 2002, Loreto et al., 2000).

The publication record supports Trousseau's initial observation and thromboembolism (TE) or deep vein thrombosis (DVT) is frequently associated with undiagnosed occult cancers and a poor patient prognosis (Bergqvist et al., 2007, Varki, 2007, Sorensen et al., 2000a, 2000b, Monreal et al., 1997, Aderka et al., 1986). It is an unfortunate irony that Trousseau, who supported this association so intensely and suggested that cancer should be suspected in all cases of TE, would himself succumb to gastric cancer a year after suffering thrombophlebitis arising from venous thrombosis, the formation of a clot in a vein, in his left arm.

Numerous clinical and pathologic observations have confirmed an increased incidence of clinically important thrombosis ranges from 5% to 60% in various malignancies, with cancer patients appearing twice as likely to develop symptomatic VTE compared to patients without malignancy thus highlighting the involvement of coagulation and fibrinolytic systems in cancer development (Sutherland et al., 2003).

Thrombocytosis has been observed with a variety of cancers in which it has been associated with poor prognosis. These include:

- Lung, (Tomita et al., 2008, Aoe et al., 2004, Pedersen and Milman, 1996)
- Breast (Pedersen and Milman, 1996),
- Gastric, (Heras et al., 2010, Ikeda et al., 2002)
- Colon/colorectal, (Kandemir et al., 2005)
- Renal (Erdemir et al., 2007, Suppiah et al., 2006, Bensalah et al., 2006)
- Pancreatic (Suzuki et al., 2004) and
- Oral squameous cell cancers (Lu et al., 2007)

Thrombocytosis has also been observed in gynaecologic cancers, in which it is associated with poor prognosis. These cancers include:

- Ovarian (Lee et al., 2011, Crasta et al., 2010, Kuyumcuoglu et al., 2010, Gungor et al., 2009, Soonthornthum et al., 2007, Li et al., 2004),
- Cervical (Rodriguez et al., 1994),
- Endometrial (Altieri et al., 2003, Tamussino et al., 2001)
- Vulval (Lavie et al., 1999) and
- Uterine cancers (Lerner et al., 2007)

In the context of ovarian cancer it has been observed that between one-fifth and half of patients presenting with ovarian neoplasms are found to have reactive (secondary) thrombocytosis (Soonthornthum et al., 2007, Zeimet et al., 1994, Li et al., 2004, Lerner et al., 2007).

A high platelet count is associated with poor prognosis in many cancers and it is hypothesised that this may be associated with a phenomenon known as tumour cell induced platelet aggregation (TCIPA).

1.3.3.1 Tumour Cell Induced Platelet Activation

Many forms of cancer have been shown to be associated with elevated platelet counts, the resulting pro-thrombotic state associated with increased risk of VTE and worse patient outcome.

The connection between platelets and malignancy associated thrombi/emboli and cancer CTCs has since been further investigated and a phenomenon called Tumour Cell Induced Platelet Aggregation (TCIPA) has been described whereby cancer cells have been shown to be able to induce platelet aggregation or adhesion to their surface (Bazou et al., 2011, Chang et al., 2009, Tsuruo and Fujita, 2008, Alonso-Escolano et al., 2006, 2004a, Medina et al., 2006, Camerer et al., 2004, Jurasz et al., 2001a, 2001b, Swaim et al., 1996, Heinmoller et al., 1996, 1995, Chiang et al., 1995, 1994, Radomski et al., 1991).

It is hypothesised that this process may provide several advantages to the metastasising CTC to overcome the challenge of successful haematogenous dissemination by;

- Assisting to shield cancer cells from the high shear forces they are exposed to on entry to the circulation. These high shear forces frequently force intravasated cancer cells to adopt a cylindrical rather than circular shape when faced with passage through small vessels, thus resulting in their death (L. Weiss, 1992, Barbera-Guillem and Weiss, 1993).

- Increasing the size of a tumour embolus and facilitating adhesion of the platelet aggregate to the vascular endothelium, allowing for successful embolisation in the microvasculature at a site suitable for extravasation and establishment of a secondary tumour site (Konstantopoulos and Thomas, 2009, Rickles et al., 2003b, Malik, 1983).

- Enhancing the growth, proliferation, angiogenesis and cancer cells' capability to extravasate from the vasculature and invade into the tissues to establish a secondary tumour, through release of release a number of growth factors and induction of increased protease expression by the cloaked cancer cell (Bambace

and Holmes, 2011, Holmes et al., 2009, Alonso-Escolano et al., 2006, Dineen et al., 2009).

- Enhancing extravasation through production of heparinase, which acts to encourage endothothelial cell retraction and sub-endothelial matrix degradation (Goldshmidt et al., 2002, Eldor et al., 1987).

TCIPA is also proposed to assist metastasising CTCs in evading the immune system, by co-opting blood platelets for use as a 'platelet cloak', abrogating the effects of TNF-α and NK-cells in mediating tumour cell destruction (Placke et al., 2011, Nieswandt et al., 1999, Philippe et al., 1993, Shau et al., 1993, Zheng et al., 2009b).

It has been suggested that the platelet cloak may also contribute to the development of some cancers by acting as a 'sponge' for chemotherapeutic agents, thus reducing the concentration of drug exposed to the CTC and resulting in reduced efficacy of preventing further metastatic spread. Thus the platelet cloak may play a crucial role in tumour cell embolisation in the vasculature and contribute significantly to metastatic load in malignancy.

A majority of studies examining TCIPA to date have focussed on determining the initiators and mediators underpinning the phenomenon. These studies have identified many molecules produced by cancer cells as potential pro-thrombotic initiators, including tumour cell expressed tissue factor (TF) (Rao, 1992, Mueller et al., 1992), thrombin (Pearlstein et al., 1981) , PAR4 (Camerer et al., 2004), aggrus/podoplannin (Suzuki-Inoue et al., 2007, Tsuruo and Fujita, 2008), matrix metalloproteinases (MMPs) and signalling molecules such as ADP (Medina et al., 2006, Jurasz et al., 2003, 2001a, Bastida et al., 1982). Physical mediators involved in the adhesion/aggregation process have been identified, with prime movers including vWF (Jurasz et al., 2001b, Oleksowicz et al., 1999), GP1bα, GPIIbIIIa/$\alpha_{II\beta}\beta_3$ (Amirkhosravi et al., 2003, Cohen et al., 2000), GPVI, p-selectin (Borsig et al., 2002, 2001), αVβ3 (Pidgeon et al., 2003, Felding-Habermann et al., 2001), β_3 integrin, mucins and selectins (Wahrenbrock et al., 2003).

Recently the role of these molecules has been discussed and reviewed by (Gay and Felding-Habermann, 2011, Erpenbeck and Schön, 2010, Falanga et al., 2009, Tsuruo and Fujita, 2008, Pearlstein et al., 1984, Konstantopoulos and Thomas, 2009), providing a comprehensive overview of the current understanding of the initiators and physical mediators of cancer cell-platelet interactions.

Despite ever more detailed description of the mechanisms underlying TCIPA and increased documentation of advantages it affords to platelet cloaked cancer cells, exceptionally little is yet known regarding the molecular basis for the improved metastatic potential of cancer cells that become coated in platelets during their time in the circulatory system.

These pro-metastatic changes positively affect the cancer cells' capability to evade both immune and cytotoxic drug driven death, to adhere to the endothelium, to induce angiogenesis and set up a new secondary metastasis following extravasation.

Prior to completion of this study, the molecular changes occurring in the cancer cell(s) at the core of the CTC-platelet aggregate were largely unknown and limited to a solitary gene, MMP9, described in one study to be transcriptionally up-regulated in cancer cells as a result of TCIPA (Alonso-Escolano et al., 2006).

1.4 Aims

This thesis proposes to forward the understanding of the interaction of cancer cells and platelets in the context of ovarian cancer through:

- Investigation of the relationship between ovarian cancer and thrombocytosis in the Irish population through performance of a retrospective study of archival clinical samples and associated patient data.

- Examination of the dynamics of TCIPA via an *in vitro* model system, utilising a panel of ovarian epithelial cell lines.

- Determining the molecular basis of changes resulting from TCIPA-associated tumour cell 'cloaking' on ovarian cancer cells through whole transcriptome analysis.

CHAPTER TWO

MATERIALS AND METHODOLOGY

2 Materials and Methodology

The contents of this chapter are a full and comprehensive account of the methods and materials employed in the completion of this thesis. New and more modern techniques employed are supported by background information. Where techniques have been used in more than one chapter the full description of the technique is limited to this chapter or specifics provided but only where relevant.

2.1 Archival Tissue Collection

2.1.1 Formalin Fixed Paraffin Embedded Tissue

Formalin fixed paraffin embedded (FFPE) ovarian samples were selected from the pathology files of St. James's Hospital, Dublin. Haematoxylin and eosin (H&E) stained slides for each sample were classified according to WHO classification (Tavassoli, 2003) by a qualified pathologist (Dr. Richard Flavin of St. James's Hospital, Dublin, Ireland).

2.1.2 FFPE Sample Preparation

Five to eight 10μm sections were cut from selected FFPE samples using a Leica RM2235 rotary microtome (Leica Biosystems, Nussloch, Germany).

- The smooth hand wheel was turned until the specimen holder is in the uppermost position and the hand wheel lock applied.
- The sample block to be cut was placed in specimen holder and the cut depth to 10μm using the cutting dial.
- The knife guard was moved to the down position allowing a microtome blade to be slid horizontally into position and clamped parallel to the upper edge in the knife holder.
- The brake mechanism was released allowing the coarse driving wheel, capable of advancing the sample 30μm per revolution to bring the sample closer to the cutting blade. Once the blade was observed to have begun cutting the sample

block the smooth turning hand wheel was used to advance the sample a distance of 10μm.

- Once the requisite number of complete sections had been recovered the specimen holder was returned to the uppermost position, the hand wheel lock applied, the knife guard raised and sections transferred to a labelled 2ml DNAse and RNAse free micro-centrifuge tube.
- Prior to the next sample being cut the specimen holder was run backwards using the coarse driving wheel to ensure the knife was positioned away from the sample block before cutting proceeds.

Following completion of sectioning activities the specimen holder was returned to the uppermost position, the wheel lock applied and the sample removed. The knife was released from its clamp, returned to its case and the knife guard returned to the up position. All section waste was collected into the waste tray and discarded and the microtome cleaned.

2.2 Nucleic Acid Extraction

To successfully make use of many modern molecular biology techniques, especially those required to investigate and analyse gene expression such as microarray or quantitative polymerase chain reaction (PCR) or other aspects of genomics such as mutation or methylation analysis, it is critical that nucleic acids of high quantity and quality can be extracted from experimental materials.

While high quality RNA can be routinely extracted from cell lines and fresh tissues using kits such as the QIAGEN® RNeasy® Mini Kit, FFPE materials whose RNA molecules have been chemically modified and degraded during the fixation and embedding process require specific and specialised reagents to maximise the quantity and quality of RNA extracted. The Ambion® RecoverAll™ Total Nucleic Acid Isolation Kit specifically optimised for DNA or RNA isolation from FFPE materials was used in this thesis. The protocols for the nucleic acid extraction/isolation kits used are outlined in the following subsections.

2.2.1 RNA Extraction From FFPE Tissues

Total RNA (tRNA), including mRNA and small RNA species such as microRNA (miRNA) were extracted from FFPE materials (prepared as per section 2.1) using Ambion® RecoverAll™ Total Nucleic Acid Isolation Kits.

2.2.1.1 Ambion® RecoverAll™ Total Nucleic Acid Isolation Kit

Total RNA extraction from FFPE materials using the Ambion® RecoverAll™ total nucleic acid isolation kit was performed following the manufacturers recommended protocol (Appendix Section 7.1).

2.2.2 RNA Extraction from Cell Lines

In order to determine the protocol which returned optimal RNA quantity and quality two nucleic acid extraction kits were tested for use in this thesis.

The kits in question are the QIAGEN® RNeasy® Mini Kit used with QIAGEN® QIAshredder™ columns for sample homoginisation and the Ambion® *mir*Vana™ miRNA Isolation Kit. The *mir*Vana™ Kit unlike the RNeasy® kit included optional procedures for enrichment of miRNA species or for total RNA isolation, the latter of which was performed for to allow comparison of the efficacy of the two products for total RNA isolation.

2.2.2.1 QIAGEN® RNeasy® Mini Kit

Total RNA extraction from cell lines using the Qiagen®RNeasy Mini kit was performed following the manufacturers recommended protocol (Appendix Section 7.2).

2.2.2.2 Ambion® *mir*Vana™ miRNA Isolation Kit

Total RNA extraction from cell lines using the Qiagen®RNeasy Mini kit was performed following the manufacturers recommended protocol (Appendix Section 7.27.3).

2.3 Nucleic Acid Quantitation and Assessment

2.3.1 Nano-Drop™ 2000 Spectrophotometer

Nucleic acid samples were assessed for quantity and quality using a Thermo Fisher NanoDrop™ 2000 UV-Vis spectrophotometer (Thermo Fisher Scientific Inc., Wilmington, DE, USA). The 2000 UV-Vis spectrophotometer is the next generation instrument of the NanoDrop 1000. It is capable of all the functions of the unit it succeeds but requires less time; requiring <5 seconds per sample, a smaller sample size; as little as 0.5µl for higher concentration samples, a broader spectrum (190-840nm vs 220-750nm), a broader concentration dynamic range (2ng/µl to 15,000ng/µl dsDNA), and enhanced software that allows for custom methods.

2.3.1.1 Loading Samples

- With the NanoDrop™ 2000 spectrophotometer unit, operating PC and NanoDrop™ operating software turned on the unit is directed to measure the appropriate sample type.
- Details of the sample to be measured were entered in the Sample Name field in the NanoDrop™ software window.
- With the sampling arm open, 1µl of sample is pipetted directly onto the lower measurement pedestal (Figure 2-1a).
- The sampling arm is gently closed resulting in a column forming as a result of sample surface tension (Figure 2-1b).
- The pedestal then moves automatically to adjust for an optimal path length (Figure 2-1c).
- The software is used to take the measurement and when complete, the sampling arm is raised and the pedestal surfaces are simply wiped with a soft clean wipe before going on to the next sample. This prevents carryover between samples impacting on successive sample measurements.

Figure 2-1

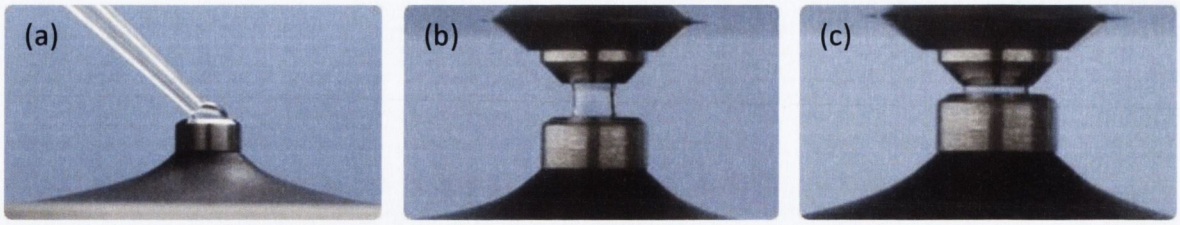

Figure 2-1: NanoDrop™ Spectrophotometer Sample Loading.

Following sample placement on the lower measurement pedestal (a) the upper sampling arm is closed resulting in the formation of a column between the upper and lower measurement pedestals (b). The lower measurement pedestal then adjusts its height to that optimal for the sample type to be measured (c). Adapted from www.chem.agilent.com.

2.3.1.2 Blank Measurement

- The surface of the upper and lower pedestal surfaces were gently cleaned using DNase and RNase free water and a soft clean wipe.
- Using the operating PC, the NanoDrop™ 2000 software was opened and the application of interest selected and the instrument initialized following software prompts.
- After initialisation 1µl volume of blanking solution, typically the solution in which samples were prepared, was transferred to the lower pedestal lower the arm, the upper sample arm lowered and the 'Blank' button clicked to calibrate the unit against this blank. This ensures that non-specific fluorescence is not a concern going forward.
- The sampling arm was raised and the blanking solution cleaned away using a laboratory wipe.
- A new 1µl volume of blanking solution was analysed as it were a sample using the 'Measure' function in the NanoDrop™ software. This should result in a spectrum with a relatively flat baseline. The blanking solution was cleaned away as before and the process repeated as necessary until the spectrum is flat.

2.3.1.3 Sample Measurement

- After blank calibration and measurement load samples as outlined above in section 2.3.1.1.
- 1µl of sample is sufficient to return accurate and reproducible results in aqueous nucleic acid sample analyses.
- After analysis of individual groups of samples and/or at 30 minute intervals, a blanking solution measurement was taken to ensure there was no drift in sampling accuracy.

Results:

- A260: Absorbance of the sample at 260nm as if measured by a 10mm path. This is actually 10x the absorbance actually measured at the 1mm path length and 50x that measured using the 0.2mm path length.
- A280: Absorbance of the sample at 280nm as if measured by a 10mm path. This is actually 10x the absorbance actually measured at the 1mm path length and 50x that measured using the 0.2mm path length.
- 260/280: The ratio of absorbance at 260 nm and 280 nm is used to assess the purity of DNA and RNA. A ratio of ~1.8 and a ratio of ~2.0 are generally accepted as "pure" for DNA and RNA respectively. If the ratio is appreciably lower in either case, it may indicate the presence of protein, phenol or other contaminants that absorb strongly at or near 280 nm.
- 260/230: This ratio of absorbance at 260 nm and 230 nm is used as a secondary measure of nucleic acid purity. The 260/230 values for "pure" nucleic acid are often higher than the respective 260/280 values.
- Concentration: This is the calculated nucleic acid concentration of the measured sample provided as ng/µl as default.

2.3.2 Agilent Bioanalyser

Produced by Agilent (Santa Clara, CA, USA) the 2100 Bioanalyzer is a lab-on-a-chip microfluidics-based platform for sizing, quantification and quality control of nucleic acids and proteins through electrophoretic separation. It is capable of delivering fast, automated, high quality digital data instead of subjective, time-consuming results associated with labour intensive traditional gels separation techniques. RNA integrity and concentration was analysed using an Agilent Bioanalyser 2100 unit following the protocol below. Samples are loaded into a chip and placed into the Bioanalyzer, where they are individually analysed and a pseudo-gel image is created and bands are sized, quantified and integrity assessed.

2.3.2.1 Stock Reagent Preparation

- On receipt of a new Bioanalyser RNA 6000 Nano kit (Agilent, Santa Clara, CA, USA) the provided RNA ladder was transferred to an RNase- and DNase-free microcentrifuge tube.
- The RNA ladder was heat denatured in a heat block at 70°C for 2 minutes and placed directly on ice.
- 2µl aliquots were prepared in 500µl DNase and RNase free tubes and stored at -80°C

2.3.2.2 Chip Priming Station Setup

- When using a new assay kit the syringe was replaced. The old syringe was unscrewed from the chip priming station lid and discarded. The plastic cap was removed from a new syringe, inserted into the hole of the lock adapter and screwed tightly into place on the chip priming station lid.
- If required the base plate was adjusted to accommodate the appropriate microfluidic chip for the application required. The chip priming station was opened by pulling the latch, then the screw at the underside of the base plate was

opened using a screw driver. The base plate was lifted and reinserted in position required, retightening the screw afterwards.

- The syringe clip was adjusted by releasing the lever of the clip and slid to the top position for use with RNA Nano microfluidic chips.

2.3.2.3 Electrode Decontamination

In order to prevent decomposition of RNA samples during analysis an electrode decontamination procedure was followed on a daily basis prior to running any Bioanalyser assays.

- An electrode cleaning chip was carefully filled by pipette with 350µl RNase Zap® (Ambion Inc, Austin, TX, USA).
- The lid of the Bioanalyser 2100 unit was opened and the electrode cleaning chip placed in position.
- The lid was closed and left for 1 minute.
- The lid was opened and the cleaning chip removed and labelled for future reference and reuse.
- Another electrode cleaning chip was carefully filled by pipette with 350µl DNase and RNase free water.
- The chip was placed in the Bioanalyser and the lid closed and left for 15 seconds.
- The lid was opened and the cleaning chip removed and the lid closed after a further 15 seconds to allow any residual water on the electrodes to evaporate. The electrode cleaning chip was labelled for future reference and reuse.

2.3.2.4 Gel Preparation

- All reagents were allowed to equilibrate to room temperature for 30 minutes prior to use.
- 550µl Agilent RNA 6000 Nano gel matix was placed into the top of a spin filter assembly provided and the cap closed.

- The spin filter assembly was transferred to a microcentrifuge and centrifuged at 1500 x *g* for 10 minutes.
- The filtered gel was separated into 65µl aliquots in 500µl tubes (included with the kit) and stored at 4°C to be used within one month of preparation.

2.3.2.5 Gel-Dye Mix Preparation

As components of the kit contain Dimethyl Sulfoxide (DMSO), a potential mutagen capable of facilitating transport of organic molecules into tissues appropriate hand and eye protection are required and good laboratory practice followed when handing and using reagents and samples.

- All reagents were allowed to equilibrate to room temperature for 30 minutes prior to use, protecting the dye concentrate from light exposure during this time.
- The RNA 6000 Nano Dye Concentrate was vortexed and centrifuged for 10 seconds.
- 1µl of dye concentrate was added into a 65µl aliquot of filtered gel (prepared as described in section 2.3.2.3 above) and the cap closed.
- The gel-dye solution was thoroughly vortexed and well and centrifuged at 13,000 g for 10 minutes at room temperature.
- The prepared gel-dye mix must be protected from light exposure and used within one day.

2.3.2.6 Gel Dye Mix Loading

Before loading the gel-dye mix the positions of the chip station base plate and the syringe clip were in the correct positions at (C) and the uppermost position respectively (Figure 2-2(a) and (b).

Figure 2-2

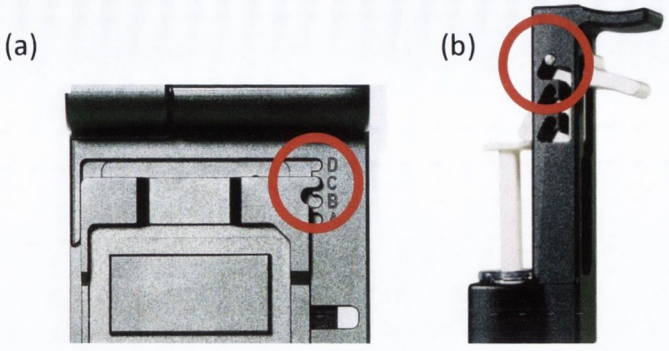

Figure 2-2: Bioanalyser 2100 Chip Station Setup.

Prior to beginning RNA analysis using the Bioanalyser 2100 and RNA 6000 Nano kit the base plate (a) and syringe clip (b) in must be set to the required positions indicated.

- A new RNA 6000 Nano chip was placed on the chip priming station.
- 9µl of room temperature gel-dye mix was pipette into the bottom of the well marked G.
- Making sure that the plunger is positioned at 1ml the chip priming station was then closed.
- A laboratory timer was set to 30 seconds and the syringe plunger depressed until held by the clip.
- Once the timer indicated 30 seconds had elapsed the clip was released.
- The plunger was visually observed to return to at minimum the 0.3ml mark and after 5 seconds was pulled slowly back to the 1ml position.
- The chip priming station was then opened and 9µl of gel-dye mix pipette into the bottom of the wells marked G.

2.3.2.7 RNA Nano Marker Loading

- 5µl of the RNA 6000 Nano Marker was pipetted into the bottom of the well marked with the ladder symbol and into each of the twelve sample wells.
- It is important that all wells are filled. Unused wells must be filled with 6µl RNA 6000 Nano Marker as empty wells will result in the chip failing to run properly.

2.3.2.8 Ladder and Sample Loading

- An aliquot of heat denatured RNA ladder was thawed on ice.
- 1µl of RNA ladder was pipetted into the well marked with a ladder symbol .
- 1µl of RNA sample was pipetted into a sample well for each sample being analysed.
- A timer was set for 1 minute and the chip placed in the adapter on the IKA vortex mixer ensuring the chip was held securely in place. The chip was then vortexed at 2400 RPM for 1 minute.
- The chip was then transferred to the Agilent Bioanalyser 2100 unit. The unit lid was opened and the chip placed in the receptacle and the lid carefully closed.
    - The chip will only fit in one orientation and the device electrodes will fit into the chip wells as the lid is closed.

2.3.2.9 Bioanalyser 2100 Software Operation

After powering up the Bioanalyser 2100 unit and the operating PC, the Agilent 2100 Expert software was initialised.

The software provides a graphical indication of the status of the Bioanalyser unit; no instrument detected, instrument detected with lid open, instrument detected with lid closed or instrument detected with lid closed and chip inserted (Figure 2-3).

Figure 2-3

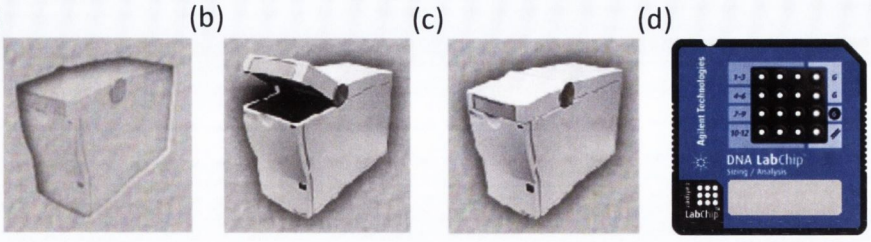

Figure 2-3: Bioanalyser 2100 Instrument Indicator Icons.

The icons above displayed in the '*Instrument*' context of Agilent 2100 Expert software indicate the current status of the Bioanalyser 2100 instrument. Icon (a) indicates the unit is not connected or switched on, icon (b) indicates the unit is detected and the lid is open, (c) indicates the unit is detected and the lid is closed and (d) indicates the unit is detected with the lid closed and a chip has been inserted in the chip receptacle. It is critical to note that the chip image displayed is determined by the assay type to be run as selected using the software. If the chip image displayed is incorrect the user must change the assay setting to that appropriate for their application before proceeding any further.

- In the 'Instrument' context the assay type appropriate to the application required was selected in the assay menu.
- The 'Start' button was clicked to initialise the chip run and the incoming raw signals displayed in the 'Instrument' context as the ladder and subsequently samples are analysed.
- Sample information including sample names and relevant comments were entered in the 'Chip Summary' tab selected in the 'Assay' context.
- Once the chip run finished the chip was removed from the Bioanalyser 2100 unit and disposed of following good laboratory practice.
- Results of the run were checked in the 'Gel' or 'Electropherogram' tabs in the 'Data' context. The electropherogram of the ladder should closely resemble that shown in Figure 2-4(A).
- Specific sample results were viewed in the 'Results' sub-tab. The electropherogram for a sample well containing total RNA should closely resemble that shown in Figure 2-4(B).

Figure 2-4

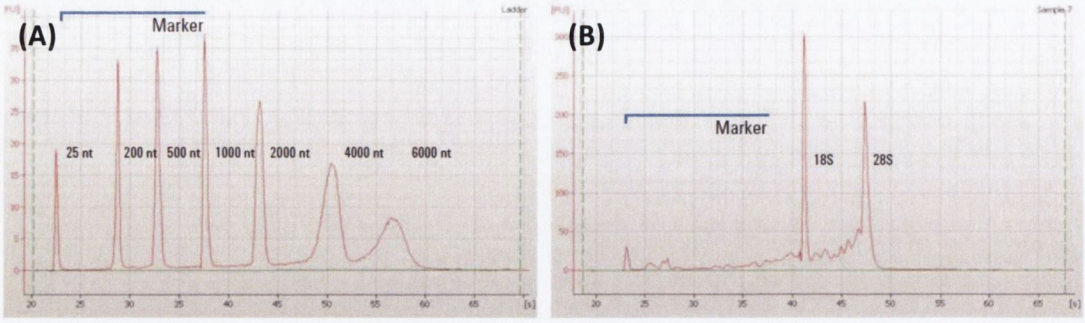

Figure 2-4: Agilent 2100 Bioanalyser Exemplar Electropherograms.

Following RNA chip assay results for the RNA ladder (A) and RNA samples (B) can be viewed in the '*Results*' sub-tab. The RNA ladder image should return an output similar to that above with seven well defined spikes representing nucleotide (nt) sizes between 25nt and 6000nt.

Similarly total RNA sample results should return an electropherogram chart displaying three peaks, a minor marker peak at two ribosomal peaks indicative of 18s and 28s ribosomal RNA.

In selecting the 'Results' sub-tab values for the sample RNA concentration, ribosomal ration and RNA Integrity Number (RIN) was displayed.

The RIN calculation achieved by a proprietary algorithm utilised by the 2100 Expert software which determines RNA integrity based on several critical features extrapolated from electrophoretic traces.

The algorithm design means that RIN can be considered as a standard integrity measure that is independent of confounding factors such as variation of sample concentration, instrument or analyst. The RIN scale is from 1 to 10, with 1 being the most degraded and 10 being the most intact.

2.4 Gene Expression Analysis

Several methods were employed in the completion of this thesis to analyse levels of mRNA expression. These methods are described in the following section of the thesis.

2.4.1 TaqMan® PCR

A TaqMan® PCR based assay was selected for use in mRNA expression quantitation in this study. This technique was selected for several reasons. Given the comparatively low nucleic acid yields typically recovered from archival FFPE materials this technique is exquisitely suitable given the low sample quantities required, as little as a few nanograms of sample target RNA is sufficient. Also, TaqMan PCR products are small, often 200 base pairs (bp) or less, and this feature can allow the amplification of partially degraded nucleic acids such as those extracted from FFPE material.

TaqMan® RT-PCR exploits the dual 5' polymerisation and exonuclease functionality of AmpliTaq Gold® DNA Polymerase to detect amplification of a PCR product in real-time by hybridisation and cleavage of a dual labelled fluorogenic TaqMan® probe.

The TaqMan® probe is composed of a short oligonucleotide sequence, 20 - 25 bp in length, bookended by a 5' and a 3' fluorescent molecule and a 3' blocking phosphate to prevent nucleotide extension. During the PCR reaction the probe is designed to hybridise within the target sequence of the forward and reverse primers.

When intact, the probe utilises a phenomenon known as fluorescence resonance energy transfer (FRET); where the proximity of the 5' end fluorescent molecule, known as the reporter dye, to the 3' end fluorescent molecule, known as the quencher dye, results in energy transfer between the two molecules which suppresses the fluorescent emission from the reporter dye (Förster, 1948, Lakowicz and Masters, 2008).

During PCR the primers bind to the target sequence, sequence elongation occurs and probe specifically anneals to the sequence between the forward and reverse primer sites.

As elongation progresses the hybridised probe is cleaved due to the 5'-3' exonuclease activity of the AmpliTaq Gold® DNA Polymerase. This results in the separation of the reporter and quencher molecules, which allows increased fluorescent emission from the released reporter molecule. Therefore the accumulation of PCR product is directly proportional to the increase in the fluorescent emission from the reporter dye.

The real-time PCR instrument (7900HT sequence detection system (Applied Biosystems/Life Technologies Corp., Carlsbad, CA, USA) detects fluorescence from the unquenched FAM, monitoring it in real-time. As the polymerase reaction continues the probe remnants are displaced by from the target and strand polymerisation continues. As a result of the probes' 3' blocking phosphate polymerase driven extension of the probe is prevented (Figure 2-5).

Figure 2-5

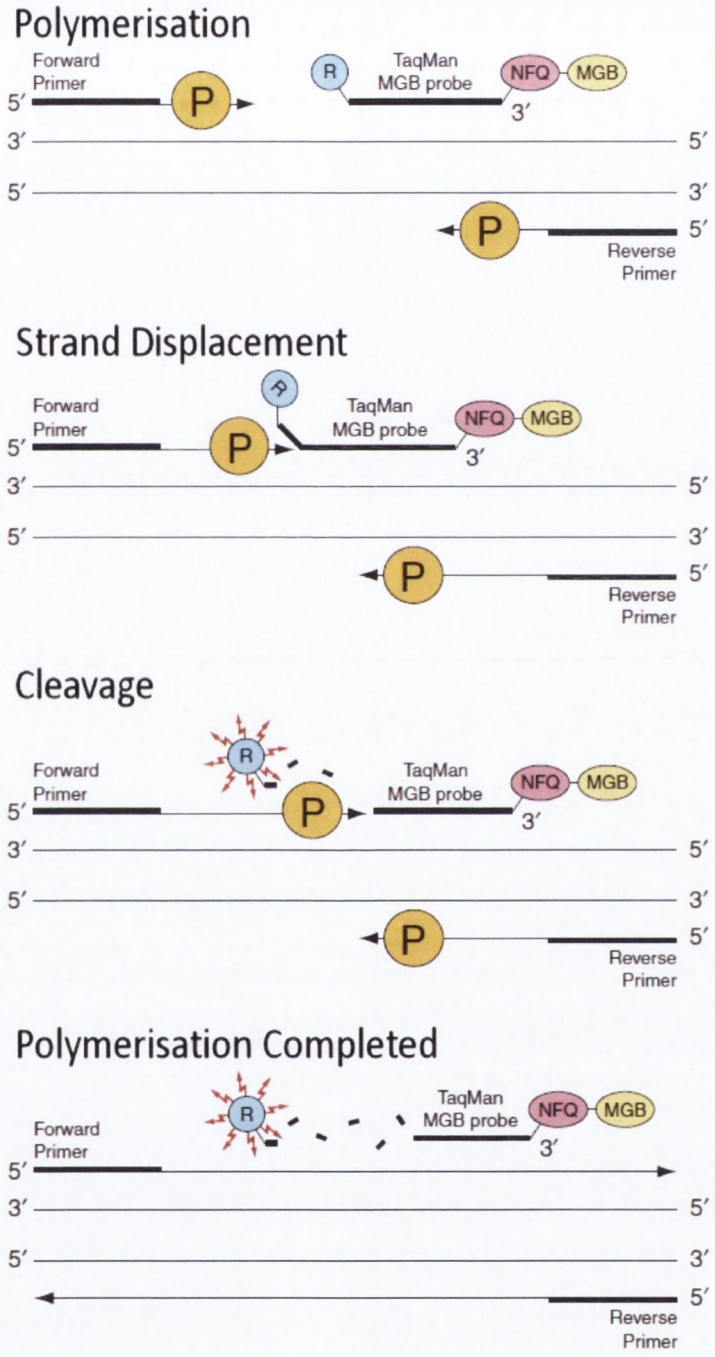

Figure 2-5: Graphical Illustration of Applied Biosystems TaqMan® RT-PCR.

Following binding to the target sequence Taq polymerase enzyme driven elongation occurs between the forward and reverse primers. The target bound probe has both 5′ dye and 3′ quencher intact and reporter emission is prevented. As extension/polymerisation continues Taq exonuclease activity cleaves the reporter dye from the probe. The resulting separation of dye and quencher allows fluorescence of the dye.

2.4.1.1 TaqMan® RT-PCR Primers and Probes

TaqMan® Gene Expression Assays are available as sets of custom or pre-optimized PCR primer sets and probes for real-time PCR applications and formulated at 20X concentration. Each assay contains three target-specific oligonucleotides: and unlabeled PCR primer pair and a TaqMan® probe (as described above). A TaqMan® probe typically has a 5' FAM™ or VIC® dye label and 3' non-fluorescent quencher (NFQ) minor groove binder (MGB) moieties.

As probe hybridisation prior to primer binding and elongation is critical the probe melting temperature approximately 10°C higher than that of the primers. This is achieved by incorporation of a 3' minor groove binding (MGB) molecule results in tighter probe/target binding that stabilizes probe–target hybrids, reduces background fluorescence and effectively raises their melting temperature, ensuring the probe remains bound to the target molecule (Livak et al., 1995) and prevents the generation of PCR products without fluorescence.

All but one primer-probe set utilised were predesigned assays by Applied Biosystems. A custom primer-probe set was designed to detect ret/PTC3 transcript expression. The primer probe sequence used was identical to that utilised by Finn et al. (Finn et al., 2003, Finn et al., 2004) designed to span the fusion points of chimeric transcripts.

All other primers and probes used throughout this study, including gene targets of interest and endogenous controls were commercial pre-designed primer and probe mixes (20X) obtained from Applied Biosystems (Foster City, CA, USA).

2.4.1.2 Custom TaqMan® Gene Expression Assay Preparation

When utilising custom designed TaqMan® assays lyophilised primers and probes were first reconstituted with nuclease free H_2O. Custom primers were provided as lyophilised 10nMol powder and reconstituted to 18µM solution in a final volume of 550µl. Custom probes were provided as lyophilised 6nMol powder and reconstituted to 5µM solution in a final volume of 1200µl. These concentrations were in keeping with Applied Biosystems

assay development guidelines, which result in an assay working concentration after 1:20 dilution of 900nM for primers and a 250nM for the probe which has been shown to provide highly reproducible and sensitive assays.

2.4.1.3 Real-time Quantitative TaqMan® RT-PCR

TaqMan® RT-PCR is a real-time PCR technique and therefore data is collected throughout the PCR process, rather than at the end of a set of PCR cycles. Consequently reactions are characterised by the point in time during PCR cycling when amplification of a target is first significantly detected by concomitant probe fluorescence. The higher the starting copy number of the nucleic acid target, the sooner a significant increase in fluorescence is observed.

The initial cycles of PCR return little change in detected fluorescence signal defining the baseline for the amplification plot over which detected increases in probe fluorescence in successive cycles indicate accumulation of amplified target. A fixed threshold can be set above the baseline and the fractional cycle number at which fluorescence passes this fixed threshold defined the threshold cycle or C_T (Figure 2-6).

A C_T value of 40 indicates that the gene target has failed to reach the threshold cycle over 40 rounds of amplification. This is accepted as an indication the target failed to amplify, typically as a result of target (sample) degradation, or in no template or reverse transcriptase controls.

Figure 2-6

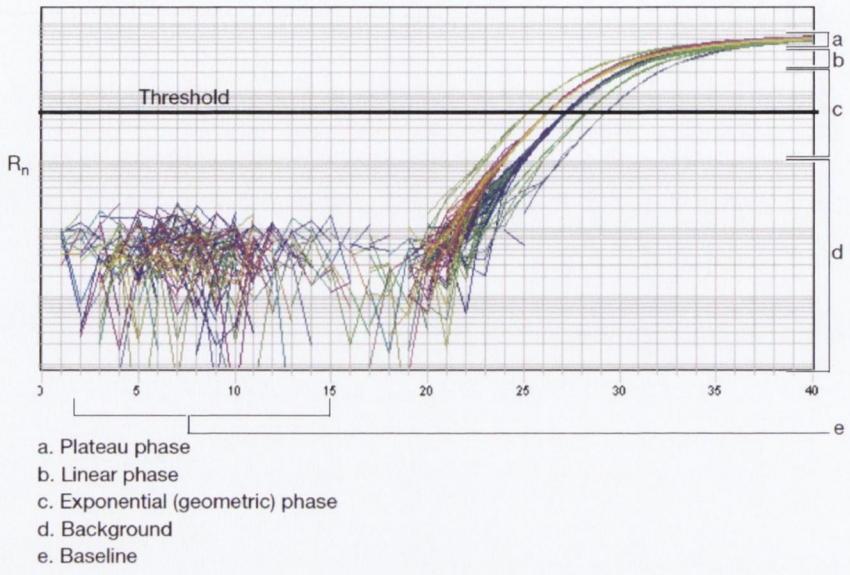

Figure 2-6: Typical TaqMan® Gene Expression Assay Amplification Plot.

Figure 2.6 indicates a typical TaqMan® Gene Expression Assay amplification plot. Indicated are plateau, linear and exponential phases (a-c), background fluorescence (d) and baseline fluorescence (e). Also indicated is threshold fluorescence used to determine Threshold Cycle (C_T) values.

2.4.1.4 Relative Gene Expression

The Applied Biosystems Prism 7900HT Detection system utilised supports real-time relative quantitation of nucleic acids using TaqMan® RT-PCR chemistries and the comparative C_T method for relative quantitation.

2.4.1.4.1 Comparative C_T Method

Relative quantification of the target genes using the comparative C_T method was first described in 2001 (Livak and Schmittgen, 2001). This method describes the change in target genes relative to a reference group, typically an untreated control, non-disease 'normal' sample or sample at T=0 in a time course study. Therefore the calibrator sample

is 1X expression and all other samples investigated are expressed as a fold difference relative to the calibrator.

The comparative C_T method calculates relative gene expression using the following equation:

$$\textbf{Relative Quantity} = 2^{-\Delta\Delta C_T}$$

ΔCT is achieved by subtracting the endogenous control C_T from your sample gene of interest C_T.

$$\Delta C_T = (\text{SAMPLE GENE } C_T - \text{SAMPLE ENDOGENOUS CONTROL } C_T)$$

In this study the ΔC_T for samples and calibrators represented an average value of at least three biological replicates. To determine the relative expression between a sample one must then compare it against a calibrator sample. Thus;

$$\Delta\Delta C_T = \Delta C_T \text{ (Sample)} - \Delta C_T \text{ (Calibrator)}$$

Using the $2^{-\Delta\Delta C_T}$ calculation the difference in gene expression is presented as a fold change difference normalised against an endogenous control reference gene in an untreated/normal/T=0 control sample.

Relative quantitation using the 7900HT instrument is achieved through the use of TaqMan® gene expression assay of samples as described previously. Samples containing cDNA, gene expression master mix and assays containing probe and primer sets for specific nucleic acid sequences were loaded into the instrument. Using Applied Biosystems SDS software samples and assays were labelled as samples or calibrators and the assays defined as endogenous controls or as experimental gene targets. During the instrument run it records the emission resulting from the cleavage of TaqMan® probes in the presence of their target sequence over successive cycles of PCR.

After the run the instrument processes raw fluorescence data to produce threshold cycle (C_T) values for each sample. The SDS software calculates relative expression levels from the C_T values of the endogenous control gene in the calibrator sample against those C_T values determined for gene targets in other samples. Relative quantitation values (gene fold changes) can be achieved manually by collation of C_T values and inputting them into the $2^{-\Delta\Delta C_T}$ formula, alternatively the SDS software can collect the data and produce the RQ values.

For analysis of large studies C_T and relative quantitation data can be exported from Applied Biosystems SDS software and entered in third party software such as TIBCO Spotfire™ for Functional Genomics.

2.4.1.5 cDNA Synthesis

Applied Biosystems' High Capacity cDNA Reverse Transcription Kit (Applied Biosystems/Life Technologies Corp., Carlsbad, CA, USA) was used to convert tRNA into cDNA. This kit uses random primers to initiate cDNA synthesis as this ensures that the first strand synthesis occurs efficiently with all species of RNA molecules including messenger RNA (mRNA) and ribosomal RNA (rRNA). The cDNA synthesis protocol is outlined below.

2X Master Mix Preparation

RNase and DNase free consumables were used in the preparation of a 2X Reverse Transcription Master Mix to minimise degradation of nucleic acids and maximise cDNA yields.

- Kit components were allowed to thaw on ice.
- The volumes of the components required to prepare cDNA for each sample were calculated based on the volumes indicated in Table 2-1.
- 2X Reverse Transcription Master Mix was prepared in DNase and RNase free plastics and kept on ice until required.

Table 2-1

Component	Volume Required Per Sample
10X RT Buffer	2.0µl
25X dNTP Mix (100mM)	0.8µl
10X Random Primers	2.0µl
MultiScribe™ Reverse Transcriptase	1.0µl
DNase and RNase Free H_2O	4.2µl
Total Reaction Volume	**10.0µl**

Table 2-1: 2X Reverse Transcriptase Master Mix

cDNA Reverse Transcription Reaction

- 10µl of 2X reverse transcription master mix was transferred to a 200µl PCR tube.
- 10µl of sample tRNA was pipette into the PCR tube and mixed by pipetting the mixture up and down three times to mix.
- The PCR tube was sealed, briefly centrifuged to deposit the RNA/Master Mix solution at the bottom of the tube and eliminate any air bubbles. The tube(s) were placed on ice until ready to transfer to a thermal cycler.
- The cDNA reaction was performed on the 9600 Thermal Cycler (Applied Biosystems/Life Technologies Corp., Carlsbad, CA, USA) as follows: the reaction volume was set at 20µl and the cycling parameters to 25°C for 10 minutes, 37°C for 120 minutes, 85°C for 5 minutes to deactivate the enzyme, and cooling to 4°C.
- After the reaction was completed cDNA quantified by NanoDrop and stored at -20°C until required.

2.4.1.6 Pre-amplification of cDNA

In instances where sample tRNA is high value arising from small quantities being extracted from small amounts of available sample such as from FFPE or laser capture

microdissected materials, where tRNA may also be degraded, the decision may be taken to pre-amplify (pre-amp) gene targets prior to real-time PCR assay.

The TaqMan® PreAmp Master Mix kit allows for multiplex pre-amplification of up to 100 gene targets from reverse transcribed cDNA prior to real-time TaqMan® PCR assay. This technique uniformly amplifies multiple gene targets retaining the gene expression profile of the original cDNA sample whilst increasing the volume of sample available to use downstream applications such as TaqMan® gene expression assay.

Pooled Assay Mix Preparation

- 10µl of each 20X TaqMan® gene expression assay to be used was transferred to a 2ml nuclease free tube and the final volume adjusted to 1ml using 1X Tris EDTA (TE) buffer pH 8.0.

Pre-amplification PCR Protocol

- For each sample, reagents (Table 2-2) were prepared in a nuclease free micro-centrifuge tube and transferred to a 96 well reaction plate.
- The reaction plate was sealed and kept on ice until ready to transfer to an Applied Biosystems 9600 Thermal Cycler.
- The reaction volume was set as 50µl and cycling conditions were set at 95°C for 10 minutes followed by fourteen cycles of 95°C for 15 seconds and 60°C for 4 minutes.
- Upon completion the reaction plate was placed on ice and pre-amplified samples transferred to pre-labelled nuclease free tubes and diluted 1:20 with 1X TE buffer.

Table 2-2

Component	Volume Required Per Sample
TaqMan® PreAmp Master Mix 2X	25.0µl
Pooled Assay Mix (0.2X each assay)	12.5µl
1-250ng cDNA sample + nuclease free H_2O	12.5µl
Total Reaction Volume	**50µl**

Table 2-2: TaqMan® PreAmp Reaction Preparation

Table 2-2 indicates the components and their volumes required for pre-amplification of gene targets in valuable samples prior to real-time PCR based gene expression assay analysis.

2.4.1.7 TaqMan® RT-PCR Protocol

The final in TaqMan® Gene Expression assays is target amplification using cDNA prepared by reverse transcription of tRNA or preAmplified cDNA product if target pre-amplification is required. In this step the DNA polymerase in TaqMan® Gene Expression Master Mix amplifies the cDNA using target gene sequence specific primer and probe sets from the TaqMan® Gene Expression Assay mix. Performing this step for singleplex assays in a 96 well reaction plate format requires the following.

Reaction Plate Preparation

- The TaqMan® Gene Expression Master Mix was thoroughly mixed by swirling the bottle.
- Frozen TaqMan® reagents were thawed on ice, resuspended by vortexing and centrifuged briefly.
- To ensure optimal performance in TaqMan® Gene Expression assays 10-100ng of cDNA was used per 20µl reaction volume. Where target pre-amplification had been performed kit manufacturer's instructions were followed.

- The reaction mix was prepared so that each PCR reaction contained the components listed in Table 2-3.
- The reaction mix for each sample was prepared separately in a nuclease free microcentrifuge tube, the solutions mixed by gentle pipetting and the tubes capped.
- The tubes were briefly centrifuged to collect all the contents at the bottom of the tube and eliminate any air bubble and the solution transferred to the wells of a 96 well optically clear reaction plate (Applied Biosystems/Life Technologies Corp., Carlsbad, CA, USA).
- The plate was sealed using an optical adhesive cover (Applied Biosystems/Life Technologies Corp., Carlsbad, CA, USA), briefly vortexed to ensure effective mixing and centrifuged to eliminate air bubbles from the solutions.

Table 2-3

Component	Volume per 20µl Reaction Volume (cDNA Template)	Volume per 20µl Reaction Volume (Pre-amplified Template)
TaqMan® Gene Expression Master Mix (2X)	10µl	10µl
TaqMan® Gene Expression Assay (20X)	1µl	1µl
cDNA Template (1-100ng)	≤9µl	N/a
PreAmp PCR cDNA Product	N/a	5µl
Nuclease Free H20	To F_V = 20µl	4µl
Total Reaction Volume	**20µl**	**20µl**

Table 2-3: TaqMan® Real-time PCR Setup for a 20µl Reaction Volume.

Note: The volumes of template used varies depending on the use of reverse transcription derived cDNA or cDNA which has undergone pre-amplification of gene targets prior to TaqMan® Gene Expression Assay analysis.

TaqMan Real-time PCR Reaction

The RT-PCR reaction was performed on the 7900HT (Applied Biosystems/Life Technologies Corp., Carlsbad, CA, USA) under the following thermal cycling conditions:

- 50°C for 1 minute (UNG activation),
- 95°C for 10 minutes (AmpliTaq Gold activation) and
- 40 cycles of 95°C for 15 seconds and 1 minute at 60°C (melting and annealing/extension).

Experimental controls included in each TaqMan® PCR were a no template control. Endogenous controls used in this study included FAM labelled TaqMan® primer/probe sets for Cycling Dependant Kinase 1B (CDKN1B) or Glyceraldehyde-3-phosphate dehydrogenase (GAPDH). All were assayed in a separate TaqMan® PCR reaction to the target gene. All target and control reactions were performed in triplicate.

2.4.2 Fluidigm® High Throughput Real-Time PCR

Fluidigm® Dynamic Array™ microfluidic technologies allow flexible, multiplex and low cost use of existing real-time quantitative PCR technologies and assays.

2.4.2.1 Fluidigm® 48.48 Dynamic Array™

Two forms of high throughput microfluidic array have been developed by Fluidigm® for qPCR applications: a 48.48 Dynamic Array™ capable of interrogating 48 independent samples against 48 qPCR gene expression assays and a 96.96 Dynamic Array™ similarly capable of interrogating 96 independent samples against 96 qPCR gene expression assays thus reducing the time and volumes required to perform 2304 or 9216 qPCR reactions respectively.

This Dynamic Array™ technology uses integrated fluidics circuits (IFC) to combine the multiple samples and qPCR assays allowing easy high throughput multiplexing saving significant cost of time and materials over conventional qPCR techniques, providing up to twenty four times more data in a single run than a 384 well plate.

The Dynamic Arrays require proprietary equipment to allow their use: the IFC controller, used to pressure load samples and primer-probe sets resulting in their mixing in 9nl

volumes in each reaction chamber, and the BioMark™ Real-Time PCR System for thermal cycling and real-time fluorescence detection.

2.4.2.2 cDNA Synthesis

See section 2.4.1.5

2.4.2.3 Pre-amplification of cDNA

Pre-amplification of gene targets using cDNA reverse transcribed from sample tRNA was performed using the same TaqMan® PreAmp Master Mix kit and having prepared a Pooled Assay Mix as described in Section 2.4.1.6. The volumes required for pre-amplification of targets prior to Fluidigm® Real-Time Dynamic Array™ assay are described in Table 2-4.

Table 2-4

Component	Volume Required Per Sample
TaqMan® PreAmp Master Mix 2X	2.5µl
Pooled Assay Mix (0.2X each assay)	1.25µl
1-250ng cDNA sample + nuclease free H_20	1.25µl
Total Reaction Volume	**5µl**

Table 2-4: Fluidigm® Sample cDNA Pre-Amplification Reaction Preparation.

- For each sample, reagents were prepared in a nuclease free micro-centrifuge tube and transferred to a 96 well reaction plate.
- The reaction plate was sealed and kept on ice until ready to transfer to an Applied Biosystems 9600 Thermal Cycler.
- The reaction volume was set as 5µl and cycling conditions were set at 95°C for 10 minutes followed by fourteen cycles of 95°C for 15 seconds and 60°C for 4 minutes.

Upon completion the reaction plate was placed on ice, the pre-amplified samples transferred to pre-labelled nuclease free tubes and diluted 1:5 with 20µl 1X TE buffer

pH8.0. The pre-amplified sample can be used immediately or stored at -20°C until required.

2.4.2.4 Fluidigm® Real-Time PCR Protocol

TaqMan® Gene Expression assays (20x) were diluted to a final concentration of 10x using Fluidigm® DA Assay Loading Reagent: 2.5µl 20x assay + 2.5µl DA Assay Loading Reagent. The diluted pre-amp cDNA products (section 2.5.2.3) were combined with real-time qPCR reagents as per Table 2-5.

Table 2-5

Component	Volume (µl) Per Sample
Diluted Pre-Amplified Sample cDNA	2.25
2x Universal PCR Master Mix (Applied Biosystems)	2.5
Fluidigm® Sample Loading Reagent	0.25
Total	**5**

Table 2-5: Reagent Volumes required for Fluidigm® Real-time PCR.

- The dynamic array™ was primed to prevent the premature mixing of samples and assays.
- 5µl of samples pre-mixed with master mix was pipetted into sample inlets on the right hand side of the dynamic array™.
- Primer-probe sets (5µl) were pipetted into primer-probe inlets on the opposite side of the array.
- The dynamic array™ was placed on the IFC controller and the software interface used to pressure load the assay components into the array reaction chambers. This automatically combines assay components (sample/mastermix and primer-probe sets) on-chip.
- The array was placed in the BioMark™ Real-Time PCR system for thermal cycling and fluorescence detection.

- Fluidigm® Real-Time PCR Analysis software (ver 3.02) was used to view and analyse amplification curves, heat maps and C_T data for the qPCR run. Subsequent fold change calculations were performed using Microsoft Office Excel.

2.4.3 Affymetrix® GeneChip® Human Exon 1.0 ST Array Analysis

2.4.3.1 Affymetrix® GeneChip® Human Exon 1.0 ST Array Technology

The Affymetrix® GeneChip® Human Exon 1.0 ST array is the most current interation of a technology derived from the technique of southern blotting, whereby fragmented DNA was attached to a substrate and probed for a known gene or fragment of interest. In the context of Affymetrix® GeneChip® technologies the Human Exon 1.0 ST array a significant improvement on the preceding Human Genome U133 plus 2.0 array which was 3' biased (i.e. the probesets for a gene were localised in the extreme 3' end of the transcript).

This older assay technology used expression at the 3' end to approximate expression of the entire gene and was capable of providing valuable insight into global gene expression. However, this technology made several assumptions: that the 3' end of each gene is clearly defined, that each transcript has an intact poly-A tail and that the entire length of the gene is expressed as a single unit. However, we know that this does not apply to all genes or all samples, indeed than 60% of genes are known to be alternatively spliced (Lee and Roy, 2004, Johnson et al., 2003, Kim and Lee, 2008, Modrek and Lee, 2002) with hundreds of thousands of transcript variants with potentially distinct functions.

Furthermore, classical 3' expression microarrays cannot discriminate between alternatively spliced transcripts that have identical 3' ends and transcripts lacking a 3' exon because of alternative splicing, non-polyadenylation, genomic deletions or other non-canonical genomic events are not detected in 3' based expression experiments.

The Human Exon 1.0 ST array is a whole transcript (WT) assay technology which uses probesets at several points along the length of a transcript, approximately four probes per exon and roughly 40 probes per gene, allowing both robust gene level expression profile studies and expression profiles investigation of the following alternative splicing events:

- Exon skipping
- Intron retention

- Mutually exclusive exon usage
- Alternative promoter usage
- Alternative polyadenylation
- Alternative splicing donor/acceptor site with changes over 25 bp

This difference in design and improvement over previous U133 plus 2.0 assay technology is illustrated in Figure 2-7.

Figure 2-7

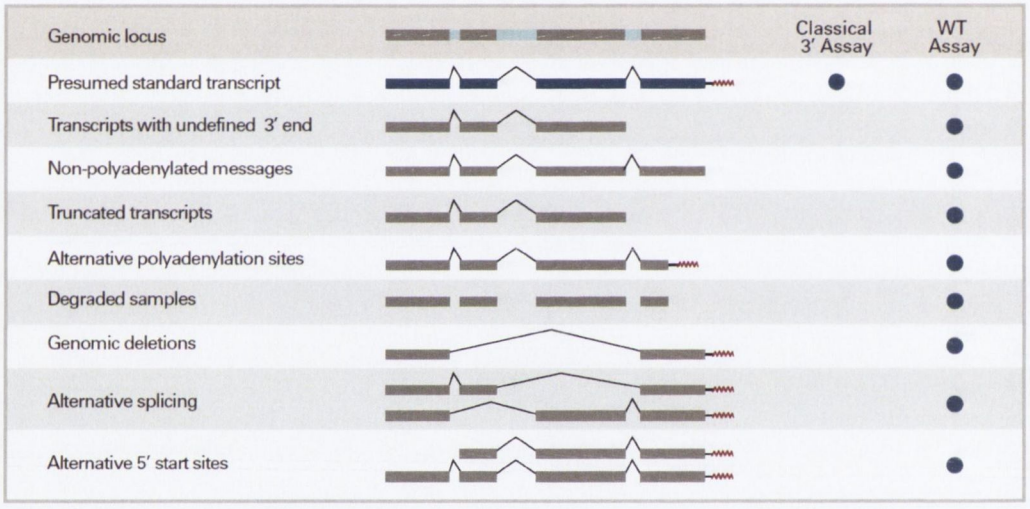

Figure 2-7: Detection capacity of Whole Transcript (WT) versus 3′ assay technologies.

Whole transcript (WT) analysis allows analysis of the level of gene expression but with increased resolution allowing determination of the nature of the transcript including splice variants, truncated transcripts and detection of deletions.

Human Exon 1.0 ST Design

The Human Exon 1.0 ST Array probes sequences are based on a combination of empirical data and predicted data.

- Empirical evidence based data include:

- the annotations against the build 34 of the human genome sequence (hg16, build 34, July 2003)
- cDNA-based content including the more established RefSeq mRNAs (Cumulative update, February 7th, 2004), GenBank® mRNAs (release 139), and ESTs from dbEST (February 5th, 2004). In addition, mouse and rat cDNAs have been mapped onto the human genome using genome synteny maps from the UCSC Genome Bioinformatics group.

- Predicted gene structure sequences include those from:
  - GENSCAN
  - Ensembl
  - Vega
  - geneid and sgp
  - TWINSCAN
  - Exoniphy
  - MicroRNA Registry
  - MITOMAP

The consolidation of several input sequences and annotation sources is a significant feature of the exon array and provides targets that are divided into contiguous, non-overlapping Probe Selection Regions (PSRs). These were identified by projecting all the input annotations onto the genome and inferring exonic, intronic and intergenic regions. Transcribed blocks (exonic clusters) were then further divided into PSRs where hard and soft edges were identified. Hard edges are end of sequences identifying PSR boundaries that evidence indicates cannot be extended such as 3' and 5' splice sites, CDS start/stop sites, poly adenylation sites and internal splice sites. Soft edges are end of sequences that can be extended by another source of evidence that may not result in a PSR boundary.

Based on data from these sources each array contains 5,362,207 unique 25-mer oliognucleotide probes, constituting 1.4 million probesets, themselves grouping into 1,084,639 exon clusters (i.e. probing one or more overlapping exons) and 150,000 transcript clusters (groups of putative alternatively spliced transcripts of a gene) allowing

not only gene level expression analysis but the most detailed exon level transcript analysis available using microarray technology.

After *in silico* array design and validation, the array is manufactured using the same photolithographic and combinatorial chemistry methods used to manufacture previous GeneChip® arrays although at a higher probe density/smaller feature size than previously employed.

Unlike the U133 plus 2.0 array which preceded it, the Human Exon array uses four perfect match probes for each probeset instead of the previous design which employed 11 probe pairs. While it is accepted that using multiple probes for each probe set generates more robust quantitative information and that reducing the number of probes results in lower sensitivity and specificity, human exon array performance is expected to be recovered because of the multiple PSRs representing each gene with the gene-level performance comparable to that obtained on the HG-U133 Plus 2.0 Array.

The Human Exon 1.0 ST array also differs significantly to previous GeneChip® technologies in how background correction is achieved. Previously chips included both perfect match probes and corresponding mismatch probes whose fluorescence was subtracted from their corresponding perfect match probe fluorescence. Human Exon 1.0 ST arrays include two groups of probes used to achieve background fluorescence correction: antigenomic background probes and genomic background probes. Antigenomic probes are directed against signals not in the human genome (mouse, rat, drosphila, C. *elegans*, S. *cervisae*, arabidosis, E. *coli*) and not expected to cross hybridise to human sequences. For each of the 26 possible combinations of GC count (from no GC presence to a 25bp oligo containing only G or C) approximately 1000 25mer probes are placed on the array. Genomic background probes are used in place of specific mismatch probes. Unlike the antigenomic background probes the genomic background probes are mismatch probes of which their perfect match counterparts do match the human genome but at regions less likely to be expressed. As per the antigenomic background probes, approximately 1000 25mer probes derived from the 26 possible combinations of GC content were placed on the array.

These two collections of probes are used to estimate specific by comparing perfect match probe intensity to the median intensity of all background probes of matching GC content. This method has been shown to be an effective replacement for the previous mismatch/perfect match method used in previous array designs.

Other control probes included on the array include:

- Affymetrix Controls:
    - Antisense, perfect match and mismatch probes for bacterial spikes: bioB, bioC, BioD and cre used for hybridisation and wash step evaluation. (See section 2.5.3.4 for further details).
    - Sense target probes for poly-A controls: dap, lys, phe and thr used for trouble shooting the entire experimental procedure. (See section 2.5.3.2 for further details).

- Intron/Exon Controls: Probesets were generated for the consensus sequences of the HG-U133 plus 2.0 array normalisation control genes. All of the exons in addition to 100bp long interonic regions were used as PSRs to select perfect match probes as controls.

- Unmapped Human mRNA: putative full length human mRNA sequences which did not align to the human genome were tiled on the array with one perfect match sense probe set for every 5bp for the last 600 bp of the transcript.

Other key features of Human Exon 1.0 ST Arrays include:

- GeneChip® Hybridisation Oven 640: Employed to provide a temperature controlled environment for the hybridisation of samples to GeneChip® arrays, ensuring consistent hybridisation performance across arrays/experiments.

- High resolution GeneChip® 3000 7G scanner: Capable of accurately and precisely scanning at resolutions as low as 0.51µm easily imaging the 5µm features present

on the Human Exon 1.0 ST array, themselves less than half the size of the 11µm features present on the preceding U133 plus 2.0 array.

- GeneChip® Fluidics Station: Allowing highly reproducible, automated, simultaneous loading and detection of solutions required for and processing of up to four GeneChip® arrays.

- Affymetrix® GeneChip® Software: Affymetrix® GeneChip® Command Console® (AGCC) and Affymetrix Expression Console™ (EC) – software solutions allowing the user simple and easy to use applications for GeneChip® sample/experiment registration, control of fluidics modules, array scanning and subsequent quality control of both gene-level and exon-level data.

2.4.3.2 Day 1 Workflow

The workflow for the first day of Affymetrix Human Exon Array analysis of whole transcriptome expression is indicated in Figure 2-8. The observed protocol was that prescribed by Affymetrix® for the GeneChip® Human Exon 1.0 ST Array (Appendix Section 7.4.1).

Briefly, following assessment and adjustment of sample tRNA and control tRNA and preparation of Poly-A controls, starting template tRNA is 'spiked' with the Poly-A controls. These *in vitro* synthesised polyadenylated transcripts of exogenous *B. Subtilis* genes (*lys*, *phe*, *thr* and *dap*) are premixed at staggered concentrations and serve to monitor the eukaryotic sample preparation and labelling process and assess assay success independent of starting RNA quality. First strand cDNA is then synthesised using the Poly-A spiked tRNA as a template.

This single stranded cDNA is created with a T7 promoter sequence and is used as a template in a following second strand cDNA synthesis step where any remaining original RNA is also eliminated by RNase H mediated degradation.

The synthesised double stranded cDNA (dscDNA) is finally used as a template for antisense cRNA synthesis over a 16 hour overnight *In Vitro* Transcription (IVT) reaction.

Figure 2-8

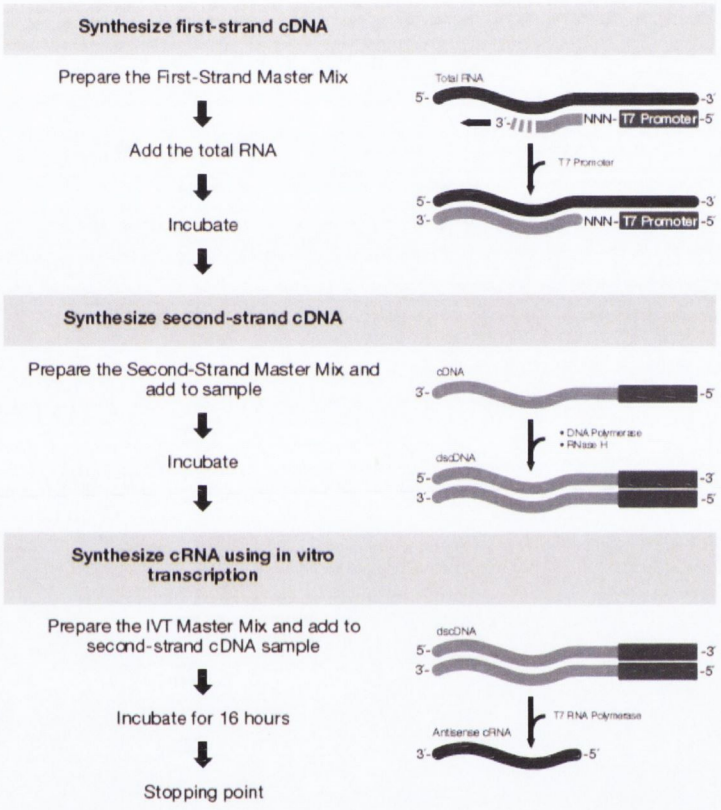

Figure 2-8: Affymetrix® GeneChip® Human Exon 1.0 ST Array Day 1 Workflow

2.4.3.3 Day 2 Workflow

The workflow for the second day of Affymetrix Human Exon 1.0 ST Array analysis of whole transcriptome expression is indicated in Figure 2-9. The protocol observed was that prescribed by Affymetrix® for the GeneChip® Human Exon 1.0 ST Array (Appendix Section 7.4.2).

Briefly, previously synthesised cRNA undergoes a purification step utilising magnetic bead separation technologies to positively select cRNA from any remaining cDNA that may be present.

Following assessment of purified cRNA quantity and size characteristics by Nanodrop and Bioanalyser assay, the cRNA is used as a template for second cycle cDNA synthesis using random primer driven reverse transcription.

Following cDNA synthesis residual cRNA is eliminated by RNase H mediated degradation and the synthesised cDNA undergoes a purification step utilising magnetic bead separation technologies to positively select cDNA from any contaminants that may be present.

The cDNA is then subject to assessment by Nanodrop and Bioanalyser assay for quantity and size characteristics before being fragmented and progressing onto labelling and hybridisation steps on day three.

Figure 2-9

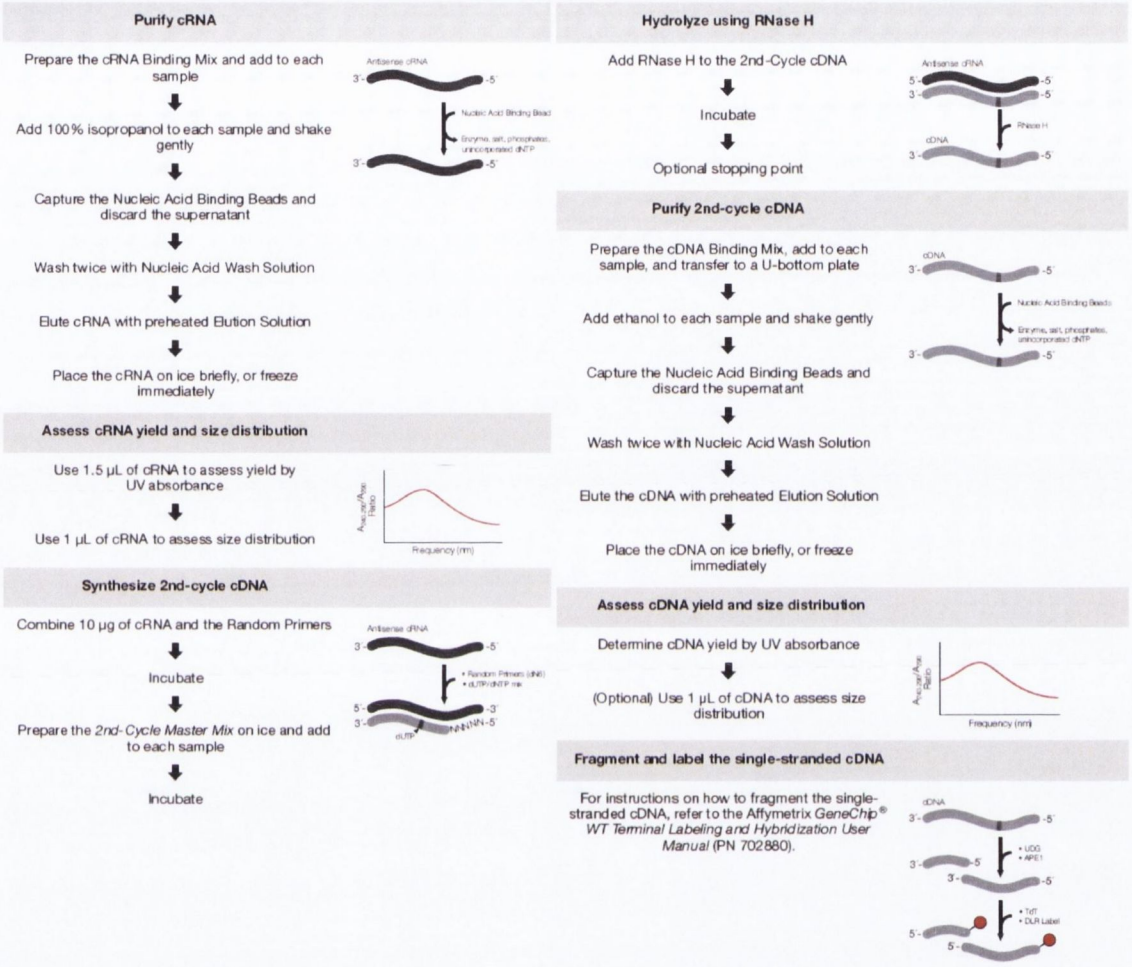

Figure 2-9: Affymetrix® GeneChip® Human Exon 1.0 ST Array Day 2 Workflow.

2.4.3.4 Day 3 Workflow

The third day of the Human Exon Array preparation involves the labelling of fragmented cDNA and hybridisation to the GeneChip® array. The protocol observed was that prescribed by Affymetrix® for the GeneChip® Human Exon 1.0 ST Array (Appendix Section 7.4.3).

Briefly, using the Affymetrix® GeneChip® WT Terminal Labelling Kit fragmented cDNA was labelled using terminal deoxynucleotidyl transferase (TdT) in the presence of a proprietary biotinylated labelling reagent (Biotin Allonamide Triphosphate, BAT). Following labelling samples are hybridised onto GeneChip® Human Exon 1.0 ST Arrays in

the presence of a synthetic control oligonucleotide (Oligo B2) and four *E. coli* derived hybridisation controls (bioB, bioC, bioD and cre). These non-eukaryotic controls serve as controls for alignment for image analysis (Oligo B2) and for hybridisation, washing and staining procedures (bioB, bioC, bioD and cre).

2.4.3.5 Day 4 Workflow

On the fourth day of Affymetrix® GeneChip® array labelled, fragmented cDNA has been hybridised to probes on the GeneChip® array over 17 hours ±1 hour. After aspirating the Hybridisation Cocktail from the array the GeneChip® is subject to a series of washes (non-stringent and stringent) and staining with a streptavidin phycoreythrin (SAPE) conjugate using a GeneChip® Fluidics Station 450 before scanning on a GeneChip® Scanner. The protocol observed was that prescribed by Affymetrix® for the GeneChip® Human Exon 1.0 ST Array (Appendix Section 7.4.4).

2.4.3.6 *In Silico* Analysis

2.4.3.6.1 Quality Control

Quality control analysis was performed on GeneChip® array data using the Affymetrix Expression Console™ (EC) software before progressing onto subsequent in depth analysis using third party software. This was accessed from the AGCC toolbar via the Expression Console™ icon. 

- The previously generated .cel files of arrays to be analysed were loaded into a new EC study and multi chip analysis performed.
- The probeset summarisation of choice was then selected using the analysis menu. Options available with GeneChip® Human Exon 1.0 ST arrays include:
    - Gene
    - Exon
    - Controls Only
        - For the purposes of this thesis Gene level analysis was employed.
- The annotation level, **Core** or **Extended** was then selected from the dropdown list.

- **Core:** limits analysis to exon-level probe sets supported by the most reliable evidence from RefSeq and that map to BLAST-like alignment tool (BLAT) alignments of mRNA with GenBank annotated full-length coding sequence (CDS) regions.
- **Extended:** limits analysis to transcripts that are defined by exon-level probe sets that map to cDNA alignments and their annotations based on cDNA alignments, in addition to transcripts defined by the core category. Examines probesets supported by other cDNA evidence (from other Genbank mRNAs not annotated as full-length, EST sequences, ENSEMBL gene collections, syntenically mapped mRNA from Mouse, Rat, or Human, mitoMap mitochondrial genes, microRNA registry genes, vegaGene, and vegaPseudoGene records) beyond what is used to support core probe sets.
  - For the purposes of this thesis Core Annotation analysis was employed.

- Following analysis various metrics were generated by selecting: Graph, Line Graph – Report Metrics.

A brief summary of the different quality control metrics, their meaning and function are described below.

Probe Level Metrics

- pm_mean: This first quality assessment metric is the mean of the raw intensity of all the perfect match (PM) probes on the array prior to any intensity transformations (e.g. as occurs during normalisation). These values can be used to determine if a chip is unusually bright or dim, which in itself may not present a problem but may warrant scrutiny of probeset based metrics to ensure further irregularities do not occur.

- Box Plot – Probe Cell Intensity/Relative Probe Cell Intensity: Using the Graph function and selecting Box Plot – Probe Cell Intensity or Box Plot Relative Probe Cell Intensity allows the generation of box plot graphs from either CEL or CHP files. These graphs allow visual identification of individual arrays that are dramatically

different from the others and critically if different from other replicates in the same group. Relative Probe Cell Intensity box plots compare the distribution of intensities on each array to the median probe intensity value for the group assisting in identifying possible outlier arrays that may warrant further investigation.

Probeset Summarisation Based Metrics

This set of metric is based on summarisation of probeset results. Theses metrics are largely performed for different groupings of probesets for Poly-A or hybridisation controls.

- pos_vs_neg_auc: This metric examines the area under the curve (AUC) for a plot comparing positive control signal values (from putative exon based probe sets from putative housekeeping genes) and negative control signal values (from putative intron based probe sets from putative housekeeping genes). The curve is generated by evaluating how well the positive and negative control signals separate with the assumption that negative control signal is a measure of false positives and positive control signal is a measure of true positives. An AUC of 1.0 reflects perfect/complete separation whereas 0.5 indicates no separation. The AUC may vary with tissue type and RNA quality however AUC values of 0.80 to 0.90 are typical.
- X_mean: This is the mean signal value for all the probesets analysed for the category 'X'.
- X_mad_residual_mean: This is the mean of the absolute value of deviation of the residuals from the median for all probesets analysed for the category 'X'.
- Different probes will return different signal intensities when hybridised to a common target. To account for these variations in intensity an RMA algorithm creates a model for individual probe responses. The difference between the actual probe signal intensities and the algorithm predicted value is the 'residual'. If the residual for a probe on any given chip is very different from the median probe intensity it means it is a poorer fit to the model. As such, calculating the mean of all the absolute value of all the deviations results in a metric describing how well

or poorly all the probes on a given chip fit the model, with an excessively high mean absolute deviation of residuals from the median indicating possible problematic data on that chip.

- X_rle_mean: This is the mean absolute relative log expression (RLE) for all the probesets analysed for category 'X'. This metric is generated by using the signal estimate generated for a particular probeset on a chip and calculating the difference in Log_2 from the median signal value of that probeset over all the chips in a study. The mean is then calculated from the absolute RLE for all the probesets analysed from category 'X'. When only replicates from a tissue or cell line are analysed together the mean absolute RLE should be consistently low, indicating low variation in the biological replicates.

Probeset Quality Metrics

Quality control assessment also includes metrics describing individual probeset signals for Affymetrix controls, including the bac (bacterial) spike and poly-A spike probesets. Any probeset of interest can be graphed using the Expression Console software by selecting 'Graph, Probeset list' from the programme window. The primary use of analysing specific probeset values is in determining if expected behaviours, such as consistent expression of housekeeping genes and rank ordering of spike probesets is present.

Probeset Categories

When examining probeset quality metrics values are frequently reported on, not just for all the probesets analysed but also for subsets of interest of particular probesets. These may be used to assist in trouble shooting in the event of a poorly performing sample.

- all_probeset: is all the probesets analyzed. In most cases, this category is the bulk of probesets that will be carried into downstream statistical analysis. Thus the metrics reported for this category will be the most representative of the quality of the data being used downstream.

- bac_spike: is the set of probesets which hybridize to the pre-labeled bacterial spike controls (BioB, BioC, BioD, and Cre). This category is useful in identifying problems with the hybridization and/or chip. Metrics in this category will have more variability than other categories (*i.e.,* positive controls, all probesets) due to the limited number of spikes and probesets for this category.
- polya_spike: is the set of polyadenylated RNA spikes (Lys, Phe, Thr, and Dap). This category is useful in identifying problems with the target prep. Metrics in this category will have more variability than other categories (*i.e.,* positive controls, all probesets) due to the limited number of spikes and probesets for this category.
- neg_control: is the set of putative intron based probe sets from putative housekeeping genes. Specifically, these are a number of species specific probesets shown to have constitutive expression over a large number of samples on 3' IVT arrays, the genes for these probesets identified and multiple four probe probesets were selected against their putative intronic regions. Thus in any given sample some (or many) of these putative intronic regions may be transcribed and retained. This probeset collection provides a moderately large collection which in general has very low signal values and can thus be used to estimate the false positive rate for the pos_vs_neg_auc metric.
- pos_control: similar to the neg_control probeset, this is a set of putative exon based probe sets from putative housekeeping genes. In this instance species specific four probe probesets were selected for putative exonic regions in these genes which were previously identified as having constitutive expression over a large number of samples. This collection makes up a moderately large selection of probesets with target present which tend to have moderate to high signal values. These probesets are used to estimate the true positive rate for the pos_vs_neg_auc metric.

Metrics based on the pos_control and all_probeset categories provide a means to assess the overall quality of the data from each chip. They will reflect the quality of the experiment as a whole, from input tRNA, target prep, chip, hybridization, scanning through to grid alignment and indicate towards the nature of the data prior to downstream statistical analysis.

The polya_spike category is useful for identifying potential problems with the target prep phase of the experiment; the bac_spike category is useful for identifying potential problems with the hybridization and chip. The caveat with these two categories is the limited number of spikes. Thus they should be used to troubleshoot problems whereas the pos_control and all_probeset categories should be used to assess overall quality.

2.4.3.6.2 Biotique Systems XRAY

Having passed quality control assessment GeneChip® data was progressed to in depth analysis using Boutique Systems XRAY software (Biotique Systems Inc., Reno, NV, USA). Data from resting, untreated cell lines was compared against data generated using cells exposed to experimental treatments. Genes were determined to be differentially expressed if they possessed a *p*-value of ≤0.05 and a fold change of ≥1.5.

The 6 input CEL files, three replicates of each condition were analyzed with the Affymetrix Human Exon 1.0 ST array to identify genes that were significantly differentially expressed significant between the groups of interest (Gardina, et al 2006; Huang, et al 2007; Clark et al 2007).

Array Normalization

The input files were normalized with full quantile normalization (Irizarry et al., 2003b). For each input array, for each probe expression value, the array ith percentile probe value was replaced with the average of all array ith percentile points.

Probe Score Transformation and GC Filtering

The 5,359,576 probes were manipulated into the analysis values as follows. Probes with GC count less than 6 and greater than 17 were excluded from the analysis. Probe scores were then transformed by taking the Natural Logarithm of 0 plus the probe score.

Background Correction

Unlike previous GeneChip® array types, Exon arrays do not use individual mis-match probes to determine and allow correction for background signal. Background is established from a pool of probes specifically designed for that purpose. Background probes are stratified by CG content and each probe score was corrected for background by subtracting the median expression score of background probes with similar GC content.

Multiple Tests Correction

Under proper randomization conditions, for each gene we test, the probability of a 'false-positive' (or 'Type I Error') is 0.05. This is taken to understand that from 100 test observations, 5 would incorrectly show to be significant. Because array based technologies allow the testing of a large number of "independent" genes (approximately 30,000), this significance value may be misleading since the probability of finding a false-positive will grow as more genes are tested, with 1,500 false positives potentially indicated (Glantz, 1997). To correct for this we use the Benjamini and Hochberg False Discovery Rate (FDR) method outlined by Benjamini and Hochberg (Benjamini and Hochberg, 1995) and originally proposed by Simes (Simes, 1986) that controls the family wide error rate in a weak sense.

The "False Discovery Rate" of expected proportion of false positives is controlled - by contrast methods like the Bonferroni correction control false discoveries in the "strong sense" and bound the probability of occurrence of ANY false positives. The Bonferroni method tends to be too conservative, potentially so much so that the probability of detecting a true association can in some instances be reduced to zero for these types of studies.

2.5 Cell Culture

Several cell lines were used over the completion of this thesis. These include cell lines representing ovarian tissues (HIOE-80, 59M, SK-OV 3, A2780 and A2780cis) and thyroid tissues (Nthy-ori 3-1). These cells were used in the evaluation of cell lines interaction with platelets isolated from whole blood through completion of both *in vitro* cell based assays and molecular based gene expression assay and microarray based investigations.

2.5.1 Cell lines

- HIOE-80: A gift from the Fox Chase Cancer Centre, Philadelphia, PA, this cell line represents normal human ovarian epithelial cells. Human ovarian surface epithelial (HOSE) cells were prepared from prophylactic oophorectomies and immortalised by transfection with a plasmid encoding for the Simian Virus 40 (SV40) large T antigen. It is moderately well characterised and is known to be non-tumorigenic in nude mice.

- 59M: (HPACC, Salisbury, UK) This cell line represents human ovarian epithelial carcinoma, originally isolated from ascites of a 65 year old patient with metastatic ovarian cancer and is well characterised, known to be tumorigenic in nude mice.

- SK-OV-3: (ATCC, Manassas, VA, USA) represents a human ovarian epithelial adenocarcinoma, originally isolated from ascites of a 64 year old patient with metastatic ovarian cancer. This cell line is well characterised and is known to be resistant to tumour necrosis factor (TNF) and several cytotoxic agents including diphtheria toxin, cisplatin and adriamycin. In culture it is observed to form moderately well-differentiated adenocarcinoma consistent with ovarian primary cells and is tumorigenic in nude mice.

- A2780 and A2780cis: are cell lines derived from a primary ovarian epithelial tumour in an untreated patient.

- Nthy-ori 3-1: (HPACC, Salisbury, UK) is a human follicular epithelial cell line derived from normal adult thyroid tissue and immortalised by transfection with a plasmid encoding from the SV40 large T antigen. This cell line has been highly characterised and found to be non-tumorigenic but following irradiation may undergo malignant transformation due to ret/PTC oncogene rearrangement (Finn et al., 2004).

All cell lines were grown in a humidified atmosphere containing 5% CO_2 at 37°C in the appropriate full growth media.

2.5.2 Cell Culture Media and Other Solution Formulation

- HIOE-80: This cell line was maintained in a 1:1 mixture of medium 199 and MCDB 105 supplemented with 10% foetal bovine serum, 2mM L-glutamine, 100 units/ml penicillin, 100µg/ml streptomycin and 0.2 IU of recombinant human insulin per ml. As this media formulation is not commercially available it is necessary to prepare it prior to use following the following protocol.

    - 900ml room temperature (15-20°C) double distilled water was transferred to a 1.5L beaker.
    - Powdered MCDB 105 medium (Sigma Aldrich, St Louis, MO, USA) was added whilst stirring until dissolved. No sodium bicarbonate supplementation is required.
    - The pH of the media was adjusted to pH7.0. As a result of subsequent filtration the pH rises to a working pH of 7.3.
    - Double distilled water was added to reach a final volume of 1000ml.
    - 220ml of MCDB 105 was mixed with 220ml M199 media (Sigma Aldrich, St Louis, MO, USA) in the upper chamber of a Millipore Stericup® vacuum filter unit (Millipore, Billerica, MA, USA) and immediately sterilised by 0.22 micron filtration into a sterile 500ml collection bottle. The volume prepared allowed for four bottles of media to be prepared with remaining

media being used in the preparation of cryoprotectant media or trypsin neutralising solution (TNS).

- Prior to use 10mls penicillin/streptomycin (Sigma Aldrich, St Louis, MO, USA), 540µl of human recombinant insulin (10mg/ml) (Sigma Aldrich, St Louis, MO, USA) and 50mls Foetal Bovine Serum (FBS) were added to make prepare a working stock of full growth media.

- 59M: This cell line was maintained in DMEM, 1g glucose/L (Sigma Aldrich, St Louis, MO, USA), supplemented with 10% FBS, 2mM L-glutamine, 100 units/ml penicillin, 100µg/ml streptomycin.

- SK-OV 3: This cell line was maintained in McCoy's 5A media (Sigma Aldrich, St Louis, MO, USA), supplemented with 10% FBS, 100 units/ml penicillin, 100µg/ml streptomycin.

- A2780 and A2780cis: These cell lines were maintained in RPMI 1640 media (Sigma Aldrich, St Louis, MO, USA) supplemented with 10% FBS, 2mM L-glutamine, 100 units/ml penicillin, 100µg/ml streptomycin. Every third passage the A2780cis cell line was maintained in media supplemented with 1µM cisplatin to maintain chemoresistance.

- Nthy-ori 3-1: This cell line was maintained in RPMI 1640 media (Sigma Aldrich, St Louis, MO, USA) supplemented with 10% FBS, 2mM L-glutamine, 100 units/ml penicillin, 100µg/ml streptomycin.

All prepared media was stored at 4°C and warmed to 37°C in a water bath prior to use.

2.5.2.1 Cisplatin Solution Preparation

To maintain chemo-resistance in the A2780cis cell line the cells required exposure to 1µM cisplatin every 2-3 passages. This was performed by supplementing 29.7ml full growth media (described in Section 2.5.2) with 300µl of a 100µM

cisplatin/0.9% saline solution. This was prepared according to the following protocol.

- 270mg NaCl (Sigma Aldrich, St Louis, MO, USA) was dissolved in 20ml room temperature sterile water (Sigma Aldrich, St Louis, MO, USA).
- 900µg cisplatin (Sigma Aldrich, St Louis, MO, USA) was transferred to the saline solution and the pH adjusted to 7.6.
- The solution was adjusted to a final volume of 30ml using room temperature sterile water.
- The cisplatin solution was then filtered through a 0.22 micron filter, 300µl aliquots prepared in 1ml microcentrifuge tubes and stored at -20°C until required.

2.5.2.2 Cryopreservation Media

To ensure cell survival during the preparation of frozen stocks and the recovery of frozen stocks from liquid nitrogen storage a cryopreservative media was prepared for each cell line.

- 28ml basal (unsupplemented) cell culture media (70% F_v) was transferred to a sterile 50ml skirted centrifuge tube.
- 8ml FBS (20% F_v) was added and gently mixed by inversion.
- 4ml Dimethyl sulfoxide (DMSO) (10% F_v) was added and the mixture mixed by inversion
- Cryopreservation media was stored at -20°C until required.

2.5.2.3 Trypsin Neutralising Solution

In order to neutralise the protease activity of trypsin used during passaging of cell lines, and prevent damage of cell cultures Trypsin Neutralising Solution (TNS) was prepared.

- 30ml basal (unsupplemented) cell culture media (80% F_v) was transferred to a sterile 50ml skirted centrifuge tube.
- 7.5ml FBS was added to the media and gently mixed by inversion.
- Trypsin Neutralising Solution was stored at -20°C.

2.5.3 Adherent Cell Line Passage

- Cell culture media, trypsin-EDTA and TNS was pre-warmed at 37°C in a water bath. PBS was warmed to RT for 30 minutes prior to use.
- Add 15ml cell culture media to two 75cm^2 (T75) cell culture flasks and transfer to a humidified cell culture incubator at 37°C, 5% CO^2.
- Old cell media was removed from each flask to a waste bottle containing a chlorinating disinfectant (Guest Medical Ltd, Kent, UK).
- Cells were washed with 5ml of phosphate buffered saline (PBS).
- The PBS was removed to the waste bottle.
- 5ml of 1x trypsin-EDTA (Sigma Aldrich, St Louis, MO, USA) was added the cells and the flask incubated for 3-4 minutes at 37°C.
- The flasks were assessed by light microscopy to determine cell detachment and the flasks lightly tapped to encourage detachment from the growth surface.
- When >90% of cells were observed to be detached 5ml TNS was added to the flask. The cell suspension (10ml) was transferred to a 15ml centrifuge tube and centrifuged at 300 x *g* for 5mins.
- The supernatant was removed to the waste bottle and the cell pellet resuspended in 2ml of complete medium.
- Cells were seeded to the pre-warmed cell culture flasks according to the splitting instructions appropriate for each cell line. E.g. transferring 500µl of cell suspension to a flask equates to seeding at approximately 25% confluence or a 1:4 split and similarly transferring 250µl of cell suspension to a flask equates to seeding at approximately 12.5% confluence or a 1:8 split.

2.5.4 Non-Enzymatic Cell Detachment

When cells were required for assay and maintenance of membrane bound protein integrity was paramount non-enzymatic detachment of cells from growth plates was performed.

- Cells were grown to ≥ 80% confluence on 75cm^2 cell culture flasks.
- Cells were washed with 10ml room temperature Ca^{2+} and Mg^{2+} free PBS.
- 5mls PBS/7mM EDTA was applied to the cells and the flask incubated at 37°C 5% CO_2 for 15 minutes.
- 20ml room temperature PBS (containing Ca^{2+} and Mg^{2+}) were added to the cell suspension and transferred to a 50ml centrifuge tube and centrifuged at 300g for 5 minutes.
- The cell pellet was gently resuspended in 5mls PBS (containing Ca^{2+} and Mg^{2+}) by pipetting and centrifuged at 300 x *g* for 5 minutes.
- The cell pellet was gently resuspended in 1ml of PBS, Tyrode's Buffer or JNL as the subsequent experiment required, counted as per Section 2.5.5 and adjusted the required concentration.
- Cells were maintained on ice prior to use.

2.5.5 Cell Counting

After pelleting cells by centrifugation following enzymatic/non-enzymatic detachment from tissue culture flasks, cells were resuspended in 1ml of pre-warmed media, mixing well by pipetting.

- The cells are counted using a haemocytometer as follows:

    - Add 90µl of media to a 1ml microcentrifuge tube.
    - Add 10µl of the cell suspension to the microcentrifuge and mix by gentle pipetting. This is a 1:10 dilution of the original cell suspension.
    - Clean the haemocyctometer with Trigene detergent (Medichem International, Kent, UK) and 70% ethanol.
    - Place a cover slip over the haemocytometer.
    - Add 20µl of the diluted cell suspension to the haemocytometer by placing the pipette tip at the edge of the cover slip and the haemocytometer chamber will fill by capillary action.
    - Cells are counted in the sixteen small squares (indicated in yellow in Figure 2.6) within an A square (indicated in red in Figure 2-10).
    - The number of cells in three A squares was counted averaged and the following formula used to calculate the number of cells per ml.

Average number of cells per A square x 10^4 x Dilution factor= number of cells per ml of cell suspension

    - cells or dilution required to achieve a desired cell concentration can then be calculated.

Figure 2-10

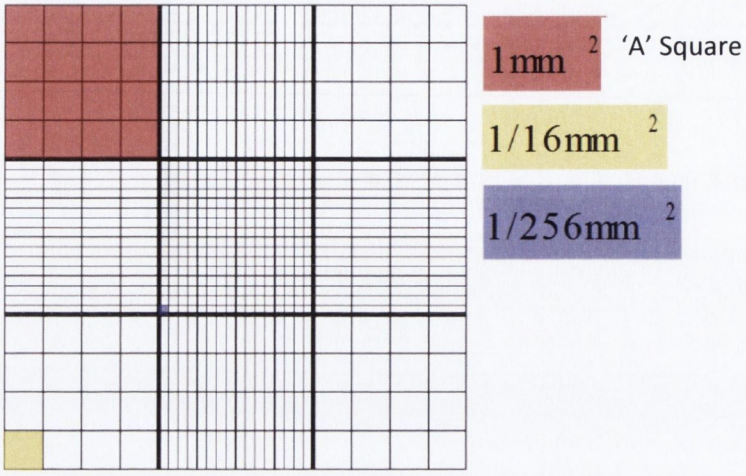

Figure 2-10: Graphical illustration of a haemocytometer counting chamber.

2.5.6 Freezing Cells Stocks

- Cryopreservation media was thawed on ice for 30-45 minute prior to use.
- Following detachment of cells from tissue culture flask and pelleting by centrifugation cells were resuspended in 2ml cryopreservation media.
- 1ml of the cell suspension was transferred to two cryovials and the cryovials placed on ice for 10 minutes.
- The cryovials were placed at -20°C for one hour, kept overnight at -80°C and transferred the following day to a liquid nitrogen storage tank for long-term storage.

2.5.7 Thawing Cells from Frozen Stocks

- Warm cell culture media for 30 minutes at 37°C in a water bath.
- Add 15ml cell culture media to two 75cm^2 (T75) cell culture flasks and transfer to a humidified cell culture incubator at 37°C, 5% CO^2.

- Remove one cryovial of cells (1ml volume) from liquid N^2 storage and bring to room temperature in a 37°C water bath. It is critical to perform this and the subsequent step as quickly as possible as the DMSO in the cryopreservation solution is toxic to the cells at room temperature.
- The thawed cells were added in a drop-wise manner to 8mls of warm media in a 15ml centrifuge tube by pipette and mixed by inverting. The cell suspension was centrifuged at 300 x *g* for four minutes.
- The pellet was resuspended in 1ml of cell culture media and 500µl of cell suspension transferred to each of the T75 flasks prepared previously.
- Cells will adhere to the base of the flask and were grown to confluence
- Media was changed initially after three days and at 2-3 day intervals until confluent and requiring further passaging.

2.5.8 Mycoplasma Testing

Mycoplasma are very small (0.15–0.3 µm) cell wall-less bacteria. Due to their size they are sometimes not removed by common filtration practices and should they contaminate a cell culture they pose a significant problem. Mycoplasma infection of cell cultures is frequently invisible by conventional microscopy but the effect on cultures ranges from altering cell metabolism and proliferation by withdrawl of nutrients and production of toxic metabolites and alterations in gene expression and DNA structure including chromosomal aberrations. Thus a mycoplasma infection can significantly alter cells responses and can significantly affect the accuracy of gene expression and microarray based studies. Due to the risk of cross contamination if discovered cultures are destroyed rather than attempts made to remove mycoplasma species.

In order to detect possible mycoplasma infections the Roche Mycoplasma Detection Kit (Roche Diagnostics, Mannheim, Germany) was employed following the manufacturers protocol (Appendix Section 7.4.5). This enzyme-linked immunosorbent assay (ELISA) kit allows for the detection of the four most common mycoplasma/acholeplasma contaminants found in cell culture (*M. arginini, M. hyorhinis, A. laidlawii, M. orale*).The principle behind this assay is illustrated in Figure 2-11.

Figure 2-11

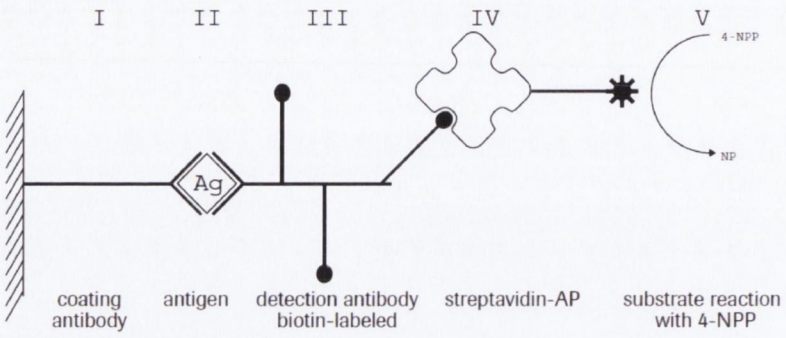

Figure 2-11: Graphical illustration of ELISA based mycoplasma detection.

The surface of a microplate well is coated with a mycoplasma species specific coating antibody. Non-specific binding is impaired by blocking non-specific binding sites and subsequent incubation of test samples/controls will result in binding of present mycoplasma/mycoplasma fragments to the coating antibody.

A biotinylated secondary mycoplasma species specific antibody is then applied providing a binding site for streptavadin-Alkaline Phosphatase (Strep-AP). When presented with 4-NitroPhenolPhosphate (4-NPP) substrate it produces the metabolite 4-NitroPhenol (NP) which can be then detected by absorbance at 405nm.

2.5.9 Thyrocyte γ-Irradiation

- Nthy-ori 3-1 cells were cultured in full media in 75cm^2 cell culture flasks until approaching confluence.
- Irradiation was performed with permission from Prof. Kingston Mills and assistance from Dr. Neil Marshall, Dept. of Biochemistry, Trinity College Dublin using the Gammacell 3000 Elan (MDS Nordion, Ottawa, Canada), which uses a ^{137}Cs γ source.
- The cells were passaged and re-suspended briefly in PBS/10% FCS. Cells were maintained in full growth media in a humidified incubator at 37°C, 5% CO^2.

- During subsequent passaging an aliquot of cells was removed and RNA extracted as per section 2.2.2.1 and stored at -80°C for later use in subsequent gene expression analyses.

2.6 Platelet and Platelet Releasate Isolation

2.6.1 Washed Platelet Preparation

2.6.1.1 Stock Buffer Preparation

JNL Physiological Buffer

JNL physiological buffer is a modified HEPES-Tyrodes buffer utilised in the preparation of washed (isolated) platelets from whole blood samples without inducing platelet activation.

The buffer is a modification of that utilised by Mendelsohn and colleagues (1991, 1990) and Hawiger and colleagues (1980) for the preparation of washed/filtered platelets (Dunne et al., 2012, Larkin et al., 2009, Stephens et al., 1998) with a final concentration of 130 mM NaCl, 10 mM sodium citrate, 9 mM NaHCO 3 , 6 mM D-glucose, and 0.9 mM MgCl 2 , 0.81 mM KH 2 PO 4 , and 10 mM Tris, pH 7.4. The buffer is prepared as separate 10x concentrate component solutions (JNL A-E) and combined as a final solution as described in Appendix Section 7.5.1.

Acid Citrate Dextrose (ACD)

ACD is an anticoagulant utilised to prevent the activation of platelets during the preparation of washed or filtered platelets by reversibly chelating calcium. ACD is prepared to final concentrations of citrate acid anhydrous 38mM, sodium citrate 75mM, dextrose 136mM (Appendix Section 7.5.2).

2.6.1.2 Washed Platelet Preparation From Whole Blood

- 30 ml of blood was taken from healthy female volunteers who had not taken any drugs or medication that may affect platelet function in the last within two weeks into 4.5ml acid citrate dextrose (ACD).
- 5mls of citrated blood was transferred to 15 ml falcon tubes (5 ml/tube) and subjected to centrifugation at 170 G for 10 minutes.
- The platelet rich plasma was removed and acidified to pH6.5 using ACD/PGE_1 (1μM) (Sigma-Aldrich, St Louis, MO, USA) added before being centrifuged at 720 x *g* for 10 minutes to pellet platelets.
- The platelet pellet was then gently resuspended in 2ml JNL buffer (130mM NaCl, 10mM sodium citrate, 9mM $NaHCO_3$, 6mM dextrose, 9mM $MgCl_2$, 0.81mM KH_2PO_4, 3mM KCl, 10mM Tris, pH 7.4).
- Platelet counts were standardised to a physiologically representative to 200-250 x 10^3/μl, supplemented with 1.8mM $CaCl_2$ before being allowed to rest for 30-60 minutes prior to use.

2.6.2 Gel Filtered Platelet Isolation

2.6.2.1 Sepharose Column Preparation

- Sepharose 2B (Sigma Aldrich, St Louis, MO, USA) was vigorously shaken to ensure even suspension of sepharose beads.
- 10ml Sepharose 2B was poured into a beaker and diluted with ddH_2O and poured into a 20ml column.
- The contents were allowed to settle before adding further sepharose to the column. For a starting blood volume of 30ml a 6ml packed column is desired.
- The when the desired depth of packed sepharose beads was achieved the column was then washed with 60ml (10x bead volume) with ddH_2O.
- The packed sepharose bead column was then washed with 24ml (4x bead volume) with JNL buffer, equilibrating the column to a pH of 7.4, a physiological equivalent for platelets.

2.6.2.2 Gel Filtration of Washed Platelets

- Just as the final drop of the last JNL wash was leaving the column washed platelets (as prepared in section 2.6.1) were placed gently on top of the column using a Pasteur pipette.
- As the washed platelets begin to move into the column a further volume of JNL is gently added.
- As the platelets move through the column a definite cream coloured band in the column should be visible indicating their location. As the band progresses further JNL buffer is added to the column.
- Having passed through the column the gel filtered platelets are eluted in white cloudy droplets collected in a 15ml tube.
- Prior to use the platelets were quantified using a Coulter counter, adjusted to physiological concentration and $CaCl_2$ added to a final concentration of 1.8mM.

2.6.3 Platelet Releasate Preparation

- Gel filtered platelets (as prepared in section 2.6.2) were stimulated with 20µM Thrombin Receptor Activating Peptide (TRAP,SFLLRN) (Sigma-Aldrich, St Louis, MO, USA) and 190µg/ml collagen (Bio/Data Corp., Horsham, PA, USA).
- The sample was stirred for 10 minutes (1100 RPM) at 37°C.
- The platelet aggregate was then centrifuged at 720 x *g* for 10 min.
- The supernatant (platelet releasate) was aspirated and filtered through 0.22µM pore disks to remove platelet microparticles.

2.6.4 Platelet Releasate Protein Quantitation

2.6.4.1 Bradford Protein Assay

To determine to protein content of platelet releasate Bradford bicinchoninic acid (BCA) colorometric protein assays were performed using the Pierce® BCA Protein Assay Kit (Pierce Biotechnology, Rockford, IL, USA) following the manufacturers recommended protocol (Appendix Section 7.6).

2.7 Cell-Platelet Interaction Assays

2.7.1 *In Vitro* Platelet Adhesion Assay

2.7.1.1 Cell Line Preparation

- Cell lines representing normal and malignant tissues were seeded into Nunc 96 well plates at $4x10^4$ cells/well. These plates were selected for the proprietary Nunclon Δ surface modification which facilitates cell attachment through the addition of hydroxyl groups to the plastic growth surface (Thermo Fisher Scientific Inc., 2010) thus making it hydrophilic and improving cell attachment.
- After seeding cells were grown to confluence in the appropriate full growth media.
- Prior to cells becoming confluence 100µl of fibrinogen solution (20µg/ml) was applied to one row of cells and incubated overnight, providing a positive control for platelet adhesion.
- When confluent wells containing adhering cells/fibrinogen were aspirated by pipette and washed twice with 200µl JNL buffer.
- Non-specific platelet adhesion was prevented by blocking wells with 200µl 1% PBS/BSA solution for two hours at 37°C.
- Following incubation wells were washed three times with 100µl JNL/1.8mM $CaCl_2$ (JNL/$CaCl_2$).

2.7.1.2 Platelet Preparation

- Gel filtered platelets were prepared as described in section 2.6.2.2.
- Calcein AM dye (2µg/ml) and PGE_1 (1µg/ml) was added to gel filtered platelets for 30 minutes at 37°C.
- Following incubation PGE_1 (1µg/ml) was added to the platelets and the platelets centrifuged at 720 x *g* for 10 minutes.
- Following centrifugation the supernatant was aspirated and platelets gently resuspended in fresh JNL buffer at $2x10^8$ platelets/ml and allowed to rest in the dark for 20 minutes before use.

2.7.1.3 Cancer Cell – Platelet Adhesion Assay

- Following the final JNL/$CaCl_2$ wash wells containing cells/fibrinogen were exposed to 100µl Calcein AM dye-loaded washed platelets ($1-2x10^8$/ml in JNL buffer) and incubated for 45 minutes at 37°C in the dark.
- Following incubation plates were read on a plate reader Victor^2 V Multilabel Counter (Perkin Elmer, Waltham, MA, USA) at excitation 485nm, emission 535nm providing a measurement of total platelet fluorescence.
- The dye-loaded platelet suspension was then aspirated and wells washed gently three times with 50µl JNL/$CaCl_2$.
- 100µl JNL/$CaCl_2$ was applied to each well and the plate fluorescence re-read to determine the remaining platelets adhering to cultured cells and controls.

2.7.2 Aggregometry Assay

The aggregometry assay utilised followed the protocol utilised previously by investigators examining platelet function and TCIPA (Radomski et al., 1992, Sawicki et al., 1998, Alonso-Escolano et al., 2004b, Medina et al., 2006).

- Cells were grown to 90% confluence in 75cm^2 tissue culture flasks.
- Cells were non-enzymatically detached as per Section 2.6.7 and adjusted to a final concentration of 1x10^6 cell/ml in JNL/1.8μM $CaCl_2$ Buffer.
- A series of 1:10 serial dilutions were performed to allow a set of cell concentrations to be investigated (Table 2-6).

Table 2-6

Dilution	Cell Concentration	Volume to platelet suspension (225μl)	Final Concentration/ Number of cells in suspension
Stock Suspension	1X10^6 cells/ml (stock)	25μl	1x10^5 cells/ml, 2500 cells/250μl
Dilution 1 1:10 Stock Suspension	1X10^5 cells/ml (1:10 Dil Stock)	25μl	1x10^4 cells/ml, 250 cells/250μl
Dilution 2 1:10 Dilution 1	1X10^4 cells/ml (1:10 Dil Stock)	25μl	1x10^3 cells/ml, 25 cells/250μl

Table 2-6: Serial Dilution Schema of non-enzymatically detached cells for Aggregometry Assay use.

- Washed platelets were prepared as per section 2.6.1.
- 3mg/ml fibrinogen added to reflect the physiological concentration normally present in the peripheral circulation, and allowed to rest one hour before beginning the experiment.
- JNL buffer controls (250μl) - representing 100% aggregation controls - were placed in cuvettes the control positions of a Bio/Data Corp. PAP4 aggregometer (Horsham, PA, USA).
- 225μl washed platelet suspension was transferred to cuvettes containing magnetic stir bars and placed in the sample positions of the aggregometer and baseline recorded.

- Baseline was recorded for one minute prior to the addition of cells and/or positive control TRAP and up to 30 minutes of aggregation data recorded subsequently.
- After baseline was recorded 25µl of cell line suspension or Thrombin Receptor Activating Peptide (TRAP, SFLLRN) solution (200µM stock) was added to the platelet suspension to a final concentration of 1µM and the effect on platelet activation and aggregation recorded.
- Platelet activation/aggregation was then normalized by comparing it with a maximal response, defined as that induced by TRAP.

2.7.3 Cell line-Platelet Releasate/Washed Platelet Exposure

Each of the experimental cell lines required were grown to ~90% confluence in nine $75cm^2$ cell culture flasks.

Following preparation of washed platelets and platelet releasate cells were exposed to 10mls of a 1:1000 dilution of washed platelets or 1:1000 dilution of platelet releasate prepared in pre-warmed full growth media in triplicate.

Control cells were exposed to pre-warmed full growth media. The exposure period for the experiment was 6 hours. This exposure period was selected based on work previously carried out in the lab which indicates significant alterations in gene expression may be measured over exposures of this duration (Denning et al., 2008). Following the exposure period total RNA (tRNA) was extracted following the protocol indicated in section and stored at -80°C.

2.8 Detection of Platelet Markers

2.8.1 Flow Cytometry

The ability of ovarian cancer cells to induce platelet activation and degranulation was measured by flow cytometry, using platelet surface $\alpha_{IIb}\beta_3$ or p-selectin (CD62P) expression as a marker.

- In a total reaction volume of 100µl, 10µl of non-enzymatically detached ovarian cancer cells (0 – 1.5 x 10^6/mL) was incubated with in PRP the presence of a PE labelled anti-human p-selectin antibody (1.25µg/ml), FITC labelled anti-human $\alpha_{IIb}\beta_3$ or an appropriate isotype control (1.25µg/ml).
- All incubations were performed at room temperature for 15 minutes.
- The reaction was then terminated with 1 ml of JNL buffer prior to analysis by flow cytometry.
- Samples were analysed using a BD FACS Calibur (Becton Dickinson, Palo Alto, CA, USA) within 1 hour of fixing.
- After system initialisation and priming the instrument was set to measure particle size (forward scatter, FSC), granularity (side scatter, SSC) and fluorescence.
- Using a log FSC vs. log SSC dot plot, a two dimensional analysis gate was drawn around the platelet population (Figure 2-12) and a fluorescence histogram (log FL2 vs. count) was obtained for 10,000 platelet events for each sample.

Figure 2-12

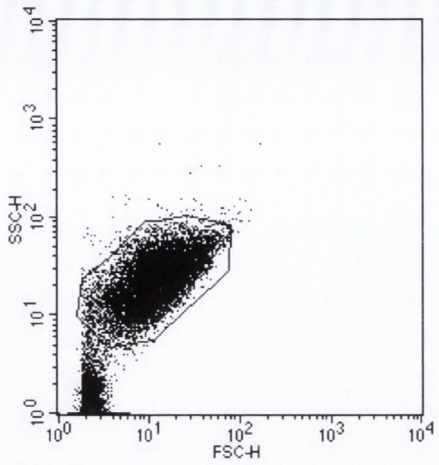

Figure 2-12: Flow Cytometry Dot plot indicating side scatter (SSC-H) and forward scatter (FSC-H) axes*.

*Representative image of a washed platelet sample, indicated by small size and little granularity.

- Data was analysed using Becton Dickinson CellQuest Pro software and expressed as percentage of platelets p-selectin positive relative to the isotype control. All values were expressed as mean ± SEM.

2.8.1.1 Antibodies

- PE labelled anti human p-selectin (mouse IgG) and PE mouse IgG isotype control antibodies were purchased from BD Pharmingen (BD Pharmingen, San Diego, CA, USA).

- FITC labelled anti-human PAC-1/$\alpha_{IIb}\beta_3$ (mouse IgM) and FITC mouse IgM isotype control antibodies were purchased from BD Pharmingen (BD Pharmingen, San Diego, CA, USA).

2.8.1.2 Flow Cytometry Assay of $\alpha_{IIb}\beta_3$/p-selectin

- Platelet Isotype Control – used to set gating properties to investigate platelets population only

- Fluorescently labelled platelets – used to determine mean platelet anti-$\alpha_{IIb}\beta_3$/p-selectin fluorescence
- Cell line Isotype controls for each cell line – used to set gating properties to selectively investigate cell populations
- FACS analysis determines platelets by size via side scatter (SSC) and anti- $\alpha_{IIb}\beta_3$/p-selectin tag fluorescence
- FACS determines cells by size via side scatter and platelet adhesion by presence of anti-$\alpha_{IIb}\beta_3$/p-selectin tag fluorescence.

The presence of $\alpha_{IIb}\beta_3$/p-selectin fluorescence is indicative of platelet presence and the intensity of fluorescence is proportional to number of platelets adhering to the cell. If required this allows the estimation of the number of platelets adhering to cells in addition to the percentage of a cell population adhering platelets to their surface.

2.8.2 Fluorescent Microscopy of Cell Surface Markers

2.8.2.1 Antibodies

- Mouse monoclonal IgG anti-human $\alpha_5\beta_1$ (α_5) integrin (ab75472) (Abcam, Cambridge, MA, USA)
- Mouse monoclonal IgG anti-human $\alpha_5\beta_3$ integrin (MAB3050) (R&D Systems Inc., Minneapolis, MN, USA)
- Alexa Fluor® 488 goat anti-mouse IgG (H+L) (A-11029) (Invitrogen/Life Technologies Corp., Carlsbad, CA, USA)

2.8.2.2 Staining and Visualisation

- Cells were non-enzymatically detached from cell culture plates as described previously adjusted to $5x10^5$ cells/ml in JNL buffer.
- 200µl of the cell suspension was transferred by pipette to a poly-L-lysine coated slide and incubated for 45 minutes at 37°C

- After incubation the slide was washed gently with JNL and adhering cells fixed by incubation with 200µl 3.7 % PFA for 15 minutes at room temperature.
- After incubation the slide was washed gently with JNL. Cells were blocked by incubation with 5% goat serum for 30 minutes at 37°C after which excess goat serum was tapped off.
- The primary antibody was made to 1.25µg/ml in PBS/5% goat serum and incubated for 2 hours at 37°C.
- After incubation which the primary antibody was tapped off and the secondary antibody (1.25µg/mL in PBS/5% goat serum) applied to the slide and incubated for 45 minutes at room temperature.
- Following secondary antibody incubation the slide was gently washed with JNL, a cover slip placed on the slide using DAKO mounting media (Invitrogen/Life Technologies Corp., Carlsbad, CA, USA).

2.9 Cell Growth and Proliferation Assays

2.9.1 Roche Cell Proliferation Assay 1 (MTT)

To optimise the concentration of platelets/platelet releasate cells were to be exposed to in subsequent whole transcriptome assay investigations a series of cell proliferation assays were performed to determine the maximum concentration that could be applied to cells without negatively impacting on cell growth or survival and so determine the concentration to be used in subsequent gene expression based studies. The Roche Cell Proliferation Assay 1 was used following the manufacturers recommended protocol (Appendix Section 7.7).The assay exploits the cleavage of the yellow tetrazolium salt ((3-[4,5-dimethylthiazol-2-yl]-2,5-diphenyl tetrazolium bromide), MTT) to purple formazan crystals by metabolically active cells. These formazan crystals are subsequently solubilised and the resulting coloured solution quantified using a multi-well plate reader. This assay type has previously been shown to be suitable for use with ovarian cell types (Spinner, 2001).

2.10 Apoptosis Assay

Apoptosis is the term used to describe the orchestrated controlled death of cells in response to either physiological or patho-physiological stimuli.

Apoptotic cells may be identified microscopically arising from the characteristic appearance of nuclear chromatin condensation and fragmentation, membrane 'blebbing', however this method may be subjective and is limited to a narrow time window when the morphological changes are at their greatest. Other methods used include analysis of DNA by electrophoretic and fragmentation assays based on tritiated thymidine (^{3}H-thymidine) or 5-Bromo-2'-deoxy-uridine (BRdU) and separation of fragmented DNA (from apoptotic cells) from unfragmented DNA (from non-apoptotic cells).

One of the hallmarks of apoptosis, DNA degradation is in the early part stages of the process selective to the internucleosomal DNA regions. During DNA degradation cleavage may yield double-stranded and single-stranded DNA breaks or 'nicks' at which modified nucleotides may be used to detect breaks through labelling the free 3'-OH termini by exploiting the activity of the enzyme terminal deoxynucleotidyl transferase (TdT). TdT catalyzes template-independent polymerization of deoxyribonucleotides to the 3'-end of single- and double-stranded DNA. This method has also been termed TUNEL (TdT-mediated dUTP-X nick end labelling).

Two different TUNEL based assays were used in the completion of this thesis; the Roche *In Situ* Cell Death Detection Kit, TMR red (Roche Applied Science, Indianapolis, IN, USA) allowing determination of apoptotic cells using fluorescence microscopy and the BD Pharmagen APO-Direct Kit (Becton Dickinson, Franklin Lakes, NJ USA) allowing analysis of apoptosis by flow cytometry. Manufacturers recommended protocols for both kits were observed for these investigations (Appendix Sections 7.8 and 7.9).

CHAPTER THREE

Thrombocytosis and Platelet Related Gene Expression in Ovarian Cancer

A Retrospective Study in an Irish Population.

3 Thrombocytosis and Platelet Related Gene Expression in Ovarian Cancer

3.1 Background

Between 20-50% of patients presenting with ovarian cancer are found to have (reactive/secondary) thrombocytosis – a blood platelet concentration of 400 x 10^9/L or greater (Soonthornthum et al., 2007, Zeimet et al., 1994).

Thrombocytosis has been observed in a variety of cancers including lung, breast, gastric, colon, renal, pancreatic and gynaecologic cancers including ovarian, cervical, endometrial and vulval cancers (Tamussino et al., 2001, Aoe et al., 2004, Ikeda et al., 2002, Erdemir et al., 2007, Lavie et al., 1999, Gungor et al., Kandemir et al., 2005, Rodriguez et al., 1994). This 'malignancy-associated' elevated platelet count is associated with poor prognosis in many cancers.

This thrombocytosis is hypothesised to be associated with the phenomenon of tumour cell induced platelet aggregation (TCIPA). This is a process by which tumour cells may co-opt blood platelets forming a 'platelet cloak', (a covering of aggregated platelets) and augmenting cancer cell metastatic potential by enabling them to evade the immune system, abrogating the effects of chemotherapeutic agents and allowing cancer cells to travel within the vasculature until a downstream metastatic site is reached.

Thus the platelet cloak may play a crucial role in tumour cell embolisation in the vasculature and contribute significantly to metastatic load in a given tumour system. The platelet cloak may allow extravasation of tumour cells through the endothelium and establishment of a secondary tumour, though this may be further modified by the balance of positive and negative growth factors in the local environment in which they find themselves (Philippe et al., 1993, Nieswandt et al., 1999).

Platelets and the platelet cloak phenomenon can also release growth factors and cytokines, e.g. VEGF and PDGF, and encourage tumour growth and vascularity at the site of metastasis. Cancer cells may not only utilise platelets once in the process of

haematogenous dissemination and metastasis, but prior to extravasation may also co-opt normal cells in the surrounding stroma such as pericytes, fibroblasts and some immune cells to aid in driving angiogenesis, proliferation and invasion through produced mitogens and growth factors.

This study investigates a panel of target genes; PDGFA, PDGFB, PDGFRA, PDGFRB, VEGF, CA125, and THPO which may contribute to malignant progression and spread of ovarian cancer. These genes were selected on the basis of their potential involvement in platelet-cancer cell signalling (PDGFA/B, PDGFRA/B), involvement in other hormone sensitive cancers such as prostate, breast and thyroid cancers (PDGFA/B, PDGFRA/B, VEGF), possible impact on platelet production (THPO) and role as prognostic markers of ovarian cancer outcome (CA125, VEGF) (Singh et al., 2002, Wang et al., 2008, Roussidis et al., 2007).

3.1.1 Platelet Derived Growth Factor (PDGF) and Platelet Derived Growth Factor Receptors (PDGFR)

PDGF was the first component of platelet releasate identified (Ross and Glomset, 1973) and was observed to be a potent mitogen at mesenchymal cells (Ross et al., 1974, Kohler and Lipton, 1974). Leading on from these initial descriptions of PDGF and its activity it was subsequently described as a component of platelet α-granules released during platelet activation during clot formation (Kaplan et al., 1979a, Kaplan et al., 1979b).

The PDGF family is represented by four ligands (PDGFA-D) (Fredriksson et al., 2004). PDGFA and PDGFB were the first PDGF proteins identified and characterised. They dimerise to form AA or BB homodimers or a AB heterodimer functional PDGF molecule. In platelet releasate the primary PDGF isoform present is the PDGFAB heterodimer accounting for ~70% of the PDGF protein present, the remaining being largely PDGFBB homodimer protein (Ross, 1989).

PDGFC and PDGFD are more recently described than PDGFA and PDGFB and differ significantly in their activation and roles. Both are exclusively produced as inactive homodimers requiring proteolytic activation (Li et al., 2000, Bergsten et al., 2001, Reigstad et al., 2005, Li and Eriksson, 2003), with identified roles varying from palatogenesis (Ding et al., 2004), renal development (Eitner et al., 2003, Changsirikulchai et al., 2002) along with recent suggestions of potential contributory roles in cancer development through pro-angiogenic signalling (Hou et al., 2010, Cao et al., 2002), fibroblast and macrophage recruitment (Uutela et al., 2004, Anderberg et al., 2009) an addition to potential utilisation of a wide range of other pro-oncogenic pathways (Wang et al., 2010b).

PDGF ligands signal through two homo- or hetero-dimeric receptor tyrosine kinases (RTK) PDGF receptors, PDGFRα and PDGFRβ. These are encoded for by two separate genes, PDGFRA and PDGFRB (Matsui et al., 1989, Heldin et al., 1992). Activation of the receptors results in initiation of intracellular signalling pathways, primarily MAPK and PI3K. These

signalling pathways drive functions including cell growth, proliferation, migration and differentiation (Williams, 1989, Claesson-Welsh, 1996).

All PDGF ligands mediate their signalling through the three potential receptor complexes with varying ability and affinity (Hoch and Soriano, 2003).

- PDGFRαα: transduces PDGFAA, PDGFAB, PDGFBB and PDGFCC signalling.
- PDGFRαβ: transduces PDGFAB, PDGFBB, PDGFCC and PDGFDD signalling.
- PDGFRββ: transduces PDGFBB and PDGFDD signalling only.

PDGFAA binds only to PDGFRαα and PDGFAB having a PDGFB monomer in its construction. It is able to signal through both PDGFRαα and PDGFRαβ while PDGFBB is the only PDGF that can bind all three receptor combinations with high affinity. PDGFCC is observed to specifically interact with PDGFRαα and -αβ, but not with -ββ, and such resembles PDGF-AB in its receptor binding ability. PDGF-DD binds to PDGFR-ββ with high affinity and to PDGFRαβ to a lesser degree (illustrated in Figure 3-1) (Shim et al., 2010).

Figure 3-1

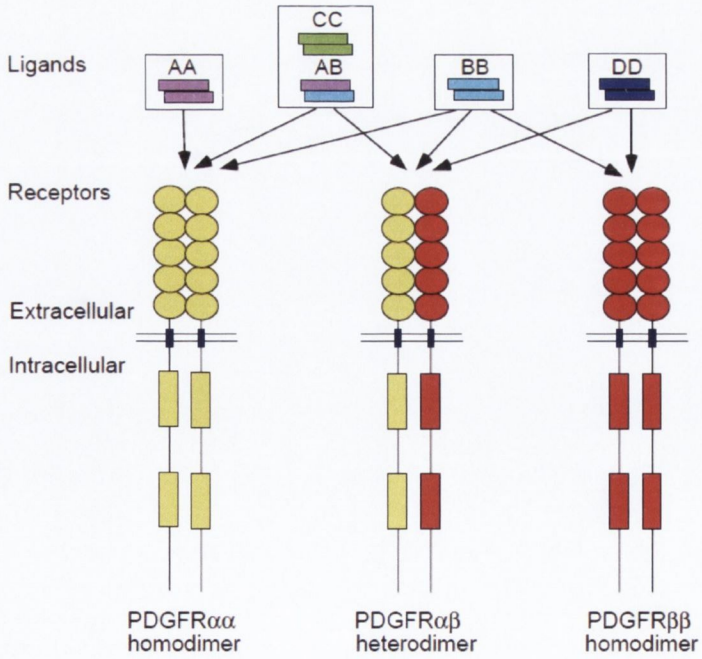

Figure 3-1: PDGF Signalling mediated by PDGF Receptors.

Image from Hoch and Soriano (2003).

Over-expression of PDGFA/B and their receptors has previously been observed in 73% of ovarian cancers, where approximately 50% will have co expressed PDGFRα, which may have up to a six fold increase in expression compared to normal ovarian tissues (Henriksen et al., 1993, Matei et al., 2003, Schilder et al., 2008). This is associated with reduced survival in patients. PDGF signalling may be autocrine and/or paracrine and has been shown to be a key modulator in tumour angiogenesis. It recruits perivascular progenitor cells (PC) to the site of new vessel generation and is a potent mitogen of ovarian epithelial cells (Pietras et al., 2008, Kuhnert et al., 2008, Dabrow et al., 1998, George, 2003).

The PDGF/PDGFR signalling system is a promising target for therapeutic intervention (Raica and Cimpean, 2010, Östman and Heldin, 2007, Board and Jayson, 2005, Burger, 2011, Duhoux and Machiels, 2010), though PDGFR specific targeting for ovarian cancer may not be as preferable as dual/multi targeting along with VEGF, fibroblast growth factor (FGF) based on recent PDGFRB inhibition studies which showed increased ascites or fluid retention in patients, which are themselves symptoms of ovarian cancer (Jayson et al., 2005). Similarly despite promising *in vitro* and animal studies, PDGFRB specific inhibition utilising tandutinib was associated with accelerated progression in prostate cancer in a recent trial (Mathew et al., 2011), suggesting that the utilisation of PDGFR specific inhibitors require further investigation before they can be selected for use in cancer treatment despite promising pre-clinical studies.

Imatinib mesylate (Gleevec) has also been investigated for inhibition of PDGF signalling in cancer treatment. Imatinib is a small inhibitory molecule with inhibition effects at both PDGFRA and PDGFRB in addition to primary targets BCR-ABL and c-KIT. Recent *in vitro* studies have suggested a potential role for incorporation of imatinib treatment in conjunction with conventional chemotherapy in several cancers, including ovarian cancer following favourable results in cell line based investigations. Arising from the interaction between PDGF and VEGF pathways, PDGFR inhibition utilising imatinib mesylate has been considered as a target for inhibiting VEGF mediated angiogenic signalling in head and neck squamous cell carcinoma (HNSCC) (Bran et al., 2009). This study revealed promising results with reduced PDGF and VEGF production in treated cells and reduced VEGF expression following imatinib treatment. Similar results have been reported in ovarian

cancer by Mundehenke and colleagues (2008) who report synergistic effects of imatinib when combined with carboplatin and cisplatin treatment of ovarian cancer leading to reduced tumour size and pro-apoptotic changes, though realizing that further clinical investigation is required before being widely utilised as a treatment. Highlighting the variability in imatinib efficacy in different tumour types, even those of a different histology but arising in the same organ, a study investigating the efficacy of imatinib on ovarian granulosa tumours determined that these molecules were ineffective in treating this form of ovarian cancer (Chu et al., 2008).

One of the latest drugs to be tested allowing multiple RTK inhibition is Vargatef (intedanib, BIBF 1120), a VEGFR, PDGFR and epidermal growth factor receptor (EGFR) blocking molecule. This has been examined in cell line and animal xenograft models and has shown anti-proliferative and anti-angiogenic efficacy (Hilberg et al., 2008, Santos et al., 2011). Investigation has been focussed on potential use in a range of solid cancers including non-small-cell lung cancer (NSCLC) (Reck, 2010, Ellis et al., 2010), multiple myeloma (Kropff et al., 2009), hepatocellular, renal cell, and colorectal cancer (Mross et al., 2010), gynaeocological malignancies (epithelial ovarian cancer, endometrial carcinoma, mixed mesenchymal tumor or cervical carcinoma) (du Bois et al., 2010) and has recently entered AGO-OVAR 12/LUME-Ovar 1 phase 3 clinical trials for the treatment of ovarian cancer (Antoniu and Kolb, 2010, Boehringer-Ingelheim, 2009).

3.1.2 Vascular Endothelial Growth Factor (VEGF)

VEGF was first characterised twenty-two years ago where it was described as 'a novel heparin binding growth factor specific for vascular endothelial cells' since which it has been described extensively for its role in stimulating the proliferation and migration of endothelial cells and inducing angiogenesis as a result in both normal and tumour tissues (Ferrara and Henzel, 1989, Ferrara and Gerber, 2001).

VEGF is represented by a family of five ligands, VEGF-A, -B, -C, -D and –E, which mediate their signalling through three tyrosine kinase receptors, VEGFR1, VEGFR2 and VEGFR3. VEGF-A is the best characterised of the ligands and is the dominant VEGF isoform responsible for angiogenesis, achieved by signalling through VEGFR1 and VEGFR2. While having a lower affinity for VEGFA than VEGFR1, VEGFR2 is the dominant transducer of angiogenic signalling within cells in this interaction (Ferrara and Kerbel, 2005, Lohela et al., 2009). VEGF-C/VEGFR3 signalling has also been described to play a role in some cancers though it's signalling effects play a more significant role in lymphaniogenesis rather than angiogenesis (Su et al., 2007, Achen et al., 2006, Tanaka et al., 2010, Shibuya and Claesson-Welsh, 2006)

As a result of the major role played by VEGF in driving the development of blood vessels in tissues, and specifically in cancerous tissue where formation of a growth sustaining tumour blood supply has long been considered critical for malignant tumour growth beyond a size of 200μm (Folkman, 1971, Folkman et al., 1989), VEGF has been a target for anti-angiogenic therapy. Arising from the focus on VEGF for therapeutic intervention bevacizumab (Avastin) developed and directed at VEGF-A, was the first monoclonal antibody directed for use as an anti-angiogenic medicine to be introduced for use in clinical treatment of some solid cancers following US FDA approval in 2004 (Shih and Lindley, 2006, Zondor and Medina, 2004, Eskander and Randall, 2011). VEGF remains a major target of anti-vascular therapy for cancer and along with PDGF (and other signalling molecules) is an ongoing target for antiangiogenic therapies for the treatment of ovarian cancer (Burger, 2011, Kumaran et al., 2009).

As with many cancers, VEGF is a primary driver of angiogenesis in ovarian cancer. Increased VEGFA expression has been documented in ovarian cancers versus benign or normal tissues and angiogenesis in ovarian cancer promotes tumour growth, ascites formation, increased metastasis (Brown et al., 2000, Ramakrishnan et al., 2005). VEGF over-expression has also been shown to be associated with increased microvessel density, malignant progression and reduced survival in ovarian cancer (Dinh et al., 2008, O'Toole et al., 2007, Jubb et al., 2006).

In addition to the angiogenic influence VEGF has it may also contribute to the increased invasive capacity of ovarian cancer cells as a result of MMP2 gelatinase induction (Zhang et al., 2006). Matrix metalloproteinases (MMPs) have been implicated in the progression of many cancers, including ovarian cancer, and have been described as potentially useful in cancer diagnostics for a range of cancers arising from frequent correlation with advanced disease and metastasis (Deryugina and Quigley, 2006).

The over-expression of VEGF in cancers has recently been associated with PDGF autocrine signalling though PDGFRA, which has been shown to be involved in increasing VEGF expression, possibly via Akt/PI3K pathway activation, with both acting to promote tumour angiogenesis (Board and Jayson, 2005, Matei et al., 2007, Matei et al., 2006). Recent evidence has also implicated VEGF signalling in mediating the reduced proliferation and impaired cytotoxicity of T cells extracted from both individuals with ovarian cancer and healthy persons (Ziogas et al., 2011). It is possible this may contribute to the tumour evasion of immune mediated destruction.

3.1.3 CA125

CA125 (Cancer Antigen 125/Mucin 16/MUC16) has been described extensively as a cancer biomarker with specific potential for use in the detection/determination of ovarian cancer. Finding better means to allow early detection of ovarian cancer has been a long term goal for researchers. The cure rate in ovarian cancer detected at an early stage can be as high as 90% to 95% (Hoskins, 1995, McLemore and Aouizerat, 2005). It is more common that the disease is detected later and so many patients face poor prognosis.

CA125 has been shown to be elevated in many cancers including endometrial, breast, lung, liver, stomach and bladder cancers but despite the involvement of this protein in cancer the significance of its role outside of biomarker has up to relatively recently been little understood.

Recently the pathophysiological role through which CA125 may contribute to ovarian cancer biology has been further elucidated, extending its importance from potential biomarker to potential target for future therapeutics. Recently CA125 production by epithelial ovarian cancer cells was described to alter the activity of peritoneal natural killer cells. NK cells mediate the destruction of cells directly by NK cytolysis and via antibody dependent cellular cytotoxicity via CD16 (Fc receptor). CA125 has been shown to reduce NK CD16 expression in vitro (Patankar et al., 2005) and expression in vivo, preferentially binding to $CD16^{+}$, $CD56^{dim}$ NK cells (Belisle et al., 2007).

Recently (2010) Siglec-9 has been identified as a receptor for CA125 on a variety of immune cells including NK cells, B Cells and monocytes possibly binding to which it is hypothesised may result in:

> *"inhibitory priming of the immune cells leading to compromised anti-tumour immunity"* (Belisle et al., 2010)

, and has been observed to reduce the number of immune activating synapses between ovarian cancer cells and NK cells (Gubbels et al., 2010).

Additionally, recent evidence suggests that CA125 expression conveys a pro-survival advantage in ovarian cancer cells. Knock down of the molecule results in impaired colony formation *in vitro* and reduced subcutaneous tumour formation *in vivo*. Cells expressing a truncated CA125 construct lacking the proteins cytoplasmic tail were observed to have impaired motility/invasiveness and tumourigenicity, recoverable in vitro when ectopically expressed (Theriault et al., 2011).

Investigating CA125 in cancer may be ideally performed through molecular biology techniques such as real-time or quantitiative PCR as examining the molecule as a protein is still affected by uncertainty of its size and structure depending on from where it was extracted and the method of investigation (Bouanene and Miled, 2010).

3.1.4 Thrombopoietin (TPO)

Thrombopoietin (TPO, mpl ligand) is the key signalling molecule produced normally in the liver and kidneys responsible for regulating the differentiation of megakaryocytes and production of platelets. In the normal regulation of thrombopoiesis TPO is primarily produced by parenchymal and sinusoidal endothelial cells in the liver and by proximal convoluted tubule cells in the kidneys (Kato et al., 1998). TPO production by these cells is controlled by a negative feedback system tied to the level of platelet production. Having driven the production of platelets to result in a normal blood platelet concentration, serum TPO is bound to the surface of platelets at the mpl receptor where it is destroyed. This reduces the amount of serum TPO that megakaryocytes may be exposed to and results in reduced platelet production. The thrombopoietin gene, THPO, provides an attractive target that may be produced by ovarian cancer cells resulting in the thrombocyctosis frequently diagnosed with the disease (Fishley and Alexander, 2004, Wendling, 1999, Kaushansky, 2003). This possibility is made more attractive given the findings of Furuhashi and colleagues (1999), who reported a TPO producing serous cystadenocarcinoma of the right ovary with peritoneal spread and throbocytosis.

More recently an investigation Tsurkishiro and colleagues (2008) examined the levels of TPO and CA125 in malignant (N=51) and benign ovarian disease (N=25). By examining serum concentrations of these variables by immuno-assay, an initial association between

TPO and CA125 production and increasing malignancy has been observed. No correlation between serum TPO and platelet count was observed, however, in this study.

It is noted that in some cancers the TPO receptor, mpl, has a contributing role in disease following the description of the c-mpl proto-oncogene in patients with AML and other myleoproliferative disorders (Li et al., 1996, Vigon et al., 1993, Wetzler et al., 1997, Schröder et al., 2000, Chelvatheebam et al., 2003).

3.1.5 Aim

The aim of this study is to examine through a retrospective study utilising clinically prepared formalin fixed paraffin embedded tissue (FFPE) samples if a relationship exists between platelets (indicated by preoperative platelet count) and a panel of target genes identified as being platelet related, as significant modulators of cancer development and/or potential biomarkers ovarian cancer in an Irish ovarian study cohort and to examine the influence of platelets on patient survival and to investigate for associations/correlation between platelet related gene expression and patient preoperative platelet count.

3.2 Materials and Methods

3.2.1 Tissue Sample Selection

Ethical approval for the study of formalin fixed, paraffin embedded (FFPE) materials was granted by the Dublin Federated Voluntary Hospitals research ethics board.

A cohort 100 FFPE ovary samples were randomly selected from the archives of St. James's Hospital (Dublin, Ireland). This total sample cohort (TSC) of archival ovarian FFPE tissues dated from 1990 to 2006 and was histologically assessed for FIGO stage by board registered histopathologist (Dr Richard Flavin, MD, PhD, FRCPath).

Further review of patient data subsequent to histological classification resulted in the elimination of any 'normal' cases or those with non-ovarian cancers; principally cervical cancer and PPC, but also included endometriosis.

This resulted in a final core sample cohort (CSC) of 91 samples: normal ovary (10), grade 2 (32), grade 2/3 (6) and grade 3 (43) ovarian cancers which were processed and subjected to RT-PCR assay.

Prior to in depth analysis quality control was performed on RT-PCR data to remove samples that failed to amplify due to sample RNA degradation from analysis. This resulted in the final analysis cohort (AC) that was subjected to final clinic-pathological and relative quantitation analysis. This process of cohort selection is illustrated in Figure 3-2.

The reference threshold value for thrombocytosis used at the site from which samples were sourced (St. James's Hospital, Dublin) is $400x10^9$ platelets per litre and this value was accepted as the threshold value for throbocytosis in this study.

Figure 3-2

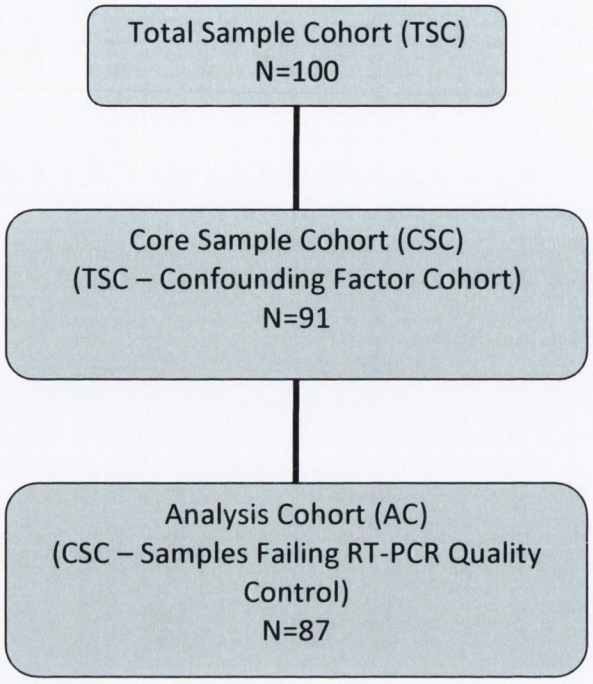

Figure 3-2: Flow chart describing progression from initial Total Sample Cohort to final Analysis Cohort.

3.2.2 FFPE Sample Preparation

A FFPE block representing ovarian tissue from each of the study cohort was retrieved from tissue archives. Five 10µm sections were prepared from each tissue block by cutting with a microtome as described in chapter 2, section 2.1.2.

3.2.3 Nucleic Acid Extraction

As described in appendix section 7.1, total RNA was extracted following manufacturer's protocols using Ambion RecoverAll kits (Ambion, Austin, TX, USA). This method of RNA extraction was selected based on previous in house research (Li et al., 2008b) which indicated RecoverAll technology was effective at recovering RNA suitable for downstream qPCR analysis FFPE samples in conjunction with target pre-amplification.

RNA quantity was assessed using a Nano-Drop® ND-1000 Spectrophotometer (Wilmington, USA). RNA was then reverse transcribed to single stranded cDNA using a

High Capacity cDNA Archive Kit (Applied Biosystems, Foster City CA, USA). cDNA samples were then PreAmplified for a panel of target genes (PDGFA, PDGFRA, PDGFB, PDGFRB, VEGFA, CA125, THPO) and endogenous controls, CDKN1B and HGPRT.

Following preamplification TaqMan® real-time PCR was performed using TaqMan® Gene Expression Master Mix and inventoried TaqMan® assays as per the plate layout in Table 3-1. and real-time PCR performed using Applied Biosystems' 7900 Real-Time PCR system.

Each assay was performed in triplicate for each sample with additional experimental controls:

- no template control performed for each individual assay.

- no reverse transcription (RT) controls performed in triplicate for both candidate endogenous control genes.

Table 3-1

Column / Row	A	B	C	D	E	F	G	H
1	PDFGA	PDFGA	PDFGA	THPO	THPO	THPO	PDGFRB	PDGFRB
2	VEGFA	VEGFA	VEGFA	PDGFRA	PDGFRA	PDGFRA	PDGFRB	HGPRT
3	PDFGB	PDFGB	PDFGB	CA125	CA125	CA125	HGPRT	HGPRT
4	THPO	THPO	THPO	PDGFRB	PDGFRB	PDGFRB	CDKN1B	CDKN1B
5	PDGFRA	PDGFRA	PDGFRA	HGPRT	HGPRT	HGPRT	CDKN1B	PDFGA
6	CA125	CA125	CA125	CDKN1B	CDKN1B	CDKN1B	VEGFA	PDGFB
7	PDGFRB	PDGFRB	PDGFRB	PDFGA	PDFGA	PDFGA	THPO	PDGFRA
8	HGPRT	HGPRT	HGPRT	VEGFA	VEGFA	VEGFA	CA125	PDGFRB
9	CDKN1B	CDKN1B	CDKN1B	PDFGB	PDFGB	PDFGB	HGPRT	CDKN1B
10	PDFGA	PDFGA	PDFGA	THPO	THPO	THPO	CDKN1B	HGPRT
11	VEGFA	VEGFA	VEGFA	PDGFRA	PDGFRA	PDGFRA	CDKN1B	HGPRT
12	PDFGB	PDFGB	PDFGB	CA125	CA125	CA125	CDKN1B	HGPRT

Table 3-1: Plate layout for TaqMan® RT-PCR.

The plate layout allows the simultaneous assay of three different biological samples (indicated in cells coloured orange, green and blue) for each of the target and endogenous control genes in triplicate and includes no template controls (indicated in white) and no RT controls (indicated in red).

3.2.4 TaqMan® Gene Expression Analysis

TaqMan® real-time PCR assays were selected for each of the target genes and endogenous controls from Applied Biosystems inventoried primer-probe assays.

Formalin fixation results in RNA modification by methoyl groups creating RNA-protein and RNA-nucleic acid cross links (Goldsworthy et al., 1999, Chaw et al., 1980, Rait et al., 2006). Combined with the frequent storage of FFPE materials at room temperature for extended periods of time FFPE sample RNA is frequently degraded to ≤300bp and extraction yields are poor (Lewis et al., 2001, Cronin et al., 2004, Goldsworthy et al., 1999, Dapson, 2007). In order to maximise the chance of successful RT-PCR of target genes, assays with an amplicon length of 100bp ± 20bp were selected for use arising from the potential of reduced transcript length of FFPE extracted RNA. The assays are listed in Table 3-2.

Table 3-2

Gene Assay	Amplicon Length	Assay ID
PDGFA Assay	93	Hs00234994_m1
PDGFB Assay	80	Hs00234042_m1
PDGFRA Assay	92	Hs00183486_m1
PDGFRB Assay	86	Hs00182163_m1
VEGF Assay	81	Hs00900058_m1
TPO Assay	103	Hs00171249_m1
CA125 Assay	84	Hs00226715_m1
CDKN1B	71	Hs00152377_m1
HGPRT Assay	100	Hs99999909_m1

Table 3-2: Applied Biosystems TaqMan® Assays for real-time PCR and relative quantitation of target genes in ovarian cancer.

3.2.5 Data Analysis

Statistical analyses for real-time PCR and sample data was performed using a combination of the Spotfire™ decision site for functional genomics (Spotfire AB, Göteborg, Sweden), Applied Biosystems Data Assist ver 2.0 (Applied Biosystems, USA), SPSS ver 16.0 (IBM SPSS, Chicago, IL, USA), and Microsoft® Excel (Microsoft® Corp., Redmond, WA, USA).

Spotfire™ allowed stringent analysis of real-time PCR data and quality control of information prior to further processing and relative quantitation calculation using Data Assist.

Data Assist was used to determine Relative Quantitation (RQ) of gene expression between sample cohorts, using the $2^{-(\Delta\Delta Ct)}$ method. The endogenous control used was determined by selection of the control with the greatest stability. Significance of results was determined by t-test. Results were exported to Microsoft Excel for further analysis and transfer to SPSS for statistical investigation.

SPSS was used to interrogate patient clinic-pathological data allowing;

- Generation and comparison of Kaplan-Meier survival curves to investigate correlation between survival metrics and tumour grade and thrombotic status.

- Investigation of correlation between gene expression levels and:

    - platelet count/thrombocytosis
    - patient clinicopathological metrics

3.3 Results

3.3.1 Clinico-pathological Characteristics of Sample Cohorts

The sample cohorts were analysed for significant descriptive statistics including the median and range for each of the following patient metrics;

- age
- platelet count
- progression free survival, and
- overall survival.

One way Analysis Of Variance (ANOVA) was performed in order to assess if there was significant differences in patient metrics associated with tumour grade.

Subsequently independent samples t-tests (two-tailed) were performed to determine if the difference in patient metrics between each pair of groups was significant.

3.3.1.1 Patient Age

Patient age information was investigated allowing the generation of a box-plot for patient age in each histological group. Generation of descriptive statistics for patient age resulted in the determination of median age and range data. This information is presented in Figure 3-3 and accompanying table.

Figure 3-3

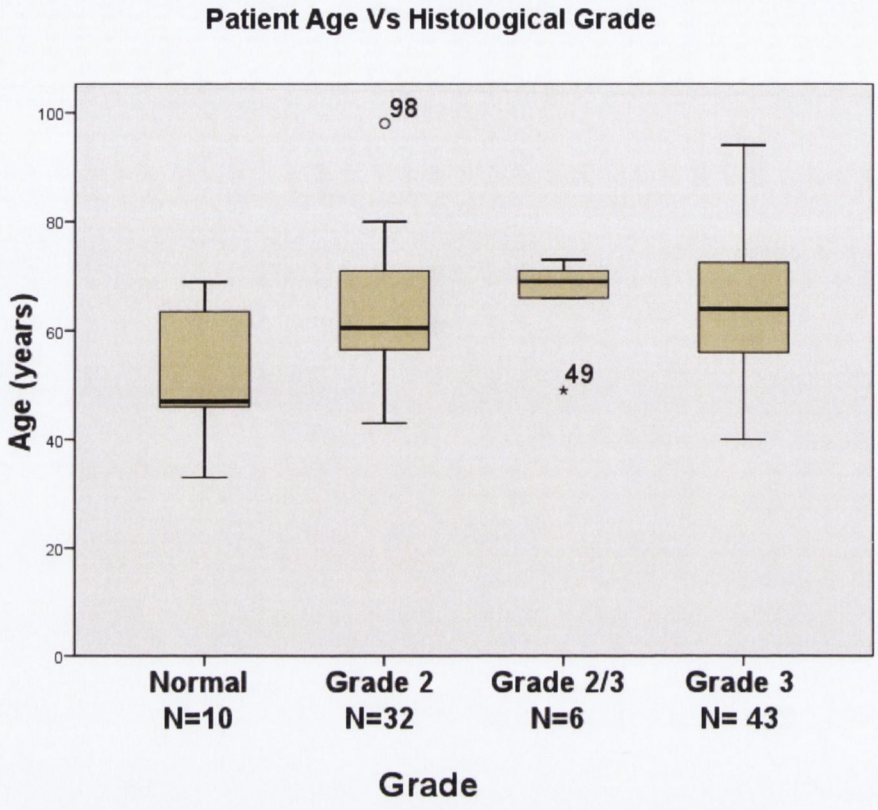

		Ovarian Cancer		
Variable	**Normal**	**Grade 2**	**Grade 2/3**	**Grade 3**
Median Age (range)	47 (33-69)	60.5 (43-98)	69 (49-73)	64 (40-94)

Figure 3-3: Patient Age Vs Histological Grade.

Patient age data was analysed using SPSS version 16.0 statistical analysis software and a boxplot graph generated. This boxplot illustrates the maximum, minimum, mean and interquartiles for patient age. Samples where outliers (values more than 1.5 inter quartile ranges (IQR's) but less than 3 IQR's from the end of the box are labelled as outliers) are indicated in the figure. All samples investigated (including outliers identified) were included in subsequent analyses.

One-way ANOVA performed to investigate patient age for variation associated with histological grade revealed no significant difference in age between groups ($p=0.133$).

T-test analysis indicates a significant difference between patient age in the normal group and ovarian cancer grades 2 and 3 groups ($p<0.05$). The difference in age between the normal and grade 2/3 borderline group approached though failed to reach significance

(p=0.053). No significant difference was determined for patient age between ovarian cancer grades 2, 2/3 borderline and 3 (Table 3-3).

Table 3-3

Grade	Normal	Grade 2	Grade 2/3	Grade 3
Normal		0.032	0.053	0.040
Grade 2	0.032		0.61	0.977
Grade 2/3	0.053	0.61		0.23
Grade 3	0.040	0.977	0.23	

Table 3-3: T-test values for differences in patient age between cohorts.

Differences in cohort age between the investigation groups was assessed by T test analysis. This analysis found significant differences in patient age between the normal ovary group and ovarian cancer groups at both grades 2 and 3. The difference between the normal group and the grade 2/3 group was not significant but approaching significance. Differences between the ovarian cancer groups were not significant.

The median age of grade 2 and grade 3 ovarian cancer patients is broadly similar to that reported in large population studies performed in the NIH SEER Programme (Kosary, 2007) and Northern Ireland Cancer Registry (Donnelly et al., 2007) which returned a median age at diagnosis of 63 years.

3.3.1.2 Preoperative Platelet Count

Preoperative platelet count information was investigated allowing the generation of a box-plot for patient age in each histological group. Generation of descriptive statistics for preoperative platelet count resulted in the determination of median figure and range data. This information is presented in Figure 3-4 and its accompanying table.

Figure 3-4

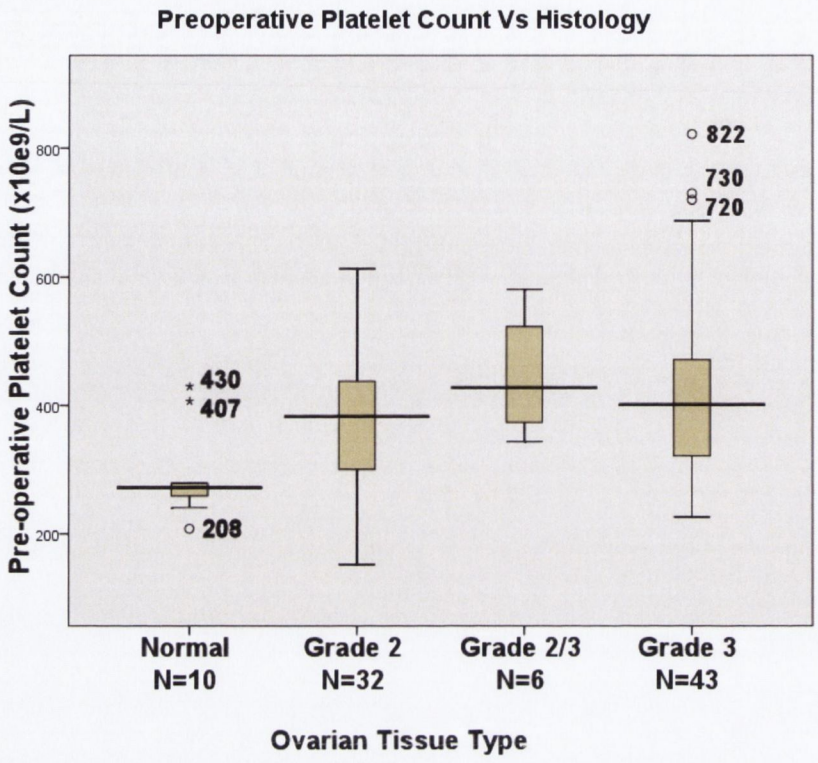

Variable	Normal	Grade 2	Grade 2/3	Grade 3
Median Platelet Count (range)	272 (208-430)	383 (152-613)	428 (344-581)	401 (226-822)

Figure 3-4: Preoperative platelet count vs Ovarian Tissue Type.

Patient preoperative platelet count was analysed using SPSS version 16.0 statistical analysis software and a boxplot graph generated. This boxplot illustrates the maximum, minimum, mean and interquartiles for preoperative platelet count. Samples where outliers (values more than 1.5 inter quartile ranges (IQR's) but less than 3 IQR's from the end of the box are labelled as outliers) are indicated in the figure. All samples investigated (including outliers identified) were included in subsequent analyses.

One-way ANOVA performed between pre-operative platelet count and histological grade indicated a significant difference between groups ($p=0.0098$). This was further expanded upon through t-test analysis (unpaired, two-tailed) between grades for differences in preoperative platelet count between cohorts. T-test analysis indicates a significant difference between preoperative platelet count in the normal group versus all other groups ($p<0.05$).

The percentage of ovarian cancer patients (cumulative, grades 2, 2/3 and 3) presenting with preoperative thrombocytosis (a platelet count greater than 400 x 10^9/L) was 48%, this is versus 20% in the normal patient cohort. Investigating each grade individually the percentage of patients revealed 40.6% of grade 2 ovarian cancers, 66% of grade 2/3 ovarian cancers and 52.5% of grade 3 ovarian cancers presenting with preoperative thrombocytosis in this study.

No significant difference in preoperative platelet count was determined between ovarian cancer grades 2, 2/3 borderline and 3. The difference between preoperative platelet count in the normal cohort was determined to be significantly different to all cancer cohorts ($p<0.05$). The p-values returned for this set of t-tests are indicated in Table 3-4.

Table 3-4

Grade	Normal	Grade 2	Grade 2/3	Grade 3
Normal		0.0296	0.0017	0.0063
Grade 2	0.0296		0.116	0.0804
Grade 2/3	0.0017	0.116		0.7313
Grade 3	0.0063	0.0804	0.7313	

Table 3-4: T-test values for differences in preoperative platelet count between cohorts.

Differences in preoperative platelet count between the investigation groups was assessed by T test analysis. This analysis found significant ($p<0.05$) differences in preoperative platelet count between the normal ovary group and ovarian cancer groups at all grades. Differences between the ovarian cancer groups were not significant ($p>0.05$). Note that previously identified outlier values were included in this analysis.

3.3.1.3 Cohort Survival

Analysis of patient data included investigation of the contribution of tumour grade to progression free survival (PFS) and overall survival (OS). Also investigated was the influence of preoperative platelet count; thrombocytotic (≥400x10^9 platelets/L) vs non-thrombocytotic on patient survival.

Prior to generation of Kaplan-Meier curves and subsequent analysis patient survival data was examined for statistical outliers (values higher or lower than 1.5 interquartile ranges

from the mean). These values were then eliminated from investigation to prevent skewing of results. Outlier investigation of PFS resulted in the elimination of one sample from the grade 2 ovarian cancer cohort (PFS ≥ 139 months) and two samples from the grade 3 ovarian cancer cohort (PFS ≥ 145) (Figure 3-5). When applied to OC, outlier investigation resulted in the elimination of one sample from the grade 2 ovarian cancer cohort (OS ≥ 139 months) and two samples from the grade 3 ovarian cancer cohort (OS ≥ 105) (Figure 3-6).

Figure 3-5

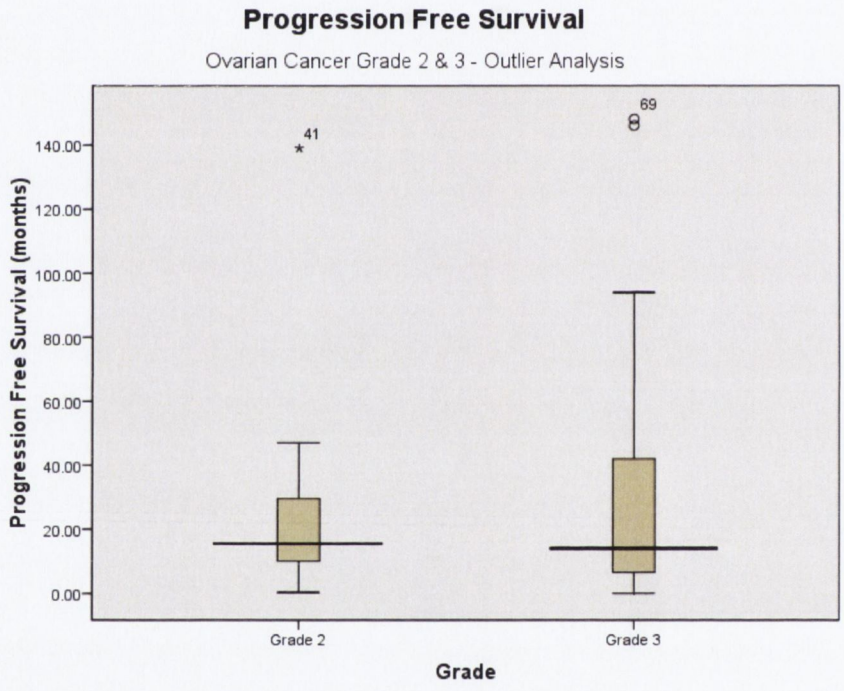

Figure 3-5: Outlier Analysis – Progression Free Survival

Figure 3-6

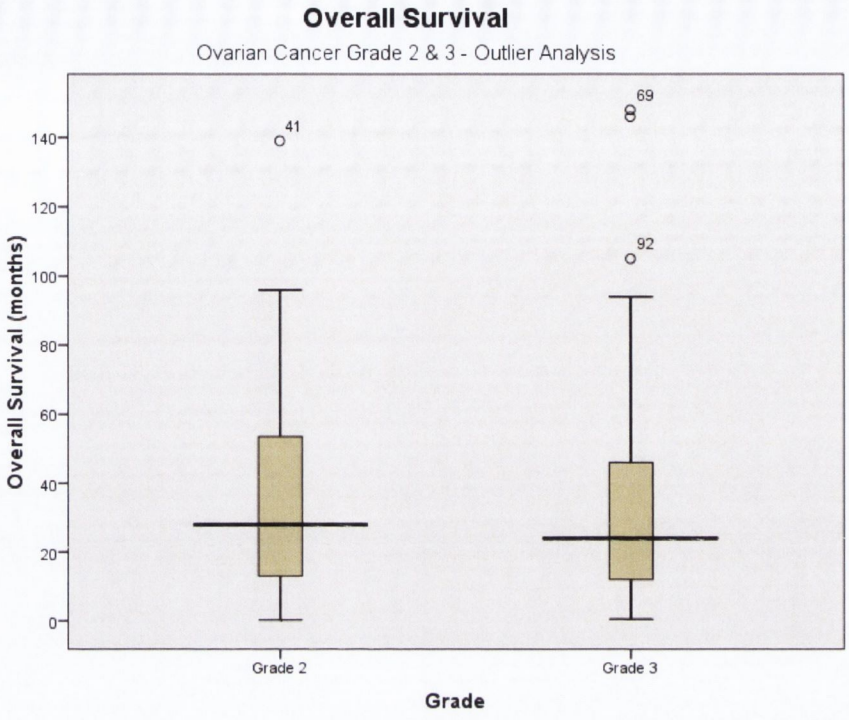

Figure 3-6: Outlier Analysis – Overall Survival.

The influence of tumour gradation on progression free and overall survival was assessed through descriptive statistic analysis, generation of Kaplan-Meier survival curves and subsequent Log Rank (Mantel-Cox) association analysis. Further investigation of patient two- and five-year survival (and the influence of preoperative thrombocytosis on these metrics) was performed by investigating the percentage of patients with an overall survival of >24 months and >60 months respectively.

Due to the smaller population size the grade 2/3 borderline cohort was not subjected to Kaplan-Meier survival curve generation.

3.3.1.4 Progression Free Survival (PFS)

The effect of tumour grade on patient progression free survival was assessed through generation of Kaplan-Meier survival curves and subsequent Log Rank (Mantel-Cox) association analysis (Figure 3-7).

Figure 3-7

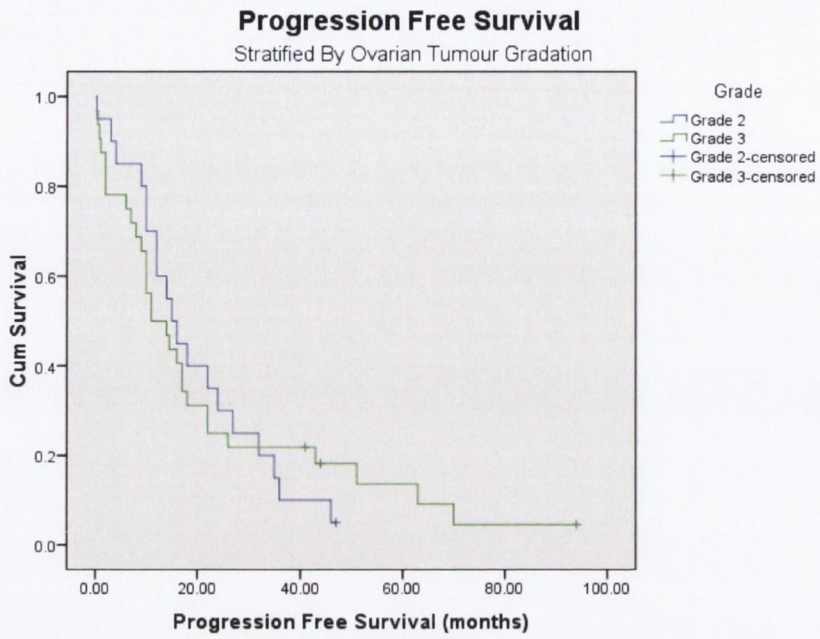

Variable	Grade 2	Grade 3
Median PFS (months) (Range)	15 (0.25-47)	11 (0-94)

Figure 3-7: Kaplan-Meier PFS Curves for ovarian cancer patients classified as either FIGO tumour grade 2 or 3.

Patient PFS data stratified by ovarian cancer tumour grade was interrogated by Kaplan-Meier survival curve and Log-Rank analysis to determine the impact of tumour grade on time to disease recurrence. The included table details PFS median and range for ovarian cancer grades 2 and 3.

Censored data refers censoring of sample data in instances where patients have not had disease recurrence, died immediately/soon after treatment in PFS analysis. It also refers to any instances in PFS analysis where values for survival data were missing or otherwise unavailable.

Statistical analysis indicates a median progression free survival of 15 months in grade 2 ovarian cancers (std. error, 2.236) compared to a median progression free survival of 11 months (std. error, 3.182) associated with grade 3 disease. Log rank analysis suggests that the tumour grade has no impact on PFS (Chi Sq. = 0.008, p=0.93).

3.3.1.5 PFS Vs Thrombocytotic Status (Stratified by Tumour Grade)

The effect of thrombocytosis on patient progression free survival in ovarian cancer was assessed through generation of Kaplan-Meier survival curves and subsequent Log Rank (Mantel-Cox) association analysis. The effect of thrombocytosis was examined separately in both grade 2 (Figure 3-8) and grade 3 (Figure 3-9) ovarian cancer allowing the median survival in the presence and absence of preoperative thrombocytosis to be determined and significance of any effect on PFS to be assessed by Log-rank analysis.

Statistical analysis indicates a median progression free survival of 12 months in grade 2 ovarian cancers (std. error = 2.887) with a normal (non-thrombocytotic) platelet count at the time of surgery. This is compared to a median progression free survival of 22 months (std. error = 7.071) associated with grade 2 disease presenting with a high preoperative platelet count.

Statistical analysis indicates a median progression free survival of 14.5 months in grade 3 ovarian cancers (std. error, 5.797) with a normal (non-thrombocytotic) platelet count at the time of surgery. This is compared to a median progression free survival of 14 months (std. error, 7.483) associated with grade 3 disease presenting with a high preoperative platelet count.

Log rank (Mantel-Cox) analysis performed to determine if significant differences in cohort survival existed based on thrombocytotic status (and adjusted for tumour grade) found that despite differences in median PFS times, thrombocytotic status has no significant impact on PFS in the ovarian cancer cohort investigated (Chi Sq. 0.78, p=0.377).

Figure 3-8

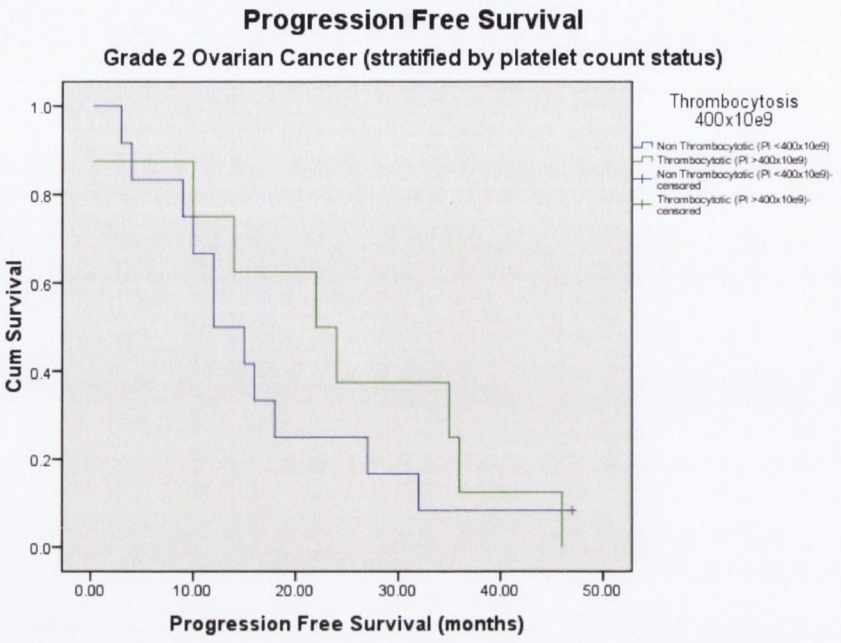

Figure 3-8: Kaplan-Meier PFS Curves for ovarian cancer patients classified as either thrombocytotic or non-thrombocytotic based on pre-operative platelet count and FIGO tumour grade 2.

Patient PFS data in grade 2 ovarian cancer was stratified by thrombocytotic status and interrogated by Kaplan-Meier survival curve and Log-Rank analysis to determine the impact of thrombocytosis on time to disease recurrence.

This statistical analysis indicated median PFS of 12 months in grade 2 ovarian cancers (std. error = 2.887) with a normal (non-thrombocytotic) platelet count and a median progression free survival of 22 months (std. error = 7.071) associated with grade 2 disease presenting with an elevated platelet count at the time of surgery.

Censored data refers censoring of sample data in instances where patients have not had disease recurrence, died immediately/soon after treatment in PFS analysis and to any instances where values for survival data were missing or otherwise unavailable.

Figure 3-9

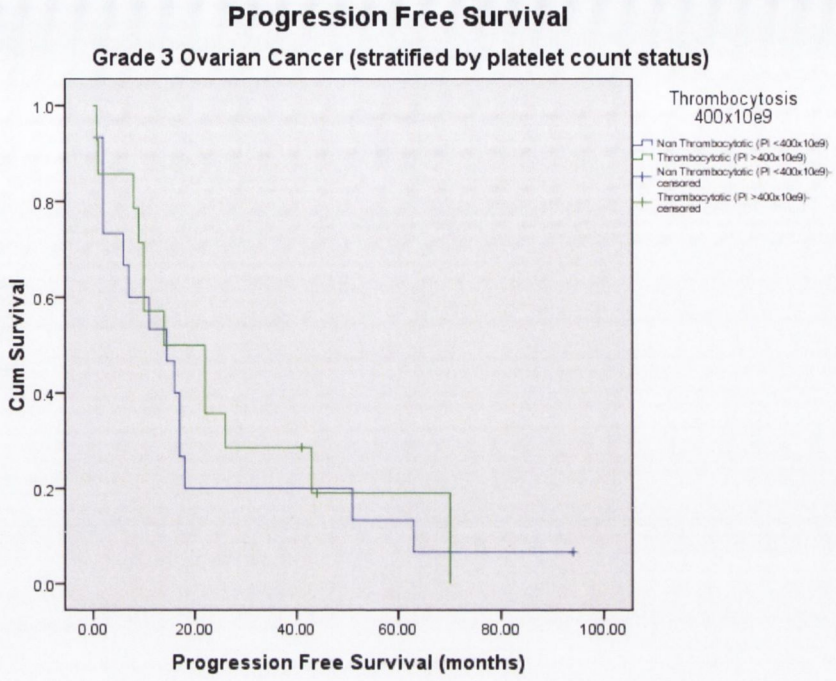

Figure 3-9: Kaplan-Meier PFS Curves for ovarian cancer patients classified as either thrombocytotic or non thrombocytotic based on pre-surgery platelet count and FIGO tumour grade 3.

Patient PFS data in grade 3 ovarian cancer was stratified by thrombocytotic status and interrogated by Kaplan-Meier survival curve and Log-Rank analysis to determine the impact of thrombocytosis on time to disease recurrence.

This statistical analysis indicated median PFS of 14.5 months in grade 3 ovarian cancers (std. error, 5.797) with a normal (non-thrombocytotic) platelet count and a median progression free survival of 14 months (std. error, 7.483) associated with grade 3 disease presenting with an elevated platelet count at the time of surgery.

Censored data refers censoring of sample data in instances where patients have not had disease recurrence, died immediately/soon after treatment in PFS analysis and to any instances where values for survival data were missing or otherwise unavailable.

3.3.1.6 Overall Survival (OS)

The influence of tumour gradation on overall survival was assessed through analysis of Kaplan-Meier survival curves and the significance of differences in OS due to

thrombocytotic status determined by subsequent Log Rank (Mantel-Cox) association analysis.

Figure 3-10

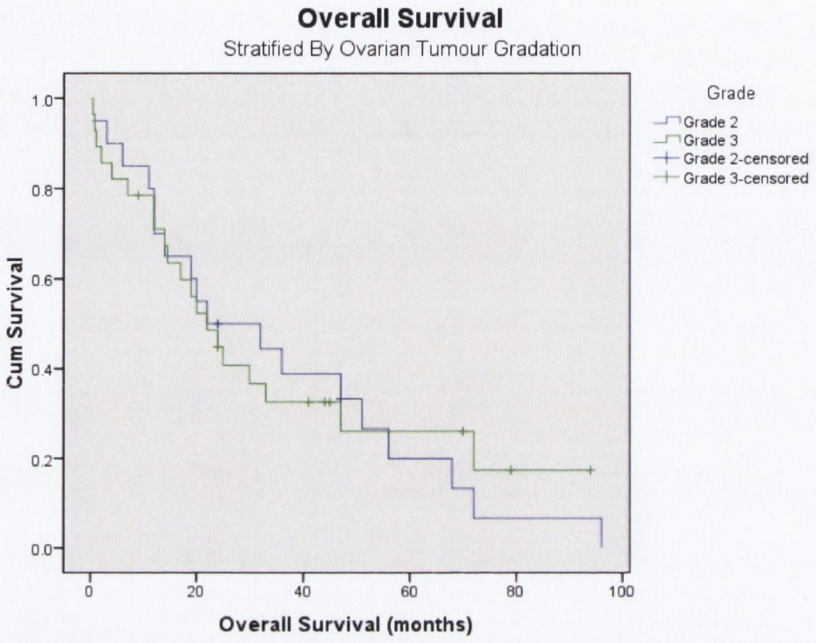

Variable	Grade 2	Grade 3
Median OS (months)	22	22
(Range)	(0-96)	(0-94)

Figure 3-10: Kaplan-Meier OS Curves for ovarian cancer patients classified as either FIGO tumour grade 2 or 3.

Patient OS data stratified by ovarian cancer tumour grade was interrogated by Kaplan-Meier survival curve and Log-Rank analysis to determine the impact of tumour grade on time to patient mortality following treatment. The included table details OS median and range for ovarian cancer grades 2 and 3.

Censored data refers censoring of sample data in instances where patients have not died in OS analysis or where values for survival data were missing or otherwise unavailable.

Statistical analysis of overall survival metrics indicates a median overall survival of 22 months in grade 2 (std. error, 12.710) and grade 3 (std. error, 4.281) ovarian cancers, and Log rank analysis determined histological classification did not influence overall survival (Log rank Chi Sq. = 0.014, p=0.905).

3.3.1.7 OS Vs Thrombocytotic Status (Stratified by Tumour Grade)

The effect of thrombocytosis on patient overall survival in ovarian cancer was assessed through generation of Kaplan-Meier survival curves and subsequent Log Rank (Mantel-Cox) association analysis. The effect of thrombocytosis was examined separately in both grade 2 (Figure 3-11) and grade 3 (Figure 3-12) ovarian cancer allowing the median survival in the presence and absence of preoperative thrombocytosis to be determined and significance of any effect on OS to be assessed by log-rank analysis.

Statistical analysis of overall survival metrics indicates a median overall survival of 20 months in grade 2 ovarian cancers (std. error, 10.235) with a normal (non-thrombocytotic) platelet count at the time of surgery. This is compared to a median overall survival of 22 months (std. error, 17.678) associated with grade 2 disease presenting with a high preoperative platelet count.

Statistical analysis of overall survival metrics indicates a median overall survival of 17 months in grade 3 ovarian cancers (std. error, 4.408) with a normal (non-thrombocytotic) platelet count at the time of surgery. This is compared to a median overall survival of 30 months (std. error, 12.796) associated with grade 3 disease presenting with a high preoperative platelet count.

Thrombocytotic status stratified by tumour grade was not associated with overall survival (Log rank Chi Sq. = 1.116, p=0.291).

Figure 3-11

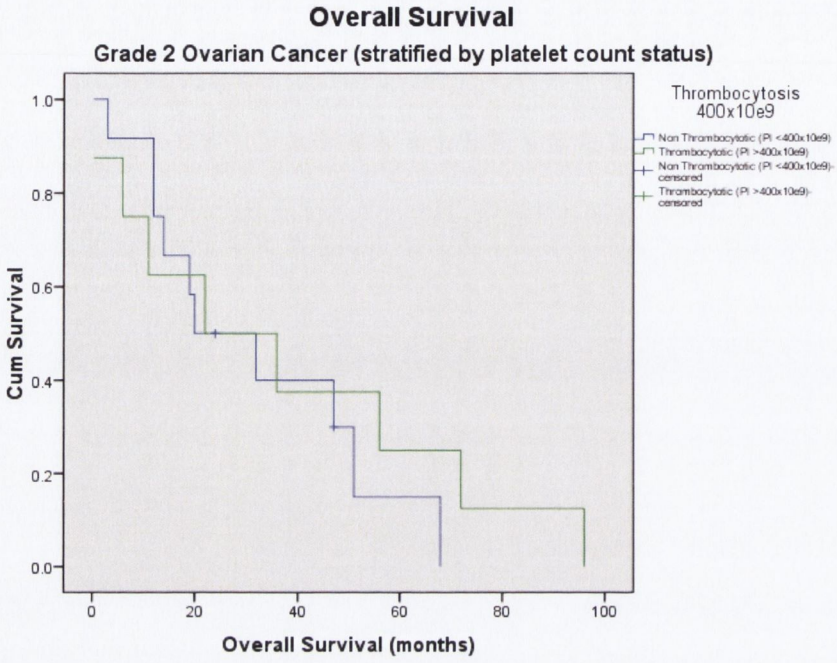

Figure 3-11: Kaplan-Meier OS Curves for ovarian cancer patients classified as either thrombocytotic or non thrombocytotic based on pre-surgery platelet count and FIGO tumour grade 2.

Patient OS data in grade 2 ovarian cancer was stratified by thrombocytotic status and interrogated by Kaplan-Meier survival curve and Log-Rank analysis to determine the impact of thrombocytosis on time to patient mortality following treatment.

This statistical analysis indicated median OS of 20 months in grade 2 ovarian cancers (std. error = 10.235) with a normal (non-thrombocytotic) platelet count and a median OS of 22 months (std. error = 17.678) associated with grade 2 disease presenting with an elevated platelet count at the time of surgery.

The two plots start at different points arising from instances of patient mortality occurring <1 month following treatment in the thrombotic group.

Censored data refers censoring of sample data in instances where patients have not died in OS analysis. It also refers to any instances in OS analysis where values for survival data were missing or otherwise unavailable.

Figure 3-12

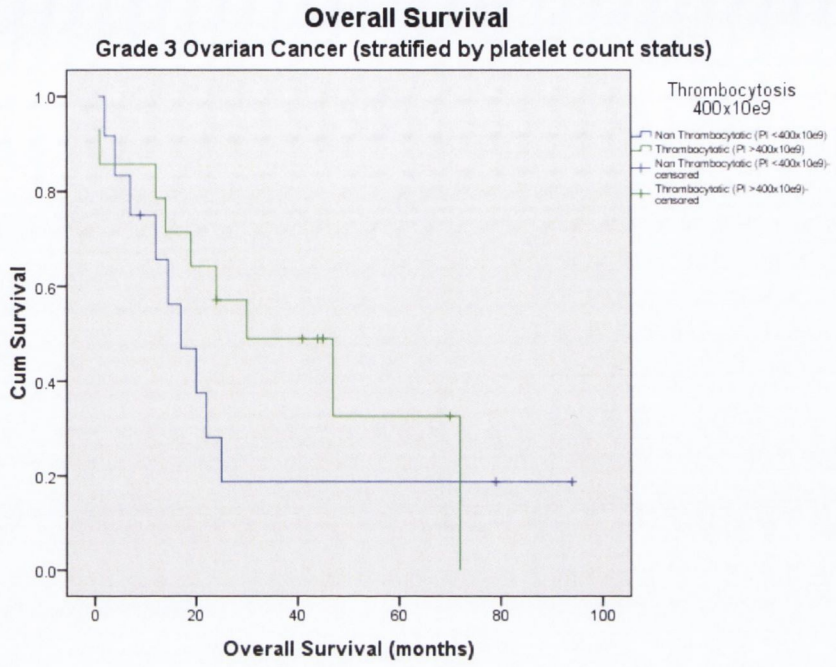

Figure 3-12: Kaplan-Meier OS Curves for ovarian cancer patients classified as either thrombocytotic or non-thrombocytotic based on pre-operative platelet count and FIGO tumour grade 3.

Patient OS data in grade 3 ovarian cancer was stratified by thrombocytotic status and interrogated by Kaplan-Meier survival curve and Log-Rank analysis to determine the impact of thrombocytosis on time to patient mortality following treatment.

This statistical analysis indicated median OS of 17 months in grade 3 ovarian cancers (std. error = 4.408) with a normal (non-thrombocytotic) platelet count and a median OS of 30 months (std. error = 12.796) associated with grade 2 disease presenting with an elevated platelet count at the time of surgery.

The two plots start at different points arising from instances of patient mortality occurring <1 month following treatment in the thrombotic group.

Censored data refers censoring of sample data in instances where patients have not died in OS analysis. It also refers to any instances in OS analysis where values for survival data were missing or otherwise unavailable.

3.3.2 Long Term Survival Analysis

Two- and five-year survival rates were calculated for FIGO grade 2 and grade 3 ovarian cancers. Normal samples were removed from analysis as they were not part of the disease cohort and the grade2/3 borderline group was excused from investigation due to small population size making comparison to the larger grade 2 and 3 cohorts difficult.

3.3.2.1 2 Year Survival Rate

Ovarian cancer was investigated for two year survival rates in grade two and grade three disease. This initial observation determined that both grades had similar two year survival rate of 52.38% and 51.61% respectively (Figure 3-13).

Figure 3-13

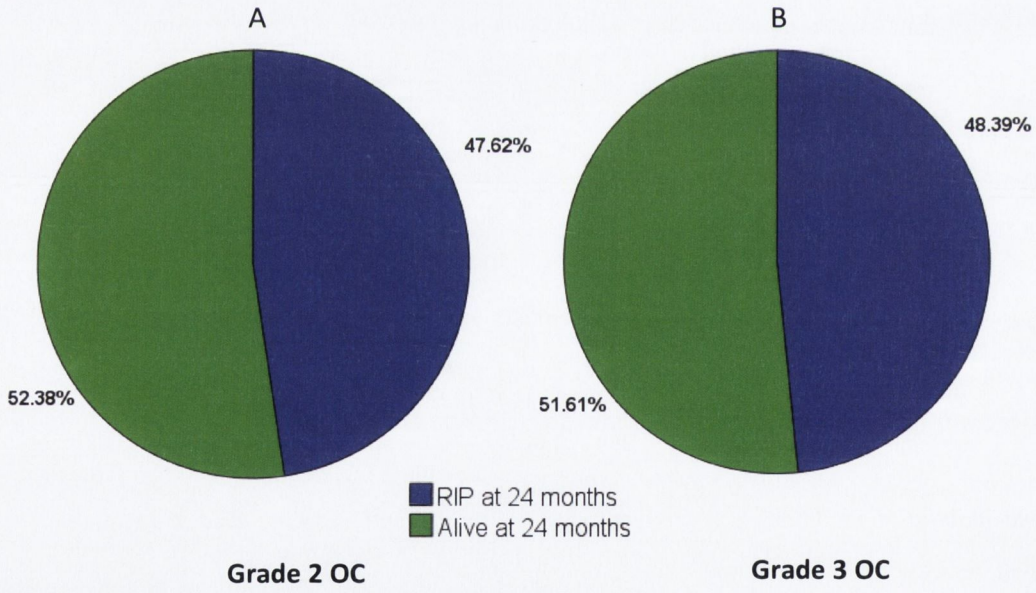

Figure 3-13: Two year survival rate in ovarian cancer stratified by FIGO disease grade.

Figure 3-13 A indicates the percentage survival/mortality in FIGO grade 2 ovarian cancer at T=24 months. Figure 3-13 B indicates the percentage survival/mortality in FIGO grade 3 ovarian cancer at T=24 months.

T-test analysis indicated the two year survival rate between the groups was not significant (p=0.958).

Patient survival data was then further assessed for the influence of preoperative thrombocytosis on survival at twenty four months for both grade 2 and grade 3 ovarian disease. When stratified to allow investigation of thrombocytotic status on survival rate individuals with preoperative thrombocytosis were observed to have a two year survival rate of 50% whereas those without preoperative thrombocytosis returned a survival rate of 53.85% (Figure 3-14).

Grade 2 Ovarian Cancer

Figure 3-14

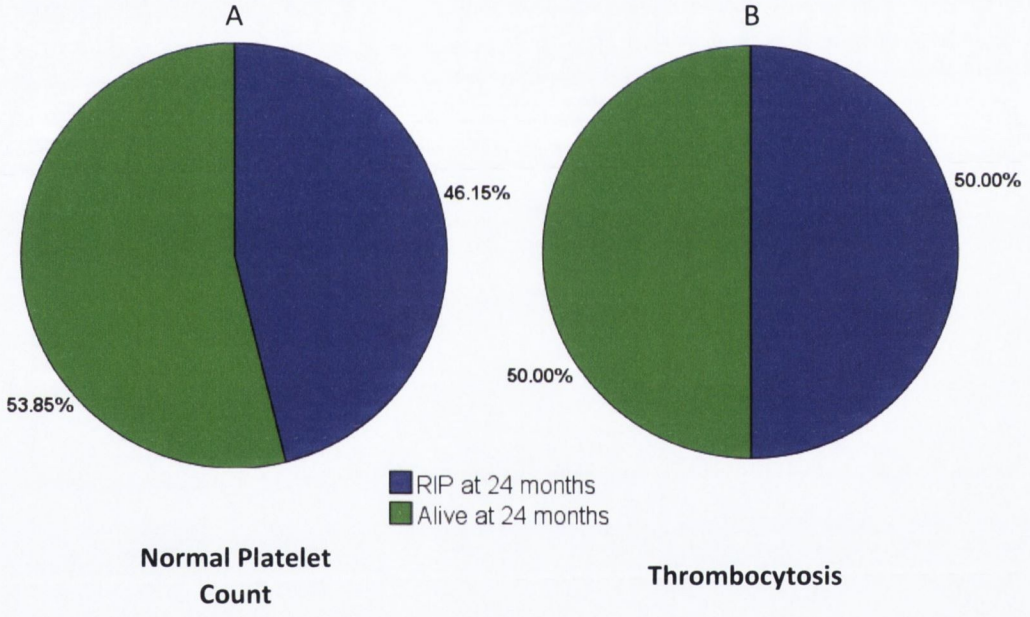

Figure 3-14: Two year survival rate in grade 2 ovarian cancer stratified by thrombocytotic status.

Figure 3-14 A indicates the percentage survival/mortality in FIGO grade 2 ovarian cancer at T=24 months in the absence of an elevated preoperative platelet count. Figure 3-14 B indicates the percentage survival/mortality in FIGO grade 2 ovarian cancer at T=24 months in the presence of an elevated preoperative platelet count.

T-test analysis for independent samples was performed in order to determine the significance of observed differences in survival between the two groups. This revealed that though thrombocytosis was associated with a 3.85% reduction in survival at two years the difference between high and low platelet count groups was not statistically significantly different (p=0.872).

Grade 3 Ovarian Cancer

Grade three ovarian cancers were observed to have a two year survival rate of 51.61% (Figure 3-13). When stratified to allow investigation of thrombocytotic status individuals with preoperative thrombocytosis were observed to have a two year survival rate of 68.75% whereas those without preoperative thrombocytosis returned a survival rate of 30.77% (Figure 3-15).

Figure 3-15

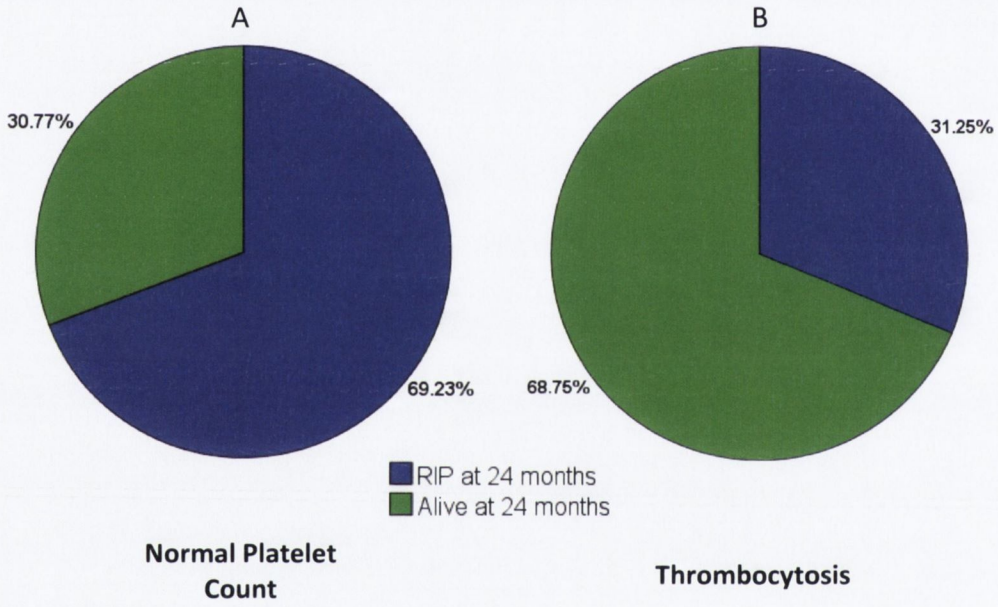

Figure 3-15: Two year survival rate in grade 3 ovarian cancer stratified by thrombocytotic status.

Figure 3-15 A indicates the percentage survival/mortality of in FIGO grade 3 ovarian cancer in the absence of an elevated preoperative platelet count (30.77%). Figure 3-15 B indicates the percentage survival/mortality in FIGO grade 3 ovarian cancers in the presence of an elevated preoperative platelet count (68.75%).

As with grade 2 ovarian cancer t-test analysis for independent samples was performed in order to determine the significance of observed differences in survival between the two groups test groups. This revealed that the difference in two year survival between high and low platelet count groups was statistically significantly different (p=0.043).

3.3.2.2 5 year Survival Rate

Ovarian cancer was investigated for two year survival rates in grade two and grade three ovarian disease. This initial observation determined that both grades had similar two year survival rate of 19.05% and 22.58% respectively (Figure 3-16).

Figure 3-16

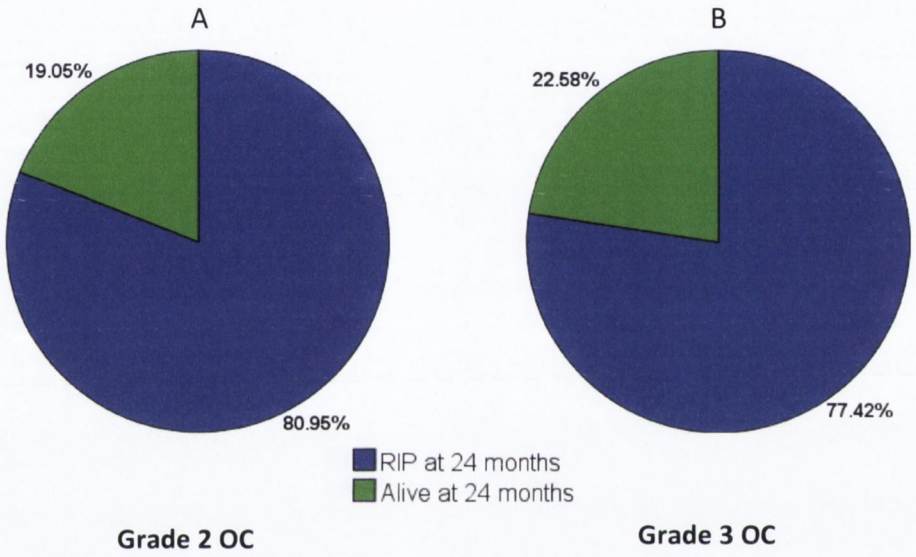

Figure 3-16: Five year survival rate in ovarian cancer grade 2 and 3.

Figure 3-16 A indicates the percentage survival/mortality in FIGO grade 2 ovarian cancer in the absence of an elevated preoperative platelet count. Figure 3-16 B indicates the percentage survival/mortality in FIGO grade 2 ovarian cancers in the presence of an elevated preoperative platelet count.

Grade two ovarian cancers were observed to have a five year survival rate of 19.05% whereas grade three ovarian cancers were observed to have a 22.58% survival rate (Figure 3-16). T-test analysis for independent samples was performed in order to determine the significance of observed differences in survival between the two groups revealed that no statistically significantly difference (p=0.765).

Grade 2 Ovarian Cancer

When stratified to allow investigation of thrombocytotic status grade 2 ovarian cancers with preoperative thrombocytosis were observed to have a two year survival rate of 25% whereas those without preoperative thrombocytosis returned a survival rate of 15.38% (Figure 3-17).

Figure 3-17

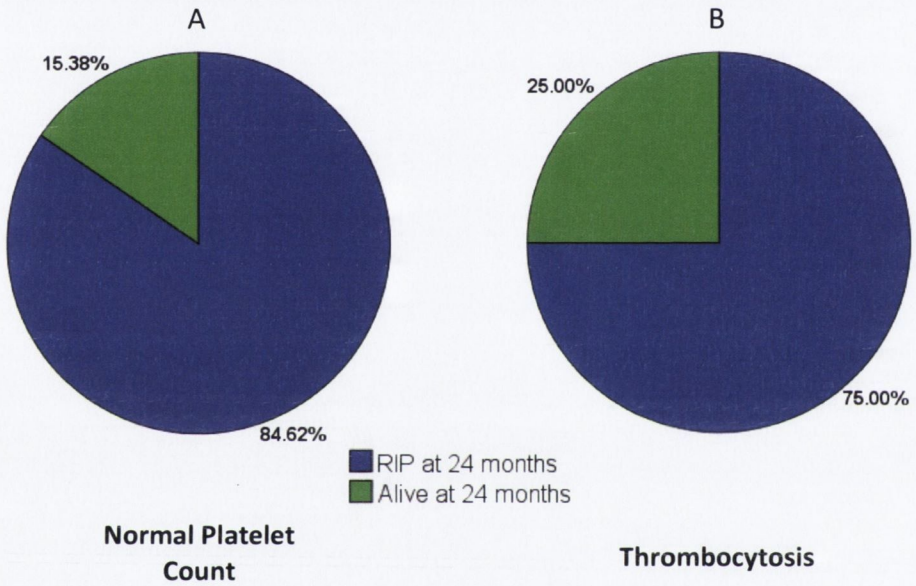

Figure 3-17: Five year survival rate in grade 2 ovarian cancer stratified by thrombocytotic status.

Figure 3-17 A indicates the percentage survival/mortality of in FIGO grade 2 ovarian cancer in the absence of an elevated preoperative platelet count. Figure 3-17 B indicates the percentage survival/mortality in FIGO grade 2 ovarian cancers in the presence of an elevated preoperative platelet count.

T-test analysis for independent samples was performed in order to determine the significance of observed differences in survival between the two groups. This revealed that though thrombocytosis was associated with close to 10% increase in survival at five years the difference between high and low platelet count groups was not statistically significantly different (p=0.608).

Grade 3 Ovarian Cancer

When stratified to allow investigation of thrombocytotic status individuals with grade 3 ovarian cancer and preoperative thrombocytosis were observed to have a five year survival rate of 25% whereas those without preoperative thrombocytosis returned a survival rate of 23.08% (Figure 3-18).

Figure 3-18

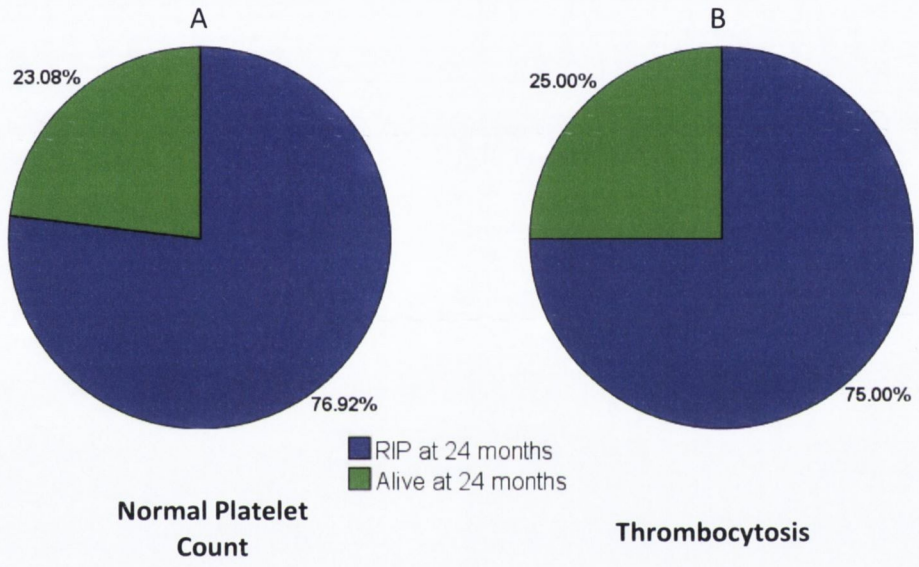

Figure 3-18: Five year survival rate in grade 3 ovarian cancer stratified by thrombocytotic status.

Figure 3-18 A indicates the percentage survival/mortality of in FIGO grade 3-18 ovarian cancer in the absence of an elevated preoperative platelet count. Figure 3-18 B indicates the percentage survival/mortality in FIGO grade 3 ovarian cancers in the presence of an elevated preoperative platelet count.

T-test analysis for independent samples was performed in order to determine the significance of observed differences in survival between the two test groups. This revealed that though thrombocytosis was associated with a 22% reduction in survival at five years the difference between high and low platelet count groups was not statistically significantly different (p=0.908). Spearman's correlation analysis was performed to determine correlations between sample metrics including: age, tumour grade, pre-operative platelet count, progression free survival and overall survival (Table 3-5).

These analyses found a statistically significant positive correlation exists between tumour grade and pre-op platelet count (corr. Coefficient = 0.284, p=0.007). No significant correlation exists between age and any other variable (p>0.05) though a negative correlation between age and OS was observed but was not statistically significant. A negative correlation was identified between pre-op platelet count and both two- and five-year survival rates though these correlations failed to reach statistical significance (p>0.05).

Additionally tumour grade negatively correlated with both PFS and OS at a non significant level. It was noted that all variables that were derivatives of each other returned statistically significant correlations (p<0.05) e.g. progression free, overall, two- and five-year survival.

Table 3-5

	Age		Grade		Pre-Op Platelet Count		PFS		OS		Two Year Survival		Five Year Survival	
	p=	Corr. Coeff.	*p*=	Corr. Coeff.	*p*=	Corr. Coeff.	*p*=	Corr. Coeff.	*p*=	Corr. Coeff.	*p*=	Corr. Coeff.	*p*=	Corr. Coeff.
Age	.	1	0.273	0.118	0.284	0.118	0.809	0.032	0.257	-0.154	0.32	-0.135	0.239	-0.16
Grade	0.273	0.118	.	1	0.007	0.284**	0.572	-0.075	0.751	-0.043	0.89	-0.019	0.871	0.022
Pre-Op Platelet Count	0.284	0.118	0.007	0.284**	.	1	0.132	0.204	0.193	0.18	0.096	0.229	0.78	0.039
PFS	0.809	0.032	0.572	-0.075	0.132	0.204	.	1	0†	0.881**	0†	0.732**	0†	0.595**
OS	0.257	-0.154	0.751	-0.043	0.193	0.18	0†	0.881**	.	1	0†	0.864**	0†	0.732**
2yr Survival	0.32	-0.135	0.89	-0.019	0.096	0.229	0†	0.732**	0†	0.864**	.	1	0†	0.512**
5yr Survival	0.239	-0.16	0.871	0.022	0.78	0.039	0†	0.595**	0†	0.732**	0†	0.512**	.	1

†$p < 0.001$

*Significance is two tailed

**Correlation Coefficient (Corr. Coeff.) is significant at the 0.01 level (two-tailed).

Table 3-5: Spearman's Correlation between patient clinicopathological metrics.

Spearman's correlation analysis was performed to examine for possible relationships between patient clinicopathological metrics. This included data from the normal group and ovarian cancer grade 2 and grade 3 groups.

3.3.3 RNA Analysis

The quantity and quality of RNA extracted from FFPE materials was examined prior to its inclusion in this study. Nanodrop™ results are shown in chapter 3 appendix Table 3-17, Table 3-18 and Table 3-19, containing details for RNA from normal, grade 2 and 2/3 and grade 3 ovarian samples respectively.

3.3.4 Real-time PCR Data Quality Control and Analysis

3.3.4.1 Quality Control

Prior to relative quantitation analysis RT-PCR data was subjected to quality control analysis to examine all interrogated samples to allow those that failed to amplify to be removed from further investigation where they would otherwise impact on subsequent relative quantitation analysis (as described previously in section 3.2.1).

RT-PCR C_T data was assessed using the RealTime Statminer function of Tibco Spotfire analysis suite revealing four samples that failed to amplify sufficiently to satisfy quality control requirements for inclusion in further relative quantitation analysis. The four samples failing QC at this point due to a >70% failure in target amplification are indicated in yellow in Figure 3-19.

Figure 3-19

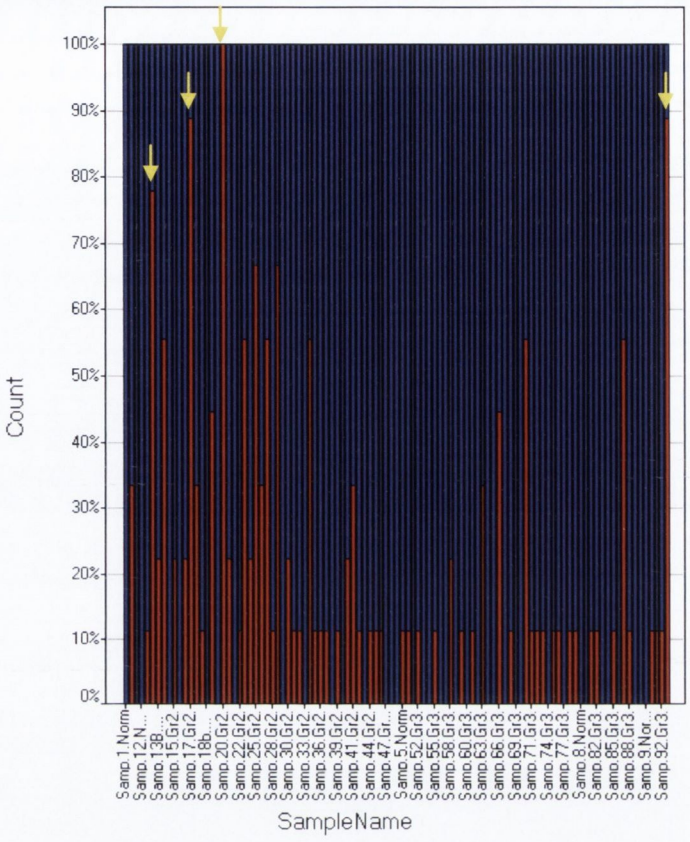

Figure 3-19: SpotFire® RealTime StatMiner™ Failed Summary

The RealTime StatMiner™ function of Tibco Spotfire® was used to interrogate RT-PCR data for samples which failed to amplify during the TaqMan reaction. Those samples with a >70%failure to amplify (C_T = 40) due to sample degradation were identified on the StatMiner™ output (indicated by yellow arrows above) and removed from subsequent investigation.

3.3.4.2 Normalisation

Sample normalisation was performed by interrogating the expression of the two candidate endogenous control genes, CDKN1B and HGPRT. Sum of stability score generated for each candidate control gene is the average pairwise variation of that gene with all other chosen candidate control genes across the samples analysed (Vandesompele et al., 2002).

The candidate endogenous control with the lowest sum of stability score, indicative of greatest stability of expression was selected as endogenous control. This was assessed using both SpotFire® (Figure 3-20) and Data Assist (Figure 3-21) prior to relative quantitation analysis.

Figure 3-20

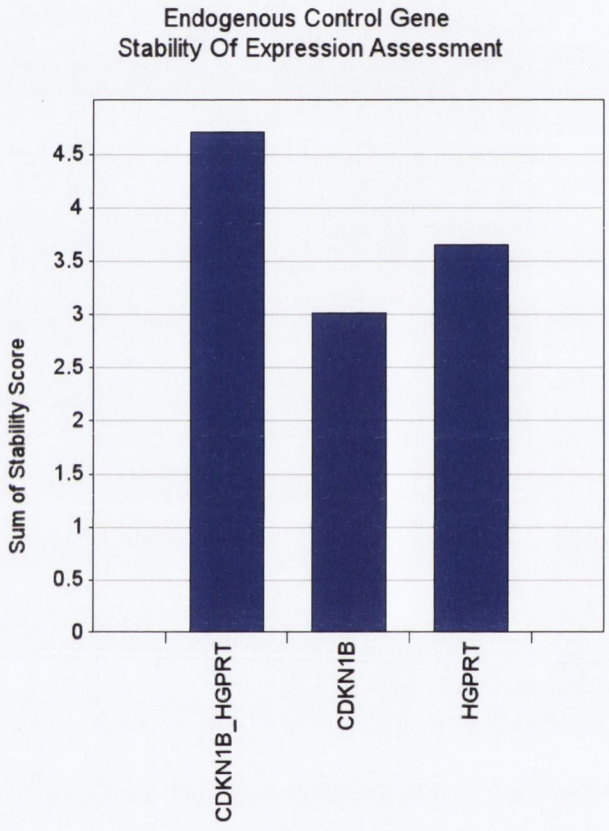

Figure 3-20: Endogenous Control Gene Stability of Expression Assessment.

TaqMan qPCR data was analysed using Tibco Spotfire® to determine the most suitable endogenous control gene for use in subsequent quantitative analyses.

The C_T data for both candidate control genes (N=3 per sample and N=87 samples) was investigated. The most suitable endogenous control gene was selected by determining the sum of stability score for each candidate control gene. The candidate control gene with the lowest sum of stability score, indicative of the least variance between samples, was accepted as the endogenous control gene for subsequent quantitative gene expression studies.

Figure 3-21

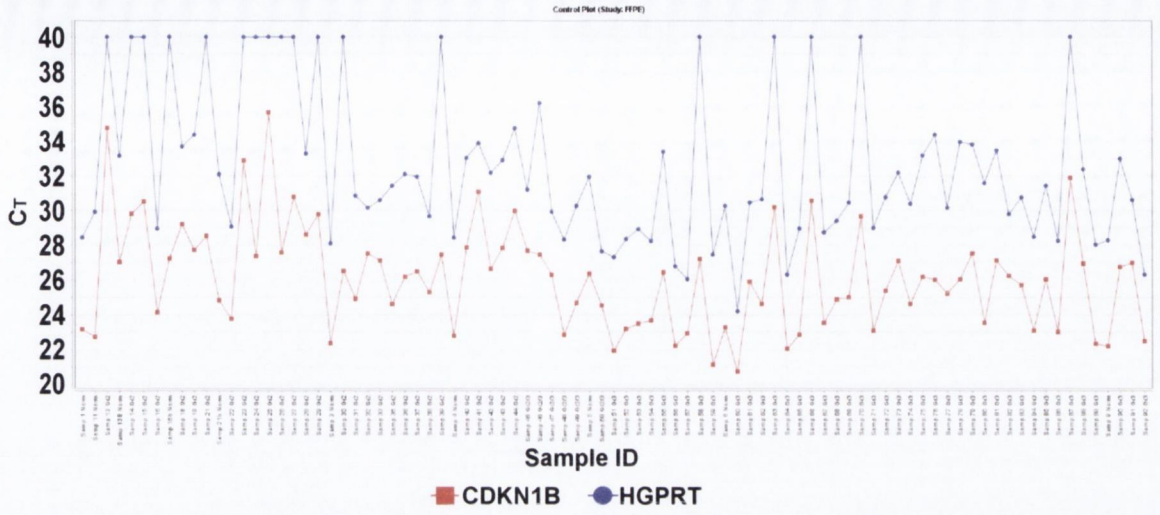

Figure 3-21: Line Graph Illustrating Candidate Endogenous Control Gene C_T values by Sample.

Applied Biosystems DataAssist™ software was utilised to interrogate the expression of candidate control genes CDKN1B and HGPRT in order to assess which was most suitable for use as endogenous control in subsequent quantitative gene expression studies.

This software allowed the generation of the above line chart illustrating the C_T value for CDKN1B (red) and HGPRT (blue) for each sample and a score of stability (off chart).

This graph indicates HGPRT failed to amplify in several samples (C_T=40) due to sample degradation. CDKN1B was successfully amplified in all samples. This finding coupled with a lower calculated sum of stability score and supported by data produced by RealTime StatMiner® analysis supported the use of CDKN1B as the endogenous control gene for us in subsequent quantitative gene expression investigations.

The line graph indicates the mean C_T value returned for both candidate endogenous control genes: CDKN1B (red) and HGPRT (blue). The graph clearly shows several samples where HGPRT failed to amplify, indicated by a C_T of 40, but where CDKN1B was successfully amplified and thus providing a suitable endogenous control gene for $\Delta\Delta C_T$ calculation and determination of comparative gene expression.

CDNK1B returned a sum of stability score less than the alternative candidate endogenous control gene, HGPRT. In addition to having a higher sum of stability value than CDKN1B, HGPRT also failed to amplify in multiple samples. Accepting both StatMiner® and

DataAssist™ results, CDKN1B was selected as endogenous control for sample normalisation when performing $\Delta\Delta C_T$ calculations.

3.3.4.3 Signal Correlation

TaqMan® real-time PCR data was then interrogated to determine intra- and inter- sample variations in C_T distribution / threshold. A high level of variation would indicate a high level of variability in this data may indicate poor success of the qPCR reaction.

Data Assist was used to produce a box and whisker plot (Figure 3-22) allowing visual assessment of samples based on the cumulative range of distribution of C_T values for every target gene in each sample and arranged by sample group/cohort. This plot revealed a low level of variation between samples indicated by close bunching of sample median and mean C_T values and with no samples range observed to fall outside the range of values reported for its biological group.

Following box and whisker analysis inter sample Pearsons' correlation analysis was performed examining the correlation of sample CT signals between each sample in each experimental cohort. This allows the generation of heat maps visually representing the correlation between samples in each cohort in addition to numeric values for the correlation between samples. Figure 3-23 illustrates the heat map generated for the grade 3 ovarian cancer cohort. Samples with a high correlation (approaching 1.0) between C_T values are indicated in shades of red, those with a moderate correlation (0.5) in darker shades and those with low correlation in shades of green (approaching 0.0).

Analysis of correlation values revealed normal ovarian samples to be a largely homogenous cohort with similar signal values (median = 0.8846). Grade 2 ovarian cancer samples returned correlation values indicative of a marginally heterogeneous cohort, possibly indicative of the grade of cancer being investigated (median = 0.7326). Grade 2/3 borderline samples returned correlation values indicative of a highly homogenous study cohort (median = 0.9181). Grade 3 ovarian cancer samples returned correlation values indicative of a largely homogenous study cohort (median = 0.8451) with few samples returning low correlation values.

Figure 3-22

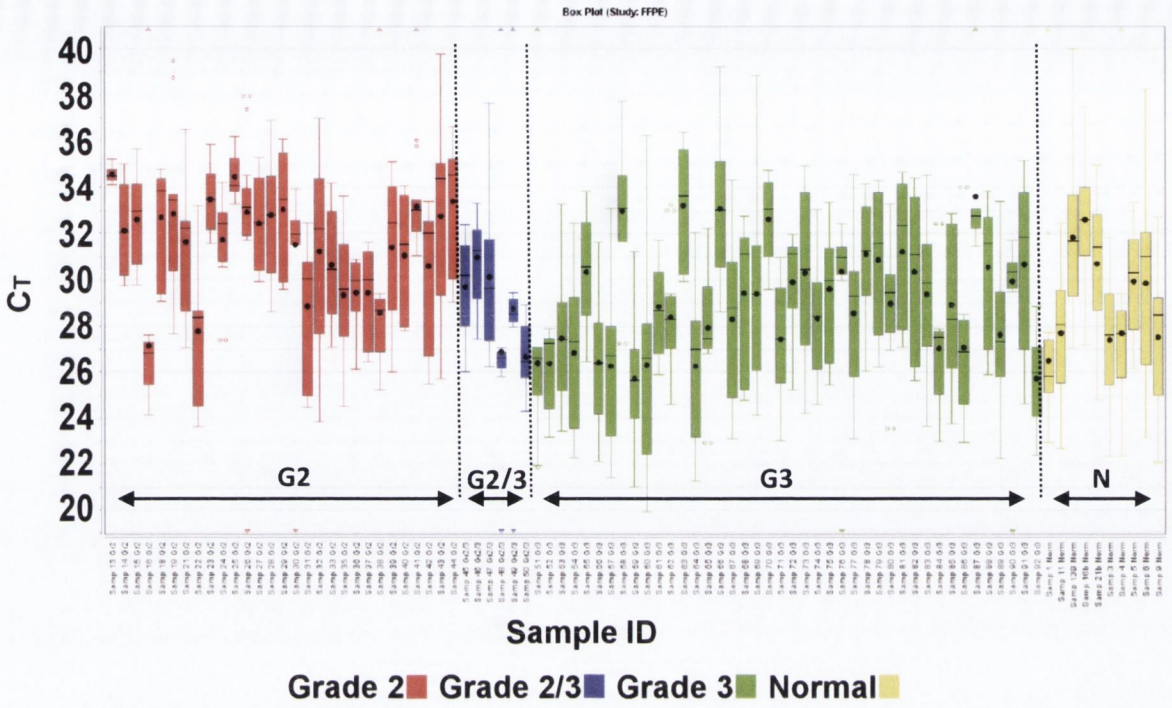

Figure 3-22: Box-and-whisker Plot displaying the overall range of C_T distribution for each sample from all genes in the experiment.

Using DataAssist™ all sample C_T data was interrogated in order to assess the level of variation in amplification data both within and between study groups. This analysis cumulatively assessed the C_T values returned for reach replicate (N=3) of each gene (N=7) for each sample (N=87), resulting in the generation of the bar chart above.

The box the middle of each plot contains 50% of the data (C_T values). The black horizontal line indicates the median C_T value, and the black dot represents the mean C_T. The ends of the vertical lines ("whiskers") indicate the minimum and maximum C_T values, unless outliers are present. The points outside the ends of the whiskers are outliers or suspected outliers. The bars are coloured based on the sample biological group: normal (yellow), grade 2 (red), 2/3 (blue) or grade 3 ovarian cancer (green) and samples are arranged to biological groups.

The chart suggests a low level of variation between samples indicated by close bunching of sample median and means C_T values and with no samples range observed to fall outside the range of values reported for its biological group.

Figure 3-23

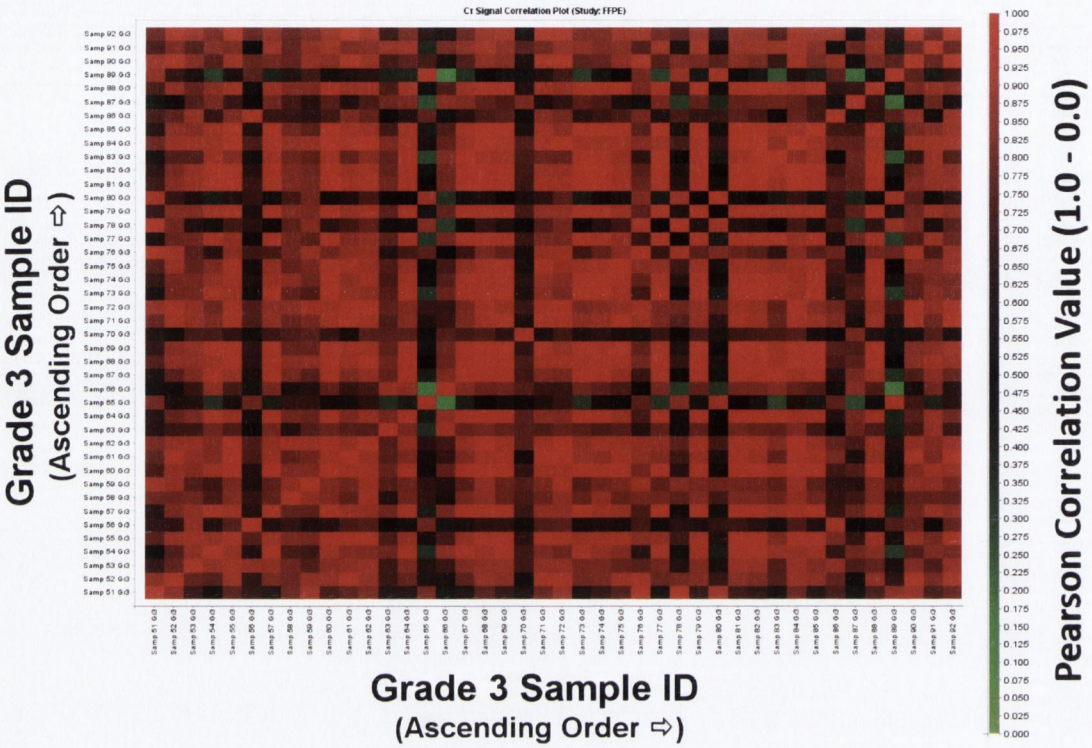

		Normal (N=10)	Grade 2 (N=29)	Grade 2/3 (N=6)	Grade 3 (N=42)
Pearson Correlation	Median	0.8847	0.7326	0.9181	0.8452
	Mean	0.8346	0.6724	0.9058	0.7991
	Max	0.9821	0.9884	0.9692	0.9951
	Min	0.3628	-0.2231	0.8017	0.1430
	SEM	0.0143	0.0085	0.0088	0.0041

Figure 3-23: Pearsons' Correlation Plot (Heat Map) of sample signal (C_T) values (ovarian cancer grade 3).

Applied Biosystems DataAssist™ was used to investigate the correlation between C_T values (cumulative) for each sample (N=87) in each of the investigation cohorts (normal ovary, grade 2, 2/3 and grade 3 ovarian cancers). DataAssist™ calculated Pearsons' correlation values for each pair of samples, enabling the further calculation of cohort correlation data (see adjoining table above), in addition to the generation of visual representations of inter-sample correlation in the form of heat maps. Figure 3-23 is an exemplar heat map illustrating patterns of correlation across samples in the grade 3 ovarian cancer group.

Red shaded squares on the heat maps indicate correlation values close to 1 (high correlation), dark squares indicate correlation values ~0.5 (moderate correlation) and green shaded squares corresponding to correlation values closer to 0.0, indicating little correlation. The analysis of correlation values revealed ovarian cohort groups returned correlation values indicated low variability in both normal and cancer cohorts

3.3.5 Gene Expression Analysis – Relative Quantitation

Real-time PCR assay of target genes indicates altered expression in all grades of ovarian cancer investigated when compared against a normal ovarian calibrator group.

The fold change (FC) in gene expression between the test groups (ovarian cancer grades 2, 2/3 and 3) compared to the calibrator (normal ovary) group for each gene and the statistical significance of the change compared to the calibrator group is given in Table 3-6, and are visually represented in Figure 3-24. Figure 3-24 indicates relative quantitation (log_{10}) of the target genes on the Y-axis and target gene on the X-axis in ovarian cancer grades 2 (red), 2/3 (blue) and 3 (green).

Figure 3-24

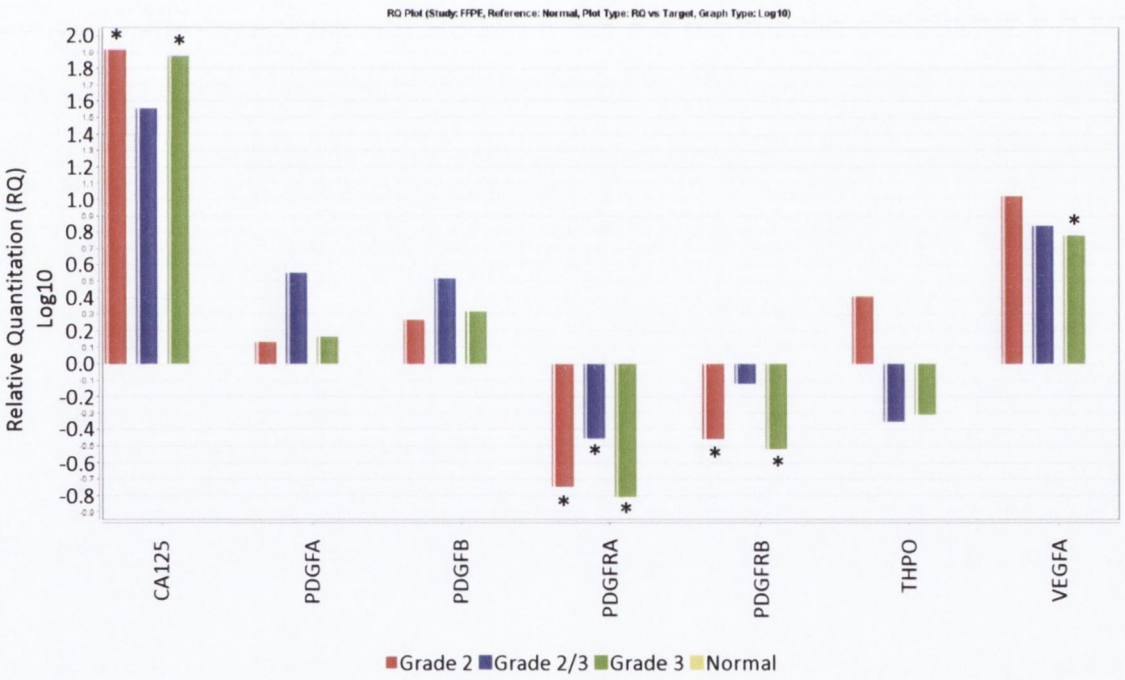

Figure 3-24: Relative Quantitation Plot. Target Gene Expression in Ovarian Cancer (FIGO grades, 2, 2/3, 3) compared to normal ovary.

DataAssist™ was used to determine differences in gene expression between the cohort groups. The normal group as a calibratior group with expression levels measured as greater or less than the expression level observed in this group. Significant increases/decreases in gene expression are indicated by asterix. Fold change differences between groups along with *p* values are given in table 3.6.

Table 3-6

	Grade 2 Vs Norm		Grade 2/3 Vs Norm		Grade 3 Vs Norm	
Gene	**FC**	**(*p*=)**	**FC**	**(*p*=)**	**FC**	**(*p*=)**
CA125	*82.4913*	*0.0029*	36.0293	0.1368	*75.6037*	*0.0000*
PDGFA	1.3545	0.4476	3.5676	0.1016	1.4538	0.3261
PDGFB	1.8458	0.0623	3.3078	0.0822	*2.0769*	*0.0072*
PDGFRA	*0.1792*	*0.0002*	*0.3518*	*0.0012*	*0.1557*	*0.0002*
PDGFRB	*0.3493*	*0.012*	0.7532	0.3196	*0.3033*	*0.0079*
THPO	2.5567	0.209	0.4448	0.2807	0.4891	0.2809
VEGFA	10.4808	0.0504	6.9026	0.0558	*5.9874*	*0.0002*

Table 3-6: Target Gene Expression in Grade 2, 2/3 borderline and grade 3 Ovarian Cancer – relative quantitation and significance compared to expression in normal ovary.

Analysis of qPCR data using Applied Biosystems DataAssist™ software enabled differences in levels of gene expression between cohort groups to be examined. The normal ovary group was used as the calibrator and the level of target gene expression described as increased or decreased in the ovairian cancer cohort groups relative to the normal calibrator.

In addition to the generation of bar graphs illustrating the comparative levels of gene expression (figure 3-24) the software also calculated the magnitude and significance of fold change differences between groups (table 3-6). This indicated several genes underwent significant alteration of expression (underlined and italicised) in the ovarian cancer cohorts compared to the normal ovary group.

The relative quantitation data indicated the following alterations in the level of expression of target genes in grade 2 ovarian cancer.

- CA125 which underwent significant up-regulation (FC > 82, $p<0.01$).
- both PDGFRA and PDGFRB which both exhibited significant down regulation of expression ($p<0.05$).
- both PDGFB and VEGFA also exhibited increased expression but fell short of significance ($p>0.05$).
- PDGFA and THPO both of which exhibited increased expression though failed to reach significance ($p>0.05$).

The relative quantitation data returned for target genes altered expression in grade 2/3 borderline ovarian cancer compared to normal ovarian samples indicates:

- statistically significant reduction in PDGFRA expression ($p<0.05$).
- increased VEGF expression approaching significance ($p=0.0558$).
- non-significant increases in CA125, PDGFA and PDGFB expression ($p>0.05$).
- non-significant reduction in THPO and PDGFRB expression.

The relative quantitation data returned for target genes altered expression in grade 3 ovarian cancer compared to normal ovarian samples indicates statistically significant alterations of expression in several genes. These include:

- CA125, VEGF and PDGFB which all showed significant increases in expression ($FC \geq 2$, $p < 0.05$)
- Significant reduction in expression of both PDGFRA and PDFGRB ($FC \leq 0.5$, $p < 0.05$).

PDGFA and THPO also exhibited altered expression (increased and decreased expression respectively) though not statistically significant.

From this data there is a clear pattern of altered gene expression in grade 2 and 3 ovarian cancer when compared against gene expression in the normal ovary. There is trend for increased PDGF expression with a concomitant reduction in PDGFR expression. CA125 and VEGF both experience large and increasingly significant increases in expression as ovarian cancer develops.

THPO, though a tantalising target due to its key role in platelet production (thrombopoiesis), indicated reduced expression occurred concurrent with disease progression though at a non-significant level.

3.3.5.1 Trends in Gene Expression

TaqMan® q-PCR analysis successfully allowed the determination of both the magnitude and significance of altered target gene expression between the normal ovary and malignant disease cohorts. Further analysis was performed on sample RQ data to allow further visualisation of the changes in gene expression described in real-time PCR results.

Relative quantitation figures for each sample were calculated utilising the $\Delta\Delta C_T$ method having randomly selecting one normal ovary sample (#9) as calibrator. The relative quantitation values were then labelled as high expression, normal expression or low expression for each gene of interest investigated in each sample. The threshold for high expression was a relative quantitation of 2 or greater and the threshold for low expression was a relative quantitation of 0.5 or lower, thus creating a margin of 'normal' relative quantitation gene expression between 0.5 and 2.0.

Due to the smaller number of samples in the grade 2/3 borderline cohort the decision was made to remove these samples from this analysis and in preference for observing the alteration gene expression as ovarian disease progresses from normal to grade two and then grade three cancers.

3.3.5.1.1 Platelet Derived Growth Factors

Real-time PCR investigation revealed the platelet derived growth factors, PDGFA and PDGFB, underwent increased expression as ovarian cancer progressed from normal tissues to later grades of ovarian malignancy. While these increases were not statistically significant in some instances, principally PDGFB, the data hints towards the possibility of a trend for increased expression of these genes that may be clearly visualised through RQ categorisation as high, normal or low expression. Figure 3-25 contains the graphs generated by this method for PDGFA and PDGFB.

Figure 3-25

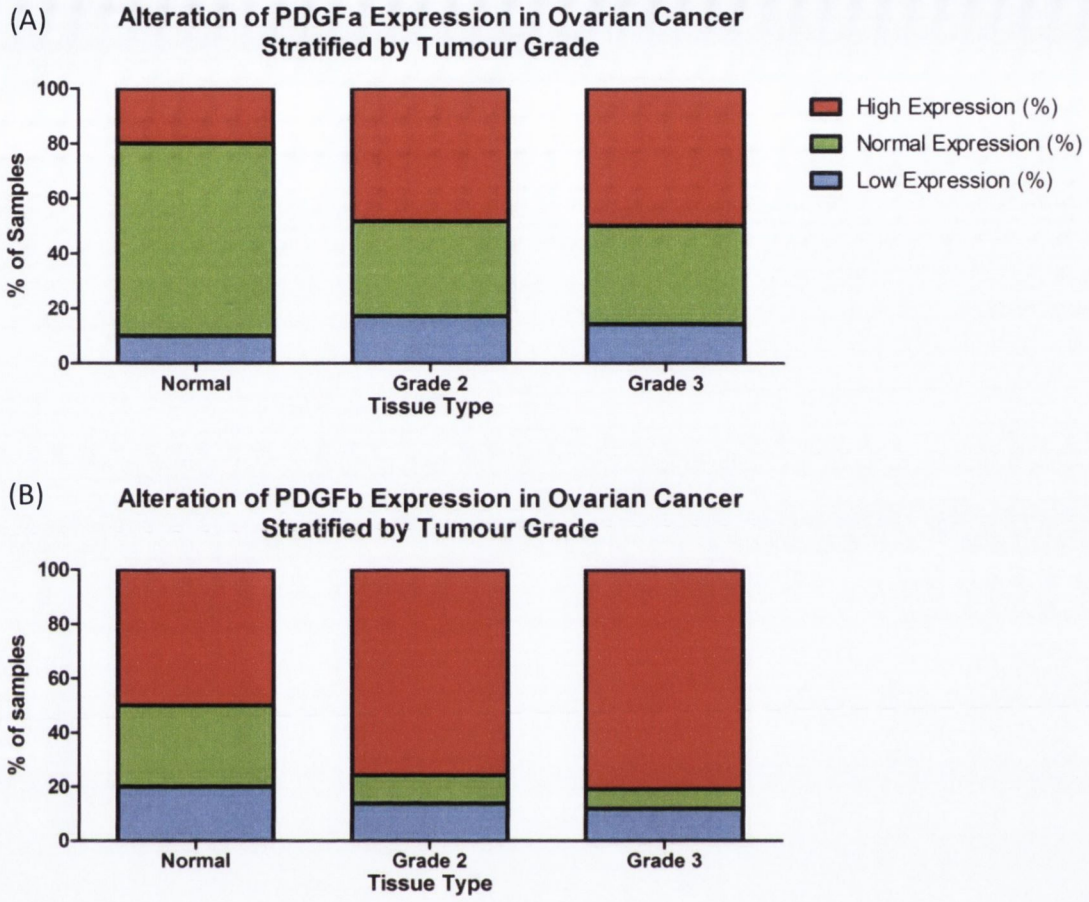

Figure 3-25: PDGFA (A) and PDGFB (B) expression categorised high to low in normal ovary and FIGO grade 2 and 3 ovarian cancers.

Relative quantitation data was calculated for each each target gene (n=7) for each sample in the normal ovary and ovarian cancer grade 2 and 3 groups (n=81) following TaqMan qPCR and using a randomly selected normal ovary sample as calibrator. The expression of each gene was categorised as high (red), normal (green) or low (blue) expression relative to the calibrator sample and stacked barcharts generated to illustrate the alteration in patterns of expression between normal ovary and ovarian cancer groups.

PDGFA and PDGFB expression was examined and was observed to undergo a trend of increased expression with increasing tumour grade compared to the normal ovary group.

Alteration of PDGFA expression during ovarian cancer progression is clearly visible in Figure 3-25 (A). The normal sample cohort returned 70% of samples expressing the gene in the 'normal' range (RQ = 2.0 – 0.5) with 10% returning a 'low' value (RQ <0.5) and 20% returning a 'high' value (RQ > 2.0). In grade 2 ovarian cancer these percentages change to

34.5%, 17.2% and 48.3% respectively with similar figures observed in grade 3 ovarian cancer (35.7% (N), 14.3% (L), 50% (H)).

This pattern of altered gene expression trending towards increased gene expression increasing tumour grade is also repeated in PDGFB expression. The normal sample cohort returned 30% of samples expressing the gene in the 'normal' range with 20% returning a 'low' value and 50% returning a 'high' value. In grade 2 ovarian cancer these percentages change to 10.3%, 13.8% and 75.9% respectively with similar figures observed in grade 3 ovarian cancer; 7.1% (N), 11.9% (L), 81% (H).

3.3.5.1.2 Platelet Derived Growth Factor Receptors

As with the platelet derived growth factors, real-time PCR analysis determined that platelet derived growth factor receptors, PDGFRA and PDGFRB, experienced altered expression as ovarian cancer progressed from normal through grades of ovarian malignancy. These changes were statistically significant reductions in expression in ovarian cancer grades 2 and 3.

As before this data indicates a trend for increased expression of these genes that may be clearly visualised through RQ categorisation as high, normal or low expression. Figure 3-26 contains the graphs generated by this method for PDGFRA and PDGFRB.

Figure 3-26

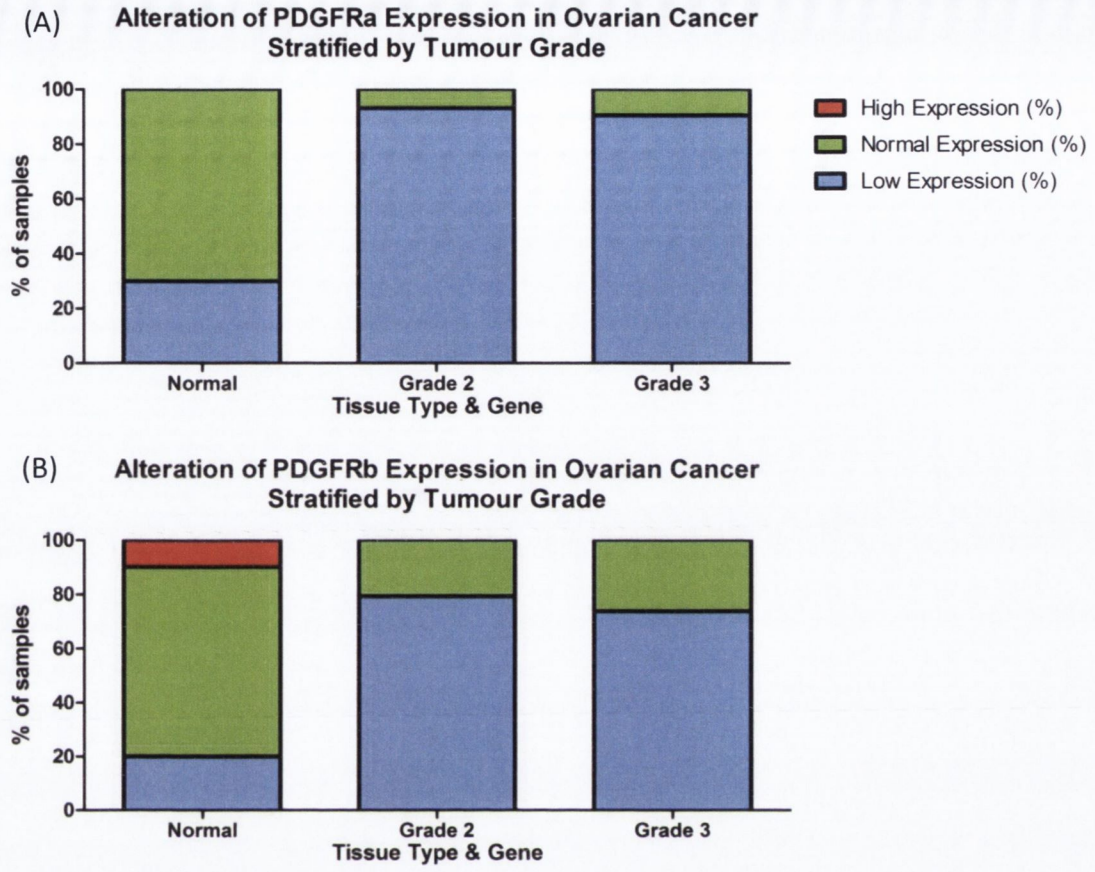

Figure 3-26: PDGFRA (A) and PDGFRB (B) expression categorised high to low in normal ovary and FIGO grade 2 and 3 ovarian cancers.

Relative quantitation data was calculated for each each target gene (n=7) for each sample in the normal ovary and ovarian cancer grade 2 and 3 groups (n=81) following TaqMan qPCR and using a randomly selected normal ovary sample as calibrator. The expression of each gene was categorised as high (red), normal (green) or low (blue) expression relative to the calibrator sample and stacked barcharts generated to illustrate the alteration in patterns of expression between normal ovary and ovarian cancer groups.

PDGFRA and PDGFRB expression was examined and was observed to undergo a trend of reduced expression with increasing tumour grade compared to the normal ovary group.

Alteration of PDGFRA expression during ovarian cancer progression is clearly visible in figure 3. (A). The normal sample cohort returned 70% of samples expressing the gene in the 'normal' range (RQ = 2.0 – 0.5) with 30% returning a 'low' value (RQ <0.5) and no samples (0%) returning a 'high' value (RQ > 2.0). In grade 2 ovarian cancer these percentages change to 6.9% (N) and 93.1% (L) with elevated expression reported in 0% of samples. Similar figures observed in grade 3 ovarian cancer; 9.5% (N) and 90.5% (L).

This pattern of altered trending towards reduced gene expression is also repeated in PDGFRB expression where low gene expression trends to be present in a greater percentage of samples with malignant disease. The normal sample cohort returned 70% of samples expressing the gene in the 'normal' range with 20% returning a 'low' value and 10% returning a 'high' value. In grade 2 ovarian cancer these percentages change to 20.7%, 79.3% and 0% respectively with similar figures observed in grade 3 ovarian cancer; 26.2% (N), 73.8% (L), 0% (H).

3.3.5.1.3 VEGFA and CA125

TaqMan® RT-PCR of target genes VEGFA and CA125 indicated both biomarkers underwent increased expression, if not always statistically significantly so in all tumour grades compared to normal ovarian tissue. Categorisation of RQ values into high, normal and low levels of gene expression allow this alteration of expression for both genes to be clearly illustrated in Figure 3-27. Similar to the platelet derived growth factor receptor genes PDGFRA and PDGFRB, cancer biomarkers VEGF and CA125 displayed large changes in the percentage of samples categorised as high, normal or low expression as ovarian tissue progressed from normal to successively more developed malignant disease.

Alteration of VEGF expression during ovarian cancer progression is clearly visible in figure 3. (A). The normal sample cohort returned 30% of samples expressing the gene in the 'normal' range, 20% returned a 'low' value and 50% returned a 'high' value. In grade 2 ovarian cancer these percentages change to 0% (N) and 13.8% (L) with high expression reported in 82.8% of samples. Similar figures observed in grade 3 ovarian cancer; 7.1% (L) and 92.9% (H).

This pattern of altered trending towards elevated gene expression is also repeated in CA125 expression where high gene expression was shown to be present in a greater percentage of samples with increasing tumour grade. The normal sample cohort returned 30% of samples expressing the gene in the 'normal' range with 50% returning a 'low' value and 20% returning a 'high' value. In grade 2 ovarian cancer these percentages

change to 10.3%, 0% and 89.7% respectively with a similar change towards increased expression observed in grade 3 ovarian cancer; 7.1% (N), 4.8% (L), 88.1% (H).

Figure 3-27

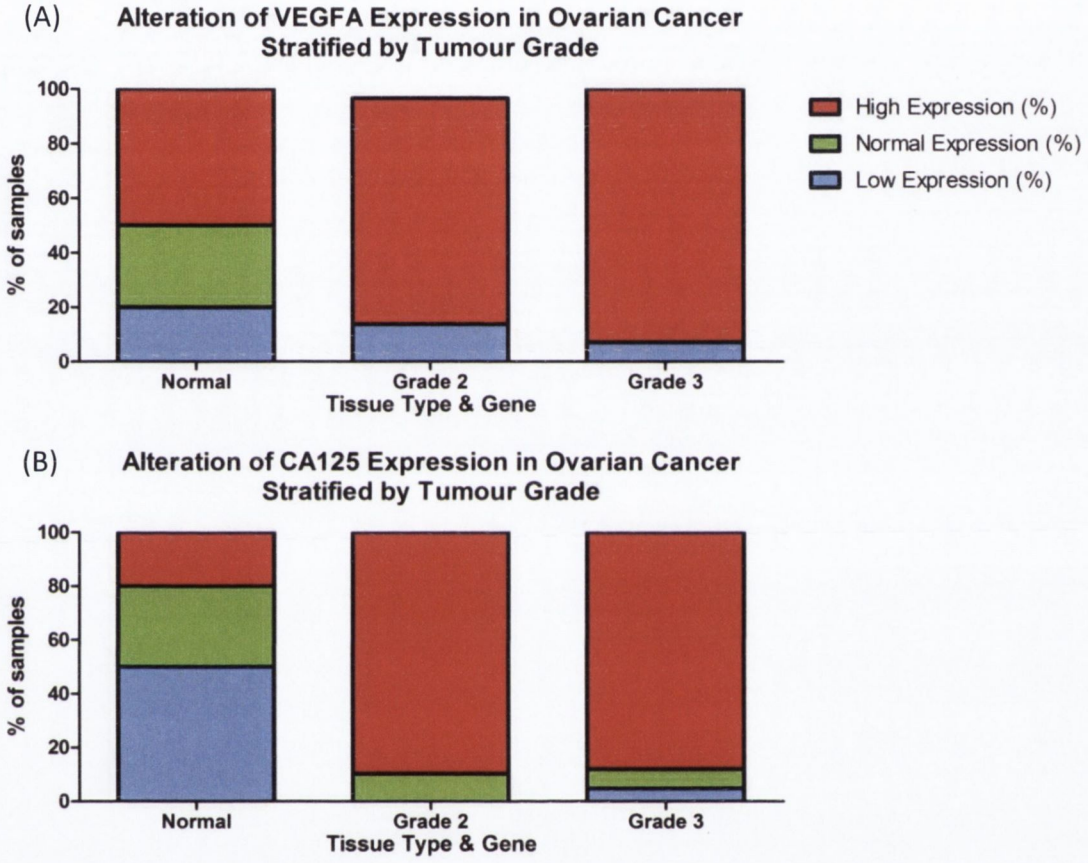

Figure 3-27: VEGFA (A) and CA125 (B) expression categorised high to low in normal ovary and FIGO grade 2 and 3 ovarian cancers.

Relative quantitation data was calculated for each each target gene (n=7) for each sample in the normal ovary and ovarian cancer grade 2 and 3 groups (n=81) following TaqMan qPCR and using a randomly selected normal ovary sample as calibrator. The expression of each gene was categorised as high (red), normal (green) or low (blue) expression relative to the calibrator sample and stacked barcharts generated to illustrate the alteration in patterns of expression between normal ovary and ovarian cancer groups.

VEGFA and CA125 expression was examined and was observed to undergo a trend of increased expression with increasing tumour grade compared to the normal ovary group.

3.3.5.1.4 Thrombopoietin

Thrombopoietin presented an attractive target for RT-PCR analysis arising from its role as primary regulator of thrombopoiesis and megakaryopoiesis and potential driver of thrombocytosis in cancer states. TaqMan® RT-PCR of the THPO gene indicated that while changes did occur they were not of a statistically significant magnitude and tended towards reduced expression in all tumour grades compared to normal ovarian tissue. As with the previous genes RQ values were categorised as high, normal and low and the percentage of samples returning these values represented on a column graph for normal ovarian tissue and both grade 2 and 3 ovarian cancer. Alteration of THPO expression during ovarian cancer progression is illustrated in Figure 3-28.

The normal sample cohort returned 20% of samples expressing the gene in the 'normal' range, 40% returned a 'low' value and 40% returned a 'high' value. In grade 2 ovarian cancer these percentages change to 17.2% (N) and 48.3% (L) with elevated expression reported in 34.5% of samples. Similar figures observed in grade 3 ovarian cancer; 31.0% (N), 50% (L) and 19% (H). This represents a very large alteration in patterns of expression

These patterns are in keeping with the alteration in expression illustrated in the Relative Quantitation Plot (Figure 3-24) generated from qPCR data and support the direction of gene expression changes in disease compared to normal ovarian tissues (Table 3-6).

Figure 3-28

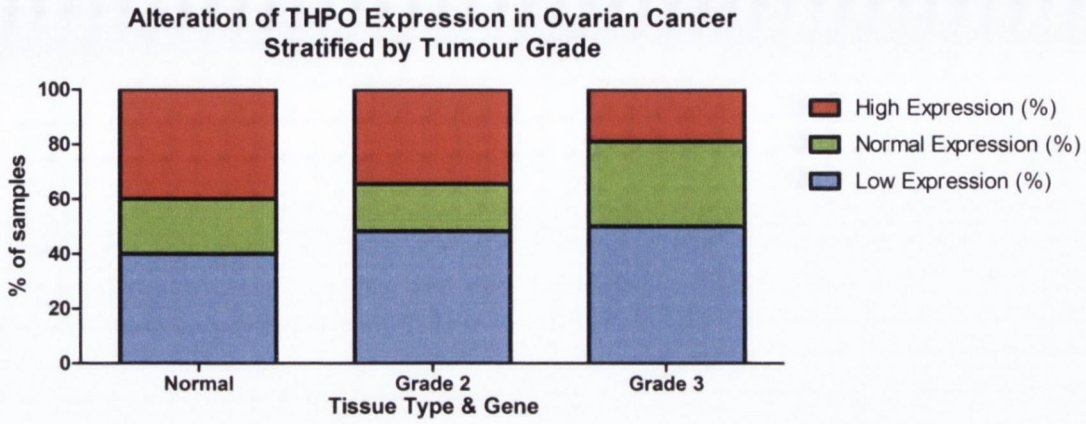

Figure 3-28: THPO expression categorised high to low in normal ovary and FIGO grade 2 and 3 ovarian cancers.

Relative quantitation data was calculated for each each target gene (n=7) for each sample in the normal ovary and ovarian cancer grade 2 and 3 groups (n=81) following TaqMan qPCR and using a randomly selected normal ovary sample as calibrator. The expression of each gene was categorised as high (red), normal (green) or low (blue) expression relative to the calibrator sample and stacked barcharts generated to illustrate the alteration in patterns of expression between normal ovary and ovarian cancer groups.

THPO expression was examined and observed to undergo a trend of reduced expression with increasing tumour grade compared to the normal ovary group.

3.3.5.2 Trends in Gene Expression - Survival

Having categorised gene expression in terms of high, normal or low levels of expression the interactions between gene expression level and survival metrics were determined through Kaplan Meier analysis and determined differences between expression levels (at each tumour grade) by log rank analysis for each target gene (Table 3-7 to Table 3-13).

This was performed using the gene expression levels previously determined having first removed those samples that failed RT-PCR QC and those samples indicated to be survival outliers removed from analysis prior to PFS and OS investigation.

Each table indicates the mean PFS and OS time in months with 95% Confidence Interval (CI) associated with low, normal and high expression of the gene investigated grade 2 and 3 ovarian cancer. Also indicated are the number of samples (N) at each expression level and log-rank analysis results (Chi square and significance); performed to determine if the differences observed between expression levels is significant.

3.3.5.2.1 PDGFA

In grade 2 ovarian cancers PDGFA appears to result in longer PFS and OS than either low or normal expression levels, though this difference is not statistically significant. In grade 3 ovarian cancers PDGFA low expression returned greater survival times for PFS than normal or high expression levels with better 95% CI values also but these differences failed to return statistical significance when tested using log rank analysis (Table 3-7).

PDGFA expression levels' effect on OS in grade 3 ovarian cancer suggests that increasing PDGFA expression level is matched with increased OS, though this was determined to be non-significant (p=0.058).

Table 3-7

Gene	Grade	Expression Level	N	Median PFS 95% CI (upper, lower)	Log Rank (χ^2, significance)	N	Median OS 95% CI (upper, lower)	Log Rank (χ^2, significance)
PDGFA	2	Low	2	10 (-,-)	0.797,0.671	3	14 (1.197,26.803)	1.363,0.506
		Normal	6	12 (12.078,17.922)		6	12 (0,74.413)	
		High	9	15 (6.933,23.067)		8	22 (7.745,36.255)	
	3	Low	4	17 (8.513,25.487)	3.8,0.15	2	7 (-,-)	5.678,0.058
		Normal	12	6 (0,16.184)		11	12 (0,26.026)	
		High	15	14.4 (5.663,23.337)		14	33 (15.592,50.408)	

Table 3-7: PDGFA: Gene Expression Level (Low, Normal, High) Vs Survival.

Comparative PDGFA expression was calculated utilising TaqMan® qPCR data and using a randomly selected normal ovary calibrator sample. Fold change (FC) differences for PDGFA expression for each sample was categorised as low (FC < 0.5), normal FC (0.5 < FC < 2.0) or high expression (FC > 2.0). SPSS software was utilised to investigate the effect of the level of PDGFA expression on patient progression free and overall survival using Kaplan-Meier analysis and determining significance by log-rank analysis. In instances where disease progression or patient mortality had not occurred or where patient survival data was missing or otherwise unavailable these samples were censored from analysis.

Table 3-7 illustrates the median PFS and OS and 95% confidence interval associated with low, normal and high PDGFA expression levels in both grade 2 and 3 ovarian cancers. The result of log-rank analysis of the significance of the differences in patient survival between gene expression levels is also given. This analysis indicates that differences in PFS and OS observed with differing levels of PDGFA expression in grade 2 and 3 ovarian cancer were not statistically significant.

3.3.5.2.2 PDGFB

In grade 2 ovarian cancers PDGFB appears to result in longer PFS and OS when expressed at a 'normal' level compared to either reduced or elevated levels of expression, though the difference in survival between groups is not statistically significant. In grade 3 ovarian cancers PDGFB expression returned greater survival times for PFS when highly expressed

than in normal or high expression levels, though with a narrower and lower 95% CI range than indicated with low expression values.

Log-rank analysis of the differences in PFS and OS between expression levels failed to return statistical significance. PDGFA expression in grade 3 ovarian cancer appear to have little effect on OS based on the median survival times returned for each expression level and this is reflected in the failure to find significant differences between the expression levels (Table 3-8).

Table 3-8

Gene	Grade	Expression Level	N	Median PFS 95% CI (upper, lower)	Log Rank (Chi Sq, *p*=)	N	Median OS 95% CI (upper, lower)	Log Rank (Chi Sq, *p*=)
PDGFB	2	Low	3	10 (-,-)	0.611,0.737	3	14 (9.199,18.801)	2.866,0.239
		Normal	1	24 (-,-)		1	96 (-,-)	
		High	13	15 (7.954,22.046)		13	22 (7.688,36.312)	
	3	Low	4	7 (0,47.180)	0.399,0.819	4	20 (-,-)	0.444,0.505
		Normal	2	6 (-,-)		1	22 (-,-)	
		High	25	11 (4.472,17.528)		22	22 (11.644,32.356)	

Table 3-8: PDGFB: Gene Expression Level (Low, Normal, High) Vs Survival.

Comparative PDGFB expression was calculated utilising TaqMan® qPCR data and using a randomly selected normal ovary calibrator sample. Fold change (FC) differences for PDGFB expression for each sample was categorised as low (FC < 0.5), normal FC (0.5 < FC < 2.0) or high expression (FC > 2.0). SPSS software was utilised to investigate the effect of the level of PDGFB expression on patient progression free and overall survival using Kaplan-Meier analysis and determining significance by log-rank analysis. In instances where disease progression or patient mortality had not occurred or where patient survival data was missing or otherwise unavailable these samples were censored from analysis.

Table 3-8 illustrates the median PFS and OS and 95% confidence interval associated with low, normal and high PDGFB expression levels in both grade 2 and 3 ovarian cancers. The result of log-rank analysis of the significance of the differences in patient survival between gene expression levels is also given. This analysis indicates that differences in PFS and OS observed with differing levels of PDGFB expression in grade 2 and 3 ovarian cancer were not statistically significant.

3.3.5.2.3 PDGFRA

Real-time PCR investigations determined PDGFRA underwent a reduction in expression in ovarian cancer grades 2 and 3 compared to normal ovarian tissue. This change in expression is reflected in the large differences in low, normal and high expression cohort sizes described in Table 3-9. These large differences make accurate comparison between the groups difficult, the investigation of the influence of PDGFRA expression on survival in ovarian cancer may benefit from increasing the size of the cohorts in future studies to overcome this issue and allow meaningful statistical analysis.

Table 3-9

Gene	Grade	Expression Level	N	Median PFS 95% CI (upper, lower)	Log Rank (χ^2, p=)	N	Median OS 95% CI (upper, lower)	Log Rank (χ^2, p=)
PDGFRA	2	Low	16	14 (8.120,19.880)	1.120,0.290	17	22 (5.315,38.685)	-,-
		Normal	1	46 (-,-)		/	N/a	
		High	/	N/a		/	N/a	
	3	Low	28	11 (5.166,16.834)	0.433,0.511	24	19 (7.443,30.557)	0.12,0.915
		Normal	3	9 (4.199,13.801)		3	24 (7.559,30.401)	
		High	/	N/a		/	N/A	

Table 3-9: PDGFRA: Gene Expression Level (Low, Normal, High) Vs Survival.

Comparative PDGFRA expression was calculated utilising TaqMan® qPCR data and using a randomly selected normal ovary calibrator sample. Fold change (FC) differences for PDGFRA expression for each sample was categorised as low (FC < 0.5), normal FC (0.5 < FC < 2.0) or high expression (FC > 2.0). SPSS software was utilised to investigate the effect of the level of PDGFRA expression on patient progression free and overall survival using Kaplan-Meier analysis and determining significance by log-rank analysis. In instances where disease progression or patient mortality had not occurred or where patient survival data was missing or otherwise unavailable these samples were censored from analysis.

Table 3-9 illustrates the median PFS and OS and 95% confidence interval associated with low, normal and high PDGFRA expression levels in both grade 2 and 3 ovarian cancers. The result of log-rank analysis of the significance of the differences in patient survival between gene expression levels is also given.

3.3.5.2.4 PDGFRB

Similar to the pattern of expression observed with PDGFRA, PDGFRB was described to undergo a reduction in expression in ovarian cancer compared to normal ovarian tissue (Table 3-10).

In grade 2 ovarian cancers the data suggests that reduced PDGFRB expression conveys a PFS advantage witnessed by a higher median PFS and improved 95% CI over 'normal' levels of expression. Similar results are returned when observing OS metrics in grade 2 ovarian cancer with low PDGFRB expression returning a higher 95% CI and median values for OS. Log rank analysis determined that the differences between expression groups were not significant for either PFS or OS.

PDGFRB expression level was observed to have little impact on PFS in Grade 3 ovarian cancer. The median values were not significantly different between low and normal levels of expression (10 months vs 11 months). 95% CI values were similar with normal expression returning a slightly improved lower value (4.80 months vs 1.02 months) suggesting a slightly extended period to relapse in patients expressing normal levels of PDGFRB.

When focus is turned to OS, a similar trend is observed with normal levels of PDGFRB expression return a higher median OS value than low levels of expression (33 months vs 14 months). Observing the differences in the 95% CI for each group, the broad values returned for low expression suggest a high variability in survival and while normal expression returned a better lower value (17.06 months vs 0 months) but smaller upper value (22.94 months vs 75.90 months) resulting in a narrower 95% CI range. Log rank analysis determined that the observed differences in PFS and OS between expression levels were not statistically significant.

Table 3-10

Gene	Grade	Expression Level	N	Median PFS 95% CI (upper, lower)	Log Rank (χ^2, p=)	N	Median OS 95% CI (upper, lower)	Log Rank (χ^2, p=)
PDGFRB	2	Low	13	22 (9.676,34.44)	1.638,0.201	13	36 (0,75.902)	0.862,0.353
		Normal	4	14 (3.22,24.78)		4	20 (17.06,22.94)	
		High	N/a	N/a		N/a	N/a	
	3	Low	21	10 (1.028,18.972)	1.241,0.265	17	14 (0,75.902)	3.428,0.064
		Normal	10	11 (4.802,17.198)		10	33 (17.06,22.94)	
		High	N/a	N/a		N/a	N/a	

Table 3-10: PDGFRB: Gene Expression Level (Low, Normal, High) Vs Survival.

Comparative PDGFRB expression was calculated utilising TaqMan® qPCR data and using a randomly selected normal ovary calibrator sample. Fold change (FC) differences for PDGFRB expression for each sample was categorised as low (FC < 0.5), normal FC (0.5 < FC < 2.0) or high expression (FC > 2.0). SPSS software was utilised to investigate the effect of the level of PDGFRB expression on patient progression free and overall survival using Kaplan-Meier analysis and determining significance by log-rank analysis. In instances where disease progression or patient mortality had not occurred or where patient survival data was missing or otherwise unavailable these samples were censored from analysis.

Table 3-10 illustrates the median PFS and OS and 95% confidence interval associated with low, normal and high PDGFRB expression levels in both grade 2 and 3 ovarian cancers. The result of log-rank analysis of the significance of the differences in patient survival between gene expression levels is also given. This analysis indicates that differences in PFS and OS observed with differing levels of PDGFRB expression in grade 2 and 3 ovarian cancer were not statistically significant.

3.3.5.2.5 CA125

RT-PCR determined a shift in expression of CA125 in normal ovarian samples including a spread across low, normal and high levels of expression to a pattern of predominantly high expression in ovarian cancer.

This is evident in the CA125 expression level cohorts and their sizes represented in grade 2 and 3 ovarian cancer in Table 3-11. This result of unbiased random sample selection ultimately presents insufficient numbers in the groups expressing CA125 at normal or low levels to allow meaningful comparison to the high expression group.

Table 3-11

Gene	Grade	Expression Level	N	Median PFS 95% CI (upper, lower)	Log Rank (χ^2, p=)	N	Median OS 95% CI (upper, lower)	Log Rank (χ^2, p=)
CA125	2	Low	2	14 (-,-)	0.221, 0.638	2	14 (-,-)	1.231,0.267
		Normal	/	N/a		/	N/a	
		High	15	15 (7.426,22.754)		15	22 (6.453,37.547)	
	3	Low	2	9 (-,-)	1.641,0.440	2	17 (-,-)	0.41, 0.98
		Normal	2	6 (-,-)		2	20 (-,-)	
		High	27	14 (6.367,21.633)		23	22 (7.732,36.268)	

Table 3-11: CA125: Gene Expression Level (Low, Normal, High) Vs Survival.

Comparative CA125 expression was calculated utilising TaqMan® qPCR data and using a randomly selected normal ovary calibrator sample. Fold change (FC) differences for CA125 expression for each sample was categorised as low (FC < 0.5), normal FC (0.5 < FC < 2.0) or high expression (FC > 2.0). SPSS software was utilised to investigate the effect of the level of CA125 expression on patient progression free and overall survival using Kaplan-Meier analysis and determining significance by log-rank analysis. In instances where disease progression or patient mortality had not occurred or where patient survival data was missing or otherwise unavailable these samples were censored from analysis.

Table 3-11 illustrates the median PFS and OS and 95% confidence interval associated with low, normal and high CA125 expression levels in both grade 2 and 3 ovarian cancers. The result of log-rank analysis of the significance of the differences in patient survival between gene expression levels is also given. This analysis indicates that differences in PFS and OS observed with differing levels of CA125 expression in grade 2 and 3 ovarian cancer were not statistically significant.

3.3.5.2.6 VEGFA

As with CA125, RT-PCR determined a shift in expression of VEGFA in normal ovarian samples including a spread across low, normal and high levels of expression to a pattern of primarily high expression in ovarian cancer. This is evident in the VEGFA expression level cohorts and their sizes represented in grade 2 and 3 ovarian cancer in Table 3-12. Due to the small sample sizes in the normal or low VEGFA expressing groups is not possible to perform meaningful statistical analysis to compare the levels of PFS/OS observed in these groups to each other or to the high VEGFA expression group.

Table 3-12

Gene	Grade	Expression Level	N	Median PFS 95% CI (upper, lower)	Log Rank (χ^2, p=)	N	Median OS 95% CI (upper, lower)	Log Rank (χ^2, p=)
VEGFA	2	Low	2	10 (-,-)	0.25, 0.617	4	12 (4.160,19.840)	0.002,0.969
		Normal	/	N/a		/	N/a	
		High	10	15		13	32 (12.049,51.951)	
	3	Low	/	N/a	8.233,0.004	/	N/a	2.592,0.107
		Normal	2	0.4 (-,-)		2	0.4 (-,-)	
		High	29	14 (8.066,19.934)		25	24 (14.757,33.243)	

Table 3-12: VEGFA: Gene Expression Level (Low, Normal, High) Vs Survival.

Comparative VEGFA expression was calculated utilising TaqMan® qPCR data and using a randomly selected normal ovary calibrator sample. Fold change (FC) differences for VEGFA expression for each sample was categorised as low (FC < 0.5), normal FC (0.5 < FC < 2.0) or high expression (FC > 2.0). SPSS software was utilised to investigate the effect of the level of VEGFA expression on patient progression free and overall survival using Kaplan-Meier analysis and determining significance by log-rank analysis. In instances where disease progression or patient mortality had not occurred or where patient survival data was missing or otherwise unavailable these samples were censored from analysis.

Table 3-12 illustrates the median PFS and OS and 95% confidence interval associated with low, normal and high VEGFA expression levels in both grade 2 and 3 ovarian cancers. The result of log-rank analysis of the significance of the differences in patient survival between gene expression levels is also given.

3.3.5.2.7 THPO

A trend of increased median survival metrics (PFS and OS) with reducing THPO expression is observed in grade 2 ovarian cancer (Table 3-13). High THPO expression results in reduced median PFS than normal or low levels of expression (12 months vs 22 months and 24 months respectively).

This trend is repeated for OS in grade 2 ovarian cancers, where normal and low levels of THPO expression return median OS values of 36 and 51 months respectively compared to 12 months reported for those exhibiting high levels of THPO expression. Log rank analysis was performed to examine these differences in PFS and OS observed with the different levels of THPO expression. This analysis determined that while the differences we're approaching significance with PFS and OSA significance values of 0.068 and 0.069 respectively that they failed to reach the threshold for statistical significance in this study.

The trend observed in grade 2 ovarian cancers for increased median PFS and OS with lower THPO expression was not evident on examining the relationship between the level of gene expression and survival in grade 3 ovarian cancers.

It is noteworthy that for several of the genes investigated such as PDGFB, PDGFRA/B, CA125 and VEGF, the proportion of samples returning a either low, normal or high level of expression can in some instances be comparatively few or even absent. This results in a reduced ability to effectively compare the impact/influence of these levels of gene expression in some circumstances.

While this reflects the natural proportion of randomly selected samples returning these differing levels of expression in the ovarian cancer cohorts it does result in a scenario where the populations compared (defined by level of gene expression) can be of very different sizes. Future studies performed that intend to examine the effect of expression level on survival may consider increasing the population size selected to increase the power of the study to assist in overcoming the natural variation in expression levels observed.

Table 3-13

Gene	Grade	Expression Level	N	Median PFS 95% CI (upper, lower)	Log Rank (χ^2, p=)	N	Median OS 95% CI (upper, lower)	Log Rank (χ^2, p=)
THPO	2	Low	9	24 (0,50.296)	5.385,0.068	9	51 (4.637,97.363)	5.343,0.069
		Normal	2	22 (-,-)		1	36 (-,-)	
		High	6	12 (9.737,14.263)		7	12 (9.434,14.566)	
	3	Low	13	10 (2.954,17.016)	2.069,0.355	9	12 (0,26.609)	0.914,0.633
		Normal	11	10 (5.954,14.046)		11	24 (12.132,35.868,)	
		High	7	18 (12.868,23.132)		7	22 (6.797,37.603)	

Table 3-13: THPO: Gene Expression Level (Low, Normal, High) Vs Survival.

Comparative THPO expression was calculated utilising TaqMan® qPCR data and using a randomly selected normal ovary calibrator sample. Fold change (FC) differences for THPO expression for each sample was categorised as low (FC < 0.5), normal FC (0.5 < FC < 2.0) or high expression (FC > 2.0). SPSS software was utilised to investigate the effect of the level of THPO expression on patient progression free and overall survival using Kaplan-Meier analysis and determining significance by log-rank analysis. In instances where disease progression or patient mortality had not occurred or where patient survival data was missing or otherwise unavailable these samples were censored from analysis.

Table 3-13 illustrates the median PFS and OS and 95% confidence interval associated with low, normal and high THPO expression levels in both grade 2 and 3 ovarian cancers. The result of log-rank analysis of the significance of the differences in patient survival between gene expression levels is also given. This analysis indicates that differences in PFS and OS observed with differing levels of THPO expression in grade 2 and 3 ovarian cancer were not statistically significant.

3.3.5.3 Gene Expression Correlation

Spearman's correlations were performed on relative quantitation data returned from RT-PCR TaqMan® assay of target genes in FFPE materials. These were performed to investigate the possible presence of an association between the expression of platelet associated genes and selected biomarkers (RQ values) and patient clinicopathological

metrics including preoperative platelet count and survival (Table 3-14) and an internal correlation investigation between the target genes themselves (Table 3-15).

While correlation investigation is a very useful tool for determining if there is a relationship between variables, a statistically significant positive or inverse correlation is not indicative of a causal relationship between the two but may inform towards future directions of work to investigate that hypothesis.

Table 3-14

			Gene Expression (RQ)						
			PDGFA	**PDGFB**	**PDGFRA**	**PDGFRB**	**THPO**	**CA125**	**VEGF**
Cohort Metrics	**Age**	Corr. Coeff	*0.191*	0.166	-0.056	0.046	0.084	*0.319***	*0.299***
		p =	*0.079*	0.129	0.610	0.674	0.441	*0.003*	*0.006*
	Age (+/- mean)	Corr. Coeff	*0.237**	0.138	0.184	*0.210**	0.096	0.035	0.124
		p =	*0.026*	0.201	0.085	*0.048*	0.370	0.744	0.253
	Grade	Corr. Coeff	0.121	0.202	*-0.277***	*-0.227**	*-0.211**	*0.291***	*0.299***
		p =	0.261	0.059	*0.008*	*0.032*	*0.048*	*0.006*	*0.005*
	Pre-Op Platelet Count	Corr. Coeff	0.032	*0.215**	-0.096	-0.101	-0.192	0.186	0.128
		p =	0.771	*0.048*	0.378	0.356	0.077	0.086	0.245
Survival Metrics	**PFS**	Corr. Coeff	0.048	0.174	0.010	-0.099	0.070	-0.089	0.143
		p =	0.726	0.199	0.940	0.464	0.603	0.513	0.298
	OS	Corr. Coeff	0.174	0.118	0.097	0.058	-0.086	-0.255	0.161
		p =	0.213	0.399	0.486	0.678	0.537	0.062	0.255
	2yr Survival	Corr. Coeff	0.126	0.079	0.078	0.083	-0.131	*-0.283**	0.050
		p =	0.369	0.574	0.573	0.550	0.346	*0.038*	0.725
	5yr Survival	Corr. Coeff	-0.040	-0.043	0.079	-0.101	-0.126	-0.065	-0.007
		p =	0.775	0.760	0.569	0.465	0.362	0.639	0.958

**Correlation is significant at the 0.01 level (2-tailed). *Correlation is significant at the 0.05 level (2-tailed).

Table 3-14: Spearmans' Correlation - Target Gene Expression (RQ values) Vs Patient Cohort and Survival Metrics.

SPSS software was used to examine the correlation between gene expression data and patient cohort and survival metrics.

Significant positive and negative correlations are indicated by italicised and underlined text in Table 3-14.

Results from the Spearmans' correlation between gene expression and patient cohort and survival metrics revealed:

- A statistically significant ($p<0.05$) positive correlation between PGDFA expression and patients age when categorised older or younger than the mean (62.85 years).
- A statistically significant ($p<0.05$) positive correlation between PDGFB expression and preoperative platelet count.
- PDGFA, PDGFB and THPO expression have a statistically significant ($p<0.05$) negative correlations with tumour grade.
- VEGFA and CA125 expression have statistically significant positive correlations with patient age and tumour grade.
- CA125 was the only target gene to return a statistically significant correlation with any survival metric; a statistically significant ($p<0.05$) negative correlation was observed between the gene and 2 year survival. CA125 was also observed to negatively correlate with overall survival but fell short of statistical significance ($p=0.062$).

Results from the Spearmans' correlation between the panel of target genes (Table 3-15) revealed several statistically significant correlations between target genes investigated in this study:

- Both PDGFA and PDGFB strongly correlated with each other, returning strong positive correlations with PDGFRB and CA125 respectively and additionally both positively correlated with VEGF expression (p for all correlations <0.01).

- Both PDGFRA and PDGFRB had a statistically significant positive correlation with each other and inverse correlation with CA125. PDGFRA was observed to have and additional statistically significant correlation with VEGF (inverse) and PDGFRB with PDGFA (positive). p for all correlations was <0.01.

- THPO had no significant correlation with any other target gene investigated.

CA125 and VEGFA returned statistically correlation with each other. As reported above bother genes returned statistically significant correlations with PDGFB (positive) and PDGFRA (inverse). CA125 also returned an inverse correlation with PDGFRB and VEGFA a positive correlation with PDGFA (p for all correlations <0.01).

Table 3-15

		Gene Expression (RQ)						
		PDGFA	**PDGFB**	**PDGFRA**	**PDGFRB**	**THPO**	**CA125**	**VEGF**
PDGFA	Corr. Coeff	1.000	*0.509***	0.157	*0.389***	0.083	0.160	*0.512***
	Sig. (2-tailed)	.	*0.000*	0.144	*0.000*	0.440	0.137	*0.000*
PDGFB	Corr. Coeff	*0.509***	1.000	0.091	0.165	0.036	*0.289***	*0.489***
	Sig. (2-tailed)	*0.000*	.	0.399	0.124	0.740	*0.006*	*0.000*
PDGFRA	Corr. Coeff	0.157	0.091	1.000	*0.723***	0.086	*-0.376***	*-0.315***
	Sig. (2-tailed)	0.144	0.399	.	*0.000*	0.421	*0.000*	*0.003*
PDGFRB	Corr. Coeff	*0.389***	0.165	*0.723***	1.000	0.070	*-0.345***	-0.049
	Sig. (2-tailed)	*0.000*	0.124	*0.000*	.	0.516	*0.001*	0.649
THPO	Corr. Coeff	0.083	0.036	0.086	0.070	1.000	0.071	0.193
	Sig. (2-tailed)	0.440	0.740	0.421	0.516	.	0.510	0.073
CA125	Corr. Coeff	0.160	*0.289***	*-0.376***	*-0.345***	0.071	1.000	*0.549***
	Sig. (2-tailed)	0.137	*0.006*	*0.000*	*0.001*	0.510	.	*0.000*
VEGF	Corr. Coeff	*0.512***	*0.489***	*-0.315***	-0.049	0.193	*0.549***	1.000
	Sig. (2-tailed)	*0.000*	*0.000*	*0.003*	0.649	0.073	*0.000*	.

**Correlation is significant at the 0.01 level (2-tailed). *Correlation is significant at the 0.05 level (2-tailed).

Table 3-15: Spearmans' Correlation - Target Gene Expression (RQ values).

SPSS software was used to examine the correlation between gene expression data and patient cohort and survival metrics.

Significant positive and negative correlations are indicated by italicised and underlined text in Table 3-15.

3.4 Discussion

One-way ANOVA results determined a significant difference in preoperative platelet count exists between the cohorts investigated in this study. Furthermore, t-test analysis determined that the preoperative platelet count of samples in the normal ovary cohort are statistically significantly different to all other groups investigated and Spearmans' correlations preformed indicate a positive correlation between preoperative platelet count and tumour grade, i.e. that an elevated platelet count is associated with increased tumour grade. This data supports the theory that blood platelets may interact with tumour cells to affect their malignant potential – in this instance promoting tumour grade progression. The assoc of elevated platelet count has been observed to correlate with higher grade and disease stage in ovarian cancer (Crasta et al., 2010, Li et al., 2004) but this is the first study using archival tissue samples to reveal this association in ovarian cancer specifically in an Irish study population.

Progression free survival analysis revealed that grade 2 ovarian cancer has an increased progression free survival over grade three ovarian cancer of 4 months though log rank analysis determined these differences to be non-significant. When further investigating PFS through stratification by thrombocytotic status differences in survival for both grade 2 and 3 ovarian cancers were again shown to be non-significant through log-rank analysis. Similarly, when overall survival analysis was performed similar results were returned with differences between grade 2 and 3 ovarian cancer and OS stratified by thrombocytotic status for both grades returning non-significant differences.

Thrombocytosis has been investigated for its prognostic significance and potential to inform on patient survival outcome in many cancers for many years and has been shown to correlate with survival in many cancers, including ovarian cancer. Preoperative thrombocytosis was present in 48% of cancer cohort patients in this study with a 40.6%, 66% and 52.5% occurrence in ovarian cancer grades 2, 2/3 and 3 respectively. Lower percentages have been reported elsewhere with Menczer et al (1998) and Li et al (2004) reporting just 24.3% and 22.4% of subjects with elevated preoperative platelet counts respectively. Taken separately however, the percentages observed in Grade 2 ovarian cancers are comparable to those recoded in investigations performed by Crasta (37.5%)

and Zeimet (38%) (Crasta et al., 2010, Zeimet et al., 1994) and with the grade 3 figure also comparable to the percentage thrombosis Zeimet described present in advanced ovarian cancers preoperatively (56.79%). This suggests that the Irish cohort studied is broadly similar in terms of preoperative thrombocytosis in ovarian cancer and comparable to others studied internationally.

To date investigations performed to examine the relationship between survival and thrombocytosis in ovarian cancer have revealed a wealth of information; however their conclusions regarding thrombocytosis and ovarian disease have often been conflicting or inconsistent.

Thrombocytosis has been shown to have varying association between patient and disease variables, including age, grade, survival, CA125 with some reporting correlations with worse prognoses/survival (Gungor et al., 2009, Haddad and Laufer, 2008, Bozkurt et al., 2004, Gerestein et al., 2009), with a relatively consistent correlation between thrombocytosis and ovarian disease vs normal/benign tissues (Menczer et al., 1998, Friebe et al., 2005, Li et al., 2004, Soonthornthum et al., 2007) but with some revealing no significant bearing on survival, a result consistent with that observed in this study (Nather et al., 2003, Zeimet et al., 1994).

It is note-worthy that variability in the accepted value for thrombocytosis between publications can make comparison of experimental results with and between publications difficult. This study used one of the two most frequently used and accepted values for thrombocytosis previously accepted in previously published, peer-reviewed research. A platelet count of greater than $450x10^9$/L, a figure frequently suggested as relevant for patient management in the clinical setting (Turgeon, 2005) and the second, a platelet count of $400x10^9$/L is frequently utilised in academic research investigations (Gungor et al., 2009, Soonthornthum et al., 2007, Li et al., 2004) and is currently the clinical threshold value for thrombocytosis utilised in sample source laboratory and the medical setting in Ireland. These values are the most prevalent in peer reviewed articles though occasionally other values have been reported on including $300x10^9$/L (Nather et al., 2003), $305x10^9$/L (Soonthornthum et al., 2007), $500x10^9$/L (Griesshammer et al., 1999).

The influence of the metric selected may have a significant effect on the outcome of some analyses. As a case in point and taking 2- and 5-year survival metrics as an example, had a platelet count of greater than $450x10^9$/L been accepted in favour of $400x10^9$/L for thrombocytosis this study would have returned quite different survival percentages (Table 3-16).

Table 3-16

			% Survival if thrombocytosis =	
Survival Metric	**Tumour Grade**	**Group**	**400 X 10^9/L**	**450 X 10^9/L**
2 Year Survival	2	Cumulative	52.39%	
		Normal	33.80%	55.60%
		High	50%	33.30%
	3	Cumulative	51.60%	
		Normal	30.77%*	45.50%
		High	68.75%*	71.40%
5 Year Survival	2	Cumulative	19.50%	
		Normal	15.38%	22.20%
		High	25%	0%
	3	Cumulative	22.58%	
		Normal	23.08%	27.30%
		High	25%	14.30%

*Statistically Significant @ $p<0.05$

Table 3-16: Survival – influence of accepted value for thrombocytosis on % survival at T= 24 and 60 months.

Table 3-16 illustrates the conflicting results that may be returned based on selection of one value for thrombocytosis over another. Accepting thrombocytosis as a platelet count of $>400x10^9$/L returns results that consistently show an elevated preoperative platelet count is associated with a higher % survival in both grade 2 and 3 ovarian cancer at 24 and 60 months post-operative.

Conversely, with the exception of survival at 24 months in the grade 3 ovarian cancer cohort, accepting thrombocytosis as a platelet count of $>450x10^9$ platelets/L returns results for survival at 24 and 60 months post-operative that indicate reduced % survival is associated with preoperative thrombocytosis.

Progression free survival (median) was shown to vary between 12 and 22 months, returning 15 months and 11 months PFS for grade 2 and 3 respectively with other values the result of variation occurring with preoperative platelet count status. This result is broadly similar to that found by Gerestein (2009) who reported a median PFS in ovarian cancer of 15 months a Dutch study population. In addition to informing on the efficacy of cancer treatment and the influence of different variables on the time to cancer recurrence/end of remission PFS has been suggested by some as informative/predictive of OS and a potential surrogate endpoint for clinical trials (Bast et al., 2007, Sargent et al., 2005, Shi and Sargent, 2009, Saad et al., 2010, Amit et al., 2010), though it is accepted that pragmatism should be shown in taking this approach as while the use of surrogate endpoints may reduce the time and cost of performing clinical trials the strength the surrogate measurement may not always be sufficiently strong or accurately reflect OS (Buyse et al., 2011, Buyse et al., 2010, Shi and Sargent, 2009).

This study revealed an overall survival time (median) in ovarian cancer of between 20 and 30 months, returning 22 months overall for both grade 2 and 3 ovarian cancer with variation with preoperative platelet count status. Overall survival reported for ovarian cancer is subject to some variability between studies though an overall survival period (months) between the low forties and mid fifties are not uncommon (Rothenberg et al., 2002, Kosary, 2007) and the values determined in this study fall short of the lower limits of this range.

Two year survival in ovarian cancer in this study returned values if 52.39% and 51.61% for grade 2 and grade 3 ovarian cancers respectively. Interrogated for differences occurring due to preoperative platelet count status two year survival was observed to range from 30.77% to 68.75%. These values are lower than those reported by Rothenberg and colleagues (2002) who found a 2 year survival with ovarian cancer of 65%-70%; a figure reportedly extendable to 92% with optimal tumour debulking, intravenous (IV) and intraperitoneal (IP) chemotherapy, and Kosary (2007) who reported a similar figure of 64% survival at two years.

This study determined five year ovarian cancer survival in the study cohorts to range between 15.3% and 25% with some variation associated with tumour gradation and preoperative platelet count status. 5 year ovarian cancer survival reported in the literature again shows variability between studies. Irish and UK five year ovarian cancer survival figures have recently been reported as:

- Ireland: 40.9% (NCRI, 2006)
- 38% England & Wales (Cooper et al., 2008)
- UK& Ire 39% ranging from 35% Wales, to 41% Ireland (Woods et al., 2010)
- 41% (UK) (Easton et al., 2011)
- Ireland: 36.1% - (NCRI, 2011b)

Extending focus to examine international and multi-country studies five year survival for ovarian cancer has revealed a range of values typically falling 40% ±4% with a few exceptions revealing higher survival figures:

- 36.3% Europe wide five year survival (Berrino et al., 2007)
- 43% survival in the USA at five years (Kosary, 2007).
- 36% to 54% over Northern and Western European countries average 41.6% (Karim-Kos et al., 2008)
- Europe wide five year survival range from 44.1% in Iceland to 63.6% Austria (Moller et al., 2009).

The five year survival percentage determined in this study is significantly less than reported in pervious investigations in Irish/UK populations and in international/multi-country studies, though it is observed that the time span investigated in other investigations is frequently more recent and/or shorter than that from which the cohorts examined in this study were selected (1990-2006) during which ovarian cancer diagnosis, treatment and care are likely to have improved.

PDGF and its receptors pose an attractive target for investigation in ovarian cancer considering their involvement in other cancers and known role as a mitogen at ovarian surface epithelium (Dabrow et al., 1998) and their importance in recruiting pericyte and vascular smooth muscle cells required for successful angiogenesis to occur (Song et al., 2005, Lindahl et al., 1997, Pietras et al., 2008, Greenberg et al., 2008).

Additionally, PDGF and its receptors provide attractive targets for investigation due to their potential contribution to enhancing cancer cell survival and metastasis arising from platelets' rich stores of PDGF (and other cytokines and mitogens) which may be locally delivered to coated cancer cells during TCIPA.

This study revealed significantly increased PDGFB expression compared to normal tissues with increasing tumour grade. PDGFB expression also correlated with pre-operative platelet count. Platelet derived growth factors have recently been shown to influence proliferation though alteration of micro RNA (miRNA) expression which in turn modify the expression of target genes. PDGFAA signalling has been shown to repress miRNA let7d expression effecting an increase in expression of cell cycle regulator cyclin D1 resulting in increased cell entry to S-phase and cell proliferation as a result. PDGFBB was shown to specifically induce *miR-146b* expression resulting in repression of EGFR expression and, it is hypothesised, may influence the balance between growth factor signalling pathways; a PDGF signalling associated mesenchymal phenotype and EGF signalling associated with epithelial phenotype (Shao et al., 2011). This implicates a possible role in platelet related PDGF signalling contributing to the Epithelial to Mesenchymal Transition (EMT) observed to occur in many cancers including ovarian cancer.

As with correlations between thrombocytosis/platelet count and ovarian cancer variables, expression of target genes investigated in this study – notably PDGF and the PDGF receptors – has returned conflicting results. Some studies have previously reported increased expression of one or both PDGFRs in ovarian cancers (Matei et al., 2003, Henriksen et al., 1993, Wilczynski et al., 2005, Rocconi et al., 2008), however in this study both PDGFRA and PDGFRB were observed to undergo reductions in expression with increasing tumour grade in comparison to normal ovarian tissues. These experimental findings are supported by histological patterns of Tissue Micro Array staining published by

the Human Protein Atlas histological staining database (Berglund et al., 2008) and is reminiscent of findings from Versnel et al (1994).

This study found that VEGF expression was significantly increased in addition to PDGFB and that the expression levels of these genes showed strong and statistically significant correlations is in agreement with observations previously made at the protein level in ovarian cancer reported by Matei et al. (2007).

These observations support the hypothesis, in the context of ovarian cancer, that tumour cells increase their production of PDGFB while becoming insensitive to autocrine signalling via reduced PDGFR expression. These may allow the generation of local microenvironments where elevated PDGF ligand availability may signal at endothelial cells, pericytes and vascular smooth muscle (VSM) cells in the nearby stroma to encourage angiogenesis and subsequent access to the circulatory system by extravasating cancer cells via newly formed 'leaky' tumour vessels. This is in part supported by observations elsewhere that PDGFB expression in ovarian cancer is increased and pericytes, essential for establishment of tumour vasculature in conjunction with endothelial cells, express PDGFRB, and interference in this signalling axis utilising imatinib mesylate inhibited pericyte and endothelial cell migration (Lu et al., 2008, Sennino et al., 2009).

Thrombocytosis may have prognostic use in ovarian cancer and as the primary driver of platelet production TPO is an attractive target for investigation. Previous studies revealed evidence of increased TPO expression in ovarian cancer in both patient serum and in tumours, however no correlations were made between thrombopoietin levels and platelet count (Tsukishiro et al., 2008, Ceresa et al., 2007, Wang et al., 1998, Furuhashi et al., 1999).

While expression was not shown to be increased in ovarian cancers in the study population, this study similarly revealed no correlation between TPO expression and patient platelet count in ovarian cancer and gene expression investigation failed to show significant differences in TPO expression in grade two and three ovarian cancer when compared to normal ovarian tissues. From these results it would appear that THPO may

be of little diagnostic value when investigating ovarian malignancy however there does appear to be potential to utilise serum TPO levels to determine malignant ovarian disease from benign ovarian cystic conditions (Tsukishiro et al., 2008) though this requires further investigation.

Thrombopoietin is not solely responsible for driving platelet production, however, with interleukin 6 (IL-6) previously identified as being involved in altering megakaryocytopoiesis via increased TPO production (Kaser et al., 2001). In ovarian cancer, serum IL-6 levels have also been shown to correlate with acites volume, tumour size and reactive thrombocytosis (Plante et al., 1994, Gastl et al., 1993). It may be possible that tumour secreted IL-6 may induce increased THPO expression in the liver and kidneys, thus helping drive cancer related thrombocytosis, a hypothesis that may be investigated in future work. In addition to effecting increases in TPO, IL-6 levels have also been shown to strongly correlate with VEGF in some cancers (Bachelot et al., 2003, Salgado et al., 1999, Benoy et al., 2002).

VEGF is a documented pro-angiogenic factor in many forms of solid tumours and high serum VEGF levels have been proposed as a negative prognostic indicator of outcome in ovarian cancer (Manenti et al., 2003) though this study revealed no correlation with VEGF and any survival metric despite elevated expression being observed in tumour cohorts compared to the normal group.

A recent investigation has suggested that VEGF expression may potentially inform the efficacy of cisplatin treatment in ovarian cancer: here a strong correlation between high VEGF expression (determined immunohistochemically) and platinating agent resistance was observed, patients with low VEGF expression were observed to have; a longer PFS (32 months vs 11 months) with a strong inverse correlation between VEGF expression and overall survival also detected (Siddiqui et al., 2011). The relationship between the level of expression of the genes investigated in this study and platinating agent/chemotherapy resistance or sensitivity fell outside of the remit of this study and this data was not collated. Additionally, the unbiased selection of samples resulted in an impaired ability to effectively compare the effect on survival of different levels of gene expression for several of the target genes including VEGFA. Determination of the effect of target gene

expression on treatment efficacy in addition to survival would be a worthwhile addition to any larger future investigation based on this study.

Several investigations performed to date have returned positive correlation of thrombocytosis with high CA125, more advanced tumour stage and grade, increased ascites & lymph node metastasis and reduced survival, with (Kuyumcuoglu et al., 2010, Li et al., 2004, Soonthornthum et al., 2007). This study reports significant positive correlation with tumour grade and negative correlation with progression free survival in ovarian cancer. No significant correlation was observed with preoperative platelet count or thrombocytosis.

3.5 Conclusion

As with similar investigations, this study is retrospective in nature and allows investigation of a variety of factors allowing associations to be investigated, but lacks the capability to definitively determine causal relationships between study variables.

This study adds to the body of work investigating variables in ovarian cancer for associations with patient outcome and other variables and confirms preoperative thrombocytosis as a potential contributor to ovarian cancer. Preoperative platelet count was discovered to be elevated in ovarian cancer groups compared to controls, and molecular investigation of gene expression variation between normal ovarian tissue and ovarian cancer of increasing grade reveals statistically significant increases in CA125, VEGF and PDGFβ expression with significant decreases in PDGFRα and PDGFRβ. While significant changes THPO expression were not observed between the experimental cohorts it is possible that tumour related IL-6 expression may contribute to malignancy related thrombocytosis through induction on THPO expression elsewhere. As such should future follow up studies be performed attempting to investigate the relationship between gene expression in ovarian cancer and preoperative thrombocytosis include IL-6 assay to examine if this gene plays a role.

This study hypothesises that the alteration in the expression levels of these genes may act towards the generation of a pro-angiogenic local micro environment to potentiate tumour growth and metastasis.

This study returned some very interesting results regarding PDGF receptor expression that may warrant further investigation in the future. PDGFR's have been identified as major therapeutic targets for the treatment of a range of cancers and should these receptors undergo reduced as opposed to increased expression in certain cancers this may have significance in selecting the treatment delivered to patients in the clinical setting.

Larger numbers of patient samples may allow further investigation and fine discrimination of the involvement of thrombocytosis in survival in ovarian cancer in the Irish population and allow refinement of the correlation of expression of target genes with disease and patient variables.

The hypothesis that platelet-tumour cell interaction may influence ovarian cancer progression arising from pro-angiogenic or pro-survival signalling though local release of platelet PDGF and/or VEGF from α-granules during TCIPA requires further attention.

To investigate the relationship between platelets and ovarian cancer further experimental work is required to investigate the physical interaction between ovarian cancer cells and platelets and how this interaction affects the cancer cells to increase their metastatic and malignant potential.

Chapter Three Appendix

Table 3-17

Sample #	Histology	Concentration (ng/µl)	A260/280
1	Normal	15.4	1.83
3	Normal	20.4	1.97
4	Normal	19.0	1.69
5	Normal	10.0	1.86
6	Normal	20.8	1.73
9	Normal	13.6	1.67
11	Normal	29.9	1.83
13B	Normal	7.80	1.41
16B	Normal	9.20	1.24
21B	Normal	13.80	1.36

Table 3-17: Concentration and A260/280 of RNA extracted from FFPE normal ovarian samples.

Table 3-18

Sample #	Histology	RNA (ng/µl)	A260/280
13	GR2	8.3	1.50
14	GR2	8.4	1.49
15	GR2	8.1	1.55
16	GR2	19.1	1.96
17	GR2	9.6	1.42
18	GR2	13.7	1.87
19	GR2	11.6	1.82
20	GR2	9.6	1.46
21	GR2	12.4	1.50
22	GR2	24.4	1.96
23	GR2	10.1	1.56
24	GR2	34.2	1.80
25	GR2	20.1	1.67
26	GR2	11.7	1.90
27	GR2	32.0	1.87
28	GR2	22.3	1.70
29	GR2	11.2	1.53
30	GR2	38.0	1.75

Sample #	Histology	RNA (ng/µl)	A260/280
31	GR2	15.0	1.63
32	GR2	11.6	1.47
33	GR2	8.3	1.36
34	GR2	8.8	1.23
35	GR2	12.5	1.34
36	GR2	5.2	0.92
37	GR2	4.6	0.90
38	GR2	29.1	1.71
39	GR2	17.9	1.61
40	GR2	10.1	1.26
41	GR2	5.2	0.97
42	GR2	10.8	1.33
43	GR2	5.2	1.11
44	GR2	9.4	1.22
45	GR2/3	105.1	1.98
46	GR2/3	45.6	1.86
47	GR2/3	29.6	1.76
48	GR2/3	8.7	1.32
49	GR2/3	11.2	1.54

Table 3-18: Concentration and A260/280 of RNA extracted from FFPE grade 2 and 2/3 ovarian tumour samples.

Table 3-19

Sample #	Histology	RNA (ng/µl)	A260/280	Sample #	Histology	RNA (ng/µl)	A260/280
50	GR3	6.9	1.07	72	GR3	39.7	1.83
51	GR3	37.3	1.55	73	GR3	52.9	1.82
52	GR3	12.1	1.31	74	GR3	28.3	1.91
53	GR3	37.1	1.83	75	GR3	19.9	1.69
54	GR3	24.5	1.78	76	GR3	22.9	1.67
55	GR3	7.7	1.32	77	GR3	125.2	1.99
56	GR3	175.1	2.03	78	GR3	7.4	1.33
57	GR3	11.8	1.57	79	GR3	49.7	1.87
58	GR3	24.0	1.69	80	GR3	19.6	1.67
59	GR3	33.9	1.71	81	GR3	20.0	1.55
60	GR3	61.7	1.93	82	GR3	65.9	1.85
61	GR3	15.1	1.88	83	GR3	2.8	0.95
62	GR3	45.8	2.03	84	GR3	36.4	1.87
63	GR3	10.8	1.67	85	GR3	8.6	1.43
64	GR3	75.7	2.14	86	GR3	5.8	1.27
65	GR3	34.8	1.92	87	GR3	17.2	1.53
66	GR3	5.7	2.10	88	GR3	5.2	1.09
67	GR3	108.6	2.04	89	GR3	6.9	1.03
68	GR3	27.1	2.13	90	GR3	3.6	1.13
69	GR3	76.0	2.11	91	GR3	6.9	1.76
70	GR3	3.7	1.28	92	GR3	19.6	1.67
71	GR3	128.5	2.00	93	GR3	7.6	1.08

Table 3-19: Concentration and A260/280 of RNA extracted from FFPE grade 3 ovarian tumour samples.

CHAPTER FOUR

PLATELET ADHESION TO OVARIAN CELL LINES

4 Platelet Adhesion to Ovarian Cell Lines

4.1 Background

Aim of this component of this thesis is to confirm and compare the interaction of platelets and experimental ovarian cell lines

A series of experimental techniques were selected for use in the experiments that from this chapter:

- A novel adhesion assay for the investigation of cell line:platelet adhesion in a static system; the basis of which is similar to that successfully employed by Biggerstaff and colleagues (2006) and is supported through peer reviewed publication elsewhere (Bazou et al., 2011) to examine adhesion/interaction between monocytes and tumour cells.

- Aggregometry; a well documented and described technique that has been used to describe the magnitude and kinetics of tumour cell induced platelet aggregation (Suzuki-Inoue et al., 2007, Alonso-Escolano et al., 2006, 2004b, Medina et al., 2006, Jurasz et al., 2003, 2001a, Radomski et al., 1991). The technique effectively allows a dynamic *in vitro* spectrophotometric analysis of the reduction of washed platelet suspension turbidity indicative and proportional to platelet aggregation in response to the addition of benign or malignant cell lines and in comparison to a blank representative of 100% aggregation.

- Flow cytometry; a robust technology allowing individual cells to be assessed for markers of platelet activation after co-incubation with fluorescently labelled washed platelets. Each observation (cell) provides an individual experimental data point, with several thousand data points observed per sample.

At the time this component of the thesis was initiated no previous study had been published examining and confirming the capability for cell lines representing ovarian epithelial cancer to induce TCIPA.

4.2 Methodology

4.2.1 Stock Solution Preparation

4.2.1.1 BSA

BSA solutions were prepared according to the Table 4-1.

Table 4-1

Solution ID	Required BSA Concentration	BSA	ddH_2O
Stock A	20% w/v	4g	20ml
Stock B	10% w/v	10ml Stock A	10ml
Stock C	5% w/v	10ml Stock B	10ml

Table 4-1: BSA Solution Preparation.

4.2.1.2 TWEEN 20

Tween solutions were prepared according to the Table 4-2. The volumes of Tween 20 were added using a P1000 pipetter. To allow easy pipetting the tip used was cut approximately 5mm short to create a wider tip diameter suitable for transferring a viscous liquid.

Table 4-2

Solution ID	Required TWEEN 20 Concentration	BSA	ddH_2O
Stock A	1% v/v	200µl	19800µl
Stock B	0.5% v/v	6ml Stock A	6ml
Stock C	0.1% v/v	2ml Stock B	8ml

Table 4-2: TWEEN 20 Solution Preparation.

4.2.1.3 FBS

FBS solutions were prepared according to the Table 4-3.

Table 4-3

Solution ID	Required BSA Concentration	BSA	ddH_2O
Stock A	20% v/v	4ml	16ml
Stock B	10% v/v	10ml Stock A	10ml
Stock C	5% v/v	10ml Stock B	10ml

Table 4-3: FBS Solution Preparation.

4.2.2 Washed Platelet Preparation

For complete details of washed platelet preparation from whole blood see chapter 2 section 2.6.1.

4.2.3 Gel Filtered Platelet Preparation

For complete details of gel filtered platelet preparation see chapter 2, section 2.6.2.2.

4.2.4 Platelet Releasate Preparation

For complete details of platelet releasate preparation see chapter 2, section 2.6.3.

4.2.5 Cell Culture

For complete details of cell culture methodology see chapter 2, section 2.5.

4.2.5.1 Thyrocyte Irradiation

For complete details of the methodology employed for γ-irradiation of thyrocyte cells see chapter 2, section 2.5.9.

4.2.6 RNA Extraction

For complete details of the methodology employed for extraction of total RNA from cell lines see chapter 2, section 2.2.2.1.

4.2.7 TaqMan® Realtime PCR

For complete details of the TaqMan® RT-PCR methodology see chapter 2, section 2.4.1.

Additional details specific to this component of the thesis include the layout for the assay plate for the purpose of ret/PTC-3 detection.

The layout of cell lines, assays and controls employed in this study is as per Table 4-4.

Table 4-4

	1	2	3	4	5	6	7	8
A	p18	p22	p26	NTC	p21	p25	Pos Con	
B	p18	p22	p26	NTC	p21	p25	Pos Con	
C	p18	p22	p26	NTC	p21	p25	Pos Con	
D	p19	p23	p17	p18	p22	p26	NTC	
E	p19	p23	p17	p18	p22	p26	NTC	
F	p19	p23	p17	p18	p22	p26	NTC	
G	p20	p24	p69	p19	p23	p17		
H	p20	p24	p69	p19	p23	p17		
I	p20	p24	p69	p19	p23	p 17		
J	p21	p25	Pos Con	p20	p24	p69		
K	p21	p25	Pos Con	p20	p24	p69		
L	p21	p25	Pos Con	p20	p24	p69		

Key:				
Cell Line	HIOE-80	4Gy Nthy-ori 3-1	Nthy-ori 3-1	
Assay	ret/PTC-3	ret/PTC-3	ret/PTC-3	
	CDKN1B	CDKN1B	CDKN1B	

Table 4-4: ret/PTC-3 TaqMan® RT-PCR Assay Plate Layout.

Cell line and assay are indicated by colour with sample passage number indicated in the plate diagram.

Positive Control was performed using a plasmid encoding for ret/PTC-3 fusion site.

No Template Control was performed using ddH_20 in place of sample tRNA.

4.2.7.1 Primers

The primer sequences used in the investigation of ret/PTC-3 transcript presence were as per used by Finn et al (2004). The primer and probe sequences for the ret/PTC-3 assay are as provided in Table 4-5. CDKN1B was selected as experimental endogenous control.

Table 4-5

ret/PTC-3 TaqMan™ Primer-probeset	
Forward Primer Sequence	AAC CAA GTT CTT CCG AGG GAA T
Probe Sequence	CCA CTT TGG ATC CTC CTG
Reverse Primer Sequence	TGT TCT CCA AGG TCT GCT TTT G

Table 4-5: ret/PTC-3 TaqMan™ Primer-probeset.

4.2.8 Platelet Adhesion Assay

For complete details for performing the platelet adhesion assay utilised in this component of the thesis see chapter 2, section 2.7.1.

4.2.9 Aggregometry Assay

For complete details for performing the aggregometry assay utilised in this component of the thesis see chapter 2, section 2.7.2.

4.2.10 Flow Cytometry Assay

For complete details for performing the flow cytometry assay utilised in this component of the thesis see chapter 2, section 2.8.1.

4.3 Results

4.3.1 In Vitro Adhesion Assay Optimisation

Initial experimentation was performed to determine if:

1. The technique for fluorescently labelling (calcein AM loading) platelets was effectively detectable using the technologies selected.
2. The suitability of cell culture optimised multi-well plates for use in the assay as ELISA plates do not allow sufficiently robust cell attachment for the application intended given the number of wash steps involved.
3. The positive and negative controls for platelet adhesion, fibrinogen (20µg/ml), and JNL buffer (vehicle only negative control).

All data was normalised against adhesion to the positive control condition (fibrinogen, 20µg/ml), revealing increased platelet adhesion to uncoated experimental wells.

This initial assay revealed that platelets successfully adhere to the experimental positive control given the employed experimental protocol. This experiment also revealed however that the surface of the unblocked/uncoated experimental wells was capable of causing platelets to adhere to it with a greater ability than that displayed by the fibrinogen coated positive control wells (Figure 4-1).

This finding necessitated the development of a blocking strategy to minimise the non-specific adhesion of platelets to the growth surface of experimental wells.

Figure 4-1

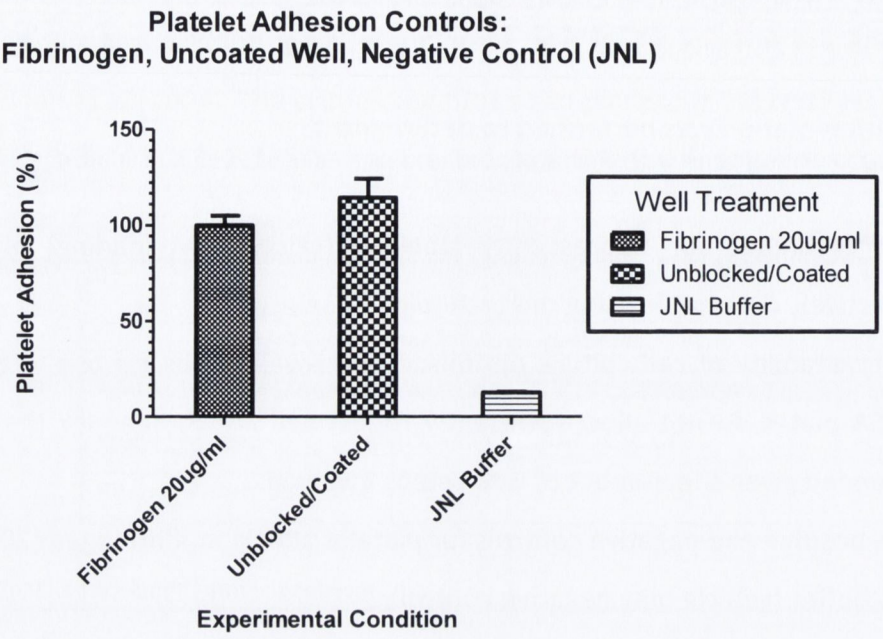

Figure 4-1: Adhesion of calcein AM loaded platelets to positive control (fibrinogen) coated and uncoated assay wells and JNL (vehicle) negative control.

Fibrinogen solution (20µg/ml) was applied to experimental positive control wells overnight at 37°C. Washed platelets were prepared and loaded with calcein AM dye. Platelet adhesion to fibrinogen coated, uncoated wells and vehicle only negative control wells was assessed.

Results support the use of fibrinogen as a positive control for platelet adhesion while indicating a necessity to develop an effective blocking strategy to minimise non-specific platlet adhesion. For all data N=4 and bars indicate mean ± SEM.

4.3.1.1 Assay Blocking Strategies

Prior to beginning in depth platelet-cancer cell adhesion investigation a series of experiments were performed to determine the optimal blocking agent available to mitigate the non-specific biding of washed/gel filtered platelets to the assay wells used in the performance of the adhesion experiments. The aim of this blocking exercise was to determine the strategy that was most efficacious at preventing non-specific binding to the plate yet having the minimal effect on adhesion to the experimental positive control, 20µg/ml fibrinogen.

All wells were washed three times with 200µl JNL buffer and 200µl blocking agent applied to all wells with the exception of no blocking agent controls and incubated for 45 minutes at 37°C. Blocking agents tested included BSA, FBS, TWEEN 20 at a range of percentage concentrations.

Following incubation of the blocking agent the wells were briefly washed x3 with 200µl JNL and calcein-AM dye loaded platelets delivered to the wells and incubated for 45 minutes at 37°C. At the end of the incubation total platelet fluorescence was measured, the wells washed 3x with JNL and residual fluorescence, indicative of platelet adhesion, measured.

4.3.1.1.1 BSA Blocking

BSA has previously been utilised as an effective blocking agent in a variety of different assay types and has been described as effective in blocking hydrophilic (and hydrophobic) surfaces similar to those employed in this study (Jeyachandran et al., 2010).

Figure 4-2 illustrates platelet adhesion to assay multi-well plates that were either pre-coated in fibrinogen or left uncoated prior to blocking with three different blocking concentrations of BSA to interrogate the efficacy of these treatments in eliminating non-specific platelet adhesion to the growth surface after subsequent platelet exposure.

All data was normalised against platelet adhesion to the positive control (fibrinogen) in the abence of a blocking concentration of BSA.

The use of 5% BSA as a blocking agent revealed least impact on platelet adhesion to the fibrinogen positive control wells compared to 10% and 20% BSA blocking which resulted in comparative reductions in platelet adhesion to fibrinogen by ~47% and ~67% respectively.

Figure 4-2

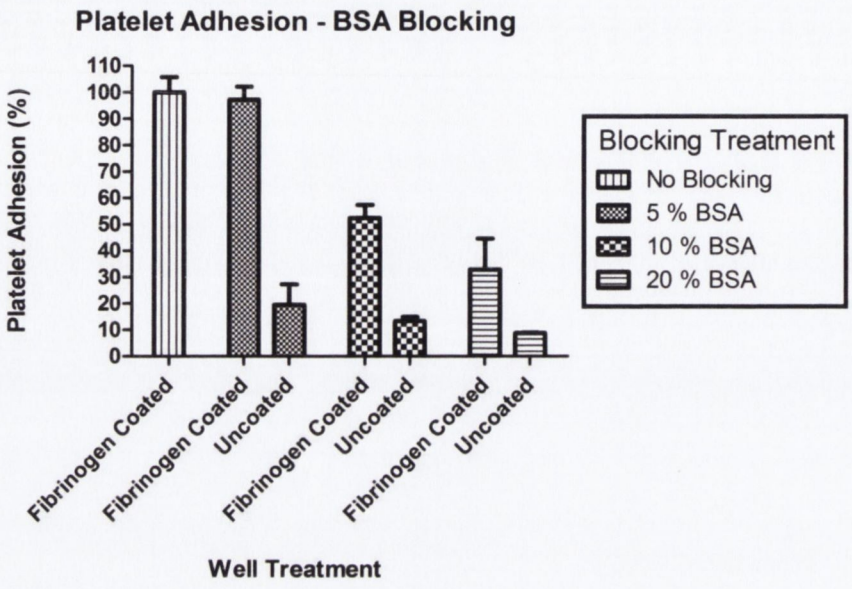

Figure 4-2: Blocking Strategy for Non-specific Platelet Adhesion – BSA.

Fibrinogen solution (20μg/ml) was applied to experimental positive control wells overnight at 37°C. Washed platelets were prepared and loaded with calcein AM dye. Platelet adhesion to fibrinogen coated and uncoated wells was assessed in the presence and absence of prior treatment with 5%, 10% and 20% BSA blocking solutions. Results were normalised to platelet adhesion to fibrinogen only. Blocking with a 5% BSA solution was observed to have least impact on platelet adhesion to the fibrinogen positive control wells compared to 10% and 20% BSA blocking which resulted in comparative reductions in platelet adhesion to fibrinogen by ~47% and ~67%. For all groups N=3 and bars indicate mean ± SEM.

4.3.1.1.2 TWEEN 20 Blocking

TWEEN 20 is a non-ionic detergent that has been used as a blocking agent in ELISA and other types of immuno-assay as an effective blocking agent to prevent non-specific binding affecting assay results (Esser, 2010). Arising from promising results as a blocking agent indicated by Esser TWEEN 20 was assessed for its potential use as a blocking agent in this study.

Figure 4-3 illustrates platelet adhesion to assay multi-well plates that were either pre-coated in fibrinogen or left uncoated prior to blocking with three different blocking

concentrations of TWEEN 20 to interrogate the efficacy of these treatments in eliminating non-specific platelet adhesion to the growth surface after subsequent platelet exposure.

As before all data was normalised against platelet adhesion to the positive control (fibrinogen) in the absence of a blocking solution of TWEEN 20. Platelet adhesion in the presence of 5% BSA solution is included for comparative purposes.

The use of TWEEN 20 as a blocking agent revealed little effect on reducing nonspecific platelet adhesion to uncoated wells. Higher blocking concentrations of TWEEN 20 returned platelet adhesion values greater than those reported for fibrinogen coated wells.

Figure 4-3

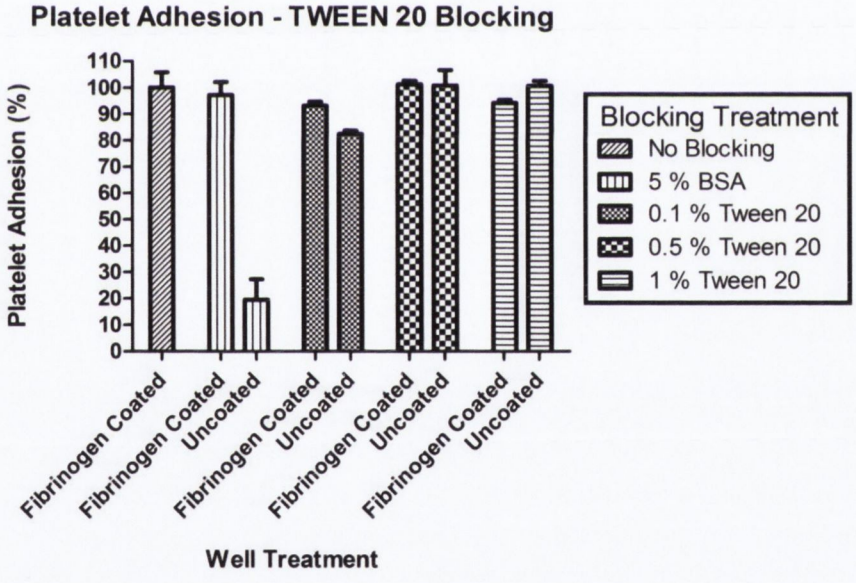

Figure 4-3: Blocking Strategy for Non-specific Platelet Adhesion – TWEEN.

Fibrinogen solution (20µg/ml) was applied to experimental positive control wells overnight at 37°C. Washed platelets were prepared and loaded with calcein AM dye. Platelet adhesion to fibrinogen coated and uncoated wells was assessed in the presence and absence of prior treatment with 0.1%, 0.5% and 1% TWEEN 20 blocking solutions. Results were normalised to platelet adhesion to fibrinogen only and indicate Tween 20 did not demonsrate efficacy in blocking nonspecific platelet adhesion.

For all groups N=3 and bars indicate mean ± SEM. Platelet adhesion in the presence of 5% BSA solution is included for comparative purposes.

4.3.1.1.3 FBS Blocking

Foetal Bovine Serum (FBS) is used in a similar manner to BSA for the purposes of blocking in many assay types. It is frequently used in those requiring effective blocking to ensure high specificity antibody binding such as ELISA, fluorescence microscopy and western blot. FBS provides a heterogeneous protein source to block binding to non-target epitopes/binding sites.

Figure 4-4

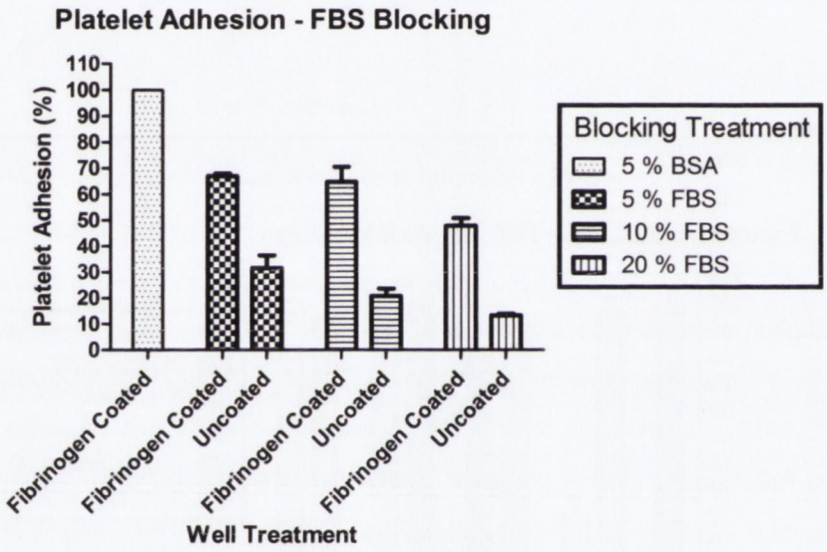

Figure 4-4: Blocking Strategy for Non-specific Platelet Adhesion – FBS.

For all groups N=4 and bars indicate mean ± SEM.

Figure 4-4 illustrates platelet adhesion to assay multi-well plates that were either pre-coated in fibrinogen or left uncoated prior to blocking with three different blocking concentrations of FBS to interrogate the efficacy of these treatments in eliminating non-specific platelet adhesion to the growth surface after subsequent platelet exposure.

As before all data was normalised against platelet adhesion to the positive control (fibrinogen) when blocked with BSA (5%).

The use of FBS as a blocking agent revealed showed efficacy in reducing non-specific platelet adhesion to the growth surface of experimental wells. At 10% and 20% concentrations the percentage of platelet adhesion to untreated wells was similar to that recorded by blocking with 5% BSA although the use of FBS reduced adhesion to the fibrinogen positive control by 33%-53% compared to that recorded with 5% BSA blocking.

Arising from this series of optimisation experiments a 5% BSA solution was selected for use as a blocking agent in all subsequent experiments with the risk of non-specific platelet adhesion to the growth surface of experimental wells further reduced by growing cells to confluence in the wells prior to performing adhesion assays.

4.3.1.2 *In Vitro* Platelet Adhesion Assay

4.3.1.3 Adhesion Assay: Preliminary Testing

Having optimised the system designed to test for platelet adhesion to experimental cell lines preliminary testing was performed.

These preliminary investigations were performed over a set of cell lines representing immortalised normal epithelium, malignantly transformed immortalised epithelium and malignant epithelial carcinoma.

The cell lines utilised were Nthy-ori 3-1, normal immortalised thyroid epithelial cells, 4Gy γ-irradiated Nthy-ori 3-1 malignantly transformed epithelial cells and 59M ovarian epithelial carcinoma cells. The Nthy-ori 3-1 thyroid line was selected due to similarities between thyroid and ovarian cancers, both may be of epithelial origin, may be hormone sensitive, can have similar underlying oncogenes such as B-type Raf kinase (BRAF) and possibly ret/PTC (Sieben et al., 2004, Nakayama et al., 2008, Flavin et al., 2009). Additionally there is evidence to support use of this cell line for transformation to create a line of increase malignant potential.

Previous work performed by Finn et al (2004) revealed that exposure of Nthy-ori 3-1 cells to a 4Gy exposure of gamma radiation resulted in the formation of the ret/PTC-3 chimeric transcripts. This transcript is prevalent in thyroid tumours detected in children following

the Chernobyl nuclear accident which resulted in significant environmental contamination of γ-radiation emitting caesium-137 (along with β-radiation emitting isotopes iodine-131 and strontium-90).

Platelet adhesion to immortalised, immortalised & transformed thyroid and malignant ovarian epithelial cell lines was assessed using the previously optimised *in vitro* fluorescent adhesion assay.

Platelet adhesion (n=8) was assessed in each condition and using freshly prepared gel filtered platelets isolated from three healthy female volunteers. Gel filtered platelets were used in order to examine the pure interaction of platelets with ovarian cancer cells i.e. that the interaction was mediated by direct platelet-cancer cell adhesion and not by other constituents of the blood such as plasma proteins such as fibrinogen. While there is little evidence of intergender differences in platelet function/activity only female donors were used in these investigations. Given current conflicting information regarding gender differences in platelet reactivity (Otahbachi et al., 2010, Eshel-Green et al., 2009, Beyan et al., 2006) the decision was made to eliminate this variable from the study of a female specific cancer by using female source platelets.

All data was normalised against platelet adhesion to the experimental positive control well coated with fibrinogen in Microsoft Excel and Graphpad Prism utilised to analyse the experiment data and generate graphs to visualise the results (Figure 4-5).

Platelet adhesion was observed to increase with increasing malignant potential from 19.6%-28%[†] to Nthy-ori 3-1 cells, increasing to 34.8%-41.7%[†] to 4Gy Nthy-ori 3-1 cells and further increased to 136.9%-164.6%[†] in the 59M cell line.

[†] Percentage platelet adhesion indicated is relative to percentage adhering to fibrinogen control (100%).

Figure 4-5

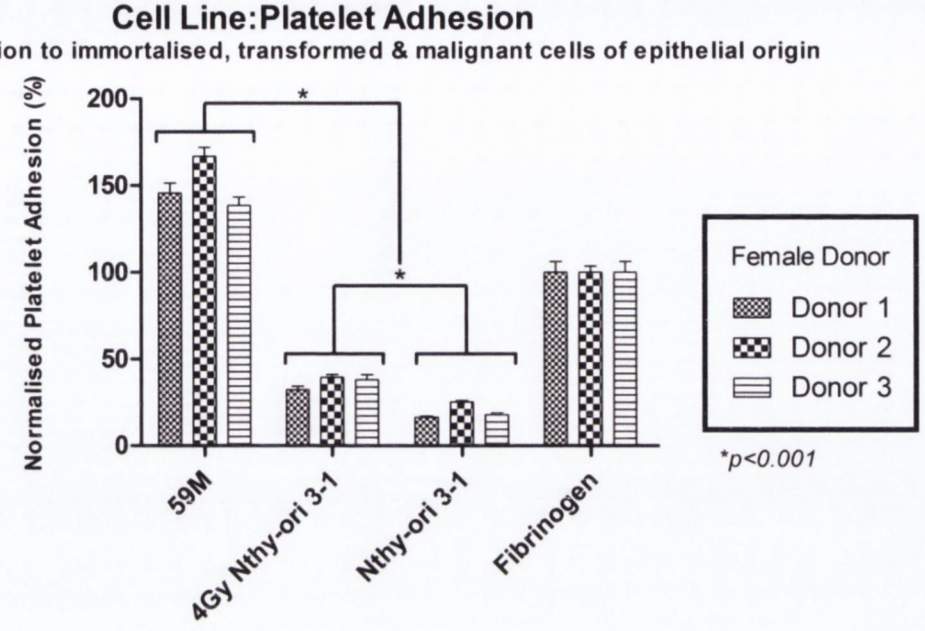

Figure 4-5: Platelet adhesion to a panel of cell lines of epithelial origin.

Washed platelets were prepared from whole blood taken from three female donors and loaded witrh calcein AM dye. Cell lines representing a spectrum of epithelial cell health; including normal thyroid epithelial cells (Nthy-ori 3-1), irradiated thyroid epithelial cells (4Gy Nthy-ori 3-1) and malignant ovarian epithelial carcinoma (59M), were grown to confluence on experimental wells (N=8) of a multiwell plate. Positive control wells were coated with fibrinogen (20μg/ml). Prior to assay of platelet adhesion all experimental wells were blocked using a 5% BSA solution. Dye loaded washed platelets were applied to cell lines and controls and co-incubated at 37°C for 45 minutes. After reading total calcein AM fluorescence experimental wells were washed and remaining fluorescence reflecting adherent platelets recorded. The percentage of platelets adhering was calculated and results normalised against platelet adhesion to fibrinogen.

Platelet adhesion was observed to increase with increasing malignant potential. The cell line representing normal epithelial cells reported 19.6%-28% platelet adhesion, increasing to 34.8%-41.7% in γ-irradiated epithelial cells and further increased to 136.9%-164.6% in the epithelial carcinoma cell line[†].

[†] Platelet adhesion as relative to that adhering to fibrinogen control (100%).

T test investigations performed on adhesion data determined the differences in platelet adhesion between immortalised and malignantly transformed cells was statistically

significant as was the difference in platelet adhesion between the ovarian carcinoma cell line and both thyroid source cell lines for each platelet donor (Table 4-6).

Table 4-6

Donor	For Comparison		*p* =	Significant
	Group 1	Group 2		
Donor1	59M	4Gy Nthy-ori 3-1	2.72463E-11	Yes
	59M	Nthy-ori 3-1	2.40334E-12	Yes
	4Gy Nthy-ori 3-1	Nthy-ori 3-1	2.21418E-06	Yes
Donor2	59M	4Gy Nthy-ori 3-1	1.05587E-12	Yes
	59M	Nthy-ori 3-1	1.05587E-12	Yes
	4Gy Nthy-ori 3-1	Nthy-ori 3-1	4.41559E-06	Yes
Donor3	59M	4Gy Nthy-ori 3-1	4.09561E-11	Yes
	59M	Nthy-ori 3-1	4.71712E-13	Yes
	4Gy Nthy-ori 3-1	Nthy-ori 3-1	1.57982E-05	Yes

Table 4-6: T-test Comparison of Platelet Adhesion to Cell Lines.

4.3.1.3.1 ret/PTC-3 Detection

Previous work performed by Finn et al (2004) indicated the presence of ret/PTC-3 transcripts in normal thyrocytes following γ-irradiation. This formation and expression of this fusion transcript is associated with malignant transformation of thyrocytes and the radiation exposure modelled that resulting from the Chernobyl nuclear accident, known to be associated with an increase in thyroid cancers.

Having identified an increased capacity for the γ-irradiated Nthy-ori 3-1 thyrocyte cell line to induce platelet adhesion to their surface qPCR was performed to investigate the presence of ret/PTC3. In order to confirm the presence of the fusion transcript in irradiated thyrocytes total RNA was extracted from cell passages prior to irradiation and from surplus cells during passaging post irradiation.

Total RNA was also extracted from human immortalised ovarian epithelial cells (HIOE-80) to act as negative controls for ret/PTC transcript presence. Total RNA was reverse

transcribed prior to assay using the Applied Biosystems High Capacity Reverse Transcription Kit.

4.3.1.3.1.1 RNA Analysis

Total RNA was assessed by Nanodrop™ to determine sample purity and concentration.

Table 4-7

Cell Line	Passage	Days Post/Prior IR	ng/µl	Δ260/280
Nthy-ori 3-1	17	0	997.8	2.12
4Gy Nthy-ori 3-1	18	3	603.9	2.14
4Gy Nthy-ori 3-1	19	7	835.1	2.13
4Gy Nthy-ori 3-1	20	11	2407	2.08
4Gy Nthy-ori 3-1	21	15	957.3	2.12
4Gy Nthy-ori 3-1	22	19	961.7	2.09
4Gy Nthy-ori 3-1	23	25	1101.1	2.12
4Gy Nthy-ori 3-1	24	28	1228.6	2.12
4Gy Nthy-ori 3-1	24	28	1244.6	2.12
4Gy Nthy-ori 3-1	25	33	1261.7	2.11
4Gy Nthy-ori 3-1	26	36	1783.8	2.11
4Gy Nthy-ori 3-1	26	36	2120.7	2.12
Nthy-ori 3-1	26	N/a	942.7	2.13
HIOE-80	69	N/a	1518.7	2.11
HIOE-80	69	N/a	1069.4	2.11

Table 4-7: Nanodrop assessment of cell line tRNA for ret/PTC-3 detection.

Table 4-7 Indicates all the cell samples from which RNA was extracted returned sufficient quantities of tRNA (603ng/µl – 2120ng/µl) and of sufficiently high purity to allow TaqMan® assays be performed with confidence in the starting materials.

4.3.1.3.1.2 TaqMan RT-PCR Results

TaqMan real-time PCR assay (Figure 4-6) for the presence of the ret/PTC-3 transcript revealed no evidence of expression of the fusion protein in γ-irradiated thyrocyctes.

Figure 4-6

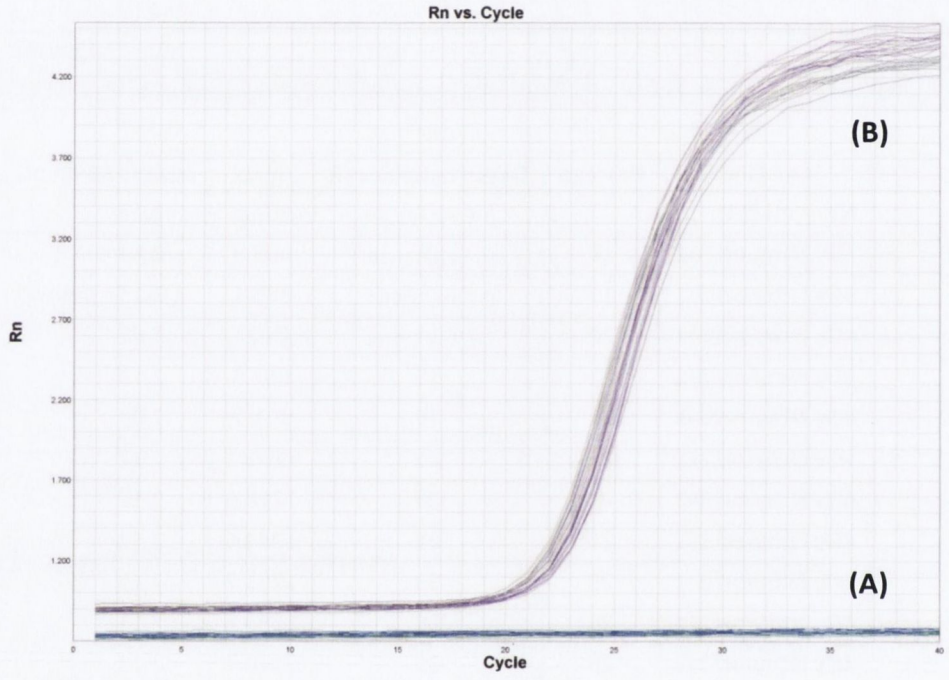

Figure 4-6: TaqMan ret/PTC-3 assay in γ-irradiated thyrocytes.

The figure indicates the fluorescent signal returned for the detection of ret/PTC-3 fusion transcripts with increasing amplification cycles (A) and fluorescent detection of the experimental endogenous control CDKN1B (B).

The 4Gy Nthy-ori 3-1 γ-irradiated cell line was observed to display an altered morphology and a propensity for more rapid cell division compared to the parental Nthy-ori 3-1 cell line. These cells required more frequent passaging when seeded at an identical density to the parental cells.

This supports the hypothesis that 4Gy γ-irradiation is capable of malignantly transforming the parental cell line into one displaying one or more of the hallmarks of cancer, in this instance, de-differentiation and increased proliferation.

The genetic changes induced by irradiation of the Nthy-ori cell line resulting in these phenotypic changes and increased capacity to induce platelet adhesion are unclear and may warrant further investigation though falling outside of the remit of this study. Whole transcriptome and/or genome analysis technologies may be efficacious in determining these γ-irradiation induced changes.

The absence of the ret/PTC-3 transcript in the tested time-course of irradiated cell passages warranted the establishment of a new panel of cells representing normal tissues and tissues of increasing malignancy.

4.3.1.4 *In Vitro* Platelet Adhesion Assay: Ovarian Cell Lines

The previously tested platelet-cell line adhesion assay was employed to assess the ability for a second panel of cell lines to adhere platelets to their surface. This second panel was specifically limited to cells of ovarian origin and included:

- HIOE-80 – normal human immortalised ovarian epithelial cells
- 59M – ovarian epithelial carcinoma
- A2780 – ovarian epithelial carcinoma
- A2780cis – cisplatin resistant daughter cell line of A2780 ovarian epithelial carcinoma.

Platelets were extracted from healthy female donors (N=3) and their adhesion to four ovarian cell lines studied (N=6). The data recorded was adjusted for blank measurements and normalised against experimental positive control wells coated in fibrinogen. Figure 4-7 illustrates the resulting graph generated using pooled data and displays mean platelet adhesion ± SEM to ovarian cell lines.

The trend for increased capacity to induce platelet adhesion with increased malignant potential previously observed utilising normal & malignantly transformed thyroid epithelial and malignant ovarian epithelial cells is present in this study.

Figure 4-7

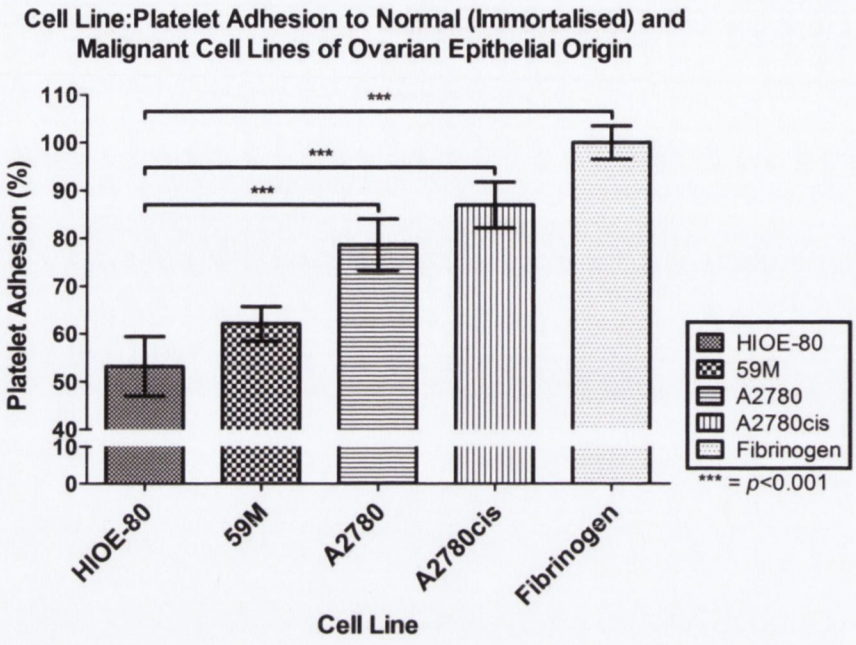

Figure 4-7: Platelet Adhesion to Ovarian Cell Lines.

Washed platelets were prepared from whole blood taken from three female donors and loaded witrh calcein AM dye. Cell lines representing a spectrum of ovarian epithelial cell health; including normal epithelial cells (HIOE-80), malignant ovarian epithelial carcinoma (59M and A2780), and malignant cisplatin resistant ovarian epithelial carcinoma, were grown to confluence on experimental wells (N=6) of a multiwell plate. Positive control wells were coated with fibrinogen (20µg/ml). Prior to assay of platelet adhesion all experimental wells were blocked using a 5% BSA solution. Dye loaded washed platelets were applied to cell lines and controls and co-incubated at 37°C for 45 minutes. After reading total calcein AM fluorescence experimental wells were washed and remaining fluorescence reflecting adherent platelets recorded. The percentage of platelets adhering was calculated and results normalised against platelet adhesion to fibrinogen.

Platelet adhesion was observed to increase with increasing malignant potential from normal ovarian epithelial cells to cisplatin resistant ovarian epithelial carcinoma cells representative of recurrent refractory ovarian malignancy.

4.3.1.4.1 Microscopic Visualisation of Platelet:Cell Line Adhesion

Bright field images of each cell line were captured following measurement of *in vitro* fluorescent assay of platelet-cell adhesion. The purpose of capturing these images was not to measure the magnitude of platelet adhesion but to visually confirm the presence of adherent platelets having performed the assay.

Representative images at 40X magnification were captured allowing visual confirmation of platelet adhesion to HIOE-80, 59M (Figure 4-8), A2780 and A2780cis cell lines (Figure 4-9).

Platelets were identified by their size and morphology. Platelets and platelet aggregeates are visible as small white objects in each image.

Figure 4-8

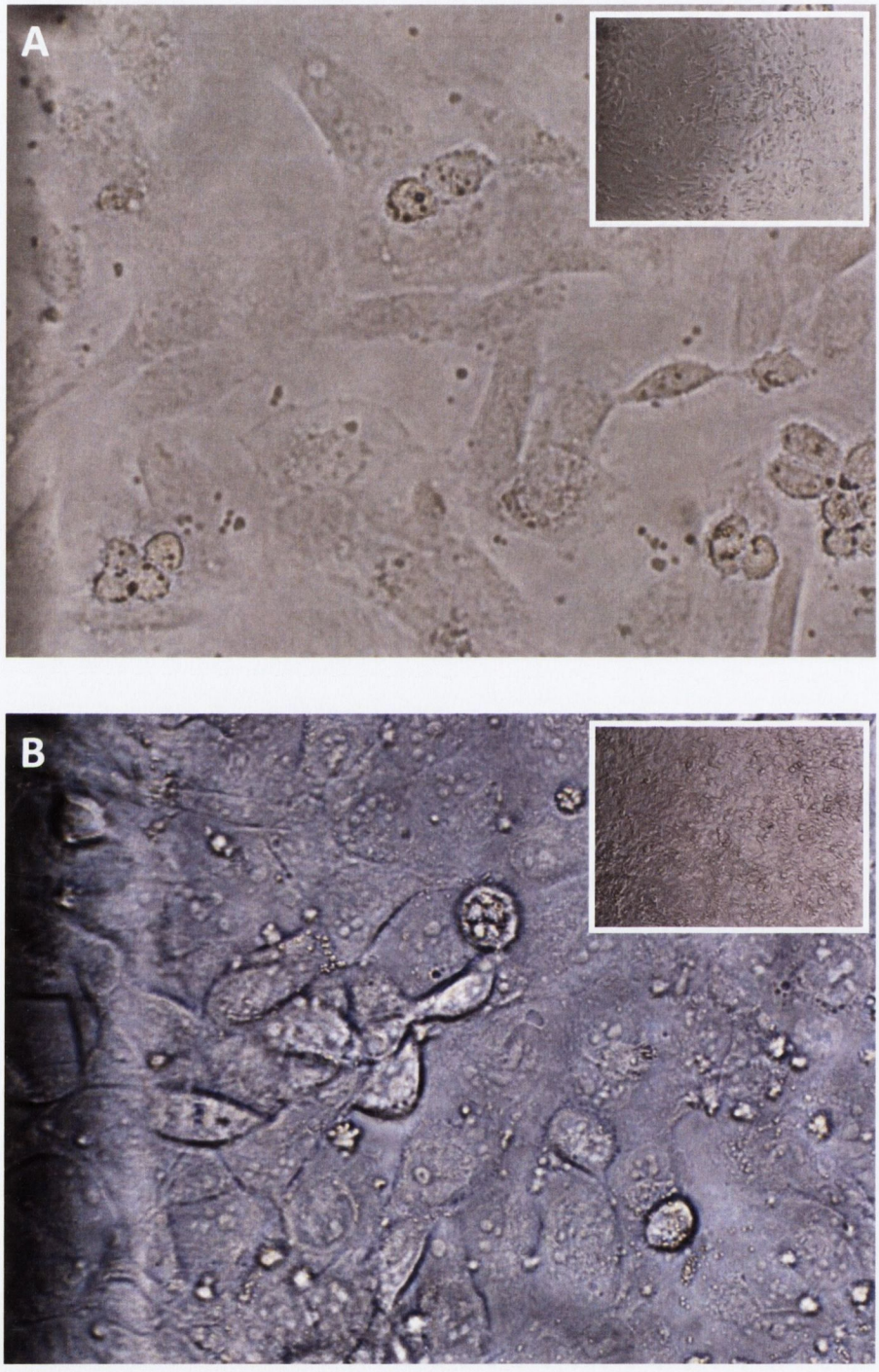

Figure 4-8: 40x Brightfield Photomicrograph of Platelet Adhesion to HIOE-80 and 59M Cells.

(A): 40x Brightfield Photomicrograph of Platelet Adhesion to HIOE-80 Cells.

(B): 40x Brightfield Photomicrograph of Platelet Adhesion to 59M Cells.

10x images (inset) illustrate the high confluence to which cells were grown prior to assay in order to minimise non specific platelet adhesion.

Figure 4-9

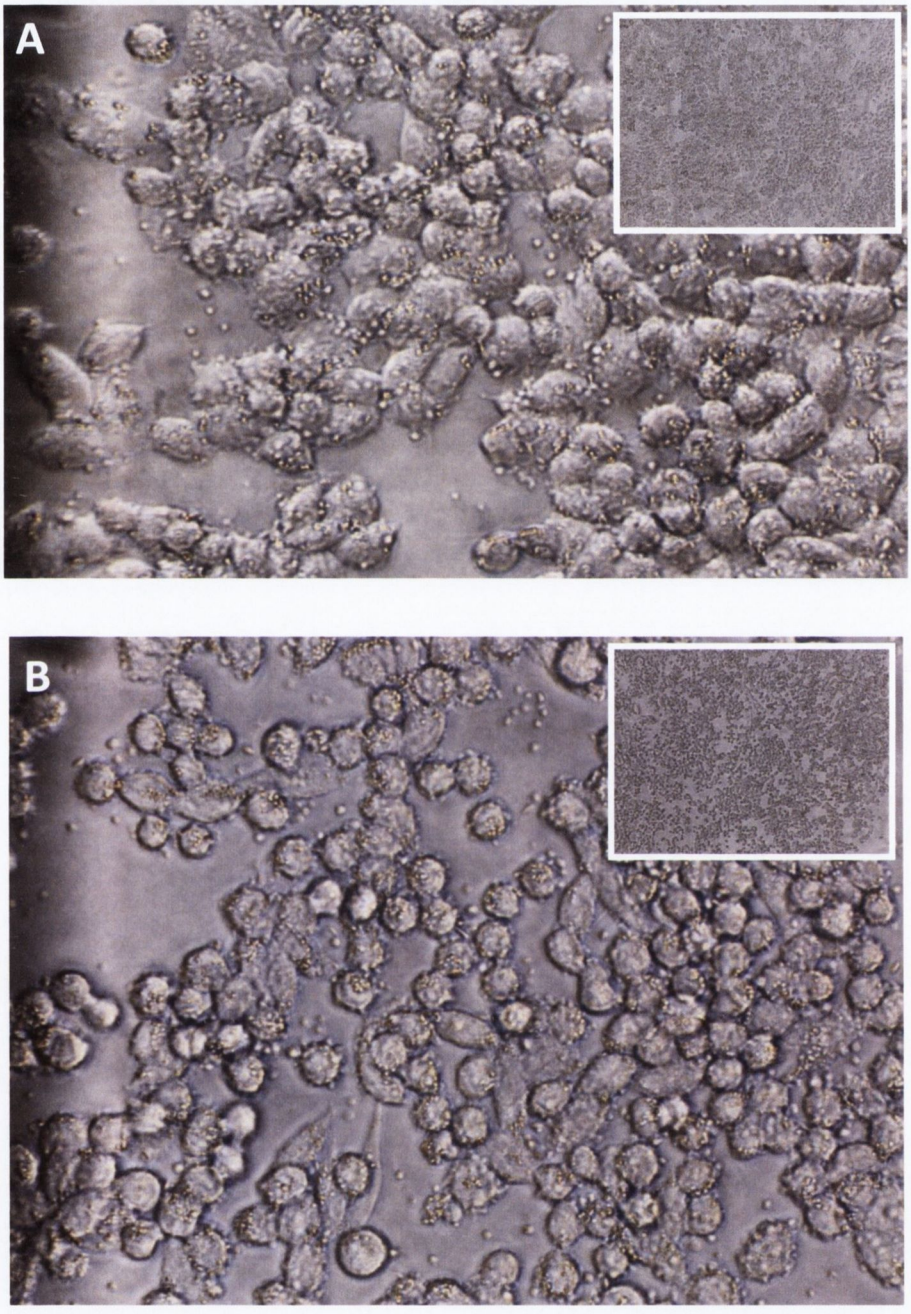

Figure 4-9: 40x Brightfield Photomicrograph of Platelet Adhesion to A2780 and A2780cis Cells.

(A): 40x Brightfield Photomicrograph of Platelet Adhesion to A2780 Cells.

(B): 40x Brightfield Photomicrograph of Platelet Adhesion to A2780cis Cells.

10x images (inset) illustrate the high confluence to which cells were grown prior to assay in order to minimise non specific platelet adhesion.

Reflecting the results recorded in the previously observed adhesion assay, HIOE-80 cells were observed to be less able to induce platelet adhesion to their surface. Photomicrographs of 59M, A2780 and A2780cis revealed platelet adhesion visibly congruent with the results of the *in vitro* adhesion assay with increased platelet adhesion easily visible in the captured photo micrographs.

Every attempt was made to ensure that cells were grown to a confluent monolayer, thus reducing the area of exposed growth surface for non-specific platelet adhesion to occur. While a contiguous cell monolayer would provide an equal area of cells to assess specific adhesion to it is clear that the cell lines utilised did not always naturally proliferate to obscure the entire growth surface, a shortcoming addressed through the incorporation of a 5% BSA blocking step in the experimental protocol.

The observed high efficacy of BSA blocking previously determined during assay optimisation is further supported by the small number of platelets adhering to unoccupied growth surface in the captured photomicrographs, most clearly seen in Figure 4-9, where platelet adhesion to exposed growth surface is minimal.

4.3.2 Aggregometry Analysis of TCIPA

To inform further to the nature of the platelet-cell line adhesion relationship a series of experiments were performed in order to determine if the capability of cells to induce adhesion to their surface/TCIPA was linear following a dose dependant relationship or if a saturation point could be reached where increased cell numbers returned no further increases in platelet adhesion. These experiments utilised a form or spectroscopy known as aggregometry, a technique used in other studies investigating platelet function and TCIPA in the past (Radomski et al., 1992, Sawicki et al., 1998, Alonso-Escolano et al., 2004b, Medina et al., 2006).

The Bio/Data Corp PAP-4 Aggregation Profiler (Bio/Data Corp., Horsham, PA, USA) utilised to perform aggregometry studies allows the simultaneous measurement of aggregation in four experimental cuvettes.

Then device allows measurement of platelet adhesion/aggregation through comparing light transmission though an experimental cuvette against a blank. Reduced turbidity of a platelet suspension arising from addition of a platelet aggregating agent results in increased light transmission proportional to platelet activation and this is compared against a vehicle only blank representing 100% aggregation and a hard copy of the data recorded over the duration of an experiment by an inbuilt printer.

This enabled cells to be assessed for their capability to induce platelet aggregation at a range of cell concentrations from $1x10^5$ cells/ml to $1x10^3$ cells/ml with the fourth cuvette exposure to Thrombin Receptor Activating Protein (TRAP) performed to confirm platelet responsiveness.

Figure 4-10 is a representative illustration of the data returned from the aggregometry experiments. The TRAP positive control returned a rapid induction of platelet aggregation (slope of aggregation = 57) and an aggregation at T=16 minutes of 76%. Cell concentrations of $1x10^5$, $1x10^4$ and $1x10^3$ cells/ml did not result in platelet aggregation being detected using this method.

Further assay of cell lines at a concentration of $1x10^5$ cells/ml ability to induce platelet aggregation similarly revealed a quick aggregation triggered by TRAP exposure (slope of aggregation = 57) with an aggregation at T=16 minutes of 92%. In this assay all cell lines investigated similarly failed to induce platelet aggregation using this technique (Figure 4-11).

The ability of cells to induce platelet aggregation given washed platelets in a physiological buffer augmented with fibrinogen was queried and further aggregometry investigation performed using platelet rich plasma (PRP) in place of washed platelets. PRP was prepared from whole blood by centrifugation and subsequent careful of the PRP fraction from red and white blood cells deposited during the process. The ability of the four cell lines investigated to induce platelet aggregation in PRP was assessed with a high cell concentration ($1x10^5$ cells/ml) failing to result in induction of platelet aggregation/activation (Figure 4-12).

Figure 4-10

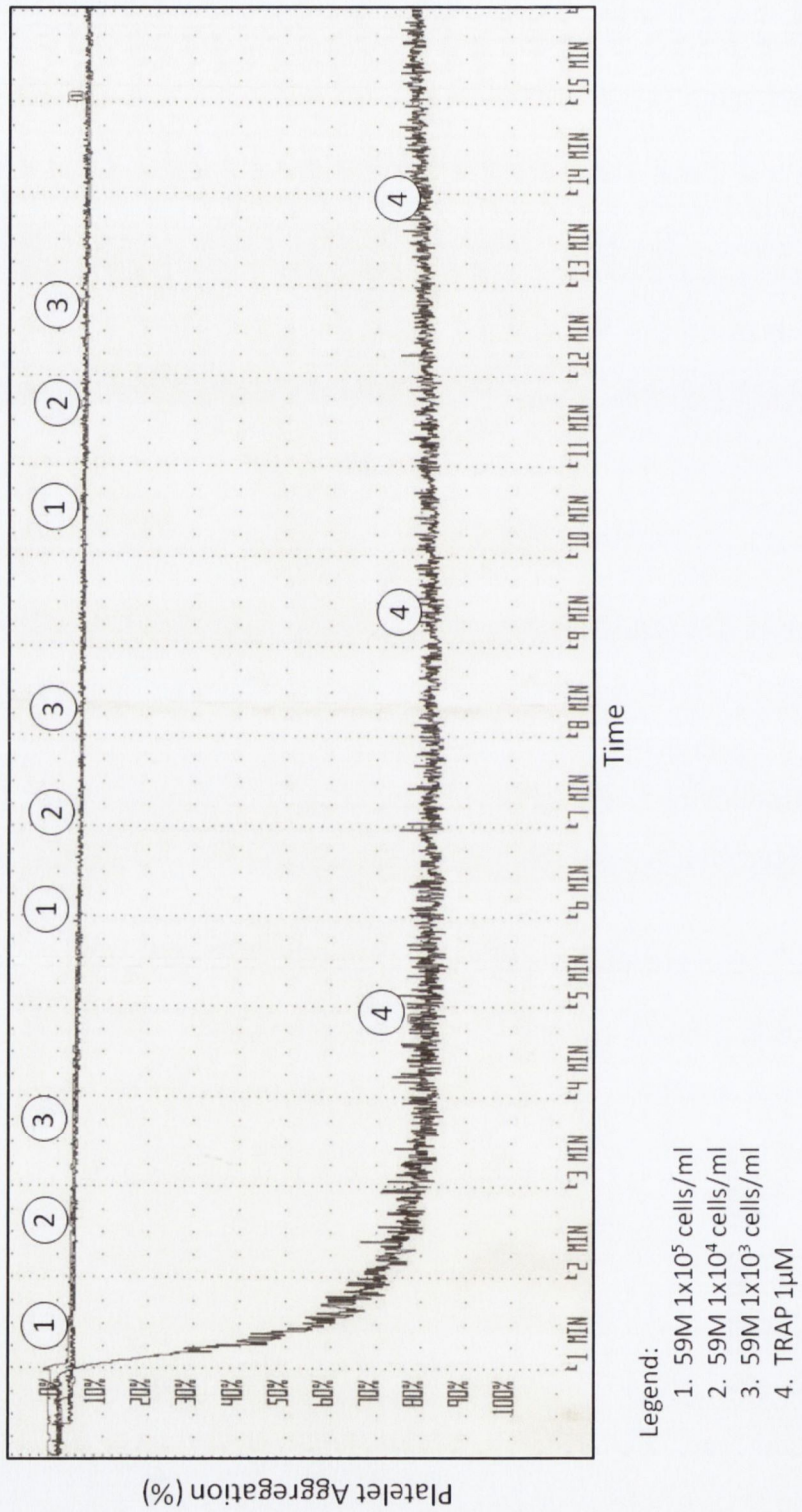

Figure 4-10: Aggregometry – 59M Ovarian Carcinoma induced Washed Platelet Aggregation.

Representative aggregometry result of one cell line (59M) at three concentrations with TRAP aggregation positive control.

Figure 4-11

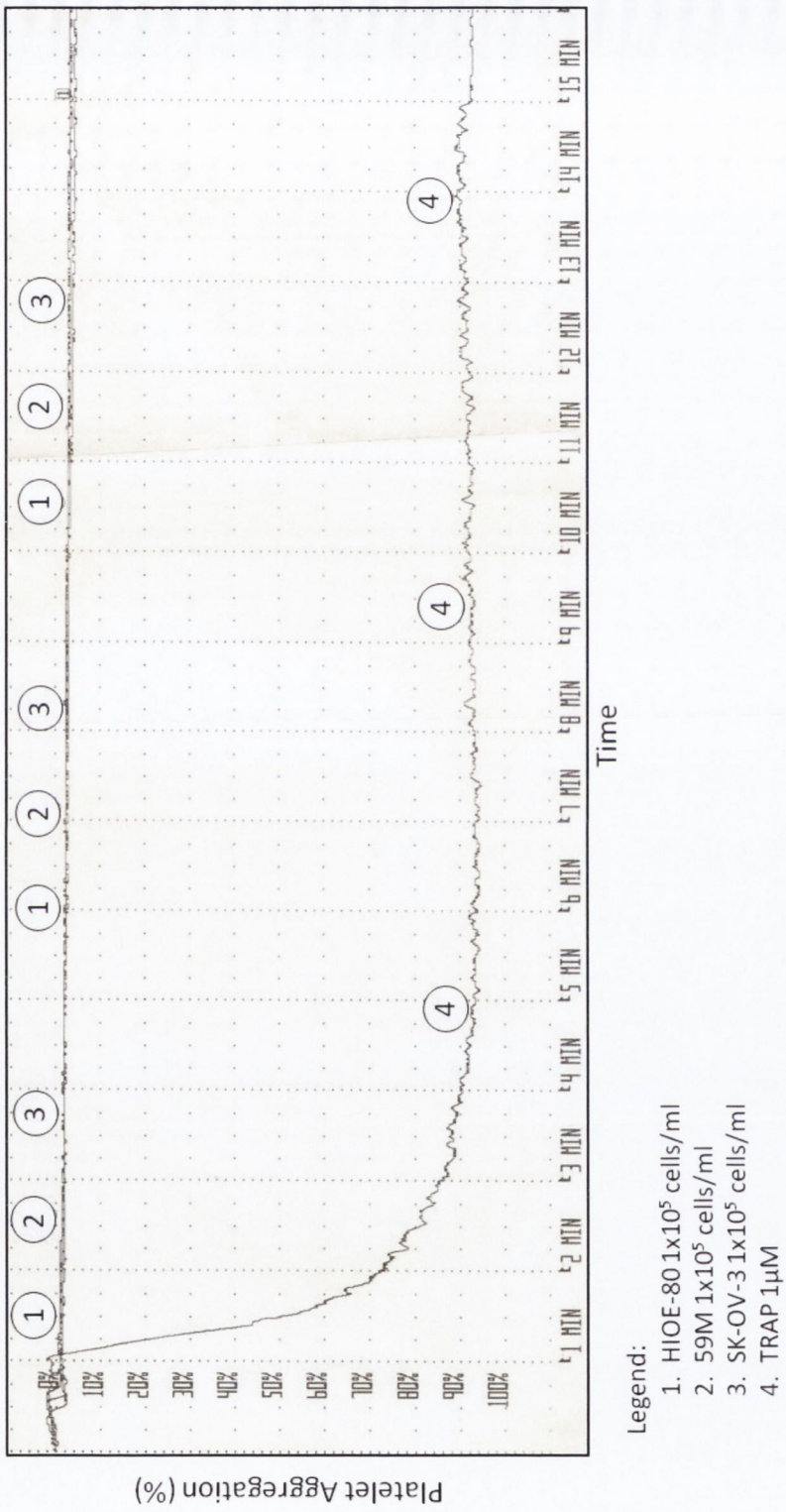

Figure 4-11: Aggregometry – Ovarian Cell Line induced Washed Platelet Aggregation

Aggregometry graph of platelet aggregation induced by the addition of three cell lines (HIOE-80, 59M & SK-OV-3) at $1x10^5$ cells/ml (F_c) with TRAP aggregation positive control.

Figure 4-12

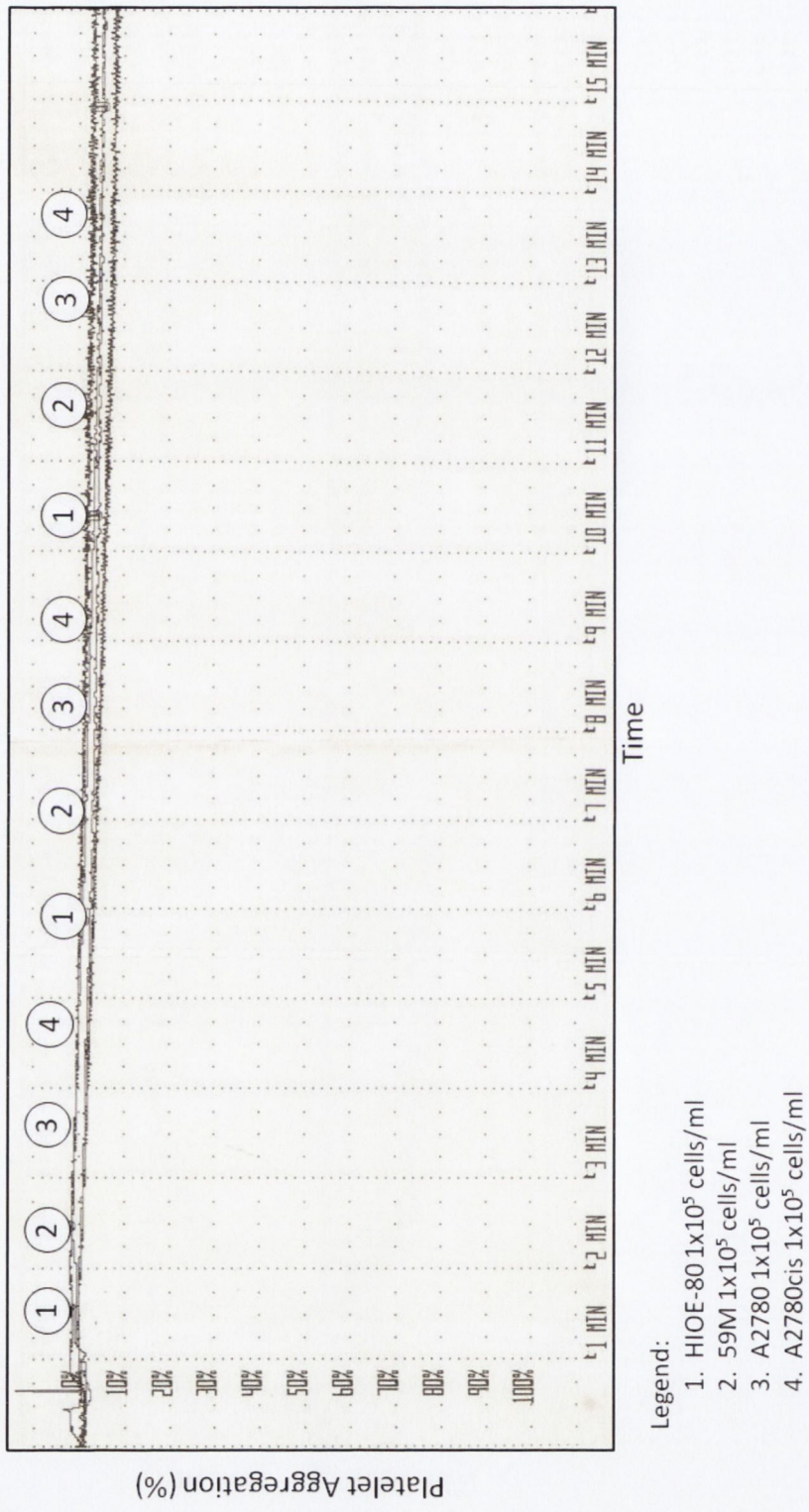

Figure 4-12: Aggregometry – Ovarian Cell Line induced Platelet Rich Plasma (PRP) Aggregation.

Aggregometry graph of platelet aggregation induced by the addition of four cell lines (HIOE-80, 59M, A2780 & A2780cis) at 1 x 10^5 cells/ml (F_c) to platelet rich plasma (PRP).

4.3.3 Flow Cytometry Analysis of Cell Line Induced Platelet Activation

Having attempted to monitor cells ability to induce platelet adhesion/aggregation though aggregometry, work progressed to investigating cells ability to induce platelet adhesion/activation through flow cytometry based experiments.

The aim of these studies was to investigate cell-platelet adhesion though analysis of cell lines following co-incubation with washed platelets and detection of adhering platelets using fluorescently labelled platelet specific markers.

Two markers were investigated:

- p-selectin - stored in resting platelets in the α-granules and is only expressed on the surface of platelets following activation and degranulation where it acts as an adhesion molecule promoting platelet adhesion to the endothelium, (Larsen et al., 1989, Hamburger and McEver, 1990) and an assisting molecule in haematogenous dissemination of circulating tumour cells (Garcia et al., 2007, Varki and Varki, 2002, Borsig et al., 2001, Kim et al., 1998).

- $\alpha_{2b}\beta_3$ – the most abundant platelet integrin receptor, it is a major platelet specific protein (Hynes, 1992). α2bβ3 is a heterodimeric receptor consisting of an α- and β-subunit for fibrinogen, fibronectin and von Willebrand Factor (Phillips et al., 1988) and is a critical mediator of outside in signalling in platelets (Shattil et al., 1998, Law et al., 1996), important for adhesion and spread in the absence of direct prior agonist signalling and supports platelet adhesion, platelet-platelet interaction and thrombus formation *in vivo* (Patel et al., 2003).

4.3.3.1 P-selectin

Flow cytometry was used to examine platelet activation resulting from TCIPA. This resulted in the generation of data reflecting the percentage of cells exhibiting p-selectin presence indicative of activated adherent platelets following platelet:cell line co-incubation.

Platelet rich plasma (PRP) was prepared from whole blood taken from healthy female donors (N=3) who had not taken any substances known to affect platelet function in the ten days prior to donation. PRP was adjusted to a platelet count of $2x10^8$ platelets/ml. Cell lines were grown under normal culture conditions, non-enzymatically detached and adjusted to concentrations between $1x10^6$ cells/ml and $1.5x10^7$ cells/ml. In a total reaction volume of 100µl, 10µl of cell line suspension was incubated with PRP for 15 minutes at room temperature in the presence of a PE conjugated mouse anti-human p-selectin/CD62 IgG antibody (BD Pharmigen, USA) or an unconjugated mouse anti-human p-selectin/CD62 IgG isotype control antibody. 100µl PRP activated by 15 minutes incubation in the presence of TRAP (20µM) was utilised as positive control for platelet activation. After 15 minutes the reaction was terminated by addition of 1 ml of JNL buffer prior to flow cytometry analysis.

Histograms describing these analyses were generated displaying gated cell counts vs p-selectin fluorescence intensity (Figure 4-13, Figure 3-14 and Figure 4-15). In all prepared histograms the TRAP positive control shows a large right shifted spike numbers of gated counts (platelets) that are activated p-selectin positive along with greater p-selectin fluorescence.

The gating data was then analysed with GraphPad Prism allowing the generation of a line graph illustrating mean % of cells presenting with a p-selectin signal indicative of activated platelets adhering to their surface. Data was adjusted for buffer control and normalised against TRAP.

Figure 4-13

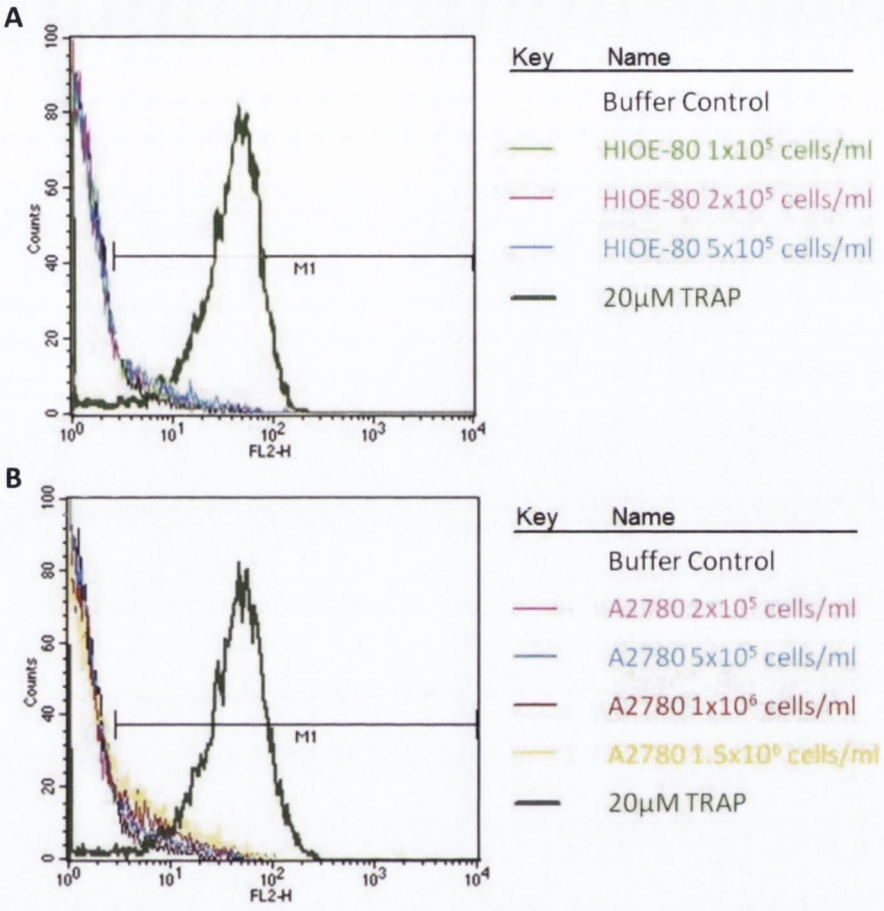

Figure 4-13: Flow Cytometry Histograms p-selectin fluorescence vs HIOE-80 and A2780 cell count.

Platelet rich plasma (PRP) was prepared from whole blood taken from healthy female donors (N=3). PRP was adjusted to $2x10^8$ platelets/ml. Cell lines were grown under normal culture conditions, non-enzymatically detached and adjusted to concentrations between $1x10^6$ cells/ml and $1.5x10^7$ cells/ml. 10µl of cell line suspension was incubated with 90 µl PRP for 15 minutes at room temperature in the presence of a PE conjugated mouse anti-human p-selectin/CD62 IgG antibody or an unconjugated mouse anti-human p-selectin/CD62 IgG isotype control antibody. 100µl PRP activated by 15 minutes incubation in the presence of TRAP (20µM) was utilised as positive control for platelet activation.

Figure 4-13 (A) is a flow cytometry histogram representative of p-selectin fluorescence resulting from increasing HIOE-80 cell exposure to washed platelets and resultant cell induced platelet aggregation. There was very little difference to buffer only control and little change in fluorescence in response to increase cell concentration. Figure 4-13 (B) is a flow cytometry histogram representative of p-selectin fluorescence resulting from increasing A2780 cell exposure to washed platelets and resultant cell induced platelet aggregation. A trend of increased numbers of gated cells presenting with p-selectin associated fluorescence is clearly visible, though the increases between cell concentrations are small.

Figure 4-14

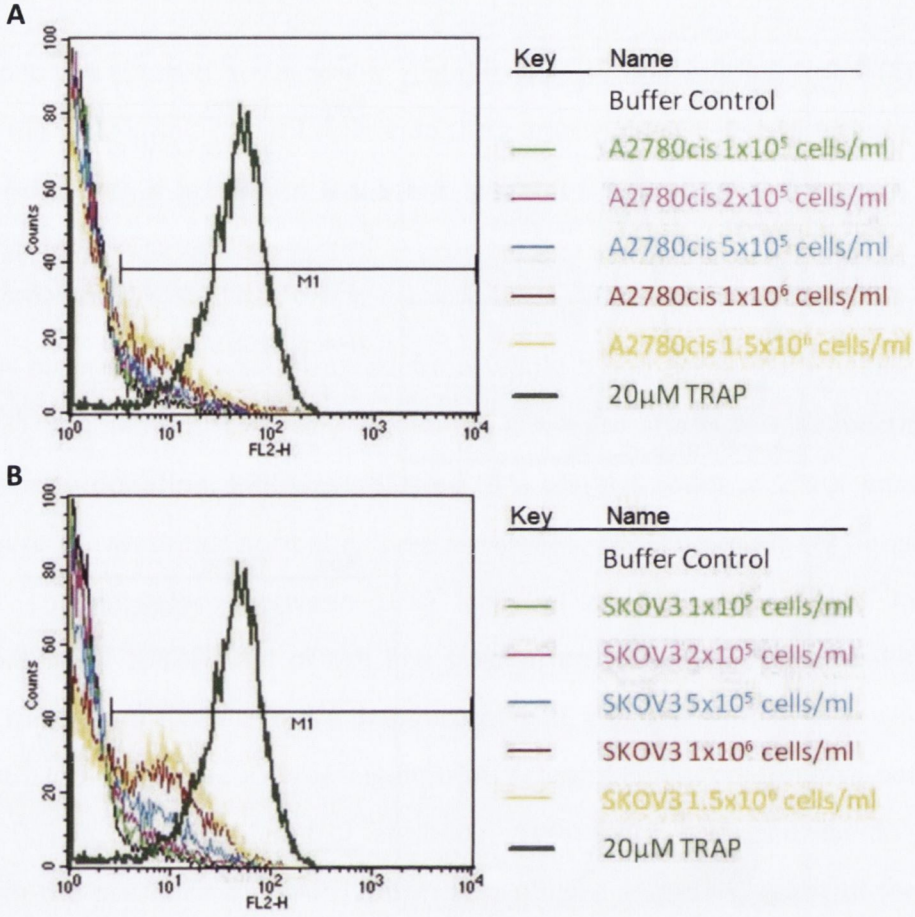

Figure 4-14: Flow Cytometry Histograms p-selectin fluorescence vs A2780cis and SK-OV-3 cell count

Platelets and cell lines were prepared as described in Figure 4-13.

Figure 4-14 (A) is a flow cytometry histogram representative of p-selectin fluorescence resulting from increasing A2780cis cell exposure to washed platelets and resultant cell induced platelet aggregation. The image clearly shows a small but stepwise increase in numbers of cells presenting with p-selectin associated fluorescence.

Figure 4-14 (B) is a flow cytometry histogram representative of p-selectin fluorescence resulting from increasing SK-OV-3 cell exposure to washed platelets and resultant cell induced platelet aggregation. A defined pattern of increased numbers of gated cells presenting with p-selectin associated fluorescence with increasing cell concentration is clearly visible.

Figure 4-15

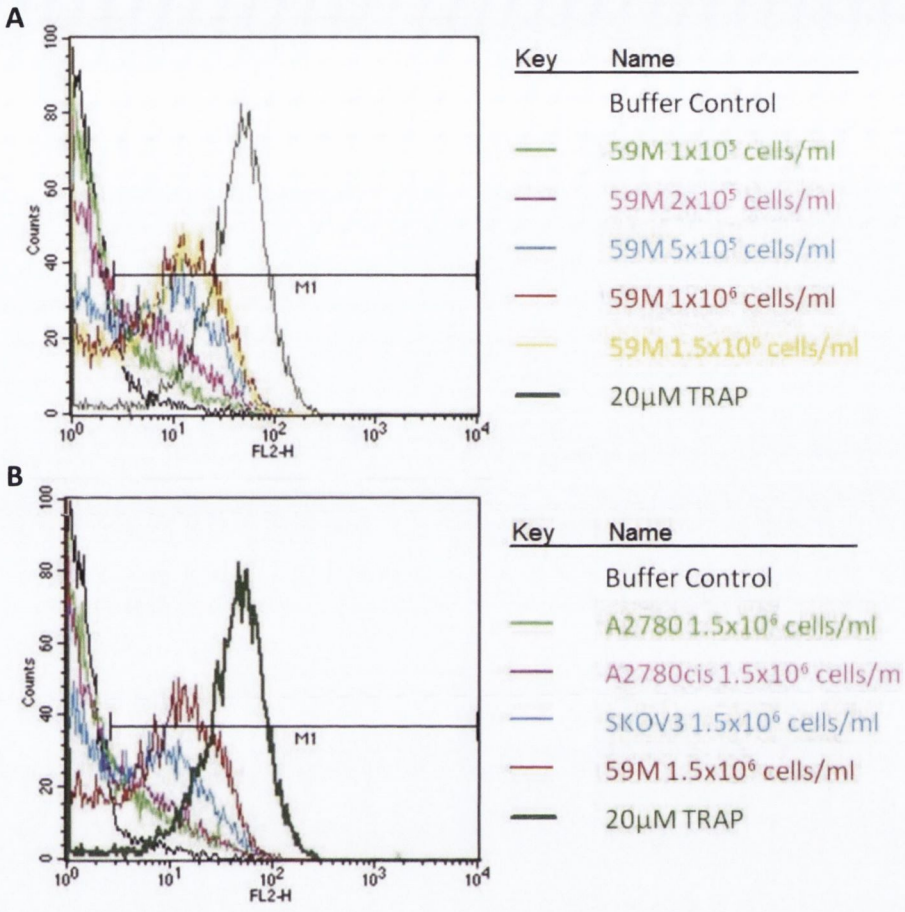

Figure 4-15: Flow Cytometry Histograms p-selectin fluorescence vs 59M cell count and a panel of cancer cell lines at 1.5x10^6 cells/ml.

Platelets and cell lines were prepared as described in Figure 4-13.

Figure 4-15 (A) is a flow cytometry histogram representative of p-selectin fluorescence resulting from increasing 59M cell exposure to washed platelets and resultant cell induced platelet aggregation. The image clearly shows a small but stepwise increase in numbers of cells presenting with p-selectin associated fluorescence.

Figure 4-15 (B) is a flow cytometry histogram representative of p-selectin fluorescence resulting from exposure of a panel of cell lines (A2780, A2780cis, SK-OV-3 & 59M) at a concentration of 1.5x10^6 cells/ml to washed platelets and resultant cell induced platelet aggregation. A defined pattern of increased p-selectin presence indicative of adherent activated platelets is visible. The A2780cis cell line displays greater p-selectin presence than the parental A2780 cell line, the SK-OV-3 cell line induced further increased p-selectin presence with the 59M cell line returning the highest values with the given cell concentration.

Figure 4-16 graphically illustrates the gating data recorded for the percentage of observations for each exposure (control or cell line) gating positive for p-selectin, indicative of adherent, activated platelets. The mean p-selectin values ± SEM illustrated are provided in Appendix Figure 4-1 at the end of this chapter.

The data was adjusted to take into account background indicated by the buffer only control.

Figure 4-16

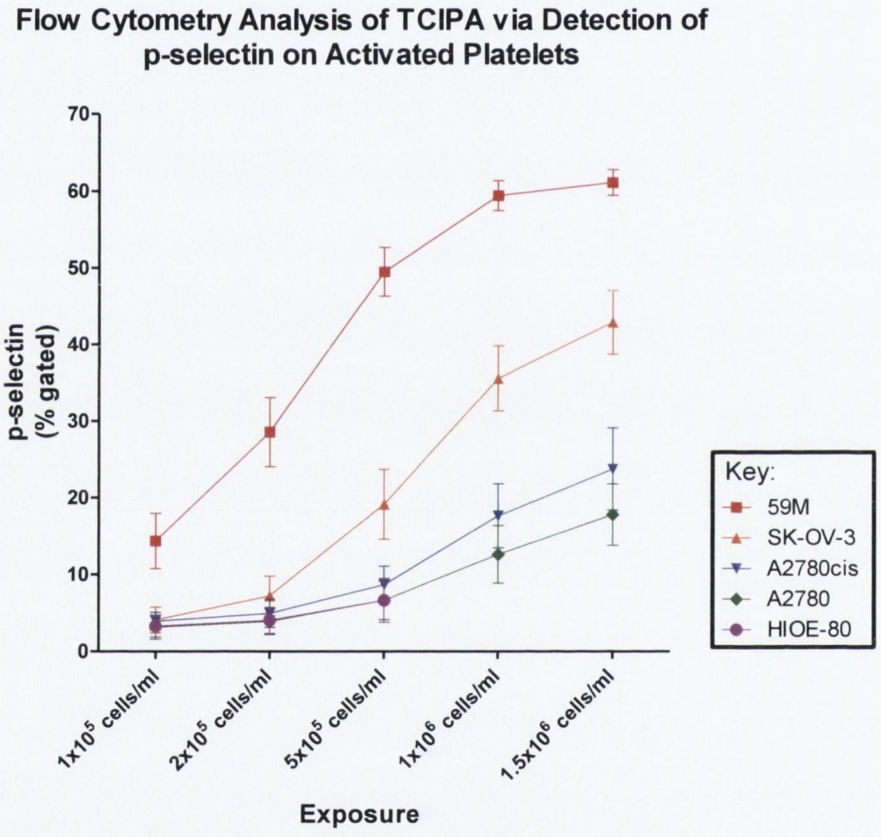

Figure 4-16: Flow Cytometry Analysis of TCIPA via activated platelet p-selectin: % Cells p-selectin positive.

Platelets and cell lines were prepared as described in Figure 4-13. Pooled flow cytometry data from 3 platelet donors compiled from the histograms shown in figures 4-13 to 4-15(A).

Data points indicate mean percentage gated cells (± SEM) positive for the presence of p-selectin, indicative of the presence of activated, adherent platelets. Data values in appendix figure 4-1 at the end of this chapter.

The 59M cell line saw a mean gated percentage indicative of adherent platelets increase from a mean of 14.38% when platelets were exposed to $1x10^5$ cells/ml to a mean of 61.12% when challenged with $1.5x10^6$ cells/ml. At each concentration greater than $1x10^5$ cells/ml the 59M cell line demonstrated a greater p-selectin presence than all other cell lines examined ($p \leq 0.05$).

The SK-OV-3 cell line returned the next highest set of p-selectin positive gating values initially returning a p-selectin positive value of 4.12% in response to $1x10^5$ cells/ml, increasing to 42.91% when platelets where exposed to the highest concentration of cancer cells at $1.5x10^6$ cells/ml.

The A2780 and the cisplatin resistant daughter cell line A2780cis returned similar p-selectin positive gating values when exposed to platelets at lower concentrations; $1x10^5$ cells/ml revealed 3.17% and 3.94% p-selectin positive gating respectively and $2x10^5$ cells/ml returned 3.93% and 4.97% p-selectin positive gating respectively. Subsequent exposures of higher cell concentrations saw a trend of further divergence of the cell lines ability to induce platelet activation with $1.5x10^6$ cells resulting in 12.63% of gated A2780 cells but 23.75% of A2780cis cells showing PE-labelled p-selectin presence, though this remains a trend as the difference between the two cell lines was not determined to be statistically significant.

The HIOE-80 cell line was examined at concentrations of $1x10^5$, $2x10^5$ and $5x10^5$ cells/ml only arising from cell numbers on the days of experimentation being insufficient to perform assays at all cell concentrations for each of the platelet donors (N=3). T-test analysis revealed no significant increase in p-selectin positive gating with increasing HIOE-80 cell concentration ($p \geq 0.05$).

4.3.3.2 $\alpha_{2b}\beta_3$

In addition to investigation of p-selectin, flow cytometry detection of TCIPA was performed as described using a FITC-labelled antibody directed towards human $\alpha_{2b}\beta_3$.

Platelet rich plasma (PRP) was prepared from whole blood taken from healthy female donors (N=3) who had not taken any substances known to affect platelet function in the seven days prior to donation. PRP was adjusted to a platelet count of $2x10^8$ platelets/ml. Cell lines were grown under normal culture conditions, non-enzymatically detached and adjusted to concentrations between $1x10^6$ cells/ml and $1.5x10^7$ cells/ml. In a total reaction volume of 100µl, 10µl of cell line suspension was incubated with PRP for 15 minutes at room temperature in the presence of a FITC conjugated mouse anti-human PAC-1/$\alpha_{2b}\beta_3$ IgM antibody (BD Pharmigen, USA) or an unconjugated mouse anti-human PAC-1/$\alpha_{2b}\beta_3$ IgM isotype control antibody. 100µl PRP activated by 15 minutes incubation in the presence of TRAP (20µM) was utilised as positive control for platelet activation. After 15 minutes the reaction was terminated by addition of 1 ml of JNL buffer prior to flow cytometry analysis.

The percentage of cell observations gating positive for platelet $\alpha_{2b}\beta_3$ were recorded for TCIPA in washed platelets extracted from three healthy female donors and data analysed using Microsoft Excel and Graphpad Prism. The data was adjusted to take into account background indicated by the buffer only control.

Figure 4-17 graphically illustrates the gating data recorded for the percentage of observations for each exposure (control or cell line) gating positive for $\alpha_{2b}\beta_3$, indicative of adherent platelets. The mean $\alpha_{2b}\beta_3$ values ± SEM illustrated are provided in Appendix Figure 4-2 at the end of this chapter.

Figure 4-17

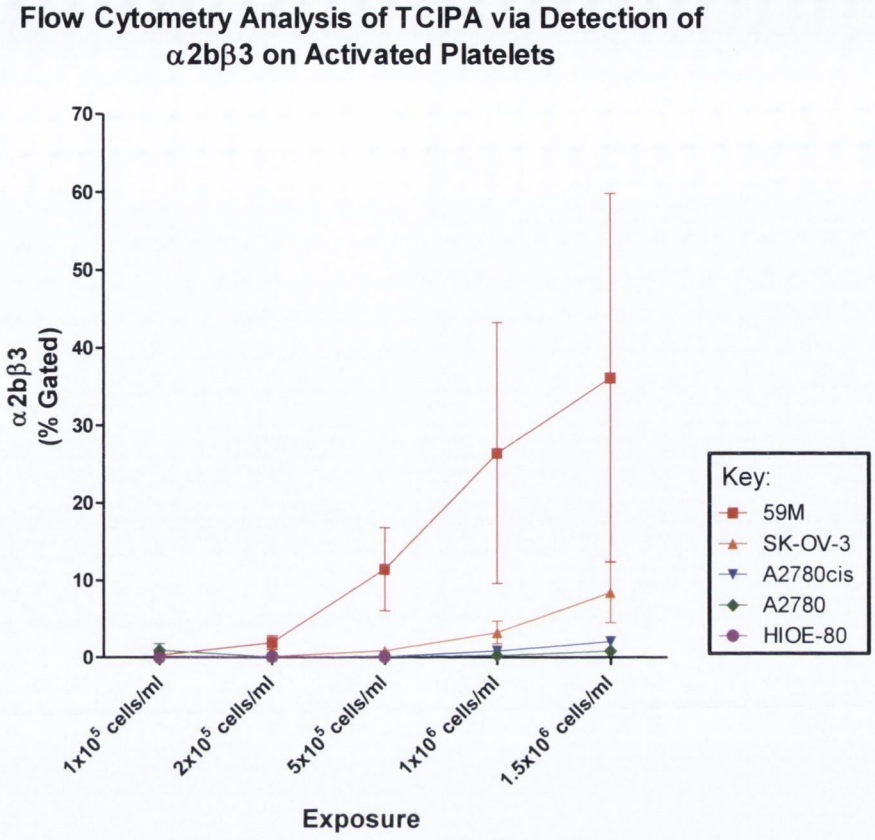

Figure 4-17: Flow Cytometry Analysis of TCIPA via activated platelet p-selectin: % Cells $\alpha_{2b}\beta_3$ positive.

Platelet rich plasma (PRP) was prepared from whole blood taken from healthy female donors (N=3). PRP was adjusted to $2x10^8$ platelets/ml. Cell lines were grown under normal culture conditions, non-enzymatically detached and adjusted to concentrations between $1x10^6$ cells/ml and $1.5x10^7$ cells/ml. 10µl of cell line suspension was incubated with 90 µl PRP for 15 minutes at room temperature in the presence of a FITC conjugated mouse anti-human PAC-1/$\alpha_{2b}\beta_3$ IgM antibody or an unconjugated mouse anti-human PAC-1/$\alpha_{2b}\beta_3$ IgM isotype control antibody. 100µl PRP activated by 15 minutes incubation in the presence of TRAP (20µM) was utilised as positive control for platelet activation.

Pooled flow cytometry data from 3 platelet donors indicating the percentage of cells positive for $\alpha_{2b}\beta_3$ presence, indicative of platelet adhesion, following cell line:PRP co-incubation. Data points indicate mean percentage gated cells (± SEM) positive for the presence of $\alpha_{2b}\beta_3$, indicative of the presence of adherent platelets. Data values in appendix figure 4-2 at the end of this chapter.

At $1x10^5$ cells/ml all cell lines returned low levels of $\alpha_{2b}\beta_3$ detection (HIOE-80; 0.003%, to 59M; 0.32%). From this concentration upwards there was an increasing trend for cells of

increasing malignant potential to gate $\alpha_{2b}\beta_3$ positive, indicative of the presence of TCIPA associated adherent platelets on their surface.

The 59M cell line saw a mean gated percentage of cells detected with $\alpha_{2b}\beta_3$ indicative of adherent platelets increase from 0.32% (mean) when platelets were exposed to $1x10^5$ cells/ml to 36.13% (mean) when challenged with $1.5x10^6$ cells/ml. Despite the observed increases in the number of 59M cells gating positive for $\alpha_{2b}\beta_3$ presence recorded at each concentration greater than $1x10^5$ cells/ml, the differences were not significantly greater that those recorded for each other cell line at the same concentrations, possibly arising from the inter-donor variation resulting in large SEM values.

The SK-OV-3 cell line returned the next highest set of $\alpha_{2b}\beta_3$ positive gating values initially returning a $\alpha_{2b}\beta_3$ positive value of 0% (mean) in response to $1x10^5$ cells/ml, increasing to 8.45% (mean) when platelets where exposed to the highest concentration of cancer cells at $1.5x10^6$ cells/ml.

The A2780 and the cisplatin resistant daughter cell line A2780cis returned low $\alpha_{2b}\beta_3$ positive gating values when exposed to platelets at lower concentrations; $1x10^5$ cells/ml revealed 0.97% and 0.037% $\alpha_{2b}\beta_3$ positive gating respectively and $2x10^5$ cells/ml returned 0.07% and 0.003% $\alpha_{2b}\beta_3$ positive gating respectively. Subsequent exposures of higher cell concentrations saw a clearer trend of increased further divergence of the cell lines ability to induce platelet activation with $1.5x10^6$ cells resulting in 0.89% of gated A2780 cells but 2.12% of A2780cis cells showing FITC-labelled $\alpha_{2b}\beta_3$ presence, though this remains a trend as the difference between the two cell lines was not determined to be statistically significant.

The HIOE-80 cell line was examined at concentrations of $1x10^5$, $2x10^5$ and $5x10^5$ cells/ml only arising from cell numbers on the day of experimentation being insufficient to perform assays at all cell concentrations for each of the platelet donors (3). Despite the five-fold increase between the lowest and highest concentration of HIOE-80 cells T-test analysis revealed no significant increase in $\alpha_{2b}\beta_3$ positive gating ($p>0.05$).

4.4 Discussion & Conclusion

The *in vitro* platelet:cell line adhesion assay developed to allow multi-well investigation of different cell lines capability to induce platelet adhesion to their surface returned valuable insight into the nature of TCIPA.

After optimisation, initial cell based assays utilised a panel of three cell lines of thyroid and ovarian origin to investigate a spectrum of epithelial health extending from normal epithelium (Nthy-ori 3-1) to malignant epithelium (carcinoma) (59M) and including γ-radiation transformed normal epithelial cells (4gy Nthy-ori 3-1) to examine the relationship between malignancy/metastatic potential and capacity to trigger TCIPA. These experiments indicated significantly increased platelet adhesion to cell lines of increasing malignant potential, with normal cells returning lowest platelet adhesion, transformed cells increased platelet adhesion and epithelial carcinoma returning further elevated levels of platelet adhesion.

Subsequent investigation for the presence of the ret/PTC-3 fusion transcript anticipated to occur based on prior work performed in the lab (Finn et al., 2004) using TaqMan® RT-PCR failed to indicate the gene rearrangement has occurred in the irradiated cells. The transformed cell line was observed during passage and maintenance to display an increased growth rate and altered morphology compared to the parental cell line. The changes underpinning these alterations of cell physiology are unknown and in depth investigation fell outside the remit of this study. Future work focussing on gene expression changes in thyrocytes induced γ radiation exposure and utilising modern whole transcriptome/genome sequencing may elucidate the cause of the changes observed in this study.

Progressing from these initial experiments a panel of exclusively ovarian cell lines was investigated for their capability to induce platelet adhesion to their surface. Normal ovarian epithelium was represented by a SV40 large T antigen immortalised cell line, HIOE-80 and malignant ovarian epithelium represented by 59M, A2780 and A2780cis cell lines. This panel of cell lines supported the previously observed trend of increased platelet adhesion to cells of greater or increasing malignant potential. Normal cells

returned a lower capacity for TCIPA than malignant cells (59M to A2780 and the cisplatin resistant A2780cis cell lines) which displayed the greatest capacity to adhere platelets. Brightfield microscopy allowed visual assessment of platelet adhesion cancer cells whilst also confirming the efficacy of the experimental blocking strategy adopted following assay optimisation experiments.

As these experiments were performed in a static test environment subsequent experimentation was performed using aggregometry in order to attempt to record the magnitude and kinetics of TCIPA induced by normal and malignant ovarian cell lines when added to washed platelets in suspension. In addition to informing about the nature of the platelet aggregation induced by the experimental cell lines with a temporal resolution not possible with the *in vitro* adhesion assay aggregometry also presented a methodology where the cells were maintained in suspension thus more closely representing cells having entered the peripheral circulation during the process of haematogenous dissemination prior to successful metastasis. Despite careful preparation of cells and platelets in line with previously published works utilising the technique (Radomski et al., 1991, Jurasz et al., 2001a, 2001b, Alonso-Escolano et al., 2004b, Medina et al., 2006) and investigating TCIPA in both washed platelets and platelet rich plasma (PRP) no aggregometry experiments were successful in recording platelet aggregation induced by the addition of any cell line. The cause of the aggregometry assay's failure to measure TCIPA in a dynamic, real-time manner was undetermined.

This technique has been successfully employed in the investigation of TCIPA by other groups in the past with marked success in recording tumour cell induction of platelet aggregation and modification of this interaction through the application of various inhibitors thus describing components of the cell-platelet interaction responsible for the phenomenon (Suzuki-Inoue et al., 2007, Alonso-Escolano et al., 2006, 2004b, Medina et al., 2006, Jurasz et al., 2003, 2001a, Radomski et al., 1991). After an extensive search no previously published scientific works have been found in the literature where aggregometry based investigations were performed using any of the experimental cell lines utilised in this thesis and investigating their ability to induce TCIPA. Of all the cell lines utilised only the 59M and SK-OV 3 cell lines have been investigated with reference to their ability to interact with platelets, specifically their interaction during TCIPA (Bazou et

al., 2011) and the contribution of platelets to ovarian tumour cell invasiveness (Holmes et al., 2009) though neither group utilised aggregometry as part of their investigations.

It is possible that with additional troubleshooting and optimisation that this technique may have generated meaningful data but as insufficient time was available to dedicate to these, it remains to be ascertained if there are specific preparation requirements of the experimental cell lines utilised in this study different to cell lines such as the MCF-7, CACO-2 and HT1080 investigated successfully elsewhere that if determined would allow successful aggregometry analysis of TCIPA and generation of data informing the speed, magnitude and potentially reversibility of TCIPA induced by HIOE-80, 59M, SK-OV-3, A2780 and A2780cis cell lines.

The final round of experiments performed utilised flow cytometry to investigate the panel of previously established cell lines capability for inducing TCIPA by detection of fluorescently labelled platelets adhering to their surface following co-incubation. Flow cytometry builds and improves upon the *in vitro* adhesion assay as it is capable of analysing each individual gated cell and taking thousands of such experimental measurements per analysed sample. In addition to generating robust data this also allows the cells to interact with platelets in suspension. Two platelet markers were selected, p-selectin and $\alpha_{2b}\beta_3$.

Both investigations revealed consistent patterns of adherent platelet detection on cell lines after co-incubation. The HIOE-80 cell line revealed the least evidence of adherent platelet presence. Both p-selectin and $\alpha_{2b}\beta_3$ flow cytometry determined the A2780 and A2780cis cell lines returned the next highest levels of adherent platelets, the cisplatin resistant daughter cell line representative of recurrent ovarian disease, notably returning a greater percentage of cells gating positive for platelets than the maternal cell line. The SK-OV 3 returned the second greatest and 59M returned the greatest percentages of gated cells determined to have adherent platelets on their surface.

There is some variation in the ability for the cell lines to induce platelet adhesion/aggregation reported by the successfully employed *in vitro* adhesion and flow cytometry assays.

Both assays support the hypothesis that cells of increased/increasing malignant potential display an increased capacity to induce platelet aggregation/adhesion to their surface. Both assays consistently report both the lowest ability for TCIPA in the HIOE-80 cell line representative of normal ovarian epithelium and the increased ability of the A2780cis cell line over the cisplatin sensitive maternal A2780 cell line. The assays differ in their ascending order of cell line platelet adhesion ability;

- the *in vitro* platelet:cell line adhesion assay determined the order to be: HIOE-80 < SK-OV 3 < 59M < A2780 < A2780cis
- the flow cytometry assay of p-selectin presence on cell lines following incubation in the presence of platelets (PRP) determined the order to be: HIOE-80 < A2780 < A2780cis < SK-OV 3 < 59M.

These differences are hypothesised to result from the differences in assay methodologies; static adherent cells vs detached cells in suspension, the latter potentially allowing the larger SK-OV 3 and 59M cells to present a greater cell surface area than the smaller A2780 and A2780cis cell lines.

Having confirmed the ability of the ovarian cell lines capability to interact with, activate and adhere platelets to their surface the capacity and nature of the TCIPA phenomenon to induce alteration of gene expression in these cell lines through whole platelet:cell signalling and platelet releasate:cell cell signalling was pursued.

Chapter Four Appendix

Appendix Figure 4-1

		Control	$1x10^5$ cells/ml	$2x10^5$ cells/ml	$5x10^5$ cells/ml	$1x10^6$ cells/ml	$1.5x10^6$ cells/ml
Mean	Buffer control	0					
SEM		0					
Mean	20µm TRAP	89.986					
SEM		1.961					
Mean	HIOE-80		3.333	4.067	6.657		
SEM			1.430	1.677	2.854		
Mean	59M		14.380	28.587	49.510	59.427	61.123
SEM			3.603	4.520	3.168	1.929	1.659
Mean	SK-OV-3		4.127	7.257	19.167	35.590	42.910
SEM			1.674	2.551	4.582	4.234	4.181
Mean	A2780		3.177	3.933	6.663	12.633	17.830
SEM			1.540	1.707	2.509	3.749	4.003
Mean	A2780cis		3.947	4.970	8.680	17.653	23.753
SEM			1.148	1.807	2.388	4.171	5.373

Appendix Figure 4-1: Flow Cytometry Assay of Platelet p-selectin.

Mean percentage of flow cytometry observations gating p-selectin positive indicative of the presence of adherent platelets after co-incubation of washed platelets with benign and malignant ovarian cell lines. Also indicated are SEM values.

Appendix Figure 4-2

		Control	$1x10^5$ cells/ml	$2x10^5$ cells/ml	$5x10^5$ cells/ml	$1x10^6$ cells/ml	$1.5x10^6$ cells/ml
Buffer control	Mean	0					
	SEM	0					
20µm TRAP	Mean	44.677					
	SEM	23.244					
HIOE-80	Mean		0.003	0.153	0.090		
	SEM		0.003	0.074	0.116		
59M	Mean		0.320	1.977	11.453	26.430	36.130
	SEM		0.223	0.895	5.358	16.826	23.678
SK-OV-3	Mean		-0.030	0.157	0.917	3.280	8.453
	SEM		0.089	0.144	0.268	1.466	3.907
A2780	Mean		0.973	0.073	0.090	0.310	0.897
	SEM		0.865	0.119	0.059	0.182	0.262
A2780cis	Mean		0.037	0.003	0.100	0.877	2.120
	SEM		0.032	0.003	0.058	0.039	0.390

Appendix Figure 4-2 : Flow Cytometry Assay of platelet $\alpha_{2b}\beta_3$.

Mean percentage of flow cytometry observations gating $\alpha_{2b}\beta_3$ positive indicative of the presence of adherent platelets after co-incubation of washed platelets with benign and malignant ovarian cell lines. Also indicated are SEM values.

CHAPTER FIVE

Tumour Cell Induced Platelet Aggregation Associated Alteration of Gene Expression in Ovarian Cancer

5 Tumour Cell Induced Platelet Aggregation Associated Alteration of Gene Expression in Ovarian Cancer

5.1 Background

In chapter four of this thesis the ability of ovarian cell lines representing a spectrum of ovarian tissue health to interact with and adhere platelets to their surface was examined. The investigations performed in this component of this thesis determined that cells of increasing malignancy or metastatic potential displayed an increased capacity to induce platelet adhesion to their surface and to induce platelet activation of adherent platelets.

This section of thesis aims to build on this information and investigate the hypothesis that tumour cell induced platelet aggregation results in altered gene expression in platelet cloaked cancer cells that may support or provide pro-tumorigenic signals which may assist in the progression of malignancy and successful establishment of metastases following dissemination through the vasculature.

This thesis aims to investigate this hypothesis by attempting to examine platelet or platelet releasate induced changes over the entire transcriptome of each of the experimental ovarian cell lines available to the study through the use of modern high resolution molecular biology assays.

5.2 Materials & Methods

5.2.1 Gel Filtered Platelet and Platelet Releasate Preparation

For complete details of washed platelet preparation from whole blood see chapter 2, section 2.6.2.

It is important to note that washed platelets and platelet releasate were isolated from three healthy female donors who had not taken any medication known to affect platelet function within 10 days of donating. These preparations were utilised as pooled gel filtered platelets and pooled platelet releasate created by combining equal volumes of individual donors washed platelets/platelet releasate.

5.2.2 Pierce® BCA (Bradford) Protein Assay

For complete details of the Pierce® BCA Protein Assay methodology see chapter 2 section 2.6.4.1.

5.2.3 Fluorescent Microscopy of Cell Surface Markers

For complete details of the methodology employed for fluorescent microscopy investigation of cell surface markers see chapter 2, section 2.8.2.

5.2.4 Roche In Situ Cell Death Detection (TUNEL) Assay

For complete details of the Roche In Situ Cell Death Detection (TUNEL) Assay methodology see chapter 7, section 7.8.

5.2.5 Roche Cell Proliferation Assay 1 (MTT)

For complete details of the Roche Cell Proliferation Assay 1 (MTT) assay methodology see chapter 2, section 2.9.1.

5.2.6 BD Pharmigen™ ApoDirect™ Flow Cytometry TUNEL Assay

For complete details of the BD Pharmigen™ ApoDirect™ Flow Cytometry TUNEL Assay methodology see chapter 7, section 7.9.

5.2.7 Nucleic Acid Extraction

For complete details of methodologies used in RNA extraction see chapter 2, section 2.2.2.1.

5.2.8 RNA Quantitation & Analysis

For complete details of methodologies employed in RNA quantitation and qualitation see chapter 2, section 2.3.

5.2.9 Affymetrix® GeneChip® Human Exon 1.0 ST Array

For complete details of the methodology employed for Affymetrix® Human Exon 1.0 ST Array investigation of whole transcriptome gene expression see chapter 2, section 2.4.3.

5.2.10 Fluidigm® Dynamic Array™

For complete details of the methodology employed for Fluidigm® Dynamic Array™ high throughput qPCR see chapter 2, section 2.4.2.

5.3 Results

5.3.1 Platelet Releasate Optimisation

Before examining cell lines response to washed platelets or platelet releasate (PLRL) the concentration of PLRL to be applied required optimisation.

As the PLRL was extracted from washed platelets at a physiologically representative concentration and was not subsequently diluted or concentrated during its preparation determining the optimal concentration of PLRL to be employed also determined the concentration of washed platelets to be used in gene expression investigations.

The concentration of platelet releasate that was used was that which resulted in no net negative alteration of cell growth or metabolism. This was selected in the absence of any published information regarding the concentration of platelet releasate at the CTC-platelet embolus during TCIPA in the dynamic flow environment of the vasculature.

The rationale for using washed platelets and PLRL prepared in JNL buffer in preference to preparing them in blood plasma as platelet rich plasma (PRP) or PLRL in plasma was informed by the expression of proteins such as αVβ3 and αV by cell lines such as the 59M (figure 5-1).

This indicated that the use of PRP in gene expression experiments be avoided due to the potential for serum components such as serum proteins fibronectin and vitronectin that can interact with αVβ3 and αV, in addition to other molecules that might signal through other receptors, to introduce signals that could possibly confound those signals of interest elicited specifically by platelet or PLRL exposure.

Figure 5-1

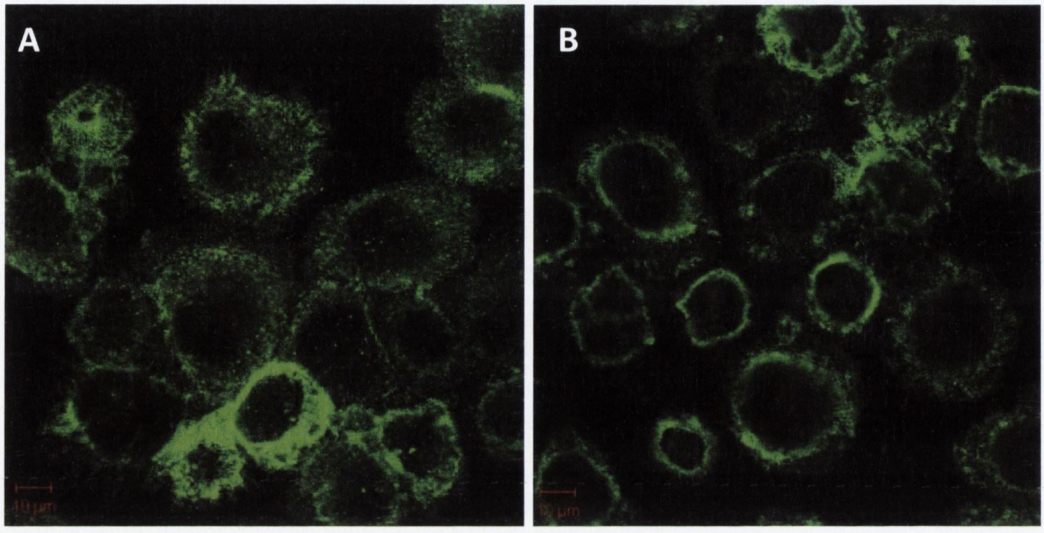

Figure 5-1: Fluorescent Photomicrographs of αVβ3 (A) and αV (B) staining in 59M cells.

Both images indicate both αVβ3 (A) and αV (B) are expressed by the 59M cell line.

Prepared with the assistance of Mr. Karl Egan, Cardiovascular Biology Group, Dept. of Molecular and Cellular Therapeutics, RCSI, Dublin.

In addition to informing against the use of platelets and PLRL prepared in PRP, αVβ3 and αV presence on the surface of these cells also eliminated these proteins as potential markers when previously assessing platelet adhesion to cell lines by flow cytometry as these integrins are also known to be present on platelet membranes.

5.3.1.1 Bradford Colorimetric Protein Assay

A Bradford colorimetric protein assay was performed (Appendix Figure 5-1 and Appendix Table 5-1) on the pooled PLRL utilised in this study. The data returned from the assay was analysed using GraphPad Prism and a linear line of best fit.

This assay determined the protein content of the pooled platelet releasate to be 244.76μg/ml.

Pooled PLRL was not investigated to determine its composition as part of this study.

5.3.1.2 Roche In Situ Cell Death Detection (TUNEL) Assay

Initial optimisation of the platelet releasate concentration interrogated the suitability of PLRL at low dilution factors (1:1, 1:3 and 1:6) in full growth media and assessing the effect of PLRL at these concentrations on cell health, specifically the induction of apoptosis, through TUNEL assay and subsequent fluorescence microscopy.

Based on protein quantitation assays, the protein concentrations applied to the cell lines were equivalent to 122.38µg/ml, 81.58µg/ml, 40.79µg/ml at 1:1, 1:3 and 1:6 dilution factors respectively.

Pairs of complementary fluorescent photomicrographs were captured of a randomly selected field of cells for each of the conditions examined. The captured digital images were analysed using Image J software (NIH, USA) allowing cell nuclei and cells undergoing apoptosis to be manually counted.The pair of images included;

- one image of Hoechst stained cell nuclei, allowing assessing the total number of cells present.
- one image of TMR red labelled DNA nick ends indicative of the number of cells undergoing apoptosis.

Figure 5-2 shows three representative sets of fluorescent photomicrographs illustrating a field of view capturing Hoechst staining (left) and TUNEL TMR red labelling (right) of a well of 59M cells cultured for 24 hours in full growth media (A), cultured in a 1:1 dilution of PLRL (B) and an exemplar positive control (DNAse 1 treatment of cells prior to TUNEL staining) (C).

This set of experiments demonstrated an apoptotic effect of high concentrations of platelet releasate on cell lines. These results are described in futher detail in sections 5.3.1.2.1 and 5.3.1.2.2.

Figure 5-2

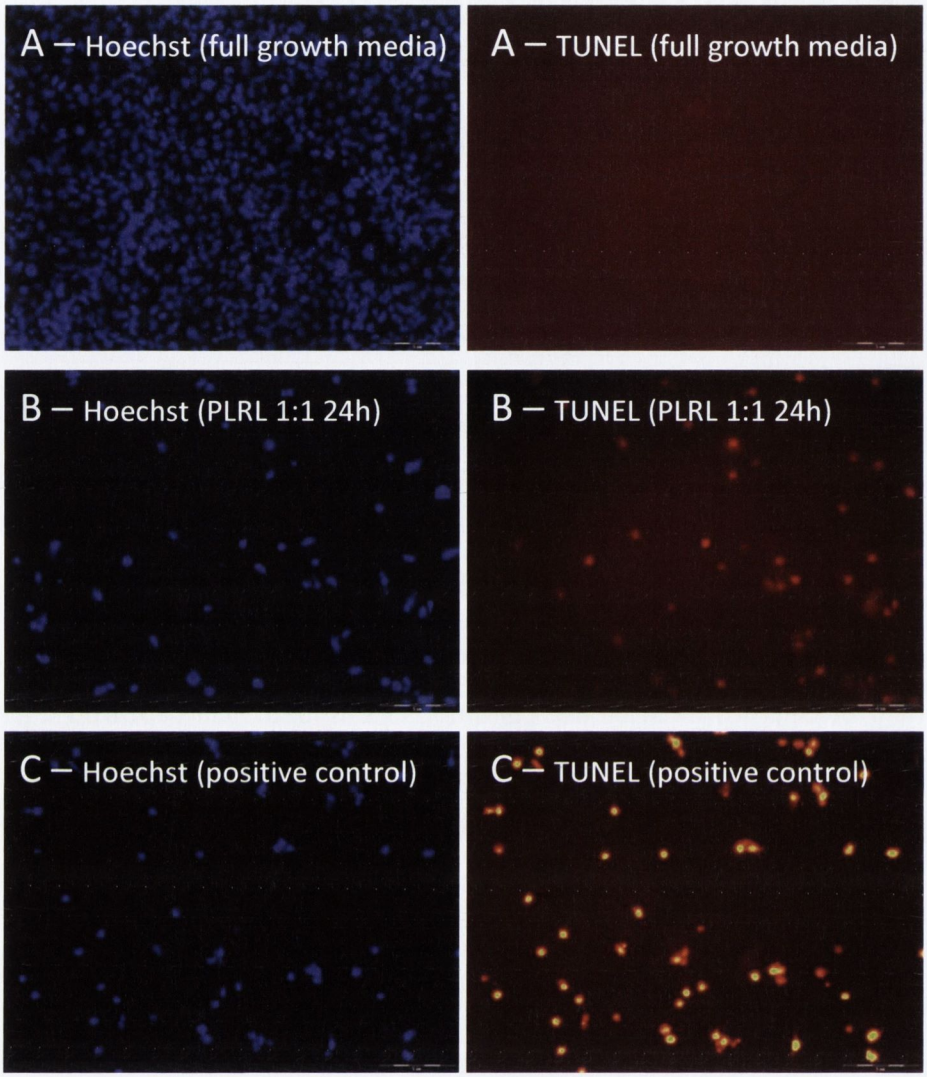

Figure 5-2: Fluorescent Photomicrographs of Hoechst Stained and TUNEL Labelled 59M cells.

The pair of images captured of 59M cells cultured in full growth media only (A) clearly show a highly confluent field of cells as indicated by the blue, Hoechst stained nuclei and an absence of apoptotic cells given the TUNEL staining revealed background colour only.

Cells cultured in a 1:1 dilution of platelet releasate in full growth media for 24 hours (B) similarly revealed the presence of cells by nuclear staining but the complementary image captured of TUNEL staining reveal bright spots indicative of TMR red labelling of DNA nick ends in cells undergoing apoptosis.

Positive control staining performed to confirm TUNEL assay labelling was effective (C). The high efficiency DNAse 1 utilised (QIAGEN) resulted resulted in very strong positive control TUNEL labelling.

5.3.1.2.1 Apoptotic Cell Count Number

Having quantified the total number of cells per field of view and the total number of cells undergoing apoptosis, the percentage of cells undergoing apoptosis in each field of view was calculated, statistical analyses performed (ANOVA) and bar charts generated to illustrate the data (Figure 5-3). The mean percentage of cells staining TUNEL positive indicative of apoptosis per field of view are indicated in Table 5-1.

Both the HIOE-80 and 59M cell lines revealed significantly greater levels of apoptosis ($p<0.001$) in cells exposed to a 1:1 dilution of PLRL compared against that observed in cells cultured in full growth media alone. The percentage of HIOE-80 and 59M cells staining TUNEL positive in response to 1:1 dilution of PLRL was 41.6% and 46.2% respectively. Both cell lines reported a reduced level of apoptosis with increased dilution factor/reduced PLRL exposure.

The A2780 and A2780cis cell lines returned data indicating a counter-intuitive increased level of apoptosis in response to increased PLRL dilution factor/reduced PLRL exposure, with a 1:3 dilution of PLRL in full growth media resulting in significantly elevated levels of apoptosis ($p<0.05$) compared to the at observed following culture in full growth media alone. The percentage of A2780 and A2780cis cells staining TUNEL positive in response to 1:3 dilution of PLRL was 14.8% and 48.3% respectively.

Figure 5-3

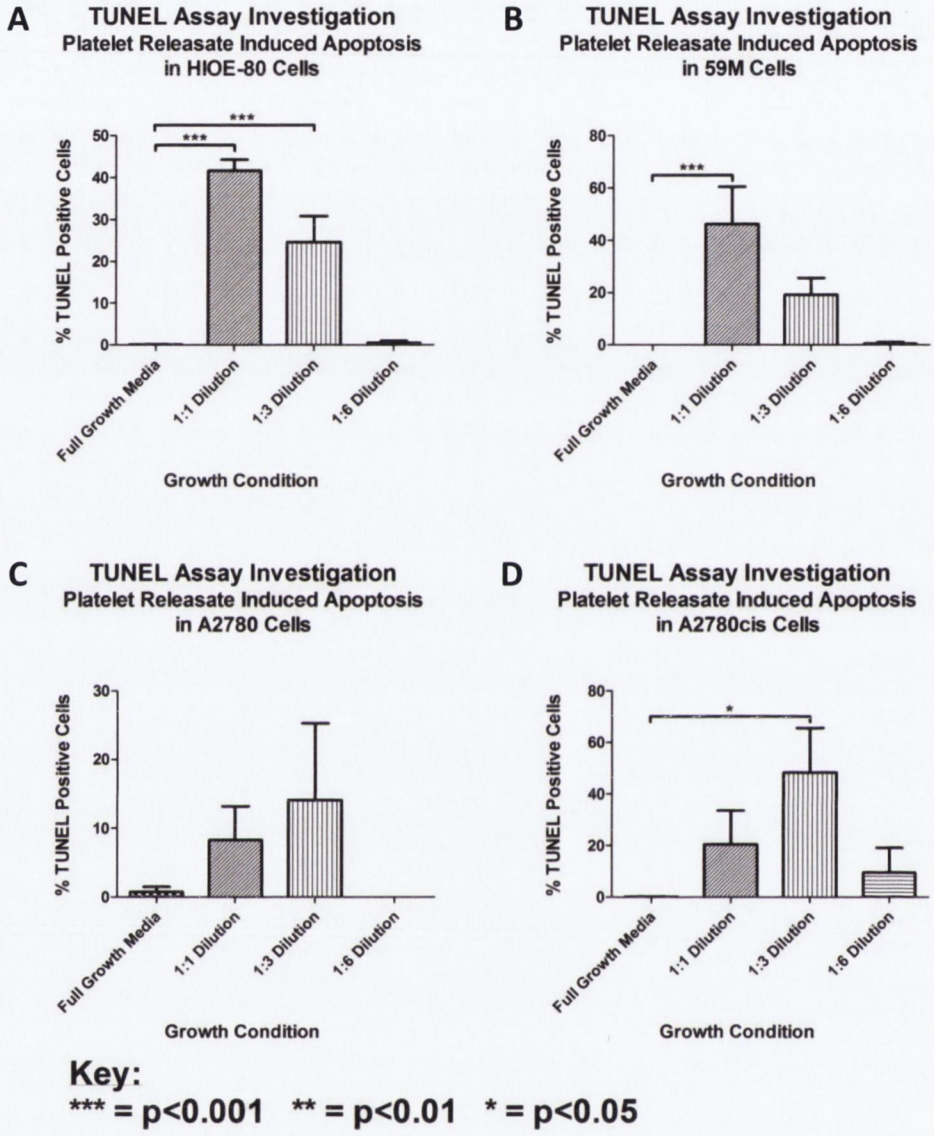

Figure 5-3: Percentage of Cells undergoing Apoptosis in Response to Platelet Releasate Exposure.

Cell lines were grown to 80% confluence on 96 well cell cluture plates under normal culture conditions. Pooled platelet releasate was prepared from gel filtered platelets extracted from whole blood from three female volunteers.

Cells were cultured in a 1:1, 1:3 or 1:6 dilution of pooled platelet releasate:full growth media or full growth media only for 24h and apoptosis examined by TUNEL labelling. N=3 was performed for each condition and mean ± SEM calculated.

TUNEL labelling revealed increased apoptosis in all cell lines in response to 1:1 and 1:3 dilutions of platelet releasate.

Table 5-1

Cell Line	Full Media	1:1 PLRL Dilution	1:3 PLRL Dilution	1:6 PLRL Dilution
HIOE-80	0.08%	41.68%	24.61%	0.49%
59M	0.23%	46.21%	19.24%	0.47%
A2780	0.74%	8.28%	14.14%	0.0%
A2780cis	0.14%	20.42%	48.32	9.57%

Table 5-1: Percentage of TUNEL positive cells in response to Platelet Releasate (PLRL) exposure.

5.3.1.2.2 Total Cell Count

Having observed the variability reported in the percentage of cells undergoing apoptosis in response to PLRL of dilution factors between 1:1 and 1:3 in full growth media the data was reassessed to examine if any confounding factors may have resulted in the irregularities previously observed.

The number of cells visible per field of view was investigated and the number of cells counted and normalised against the number visible per field of view in wells where the cells had been cultured in full growth media only. The normalised data was then analysed in GraphPad Prism (presented in Figure 5-4 & Table 5-2).

The data recorded documents a significant loss of cell numbers arising from 24 hour exposure to platelet releasate dilutions prepared in full growth media for all the cell lines investigated ($p<0.05$).

On that basis subsequent investigations were performed to determine the appropriate concentration of platelet releasate that could be applied to cell lines without negatively impacting on their growth or viability.

Figure 5-4

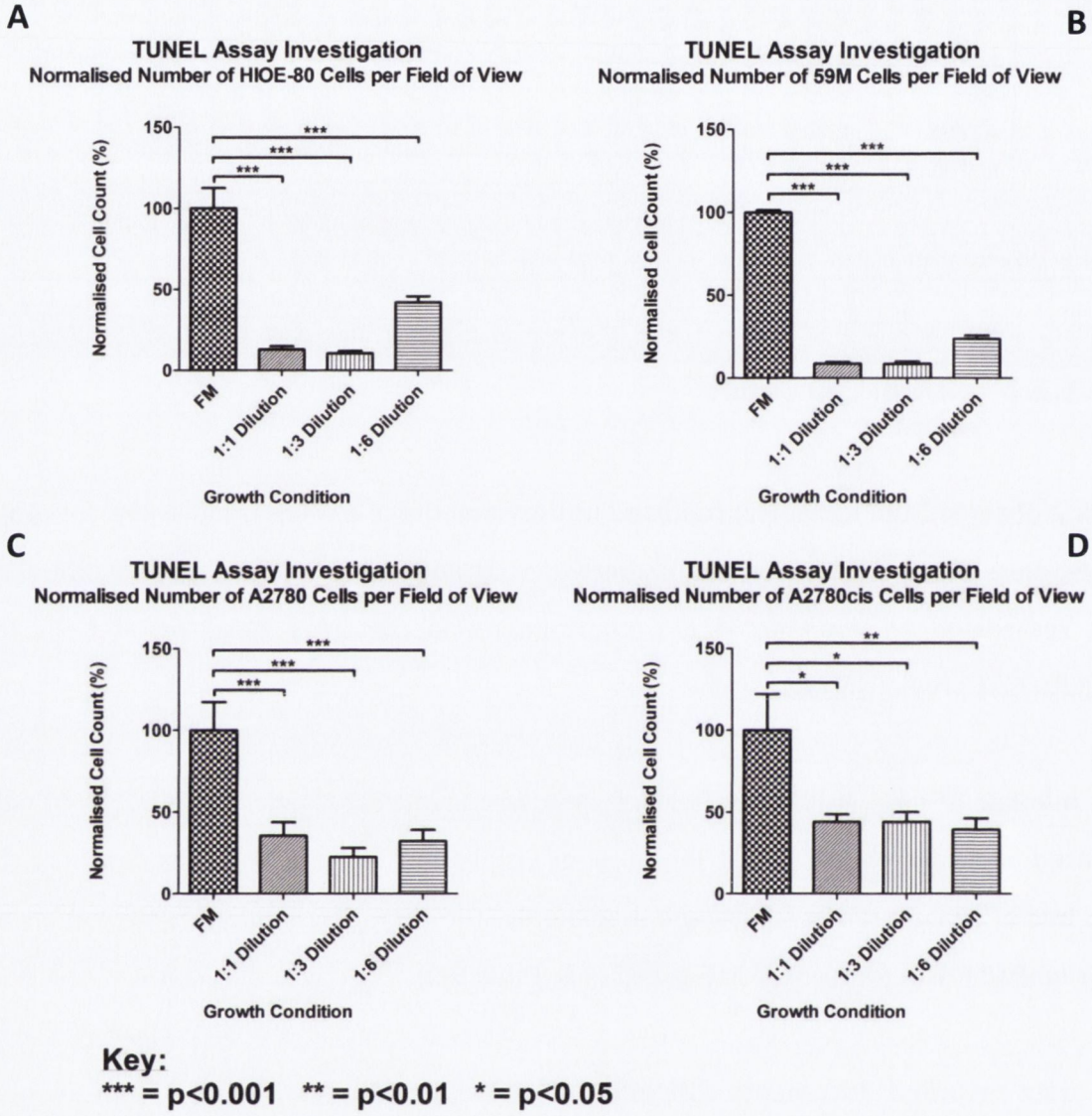

Figure 5-4: TUNEL Assay - Normalised Cell Count Per Field of View Following Culture in the Presence of Platelet Releasate.

Cell lines were grown to 80% confluence on 96 well cell cluture plates under normal culture conditions. Pooled platelet releasate was prepared from gel filtered platelets extracted from whole blood from three female volunteers.

Cells were cultured in a 1:1, 1:3 or 1:6 dilution of pooled platelet releasate:full growth media or full growth media only for 24h. N=3 was performed for each condition. Cell nucleii were Hoechst stained and mean cell count (±SEM) calculated and normalised against cell count following culture in full growth media. Hoechst staining revealed a significant loss of adherent cells in response to platelet releasate exposure in all cell lines.

Table 5-2

Cell Line	Full Media	1:1 PLRL Dilution	1:3 PLRL Dilution	1:6 PLRL Dilution
HIOE-80	100 ± 12.42	12.95 ± 1.909	10.44 ± 1.519	42.10 ± 3.599
59M	100 ± 1.256	8.671 ±0.9667	8.577 ± 1.315	23.54 ± 2.2
A2780	100 ± 17.38	35.49 ± 8.239	22.47 ± 5.632	32.21 ± 6.932
A2780cis	100 ± 22.13	43.99 ± 4.679	43.99 ± 6.037	39.35 ± 6.734

Table 5-2: TUNEL Assay - Normalised Cell Count Per Field of View (±SEM).

5.3.1.3 Roche Cell Proliferation Assay 1 (MTT Assay)

The MTT assay was selected as this form of investigation is capable of informing the impact of a treatment on cell viability through detection of a cell metabolite of MTT salts indicative of cell growth and metabolism. A reduced presence of the salt metabolite in response to a concentration of platelet releasate is accepted in these studies as indicative of reduced cell growth/viability.

After performing the assay data was collated, normalised to the experimental control exposure and analysed using GraphPad Prism. This program enabled bar charts to be generated to illustrate the data, and statistical analyses to be performed. One way ANOVA was performed to determine if a significant difference between the means of the different groups (exposures) existed and Dunnett post-test was also performed to compare data returned for all exposures against the experimental control.

Initial experiments were performed to complement the previously performed TUNEL investigation by exposing cell lines to 1:1, 1:3 or 1:6 dilutions of platelet releasate in full growth media for 24 hours and comparing cells growth/viability following the exposure period.

These exposures resulted in large (>50%) and statistically significant ($p<0.001$) reductions in cell growth/metabolism after 24 hours (illustrated in Figure 5-5). The mean normalised cell growth values (±SEM) are given in Table 5-3.

All cell lines were observed to undergo significantly reduced growth/proliferation when cultured for 24 hours at all exposures of platelet releasate supplemented growth media versus cells cultured in full growth media alone.

This is congruent with the data returned by the previously performed TUNEL assays, and reflects the observed loss of cell numbers. Another observation of note was the increased resilience of the A2780cis compared to the A2780 cell line when exposed to the same dilution of platelet releasate in full growth media for 24 hours. This may reflect the increased malignancy of the cisplatin resistant daughter cell line.

Having determined that low dilutions of pooled PLRL result apoptosis and in significant loss of cells when exposed for 24 hours by TUNEL assay this was further confirmed by MTT assay and the effect of a significantly broader range of pooled PLRL dilutions were examined on cells.

These assays were performed examining cell growth/viability following cell exposure to the following conditions:

- Pooled PLRL at a range of dilution factors in full growth media
- JNL buffer, the vehicle in which PLRL was prepared, at a range of dilution factors in full growth media

The effect on cell growth/viability following 24 hour exposure to pooled PLRL and JNL at dilutions of 1:10 to 1:500,000 in full growth media were to be investigated to determine the PLRL conditions that would later be used in gene expression investigations and to determine if exposure to the PLRL vehicle buffer, JNL, resulted in significant impact on cell physiology.

Figure 5-5

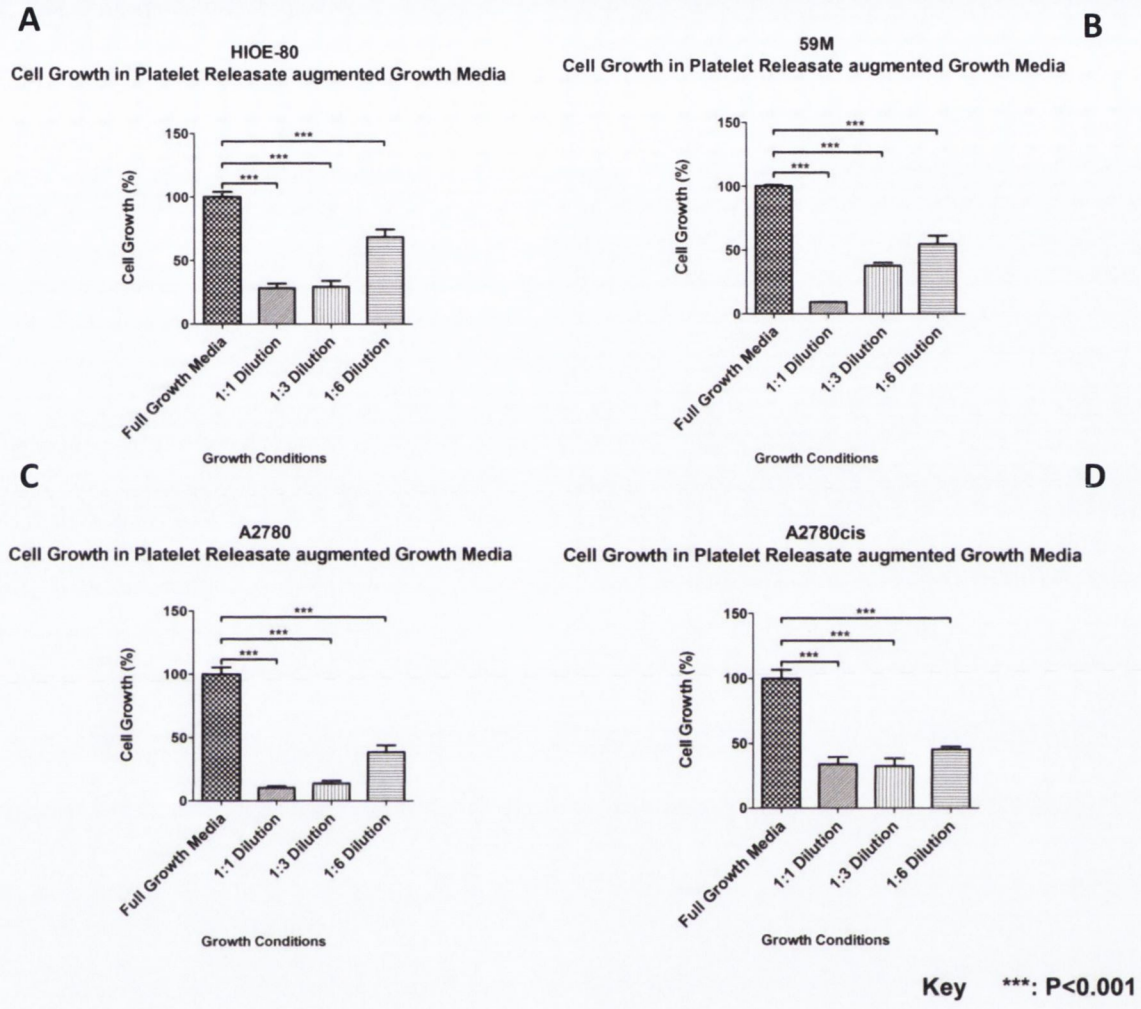

Figure 5-5: MTT Assay – Effect of platelet releasate (PLRL) on cell metabolism at dilution factors of 1:1 to 1:6 in full growth media (FM)

Cell lines were grown to 80% confluence on 96 well cell cluture plates under normal culture conditions. Pooled platelet releasate was prepared from gel filtered platelets extracted from whole blood from three female volunteers.

Cells were cultured in a 1:1, 1:3 or 1:6 dilution of pooled platelet releasate:full growth media or full growth media only for 24h. N=5 was performed for each condition. Cell metabolism/growth was assessed by MTT assay and mean cell growth (±SEM) calculated and normalised against that observed in full growth media.

MTT assay revealed a significant reduction in cell growth in response to platelet releasate exposure in all cell lines. This is linked to a loss of cell numbers arising from induction of apoptosis these exposures.

Table 5-3

Cell Line	Full Media	1:1 Dilution	1:3 Dilution	1:6 Dilution
HIOE-80	100 ± 4.177	28.29 ± 3.647	29.34 ± 4.653	68.6 ± 5.942
59M	100 ±0.9508	9.279 ± 0.1908	37.67 ± 2.298	54.67 ± 6.542
A2780	100 ± 5.6	10.22 ± 1.1319	13.68 ± 2.127	38.29 ± 5.452
A2780cis	100 ± 6.692	34.02 ± 5.525	32.48 ± 6.034	45.37 ± 2.166

Table 5-3: Cell Line Growth (mean ± SEM) in Response to Dilutions of Platelet Releasate.

5.3.1.3.1 Full Media

The effect of 24 hours exposure to platelet releasate prepared at a range of dilutions in full growth media on a panel of five cell lines (HIOE-80, 59M, SK-OV 3, A2780 and A2780cis) cell lines representing the spectrum of ovarian epithelial tissues from normal to cisplatin resistant carcinoma was assessed by MTT.

MTT assay data was corrected for negative control absorbance (wells prepared with no cells present) and normalised against absorbance returned by cells cultured in full growth media only. This data was then entered into GraphPad Prism for statistical analysis and graphical representation. This data is illustrated in table 5-4 and figure 5-6.

Table 5-4

Platelet Releasate Dilution Factor			HIOE-80	59M	SK-OV 3	A2780	A2780cis
	Full Media	Mean	100	100	100	100	100
		SEM	1.98	3.01	3.25	1.63	4.06
	1:10	Mean	70.95	94.67	94.17	77.71	94.10
		SEM	0.63	1.64	1.73	2.10	4.72
	1:50	Mean	78.12	101.37	97.27	83.81	89.16
		SEM	1.86	1.78	1.49	5.24	5.06
	1:100	Mean	80.23	100.89	100.86	96.09	91.83
		SEM	1.43	2.70	2.75	3.66	2.98
	1:500	Mean	88.26	99.42	99.15	96.82	94.86
		SEM	1.23	2.20	2.29	4.48	3.71
	1:1000	Mean	94.23	98.36	98.24	90.21	90.85
		SEM	1.46	1.49	1.31	5.27	6.71
	1:5000	Mean	95.38	99.33	98.96	95.26	82.51
		SEM	3.05	1.91	2.20	5.06	2.98
	1:10,000	Mean	99.47	98.46	98.19	87.86	88.45
		SEM	1.91	4.74	4.88	3.89	5.11
	1:50,000	Mean	100.48	92.21	97.50	96.04	87.46
		SEM	1.25	2.84	1.95	3.57	3.04
	1:100,000	Mean	107.50	100.77	100.95	95.16	83.68
		SEM	2.70	1.97	2.05	2.43	3.92
	1:500,000	Mean	113.37	94.47	97.60	96.36	88.83
		SEM	2.47	3.37	3.02	4.08	2.36

Table 5-4: MTT Assay of cell growth & proliferation in Ovarian Cell in response to culture in the presence of platelet releasate augmented full growth media.

Cell lines were grown to 80% confluence on 96 well cell cluture plates under normal culture conditions. Pooled platelet releasate was prepared from gel filtered platelets extracted from whole blood from three female volunteers.

Cells were cultured in a 1:10 to 1:500,000 dilution of pooled platelet releasate:full growth media or full growth media only for 24h. N=5 was performed for each condition. Cell metabolism/growth was assessed by MTT assay and mean cell growth (±SEM) calculated and normalised against that observed in full growth media.

MTT assay revealed a significant reduction in cell growth in response to platelet releasate exposure in all cell lines. This is linked to a loss of cell numbers arising from induction of apoptosis these exposures.

Figure 5-6

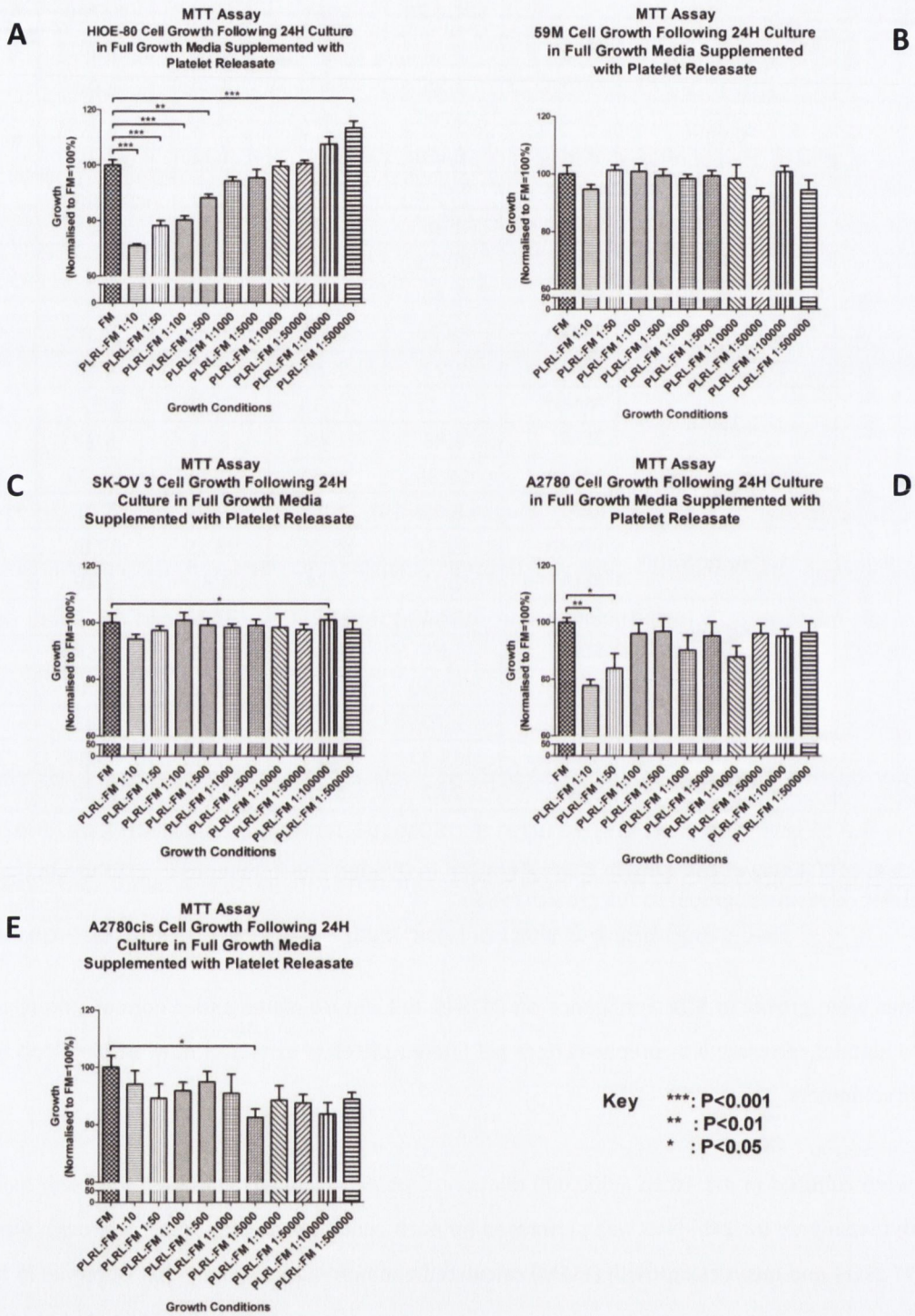

Figure 5-6: MTT Assay of cell growth & proliferation in Ovarian Cell in response to culture in the presence of platelet releasate augmented full growth media.

Cells, platelet releasate and MTT assay was performed as described in Table 5-4. Figure 5-6 illustrates the growth of HIOE-80 (A), 59M (B), SK-OV 3 (C), A2780 (D) and A2780cis (E) cell lines in the presence of Platelet Releasate (PLRL) augmented full growth media (FM). Significant differences vs growth in full growth media are annotated as follows: *p<0.05, **p<0.01, ***p<0.001.

The immortalised normal ovarian epithelial cell line, HIOE-80, demonstrated significant reductions in cell growth/viability after 24h exposure to dilutions of platelet releaseate (in full groth media) between 1:10 and 1:1000.

Both the 59M and SK-OV 3 cell lines reported little change in response to PLRL exposure and no statistically significant reduction in cell growth/viability was recorded at any concentration of platelet releasate examined.

The A2780 recorded significant reductions in cell growth/viability in response to exposure to platelet releasate dilutions of 1:10 and 1:50, a response not replicated in the cisplatin resistant A2780cis cell line.

Arising from this data a subsequent set of MTT assays were performed to further pursue the suitability of the 1:1000 dilution factor of platelet releasate in full growth media for use across the six experimental cell lines in subsequent molecular biology based investigations.

This final set of confirmatory MTT assays utilised a reduced range of platelet releasate dilutions covering four serial dilutions resulting in a range between a 1:10 and 1:10,000 dilution factors.

As with previous MTT assays cells were seeded into multi-well plates in full growth media for an exposure period of 24 hours at standard growth cell culture conditions (37°C, 5% CO_2 in a humidified cell culture incubator).

This set of assays confirmed that a 1:1000 pooled platelet releasate dilution prepared in full growth media as a maximum preparation suitable for use across the panel of cell lines to be utilised in subsequent investigations examining alterations in gene expression in response to washed platelet and platelet releasate exposure (figure 5-7).

Figure 5-7

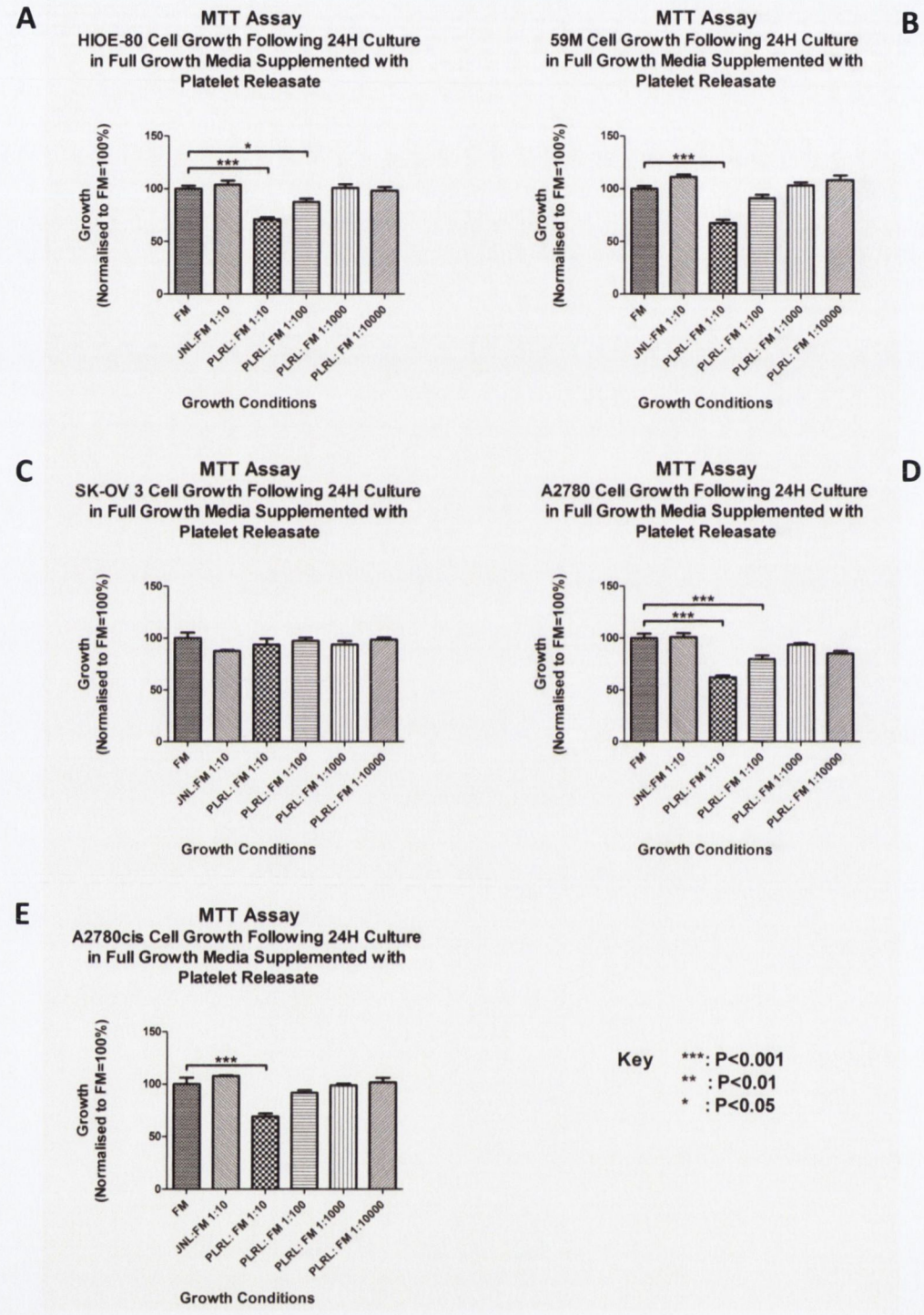

Figure 5-7: MTT Assay of cell growth & proliferation in Ovarian Cell in response to culture in the presence of platelet releasate augmented full growth media

Cells, platelet releasate and MTT assay was performed as described in Table 5-4. Figure 5-7 illustrates the growth of HIOE-80 (A), 59M (B), SK-OV 3 (C), A2780 (D) and A2780cis (E) cell lines in the presence of Platelet Releasate (PLRL) augmented full growth media (FM). Significant differences vs growth in full growth media are annotated as follows: *p<0.05, **p<0.01, ***p<0.001.

5.3.1.3.2 JNL Buffer

The effect of 24 hours exposure to JNL buffer prepared at a range of dilutions in full growth media on a panel of five cell lines (HIOE-80, 59M, SK-OV 3, A2780 and A2780cis) cell lines representing the spectrum of ovarian epithelial tissues from normal to cisplatin resistant carcinoma was assessed by MTT.

MTT assay data was corrected for negative control absorbance (wells prepared with no cells present) and normalised against absorbance returned by cells cultured in full growth media only. This data was then entered into GraphPad Prism for statistical analysis and graphical representation. This data is illustrated in figure 5-8.

This data indicates HIOE-80, 59M SKOV-3 and A2780 cell lines recorded no significant alteration to cell growth/viability following 24 hours at any JNL exposure compared to growth in full growth media alone. The A2780cis cell line reported no change in response to 24 hour JNL exposure, with the exception of 24 exposure to JNL at a dilution factor of 1:5000 in full growth media which ($p<0.01$).

These results indicate JNL buffer does not significantly negatively affect cell growth/viability.

Figure 5-8

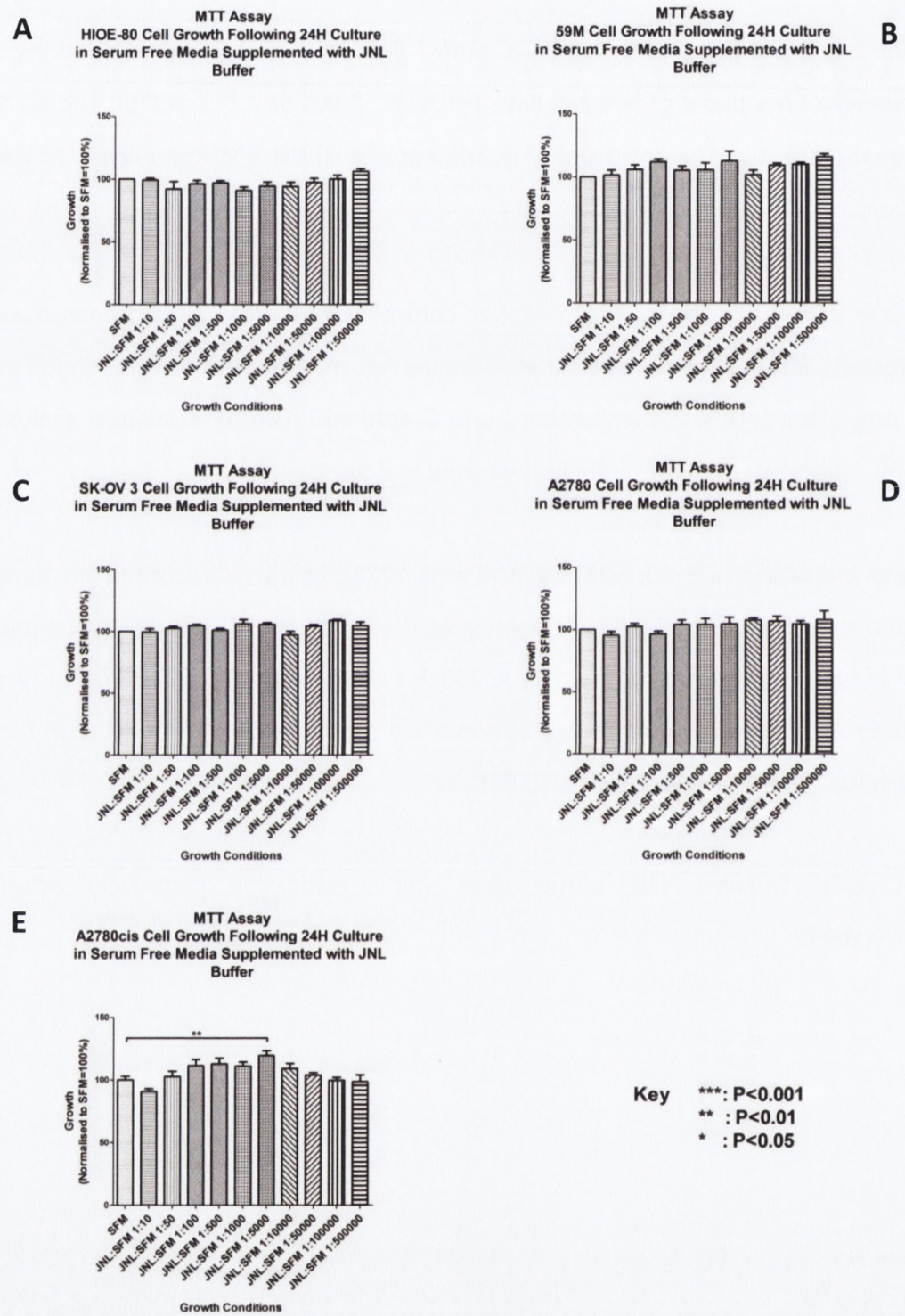

Figure 5-8: MTT Assay of cell growth & proliferation in Ovarian Cell in response to culture in the presence of JNL buffer augmented serum free growth media.

Cells, platelet releasate and MTT assay was performed as described in Table 5-4. Figure 5-8 illustrates the growth of HIOE-80 (A), 59M (B), SK-OV 3 (C), A2780 (D) and A2780cis (E) cell lines in the presence of JNL buffer augmented serum free growth media (SFM). Significant differences vs growth in SFM are annotated as follows: *p<0.05, **p<0.01, ***p<0.001.

5.3.1.4 Apoptosis detection by Flow Cytometry TUNEL Assay

Having previously confirmed a PLRL dilution of 1:1000 in full media as the highest concentration that results in no significant reduction in cell growth or metabolism over a 24 hour exposure period, the effect of this exposure period and PLRL dilution factor on cell apoptosis was assessed by flow cytometry TUNEL assay.

Each cell line was assayed in triplicate under following culture in either full growth media or PLRL supplemented full growth media for 24 hours. Positive, negative and unstained control cells were prepared in order to correctly setup the flow cytometer and set gating properties for the assay.

The results of the assay are indicated in Figure 5-9 and accompanying table. This data indicates that no cell line examined displayed any significant alteration in levels of apoptosis in response to exposure to platelet releasate at a 1:1000 dilution in full media over cell cultured in full growth media alone ($p>0.05$).

As result of significant loss of cell numbers during processing affecting flow cytometry results no data is provided for the HIOE-80 cell line. As a result of insufficient platelet releasate and time it was not possible to repeat the assay on this cell line, though the consistent results returned by the other cell lines supporting the previously performed MTT assays allows the use of the 1:1000 dilution factor of platelet releasate in full growth media.

Figure 5-9

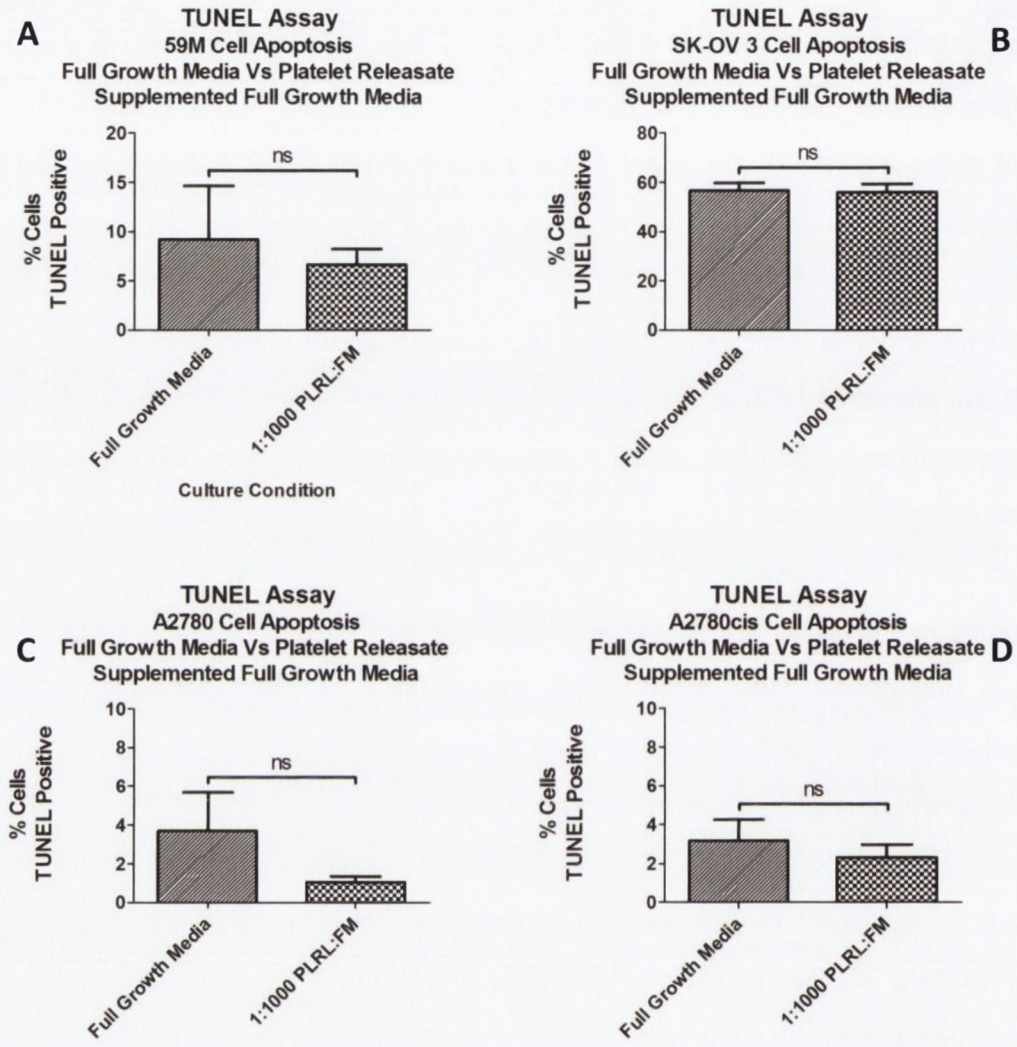

Cell Line	Culture Condition	% Cells TUNEL +ve	SEM	*p* =
59M	Full Growth Media	9.23	5.42	0.605904
	1:1000 Dilution PLRL	6.63	1.59	
A2780	Full Growth Media	3.69	2.00	0.26169
	1:1000 Dilution PLRL	1.05	0.29	
A2780cis	Full Growth Media	3.18	1.06	0.35026
	1:1000 Dilution PLRL	2.33	0.65	
SK-OV 3	Full Growth Media	53.03	3.05	0.238147
	1:1000 Dilution PLRL	59.17	1.88	

Figure 5-9: Flow Cytometry TUNEL Assay – Cell Line Apoptosis in Full Growth Media 1:1000 Dilution PLRL.

Ovarian cell lines were grown to 80% confluence in 24 well plates. Pooled platelet releasate was prepared from gel filtered platelets extracted from whole blood from three female volunteers.

Cells were cultured in a 1:1000 dilution of pooled platelet releasate:full growth media or full growth media only for 24h. N=3 was performed for each condition. Apoptosis was assessed by flow cytometry TUNEL assay and mean apoptosis (±SEM) calculated.

5.3.2 Mycoplasma Test

Due to the potential impact that mycoplasma infection could have on the gene expression in cell lines cell lines were tested for mycoplasma prior to beginning preparation for GeneChip based whole transcriptome investigations.

The Roche Mycoplasma Detection Kit (ELISA) was selected for use as it allows the fast and reliable detection of the four most common mammalian cell line contaminating mycoplasma/acholeplasma; *M. arginini* (10^6 - 10^7 CFU/ml), *M. hyorhinis* (10^6 - 10^7 colony forming units (CFU)/ml), *A. laidlawii* (10^4 - 10^5 CFU/ml), *M. orale* (10^5 - 10^6 CFU/ml).

Full growth media was freshly prepared and cell lines were seeded to cell culture plates as per standard cell culturing techniques and maintained at standard growth conditions (37°C, 5% CO_2, humidified) for two days after which time the conditioned media was extracted, transferred to sterile 15ml tubes and the cells passaged. Unconditioned media was transferred to sterile 15ml tubes to serve as experimental negative controls. The ELISA was performed as per manufacturer's instructions.

Prior to reading at 405nm sample wells were visually assessed. The solution visible in positive control wells displayed a yellow colour indicative of 4NNP conversion to NP indicative of mycoplasma presence. Conversely, the solution contained in sample and negative control wells was clear suggesting the absence of mycoplasma in these sources. The assay plates were then read at 405nm, the data recorded, adjusted for blank and results normalised against the kit positive controls. GraphPad Prism was used to interrogate the data for each cell line investigated. One way ANOVA was used to investigate for differences between the groups and Bonferroni analysis was performed to examine differences between each pair of groups.

The analysis of the data indicated no mycoplasma infection of experimental cell lines.

Figure 5-10

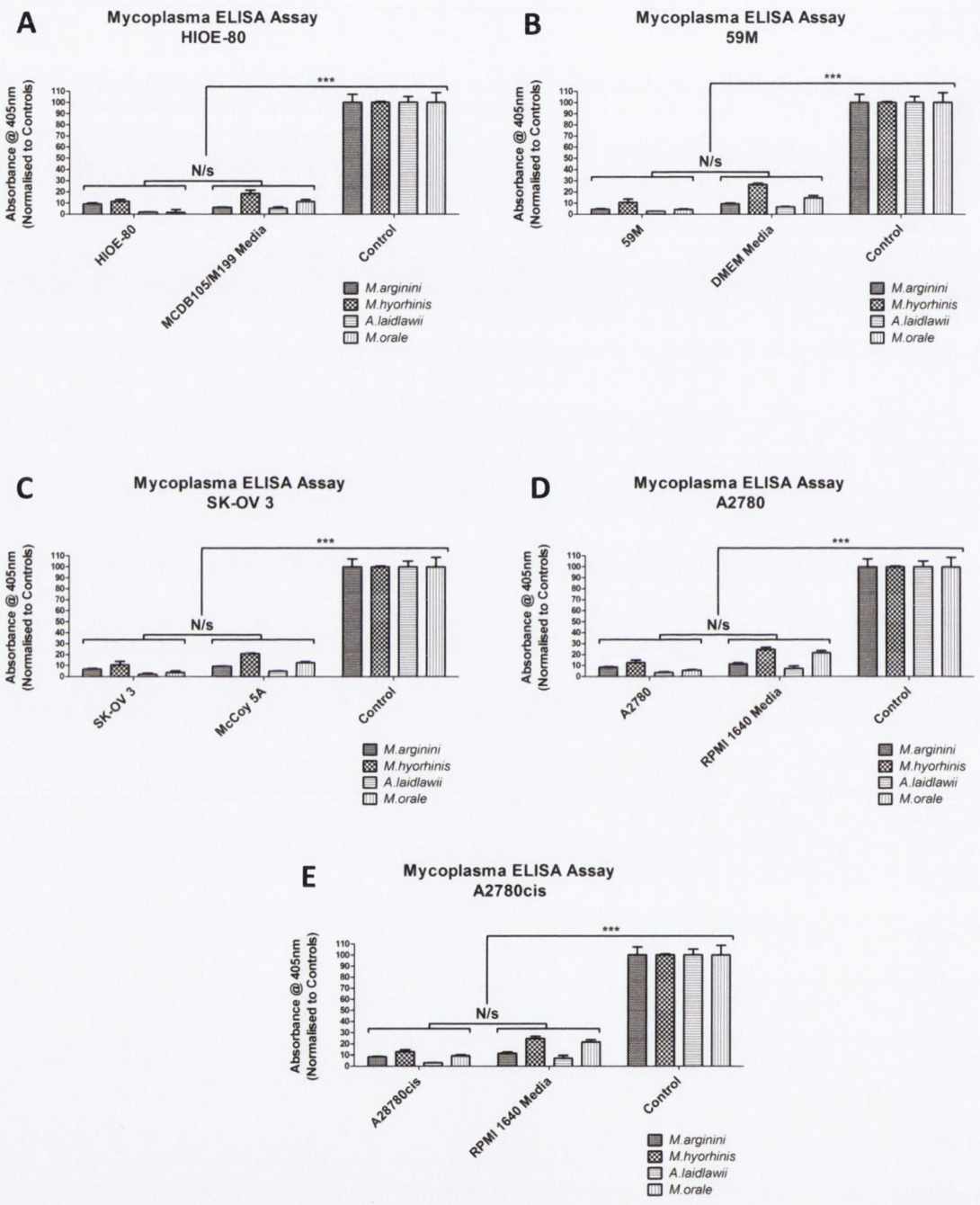

Figure 5-10: Pre-Affymetrix® GeneChip® Assay Cell Line Mycoplasma Assay.

Data recorded for mycoplasma species presence in experimental cell lines indicates no significant difference between measurements taken from cell line conditioned media and freshly prepared, unconditioned growth media. Highly significant differences were observed between these two groups in all cell lines examined and positive controls for each mycoplasma species ($p<0.001$).

5.3.3 RNA Extraction

5.3.3.1 Comparison of Extraction Methods

In order to ensure that the maximum total RNA yield was extracted from washed platelet/platelet releasate exposed cell lines different nucleic acid extraction methodologies were assessed for their ability to return high yields of high quality RNA.

The two techniques assessed were the QIAGEN® RNeasy® method utilising QIAshredder sample homogenisation and the Ambion® mirVana™ methods. Both use chemistries allowing extraction of tRNA with the latter allowing optional miRNA enrichment.

These extractions were performed in triplicate on cells recovered from T25 ($25cm^2$ growth area) flasks having been cultured to 90% confluence.

Table 5-5

Cell Line	Extraction Method	Mean Δ260/280	Mean tRNA yield (ng/µl)	SEM	*p*=
HIOE-80	QIAGEN® RNeasy®	2.06	111.90	17.32	0.04
	Ambion® mirVana™	2.05	65.50	10.61	
59M	QIAGEN® RNeasy®	2.09	158.73	13.12	0.01
	Ambion® mirVana™	2.06	104.07	5.44	
SK-OV 3	QIAGEN® RNeasy®	2.1	157.25	8.35	0.02
	Ambion® mirVana™	2.08	114.75	11.66	
A2780	QIAGEN® RNeasy®	2.09	433.07	42.67	0.004
	Ambion® mirVana™	2.09	178.47	30.85	
A2780cis	QIAGEN® RNeasy®	2.1	155.77	18.24	0.37
	Ambion® mirVana™	2.1	164.00	14.58	

Table 5-5: Comparision of total RNA extraction methods.

Both QIAGEN® and Ambion® methods resulted in extraction of RNA of high purity/low contamination as indicated by high Δ260/280 values. Having compared the yield of total RNA extracted from experimental cell lines using the QIAGEN® RNeasy® (including QIAshredder™ sample homoginisation) and Ambion® mirVana™ methods (Table 5-5) the decision was taken to utilise the QIAGEN® technique on all future RNA extractions based on the significantly greater yields reported in four out of the five cell lines ($p<0.05$).

5.3.3.2 RNA Quantitation and Integrity Assessment

Having determined the method returning the maximum tRNA yield from experimental cell lines, cells were cultured in T75 cell culture flasks until 90% confluent and subsequently exposed to a 1:1000 dilution of washed platelets or platelet releasate in full growth media for 8 hours at 37°C, 5% CO_2 in a humidified cell culture incubator. Also cultured were cells grown in full growth media only, representing normal controls. Each of the cell line culture conditions was performed in triplicate for each cell line.

Following the exposure, total RNA was extracted using QIAGEN® RNeasy® nucleic acid extraction kit methodology (Section 2.2.2.1). Following extraction, total RNA was quantified and purity assessed by NanoDrop™ (Section 2.3.1), and its integrity assessed by Agilent Bioanalyzer (Section 2.3.2). The total volume of isolated total RNA was prepared in 30µl with a loss of 1µl during NanoDrop™ quantitation.

5.3.3.2.1 NanoDrop™ RNA Assessment

Each tRNA sample isolated was subjected to NanoDrop™ quantitation prior to progressing forward for Affymetrix® GeneChip® Human Exon Array 1.0 ST sample preparation, assay and analysis.

The concentration and the Δ260/280 of tRNA recovered for each of the samples is indicated in Table 5-6.

All samples returned tRNA at concentrations of >1000ng/µl in the elution volume of 30µl. The Δ260/280 values were all high indicating a high tRNA purity.

Table 5-6

Cell Line	Sample #	Treatment	RNA (ng/µl)	Δ260/280
HIOE-80	1a	Control	2236.3	2.10
	1b	Control	2363.2	2.09
	1c	Control	1745.3	2.09
	2a	Platelet Releasate	2054	2.08
	2b	Platelet Releasate	1460	2.07
	2c	Platelet Releasate	1553.7	2.08
	3a	Washed Platelets	1541.7	2.08
	3b	Washed Platelets	1607.1	2.06
	3c	Washed Platelets	1840.2	2.08
59M	4a	Control	2397.7	2.10
	4b	Control	2500.4	2.09
	4c	Control	2577.2	2.09
	5a	Platelet Releasate	2687.5	2.10
	5b	Platelet Releasate	2475.2	2.10
	5c	Platelet Releasate	2532.3	2.11
	6a	Washed Platelets	2526.3	2.11
	6b	Washed Platelets	3248.4	2.09
	6c	Washed Platelets	3151.2	2.11
SK-OV 3	7a	Control	1185.4	2.06
	7b	Control	1555.8	2.08
	7c	Control	1391	2.07
	8a	Platelet Releasate	1153.9	2.07
	8b	Platelet Releasate	1174.2	2.08
	8c	Platelet Releasate	1182.4	2.09
	9a	Washed Platelets	1192.3	2.06
	9b	Washed Platelets	1202	2.06
	9c	Washed Platelets	1248.1	2.08
A2780	10a	Control	2068.8	2.09
	10b	Control	1686.4	2.08
	10c	Control	2073.3	2.09
	11a	Platelet Releasate	1255	2.07
	11b	Platelet Releasate	1240	2.05
	11c	Platelet Releasate	1252.8	2.03
	12a	Washed Platelets	1122.7	2.03
	12b	Washed Platelets	1121.7	2.06
	12c	Washed Platelets	982.1	2.04
A2780cis	13a	Control	2193.3	2.10
	13b	Control	2341	2.09
	13c	Control	2332.5	2.09
	14a	Platelet Releasate	1167.1	2.06
	14b	Platelet Releasate	1453.1	2.08
	14c	Platelet Releasate	2222	2.07
	15a	Washed Platelets	1994.6	2.05
	15b	Washed Platelets	1374.4	2.05
	15c	Washed Platelets	924.3	2.04

Table 5-6: Quantitation of Sample tRNA prior to Affymetrix® GeneChip® Array Assay

Total RNA was also extracted from a 1:1000 dilution of washed platelets prepared in a final volume of 10mls of full growth media reflecting both the concentration and the volume of the diluted washed platelets/platelet releasate applied to experimental cell lines.

This was performed to determine if sufficient tRNA could be detected as to possibly result in a signal originating from platelet tRNA confounding the results of subsequent Affymetrix whole transcriptome assays.

Table 5-7

Cell Line	Sample #	RNA (ng/µl)	Δ260/280
1:1000 Dilution Washed Platelets ($10ml_{FV}$)	16a	0.1	0.21
1:1000 Dilution Washed Platelets ($10ml_{FV}$)	16b	-0.1	0.30
1:1000 Dilution Washed Platelets ($10ml_{FV}$)	16c	0.2	0.22

Table 5-7: Quantitation of Total RNA of Platelet Origin.

The figures returned having attempted to recover tRNA from a 10ml volume of 1:1000 dilution of washed platelets are indicated in Table 5-7. These figures are equivalent to that of a blank control reading performed on the NanoDrop™ unit using DNAse and RNase free H_2O.

This suggests that platelet derived tRNA in the sample is either absent or present in but quantities so minute as to be undetectable using the technology available given the starting quantity of washed platelets.

Given this information and the starting tRNA quantity requirements of Affymetrix® GeneChip® assays, it is unlikely that tRNA from washed platelets is present in sufficient quantities to result in a signal that would confound that indicating changes in gene expression of experimental cell lines in response to exposure to washed platelets or platelet releasate.

5.3.3.2.2 Bioanalyser RNA Assessment

After initial NanoDrop™ tRNA quantification and purity analysis tRNA nucleic acid integrity was assessed using an Agilent Bioanalyser and RNA 6000 Nano Kit and chips. 1µl of sample tRNA was diluted 1:10 in DNase and RNase free H_2O prior to assessment so as to not exceed the concentration limit of 500ng/µl for accurate sample qualitative assessment. The RNA Integrity Number (RIN) and ribosomal ratio (Δ28S/18S) of each tRNA sample assessed is indicated in Table 5-8.

RIN utilises a proprietary Agilent algorithm to generate a value reflecting the integrity of an RNA sample based on analysis of the electrophoretic trace recorded for the sample as it is run on a Bioanalyser chip (Schroeder et al., 2006, Mueller et al., 2004). The closer the value is to 10, reflecting a perfectly intact RNA sample, the higher the sample integrity.

The RIN values returned indicate the tRNA extracted from experimental cell lines was of a high integrity and had not suffered degradation or fragmentation during extraction and processing.

The ratio of 28S to 18S ribosomal RNA (Δ28S/18S) is a secondary indicator of RNA quality when used in conjunction with Bioanalyser RIN based RNA qualitation.

The Δ28S/18S uses the rRNA ratio to infer as to the quality of the less plentiful mRNA in a tRNA sample, with a ratio of 2.0 reflecting high quality, intact RNA and a ratio of >1.0 observed to perform well in a variety of downstream applications (Ambion Inc., 2004a, 2004b).

Figure 5-11 is a representative Bioanalyser electropherogram of one sample accompanied by the ladder control indicating nucleotide sizes.

Figure 5-12 is a digital electrophoretic gel image representation of the electropherograms corresponding to a range of tRNA samples assessed at this point in tRNA assessment.

Figure 5-11

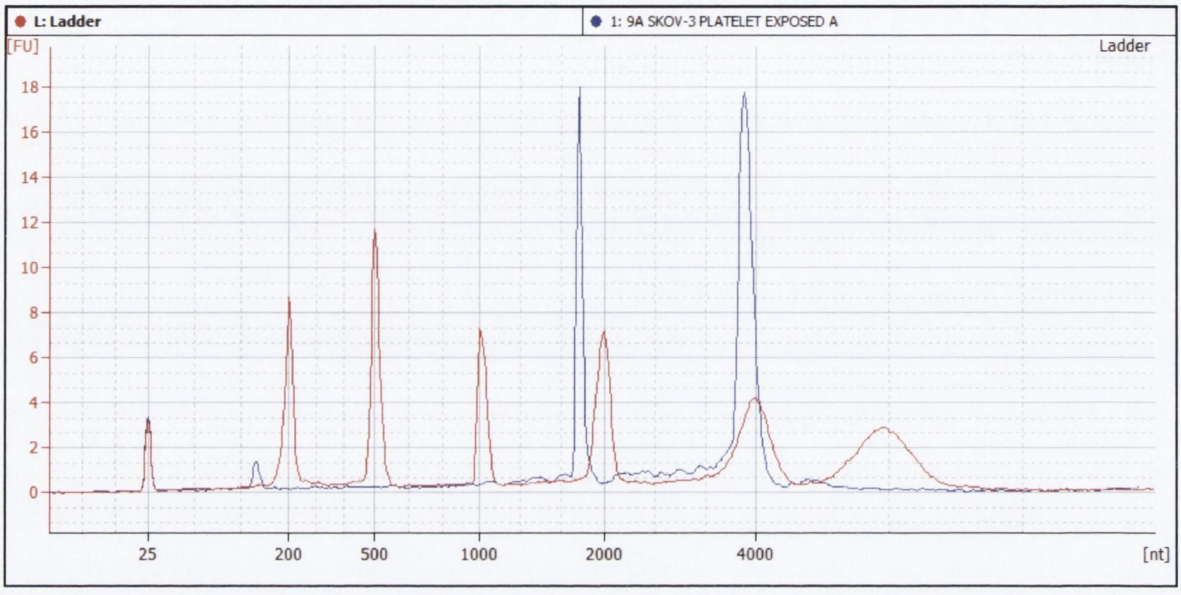

Figure 5-11: Bioanalyzer Electropherogram of sample tRNA.

Figure 5-12

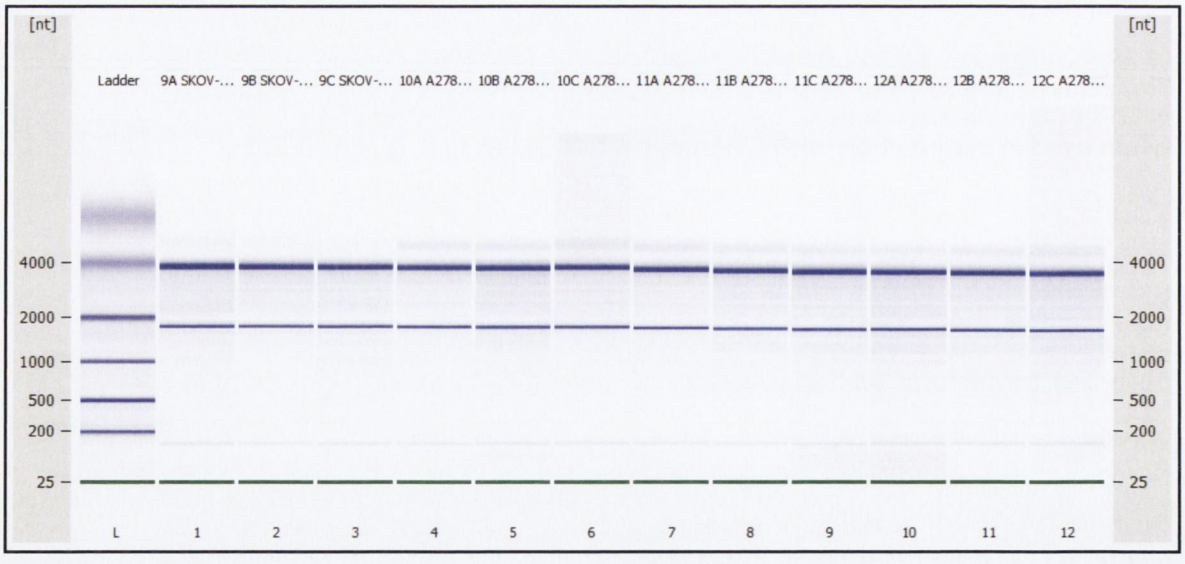

Figure 5-12: Bioanalyzer Digital Gel Image of a range of tRNA samples.

From the gel two clear bands representing 18S (lower) and 28S (upper) ribosomal RNA are clearly visible in lanes 1 to 12. The left most lane contains the nucleotide ladder ranging from nucleotides of 25nt length to 4000nt length providing standards to enable size discrimination of assayed samples in addition to sample qualitation and quantitation.

Table 5-8

Cell Line	Sample #	Treatment	RNA Integrity Number (RIN)	28S/18S rRNA Ratio
HIOE-80	1a	Control	9.8	1.9
	1b	Control	8.8	1.8
	1c	Control	9.2	1.9
	2a	Platelet Releasate	8.8	1.9
	2b	Platelet Releasate	9.1	1.9
	2c	Platelet Releasate	8.8	2.2
	3a	Washed Platelets	9.6	1.9
	3b	Washed Platelets	8.8	2.2
	3c	Washed Platelets	9.5	2.0
59M	4a	Control	9.5	2.0
	4b	Control	9.5	2.1
	4c	Control	9.4	2.1
	5a	Platelet Releasate	8.8	1.9
	5b	Platelet Releasate	8.1	1.9
	5c	Platelet Releasate	8.6	2.0
	6a	Washed Platelets	8.3	2.0
	6b	Washed Platelets	7.4	1.8
	6c	Washed Platelets	7.7	1.9
SK-OV 3	7a	Control	9.4	1.8
	7b	Control	9.0	2.0
	7c	Control	9.9	1.8
	8a	Platelet Releasate	9.4	1.9
	8b	Platelet Releasate	9.8	2.1
	8c	Platelet Releasate	10.0	2.0
	9a	Washed Platelets	9.2	2.0
	9b	Washed Platelets	9.8	1.9
	9c	Washed Platelets	9.4	2.2
A2780	10a	Control	9.6	2.0
	10b	Control	9.3	1.7
	10c	Control	10.0	1.8
	11a	Platelet Releasate	9.9	2.0
	11b	Platelet Releasate	9.5	1.8
	11c	Platelet Releasate	9.3	1.8
	12a	Washed Platelets	9.0	1.8
	12b	Washed Platelets	9.2	1.7
	12c	Washed Platelets	8.9	1.8
A2780cis	13a	Control	9.7	2.0
	13b	Control	9.8	1.9
	13c	Control	9.8	1.8
	14a	Platelet Releasate	9.7	1.9
	14b	Platelet Releasate	9.8	1.9
	14c	Platelet Releasate	9.2	1.7
	15a	Washed Platelets	8.2	1.7
	15b	Washed Platelets	9.6	1.9
	15c	Washed Platelets	9.6	2.0

Table 5-8: Integrity Assessment of Sample Total RNA prior to Affymetrix® GeneChip® Array Assay.

5.3.4 Affymetrix® GeneChip® Human Exon 1.0 ST Array

The Affymetrix® GeneChip® Human Exon 1.0 ST array was selected for use to determine the nature of changes in gene expression over the whole transcriptome in the panel of ovarian cell lines in response to exposure to washed platelets or platelet releasate.

This array type allows the investigation of whole transcript expression with increased probe coverage than is possible with previous iterations of the GeneChip® technologies and offers the possibility of additionally investigating alteration of splice variant expression if desired.

For the purposes of this study the investigation focussed on 'Core' probe-sets include probe-sets that correspond to high quality genomic features like RefSeq (www.ncbi.nlm.nih.gov) or Ensembl (www.ensembl.org) transcripts and subsequent assessment of alterations of whole transcripts. 'Full' and 'Extended' probe-sets matching less reliable annotations like EST hits and gene prediction algorithms and changes occurring in splice variant expression were not investigated.

5.3.4.1 Human Exon 1.0 ST Assay Quality Control

100ng of total RNA extracted from control cells and cells exposed to gel filtered platelets or platelet releasate was labelled using the Ambion WT Expression kit [Ambion/Life Technologies, Austin, TX, USA] including the labelling controls from the Affymetrix Gene Chip Poly-A RNA Control Kit.

As suggested by Affymetrix/Ambion, at each step of the sample preparation protocol, progress was monitored using both the Agilent 2100 Bioanalyzer and the Nanodrop™ spectrophotometer.

Quality control (QC) required:

- NanoDrop™ assessment:
  - following the first cycle RNA cleanup – to ensure that a yield of >10µg and Δ260/280 ratios of 1.8 - 2.2.
  - following the second cycle single strand cDNA cleanup – to ensure that a yield of >5µg and Δ260/280 ratios of 1.8 - 2.2.

- Bioanalyser assessment:
  - Following ssDNA fragmentation – to ensure the antisense biotin labelled cDNA to peak was observed on a Bioanalyzer to have fragmented at 40-70 bases.

Optional Bioanalyser assessments were carried out following first cycle RNA cleanup and second cycle single strand cDNA cleanup to confirm the product of these steps conformed to the expected nucleotide size distributions of 50-4500 (peaking at 200-2000nt) and 400nt respectively.

Hybridization buffer, Eukaryotic Hybridization Controls (to confirm the sensitivity of hybridization), and OligoB2 controls (used to orient and grid the array) were added to the cDNA fragments just prior to hybridization to the Affymetrix® Human Exon 1.0 ST Array. Following hybridization (45°C for 16 hours), the chips were washed and stained with a phycoerythrin-strepavidin conjugate using the Affymetrix GeneChip Fluidics Station with appropriate 64 format assay (FS450-0001) protocol.

Following staining and washing steps the Affymetrix GeneChip Scanner 3000 and Affymetrix GeneChip Operating Software was used for the management and initial processing of the expression data. All data from the 45 exon arrays was then subject to array quality control, performed using Affymetrix® Expression Console™ (v 1.1) at the transcript level using core-level probe sets.

All image plots passed visual inspection based on OligoB2 grid staining and alignment.

Bacterial (bac spike) Hybridization controls were all present with signal increases following the order BioB < BioC < BioD < Cre. A representative image of labelling controls from one set of samples (SK-OV 3 cell line, samples 7a-c, 8a-c & 9a-c) is given in Figure 5-13.

Figure 5-13

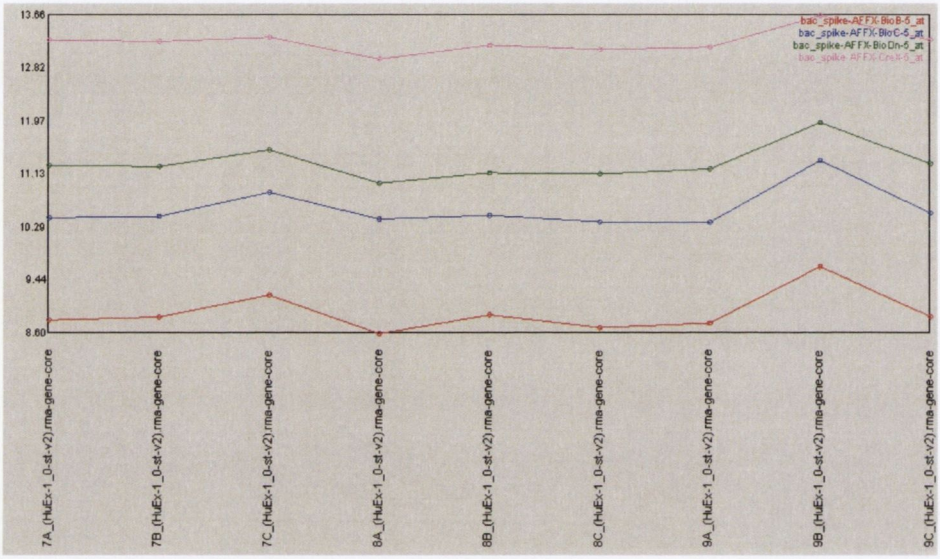

Figure 5-13: Affymetrix Quality Control - Hybridisation Control Assessment.

Hybridisation (bac spike) controls were assessed for all samples. Figure 5-13 is a representative image of hybridisation control assessment of data from SK-OV 3 samples.

The order and magnitude of signal increases (BioB < BioC < BioD < Cre) was correct, within manufactures guidelines and observed for all samples.

Labelling control signal strengths followed the order Lys < Phe < Thr< Dap. A representative image of labelling controls from one set of samples (SK-OV 3 cell line, samples 7a-c, 8a-c & 9a-c) is given in Figure 5-14.

Figure 5-14

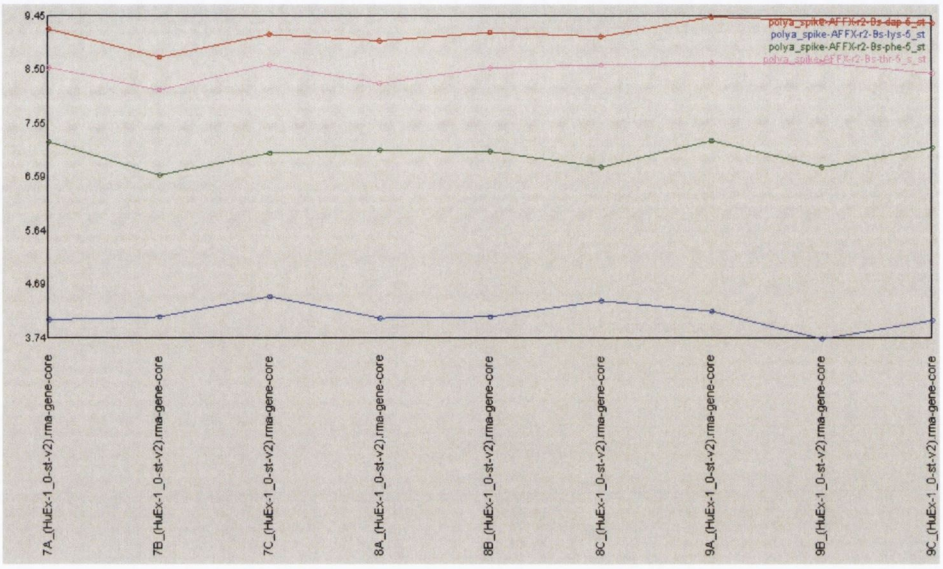

Figure 5-14: Affymetrix Quality Control - Labelling Control Assessment.

Sample labelling controls were assessed for all samples. Figure 5-14 is a representative image of hybridisation control assessment of data from SK-OV 3 samples.

The order and magnitude of signal increases (Lys < Phe < Thr< Dap) was correct, within manufactures guidelines and observed for all samples.

All controls performed for all samples at all stages of sample preparation and post hybridisation assessment were within the parameters suggested by Affymetrix.

5.3.4.2 Affymetrix Whole Transcriptome Investigation of Gene Expression

Following successful quality control standards assessment (section 5.3.4.1), the chip data was then analysed in depth using Biotique Systems XRAY analysis software.

Each cell line was examined under three different conditions;

- resting cells.
- cells exposed to platelet releasate.
- cells exposed to washed platelets.

Each condition was assayed in triplicate for each cell line resulting in the generation of 3 CEL files per condition per cell line.

XRAY software was used to compare the two exposure cohorts against the resting control and genes exhibiting a positive or negative fold change of greater than 1.5 and a significance of $p \leq 0.05$ examined.

For each group comparison 6 input CEL files (3 corresponding to resting cells, 3 corresponding to cells exposed to either washed platelets or platelet releasate) were analyzed to identify genes that were significantly differentially expressed between the groups of interest (Gardina et al., 2006, Huang et al., 2007a, Clark et al., 2007).

5.3.4.2.1 Array Normalisation

The input files were normalized with full quantile normalization (Irizarry et al., 2003a) For each input array, for each probe expression value, the array ith percentile probe value was replaced with the average of all array ith percentile points.

5.3.4.2.2 Background Correction

Background was established from a pool of probes designed for that purpose of background correction. Background probes are stratified by CG content and are defined in the HumanExon10ST_antigenomic.bgp file. Each probe score was corrected for background by subtracting the median expression score of background probes with similar GC content.

5.3.4.2.3 Probe Summarization and Transformation

The HumanExon 1.0 ST array contains 1,404,693 probe-sets, typically but not always comprised of groups of four probes. The expression score for a probe-set was defined to be the median of its probe expression scores and probe-sets with fewer than 3 probes are excluded from further analysis.

5.3.4.2.4 Experimental Design Power

The power for this experimental design to detect a genuine 25% change in gene expression at $p<0.05$ was assessed for all experiments. This is a probability score (≤ 1.0) for the experimental design to detect a statistically significant 1.25 fold change, a fold change smaller than the minimum of interest to this study, and assuming that the typical gene has 7 exons (probe-sets).

The mean probability (power) of this experimental design utilising three Human Exon 1.0ST arrays per experimental group over the ten experimental groupings being compared was 0.9841544 ± 0.006738. This means that there is across the range of group comparisons performed there is 98.41% chance that a statistically significant ($p<0.05$) fold change of 1.25 is a genuine observation of altered gene expression.

5.3.4.2.5 Bioinformatic Analysis & Literature Review

Genes identified as undergoing significant ($p<0.05$) alterations of expression with a fold change of equal to or greater than 1.5 were investigated using:

- INGENUITY® Systems (Redwood, CA, USA) Ingenuity Pathway Analysis (IPA®) software,
- the National Institute of Allergy and Infectious Diseases (NIAID) DAVID Bioinformatics Database (Huang da et al., 2009, 2008)

, and additional review of published data through directed searches of:

- the National Center for Biotechnology Information (NCBI) PubMed and
- Elsevier Science Direct publication databases.

5.3.4.3 HIOE-80

5.3.4.3.1 HIOE-80 - Washed Platelet Exposure

In order to identify genes with differential gene expression between the groups of washed platelet exposed and resting HIOE-80 cells we studied 6 hybridizations (the resting control and exposure groups, each in triplicate) on the Human Exon 1.0 ST arrays using mixed model analysis of variance.

This analysis determined 189 genes showed significant gene expression differences between the groups ($p<0.05$). Of these 189 genes observed to undergo statistically significant alteration of expression, 6 were of study interest given a fold change of greater than 1.5. These genes, their FC and significance along with their corresponding proteins are indicated in Table 5-9.

Table 5-9

Cell Line	Exposure	Gene	Protein	Fold Change (FC)	(p=)
HIOE-80	Washed Platelet	**SERPINB2**	**serpin peptidase inhibitor clade B [ovalbumin] member 2**	1.76	0.0016
		IDI1	isopentenyl-diphosphate delta isomerase 1	1.70	0.0218
		PMM2	phosphomannomutase 2	1.60	0.0188
		PCGF6	**polycomb group ring finger 6**	1.59	0.0372
		CCDC68	coiled-coil domain containing 68	1.56	0.0245
		ZNF267	**zinc finger protein 267**	1.55	0.0318

Table 5-9: Genes Undergoing Significantly Altered Expression in Response to Washed Platelet Exposure in HIOE-80 Cells.

The HIOE cell line was determined to undergo significant alteration of expression 189 genes when exposed to washed platelets compared to resting cells ($p<0.05$). Of these genes 6 showed a FC of greater than or equal to 1.5. Three of these genes (indicated in bold) were selected for subsequent validation.

5.3.4.3.2 Genes Displaying Increased Expression in HIOE-80 Cells Following Washed Platelet Exposure

SERPINB2 (PAI2)

This gene encodes for the plasminogen activator inhibitor 2 protein. This acts as an inhibitor urokinase Plasminogen Activator (uPA), a protein whose expression has been shown to correlate with negative prognoses in many cancers resulting from increased invasiveness arising from increased MMP-9 mediated extracellular matrix degredation (Hayat, 2010, Dass et al., 2008, Croucher et al., 2008).

Increased SERPINB2 expression has been reported in hepatocellular carcinoma, breast, oesophageal, lung, pancreatic and ovarian cancers where it is reported to correlate with favorable outcome or improved survival (Chambers et al., 1997, Robert et al., 1999, Duggan et al., 1997, Smith et al., 2007, Pennings et al., 2007, Lutters et al., 2003, Zhou et al., 2000, Croucher et al., 2008).

IDI1

This gene encodes for the isopentenyl-diphosphate delta isomerase 1. This protein functions as a metabolic enzyme catalyzing Isopentenyl diphosphate to dimethylallyl diphosphate in peroxisome required for activation of the isoprene biosynthetic pathway and ultimately cholesterol synthesis (Mayer et al., 1992). It has been recently reported in one study to undergo altered (reduced) expression in xenograft model of human ovarian cancer in response to 24h paclitaxel exposure (Bani et al., 2004).

PMM2

This gene encodes for the phosphomannomutase 2. This protein functions as a metabolic enzyme catalyzing isomerization of mannose 6-phosphate to mannose 1-phosphate. A deficiency in expression of this gene or defective gene product results in congenital disorder of glycosylation (carbohydrate-deficient glycoprotein syndrome (CDGS), Jaeken

Disease) (Dahl et al., 2011, Quelhas et al., 2007, Matthijs et al., 1997). No information is available describing the effect of alterated PMM2 expression in any cancer types.

PCGF6 (MBLR)

This gene encodes for the polycomb group ring finger 6. This protein functions to assist in gene expression in complexes with other proteins and functions as a transcription repressor (Akasaka et al., 2002, Lee et al., 2007).

CCDC68

This gene encodes for the coiled-coil domain containing 68 protein. There is currently little published data on the biological activity, function or localization of this protein. CCDC68 has been identified as a potential tumour suppressor gene for colon/colorectal cancer based on reduced expression/copy number in this cancer (Sheffer et al., 2009, Gerhardt et al., 2004).

ZNF267

This gene encodes for the zinc finger protein 267. This protein functions as a transcriptional regulator with specific activity in inhibiting the expression of MMP10 (Schnabl et al., 2005). Given the increased expression of MMP10 in a range of cancers including: lung (Frederick et al., 2008, Gill et al., 2004), squamous cell (Boyd et al., 2009) transitional bladder cell (Seargent et al., 2005) and oral (Yen et al., 2009) cancer/carcinomas and has been identified as upregulated in the A2780 cell line in development of cisplatin resistance (Solár and Sytkowski, 2011). It may be possible that ZNF267 fills a tumour suppressor gene function in normal tissues maintaining MMP10 expression at normal physiological levels.

5.3.4.3.3 HIOE-80 - Platelet Releasate Exposure

In order to identify genes with differential gene expression between the groups of platelet releasate exposed and resting HIOE-80 cells we studied 6 hybridizations (the resting control and exposure groups, each in triplicate) on the Human Exon 1.0 ST arrays using mixed model analysis of variance.

This analysis determined 113 genes with significant gene expression differences existed between the groups ($p<0.05$). Of these 113 genes observed to undergo statistically significant alteration of expression, 1 was of study interest given a fold change of greater than 1.5. This gene, its FC and its significance along with its corresponding protein is indicated in Table 5-10.

Table 5-10

Cell Line	Exposure	Gene	Protein	Fold Change (FC)	(p=)
HIO-80	Platelet Releasate	**LRP8**	**low density lipoprotein receptor-related protein 8 [Apo E receptor 2]**	1.50	0.0275

Table 5-10: Genes Undergoing Significantly Altered Expression in Response to Platelet Releasate Exposure in HIOE-80 Cells.

The HIOE cell line was determined to undergo significant alteration of expression 113 genes when exposed to washed platelets compared to resting cells ($p<0.05$). Of these 113 genes, one (LRP8) showed a FC of greater than or equal to 1.5.

On further analysis of genes altered in the HIOE-80 cell line LRP8 was also observed to undergo altered expression in response to washed platelet exposure (FC 1.4948, $p=0.0448$).

5.3.4.3.4 Genes Displaying Increased Expression in HIOE-80 Cells Following Platelet Releasate Exposure

LRP8

LRP8, also known as APOER2, encodes for the Apolipoprotein E receptor 2 protein. This is a cell surface protein that plays roles in both signal transduction and receptor-mediated endocytosis of specific ligands for lysosomal degradation.

The encoded protein is predominantly expressed in the brain where it plays a critical role in the migration of neurons during development by mediating signalling through it's ligand, Reelin, and also functions as a receptor for the cholesterol transport protein apolipoprotein E. (Leemhuis et al., 2010, Duit et al., 2010, Andersen et al., 2003, Kim et al., 1996).

When expressed, the protein LRP8 has been shown to mediate attenuation of platelet activation through binding of ApoE and induction of iNOS generation of nitric oxide, a potent platelet activation inhibitor (Nofer et al., 2010, Robertson et al., 2009, Riddell et al., 1999, 1997).

Increased LRP8/APOER2 expression has been reported in lung cancer where increased expression was observed to also result in altered NOTCH signalling (Garnis et al., 2005) and increased expression has been demonstrated to result in increased breast epithelial cell line (MCF 10A) migration *in vitro* (Minami et al., 2010).

Additionally LRP8/APOER2 has been observed to interact with and modify platelet activation and aggregation. It has been shown that platelets bind to dimeric β2 glycoprotein 1 via a GB1bα and apoER2 receptor complex on the platelet surface and this is capable of supporting platelet adhesion and aggregation under venous flow conditions (Urbanus et al., 2008, Pennings et al., 2007, Lutters et al., 2003) and may mediate protein C and activated protein C intracellular signalling in other cells (White et al., 2008). It has also been observed to act as a receptor for Factor X1 (FX1), a component of the intrinsic coagulation pathway (White-Adams et al., 2009).

It is not known how the increased expression of LRP8 may influence ovarian cancer though it may be hypothesised that the effect of increased LRP8 may be to increase localisation of proteins that interact with platelets to result in platelet activation and aggregation to the cell surface and thus may have a role in assisting/enabling TCIPA.

Arising from its increased expression in response to both washed platelet and platelet releasate in HIOE-80 cells it was selected for subsequent qPCR based validation.

5.3.4.4 59M

5.3.4.4.1 59M - Washed Platelet Exposure

In order to identify genes with differential gene expression between the groups of washed platelet exposed and resting 59M cells we studied 6 hybridizations (the resting control and exposure groups, each in triplicate) on the Human Exon 1.0 ST arrays using mixed model analysis of variance.

This analysis determined 275 genes with significant gene expression differences existed between the groups ($p<0.05$). Of these 275 genes observed to undergo statistically significant alteration of expression, 5 were of study interest given a fold change of greater than 1.5. These genes, their FC and significance along with their corresponding proteins are indicated in Table 5-11.

Table 5-11

Cell Line	Exposure	Gene	Protein	Fold Change (FC)	(p=)
59M	Washed Platelet	TRAF1	TNF receptor-associated factor 1	1.90	0.0056
		CCL2	chemokine [C-C motif] ligand 2	1.78	0.0281
		TNFAIP2	tumor necrosis factor alpha-induced protein 2	1.63	0.0048
		PDGFB	platelet-derived growth factor beta polypeptide	1.50	0.0397
		DSN1	DSN1 MIND kinetochore complex component homolog	-1.60	0.0350

Table 5-11: Genes Undergoing Significantly Altered Expression in Response to Washed Platelet Exposure in 59M Cells.

The 59M cell line was determined to undergo significant alteration of expression 275 genes when exposed to washed platelets compared to resting cells ($p<0.05$). Of these genes 5 showed a FC of greater than or equal to 1.5. These five genes were selected for subsequent validation.

5.3.4.4.2 Genes Displaying Increased Expression in 59M Cells Following Washed Platelet Exposure

TRAF1

This gene encodes for a member of the tissue necrosis factor receptor (TNFR) associated factor (TRAF) protein family which interact with, and mediate signal transduction from receptors of the TNFR superfamily. This protein and TRAF2 form a heterodimeric complex, which is required for TNF-alpha-mediated activation of MAPK8/JNK and NF-κB pathways. The TRAF1/TRAF2 complex also interacts with inhibitor-of-apoptosis proteins (IAPs) BIRC2 and BIRC3, recruiting them to TNFRSF1B/TNFR2 and thus mediating the anti-apoptotic signals from TNF receptors (Arlt et al., 2010, Zhang et al., 2010c, Lee and Choi, 2007, Ha et al., 2001).

Increased TRAF2 expression results in generation of a NF-κB driven anti-apoptotic and proliferative signals in cells and desensitisation to TNFα induction of apoptosis (Shin et al., 2011, Sughra et al., 2010, Lavorgna et al., 2009, Sasaki et al., 2007, Sung et al., 2007, Hodge et al., 2006, Conti et al., 2005) .

CCL2 (MCP-1)

This gene encodes for the cytokine CCL2. This protein functions as a chemotactic factor that attracts monocytes and basophils. As a result of chemokine and colony stimulating factors these monocytes differentiate into macrophages within the tissues. Many malignant solid tumours contain a large number of these tissue associated macrophages (TAMs) attract additional macrophages to the developing tumour whilst producing numerous growth factors, proteases, and cytokines that promote a more favourable tumour microenvironment potentiating tumour progression (Siveen and Kuttan, 2009, Yuan et al., 2008, Pollard, 2004, Bingle et al., 2002) and has a role in anti-autophagy signalling in cancer (Roca et al., 2008b).

In the context of cancer CCL2/MCP-1 is reported to mediate anti-autophagy, pro-migration/invasion, proliferative and pro-angiogenic signalling in *in vitro* and *in vivo*

models of prostate cancer (Roca et al., 2008a, Zhang et al., 2010a, Zhang et al., 2010b). Altered CCL2/MCP-1 expression has been reported in ovarian cancer with conflicting reports on the effect of elevated expression on disease outcome (Fader et al., 2010, Negus et al., 1995), and the effect of chemotherapy on expression levels (Coward et al., 2011, Geller et al., 2010).

Increased MCP-1 expression arising from p38-MAPK/NF-κB pathway induction has also been reported in endothelial cells in response to transient activated platelet exposure providing a possible mechanism behind the change observed in this study (Gawaz et al., 2002, Dickfeld et al., 2001).

TNFAIP2

This gene encodes for tumor necrosis factor alpha-induced protein 2. This protein functions is induced by TNF-α and other pro-inflammatory cytokines and so may act as a mediator of inflammation and angiogenesis. Its role in cancer is little understood but has recently been observed to be up-regulated in nasopharyngeal carcinoma where it correlates with increased invasion, metastasis and tumour blood vessel density (Chen et al., 2011). The influence of TNFAIP2 on ovarian cancer is yet to be described.

PDGFB

This gene encodes for the platelet derived growth factor B protein. This protein functions as platelet-derived growth factor when part of a homodimer or a heterodimer with a PDGFA polypeptide. As previously discussed in chapter 3, elevated PDGF expression has been observed in many cancers including ovarian cancer where it was identified to correlate with increased preoperative platelet count. PDGF expression in cancer is associated with pro-angiogenic signalling through the interaction of the PDGF and VEGF pathways, may contribute to anti-autophagy and anti-apoptotic signalling (Matei et al., 2007, Billie Au et al., 2005).

5.3.4.4.3 Genes Displaying Reduced Expression in 59M Cells Following Washed Platelet Exposure

DSN1

This gene encodes for the kinetochore protein that functions as part of the minichromosome instability-12 centromere complex. The encoded protein is required for proper kinetochore, and subsequent centromere, assembly and progression through the cell cycle (Przewloka et al., 2009).

Loss or reduced activity of this protein may contribute to increased genomic instability, a phenomenon associated with malignant development.

5.3.4.4.4 59M - Platelet Releasate Exposure

In order to identify genes with differential gene expression between the groups of platelet releasate exposed and resting 59M cells we studied 6 hybridizations (the resting control and exposure groups, each in triplicate) on the Human Exon 1.0 ST arrays using mixed model analysis of variance. This analysis determined 215 genes with significant gene expression differences existed between the groups ($p<0.05$). Of these 215 genes observed to undergo statistically significant alteration of expression, 13 were of study interest given a fold change of greater than 1.5.

These genes, their FC and significance along with their corresponding proteins are indicated in Table 5-12.

Table 5-12

Cell Line	Exposure	Gene	Protein	Fold Change (FC)	(*p*=)
59M	Platelet Releasate	**CCL2**	**chemokine [C-C motif] ligand 2**	1.94	0.0137
		TRAF1	**TNF receptor-associated factor 1**	1.92	0.0013
		HBEGF	**heparin-binding EGF-like growth factor**	1.67	0.0034
		CD274	**CD274 molecule**	1.64	0.0487
		ANKRD1	ankyrin repeat domain 1 [cardiac muscle]	1.60	0.0341
		TNFAIP2	**tumor necrosis factor alpha-induced protein 2**	1.59	0.0018
		BIRC3	**baculoviral IAP repeat-containing 3**	1.58	0.0303
		ICAM1	intercellular adhesion molecule 1 [CD54]	1.57	0.0012
		IRAK2	interleukin-1 receptor-associated kinase 2	1.56	0.0050
		SH2B3	**SH2B adaptor protein 3**	1.53	0.0060
		CSF2	colony stimulating factor 2 [granulocyte-macrophage]	1.52	0.0188
		GCH1	GTP cyclohydrolase 1 [dopa-responsive dystonia]	1.52	0.0211
		HIVEP1	human immunodeficiency virus type I enhancer binding protein 1	1.51	0.0212

Table 5-12: Genes Undergoing Significantly Altered Expression in Response to Platelet Releasate Exposure in 59M Cells.

The 59M cell line was determined to undergo significant alteration of expression 215 genes when exposed to platelet releasate compared to resting cells ($p<0.05$). Of these genes 13 showed a FC of greater than or equal to 1.5. Seven of these genes (indicated in bold) were selected for subsequent validation.

5.3.4.4.5 Genes Displaying Increased Expression in 59M Cells Following Platelet Releasate Exposure

CCL2

For details see Section 5.3.4.4.1 of this chapter.

TRAF1

For details see Section 5.3.4.4.1 of this chapter.

TNFAIP2

For details see Section 5.3.4.4.1 of this chapter.

HBEGF

This gene encodes for the heparin-binding EGF-like growth factor. The encoded protein is a mitogen for fibroblasts and smooth muscle cells. It is able to bind EGF receptors with higher affinity than EGF itself and is a far more potent mitogen for smooth muscle cells than EGF.

HBEGF has been identified as a potent driver of malignant development (Ongusaha et al., 2004, Ichise et al., 2010), contributes to the development of chemoresistance (Fischer et al., 2004, Wang et al., 2006) and has been considered a potential anti-cancer target (Chandler et al., 1998). In ovarian cancer it has been observed to be a primarily expressed member of the EGFR family of growth factors and where it is able to induce EMT and promotes metastasis (Yagi et al., 2008, Miyamoto et al., 2004).

CD274 (PDL-1, B7-H1)

This gene encodes for the CD274 molecule. Normally involved in the modulation the proliferation of T-cells and production of IL10 and IFNG in cancers CD274 has been identified as being involved in immune suppression and tumour immune evasion including tumour cell directed induction of T-cell apoptosis (Azuma et al., 2008, Blank et al., 2005, Dong and Chen, 2003, Dong et al., 2002). CD274 has been identified in breast cancer (Ghebeh et al., 2010, 2007, 2006), pancreatic cancer (Wang et al., 2010a, Okudaira et al., 2009, Geng et al., 2008), melanoma (Kashani-Sabet, 2010, Hino et al., 2010), renal cancer (Thompson and Kwon, 2006),cervical and ovarian cancers (Karim et al., 2009, Hamanishi et al., 2007, Tringler et al., 2006) and has been associated with tumour progression, immune evasion and anti-apoptotic signalling.

CD274 has been observed in ovarian cancer in previous studies and has been suggested as a potential diagnostic marker and target to attempt to restore anti-tumour immunity (Hamanishi et al., 2007, Tringler et al., 2006)

ANKRD1

This gene encodes for the ankyrin repeat domain 1 protein, thought play an important role in endothelial cell activation and in the negative regulation of cardiac gene expression. It has been identified as a co-activator of the p53 TSG and its induction seems to be correlated with apoptotic cell death in hepatoma cells (Kojic et al., 2010).

BIRC3 (CIAP)

This gene encodes for the baculoviral IAP repeat containing 3 protein. This molecule acts as an apoptotic suppressor. It forms a heteromeric complex with TNF receptor associated factors 1 and 2 (TRAF1 & TRAF2) which is then recruited to the tumour necrosis factor receptor 2. It interacts with and ubiquitinates SMAC/DIABLO, RIP1 and caspases -3 and -7 leading to their degradation and inhibition of apoptosis (Vanlangenakker et al., 2011, Choi et al., 2009, Bertrand et al., 2008, Hu and Yang, 2003).

ICAM1 (CD54)

This gene encodes for the intercellular adhesion molecule 1. It is the ligand for the leukocyte adhesion protein LFA-1 and is a cell adhesion, migration and signalling molecule shown to be important in normal leucocyte recruitment, endothelial cell aggregation and may contribute to migration capacity of cancer cells (Long, 2011, Lawson and Wolf, 2009, Mousa, 2008, Kobayashi et al., 2007, Yang et al., 2005). ICAM1 has been reported to undergo reduced expression in colorectal, gastric, pancreatic, breast and ovarian cancers (Fujihara et al., 1999, Sawada et al., 2006, Maeda et al., 2002, Arnold et al., 2001, Madhavan et al., 2002).

Conversely increased serum ICAM1 has been associated with metastasis, tumour spread and poor prognosis in several cancer types including NSCLC, gastric, renal and ovarian cancers (Guney et al., 2008, Alexiou et al., 2003, Perabo et al., 2001, Giavazzi et al., 1994, Banks et al., 1993, Gearing et al., 1992). The alteration of ICAM expression and/or release of soluble ICAM is hypothesised to contribute to improved metastasis through potentiating improved cancer cell extravasation through weakened intercellular interaction and through impairment of immune (NK) cell mediated cancer cell destruction (Kaihara et al., 1998).

IRAK2

This gene encodes for the interleukin-1 receptor-associated kinase 2. IRAK2 is involved in IL1 driven induction of the NFκB pathway through interaction with the IL1R.

Through interaction with the TGFβ signalling pathway IRAK2 has also been identified as a regulator of cell cycle, migration/invasion and EMT in cancer (Mullenders et al., 2010). It has also been described to have a critical role in toll-like receptor (TLR) signal transduction leading to TNFα, IFN and pro-inflammatory cytokine production (Keating et al., 2007, Flannery et al., 2011).

SH2B3 (LNK)

This gene encodes for the SH2B adaptor protein 3. This protein functions as a negative regulator of cytokine signaling. Increased SH2B3 expression leads to increased PI3K pathway activation and reduced ERK1/2 signalling resulting in reduced VCAM1 and E-selectin expression, reduced endothelial nitric oxide synthase (eNOS) expression, increased heme oxygenase-1 (HO-1) expression and reduced caspase-3 and -7 activity and reduced induction of anoikis (Chatelais et al., 2011, Liu et al., 2011, Devallière and Charreau, Wan et al., 2006, Fitau et al., 2006).

CSF2 (GMCSF)

This gene encodes for the granulocyte-macrophage colony-stimulating factor. This protein is a cytokine capable of stimulating growth and differentiation of cells of a wide range of lineages including granulocytes, macrophages, dendritic cells, eosinophils and erythrocytes.

Increased ICAM and CCL2 expression has been observed with increased GMCSF expression (Boero et al., 2010, Tanimoto et al., 2008) suggesting a potential pro-metastasis role for the protein but recently attention has focused on utilising GMCSF as a potential anti-cancer therapy using NK cells or cells modified to express the protein to attract dendritic cells and induce cell mediated immune recognition of the cancer cells (Chiang et al., 2011, Gupta and Emens, 2010, Cerullo et al., 2010).

GCH1

This gene encodes for the GTP cyclohydrolase 1 protein. GCH1 is up-regulated by interferon gamma (IFN-γ), tumour necrosis factor alpha (TNF-α), interleukin 1-beta (IL-1β), lipopolysaccharide (LPS) and phenylalanine. This up regulation stimulates production of tetrahydrobiopterin resulting in positive regulation of endothelial nitric oxide synthesis (Antoniades et al., 2008, Swick and Kapatos, 2006). It has also been implicated in modulating nociception and in the aetiology of dopamine sensitive dystonia (Latremoliere and Costigan, 2011, Hu et al., 2010).

HIVEP1

This gene encodes for the human immunodeficiency virus type I enhancer binding protein 1. This protein is structurally composed of five zinc fingers and recognises the following DNA sequence found in the enhancer elements of numerous viral promoters such as those of SV40, cytomegalovirus (CMV), or HIV1: *5'-GGGACTTTCC-3'*.

The role of this protein in malignant conditions has not described.

5.3.4.5 SK-OV 3

5.3.4.5.1 SK-OV 3 - Washed Platelet Exposure

In order to identify genes with differential gene expression between the groups of washed platelet exposed and resting SK-OV 3 cells we studied 6 hybridizations (the resting control and exposure groups, each in triplicate) on the Human Exon 1.0 ST arrays using mixed model analysis of variance.

This analysis determined 226 genes with significant gene expression differences existed between the (p<0.05). Of these 226 genes observed to undergo statistically significant alteration of expression, 1 was of study interest given a fold change of greater than 1.5.

This gene, its FC and significance along with its corresponding protein is indicated in Table 5-13.

Table 5-13

Cell Line	Exposure	Gene	Protein	Fold Change (FC)	(p=)
SK-OV 3	Washed Platelet	ASTN1	astrotactin 1	1.58	0.0030

Table 5-13: Genes Undergoing Significantly Altered Expression in Response to Washed Platelet Exposure in SK-OV 3 Cells.

The SK-OV 3 cell line was determined to undergo significant alteration of expression 226 genes when exposed to washed platelets compared to resting cells (p<0.05). Of these genes, one (ASTN1), showed a FC of greater than or equal to 1.5. This gene was selected for subsequent validation.

5.3.4.5.2 Genes Displaying Increased Expression in SK-OV 3 Cells Following Washed Platelet Exposure

Astrotactin

Astrotactin is a neuronal adhesion molecule required for the normal development of the brain (including cerebrum, hippocampus, cerebellum, and olfactory bulb) through glial-guided migration of young post-mitotic neuroblasts (Wilson et al., 2010, Adams et al., 2002, Fink et al., 1997). The role of astrotactin in malignant cells has not been described.

5.3.4.5.3 SK-OV 3 - Platelet Releasate Exposure

In order to identify genes with differential gene expression between the groups of platelet releasate exposed and resting SK-OV 3 cells we studied 6 hybridizations on the Human Exon 1.0 ST arrays using mixed model analysis of variance.

This analysis determined 348 genes with significant gene expression differences existed between the groups ($p<0.05$). Of these 348 genes observed to undergo statistically significant alteration of expression, 16 were of study interest given a fold change of greater than 1.5.

These genes, their FC and significance along with their corresponding proteins are indicated in Table 5-14.

Table 5-14

Cell Line	Exposure	Gene	Protein	Fold Change (FC)	(*p*=)
SK-OV-3	Platelet Releasate	**CRLS1**	**cardiolipin synthase 1**	1.91	0.0346
		UBLCP1	ubiquitin-like domain containing CTD phosphatase 1	1.82	0.0256
		RPL7A	ribosomal protein L7a	1.72	0.0290
		AK3	adenylate kinase 3	1.66	0.0432
		MGC71993	similar to DNA segment Chr 11 Brigham & Womens Genetics 0434 expressed	1.66	0.0299
		ANXA2	**annexin A2**	1.64	0.0225
		KIAA1324	**KIAA1324**	1.58	0.0417
		PCNP	PEST proteolytic signal containing nuclear protein	1.52	0.0455
		SLC9A8	solute carrier family 9 [sodium/hydrogen exchanger] member 8	1.52	0.0480
		TPM4	tropomyosin 4	1.51	0.0356
		ACTL6A	actin-like 6A	1.51	0.0380
		C14ORF153	chromosome 14 open reading frame 153	1.50	0.0190
		MUS81	**MUS81 endonuclease homolog**	1.50	0.0222
		CRIPAK	**cysteine-rich PAK1 inhibitor**	-1.55	0.0105
		ISOC2	**isochorismatase domain containing 2**	-1.69	0.0036
		VPS26B	**vacuolar protein sorting 26 homolog B**	-1.69	0.0402

Table 5-14: Genes Undergoing Significantly Altered Expression in Response to Platelet Releasate Exposure in SK-OV 3 Cells.

The SK-OV 3 cell line was determined to undergo significant alteration of expression 189 genes when exposed to platelet releasate compared to resting cells ($p<0.05$). Of these genes 6 were showed a FC of greater than or equal to 1.5. Seven of these genes (indicated in bold) were selected for subsequent validation.

5.3.4.5.4 Genes Displaying Increased Expression in SK-OV 3 Cells Following Platelet Releasate Exposure

CRLS1

The largest fold change observed in SK-OV 3 cell in response to platelet releasate exposure occurred for the gene encoding for Cardiolipin Synthase (CRLS1) responsible for cardiolipin (CL) production.

Anti-cardiolipin antibodies are associated with both solid and non-solid tumors and is associated with increased thrombocytosis (Miesbach, 2009). It may also have an anti-apoptotic role as reduced CL expression is associated with increased apoptosis (Choi et al., 2007).

UBLCP1

The gene encodes for ubiquitin-like domain containing CTD phosphatase 1. The repetitive C-terminal domain (CTD) of the largest RNA polymerase II (RNAP2) subunit plays a critical role in the regulation of gene expression and reversible phosphorylation at CTD heptapeptide repeat serines -2 and -5 regulate RNAP2's activity during transcription initiation, elongation and RNA processing (Lin et al., 2002, Qian et al., 2007).

The UBLCP1 protein dephosphorylates the RNAP2 CTD and so is thought to play a major role in polymerase recycling and increased expression has been observed in fast growing or tumour tissues (Zheng et al., 2005).

RPL7A (SURF3)

The gene encodes for ribosomal protein L7A. Though the location and nature of the gene has been described (Colombo et al., 1991, Giallongo et al., 1989, Yon et al., 1989, Ziemiecki et al., 1988) the function of this protein has not been elucidated.

RPL7a is highly conserved across many species including mammals, birds, xenopus, drosophila and *Schizosaccharomyces pombe* and the RPL7A/SURF3 gene product in mice has been described as a ubiquitously expressed housekeeping protein (Magoulas and Fried, 1996), as part of a Poised Gene Cassette (PGC) linked to multiple cancer pathways (Yu et al., 2008) and as an activator of the trk proto-oncogene (Ziemiecki et al., 1990).

The role of RPL7A in the aetiology of cancer is unclear though altered expression has been described in colorectal and breast cancers (increased) (Wang et al., 2000, White et al., 2009b, Zhu et al., 2001) and in osteosarcoma (reduced) (Zheng et al., 2009a). The altered expression of RPL7A has not been previously described in ovarian cancer.

AK3

The gene encodes for adenylate kinase 3. This protein is a mitochondrial enzyme that catalyses the dephosphorylation of pyrmidines from nucleotide triphosphates (NTP) to nucleotide diphosphates (NDP) and phosphorylation of adensosine monophosphate (AMP) to adenosine triphosphate (ADP) (Noma et al., 2001).

MGC71993 (RNASE K)

The gene encodes for the RNAse K enzyme, with RNase activity (Economopoulou et al., 2007). The role of the protein in malignant states has not been widely investigated though recent evidence suggests increased expression is associated with poor prognosis in ovarian cancer, and especially in chemoresistant disease (Kim et al., 2010b).

ANXA2

The gene encodes for Annexin A2, a calcium binding membrane protein capable of interacting with RNA (Filipenko et al., 2004). Increased ANXA2 expression is associated with increased cell invasion/motility in esophageal squamous cell, hepatocellular, multiple myeloma, prostate, breast, pancreatic and ovarian cancers (Feng et al., 2011, Zheng et al., 2011, Shiozawa et al., 2010, 2008, Bao et al., 2009, Nedjadi et al., 2009, Zhang et al., 2009).

Annexin A2 is hypothesised to contribute to ovarian cancer metastasis through its role in increasing the conversion of plasminogen to plasmin, itself responsible for cleaving pro-MMPs into proteolytically active mature MMP proteins and may be involved in tumour-host signalling between ovarian cancer and peritoneal cells (Lokman et al., 2011, Ween et al., 2011).

KIAA1324 (EIG121)

The gene encodes for the KIAA1324 protein. Induced by oestrogen, elevated KIAA1324 expression is observed to play a role in anti-autophagy signalling in endometrial and ovarian cancer and reduced survival in ovarian cancer (Schlumbrecht et al., 2011, 2010, Deng et al., 2010, 2005, Bauer et al., 2004).

PCNP

The gene encodes for PEST proteolytic signal containing nuclear protein. It is regulated by NIRF (IL7b) mediated ubiquitination and is thought to have a role in cell cycle regulation (Mori et al., 2002, Mori et al., 2004).

SLC9A8 (NHE8)

The gene encodes for solute carrier family 9 (sodium/hydrogen exchanger), member 8. The protein is involved in pH regulation to eliminate acids/protons generated by active metabolism, to counter adverse environmental conditions or to modulate endosome pH using a proton extruding system driven by an inward sodium ion chemical gradient (Lawrence et al., 2010, Orlowski and Grinstein, 2004).

TPM4

The gene encodes for tropomyosin 4, a protein primarily involved in calcium dependent regulation of vertebrate striated muscle contraction and stabilisation of cytoskeletal actin filaments in non-muscle cells (Marston and El-Mezgueldi, 2008, Hodgkinson, 2000, Marston et al., 1998).

Tropomyosin 4 has been described as upregulated in oesophageal squameous cell carcinoma and has more recently been investigated as a potential diagnostic and prognostic marker in the progression of cervical intraepithelial neoplasia (CIN) to squamous cervical cancer (Qi et al., 2005).

ACTL6A (ARP4, BAF53)

The gene encodes for the actin-like 6A protein. This protein plays a critical role in chromatin remodelling mediating the transcriptional activation or repression of many genes (Oma and Harata, 2011, Huang et al., 1996). ACTL6A/BAF53 has been reported to be a critical co-factor for signalling by the c-myc oncogene (Park et al., 2002).

C14ORF153 (APOP1)

The gene encodes for apoptogenic protein (Apop). This protein is an initiator of apoptosis by inducing cytochrome *c* release from mitochondria into the cytosolic space followed by activation of initiator caspase-9 and subsequent activation of the effector caspase-3 (Yasuda et al., 2006). Apop driven apoptosis is protected against by IGF1 signalling (Sun et al., 2008) resulting in the activation of the PI3K/AKT signalling pathways, known to regulate pro-survival/anti-apoptotic signalling events (Parcellier et al., 2008).

MUS81

The gene encodes for the MUS (methyl methansulfonate and ultraviolet-sensitive) 81 endonuclease homolog protein. This protein is involved in maintenance/regulation of the cell cycle. MUS81 interacts with EME1/2 and CHEK2 to form a DNA structure-specific endonuclease that recognises nick ended DNA structures including replication forks, Holliday junctions, creating double stranded breaks and allowing DNA repair to occur and replication to continue without which cells experience reduced genomic stability and increased chromosomal abnormalities (Wechsler et al., 2011, Hanada et al., 2007, McPherson et al., 2004).

MUS81 deficient mouse models have been shown to be susceptible to increased rates of spontaneous and induced cancers (Pamidi et al., 2007) arising from rereplication errors observed to occur in cell line models of MUS81 deficiency (Hiyama et al., 2006). Reduced expression of MUS81 has been described in gastric, laryngeal squameous cell hepatocellular and gastric cancers where it is associated with greater invasive capacity and worse overall survival (Wu et al., 2011, 2010, 2008, Li et al., 2008a).

Recent experimental mouse model evidence indicates that MUS81 and CHK2 may provide potential targets for cancer treatment as their dual inhibition has been observed to result in a marked reduction in genomic instability and cancer development (El Ghamrasni et al., 2011).

5.3.4.5.5 Genes Displaying Reduced Expression in SK-OV 3 Cells Following Platelet Releasate Exposure

CRIPAK

The gene encodes for cysteine-rich PAK1 inhibitor. This protein negatively regulates PAK1 (P21 Activated Kinase) (Talukder et al., 2005).

PAK1 is involved in regulating a multitude of processes including cell motility, survival and proliferation, cytoskeletal organization, gene transcription and translation (Kichina et al., 2010). PAK1 has been observed to stimulate colon cancer cell growth and invasion (Huynh et al., 2010), is capable of stimulating increased MMP9 expression (Zhou et al., 2009); the only gene confirmed to be upregulated by TCIPA prior to completion of this study.

The region surrounding the PAK1 locus (11q13.5) is disregulated in many forms of cancer, including ovarian cancer, resulting in the altered expression of many genes (Nurminen et al., 2011, Brown et al., 2008, Schwab, 1998). The gene is frequently disregulated as a result of copy number gains in ovarian cancer resulting in amplification of expression (Mayr et al., 2006, Schraml et al., 2003). Increased PAK1 expression in ovarian cancer has correlated with histological type and grade, and has been associated metastatic disease and development of chemo insensitivity, poor disease free and overall survival (Siu et al., 2010b, Siu et al., 2010a, Brown et al., 2008).

ISOC2

The gene encodes for the isochorismatase domain containing 2 protein. ISOC2 binds to and inhibits $p16^{INK4a}$, a TSG that mediates arrest of cell cycle in G1 phase by preventing the interaction of CDK-4 and -6 with Cyclin D1 to effect a decline in replicative potential of cells during apoptosis, angiogenesis and cell senescence, tumour invasion, cell spreading, and aging (Huang et al., 2007b). While reduced expression of an inhibitor of $p16^{INK4a}$ might suggest development of an anti-growth/proliferation signal there is significant evidence in the published literature that reveals elevated p16 expression/activity corresponds closely to the level of histological dysplasia and prognosis malignancy,

including cervical and ovarian cancers (Han et al., 2011, Kalof and Cooper, 2006, Giordano et al., 2008, Buchynska et al., 2007). The correlation of p16 expression to cervical cancer development is sufficiently strong that it has been suggested as a surrogate biomarker for the disease or supportive in addition to HPV oncogene detection (Haidopoulos et al., 2009, Lesnikova et al., 2009, Cuschieri and Wentzensen, 2008, Ling et al., 2008). In ovarian cancer elevated p16 is also reported (Giordano et al., 2008, Buchynska et al., 2007) and is associated with more aggressive disease and less favourable outcome.

VPS26B

The gene encodes for the vacuolar protein sorting 26 homolog B protein. It forms part of the retromer, a heteromeric protein complex consisting of three proteins – Vps26(A & B), Vps29, and Vps35 – in association with members of the sorting nexin family of proteins, which has been implicated in retrograde transport of lysosomal hydrolase receptors (IGF2R and M6PR) from endosomes to the *trans*-Golgi network (Kim et al., 2010a, Collins et al., 2008, Bonifacino and Rojas, 2006, Kerr et al., 2005). The role of this protein in the development of cancer has not been described.

5.3.4.6 A2780

5.3.4.6.1 A2780 - Washed Platelet Exposure

In order to identify genes with differential gene expression between the groups of washed platelet exposed and resting A2780 cells we studied 6 hybridizations (the resting control and exposure groups, each in triplicate) on the Human Exon 1.0 ST arrays using mixed model analysis of variance.

This analysis determined 29 genes with significant gene expression differences existed between the groups ($p<0.05$). Of these 29 genes observed to undergo statistically significant alteration of expression, none were observed to be of a fold change of greater than or equal to 1.5 and so were not investigated any further.

5.3.4.6.2 A2780 - Platelet Releasate Exposure

In order to identify genes with differential gene expression between the groups of platelet releasate exposed and resting A2780 cells we studied 6 hybridizations (the resting control and exposure groups, each in triplicate) on the Human Exon 1.0 ST arrays using mixed model analysis of variance.

This analysis determined 48 genes with significant gene expression differences existed between the groups ($p<0.05$). Of these 48 genes observed to undergo statistically significant alteration of expression, none were observed to be of a fold change of greater than or equal to 1.5 and so were not investigated any further.

5.3.4.7 A2780cis

5.3.4.7.1 A2780cis - Washed Platelet Exposure

In order to identify genes with differential gene expression between the groups of washed platelet exposed and resting A2780cis cells we studied 6 hybridizations (the resting control and exposure groups, each in triplicate) on the Human Exon 1.0 ST arrays using mixed model analysis of variance.

This analysis determined 879 genes with significant gene expression differences existed between the groups ($p<0.05$). Of these 879 genes observed to undergo statistically significant alteration of expression, 31 were of study interest given a fold change of greater than 1.5.

These genes, their FC and significance along with their corresponding proteins are indicated in Table 5-15.

Table 5-15

Cell Line	Exposure	Gene	Protein	Fold Change (FC)	(*p*=)
A2780cis	Washed Platelet	**KLK1**	**kallikrein 1**	1.63	0.0239
		ITGB2	**integrin beta 2**	1.52	0.0497
		ABCD3	ATP-binding cassette sub-family D [ALD] member 3	-1.50	0.0431
		RMND1	required for meiotic nuclear division 1 homolog	-1.50	0.0335
		ARL15	ADP-ribosylation factor-like 15	-1.50	0.0137
		RAD18	RAD18 homolog [S. cerevisiae]	-1.51	0.0327
		CAPZA1	capping protein [actin filament] muscle Z-line alpha 1	-1.51	0.0324
		SPAST	Spastin	-1.52	0.0200
		C11ORF54	chromosome 11 open reading frame 54	-1.53	0.0316
		MAD2L1	MAD2 mitotic arrest deficient-like 1 [yeast]	-1.53	0.0407
		MRPL33	mitochondrial ribosomal protein L33	-1.53	0.0328
		RNASEH2B	ribonuclease H2 subunit B	-1.53	0.0384
		DAB1	disabled homolog 1 [Drosophila]	-1.54	0.0204
		SMCHD1	structural maintenance of chromosomes flexible hinge domain containing 1	-1.54	0.0359
		DPY19L4	dpy-19-like 4 [C. elegans]	-1.56	0.0383
		EIF2B3	eukaryotic translation initiation factor 2B subunit 3 gamma 58kDa	-1.56	0.0310
		C1ORF112	chromosome 1 open reading frame 112	-1.56	0.0305
		ZNF271	zinc finger protein 271	-1.56	0.0131
		VGLL3	vestigial like 3 [Drosophila]	-1.56	0.0115
		NDUFAF1	NADH dehydrogenase [ubiquinone] 1 alpha subcomplex assembly factor 1	-1.58	0.0443
		LARP7	La ribonucleoprotein domain family member 7	-1.58	0.0400
		SNRPA1	small nuclear ribonucleoprotein polypeptide A'	-1.59	0.0276
		MED10	mediator of RNA polymerase II transcription subunit 10 homolog	-1.60	0.0114
		PTBP2	polypyrimidine tract binding protein 2	-1.60	0.0337
		STK17B	**serine/threonine kinase 17b**	-1.61	0.0304
		PRIM2A	primase polypeptide 2A 58kDa	-1.62	0.0464
		GMNN	**geminin DNA replication inhibitor**	-1.67	0.0259
		ZNF706	zinc finger protein 706	-1.68	0.0259
		CCDC76	coiled-coil domain containing 76	-1.70	0.0263
		RP9	retinitis pigmentosa 9 [autosomal dominant]	-1.71	0.0387
		NAP1L4	**nucleosome assembly protein 1-like 4**	-1.81	0.0082

Table 5-15: Genes Undergoing Significantly Altered Expression in Response to Washed Platelet Exposure in A2780cis Cells.

The A2780cis cell line was determined to undergo significant alteration of expression 897 genes when exposed to platelet releasate compared to resting cells ($p<0.05$). Of these genes 31 were showed a FC of greater than or equal to 1.5. Five of these genes (indicated in bold) were selected for subsequent validation.

5.3.4.7.2 Genes Displaying Increased Expression in A2780cis Cells Following Washed Platelet Exposure

KLK 1

The gene encodes for kallikrein 1, a serine protease. The 15 member family of kallikrein proteases have been described as having diverse contributions to the development of a diverse range of cancers including ovarian cancer. The kallikrein locus (19q13.4), the largest contiguous cluster of protease genes in the human genome, has been described as affected by genomic instability in ovarian cancer and multiple members of the kallikrein family have been observed to suffer alterations of expression (Bayani et al., 2011). In ovarian cancer kallikrein expression has largely been associated with poor prognosis, chemoresistance, increased invasiveness, tumour formation and disease recurrence.

Table 5-16 shows a selection of studies performed examining kallikrein expression in ovarian cancer in the last decade (2001-2011).

Arising from the frequent expression of these proteins in different cancers the kallikrein proteases, either singly or in groups have been suggested for potential use as cancer biomarkers, though a lack of specificity may limit their usefulness to that of a supportive biomarker for conventional biomarkers such as CA125 in ovarian cancer (Avgeris et al., 2010, Yousef and Diamandis, 2009, White et al., 2009a, Emami and Diamandis, 2008, Schmitt and Magdolen, 2009, Rosen et al., 2005).

Table 5-16

Article	Tissue	Kallikrein Gene
(Kim et al., 2001)	Ovary	↑KLK5
(Magklara et al., 2001)	Ovary	↑KLK8
(Obiezu et al., 2001)	Ovary	↑KLK4
(Yousef et al., 2001a)	Ovary	↑KLK9
(Yousef et al., 2001b)	Ovary, Breast, Testes, Prostate	↓KLK14
(Dong et al., 2003)	Ovary	↑KLK5, ↑KLK7
(Yousef et al., 2003)	Ovary	↑KLK5, ↑KLK6, ↑KLK7, ↑KLK8, ↑KLK10, ↑KLK11, ↑KLK14
(Xi et al., 2004)	Ovary	↑KLK4
(Prezas et al., 2006)	Ovary	↑KLK4, ↑KLK5, ↑KLK6, ↑KLK7
(Kountourakis et al., 2009)	Ovary	↑KLK8
(White et al., 2009b)	Ovary	↑KLK6, ↑KLK13
(White et al., 2010)	Ovary	↑KLK10
(Dorn et al., 2011)	Ovary	↑KLK5

Table 5-16: Studies of Kallikrein gene expression in ovarian cancer (2001-2011).

Table 5-16 illustrates the different kallikrein genes observed to be altered in ovarian cancer in studies performed between 2001 and 2011. The arrows indicate the direction of altered expression compared with normal tissues.

To date altered KLK1 expression has not been observed or discussed in the context of ovarian cancer.

ITGB2 (LFA-1)

The gene encodes for integrin beta 2 (complement component 3 receptor 3 and 4 subunit). This protein has significant functions in cell adhesion, migration and signalling through its function as receptor for with ICAM adhesion molecules (ICAM1, ICAM2, ICAM3 and ICAM4) and plays a significant role in mediating transendothelial migration of leucocytes (Lawson and Wolf, 2009).

It has been suggested that ICAM signalling through LFA-1 may promote cancer cell proliferation and expression of matrix metalloproteinases MMP2 and MMP9 through PI3K/AKT signalling pathway activation (Kim et al., 2006, Park et al., 2010).

5.3.4.7.3 Genes Displaying Reduced Expression in A2780cis Cells Following Washed Platelet Exposure

ABCD3 (PMP70)

This gene encodes for the ATP-binding cassette sub-family D [ALD] member 3 protein. This ABC transporter is responsible for the transport of fatty acids and/or fatty acyl-CoAs to the peroxisome and normal functioning of the organelle. Deficient or defective expression of ABCD3/PMP70 results in Zellweger Syndrome (Gartner et al., 1992, Imanaka et al., 2000).

Impaired peroxisome enzyme activity, expression and reduced peroxisome functioning has been described in a variety of cancers (Benedetti et al., 2010, Frederiks et al., 2010, el Bouhtoury et al., 1992, Yokoyama et al., 1992, Sato et al., 1992). The expression of peroxisomal enzymes is regulated by a subfamily of the ligand-activated nuclear hormone receptor superfamily, called peroxisome proliferator activated receptors (PPARs), themselves observed to be disregulated contributing to the development of many cancers including ovarian cancer (Davidson et al., 2009, Peters and Gonzalez, 2009, Krishnan et al., 2007, Sertznig et al., 2007, Vignati et al., 2006, Panigrahy et al., 2005).

RMND1

This gene encodes for the required for meiotic nuclear division 1 homolog protein. Evidence suggests this protein is involved in chromosomal separation arising from its interaction with spindle microtubules and spindle poled during cell division (Oishi et al., 2007). It has not been associated with ovarian neoplasms but has recently been identified in a candidate susceptibility locus from chronic myeloid leukaemia (Kim et al., 2011).

ARL15

This gene encodes for the ADP-ribosylation factor-like 15 protein. Genome wide association studies have suggested this protein influences circulating adiponectin levels affecting insulin sensitivity and may contribute to childhood obesity (Glessner et al., 2010, Richards et al., 2009). No role in ovarian cancer has been documented.

RAD18

This gene encodes for RAD18 homolog [S. cerevisiae], an ubiquitin ligase involved in replication damage bypass and DNA double-strand break (DSB) repair processes in mitotic cells (Inagaki et al., 2011). RAD18 plays a central role in activation of the Fanconi anemia (FA) DNA repair network through ubiquitination of proliferating cell nuclear antigen (PCNA) allowing FANC gene activation (Geng et al., 2010). Reduced expression of RAD18 may result in impaired ability to activate the FA DNA repair mechanism resulting in chromosomal instability, sensitivity to DNA crosslinking agents and cancer development.

CAPZA1

This gene encodes for capping protein [actin filament] muscle Z-line alpha 1. This protein regulates growth of the actin filament by capping the barbed end of growing actin filaments (Maun et al., 1996).

SPAST (SPG4)

This gene encodes for Spastin, an ATPase that may be involved in the assembly or function of nuclear protein complexes. Mutations in this gene are responsible for heritable spastic paraplegia (Salinas et al., 2007, Errico et al., 2002).

C11ORF54

This gene encodes for chromosome 11 open reading frame 54, an ester hydrolase (Manjasetty et al., 2006). The role played by C11ORF54 in malignancy is unknown and is undocumented in ovarian cancer though has also been observed down regulated in renal clear cell carcinoma (Sun et al., 2010).

MAD2L1 (MAD2)

This gene encodes for the MAD2 mitotic arrest deficient-like 1 protein, a homolog of yeast MAD2. This protein a component of the mitotic spindle assembly checkpoint responsible for preventing anaphase until all chromosomes are properly aligned at the metaphase plate. Reduced expression is associated with an abbreviated metaphase and insufficient mitotic arrest resulting in abnormal chromosome segregation (Agarwal et al., 2011).

MRPL33

The gene encodes for mitochondrial ribosomal protein L33. This protein is involved in ribosome biogenesis and subunit joining (Martin-Marcos et al., 2007).

RNASEH2B

The gene encodes for ribonuclease H2 subunit B, the non-catalytic subunit of RNase H2, an endonuclease that specifically mediates the excision of single ribonucleotides from DNA:RNA duplexes (Chon et al., 2009). Mutations in this gene are responsible for Aicardi-Goutieres syndrome (Crow et al., 2006).

DAB1

This gene encodes for disabled homolog 1, a human homolog of the Drosophila Disabled gene. This protein is involved in reelin directed organization of multiple neuronal types during CNS development (Senturk et al., 2011, Bar et al., 2003, Deguchi et al., 2003).

SMCHD1

This gene is predicted to encode for the structural maintenance of chromosomes flexible hinge domain containing 1 protein. No published data exists detailing the function of this protein although similar proteins have been implicated in RNA directed DNA methylation (Kanno et al., 2008).

DPY19L4

This gene encodes for the dpy-19-like 4, a human homolog of the C. elegans Dpy gene. Its role in humans is not described.

EIF2B3

This gene encodes for the eukaryotic translation initiation factor 2B subunit 3 gamma protein. The protein catalyzes the exchange of eukaryotic initiation factor 2-bound GDP for GTP. Alterations in the gene are associated with leukoencephalopathies (Matsukawa et al., 2011, Wu et al., 2009, Ohlenbusch et al., 2005).

C1ORF112

The gene encodes for the uncharacterised protein at chromosome 1 open reading frame 112. No data is available describing the nature or function of this protein.

ZNF271

The gene encodes for zinc finger protein 271. Zinc finger proteins are involved in transcriptional regulation through interaction with nucleic acids including binding to single-stranded DNA and RNA. Specific interaction and activities of ZNF271 have not been described.

VGLL3

The gene encodes for vestigial like 3 a human homolog of the Drosophila gene Vestigial. Increased expression may contribute to oncogenesis and progression of soft tissue sarcomas (Hélias-Rodzewicz et al., 2010).

NDUFAF1

The gene encodes for NADH dehydrogenase [ubiquinone] 1 alpha subcomplex assembly factor 1. This protein functions as a chaperone molecule in the intermediate assembly of the mitochondrial NADH:ubiquinone oxidoreductase complex (complex 1, C1), the largest and first of five multi-protein enzymes in the oxidative phosphorylation system along with electron carriers coenzyme Q_{10} and cytochrome *c* responsible for generation of ATP (McKenzie and Ryan, 2010, Vogel et al., 2005).

C1 components are encoded by mitochondrial genes and damaged or defective mitochondrial DNA (mtDNA) and impaired C1 has been identified in several cancers (Kirches et al., 2001, Schon, 2000, Chomyn, 2001, Fliss et al., 2000). Changes in these C1 genes and their encoded proteins may alter cellular generation of and response to reactive oxygen species (ROS), sensitivity to hypoxia, increased tumour proliferation, tumourigenicity and chemoresistance (Czarnecka et al., 2010, Lu et al., 2009, Park et al., 2009).

LARP7 (PIP7S)

The gene encodes for La ribonucleoprotein domain family member 7. This protein functions as a negative regulator of RNA Polymerase 2 (Markert et al., 2008). LARP7/PIP7S associates with and stabilises 7SK small nuclear RNA (snRNA) which sequesters and inactivates P-TEFb. P-TEFb is a general transcription factor important for the expression of a large number of genes and reduced LARP7/PIP7S expression allows the increased expression of genes tumour promoting genes such as PTHLH and TGM-2, associated with unsuppressed cell growth, leading ultimately to malignant transformation (Bayfield et al., 2010, Kohoutek, 2009, He et al., 2008a).

To date altered LARP7 expression has not been described in ovarian cancer but has been described as down regulated in early stage cervical cancer (Biewenga et al., 2008).

SNRPA1 (LEA1)

This gene encodes for the small nuclear ribonucleoprotein polypeptide A protein. This protein is a component of the spliceosome C complex – a multi-protein complex composed of snRNA and protein subunits that removes introns from post-translation pre-mRNAs and is responsible for the generation alternative splicing gene products (van Alphen et al., 2008, Fan et al., 2002).

MED10

This gene encodes for the mediator of RNA polymerase II transcription subunit 10 homolog protein. This protein is a component of the Mediator complex, a coactivator complex involved in the regulated transcription many RNA polymerase II-dependent genes (Conaway et al., 2005, Sato et al., 2003).

PTBP2 (PTB)

This gene encodes for polypyrimidine tract binding protein 2, a protein that binds to RNA intronic polypyrimidine tracts and mediates negative regulation of exon splicing.

The protein also plays an inhibitory role in modulating cell cycle as PTBP2 enhances expression of $p27^{Kip1}$, a protein that inhibits cell cycle transition through G1 to S phase through inhibition of the Cyclin E/CDK2 complex (Cho et al., 2005). Reduced $p27^{Kip1}$ has been considered a putative TSG, regulator of drug resistance in solid tumors, and promoter of apoptosis and reduced expression is associated with tumour development and progression (Lloyd et al., 1999, Levkau et al., 1998).

Though no data has been published on the role of PTBP2 in ovarian cancer, knock down of a related protein, PTBP1, in an in vitro model of ovarian cancer has reported reduced tumorigenicity (He et al., 2007).

STK17B (DRAK2)

This gene encodes for the serine/threonine kinase 17b protein also known as Death-associated protein-related apoptotic kinase-2 (DRAK2). This protein functions as a positive regulator of apoptosis and reduced expression has been observed in colorectal cancer (Doherty et al., 2009, Kuwahara et al., 2003, Sanjo et al., 1998).

PRIM2A

This gene encodes for the primase polypeptide 2A protein, also known as p58. This protein generates short RNA primers required to initiate DNA synthesis (Weiner et al., 2007).

GMNN

This gene encodes for the geminin DNA replication inhibitor. Supression of geminin leads to severe genomic instability arising from rereplication and aneuploidy in affected cells (Kaufmann et al., 2008, Tachibana et al., 2005, Zhu et al., 2004, Melixetian and Helin, 2004, Melixetian et al., 2004, Luo and Kessel, 2004, Ballabeni et al., 2004).

ZNF706

The gene encodes for zinc finger protein 706. Zinc finger proteins are involved in transcriptional regulation through interaction with nucleic acids including binding to single-stranded DNA and RNA. Specific interaction and activities of ZNF06 have not been described.

CCDC76

The gene encodes for coiled-coil domain containing 76. This protein has homology to murine transfer RNA guanosine-2'-O-methyltransferase protein, TRM13, and may be involved in methylating transfer RNA species at guanosine-4 in various transfer RNAs with a Gly, His or Pro signature.

RP9

The gene encodes for retinitis pigmentosa 9, [autosomal dominant]. The protein is a target for PIM-1 kinase and is involved in pre-mRNA splicing (Maita et al., 2004, Keen et al., 2002). The function of this gene in the development of cancer has not been described.

NAP1L4

The gene encodes for nucleosome assembly protein 1-like 4 and is involved in nucleosome formation, specifically acting as a histone chaperone protein (Okuwaki et al., 2010, Attia et al., 2011).

Though their interaction with histones 2A and histone 2A variants, histone caparones such as NAP1L4 play an important role in chromatin remodelling and disassembly which are required ahead of DNA or RNA polymerases for DNA replication or gene transcription to occur. The alteration of NAP1L4 gene expression in the context of cancer development has not been described.

5.3.4.7.4 A2780cis - Platelet Releasate Exposure

In order to identify genes with differential gene expression between the groups of platelet releasate exposed and resting A2780cis cells we studied 6 hybridizations (the resting control and exposure groups, each in triplicate) on the Human Exon 1.0 ST arrays using mixed model analysis of variance.

This analysis determined 19 genes with significant gene expression differences existed between the groups ($p<0.05$). Of these 19 genes observed to undergo statistically significant alteration of expression, none were observed to be of a fold change of greater than or equal to 1.5 and so were not investigated any further.

5.3.5 Affymetrix® Result Validation – Fluidigm® Dynamic Array™ qPCR

A technical validation of Affymetrix® GeneChip® array results was performed using Fluidigm® high throughput qPCR technology. Fluidigm qPCR was selected as the methodology for technical validation of Affymetrix results. This is due to its utilisation of an established, gold standard method of detecting changes in gene expression (TaqMan® qPCR) and in a highthroughput format using low quantities of valuable sample and reagents. Twenty five genes were selected along with two endogenous controls for analysis using the Fluidigm® 48x48 Dynamic Array™.

The genes selected and the cell lines and conditions in which significant alteration of expression were observed by Affymetrix® analyses are highlighted in bold in Tables 5-8 to 5-14.

These genes were selected based on the function of the genes observed to have under gone alteration. These included genes who have been documented in other studies to be involved in cancer biology or whose alteration of expression may potentially affect:

- cell growth/proliferation
- apoptosis/autophagy
- adhesion/migration
- alteration of cell cycle/gene transcription
- immune function
- affect platelet adhesion or function

Fluidigm® data was initially processed using proprietary software, Fluidigm® Real-time PCR Analysis (ver. 3.02), which allowed relative quantitation to be performed. Relative quantitation data was then analysed using Microsoft Excel allowing fold change values to be calculated from relative quantitation figures and comparison between the Affymetrix® and Fluidigm® derived data to take place.

All data was then entered into GraphPad Prism, statistical analysis performed and graphs generated. Conditions in which either one gene was observed to undergo a significant fold change or a single gene selected for validation were included with the other exposure data set to allow correlation analysis to be performed.

The genes selected for validation and their corresponding TaqMan® assays, along with selected endogenous controls are indicated in Table 5-17.

Table 5-17

Cell Line	Exposure	Gene	Applied Biosystems TaqMan® Assay ID
HIOE-80	Platelet Releasate	LRP8	Hs00182998_m1
	Washed Platelet	SERPINB2	Hs00234032_m1
		PCGF6	Hs00827882_m1
		ZNF267	Hs00171561_m1
59M	Platelet Releasate	CCL2	Hs00234140_m1
		TRAF1	Hs00194639_m1
		HBEGF	Hs00181813_m1
		CD274	Hs01125299_m1
		TNFAIP2	Hs00196800_m1
		BIRC3	Hs00154109_m1
		SH2B3	Hs00193878_m1
	Washed Platelet	TRAF1	Hs00194639_m1
		CCL2	Hs00234140_m1
		TNFAIP2	Hs00196800_m1
		PDGFB	Hs00234042_m1
		DSN1	Hs01566636_m1
SK-OV 3	Platelet Releasate	CRLS1	Hs00219512_m1
		ANXA2	Hs00743063_s1
		KIAA1324	Hs00331399_m1
		MUS81	Hs00228383_m1
		CRIPAK	Hs00846661_m1
		ISOC2	Hs00226771_m1
		VPS26B	Hs00364615_m1
	Washed Platelet	ASTN1	Hs00390026_m1
A2780cis	Washed Platelet	KLK1	Hs00168490_m1
		ITGB2	Hs00164957_m1
		STK17B	Hs00177790_m1
		GMNN	Hs00992846_m1
		NAP1L4	Hs00237196_m1
Endogenous Control	N/A	CDKN1B	Hs00152377_m1
		GAPDH	Hs99999905_m1

Table 5-17: Table of Genes Selected for Fluidigm technical validation of Affymetrix® GeneChip Human Exon 1.0 ST array results.

5.3.5.1 HIOE-80

Figure 5-15 and accompanying table illustrate the results of the Fluidigm qPCR technical validation of genes altered in the HIOE-80 cell line in response to exposure to washed platelets or platelet releasate.

Pearson's correlation analysis determined a strong correlation between the two sets of fold change values of 0.855. A two tailed t-test determined that this correlation was not statistically significant however (p>0.5).

Figure 5-15

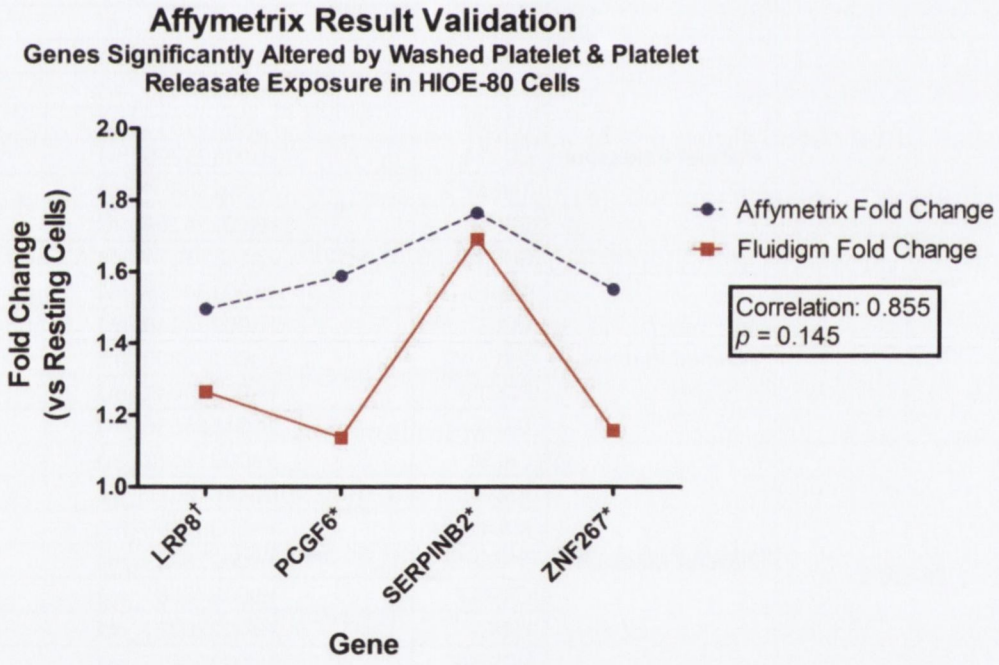

	Affymetrix Fold Change	p=	Fluidigm Fold Change	p=
LRP8†	1.50	0.0275	1.61	0.0000
PCGF6*	1.59	0.0372	1.14	0.0077
SERPINB2*	1.76	0.0016	1.69	0.0000
ZNF267*	1.55	0.0318	1.16	0.0000

† Platelet Exposure

* Washed Platelet Exposure

Figure 5-15: Fluidigm High Throughput qPCR Validation of Genes Undergoing Altered Expression in HIOE-80 Cells in response to Washed Platelet and Platelet Releasate Exposure.

5.3.5.2 59M

Figure 5-16 and accompanying table illustrate the results of the Fluidigm qPCR technical validation of genes altered in the 59M cell line in response to exposure to washed platelets or platelet releasate.

Examining the fold changes reported for genes undergoing altered expression in response to washed platelet exposure (Figure 5-16 (A)) Pearson's correlation analysis determined a very strong correlation between the two sets of fold change values of 0.982. A two tailed t-test determined that this correlation was statistically significant ($p<0.01$).

Examining the fold changes reported for genes undergoing altered expression in response to platelet releasate exposure (Figure 5-16 (B)) Pearson's correlation analysis again determined a strong correlation between the two sets of fold change values of 0.804. A two tailed t-test determined that this correlation was statistically significant ($p<0.05$).

Figure 5-16

A

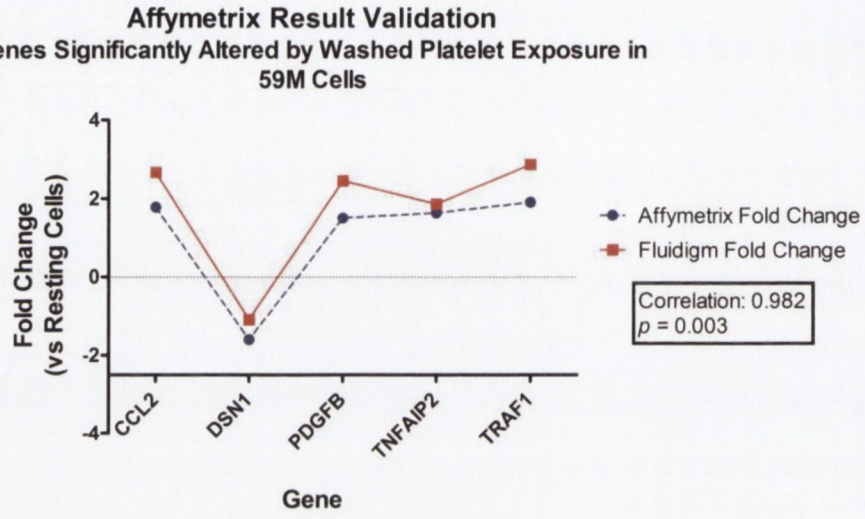

	Affymetrix Fold Change	p=	Fluidigm Fold Change	p=
CCL2	1.78	0.0281	2.67	0.0000
DSN1	-1.60	0.0350	-1.09	0.0036
PDGFB	1.50	0.0397	2.45	0.0000
TNFAIP2	1.63	0.0048	1.86	0.0000
TRAF1	1.90	0.0056	2.87	0.0000

B

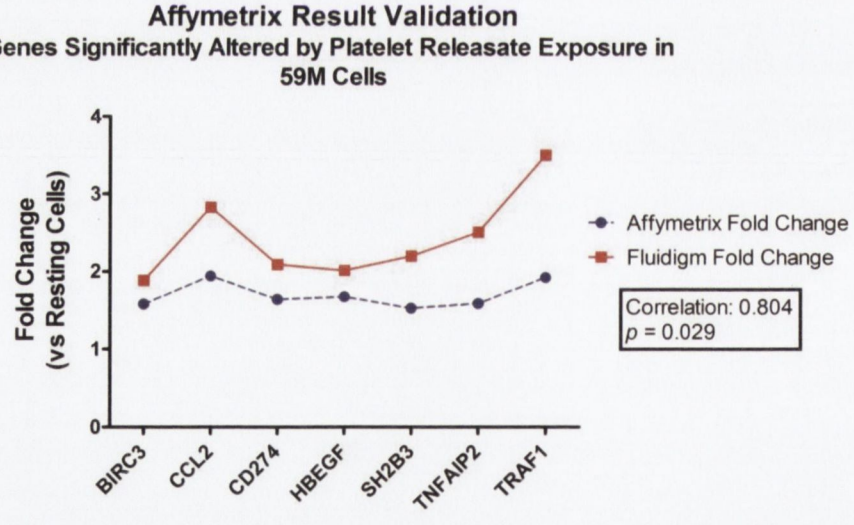

	Affymetrix Fold Change	p=	Fluidigm Fold Change	p=
BIRC3	1.58	0.0303	1.88	0.0000
CCL2	1.94	0.0137	2.83	0.0000
CD274	1.64	0.0487	2.09	0.0000
HBEGF	1.67	0.0034	2.01	0.0000
SH2B3	1.53	0.0060	2.20	0.0000
TNFAIP2	1.59	0.0018	2.51	0.0000
TRAF1	1.92	0.0013	3.50	0.0000

Figure 5-16: Fluidigm High Throughput qPCR Validation of Genes Undergoing Altered Expression in 59 Cells in response to Washed Platelet (A) and Platelet Releasate (B) Exposure.

5.3.5.3 SK-OV 3

Figure 5-17 and accompanying table illustrate the results of the Fluidigm qPCR technical validation of genes altered in the SK-OV 3 cell line in response to exposure to washed platelets or platelet releasate.

Examining the fold changes reported for genes undergoing altered expression in response to washed platelet and platelet releasate exposure (Figure 5-17) Pearson's correlation analysis determined a moderate correlation between the two sets of fold change values of 0.320. A two tailed t-test determined that this correlation was not statistically significant ($p>0.05$).

Figure 5-17

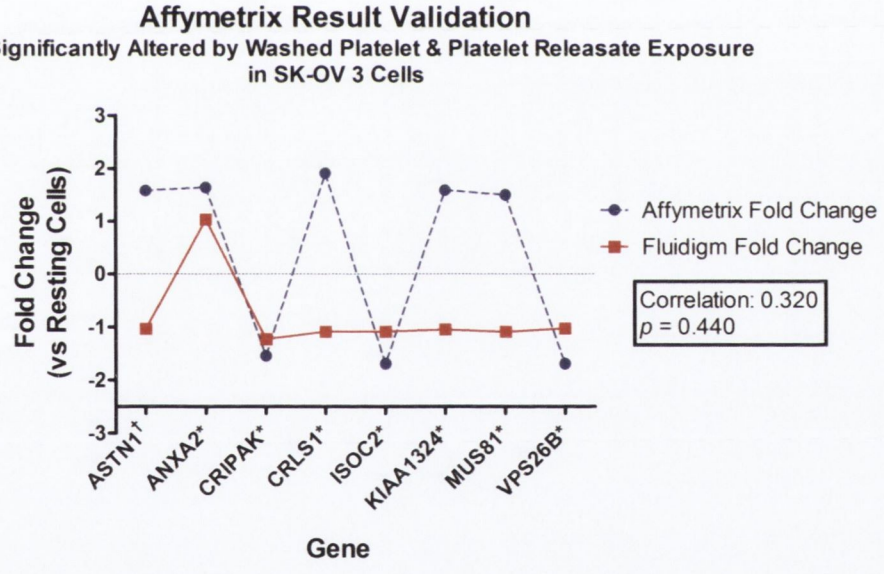

	Affymetrix Fold Change	p=	Fluidigm Fold Change	p=
ANXA2*	1.64	0.0225	1.04	0.3191
ASTN1†	1.58	0.0030	-1.03	0.9001
CRIPAK*	-1.55	0.0105	-1.23	0.0007
CRLS1*	1.91	0.0346	-1.09	0.0338
ISOC2*	-1.69	0.0036	-1.09	0.0000
KIAA1324*	1.58	0.0417	-1.05	0.1362
MUS81*	1.50	0.0222	-1.09	0.0809
VPS26B*	-1.69	0.0402	-1.03	0.5467

† Platelet Exposure

* Washed Platelet Exposure

Figure 5-17: Fluidigm High Throughput qPCR Validation of Genes Undergoing Altered Expression in SK-OV 3 Cells in response to Washed Platelet and Platelet Releasate Exposure.

5.3.5.4 A2780cis

Figure 5-18 and accompanying table illustrate the results of the Fluidigm qPCR technical validation of genes altered in the A2780cis cell line in response to exposure to washed platelets or platelet releasate.

Examining the fold changes reported for genes undergoing altered expression in response to washed platelet and platelet releasate exposure (Figure 5-18) Pearson's correlation analysis determined a moderate correlation between the two sets of fold change values of 0.550. A two tailed t-test determined that this correlation was not statistically significant ($p>0.05$).

Figure 5-18

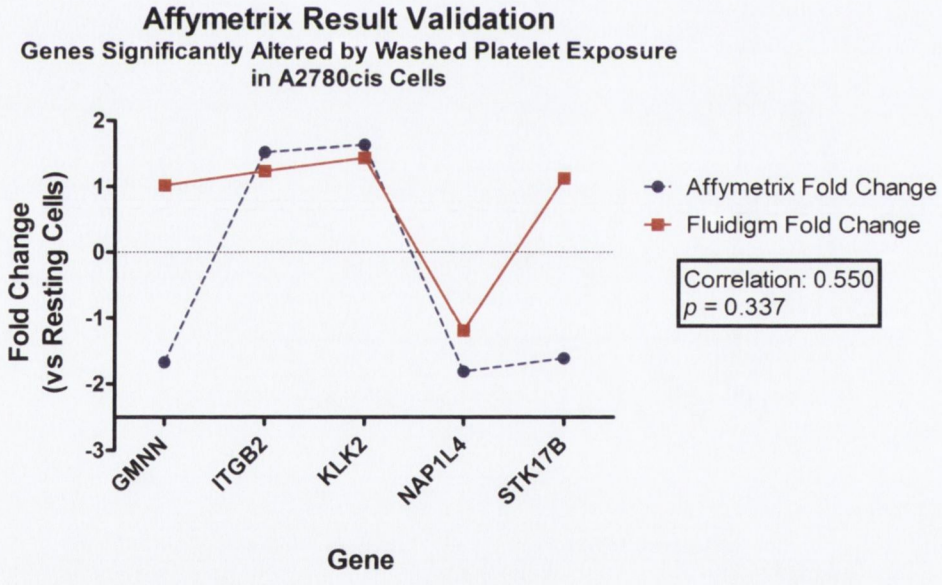

	Affymetrix Fold Change	p=	Fluidigm Fold Change	p=
GMNN	-1.67	0.0259	1.02	0.4974
ITGB2	1.52	0.0497	1.23	0.0000
KLK1	1.63	0.0239	1.44	0.0309
NAP1L4	-1.81	0.0082	-1.19	0.0054
STK17B	-1.61	0.0304	1.13	0.0019

Figure 5-18: Fluidigm High Throughput qPCR Validation of Genes Undergoing Altered Expression in A2780cis Cells in response to Washed Platelet Exposure.

5.4 Discussion

Initial experiments performed in this component of the thesis were focussed on determining the optimal platelet and washed platelet exposure that would be used to examine the effect of these exposures on gene expression in ovarian cell lines.

As there was no published data informing a standard or estimated number of platelets adhering to cells during TCIPA or the concentration of platelet releasate to which they may be exposed during the period of platelet aggregation a series of MTT and TUNEL assays were performed. These enabled a dilution factor of platelet releasate prepared in full growth media to be determined that could be used across the panel of experimental cell lines that would not negatively impact on cell growth/viability and that would not result in increased levels of apoptosis over that normally present in standard cell culture conditions. This was established at a 1:1000 dilution, equivalent to a platelet releasate protein concentration of 0.244μg/ml based on BCA assay quantitation of undiluted pooled platelet releasate protein content (Section 5.3.1.1).

The specific composition of the platelet releasate was not examined as part of this thesis, although investigations performed by other groups have shown platelet releasate to contain a wide variety of signalling molecules in addition to those pro-thrombotic mediators that assist in the platelet function of clot formation. These include chemokines and angiogenic regulators such as PDGF, TGFβ, cyclophilin A, VEGF, angiopoietin, thrombospondin, platelet factor 4 (PF4), FGF and endostatin, and immune modulators such as neutrophil-activating peptide 2 (NAP2) (Battinelli et al., 2011, García and Senis, 2011, Kamykowski et al., 2011, Peterson et al., 2010, Dineen et al., 2009, Falanga et al., 2009, Holmes et al., 2009, Piersma et al., 2009, Coppinger et al., 2007, 2004).

After further review of flow cytometry as a technique for investigating apoptosis in cell lines it is arguable that it may be more suited to investigations of non-adherent (suspension) cell lines due to some technical difficulties and considerations that may arise when investigating apoptosis in adherent cell types.

These include the risk of;

- generating false positive arising from cells becoming damaged during detachment and pipetting
- loss of detached apoptotic cells in supernatants
- uneven staining of clumped cells impacting adhesion of cells

While the chemistries and techniques utilised in this investigation were demonstrated to be efficacious in interrogating apoptosis in 80% of the experimental cell lines, future investigations of cell line apoptosis when exposed to platelet releasate may utilise high throughput microscopy technologies such as the GE IN Cell high content screening technologies. The quantitative capability of this technology is comparable to that offered by flow cytometry and has the potential to analyse each cell presented on an experimental plate. It also offers the added advantage of allowing adherent cells to be stained and analysed for the detection of apoptosis on plate eliminating the comparatively high level of processing (detachment & pipetting) steps required for flow cytometry analysis of adherent cell line apoptosis.

Having optimised the conditions at which cell lines would be exposed to washed platelets or platelet releasate, cell lines were assessed for the presence of mycoplasma species which would potentially impact on gene expression data arising from planned subsequent Affymetrix® GeneChip® based investigations. This examination of cell line health determined that there was no mycoplasma infection of experimental cell lines.

Following an 8 hour exposure of cell lines to washed platelets or platelet releasate total RNA was extracted and changes in gene expression over the entire transcriptome assessed using Affymetrix® GeneChip® Human Exon Arrays. This allowed comparison to be made between gene expression in exposure groups and that in resting cells cultured in full growth media only.

This investigation revealed context specific changes in gene expression across the different cell lines.

The HIOE-80 cell line was observed to undergo alteration in the levels of expression of genes involved in cell metabolism, gene expression, cell growth and proliferation and migration in response to washed platelet exposure. Platelet releasate exposure returned only one gene that met the threshold level of a fold change >1.5 and significance of $p<0.05$, LRP8/APOER2, which has been described as potentially affecting platelet function.

The 59M cell line was observed to undergo alteration in the levels of expression of a wide variety of genes in response to both exposures. Washed platelet exposure resulted in altered expression of genes involved in the regulation of cell cycle, cell growth and proliferation, anti-apoptotic signalling and angiogenesis. Platelet releasate exposure resulted in the altered expression of genes involved in the regulation cell cycle, cell growth and proliferation, anti-apoptotic signalling, migration/invasion, immune evasion and potentially platelet function.

The SK-OV 3 cell line was observed to undergo alteration of gene expression primarily in response to platelet releasate exposure. The genes affected had diverse functions and were involved in metabolism, gene expression and cell cycle, cell growth and proliferation, anti-apoptotic signalling, migration/invasion and potentially platelet function.

The A2780 cell line was observed to undergo alteration in the levels of expression of genes of no genes in response to either exposure but the cisplatin resistant daughter cell line representative of recurrent ovarian disease, A2780cis, was observed to undergo alteration in the levels of expression of genes involved in metabolism, gene expression, cell cycle, cell growth and proliferation, anti-apoptotic signalling, and cell migration/invasion in response to washed platelet exposure only.

These responses summarised in figure 5-19.

Figure 5-19

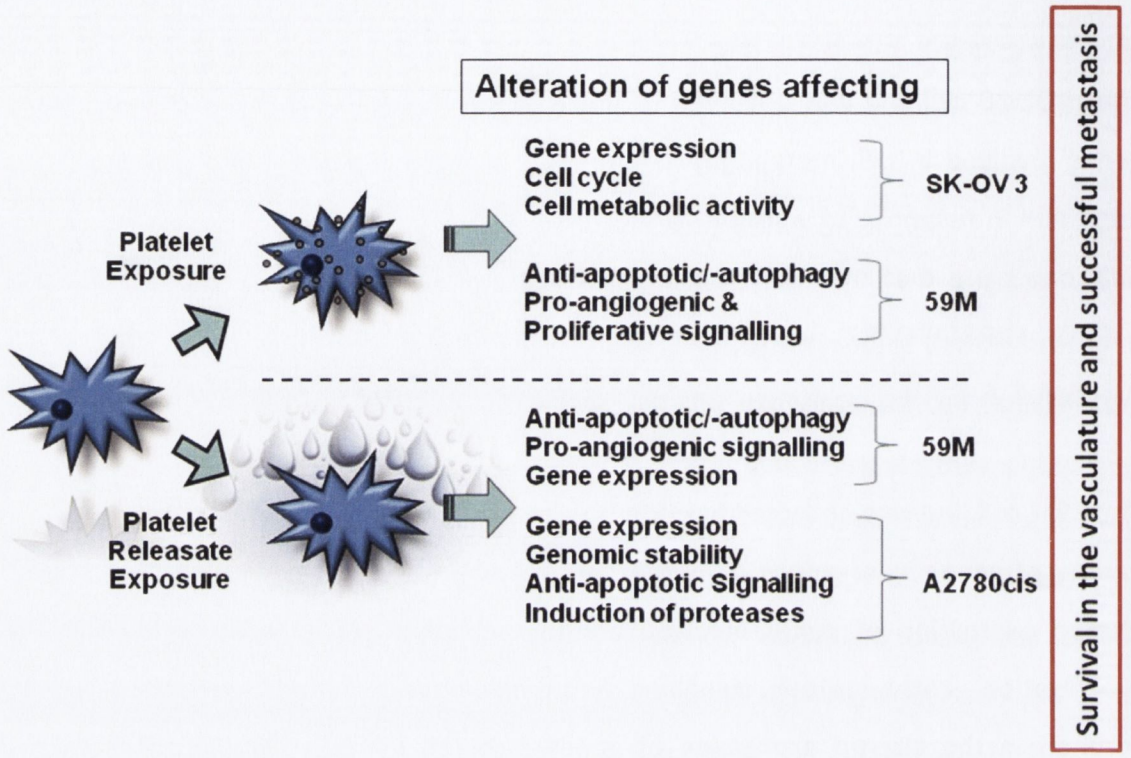

Figure 5-19: Summarisation of Gene Expression Changes Observed in Ovarian Cell Lines in Response to Washed Platelet/Platelet Releasate Exposure.

Fluidigm® Dynamic Arrays® were utilised to perform high throughput qPCR for technical validation of Affymetrix results. Fold change values for samples revealed a close correlation between Affymetrix and Fluidigm® data sets for those genes observed to have undergone altered expression in the HIOE-80, 59M, and A2780cis cell lines. The correlation for genes observed to undergo significant alteration of expression in both the 59M ovarian carcinoma cell lines was high (>0.8) and was statistically significant ($p<0.05$).

Discrepancies between expression calculated by Affymetrix and TaqMan® analyses are likely due to inherent differences between the two technologies, the different resolution of the assays or the 3' biased design of Affymetrix microarray.

Platelet releasate was generated utilising Thrombin Receptor Activating Peptide (TRAP) and collagen. It was not possible to subsequently remove the TRAP from this solution. Future investigations may consider interrogating resting cancer cells for the expression of thrombin receptors, PAR 1, 3 and 4. Subject to the results of this investigation, research may either continue with the current protocol or consider an alternative mechanism of inducing platelet activation to overcome this potential shortcoming in the current work.

Despite an extensive history of investigations examining and characterising the initiators and physical mediators the interaction of cancer cells and platelets, a relationship first described by Trousseau 146 years previous (Trousseau, 1865), at the time of study completion, just one gene, MMP9, had been confirmed at the mRNA level to undergo altered expression in response to tumour cell induced platelet aggregation (Alonso-Escolano et al., 2006).

The previous chapter of this thesis has documented a potent, dynamic interaction between ovarian cancer cells and platelets *in vitro*, and that that this interaction involves platelet adhesion, platelet activation and degranulation. This chapter has examined the molecular impact of TCIPA on the platelet-cloaked cancer cell and for the first time suggests that TCIPA may result in reciprocal platelet-induced cancer cell priming (PICCP), arising from induction of pro-survival and pro-angiogenic signalling, that could potentially promote ovarian cancer cell metastasis.

Chapter Five Appendix

Appendix Figure 5-1

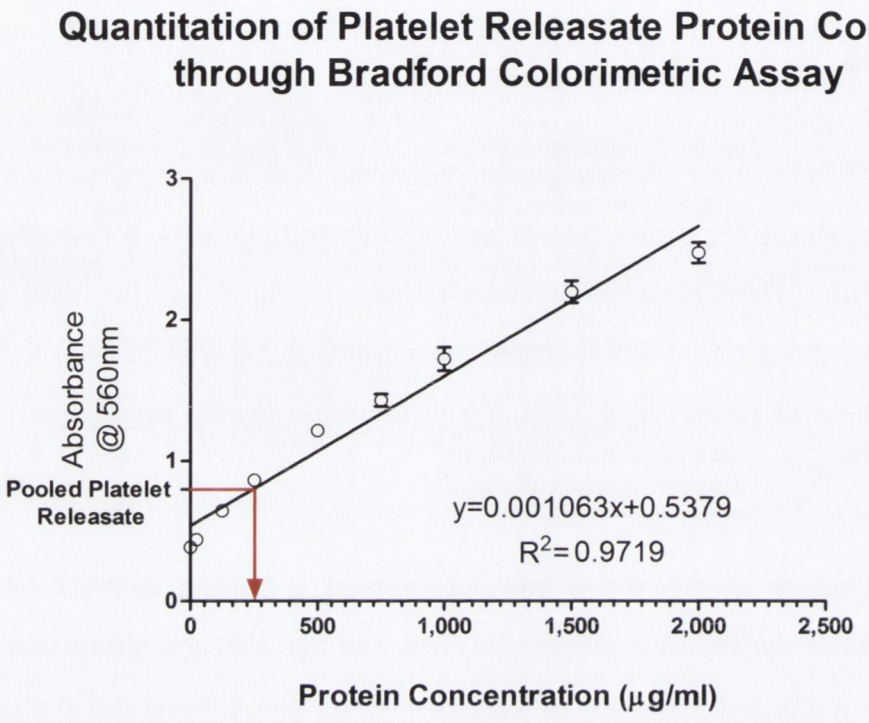

Appendix Figure 5-1: Bradford Assay – Quantitation of Platelet Releasate Protein Content.

Utilising the Bradford colorimetric assay absorbance values at 560nm for albumen standards of known concentration between 25µg/ml and 2000µg/ml a linear line of best fit and its equation of the line generated in GraphPad Prism. This equation was subsequently used to determine the protein concentration of unknown platelet releasate samples.

The R^2 value was also generated, the figure reflecting how close the data fits to the line of best fit. A high R^2 value (close to 1.0) in the context of standard curve preparation is generally considered an indicator of the accuracy of preparation in the preparation of the standards.

Appendix Table 5-1

		Absorbance @ 560nm		
Sample	**Protein (µg/ml)**	**Read 1**	**Read 2**	**Read 3**
Standard	0	0.359	0.396	0.398
Standard	25	0.440	0.435	0.445
Standard	125	0.631	0.648	0.659
Standard	250	0.813	0.886	0.888
Standard	500	1.146	1.236	1.265
Standard	750	1.350	1.499	1.449
Standard	1000	1.559	1.771	1.836
Standard	1500	2.046	2.253	2.296
Standard	2000	2.330	2.554	2.542
Pooled Platelet Releasate	244.7*	0.722	0.818	0.854
Donor 1 Platelet Releasate	154.1*	0.645	0.782	0.678
Donor 2 Platelet Releasate	322.2*	0.853	0.884	0.904
Donor 3 Platelet Releasate	192.3*	0.719	0.763	0.745

Appendix Table 5-1: Bradford Assay - Quantitation of Platelet Releasate Protein Content.

Using the absorbance figures returned at 560nm by protein standards from 25 to 2000µg/ml and the subsequently derived equation of the line corresponding to the standard curve (figure 5-19), the absorbance returned by individual and pooled platelet releasate samples was used to determine their corresponding protein concentration.

The composition of the protein releasate samples was not determined as part of this study.

CHAPTER SIX

DISCUSSION AND CONCLUSION

6. Discussion and Conclusion

6.1 Background

The three biological observations which make up the scientific underpinnings of the principal phenomenon of interest to this thesis, tumour cell induced platelet aggregation, can be traced back one hundred and forty-six years. The earliest of these is Trousseau's observation of increased venous thrombosis in individuals with cancer in 1865. The same year saw the publication of Schultz's description of platelets, but it was to be almost two decades before Bizzozero would publish a substantially more complete characterisation of the nature, role and importance of the platelet in 1882. The intervening period would see the observation by Australian physician Thomas Ashworth in 1869 of cancer cells, more recently termed circulating tumour cells, in the blood of a patient with metastatic disease.

Thus the scene was set where research performed in the 20th century would later inform the existence of TCIPA, whereby CTCs may exploit platelets during haematogenous dissemination, inducing their aggregation/adhesion to the CTC surface, resulting in the formation of a platelet-CTC embolus which confers an increased capability for the malignancy to successfully spread and establish secondary tumours away from the primary site.

The last thirty years, and in particular the last decade, have seen increasing numbers of publications examining the core components of TCIPA: circulating tumour cells and thrombocytosis/thrombosis in cancer. While the significance of CTCs in cancer and awareness of the pro-thrombotic state associated with many cancers have been more greatly appreciated in recent years, as witnessed by increased numbers of publications in both areas, the association between these aspects of malignancy and TCIPA would appear to be infrequently made. This has ensured that research into the basis of cancer cells' ability to aggregate platelets to their surface and the pro-metastatic effects this conveys by the formation of a 'platelet cloak' remains a niche venture, which is reflected in the consistent but comparatively few number of publications made on the topic in the same time frame (Figure 6-1).

Figure 6-1

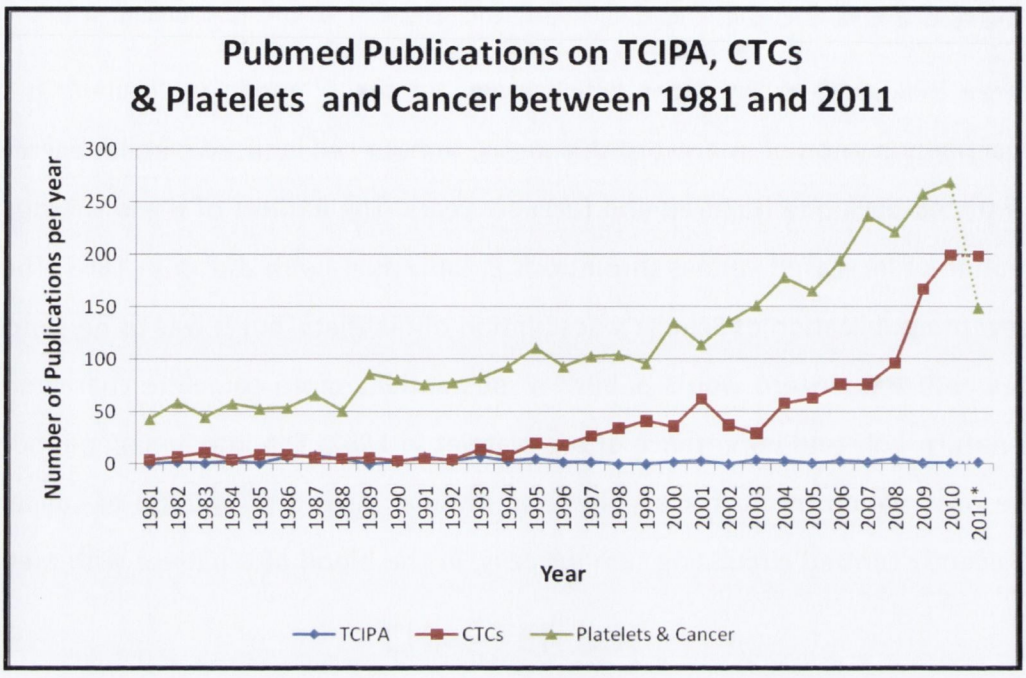

Figure 6-1: Number of Publications by year between 1981 and 2011 examining TCIPA, CTC's or Platelets & Cancer.

A clear trend is visible whereby the numbers of studies investigating or reporting on circulating tumour cells or thrombocytosis/thrombosis in cancer have risen considerably in the last decade, whereas the number of studies examining or reporting tumour cell induced platelet aggregation has remained at a low level.

The PubMed publication figures are based on database searches utilising the following queries: *"circulating tumor cells" OR "circulating tumour cells"* (CTC), *"tumour cell induced platelet aggregation" OR "tumor cell induced platelet aggregation"* (TCIPA) and *"thrombocytosis" OR "thrombosis" AND "carcinoma"* (Platelets & Cancer). *2011 figures correct to September 2011.

6.2 Aims of the Thesis

The introduction of this thesis outlined the nature of ovarian cancer, the significant cost of life and health associated with the disease, the inability to effectively screen for ovarian cancer, the resulting high frequency of late stage disease diagnosis and the challenge of providing effective treatment arising from the propensity for ovarian disease to develop resistance to chemotherapeutic interventions.

The introduction also outlined the relationship between cancer states and platelets, with focus given to the propensity for malignancy to be associated with elevated platelet counts; itself associated with greater metastases and worse patient prognosis and outcome. This is hypothesised to arise from the ability of some cancers to induce platelet aggregation/adhesion to their surface as CTCs undergo haematogenous dissemination through the vasculature.

The aims of this thesis were to examine the relationship between ovarian cancer and platelets in the Irish population utilising archival samples and corresponding patient data, to investigate the interaction between ovarian cancer cells and platelets with regard to TCIPA and finally to determine and characterise the molecular basis of the increased capacity to metastasise associated with TCIPA/thrombocytosis in ovarian cancer. These studies utilised a variety of techniques, including conventional and high-throughput forms of TaqMan® RT-PCR, a novel *in vitro* fluorescent platelet-cancer cell adhesion assay, flow cytometry and whole transcriptome microarray analysis.

6.3 Overview of Results & Conclusions

6.3.1 Chapter 3

Experiments and investigations performed in chapter three endeavoured to examine the relationship between ovarian cancer and platelets in the Irish population through a retrospective examination of preoperative platelet count/thrombocytosis and patient outcome, and correlation of patient platelet metrics and survival with the expression of a panel of related genes through RT-PCR analysis. This is was the first study of its kind performed examining these associations in the context of ovarian cancer in an Irish population.

This study revealed significant differences in the level of expression of several genes between ovarian cancer (grade 2 and 3) compared to expression levels in normal samples. These differences in expression were further investigated and trends towards increased expression (≥2x) with increasing tumour gradation were observed for the genes PDGFA, PDGFB, CA125 and VEGFA. A trend for reduced expression with increased tumour grade was observed for the genes PDGFRA, PDGFRB and THPO. The investigations revealed a positive correlation between PDGFB expression and preoperative platelet count, and expression of CA125 and VEGFA was observed to positively correlate with tumour grade.

No correlation was observed between the level of gene expression of target genes and patient survival (PFS, OS, 2- and 5-year survival), with the exception of CA125, which returned a statistically significant negative correlation with 2-year survival. While thrombocytosis was more prevalent in ovarian cancer groups than the normal sample group, no significant correlation was observed between thrombocytosis and PFS, OS, 2- or 5-year survival.

This component of the thesis revealed the presence of ovarian cancer related thrombocytosis indicating the presence of a relationship between the development of this form of malignancy and induction of megakaryopoiesis. The study results indicate this is not the result of tumour associated expression of thrombopoietin, the primary driver of

platelet production, the expression of which was not observed to correlate with platelet count/preoperative platelet count.

The study also revealed the increased expression of PDGF genes with a concurrent reduction in expression of genes encoding for PDGFRs. The altered expression of these genes is hypothesised to result in the generation of a pro-angiogenic local micro environment to potentiate tumour growth and metastasis. Given the focus PDGFRs have received as potential targets for new, targeted cancer therapies, these results may be of significant clinical relevance, as should reduced PDGFR expression be a frequent feature of ovarian cancer development, the efficacy of these new therapies may be reduced.

The investigation of the effect of thrombocytosis on patient survival revealed variation in cancer grade-related long term (2- and 5-year) survival rates arising from the metric accepted for thrombocytosis. The value for thrombocytosis commonly used in the Irish medical system ($400x10^9$ platelets/L) and the figure utilised in other countries, including the United Kingdom ($450x10^9$ platelets/L) (Harrison et al., 2010), returned contrasting results; the latter value defining reduced survival with increased tumour grade with greater clarity. This finding may have immediate and direct clinical relevance in terms of patient treatment, prognosis and monitoring.

6.3.2 Chapter 4

Progressing from the previous chapter, which revealed a correlation between tumour grade and expression of PDGFB and preoperative platelet count, chapter four of this thesis investigated the relationship between ovarian cancer and platelets with specific regard to the ability for ovarian epithelial cancer to induce tumour cell induced platelet aggregation.

To examine this interaction a novel *in vitro* assay, capable of determining the presence of fluorescently labelled platelets adhering to the surface of ovarian cell lines representing normal epithelial tissue and ovarian epithelial malignancy, was developed and optimised. This assay revealed that normal ovarian epithelial cells (HIOE-80) had little capability to induce platelet adhesion, whereas cell lines representing ovarian epithelial cancer (59M, A2780, A2780cis) were able to induce platelet adhesion to their surface during a co-incubation period. A positive relationship between malignant/metastatic potential and capacity for platelet adhesion was also identified.

Subsequent to *in vitro* assay of cell line-platelet adhesion, the capacity of cell lines to activate platelets was investigated by flow cytometry analysis. The presence of fluorescently labelled platelet p-selectin during analysis of ovarian cell lines following platelet exposure was indicative of the presence of activated adherent platelets. The results of these assays supported the observation that increased cancer cell malignancy conveys an increased capacity for adherent interaction with, and activation of, platelets.

At the time of initiation this was the first study to examine cell lines representing ovarian epithelial cancer for their capability to initiate TCIPA when exposed to platelets and is the first study where increasing cancer cell line malignancy/metastatic potential has been shown to be related to increased capacity to induce TCIPA.

6.3.3 Chapter 5

Having documented the capability of cancer cell lines to induce platelet adhesion/aggregation and platelet activation in chapter four, the fifth chapter of this thesis aimed to definitively determine the molecular basis of the increased capacity for ovarian cancer to successfully metastasise in the presence of elevated platelet counts.

This is hypothesised to be attributable to the induction of TCIPA during haematogenous dissemination, during which both platelet-cancer cell physical interaction and platelet related signalling effects result in:

- release of proliferative and pro-angiogenic signalling molecules from the α- and dense granules of activated platelets
- impaired immune system-mediated cancer cell destruction and abrogation of the efficacy of chemotherapies
- protection from shearing forces in the circulatory system
- embolus formation resulting in assistance in mechanical arrest at peripheral sites where secondary tumours may extravasate and establish metastases.

Prior to this thesis the molecular basis of the effects of TCIPA on the platelet cloaked cancer cell which result in an improved capability for metastasis was limited to a single observation at the mRNA level that MMP9 expression was increased in the MCF-7 breast cancer cell line in response to platelet exposure (Alonso-Escolano et al., 2006).

The fifth chapter of this thesis aimed to substantially improve the understanding of the effect of tumour cell induced platelet aggregation on the platelet cloaked cancer cell by employing GeneChip® microarray technologies to interrogate the changes occurring over the whole transcriptome as a result of TCIPA, or exposure to platelet releasate, in the panel of ovarian epithelial cell lines previously utilised in chapter four.

As the number of platelets adhering to cells during TCIPA was a previously unquantified variable, initial experiments were performed to determine the maximum concentration of platelet releasate to which cells would also be exposed. This would also directly inform the equivalent concentration of platelets to which cells would be exposed. The concentration used was the highest observed not to result in a negative impact on cell growth/metabolism, or result in increased rates of apoptosis across the panel of cell lines.

Having determined the optimal concentration, the panel of ovarian epithelial cell lines was exposed to platelet releasate and platelets, and changes in gene expression were assessed using Affymetrix® GeneChip® Human Exon 1.0 ST arrays. A diverse and context-specific response to platelet and platelet releasate exposure across the range of cell lines was observed.

The nature of the genes observed to undergo altered expression in response to cell exposure to platelets or platelet releasate indicate the capacity for tumour cell induced platelet aggregation to result in altered expression of genes affecting pathways associated with all aspects of Hanahan and Weinberg's revised hallmarks of cancer (2011), including the recently added enabling hallmarks and enabling characteristics (Figure 6-2).

Figure 6-2

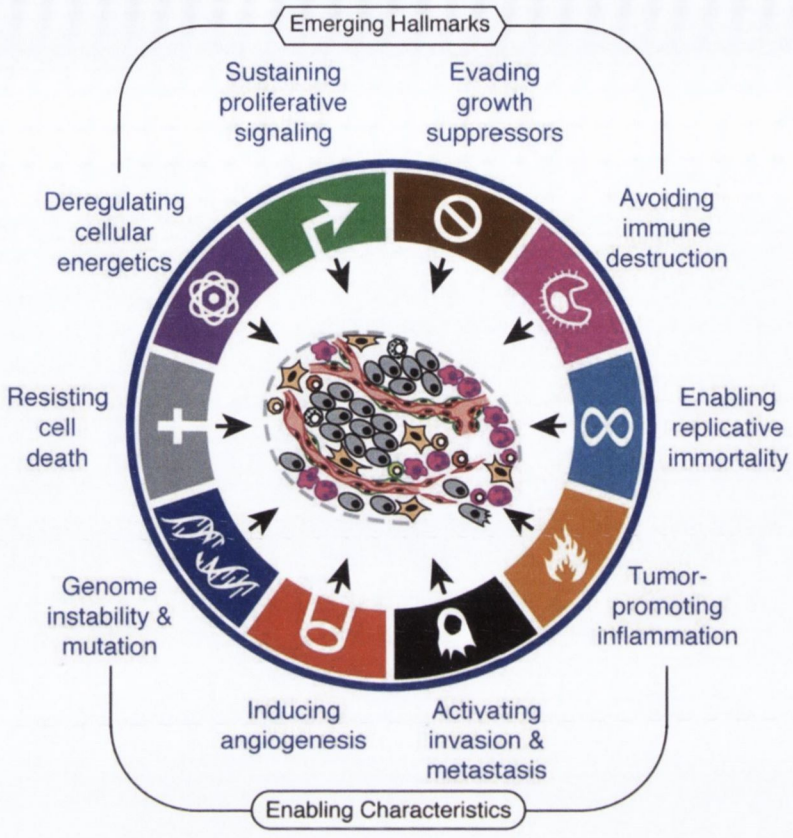

Figure 6-2: Hanahan & Weinberg's Hallmarks of Cancer.

Adapted from Hanahan & Weinberg (2011).

The HIOE-80 cell line representing normal ovarian epithelial cells revealed a small number of genes undergoing altered expression in response to washed platelet exposure, primarily involving upregulation of genes involved in metabolism and gene transcription, including two genes observed to have roles in reducing uPA and matrix metalloproteinase expression. Exposure to platelet releasate revealed the significant alteration of a single gene, LRP8, encoding for the apolipoprotein E receptor, which may alter platelet function or adhesion.

An examination of the effect of platelet or platelet releasate exposure on cell lines representing ovarian epithelial cancers revealed:

- 59M - a response was observed to both exposures. The genes undergoing increased expression were involved in anti-apopotic and anti-autophagy signalling,

proliferative and pro-inflammatory signalling, immune suppression, cell adhesion, migration and invasion. Decreased expression was observed in genes involved in maintaining genomic stability.

- SK-OV 3 – this cell line was observed to respond primarily to the platelet releasate exposure. This resulted in the increased expression of genes associated with thrombocytosis in ovarian cancer, genes involved in anti-apoptotic and anti-autophagy signalling, gene transcription and cell cycle maintenance and proliferation, cell metabolism and pH regulation, cell motility and invasion. Reduced expression was observed in genes responsible for inhibiting PAK1, a gene affecting the expression of genes involved in a variety of cellular functions including proliferation, survival and motility and MMP9 expression and associated with insensitivity to chemotherapy and poorer patient outcome.

- A2780 – this cell line revealed no significant alteration in gene expression in response to either exposure.

- A2780cis – unlike the A2780 cell line from which it was derived, this cisplatin resistant cell line representative of recurrent chemotherapy-insensitive ovarian disease saw a greater number of genes undergo reduced expression than increased expression. Those genes that saw increased expression include a member of the kallikrein serine protease family frequently described to be increased in many cancers, including ovarian cancer, and associated with more aggressive disease and worse outcome. Also increased was LFA-1 expression, with possible roles in cell adhesion, migration and mediation of matrix metalloproteinase expression. Genes undergoing reduced expression were observed to be involved in maintenance of genomic stability, cell cycle control, gene transcription and positive regulation of apoptosis.

A selection of the genes observed to undergo significantly altered expression were chosen for high throughput TaqMan™ assay using Fluidigm microfluidic platform technologies in order to technically validate the results observed. The fold changes returned by both technologies were observed to correlate well for most genes with

differences, where present, hypothesised to be the result of inherent differences in the resolution and design between the two technologies.

This study definitively demonstrates for the first time that the significance of TCIPA extends far beyond the benefits arising from the physical formation of platelet-cancer cell emboli in supporting successful metastasis of ovarian cancer.

This study has determined that TCIPA results in a dynamic alteration of gene expression in cancer cells exposed to platelets or platelet releasate *in vitro.* Many of the genes affected were observed to be associated with the development of different hallmarks of cancer and may form the molecular basis of the enhanced capability for the successful metastasis of CTCs in the prothrombotic/thrombocytotic background present in malignancy.

6.4 Future Work

The work outlined in this thesis has produced some interesting, exciting and novel data regarding the interaction of platelets with ovarian cancer. Arising from the results reported, a range of future opportunities are present for continuation of this research.

6.4.1 Ovarian Cancer Archival Studies

The research documented in the third chapter of this thesis offers several avenues for further exploration. Increasing the number of samples and corresponding data to supporting the already documented population would increase information regarding the correlation of preoperative thrombocytosis with patient survival and prognosis. Further investigation of the levels of expression of genes involved in megakaryopoiesis may determine the role of the tumour in driving the increased production of platelets observed in many ovarian cancers. With the incorporation of more patient clinical data, to include observations of chemosensitivity/resistance and extent of metastasis, correlations between these variables and thrombocytosis in Irish ovarian cancers may be pursued.

6.4.2 *In vitro* TCIPA Studies

While significant novel and exciting data regarding the interaction of normal and malignant ovarian cell lines with platelets was discovered in the completion of this thesis, a veritable smörgåsbord of potential experimental work exists for future investigation.

Full troubleshooting and optimisation of the aggregometry technique attempted in this study may allow future investigations to examine differences in cell line capability for induction of TCIPA through monitoring the rate and magnitude of aggregation in real time. This technique may also allow the future examination of the efficacy of anti-platelet aggregation/activation molecules to inhibit or to 'decloak' ovarian cancer cells which have induced TCIPA.

Arising from the recent observation made by Rothwell and colleagues (2011) that low-dose aspirin is associated with reduced risk of death from several forms of cancer (oesophageal, pancreatic, brain, lung, stomach, colorectal and prostate cancers), examining the result of low dose aspirin intake on TCIPA in future studies would be of specific interest. Rothwell's study has received a significant amount of commentary and analysis since publication, garnering interest and criticism in equal measure and renewing interest in aspirin as a potential agent for the prevention and treatment of cancer (Tagliabue and Pugliano, 2011, Kraus and Arber, 2011, Berg and Soreide, 2011, Moayyedi and Jankowski, 2010, Langley et al., 2011). Studies published subsequently have shown anti-cancer benefits of low-dose aspirin regimens in lung, breast, pancreatic and melanoma cancers (Tan et al., 2011, Curiel-Lewandrowski et al., 2011, Luo et al., Xu et al., 2011). Aspirin has been demonstrated to have anticancer effects on ovarian cell lines through COX-2 inhibition and regular use has also been demonstrated to result in reduced risk of ovarian cancer (Prizment et al., 2010, Drake and Becker, 2002, Rodríguez-Burford et al., 2002).

The function of aspirin as an inhibitor of platelet activation, and so a potential inhibitor of TCIPA, in the prevention of cancer progression has not been investigated and may be form part of future work. This may include the use of platelets isolated from the blood of individuals taking aspirin daily, or exposure of isolated platelets to low doses of aspirin, prior to exposure to ovarian cancer cells and comparing TCIPA against appropriate controls.

Finally, having optimised and examined the induction of TCIPA by ovarian cells using aggregometry and the efficacy of inhibitors of platelet aggregation in preventing or disrupting the interaction, the formation of the platelet cloak might be visualised in real-time through the use of microfluidic lab-on-chip type devices capable of replicating the flow and shear forces *in vitro* which are normally present in the circulation during haematogenous spread of CTCs.

6.4.3 TCIPA Induced Alteration of Cancer Cell Gene Expression

Many options are available for progression of the work performed in chapter five of this thesis, which revealed the capability of TCIPA to induce altered expression of genes in the platelet-cloaked cancer.

Initial work may involve repeating the exposure of the panel of cell lines to washed platelets or platelet releasate and examining whether the exposure results in quantifiable increases in invasive capacity, by performing transendothelial migration assays as an *in vitro* model of extravasation. As Holmes and colleagues have previously indicated an increase in invasive capacity of SK-OV 3 cells after exposure to TRAP activated platelets, it would be very interesting to investigate whether platelet activation arising from TCIPA alone results in similar increases in invasive ability (Holmes et al., 2009).

A gold standard set of future experiments may utilise normal and malignant primary ovarian epithelial cells isolated from women undergoing prophylactic oopherectomy and cancer debulking surgeries. Examining the capacity of these cells to induce TCIPA and the alteration of gene expression resulting from TCIPA using donor matched platelets may verify those previously reported in cell line models of TCIPA in ovarian cancer.

Finally, the experiments performed examining TCIPA in chapters four and five may be repeated to examine the interaction of platelets and cell lines representing other cancers known to undergo haematogenous dissemination during metastasis and the effect of TCIPA on gene expression in these model systems.

6.5 Translational Benefits of TCIPA Research

The investigations performed in the completion of this thesis have the potential to significantly impact the health and disease outcomes of those with ovarian cancer.

Results of investigations performed using archival clinical samples determined altered expression of platelet derived growth factors and their receptor as cancer grade progressed, with the former undergoing increased expression and the latter undergoing reduced expression. As the interference with, or inhibition of, these receptors has specifically been considered a potential goal of targeted adjunct therapies in support of conventional treatment of ovarian cancer, the reduced expression of these proteins may have significant impact on the efficacy of these treatments. Additionally the threshold value for thrombocytosis utilised in the Irish clinical setting, $400x10^9$ platelets/L, was observed to be less sensitive in detecting differences in long term survival between tumour grades than the elsewhere used value of $450x10^9$ platelets/L. It is contended that the latter value should be promptly accepted as a standard metric for thrombocytosis in patients diagnosed with ovarian cancer due to significance in outcome and prognosis.

The results of investigations examining ovarian cancer cells' capacity to induce TCIPA and their altered gene expression arising from TCIPA may have exceptionally powerful translational significance for ovarian cancer screening, treatment and monitoring.

In 2011 Veridex, a Johnson and Johnson subsidiary company, was given FDA approval for the marketing of a microfluidic system, CellSearch™, capable of isolating CTCs from whole blood of patients diagnosed with metastatic breast colorectal or prostate cancers. The CellSearch™ system uses a system of positive and negative selection of epithelial and non-epithelial surface markers to capture and subsequently identify tumour cells of epithelial origin (CD45 negative, epithelial cell adhesion molecule (EpCAM) and cytokeratins 8/18 and 19 positive) (Veridex LLC, 2011).

The CellSearch™ platform has been shown to be capable of isolating CTCs of various cancer types and that the number of CTCs detected is a strong independent predictor of patient prognosis, with >5 CTC/7.5ml whole blood associated with shortened PFS and OS

periods. The system is suggested to provide a more accurate prognosis than conventional imaging techniques and has demonstrated a capability for monitoring the efficacy of treatment. It has the potential to indicate early recurrence through CTC monitoring throughout the treatment period and in follow up (Hartkopf et al., 2011, Budd et al., 2006, Allard et al., 2004).

This thesis has demonstrated that ovarian cancer cells have the capacity to induce platelet adhesion and activation and that this can result in altered gene expression effecting increased malignant potential. Should CTCs in a patient sample be coated in a platelet 'cloak', having induced TCIPA, the metastasising tumour cell may not be detected using this type of technology without refinement, and the number of CTCs detected may not accurately reflect the true circulating tumour cell burden.

A recent publication utilising the CellSearch™ system supports the use of this technology for use in ovarian cancer. Interestingly, while this study by Poveda and colleagues determined that the number of CTCs in ovarian cancer was a strong negative prognostic indicator of survival in ovarian cancer (supporting previously observations between CTC burden and prognosis), the study also noted that comparatively few CTCs were detected in ovarian cancer compared with other cancers resulting in the use of a lower CTC threshold >2 CTC/7.5ml in the investigation (Poveda et al., 2011). It is not known if the reduced number of detected ovarian CTCs is attributable to an actual low number of CTCs, some other aspect of cancer biology, or TCIPA-cloaked ovarian CTCs escaping detection and isolation by the current CellSearch™ configuration of reagents.

The results of this thesis may prove pivotal in addressing shortfalls in systems investigating CTCs. If the capability for detection and assessment of platelet cloaked CTCs is added to diagnostic and monitoring tools such as the Veridex CellSearch™ platform it may allow more accurate determination of metastatic tumour load, better monitoring and quantitation of the treatment efficacy, monitoring of remission and early determination of disease recurrence.

6.6 Ovarian Cancer and CTC Studies in the Societal Context

The interaction of science and society in the dissemination and understanding of developments in research involved in or relating to ovarian cancer and CTCs has been significantly improved in recent times.

The latter part of 2010 and early part of 2011 saw significant worldwide coverage of the study performed by Rothwell and colleagues (2011) indicating the survival benefits associated with long term low-dose aspirin in reducing the risk of cancer death (Moore, 2010, Kay, 2010, Roni, 2010, Kelland, 2010). Given the inhibitory effect aspirin has on platelet activation, it may be possible that low dose aspirin may mediate its effect in reducing the risk of cancer mortality through both effects at the cancer cell and in inhibition of TCIPA assisted CTC metastasis.

Public awareness regarding CTCs was also increased with the widespread reporting of the Johnson & Johnson/Veridex collaboration with Massachusetts General Hospital to develop a 'liquid biopsy' for the capture and subsequent analysis of CTCs from whole blood building on the experience and technology developed for the Veridex CellScan™ system (Johnson & Johnson Inc., 2011). This collaboration was reported worldwide through print, broadcast and online news media (Forgione, 2011, Gardner, 2011, Marchione, 2011, Sheridan, 2011, Clarke, 2011, Swaine, 2011, Thomas-Peter, 2011).

Additionally, the awareness and understanding of ovarian cancer through the media has taken significant steps forward, with Irish media outlets reporting on medico-scientific developments in ovarian cancer with increased frequency (Beckford, 2011, McDonagh, 2011, Radowitz, 2011a, 2011b, Press Association, 2010).

It is clear that there is a significant and positive engagement between those involved in clinical research and the public. The public is becoming increasingly aware of developments in ovarian cancer and circulating tumour cells, with investigation into TCIPA likely to garner increased public dissemination and awareness with increased future research attention.

6.7 Conclusions

The field of tumour cell induced platelet aggregation research has several interests arising from the multi-factorial nature of the phenomenon. Common goals include determining the root of tumour associated thrombocytosis, the mechanisms underlying tumour cells' ability to induce platelet aggregation to their surface in the peripheral circulation and to determine the molecular basis of the increased metastatic ability observed to result from thrombocytotic/pro-thrombotic cancer states.

A retrospective investigation performed in this thesis revealed that tumour grade and levels of tumour-expressed PDGFB correlated with patient thrombocytosis in ovarian cancer. *In vitro* investigation determined that increased ovarian epithelial malignancy conveys an increased capacity for platelet aggregation/adhesion and activation. The effect of tumour cell induced platelet aggregation on the platelet cloaked cancer cell was documented for the first time, revealing a dynamic alteration of genes affecting many of the processes proposed to promote malignant progression. There is significant scope for continuation of this research, to further elaborate and characterise of the role and effect of TCIPA in ovarian cancer, before progressing to characterise the interaction and its influence on metastasising CTCs in other forms of cancer.

Circulating tumour cells have significance as prognostic indicators of cancer survival and as potential markers in disease management and surveillance in current state of the art diagnostic systems. The optimisation of these advanced systems to detect platelet cloaked CTCs, which may be of high metastatic potential arising from their 'molecular priming' due to their interaction with platelets, may lead to better clinically important representation of disease burden, thus guiding treatment and monitoring.

In conclusion, the research performed in the completion of this thesis fulfilled the aims set out at the beginning of the project, whilst generating novel and exciting results with potentially significant clinical relevance.

Bibliography

ACHEN, M. G., MANN, G. B. & STACKER, S. A. 2006. Targeting lymphangiogenesis to prevent tumour metastasis. *Br J Cancer,* 94**,** 1355-60.

ADAMI, H. O., HSIEH, C. C., LAMBE, M., TRICHOPOULOS, D., LEON, D., PERSSON, I., EKBOM, A. & JANSON, P. O. 1994. Parity, age at first childbirth, and risk of ovarian cancer. *Lancet,* 344**,** 1250-4.

ADAMS, N. C., TOMODA, T., COOPER, M., DIETZ, G. & HATTEN, M. E. 2002. Mice that lack astrotactin have slowed neuronal migration. *Development,* 129**,** 965-972.

ADERKA, D., BROWN, A., ZELIKOVSKI, A. & PINKHAS, J. 1986. Idiopathic deep vein thrombosis in an apparently healthy patient as a premonitory sign of occult cancer. *Cancer,* 57**,** 1846-9.

AGARWAL, N., TOCHIGI, Y., ADHIKARI, A. S., CUI, S., CUI, Y. & IWAKUMA, T. 2011. MTBP plays a crucial role in mitotic progression and chromosome segregation. *Cell Death Differ,* 18**,** 1208-1219.

AGGARWAL, P. & KEHOE, S. 2010. Serum tumour markers in gynaecological cancers. *Maturitas,* 67**,** 46-53.

AGUR, A. M. R. & DALLEY, A. F. 2009. *Grant's atlas of anatomy,* Philadelphia, Wolters Kluwer Health/Lippincott Williams & Wilkins.

AKASAKA, T., TAKAHASHI, N., SUZUKI, M., KOSEKI, H., BODMER, R. & KOGA, H. 2002. MBLR, a new RING finger protein resembling mammalian Polycomb gene products, is regulated by cell cycle-dependent phosphorylation. *Genes to cells : devoted to molecular & cellular mechanisms,* 7**,** 835-50.

AKTAS, B., KASIMIR-BAUER, S., HEUBNER, M., KIMMIG, R. & WIMBERGER, P. 2011. Molecular Profiling and Prognostic Relevance of Circulating Tumor Cells in the Blood of Ovarian Cancer Patients at Primary Diagnosis and After Platinum-Based Chemotherapy. *International Journal of Gynecological Cancer,* 21**,** 822-830 10.1097/IGC.0b013e318216cb91.

AL-AGHA, O. M. & BLAKE GILKS, C. 2011. High-Grade Serous Carcinoma Involving Fallopian Tube, Ovary and Peritoneum. *Surgical Pathology Clinics,* 4**,** 375-396.

ALETTI, G. D., GALLENBERG, M. M., CLIBY, W. A., JATOI, A. & HARTMANN, L. C. 2007. Current Management Strategies for Ovarian Cancer. *Mayo Clinic Proceedings,* 82**,** 751-770.

ALEXIOU, D., KARAYIANNAKIS, A. J., SYRIGOS, K. N., ZBAR, A., SEKARA, E., MICHAIL, P., ROSENBERG, T. & DIAMANTIS, T. 2003. Clinical Significance of Serum Levels of E-Selectin, Intercellular Adhesion Molecule-1, and Vascular Cell Adhesion Molecule-1 in Gastric Cancer Patients. *Am J Gastroenterol,* 98, 478-485.

ALLARD, W. J., MATERA, J., MILLER, M. C., REPOLLET, M., CONNELLY, M. C., RAO, C., TIBBE, A. G. J., UHR, J. W. & TERSTAPPEN, L. W. M. M. 2004. Tumor Cells Circulate in the Peripheral Blood of All Major Carcinomas but not in Healthy Subjects or Patients With Nonmalignant Diseases. *Clinical Cancer Research,* 10, 6897-6904.

ALONSO-ESCOLANO, D., MEDINA, C., CIESLIK, K., RADOMSKI, A., JURASZ, P., SANTOS-MARTINEZ, M. J., JIFFAR, T., RUVOLO, P. & RADOMSKI, M. W. 2006. Protein Kinase C{delta} Mediates Platelet-Induced Breast Cancer Cell Invasion. *J Pharmacol Exp Ther,* 318, 373-380.

ALONSO-ESCOLANO, D., STRONGIN, A. Y., CHUNG, A. W., DERYUGINA, E. I. & RADOMSKI, M. W. 2004a. Membrane type-1 matrix metalloproteinase stimulates tumour cell-induced platelet aggregation: role of receptor glycoproteins. *British Journal of Pharmacology,* 141, 241-52.

ALONSO-ESCOLANO, D., STRONGIN, A. Y., CHUNG, A. W., DERYUGINA, E. I. & RADOMSKI, M. W. 2004b. Membrane type-1 matrix metalloproteinase stimulates tumour cell-induced platelet aggregation: role of receptor glycoproteins. *Br J Pharmacol,* 141, 241-52.

ALTIERI, A., FRANCESCHI, S., FERLAY, J., SMITH, J. & VECCHIA, C. L. 2003. Epidemiology and aetiology of gestational trophoblastic diseases. *The Lancet Oncology,* 4, 670-678.

AMBION INC. 2004a. Assessing RNA Quality. *TechNotes* [Online], 11. Available: http://www.ambion.com/techlib/tn/111/8.html.

AMBION INC. 2004b. Determinants of RNA Integrity and Purity. *TechNotes* [Online], 11. Available: http://www.ambion.com/techlib/tn/112/10.html.

AMERICAN CANCER SOCIETY. 2010. Ovarian Cancer. Available: http://documents.cancer.org/acs/groups/cid/documents/webcontent/003130-pdf.pdf.

AMERICAN CANCER SOCIETY. 2011. Cancer Facts and Figures 2011. Available: http://www.cancer.org/acs/groups/content/@epidemiologysurveilance/documents/document/acspc-029771.pdf.

AMIRKHOSRAVI, A., MOUSA, S. A., AMAYA, M., BLAYDES, S., DESAI, H., MEYER, T. & FRANCIS, J. L. 2003. Inhibition of tumor cell-induced platelet aggregation and lung metastasis by the oral GpIIb/IIIa antagonist XV454. *Thrombosis and Haemostasis,* 90, 549-54.

AMIT, O., BUSHNELL, W., DODD, L., ROACH, N. & SARGENT, D. 2010. Blinded Independent Central Review of the Progression-Free Survival Endpoint. *Oncologist,* 15, 492-495.

ANDERBERG, C., LI, H., FREDRIKSSON, L., ANDRAE, J., BETSHOLTZ, C., LI, X., ERIKSSON, U. & PIETRAS, K. 2009. Paracrine signaling by platelet-derived growth factor-CC promotes tumor growth by recruitment of cancer-associated fibroblasts. *Cancer Research,* 69, 369-78.

ANDERSEN, O. M., BENHAYON, D., CURRAN, T. & WILLNOW, T. E. 2003. Differential Binding of Ligands to the Apolipoprotein E Receptor 2†. *Biochemistry,* 42, 9355-9364.

ANTONIADES, C., SHIRODARIA, C., VAN ASSCHE, T., CUNNINGTON, C., TEGEDER, I., LÖTSCH, J., GUZIK, T. J., LEESON, P., DIESCH, J., TOUSOULIS, D., STEFANADIS, C., COSTIGAN, M., WOOLF, C. J., ALP, N. J. & CHANNON, K. M. 2008. GCH1 Haplotype Determines Vascular and Plasma Biopterin Availability in Coronary Artery Disease: Effects on Vascular Superoxide Production and Endothelial Function. *Journal of the American College of Cardiology,* 52, 158-165.

ANTONIOU, A., PHAROAH, P. D., NAROD, S., RISCH, H. A., EYFJORD, J. E., HOPPER, J. L., LOMAN, N., OLSSON, H., JOHANNSSON, O., BORG, A., PASINI, B., RADICE, P., MANOUKIAN, S., ECCLES, D. M., TANG, N., OLAH, E., ANTON-CULVER, H., WARNER, E., LUBINSKI, J., GRONWALD, J., GORSKI, B., TULINIUS, H., THORLACIUS, S., EEROLA, H., NEVANLINNA, H., SYRJAKOSKI, K., KALLIONIEMI, O. P., THOMPSON, D., EVANS, C., PETO, J., LALLOO, F., EVANS, D. G. & EASTON, D. F. 2003. Average risks of breast and ovarian cancer associated with BRCA1 or BRCA2 mutations detected in case Series unselected for family history: a combined analysis of 22 studies. *American journal of human genetics,* 72, 1117-30.

ANTONIU, S. A. & KOLB, M. R. 2010. Intedanib, a triple kinase inhibitor of VEGFR, FGFR and PDGFR for the treatment of cancer and idiopathic pulmonary fibrosis. *IDrugs,* 13, 332-45.

AOE, K., HIRAKI, A., UEOKA, H., KIURA, K., TABATA, M., TANAKA, M. & TANIMOTO, M. 2004. Thrombocytosis as a Useful Prognostic Indicator in Patients with Lung Cancer. *Respiration,* 71, 170-173.

ARLT, A., MUERKOSTER, S. S. & SCHAFER, H. 2010. Targeting apoptosis pathways in pancreatic cancer. *Cancer Lett.*

ARNOLD, J. M., CUMMINGS, M., PURDIE, D. & CHENEVIX-TRENCH, G. 2001. Reduced expression of intercellular adhesion molecule-1 in ovarian adenocarcinomas. *Br J Cancer,* 85, 1351-1358.

ASHWORTH, T. 1869. A case of cancer in which cells similar to those in the tumours were seen in the blood after death. *Aus Med J,* 14, 146–149.

ATTIA, M., FÖRSTER, A., RACHEZ, C., FREEMONT, P., AVNER, P. & ROGNER, U. C. 2011. Interaction between Nucleosome Assembly Protein 1-like Family Members. *Journal of Molecular Biology,* 407, 647-660.

AVGERIS, M., MAVRIDIS, K. & SCORILAS, A. 2010. Kallikrein-related peptidase genes as promising biomarkers for prognosis and monitoring of human malignancies. *Biological Chemistry,* 391, 505-511.

AZUMA, T., YAO, S., ZHU, G., FLIES, A. S., FLIES, S. J. & CHEN, L. 2008. B7-H1 is a ubiquitous antiapoptotic receptor on cancer cells. *Blood,* 111, 3635-3643.

BACHELOT, T., RAY-COQUARD, I., MENETRIER-CAUX, C., RASTKHA, M., DUC, A. & BLAY, J. Y. 2003. Prognostic value of serum levels of interleukin 6 and of serum and plasma levels of vascular endothelial growth factor in hormone-refractory metastatic breast cancer patients. *Br J Cancer,* 88, 1721-6.

BALLABENI, A., MELIXETIAN, M., ZAMPONI, R., MASIERO, L., MARINONI, F. & HELIN, K. 2004. Human geminin promotes pre-RC formation and DNA replication by stabilizing CDT1 in mitosis. *EMBO J,* 23, 3122-32.

BAMBACE, N. M. & HOLMES, C. E. 2011. The platelet contribution to cancer progression. *J Thromb Haemost,* 9, 237-49.

BANI, M. R., NICOLETTI, M. I., ALKHAROUF, N. W., GHILARDI, C., PETERSEN, D., ERBA, E., SAUSVILLE, E. A., LIU, E. T. & GIAVAZZI, R. 2004. Gene expression correlating with response to paclitaxel in ovarian carcinoma xenografts. *Molecular Cancer Therapeutics,* 3, 111-121.

BANKS, R. E., GEARING, A. J., HEMINGWAY, I. K., NORFOLK, D. R., PERREN, T. J. & SELBY, P. J. 1993. Circulating intercellular adhesion molecule-1 (ICAM-1), E-selectin and vascular cell adhesion molecule-1 (VCAM-1) in human malignancies. *British Journal of Cancer,* 68, 122-4.

BAO, H., JIANG, M., ZHU, M., SHENG, F., RUAN, J. & RUAN, C. 2009. Overexpression of Annexin II affects the proliferation, apoptosis, invasion and production of proangiogenic factors in multiple myeloma. *International Journal of Hematology,* 90, 177-185.

BAR, I., TISSIR, F., LAMBERT DE ROUVROIT, C., DE BACKER, O. & GOFFINET, A. M. 2003. The Gene Encoding Disabled-1 (DAB1), the Intracellular Adaptor of the Reelin Pathway, Reveals Unusual Complexity in Human and Mouse. *Journal of Biological Chemistry,* 278, 5802-5812.

BARBERA-GUILLEM, E. & WEISS, L. 1993. Cancer-cell traffic in the liver. III Lethal deformation of B16 melanoma cells in liver sinusoids. *Int J Cancer,* 54, 880-4.

BAST, R. C., JR., BADGWELL, D., LU, Z., MARQUEZ, R., ROSEN, D., LIU, J., BAGGERLY, K. A., ATKINSON, E. N., SKATES, S., ZHANG, Z., LOKSHIN, A., MENON, U., JACOBS, I. & LU, K. 2005. New tumor markers: CA125 and beyond. *International journal of gynecological cancer : official journal of the International Gynecological Cancer Society,* 15 Suppl 3**,** 274-81.

BAST, R. C., THIGPEN, J. T., ARBUCK, S. G., BASEN-ENGQUIST, K., BURKE, L. B., FREEDMAN, R., HORNING, S. J., OZOLS, R., RUSTIN, G. J., SPRIGGS, D., WENZEL, L. B. & PAZDUR, R. 2007. Clinical trial endpoints in ovarian cancer: report of an FDA/ASCO/AACR Public Workshop. *Gynecol Oncol,* 107**,** 173-6.

BASTIDA, E., ORDINAS, A., GIARDINA, S. L. & JAMIESON, G. A. 1982. Differentiation of platelet-aggregating effects of human tumor cell lines based on inhibition studies with apyrase, hirudin, and phospholipase. *Cancer Research,* 42**,** 4348-52.

BATTINELLI, E. M., MARKENS, B. A. & ITALIANO, J. E. 2011. Release of angiogenesis regulatory proteins from platelet alpha granules: modulation of physiologic and pathologic angiogenesis. *Blood,* 118**,** 1359-1369.

BAUER, M., AUST, G. & SCHUMACHER, U. 2004. Different transcriptional expression of KIAA1324 and its splicing variants in human carcinoma cell lines with different metastatic capacity. *Oncol Rep,* 11**,** 677-80.

BAYANI, J., MARRANO, P., GRAHAM, C., ZHENG, Y., LI, L., KATSAROS, D., LASSUS, H., BUTZOW, R., SQUIRE, J. A. & DIAMANDIS, E. P. 2011. Genomic instability and copy-number heterogeneity of chromosome 19q, including the kallikrein locus, in ovarian carcinomas. *Molecular oncology,* 5**,** 48-60.

BAYFIELD, M. A., YANG, R. & MARAIA, R. J. 2010. Conserved and divergent features of the structure and function of La and La-related proteins (LARPs). *Biochimica et biophysica acta,* 1799**,** 365-78.

BAZOU, D., SANTOS-MARTINEZ, M. J., MEDINA, C. & RADOMSKI, M. W. 2011. Elucidation of flow-mediated tumour cell-induced platelet aggregation using an ultrasound standing wave trap. *British Journal of Pharmacology,* 162**,** 1577-1589.

BECKFORD, M. 2011. Women at risk of cancer 'should have ovaries removed. *The Irish Independent*, 06/09/2011.

BELISLE, J. A., GUBBELS, J. A., RAPHAEL, C. A., MIGNEAULT, M., RANCOURT, C., CONNOR, J. P. & PATANKAR, M. S. 2007. Peritoneal natural killer cells from epithelial ovarian cancer patients show an altered phenotype and bind to the tumour marker MUC16 (CA125). *Immunology,* 122**,** 418-29.

BELISLE, J. A., HORIBATA, S., JENNIFER, G. A., PETRIE, S., KAPUR, A., ANDRE, S., GABIUS, H. J., RANCOURT, C., CONNOR, J., PAULSON, J. C. & PATANKAR, M. S. 2010.

Identification of Siglec-9 as the receptor for MUC16 on human NK cells, B cells, and monocytes. *Mol Cancer,* 9, 118.

BELL, D. A. 2005. Origins and molecular pathology of ovarian cancer. *Mod Pathol,* 18, S19-S32.

BENEDET, J. L., PECORELLI, S., NAGAN, H. Y. & HACKER, N. F. 2006. *Staging Classifications and Clinical Practice Guidelines for Gynaecological Cancers,* International Federation of Gynecology & Obstetrics.

BENEDETTI, E., GALZIO, R., LAURENTI, G., D'ANGELO, B., MELCHIORRE, E., CIFONE, M. G., FANELLI, F., MUZI, P., COLETTI, G., ALECCI, M., SOTGIU, A., CERU, M. P. & CIMINI, A. 2010. Lipid metabolism impairment in human gliomas: expression of peroxisomal proteins in human gliomas at different grades of malignancy. *International journal of immunopathology and pharmacology,* 23, 235-46.

BENJAMINI, Y. & HOCHBERG, Y. 1995. Controlling the False Discovery Rate: A Practical and Powerful Approach to Multiple Testing. *Journal of the Royal Statistical Society. Series B (Methodological),* 57, 289-300.

BENOY, I., SALGADO, R., COLPAERT, C., WEYTJENS, R., VERMEULEN, P. & DIRIX, L. 2002. Serum Interleukin 6, Plasma VEGF, Serum VEGF, and VEGF Platelet Load in Breast Cancer Patients. *Clinical Breast Cancer,* 2, 311-315.

BENSALAH, K., LERAY, E., FERGELOT, P., RIOUX-LECLERCQ, N., TOSTAIN, J., GUILLE, F. & PATARD, J. J. 2006. Prognostic value of thrombocytosis in renal cell carcinoma. *The Journal of urology,* 175, 859-63.

BERAL, V. 2007. Ovarian cancer and hormone replacement therapy in the Million Women Study. *The Lancet,* 369, 1703-1710.

BERAL, V., DOLL, R., HERMON, C., PETO, R. & REEVES, G. 2008. Ovarian cancer and oral contraceptives: collaborative reanalysis of data from 45 epidemiological studies including 23,257 women with ovarian cancer and 87,303 controls. *Lancet,* 371, 303-14.

BERG, M. & SOREIDE, K. 2011. Prevention: Will an aspirin a day keep the colorectal cancer away? *Nat Rev Clin Oncol,* 8, 130-131.

BERGLUND, L., BJORLING, E., OKSVOLD, P., FAGERBERG, L., ASPLUND, A., SZIGYARTO, C. A., PERSSON, A., OTTOSSON, J., WERNERUS, H., NILSSON, P., LUNDBERG, E., SIVERTSSON, A., NAVANI, S., WESTER, K., KAMPF, C., HOBER, S., PONTEN, F. & UHLEN, M. 2008. A genecentric Human Protein Atlas for expression profiles based on antibodies. *Mol Cell Proteomics,* 7, 2019-27.

BERGQVIST, D., CAPRINI, J. A., DOTSENKO, O., KAKKAR, A. K., MISHRA, R. G. & WAKEFIELD, T. W. 2007. Venous Thromboembolism and Cancer. *Current Problems in Surgery,* 44, 157-216.

BERGSTEN, E., UUTELA, M., LI, X., PIETRAS, K., OSTMAN, A., HELDIN, C.-H., ALITALO, K. & ERIKSSON, U. 2001. PDGF-D is a specific, protease-activated ligand for the PDGF [beta]-receptor. *Nat Cell Biol,* 3, 512-516.

BERNE, R. M. 2004. *Physiology,* St. Louis, Mo., Mosby.

BERRINO, F., DE ANGELIS, R., SANT, M., ROSSO, S., BIELSKA-LASOTA, M., COEBERGH, J. W. & SANTAQUILANI, M. 2007. Survival for eight major cancers and all cancers combined for European adults diagnosed in 1995-99: results of the EUROCARE-4 study. *Lancet Oncol,* 8, 773-83.

BERTRAND, M. J. M., MILUTINOVIC, S., DICKSON, K. M., HO, W. C., BOUDREAULT, A., DURKIN, J., GILLARD, J. W., JAQUITH, J. B., MORRIS, S. J. & BARKER, P. A. 2008. cIAP1 and cIAP2 Facilitate Cancer Cell Survival by Functioning as E3 Ligases that Promote RIP1 Ubiquitination. *Molecular cell,* 30, 689-700.

BEYAN, C., KAPTAN, K., IFRAN, A., SAVASCI, S., OZTURK, Y. & OKMEN, B. 2006. Effect of sex difference on platelet aggregation using an optical method in healthy subjects. *Clin Lab Haematol,* 28, 14-6.

BHARADWAJ, R. & YU, H. 2004. The spindle checkpoint, aneuploidy, and cancer. *Oncogene,* 23, 2016-2027.

BIAGI, J. J., OZA, A. M., CHALCHAL, H. I., GRIMSHAW, R., ELLARD, S. L., LEE, U., HIRTE, H., SEDERIAS, J., IVY, S. P. & EISENHAUER, E. A. 2011. A phase II study of sunitinib in patients with recurrent epithelial ovarian and primary peritoneal carcinoma: an NCIC Clinical Trials Group Study. *Annals of oncology : official journal of the European Society for Medical Oncology / ESMO,* 22, 335-40.

BIEWENGA, P., BUIST, M. R., MOERLAND, P. D., VAN THEMAAT, E. V. L., VAN KAMPEN, A. H. C., TEN KATE, F. J. W. & BAAS, F. 2008. Gene expression in early stage cervical cancer. *Gynecologic Oncology,* 108, 520-526.

BIGGERSTAFF, J. P., WEIDOW, B., VIDOSH, J., DEXHEIMER, J., PATEL, S. & PATEL, P. 2006. Soluble fibrin inhibits monocyte adherence and cytotoxicity against tumor cells: implications for cancer metastasis. *Thrombosis journal,* 4, 12.

BILLIE AU, P. Y., MARTIN, N., CHAU, H., MOEMENI, B., CHIA, M., LIU, F.-F., MINDEN, M. & YEH, W.-C. 2005. The oncogene PDGF-B provides a key switch from cell death to survival induced by TNF. 24, 3196-3205.

BINGLE, L., BROWN, N. J. & LEWIS, C. E. 2002. The role of tumour-associated macrophages in tumour progression: implications for new anticancer therapies. *The Journal of Pathology,* 196**,** 254-265.

BLANK, C., GAJEWSKI, T. F. & MACKENSEN, A. 2005. Interaction of PD-L1 on tumor cells with PD-1 on tumor-specific T cells as a mechanism of immune evasion: implications for tumor immunotherapy. *Cancer Immunology, Immunotherapy,* 54**,** 307-314.

BOARD, R. & JAYSON, G. C. 2005. Platelet-derived growth factor receptor (PDGFR): a target for anticancer therapeutics. *Drug Resist Updat,* 8**,** 75-83.

BOEHRINGER-INGELHEIM. 2009. *Lume Clinical Trial Programme: AGO-OVAR 12 / LUME-Ovar 1* [Online]. Ingelheim am Rhein, Germany Boehringer Ingelheim. Available: http://www.inoncology.com/content/dam/internet/opu/oncology/com_EN/documents/LUME_OVAR.pdf.

BOERO, S., SILVESTRI, M., ULLMANN, N. & ROSSI, G. A. 2010. Modulation by flunisolide of tumor necrosis factor-alpha-induced stimulation of airway epithelial cell activities related to eosinophil inflammation. *The Journal of asthma : official journal of the Association for the Care of Asthma,* 47**,** 381-7.

BONIFACINO, J. S. & ROJAS, R. 2006. Retrograde transport from endosomes to the trans-Golgi network. *Nat Rev Mol Cell Biol,* 7**,** 568-579.

BORSIG, L., WONG, R., FERAMISCO, J., NADEAU, D. R., VARKI, N. M. & VARKI, A. 2001. Heparin and cancer revisited: mechanistic connections involving platelets, P-selectin, carcinoma mucins, and tumor metastasis. *Proceedings of the National Academy of Sciences of the United States of America,* 98**,** 3352-7.

BORSIG, L., WONG, R., HYNES, R. O., VARKI, N. M. & VARKI, A. 2002. Synergistic effects of L- and P-selectin in facilitating tumor metastasis can involve non-mucin ligands and implicate leukocytes as enhancers of metastasis. *Proc Natl Acad Sci U S A,* 99**,** 2193-8.

BOUANENE, H. & MILED, A. 2010. Conflicting views on the molecular structure of the cancer antigen CA125/MUC16. *Disease Markers,* 28**,** 385-394.

BOYD, S., VIROLAINEN, S., PÄRSSINEN, J., SKOOG, T., VAN HOGERLINDEN, M., LATONEN, L., KYLLÖNEN, L., TOFTGARD, R. & SAARIALHO-KERE, U. 2009. MMP-10 (Stromelysin-2) and MMP-21 in human and murine squamous cell cancer. *Experimental Dermatology,* 18**,** 1044-1052.

BOYLE, P., LEVIN, B., INTERNATIONAL AGENCY FOR RESEARCH ON CANCER. & WORLD HEALTH ORGANIZATION. 2008. *World cancer report 2008,* Lyon
Geneva, International Agency for Research on Cancer ;
Distributed by WHO Press.

BOZKURT, N., YUCE, K., BASARAN, M., KOSE, F. & AYHAN, A. 2004. Correlation of platelet count with second-look laparotomy results and disease progression in patients with advanced epithelial ovarian cancer. *Obstet Gynecol,* 103, 82-5.

BRAN, B., BRAN, G., HORMANN, K. & RIEDEL, F. 2009. The platelet-derived growth factor receptor as a target for vascular endothelial growth factor-mediated anti-angiogenetic therapy in head and neck cancer. *Int J Oncol,* 34, 255-61.

BREWER, D. B. 2006. Max Schultze (1865), G. Bizzozero (1882) and the discovery of the platelet. *British Journal of Haematology,* 133, 251-258.

BROWN, L. A., KALLOGER, S. E., MILLER, M. A., SHIH, I.-M., MCKINNEY, S. E., SANTOS, J. L., SWENERTON, K., SPELLMAN, P. T., GRAY, J., GILKS, C. B. & HUNTSMAN, D. G. 2008. Amplification of 11q13 in ovarian carcinoma. *Genes, Chromosomes and Cancer,* 47, 481-489.

BROWN, M. R., BLANCHETTE, J. O. & KOHN, E. C. 2000. Angiogenesis in ovarian cancer. *Baillieres Best Pract Res Clin Obstet Gynaecol,* 14, 901-18.

BUCHYNSKA, L. G., NESINA, I. P., YURCHENKO, N. P., BILYK, O. O., GRINKEVYCH, V. N. & SVINTITSKY, V. S. 2007. Expression of p53, p21WAF1/CIP1, p16INK4A and Ki-67 proteins in serous ovarian tumors. *Experimental oncology,* 29, 49-53.

BUDD, G. T., CRISTOFANILLI, M., ELLIS, M. J., STOPECK, A., BORDEN, E., MILLER, M. C., MATERA, J., REPOLLET, M., DOYLE, G. V., TERSTAPPEN, L. W. M. M. & HAYES, D. F. 2006. Circulating Tumor Cells versus Imaging—Predicting Overall Survival in Metastatic Breast Cancer. *Clinical Cancer Research,* 12, 6403-6409.

BURGER, R. A. 2011. Overview of anti-angiogenic agents in development for ovarian cancer. *Gynecol Oncol,* 121, 230-8.

BUYSE, M., QUINAUX, E., HENDLISZ, A., GOLFINOPOULOS, V., TOURNIGAND, C. & MICK, R. 2011. Progression-Free Survival Ratio As End Point for Phase II Trials in Advanced Solid Tumors. *Journal of Clinical Oncology.*

BUYSE, M., SARGENT, D. J., GROTHEY, A., MATHESON, A. & DE GRAMONT, A. 2010. Biomarkers and surrogate end points - the challenge of statistical validation. *Nat Rev Clin Oncol,* 7, 309-317.

CAINE, G. J., STONELAKE, P. S., REA, D. & LIP, G. Y. 2003. Coagulopathic complications in breast cancer. *Cancer,* 98, 1578-86.

CAMERER, E., QAZI, A. A., DUONG, D. N., CORNELISSEN, I., ADVINCULA, R. & COUGHLIN, S. R. 2004. Platelets, protease-activated receptors, and fibrinogen in hematogenous metastasis. *Blood,* 104, 397-401.

CAMPEAU, P. M., FOULKES, W. D. & TISCHKOWITZ, M. D. 2008. Hereditary breast cancer: new genetic developments, new therapeutic avenues. *Human genetics,* 124**,** 31-42.

CANNISTRA, S. A., MATULONIS, U. A., PENSON, R. T., HAMBLETON, J., DUPONT, J., MACKEY, H., DOUGLAS, J., BURGER, R. A., ARMSTRONG, D., WENHAM, R. & MCGUIRE, W. 2007. Phase II study of bevacizumab in patients with platinum-resistant ovarian cancer or peritoneal serous cancer. *Journal of clinical oncology : official journal of the American Society of Clinical Oncology,* 25**,** 5180-6.

CAO, R., BRAKENHEILM, E., LI, X., PIETRAS, K., WIDENFALK, J., ÖSTMAN, A., ERIKSSON, U. & CAO, Y. 2002. Angiogenesis stimulated by PDGF-CC, a novel member in the PDGF family, involves activation of PDGFR-αα and -αß receptors. *The FASEB Journal,* 16**,** 1575-1583.

CAZZOLA, M. 2008. Molecular basis of thrombocytosis. *Haematologica,* 93**,** 646-8.

CENTRAL STATISTICS OFFICE (IRELAND) 2012. *This is Ireland : highlights from Census 2011, part 1,* Dublin, Stationery Office.

CERESA, I. F., NORIS, P., AMBAGLIO, C., PECCI, A. & BALDUINI, C. L. 2007. Thrombopoietin is not uniquely responsible for thrombocytosis in inflammatory disorders. *Platelets,* 18**,** 579 - 582.

CERULLO, V., PESONEN, S., DIACONU, I., ESCUTENAIRE, S., ARSTILA, P. T., UGOLINI, M., NOKISALMI, P., RAKI, M., LAASONEN, L., SÄRKIOJA, M., RAJECKI, M., KANGASNIEMI, L., GUSE, K., HELMINEN, A., AHTIAINEN, L., RISTIMÄKI, A., RÄISÄNEN-SOKOLOWSKI, A., HAAVISTO, E., OKSANEN, M., KARLI, E., KARIOJA-KALLIO, A., HOLM, S.-L., KOURI, M., JOENSUU, T., KANERVA, A. & HEMMINKI, A. 2010. Oncolytic Adenovirus Coding for Granulocyte Macrophage Colony-Stimulating Factor Induces Antitumoral Immunity in Cancer Patients. *Cancer Research,* 70**,** 4297-4309.

CHAMBERS, S. K., IVINS, C. M. & CARCANGIU, M. L. 1997. Expression of plasminogen activator inhibitor-2 in epithelial ovarian cancer: A favorable prognostic factor related to the actions of CSF-1. *International Journal of Cancer,* 74**,** 571-575.

CHAN, D. W., SHIH, I.-M., SOKOLL, L. J. & ROBERT C BAST, J. 2007. National Academy of Clinical Biochemistry Guidelines for the Use of Tumor Markers in Ovarian Cancer. *In:* DIAMANDIS, E. P., STURGEON, C. & HOFFMAN, B. (eds.) *NACB: Practice Guidelines And Recommendations For Use Of Tumor Markers In The Clinic.*

CHAN, J. K., CHEUNG, M. K., HUSAIN, A., TENG, N. N., WEST, D., WHITTEMORE, A. S., BEREK, J. S. & OSANN, K. 2006. Patterns and Progress in Ovarian Cancer Over 14 Years. *Obstet Gynecol,* 108**,** 521-528.

CHAN, J. K., TEOH, D., HU, J. M., SHIN, J. Y., OSANN, K. & KAPP, D. S. 2008. Do clear cell ovarian carcinomas have poorer prognosis compared to other epithelial cell types? A study of 1411 clear cell ovarian cancers. *Gynecologic Oncology,* 109, 370-376.

CHANDLER, L. A., SOSNOWSKI, B. A., MCDONALD, J. R., PRICE, J. E., AUKERMAN, S. L., BAIRD, A., PIERCE, G. F. & HOUSTON, L. L. 1998. Targeting tumor cells via EGF receptors: Selective toxicity of an HBEGF-toxin fusion protein. *International Journal of Cancer,* 78, 106-111.

CHANG, M. C., CHAN, C. P., HO, Y. S., LEE, J. J., LIN, P. S., LIN, B. R., HUANG, Y. L., HAHN, L. J., YEH, H. W., WANG, Y. J. & JENG, J. H. 2009. Signaling pathways for induction of platelet aggregation by SAS tongue cancer cells--a mechanism of hematogenous metastasis. *Journal of oral pathology & medicine : official publication of the International Association of Oral Pathologists and the American Academy of Oral Pathology,* 38, 434-40.

CHANGSIRIKULCHAI, S., HUDKINS, K. L., GOODPASTER, T. A., VOLPONE, J., TOPOUZIS, S., GILBERTSON, D. G. & ALPERS, C. E. 2002. Platelet-derived growth factor-D expression in developing and mature human kidneys. *Kidney Int,* 62, 2043-2054.

CHATELAIS, M., DEVALLIÈRE, J., GALLI, C. & CHARREAU, B. 2011. Gene transfer of the adaptor Lnk (SH2B3) prevents porcine endothelial cell activation and apoptosis: implication for xenograft's cytoprotection. *Xenotransplantation,* 18, 108-120.

CHATTERJEE, M., HUANG, Z., ZHANG, W., JIANG, L., HULTENBY, K., ZHU, L., HU, H., NILSSON, G. P. & LI, N. 2011. Distinct platelet packaging, release, and surface expression of proangiogenic and antiangiogenic factors on different platelet stimuli. *Blood,* 117, 3907-11.

CHAW, Y. F., CRANE, L. E., LANGE, P. & SHAPIRO, R. 1980. Isolation and identification of cross-links from formaldehyde-treated nucleic acids. *Biochemistry,* 19, 5525-31.

CHELVATHEEBAM, S., LANGABEER, S. E., HILLS, R. K., GREENWELL, P. & LINCH, D. C. 2003. Incidence and prognostic significance of C-MPL expression in acute myeloid leukemia. *Leukemia Research,* 27, 869-870.

CHEN, J. & LOPEZ, J. A. 2005. Interactions of platelets with subendothelium and endothelium. *Microcirculation,* 12, 235-46.

CHEN, L.-C., CHEN, C.-C., LIANG, Y., TSANG, N.-M., CHANG, Y.-S. & HSUEH, C. 2011. A novel role for TNFAIP2: its correlation with invasion and metastasis in nasopharyngeal carcinoma. *Mod Pathol,* 24, 175-184.

CHIANG, C. L.-L., KANDALAFT, L. E. & COUKOS, G. 2011. Adjuvants for Enhancing the Immunogenicity of Whole Tumor Cell Vaccines. *International Reviews of Immunology,* 30, 150-182.

CHIANG, H. S., SWAIM, M. W. & HUANG, T. F. 1994. Characterization of platelet aggregation induced by human colon adenocarcinoma cells and its inhibition by snake venom peptides, trigramin and rhodostomin. *British Journal of Haematology,* 87, 325-31.

CHIANG, H. S., SWAIM, M. W. & HUANG, T. F. 1995. Characterization of platelet aggregation induced by human breast carcinoma and its inhibition by snake venom peptides, trigramin and rhodostomin. *Breast cancer research and treatment,* 33, 225-35.

CHO, S., KIM, J. H., BACK, S. H. & JANG, S. K. 2005. Polypyrimidine tract-binding protein enhances the internal ribosomal entry site-dependent translation of p27Kip1 mRNA and modulates transition from G1 to S phase. *Molecular and cellular biology,* 25, 1283-97.

CHOI, S. Y., GONZALVEZ, F., JENKINS, G. M., SLOMIANNY, C., CHRETIEN, D., ARNOULT, D., PETIT, P. X. & FROHMAN, M. A. 2007. Cardiolipin deficiency releases cytochrome c from the inner mitochondrial membrane and accelerates stimuli-elicited apoptosis. *Cell Death Differ,* 14, 597-606.

CHOI, Y. E., BUTTERWORTH, M., MALLADI, S., DUCKETT, C. S., COHEN, G. M. & BRATTON, S. B. 2009. The E3 ubiquitin ligase cIAP1 binds and ubiquitinates caspase-3 and -7 via unique mechanisms at distinct steps in their processing. *The Journal of biological chemistry,* 284, 12772-82.

CHOMYN, A. 2001. Mitochondrial Genetic Control of Assembly and Function of Complex I in Mammalian Cells. *Journal of Bioenergetics and Biomembranes,* 33, 251-257.

CHON, H., VASSILEV, A., DEPAMPHILIS, M. L., ZHAO, Y., ZHANG, J., BURGERS, P. M., CROUCH, R. J. & CERRITELLI, S. M. 2009. Contributions of the two accessory subunits, RNASEH2B and RNASEH2C, to the activity and properties of the human RNase H2 complex. *Nucleic acids research,* 37, 96-110.

CHOUDHARY, S., FASIH, N., INNES, M. M. & MARGINEAN, C. 2009. Imaging of ovarian teratomas: Appearances and complications. *Journal of Medical Imaging and Radiation Oncology,* 53, 480-488.

CHU, S., ALEXIADIS, M. & FULLER, P. J. 2008. Expression, mutational analysis and in vitro response of imatinib mesylate and nilotinib target genes in ovarian granulosa cell tumors. *Gynecologic Oncology,* 108, 182-190.

CIBULA, D., GOMPEL, A., MUECK, A. O., LA VECCHIA, C., HANNAFORD, P. C., SKOUBY, S. O., ZIKAN, M. & DUSEK, L. 2010. Hormonal contraception and risk of cancer. *Human Reproduction Update,* 16, 631-650.

CIBULA, D., WIDSCHWENDTER, M., MÁJEK, O. & DUSEK, L. 2011a. Tubal ligation and the risk of ovarian cancer: review and meta-analysis. *Human Reproduction Update,* 17, 55-67.

CIBULA, D., ZIKAN, M., DUSEK, L. & MAJEK, O. 2011b. Oral contraceptives and risk of ovarian and breast cancers in BRCA mutation carriers: a meta-analysis. *Expert Review of Anticancer Therapy,* 11, 1197-1207.

CLAESSON-WELSH, L. 1996. Mechanism of action of platelet-derived growth factor. *The International Journal of Biochemistry & Cell Biology,* 28, 373-385.

CLARK, T. A., SCHWEITZER, A. C., CHEN, T. X., STAPLES, M. K., LU, G., WANG, H., WILLIAMS, A. & BLUME, J. E. 2007. Discovery of tissue-specific exons using comprehensive human exon microarrays. *Genome biology,* 8, R64.

CLARKE, T., STEENHUYSEN, J. 2011. *J&J pushes ahead with "liquid biopsy" research* [Online]. Thomson Reuters. Available: http://www.reuters.com/article/2011/01/03/jj-idUSN0318321220110103 [Accessed 5 January 2011].

COHEN, S. A., TRIKHA, M. & MASCELLI, M. A. 2000. Potential future clinical applications for the GPIIb/IIIa antagonist, abciximab in thrombosis, vascular and oncological indications. *Pathol Oncol Res,* 6, 163-174.

COHEN, S. J., PUNT, C. J. A., IANNOTTI, N., SAIDMAN, B. H., SABBATH, K. D., GABRAIL, N. Y., PICUS, J., MORSE, M., MITCHELL, E., MILLER, M. C., DOYLE, G. V., TISSING, H., TERSTAPPEN, L. W. M. M. & MEROPOL, N. J. 2008. Relationship of Circulating Tumor Cells to Tumor Response, Progression-Free Survival, and Overall Survival in Patients With Metastatic Colorectal Cancer. *Journal of Clinical Oncology,* 26, 3213-3221.

COLLINS, B. M., NORWOOD, S. J., KERR, M. C., MAHONY, D., SEAMAN, M. N. J., TEASDALE, R. D. & OWEN, D. J. 2008. Structure of Vps26B and Mapping of its Interaction with the Retromer Protein Complex. *Traffic,* 9, 366-379.

COLOMBO, P., YON, J. & FRIED, M. 1991. The organization and expression of the human L7a ribosomal protein gene. *Biochimica et biophysica acta,* 1129, 93-5.

CONAWAY, R. C., SATO, S., TOMOMORI-SATO, C., YAO, T. & CONAWAY, J. W. 2005. The mammalian Mediator complex and its role in transcriptional regulation. *Trends in Biochemical Sciences,* 30, 250-255.

CONTI, A., AGEUNNOUZ, M., LA TORRE, D., CARDALI, S., ANGILERI, F. F., BUEMI, C., TOMASELLO, C., IACOPINO, D. G., D'AVELLA, D., VITA, G. & TOMASELLO, F. 2005. Expression of the tumor necrosis factor receptor-associated factors 1 and 2 and regulation of the nuclear factor-kappaB antiapoptotic activity in human gliomas. *Journal of neurosurgery,* 103, 873-81.

COOPER, N., QUINN, M. J., RACHET, B., MITRY, E. & COLEMAN, M. P. 2008. Survival from cancer of the ovary in England and Wales up to 2001. *Br J Cancer,* 99 Suppl 1, S70-2.

COPPINGER, J. A., CAGNEY, G., TOOMEY, S., KISLINGER, T., BELTON, O., MCREDMOND, J. P., CAHILL, D. J., EMILI, A., FITZGERALD, D. J. & MAGUIRE, P. B. 2004. Characterization of the proteins released from activated platelets leads to localization of novel platelet proteins in human atherosclerotic lesions. *Blood,* 103, 2096-2104.

COPPINGER, J. A., O'CONNOR, R., WYNNE, K., FLANAGAN, M., SULLIVAN, M., MAGUIRE, P. B., FITZGERALD, D. J. & CAGNEY, G. 2007. Moderation of the platelet releasate response by aspirin. *Blood,* 109, 4786-92.

COWARD, J., KULBE, H., CHAKRAVARTY, P., LEADER, D. A., VASSILEVA, V., LEINSTER, D. A., THOMPSON, R., SCHIOPPA, T., NEMETH, J. A., VERMEULIN, J., SINGH, N., AVRIL, N. E., CUMMINGS, J., REXHEPAJ, E., JIRSTROM, K., GALLAGHER, W. M., BRENNAN, D. J., MCNEISH, I. A. & BALKWILL, F. R. 2011. Interleukin-6 as a therapeutic target in human ovarian cancer. *Clinical Cancer Research.*

CRASTA, J. A., PREMLATHA, T. S., KRISHNAN, S. M., VALLIKAD, E. & RAMESHKUMAR, K. 2010. Significance of preoperative thrombocytosis in epithelial ovarian cancer. *Indian J Pathol Microbiol,* 53, 54-6.

CRISTOFANILLI, M., BUDD, G. T., ELLIS, M. J., STOPECK, A., MATERA, J., MILLER, M. C., REUBEN, J. M., DOYLE, G. V., ALLARD, W. J., TERSTAPPEN, L. W. M. M. & HAYES, D. F. 2004. Circulating Tumor Cells, Disease Progression, and Survival in Metastatic Breast Cancer. *New England Journal of Medicine,* 351, 781-791.

CRONIN, M., PHO, M., DUTTA, D., STEPHANS, J. C., SHAK, S., KIEFER, M. C., ESTEBAN, J. M. & BAKER, J. B. 2004. Measurement of gene expression in archival paraffin-embedded tissues: development and performance of a 92-gene reverse transcriptase-polymerase chain reaction assay. *Am J Pathol,* 164, 35-42.

CROUCHER, D. R., SAUNDERS, D. N., LOBOV, S. & RANSON, M. 2008. Revisiting the biological roles of PAI2 (SERPINB2) in cancer. *Nat Rev Cancer,* 8, 535-545.

CROW, Y. J., LEITCH, A., HAYWARD, B. E., GARNER, A., PARMAR, R., GRIFFITH, E., ALI, M., SEMPLE, C., AICARDI, J., BABUL-HIRJI, R., BAUMANN, C., BAXTER, P., BERTINI, E., CHANDLER, K. E., CHITAYAT, D., CAU, D., DERY, C., FAZZI, E., GOIZET, C., KING, M. D., KLEPPER, J., LACOMBE, D., LANZI, G., LYALL, H., MARTINEZ-FRIAS, M. L., MATHIEU, M., MCKEOWN, C., MONIER, A., OADE, Y., QUARRELL, O. W., RITTEY, C. D., ROGERS, R. C., SANCHIS, A., STEPHENSON, J. B., TACKE, U., TILL, M., TOLMIE, J. L., TOMLIN, P., VOIT, T., WESCHKE, B., WOODS, C. G., LEBON, P., BONTHRON, D. T., PONTING, C. P. & JACKSON, A. P. 2006. Mutations in genes encoding ribonuclease H2 subunits cause Aicardi-Goutieres syndrome and mimic congenital viral brain infection. *Nature genetics,* 38, 910-6.

CRUM, C. P., DRAPKIN, R., MIRON, A., INCE, T. A., MUTO, M., KINDELBERGER, D. W. & LEE, Y. 2007. The distal fallopian tube: a new model for pelvic serous carcinogenesis. *Current Opinion in Obstetrics and Gynecology,* 19, 3-9 10.1097/GCO.0b013e328011a21f.

CURIEL-LEWANDROWSKI, C., NIJSTEN, T., GOMEZ, M. L., HOLLESTEIN, L. M., ATKINS, M. B. & STERN, R. S. 2011. Long-Term Use of Nonsteroidal Anti-inflammatory Drugs Decreases the Risk of Cutaneous Melanoma: Results of a United States Case-Control Study. *J Invest Dermatol,* 131, 1460-1468.

CUSCHIERI, K. & WENTZENSEN, N. 2008. Human Papillomavirus mRNA and p16 Detection as Biomarkers for the Improved Diagnosis of Cervical Neoplasia. *Cancer Epidemiology Biomarkers & Prevention,* 17, 2536-2545.

CZARNECKA, A. M., CZARNECKI, J. S., KUKWA, W., CAPPELLO, F., SCINSKA, A. & KUKWA, A. 2010. Molecular oncology focus - is carcinogenesis a 'mitochondriopathy'? *Journal of biomedical science,* 17, 31.

D'ANDREA, A. D. & GROMPE, M. 2003. The Fanconi anaemia/BRCA pathway. *Nature reviews. Cancer,* 3, 23-34.

DABROW, M. B., FRANCESCO, M. R., MCBREARTY, F. X. & CARADONNA, S. 1998. The effects of platelet-derived growth factor and receptor on normal and neoplastic human ovarian surface epithelium. *Gynecol Oncol,* 71, 29-37.

DAHL, R., BRAVO, Y., SHARMA, V., ICHIKAWA, M., DHANYA, R. P., HEDRICK, M., BROWN, B., RASCON, J., VICCHIARELLI, M., MANGRAVITA-NOVO, A., YANG, L., STONICH, D., SU, Y., SMITH, L. H., SERGIENKO, E., FREEZE, H. H. & COSFORD, N. D. 2011. Potent, selective, and orally available benzoisothiazolone phosphomannose isomerase inhibitors as probes for congenital disorder of glycosylation Ia. *Journal of medicinal chemistry,* 54, 3661-8.

DALY, M. E. 2011. Determinants of platelet count in humans. *Haematologica,* 96, 10-13.

DAPSON, R. 2007. Macromolecular changes caused by formalin fixation and antigen retrieval. *Biotechnic & Histochemistry,* 82, 133-140.

DASS, K., AHMAD, A., AZMI, A. S., SARKAR, S. H. & SARKAR, F. H. 2008. Evolving role of uPA/uPAR system in human cancers. *Cancer treatment reviews,* 34, 122-136.

DAVIDSON, B., HADAR, R., STAVNES, H. T., TROPE, C. G. & REICH, R. 2009. Expression of the peroxisome proliferator-activated receptors-alpha, -beta, and -gamma in ovarian carcinoma effusions is associated with poor chemoresponse and shorter survival. *Human pathology,* 40, 705-13.

DE BONO, J. S., SCHER, H. I., MONTGOMERY, R. B., PARKER, C., MILLER, M. C., TISSING, H., DOYLE, G. V., TERSTAPPEN, L. W. W. M., PIENTA, K. J. & RAGHAVAN, D. 2008.

Circulating Tumor Cells Predict Survival Benefit from Treatment in Metastatic Castration-Resistant Prostate Cancer. *Clinical Cancer Research,* 14, 6302-6309.

DEGUCHI, K., INOUE, K., AVILA, W. E., LOPEZ-TERRADA, D., ANTALFFY, B. A., QUATTROCCHI, C. C., SHELDON, M., MIKOSHIBA, K., D'ARCANGELO, G. & ARMSTRONG, D. L. 2003. Reelin and disabled-1 expression in developing and mature human cortical neurons. *Journal of neuropathology and experimental neurology,* 62, 676-84.

DENG, L., BROADDUS, R. R., MCCAMPBELL, A., SHIPLEY, G. L., LOOSE, D. S., STANCEL, G. M., PICKAR, J. H. & DAVIES, P. J. 2005. Identification of a novel estrogen-regulated gene, EIG121, induced by hormone replacement therapy and differentially expressed in type I and type II endometrial cancer. *Clin Cancer Res,* 11, 8258-64.

DENG, L., FENG, J. & BROADDUS, R. 2010. The novel estrogen-induced gene EIG121 regulates autophagy and promotes cell survival under stress. *Cell Death Dis,* 1, e32.

DENNING, K., SMYTH, P., CAHILL, S., LI, J., FLAVIN, R., AHERNE, S., JJ, O. L. & SHEILS, O. 2008. ret/PTC-1 expression alters the immunoprofile of thyroid follicular cells. *Mol Cancer,* 7, 44.

DERYUGINA, E. I. & QUIGLEY, J. P. 2006. Matrix metalloproteinases and tumor metastasis. *Cancer Metastasis Rev,* 25, 9-34.

DEVALLIÈRE, J. & CHARREAU, B. The adaptor Lnk (SH2B3): An emerging regulator in vascular cells and a link between immune and inflammatory signaling. *Biochemical Pharmacology,* In Press, Corrected Proof.

DICKFELD, T., LENGYEL, E., MAY, A. E., MASSBERG, S., BRAND, K., PAGE, S., THIELEN, C., LANGENBRINK, K. & GAWAZ, M. 2001. Transient interaction of activated platelets with endothelial cells induces expression of monocyte-chemoattractant protein-1 via a p38 mitogen-activated protein kinase mediated pathway. Implications for atherogenesis. *Cardiovascular research,* 49, 189-99.

DINEEN, S. P., ROLAND, C. L., TOOMBS, J. E., KELHER, M., SILLIMAN, C. C., BREKKEN, R. A. & BARNETT, C. C., JR. 2009. The acellular fraction of stored platelets promotes tumor cell invasion. *The Journal of surgical research,* 153, 132-7.

DING, H., WU, X., BOSTROM, H., KIM, I., WONG, N., TSOI, B., O'ROURKE, M., KOH, G. Y., SORIANO, P., BETSHOLTZ, C., HART, T. C., MARAZITA, M. L., FIELD, L. L., TAM, P. P. L. & NAGY, A. 2004. A specific requirement for PDGF-C in palate formation and PDGFR-[alpha] signaling. *Nat Genet,* 36, 1111-1116.

DINH, P., HARNETT, P., PICCART-GEBHART, M. J. & AWADA, A. 2008. New therapies for ovarian cancer: cytotoxics and molecularly targeted agents. *Crit Rev Oncol Hematol,* 67, 103-12.

DINIZ, P. M., CARVALHO, J. P., BARACAT, E. C. & CARVALHO, F. M. 2011. Fallopian tube origin of supposed ovarian high-grade serous carcinomas. *Clinics (Sao Paulo),* 66, 73-6.

DOHERTY, G. A., BYRNE, S. M., AUSTIN, S. C., SCULLY, G. M., SADLIER, D. M., NEILAN, T. G., KAY, E. W., MURRAY, F. E. & FITZGERALD, D. J. 2009. Regulation of the apoptosis-inducing kinase DRAK2 by cyclooxygenase-2 in colorectal cancer. *British Journal of Cancer,* 101, 483-91.

DONG, H. & CHEN, L. 2003. B7-H1 pathway and its role in the evasion of tumor immunity. *Journal of Molecular Medicine,* 81, 281-287.

DONG, H., STROME, S. E., SALOMAO, D. R., TAMURA, H., HIRANO, F., FLIES, D. B., ROCHE, P. C., LU, J., ZHU, G., TAMADA, K., LENNON, V. A., CELIS, E. & CHEN, L. 2002. Tumor-associated B7-H1 promotes T-cell apoptosis: A potential mechanism of immune evasion. *Nat Med,* 8, 793-800.

DONG, Y., KAUSHAL, A., BRATTSAND, M., NICKLIN, J. & CLEMENTS, J. A. 2003. Differential splicing of KLK5 and KLK7 in epithelial ovarian cancer produces novel variants with potential as cancer biomarkers. *Clin Cancer Res,* 9, 1710-20.

DONNELLY, D. W., GAVIN, A. T. & COMBER, H. 2009. Cancer in Ireland 1994-2004: A comprehensive report. Northern Ireland Cancer Registry/National Cancer Registry, Ireland.

DONNELLY, D. W., GAVIN, A. T., N. IRELAND CANCER REGISTRY. & QUEEN'S UNIVERSITY OF BELFAST. 2007. *Survival of cancer patients in Northern Ireland : 1993-2004,* [Belfast], Northern Ireland Cancer Registry.

DORN, J., MAGDOLEN, V., GKAZEPIS, A., GERTE, T., HARLOZINSKA, A., SEDLACZEK, P., DIAMANDIS, E. P., SCHUSTER, T., HARBECK, N., KIECHLE, M. & SCHMITT, M. 2011. Circulating biomarker tissue kallikrein-related peptidase KLK5 impacts ovarian cancer patients' survival. *Annals of Oncology,* 22, 1783-1790.

DRAKE, J. G. & BECKER, J. L. 2002. Aspirin-induced inhibition of ovarian tumor cell growth. *Obstetrics and gynecology,* 100, 677-82.

DRAKE, R. L., VOGL, W., MITCHELL, A. W. M. & GRAY, H. 2005. *Gray's anatomy for students,* Philadelphia, Elsevier/Churchill Livingstone.

DU BOIS, A., HUOBER, J., STOPFER, P., PFISTERER, J., WIMBERGER, P., LOIBL, S., REICHARDT, V. L. & HARTER, P. 2010. A phase I open-label dose-escalation study of oral BIBF 1120 combined with standard paclitaxel and carboplatin in patients with advanced gynecological malignancies. *Annals of Oncology,* 21, 370-375.

DU BOIS, A., MARTH, C., PFISTERER, J., HARTER, P., HILPERT, F., ZEIMET, A. G. & SEHOULI, J. 2011. Neoadjuvant Chemotherapy Cannot Be Regarded as Adequate Routine

Therapy Strategy of Advanced Ovarian Cancer. *International Journal of Gynecological Cancer,* 21, 1165-1168 10.1097/IGC.0b013e31821d419a.

DUGGAN, C., KENNEDY, S., KRAMER, M. D., BARNES, C., ELVIN, P., MCDERMOTT, E., O'HIGGINS, N. & DUFFY, M. J. 1997. Plasminogen activator inhibitor type 2 in breast cancer. *British Journal of Cancer,* 76, 622-7.

DUHOUX, F. P. & MACHIELS, J. P. 2010. Antivascular therapy for epithelial ovarian cancer. *J Oncol,* 2010, 372547.

DUIT, S., MAYER, H., BLAKE, S. M., SCHNEIDER, W. J. & NIMPF, J. 2010. Differential functions of ApoER2 and very low density lipoprotein receptor in Reelin signaling depend on differential sorting of the receptors. *The Journal of biological chemistry,* 285, 4896-908.

DUNNE, E., SPRING, C. M., REHEMAN, A., JIN, W., BERNDT, M. C., NEWMAN, D. K., NEWMAN, P. J., NI, H. & KENNY, D. 2012. Cadherin 6 Has a Functional Role in Platelet Aggregation and Thrombus Formation. *Arteriosclerosis, Thrombosis, and Vascular Biology,* 32, 1724-1731.

EASTON, D., GAYTHER, S., KEHOE, S., POOLE, J. & GREENBERG, D. 2011. Ovarian Cancer UK. *CancerStats.* Cancer Research UK.

ECONOMOPOULOU, M. A., FRAGOULIS, E. G. & SIDERIS, D. C. 2007. Molecular cloning and characterization of the human RNase kappa, an ortholog of Cc RNase. *Nucleic acids research,* 35, 6389-98.

EDGE, S. B. & AMERICAN JOINT COMMITTEE ON CANCER. 2010. *AJCC cancer staging manual,* New York ; London, Springer.

EITNER, F., OSTENDORF, T., KRETZLER, M., COHEN, C. D., ERIKSSON, U., GRÖNE, H.-J. & FLOEGE, J. 2003. PDGF-C Expression in the Developing and Normal Adult Human Kidney and in Glomerular Diseases. *Journal of the American Society of Nephrology,* 14, 1145-1153.

EL BOUHTOURY, F., KELLER, J. M., COLIN, S., PARACHE, R. M. & DAUCA, M. 1992. Peroxisomal enzymes in normal and tumoral human breast. *The Journal of Pathology,* 166, 27-35.

EL GHAMRASNI, S., PAMIDI, A., HALABY, M. J., BOHGAKI, M., CARDOSO, R., LI, L., VENKATESAN, S., SETHU, S., HIRAO, A., MAK, T. W., HANDE, M. P., HAKEM, A. & HAKEM, R. 2011. Inactivation of chk2 and mus81 leads to impaired lymphocytes development, reduced genomic instability, and suppression of cancer. *PLoS genetics,* 7, e1001385.

ELDOR, A., BAR-NER, M., YAHALOM, J., FUKS, Z. & VLODAVSKY, I. 1987. Role of heparanase in platelet and tumor cell interactions with the subendothelial extracellular matrix. *Semin Thromb Hemost,* 13, 475-88.

ELLIS, P. M., KAISER, R., ZHAO, Y., STOPFER, P., GYORFFY, S. & HANNA, N. 2010. Phase I Open-Label Study of Continuous Treatment with BIBF 1120, a Triple Angiokinase Inhibitor, and Pemetrexed in Pretreated Non–Small Cell Lung Cancer Patients. *Clinical Cancer Research,* 16, 2881-2889.

EMAMI, N. & DIAMANDIS, E. P. 2008. Utility of kallikrein-related peptidases (KLKs) as cancer biomarkers. *Clin Chem,* 54, 1600-7.

ERDEMIR, F., KILCILER, M., BEDIR, S., OZGOK, Y., COBAN, H. & ERTEN, K. 2007. Clinical Significance of Platelet Count in Patients with Renal Cell Carcinoma. *Urologia Internationalis,* 79, 111-116.

ERPENBECK, L. & SCHÖN, M. P. 2010. Deadly allies: the fatal interplay between platelets and metastasizing cancer cells. *Blood,* 115, 3427-3436.

ERRICO, A., BALLABIO, A. & RUGARLI, E. I. 2002. Spastin, the protein mutated in autosomal dominant hereditary spastic paraplegia, is involved in microtubule dynamics. *Human Molecular Genetics,* 11, 153-63.

ESHEL-GREEN, T., BERNY, M. A., CONLEY, R. B. & MCCARTY, O. J. 2009. Effect of sex difference on platelet adhesion, spreading and aggregate formation under flow. *Thromb Haemost,* 102, 958-65.

ESKANDER, R. N. & RANDALL, L. M. 2011. Bevacizumab in the treatment of ovarian cancer. *Biologics,* 5, 1-5.

ESSER, P. 2010. Blocking Agent and Detergent in ELISA. *Thermo Scientific Nunc Bulletin, No.8.* Thermo Fisher Scientific Inc.

FADER, A. N., RASOOL, N., VAZIRI, S. A. J., KOZUKI, T., FABER, P. W., ELSON, P., BISCOTTI, C. V., MICHENER, C. M., ROSE, P. G., ROJAS-ESPAILLAT, L., BELINSON, J. L., GANAPATHI, M. K. & GANAPATHI, R. 2010. CCL2 Expression in Primary Ovarian Carcinoma Is Correlated with Chemotherapy Response and Survival Outcomes. *Anticancer Research,* 30, 4791-4798.

FALANGA, A., PANOVA-NOEVA, M. & RUSSO, L. 2009. Procoagulant mechanisms in tumour cells. *Best practice & research. Clinical haematology,* 22, 49-60.

FAN, T., ZHAO, Q., CHEN, J. J., CHEN, W. T. & PEARL, M. L. 2009. Clinical significance of circulating tumor cells detected by an invasion assay in peripheral blood of patients with ovarian cancer. *Gynecol Oncol,* 112, 185-91.

FAN, Y., NEWMAN, T., LINARDOPOULOU, E. & TRASK, B. J. 2002. Gene content and function of the ancestral chromosome fusion site in human chromosome 2q13-2q14.1 and paralogous regions. *Genome Res,* 12, 1663-72.

FEHM, T., BECKER, S., BACHMANN, C., BECK, V., GEBAUER, G., BANYS, M., WALLWIENER, D. & SOLOMAYER, E. F. 2006. Detection of disseminated tumor cells in patients with gynecological cancers. *Gynecologic Oncology,* 103, 942-947.

FELDING-HABERMANN, B., O'TOOLE, T. E., SMITH, J. W., FRANSVEA, E., RUGGERI, Z. M., GINSBERG, M. H., HUGHES, P. E., PAMPORI, N., SHATTIL, S. J., SAVEN, A. & MUELLER, B. M. 2001. Integrin activation controls metastasis in human breast cancer. *Proc Natl Acad Sci U S A,* 98, 1853-8.

FENG, J. G., LIU, Q., QIN, X., GENG, Y. H., ZHENG, S. T., LIU, T., SHEYHIDIN, I. & LU, X. M. 2011. Clinicopathological pattern and Annexin A2 and Cdc42 status in patients presenting with differentiation and lymphnode metastasis of esophageal squamous cell carcinomas. *Molecular biology reports.*

FERLAY J, SHIN HR, BRAY F, FORMAN D, MATHERS C & DM, P. 2010. Cancer Incidence and Mortality Worldwide: IARC CancerBase No. 10. *GLOBOCAN 2008 v1.2.* International Agency for Research on Cancer.

FERLAY, J., AUTIER, P., BONIOL, M., HEANUE, M., COLOMBET, M. & BOYLE, P. 2007. Estimates of the cancer incidence and mortality in Europe in 2006. *Ann Oncol,* 18, 581-592.

FERRARA, N. & GERBER, H. P. 2001. The role of vascular endothelial growth factor in angiogenesis. *Acta Haematologica,* 106, 148-56.

FERRARA, N. & HENZEL, W. J. 1989. Pituitary follicular cells secrete a novel heparin-binding growth factor specific for vascular endothelial cells. *Biochem Biophys Res Commun,* 161, 851-8.

FERRARA, N. & KERBEL, R. S. 2005. Angiogenesis as a therapeutic target. *Nature,* 438, 967-974.

FILIPENKO, N. R., MACLEOD, T. J., YOON, C.-S. & WAISMAN, D. M. 2004. Annexin A2 Is a Novel RNA-binding Protein. *Journal of Biological Chemistry,* 279, 8723-8731.

FINK, J. M., HIRSCH, B. A., ZHENG, C., DIETZ, G., HATTEN, M. E. & ROSS, M. E. 1997. Astrotactin (ASTN), a Gene for Glial-Guided Neuronal Migration, Maps to Human Chromosome 1q25.2. *Genomics,* 40, 202-205.

FINN, S. P., SMYTH, P., O'LEARY, J., SWEENEY, E. C. & SHEILS, O. 2003. Ret/PTC chimeric transcripts in an Irish cohort of sporadic papillary thyroid carcinoma. *J Clin Endocrinol Metab,* 88, 938-41.

FINN, S. P., SMYTH, P., O'REGAN, E., CAHILL, S., FLAVIN, R., O'LEARY, J. & SHEILS, O. 2004. Array comparative genomic hybridisation analysis of gamma-irradiated human thyrocytes. *Virchows Arch,* 445, 396-404.

FISCHER, O. M., HART, S., GSCHWIND, A., PRENZEL, N. & ULLRICH, A. 2004. Oxidative and osmotic stress signaling in tumor cells is mediated by ADAM proteases and heparin-binding epidermal growth factor. *Molecular and cellular biology,* 24, 5172-83.

FISHLEY, B. & ALEXANDER, W. S. 2004. Thrombopoietin signalling in physiology and disease. *Growth Factors,* 22, 151-5.

FITAU, J., BOULDAY, G., COULON, F., QUILLARD, T. & CHARREAU, B. 2006. The Adaptor Molecule Lnk Negatively Regulates Tumor Necrosis Factor-α-dependent VCAM-1 Expression in Endothelial Cells through Inhibition of the ERK1 and -2 Pathways. *Journal of Biological Chemistry,* 281, 20148-20159.

FLANNERY, S. M., KEATING, S. E., SZYMAK, J. & BOWIE, A. G. 2011. Human Interleukin-1 Receptor-associated Kinase-2 Is Essential for Toll-like Receptor-mediated Transcriptional and Post-transcriptional Regulation of Tumor Necrosis Factor α. *Journal of Biological Chemistry,* 286, 23688-23697.

FLAVIN, R., JACKL, G., FINN, S., SMYTH, P., RING, M., O'REGAN, E., CAHILL, S., UNGER, K., DENNING, K., JINGHUAN LI, AHERNE, S., TALLINI, G., GAFFNEY, E., O'LEARY, J. J., ZITZELSBERGER, H. & SHEILS, O. 2009. RET/PTC Rearrangement Occurring in Primary Peritoneal Carcinoma. *International Journal of Surgical Pathology,* 17, 187-197.

FLISS, M. S., USADEL, H., CABALLERO, O. L., WU, L., BUTA, M. R., ELEFF, S. M., JEN, J. & SIDRANSKY, D. 2000. Facile detection of mitochondrial DNA mutations in tumors and bodily fluids. *Science,* 287, 2017-9.

FOLKMAN, J. 1971. Tumor angiogenesis: therapeutic implications. *N Engl J Med,* 285, 1182-6.

FOLKMAN, J., WATSON, K., INGBER, D. & HANAHAN, D. 1989. Induction of angiogenesis during the transition from hyperplasia to neoplasia. *Nature,* 339, 58-61.

FORGIONE, M. 2011. *Blood test in development appears to be able to detect a single cancer cell* [Online]. Los Angeles Times. Available: http://articles.latimes.com/2011/jan/05/news/la-heb-cancer-blood-test-20110105 [Accessed 5 January 2011].

FÖRSTER, T. 1948. Zwischenmolekulare Energiewanderung und Fluoreszenz. *Annalen der Physik,* 437, 55-75.

FREDERICK, L. A., MATTHEWS, J. A., JAMIESON, L., JUSTILIEN, V., THOMPSON, E. A., RADISKY, D. C. & FIELDS, A. P. 2008. Matrix metalloproteinase-10 is a critical effector of protein kinase C[iota]-Par6[alpha]-mediated lung cancer. *Oncogene,* 27, 4841-4853.

FREDERIKS, W. M., BOSCH, K. S., HOEBEN, K. A., VAN MARLE, J. & LANGBEIN, S. 2010. Renal cell carcinoma and oxidative stress: The lack of peroxisomes. *Acta Histochemica,* 112, 364-371.

FREDRIKSSON, L., LI, H. & ERIKSSON, U. 2004. The PDGF family: four gene products form five dimeric isoforms. *Cytokine Growth Factor Rev,* 15, 197-204.

FRIEBE, Z., WATROWSKI, R., BEMBNISTA, M., ROKOWSKA, A., WLOSIINSKA, J. & DEMBINSKA, M. 2005. [Correlation between platelet count and CA-125 in ovarian cancer]. *Ginekol Pol,* 76, 187-94.

FRIEDLANDER, M., HANCOCK, K. C., RISCHIN, D., MESSING, M. J., STRINGER, C. A., MATTHYS, G. M., MA, B., HODGE, J. P. & LAGER, J. J. 2010. A Phase II, open-label study evaluating pazopanib in patients with recurrent ovarian cancer. *Gynecologic Oncology,* 119, 32-7.

FUERTES, M. A., CASTILLA, J., ALONSO, C. & PREZ, J. M. 2003. Cisplatin Biochemical Mechanism of Action: From Cytotoxicity to Induction of Cell Death Through Interconnections Between Apoptotic and Necrotic Pathways. *Current Medicinal Chemistry,* 10, 257-266.

FUJIHARA, T., YASHIRO, M., INOUE, T., SAWADA, T., KATO, Y., OHIRA, M., NISHIGUCHI, Y., ISHIKAWA, T., SOWA, M. & CHUNG, K. H. 1999. Decrease in ICAM-1 expression on gastric cancer cells is correlated with lymph node metastasis. *Gastric cancer : official journal of the International Gastric Cancer Association and the Japanese Gastric Cancer Association,* 2, 221-225.

FURUHASHI, M., MIYABE, Y. & ODA, H. 1999. A Case of Thrombopoietin-Producing Ovarian Carcinoma Confirmed by Immunohistochemistry. *Gynecologic Oncology,* 74, 278-281.

GARCÍA, Á. & SENIS, Y. A. 2011. *Platelet proteomics : principles, analysis, and applications,* Hoboken, N.J., John Wiley & Sons.

GARCIA, J., CALLEWAERT, N. & BORSIG, L. 2007. P-selectin mediates metastatic progression through binding to sulfatides on tumor cells. *Glycobiology,* 17, 185-196.

GARCIA, M. J. & BENITEZ, J. 2008. The Fanconi anaemia/BRCA pathway and cancer susceptibility. Searching for new therapeutic targets. *Clinical & translational oncology : official publication of the Federation of Spanish Oncology Societies and of the National Cancer Institute of Mexico,* 10, 78-84.

GARDINA, P. J., CLARK, T. A., SHIMADA, B., STAPLES, M. K., YANG, Q., VEITCH, J., SCHWEITZER, A., AWAD, T., SUGNET, C., DEE, S., DAVIES, C., WILLIAMS, A. & TURPAZ, Y. 2006. Alternative splicing and differential gene expression in colon cancer detected by a whole genome exon array. *BMC Genomics,* 7, 325.

GARDINER, C. 2007. Family history of gynaecological cancers. *Obstetrics, Gynaecology & Reproductive Medicine,* 17, 356-361.

GARDNER, A. 2011. *Scientists Aim for Test That Spots Single Cancer Cell in Blood Sample* [Online]. Bloomberg Businessweek. Available: http://www.businessweek.com/lifestyle/content/healthday/648465.html [Accessed 5 January 2011].

GARNIS, C., CAMPBELL, J., DAVIES, J. J., MACAULAY, C., LAM, S. & LAM, W. L. 2005. Involvement of multiple developmental genes on chromosome 1p in lung tumorigenesis. *Human Molecular Genetics,* 14, 475-482.

GARTNER, J., MOSER, H. & VALLE, D. 1992. Mutations in the 70K peroxisomal membrane protein gene in Zellweger syndrome. *Nature genetics,* 1, 16-23.

GASIC, G. J., GASIC, T. B. & STEWART, C. C. 1968. Antimetastatic effects associated with platelet reduction. *Proc Natl Acad Sci U S A,* 61, 46-52.

GASTL, G., PLANTE, M., FINSTAD, C. L., WONG, G. Y., FEDERICI, M. G., BANDER, N. H. & RUBIN, S. C. 1993. High IL-6 levels in ascitic fluid correlate with reactive thrombocytosis in patients with epithelial ovarian cancer. *Br J Haematol,* 83, 433-41.

GAWAZ, M., PAGE, S., MASSBERG, S., NOTHDURFTER, C., WEBER, M., FISHER, C., UNGERER, M. & BRAND, K. 2002. Transient platelet interaction induces MCP-1 production by endothelial cells via I kappa B kinase complex activation. *Thrombosis and Haemostasis,* 88, 307-14.

GAY, L. J. & FELDING-HABERMANN, B. 2011. Contribution of platelets to tumour metastasis. *Nat Rev Cancer,* 11, 123-134.

GEARING, A. J. H., HEMINGWAY, I. A. N., PIGOIT, R. O. D., HUGHES, J., REES, A. J. & CASHMAN, S. J. 1992. Soluble Forms of Vascular Adhesion Molecules, E-Selectin, ICAM-1, and VCAM-1: Pathological Significance. *Annals of the New York Academy of Sciences,* 667, 324-331.

GELLER, M. A., BUI-NGUYEN, T. M., ROGERS, L. M. & RAMAKRISHNAN, S. 2010. Chemotherapy Induces Macrophage Chemoattractant Protein-1 Production in Ovarian Cancer. *International Journal of Gynecological Cancer,* 20, 918-925 10.1111/IGC.0b013e3181e5c442.

GENG, L., HUANG, D., LIU, J., QIAN, Y., DENG, J., LI, D., HU, Z., ZHANG, J., JIANG, G. & ZHENG, S. 2008. B7-H1 up-regulated expression in human pancreatic carcinoma tissue associates with tumor progression. *Journal of Cancer Research and Clinical Oncology,* 134**,** 1021-1027.

GENG, L., HUNTOON, C. J. & KARNITZ, L. M. 2010. RAD18-mediated ubiquitination of PCNA activates the Fanconi anemia DNA repair network. *The Journal of Cell Biology,* 191**,** 249-257.

GEORGE, D. 2003. Targeting PDGF receptors in cancer--rationales and proof of concept clinical trials. *Adv Exp Med Biol,* 532**,** 141-51.

GERESTEIN, C. G., EIJKEMANS, M. J. C., DE JONG, D., VAN DER BURG, M. E. L., DYKGRAAF, R. H. M., KOOI, G. S., BAALBERGEN, A., BURGER, C. W. & ANSINK, A. C. 2009. The prediction of progression-free and overall survival in women with an advanced stage of epithelial ovarian carcinoma. *BJOG: An International Journal of Obstetrics & Gynaecology,* 116**,** 372-380.

GERHARDT, A., USENER, D., KEESE, M., STURM, J., SCHADENDORF, D. & EICHMÜLLER, S. 2004. Tissue expression and sero-reactivity of tumor-specific antigens in colorectal cancer. *Cancer Letters,* 208**,** 197-206.

GERSHENSON, D. M. 2007. Management of Ovarian Germ Cell Tumors. *Journal of Clinical Oncology,* 25**,** 2938-2943.

GHEBEH, H., LEHE, C., BARHOUSH, E., AL-ROMAIH, K., TULBAH, A., AL-ALWAN, M., HENDRAYANI, S. F., MANOGARAN, P., ALAIYA, A., AL-TWEIGERI, T., ABOUSSEKHRA, A. & DERMIME, S. 2010. Doxorubicin downregulates cell surface B7-H1 expression and upregulates its nuclear expression in breast cancer cells: role of B7-H1 as an anti-apoptotic molecule. *Breast Cancer Res,* 12**,** R48.

GHEBEH, H., MOHAMMED, S., AL-OMAIR, A., QATTAN, A., LEHE, C., AL-QUDAIHI, G., ELKUM, N., ALSHABANAH, M., BIN AMER, S., TULBAH, A., AJARIM, D., AL-TWEIGERI, T. & DERMIME, S. 2006. The B7-H1 (PD-L1) T lymphocyte-inhibitory molecule is expressed in breast cancer patients with infiltrating ductal carcinoma: correlation with important high-risk prognostic factors. *Neoplasia,* 8**,** 190-8.

GHEBEH, H., TULBAH, A., MOHAMMED, S., ELKUM, N., BIN AMER, S. M., AL-TWEIGERI, T. & DERMIME, S. 2007. Expression of B7-H1 in breast cancer patients is strongly associated with high proliferative Ki-67-expressing tumor cells. *International Journal of Cancer. Journal International Du Cancer,* 121**,** 751-8.

GIALLONGO, A., YON, J. & FRIED, M. 1989. Ribosomal protein L7a is encoded by a gene (Surf-3) within the tightly clustered mouse surfeit locus. *Molecular and cellular biology,* 9**,** 224-31.

GIAVAZZI, R., NICOLETTI, M. I., CHIRIVI, R. G., HEMINGWAY, I., BERNASCONI, S., ALLAVENA, P. & GEARING, A. J. 1994. Soluble intercellular adhesion molecule-1 (ICAM-1) is released into the serum and ascites of human ovarian carcinoma patients and in nude mice bearing tumour xenografts. *European journal of cancer,* 30A, 1865-70.

GILL, J. H., KIRWAN, I. G., SEARGENT, J. M., MARTIN, S. W., TIJANI, S., ANIKIN, V. A., MEARNS, A. J., BIBBY, M. C., ANTHONEY, A. & LOADMAN, P. M. 2004. MMP-10 is overexpressed, proteolytically active, and a potential target for therapeutic intervention in human lung carcinomas. *Neoplasia,* 6, 777-85.

GINSBERG, M. H., LOFTUS, J. & PLOW, E. F. 1988. Platelets and the adhesion receptor superfamily. *Progress in Clinical and Biological Research,* 283, 171-95.

GINSBERG, M. H., XIAOPING, D., O'TOOLE, T. E., LOFTUS, J. C. & PLOW, E. F. 1993. Platelet integrins. *Thrombosis and Haemostasis,* 70, 87-93.

GIORDANO, G., AZZONI, C., D'ADDA, T., ROCCO, A., GNETTI, L., FROIO, E., MERISIO, C. & MELPIGNANO, M. 2008. Human papilloma virus (HPV) status, p16INK4a, and p53 overexpression in epithelial malignant and borderline ovarian neoplasms. *Pathology, research and practice,* 204, 163-74.

GLANTZ, S. A. 1997. *Primer of biostatistics,* New York ; London, McGraw-Hill, Health Professions Division.

GLESSNER, J. T., BRADFIELD, J. P., WANG, K., TAKAHASHI, N., ZHANG, H., SLEIMAN, P. M., MENTCH, F. D., KIM, C. E., HOU, C., THOMAS, K. A., GARRIS, M. L., DELIARD, S., FRACKELTON, E. C., OTIENO, F. G., ZHAO, J., CHIAVACCI, R. M., LI, M., BUXBAUM, J. D., BERKOWITZ, R. I., HAKONARSON, H. & GRANT, S. F. 2010. A genome-wide study reveals copy number variants exclusive to childhood obesity cases. *American journal of human genetics,* 87, 661-6.

GOLDSHMIDT, O., ZCHARIA, E., ABRAMOVITCH, R., METZGER, S., AINGORN, H., FRIEDMANN, Y., SCHIRRMACHER, V., MITRANI, E. & VLODAVSKY, I. 2002. Cell surface expression and secretion of heparanase markedly promote tumor angiogenesis and metastasis. *Proc Natl Acad Sci U S A,* 99, 10031-6.

GOLDSWORTHY, S. M., STOCKTON, P. S., TREMPUS, C. S., FOLEY, J. F. & MARONPOT, R. R. 1999. Effects of fixation on RNA extraction and amplification from laser capture microdissected tissue. *Mol Carcinog,* 25, 86-91.

GRAM, I. T., LUKANOVA, A., BRILL, I., BRAATEN, T., LUND, E., LUNDIN, E., OVERVAD, K., TJØNNELAND, A., CLAVEL-CHAPELON, F., CHABBERT-BUFFET, N., BAMIA, C., TRICHOPOULOU, A., ZYLIS, D., MASALA, G., BERRINO, F., GALASSO, R., TUMINO, R., SACERDOTE, C., GAVRILYUK, O., KRISTIANSEN, S., RODRÍGUEZ, L., BONET, C., HUERTA, J. M., BARRICARTE, A., SÁNCHEZ, M.-J., DORRONSORO, M., JIRSTRÖM, K., ALMQUIST, M., IDAHL, A., BUENO-DE-MESQUITA, H. B., BRAEM, M., ONLAND-

MORET, C., TSILIDIS, K. K., ALLEN, N. E., FEDIRKO, V., RIBOLI, E. & KAAKS, R. 2011. Cigarette smoking and risk of histological subtypes of epithelial ovarian cancer in the EPIC cohort study. *International Journal of Cancer*, n/a-n/a.

GREENBERG, J. I., SHIELDS, D. J., BARILLAS, S. G., ACEVEDO, L. M., MURPHY, E., HUANG, J., SCHEPPKE, L., STOCKMANN, C., JOHNSON, R. S., ANGLE, N. & CHERESH, D. A. 2008. A role for VEGF as a negative regulator of pericyte function and vessel maturation. *Nature,* 456, 809-13.

GRIESSHAMMER, M., BANGERTER, M., SAUER, T., WENNAUER, R., BERGMANN, L. & HEIMPEL, H. 1999. Aetiology and clinical significance of thrombocytosis: analysis of 732 patients with an elevated platelet count. *J Intern Med,* 245, 295-300.

GROSS, A. L., KURMAN, R. J., VANG, R., SHIH IE, M. & VISVANATHAN, K. 2010. Precursor lesions of high-grade serous ovarian carcinoma: morphological and molecular characteristics. *J Oncol,* 2010, 126295.

GUBBELS, J. A., FELDER, M., HORIBATA, S., BELISLE, J. A., KAPUR, A., HOLDEN, H., PETRIE, S., MIGNEAULT, M., RANCOURT, C., CONNOR, J. P. & PATANKAR, M. S. 2010. MUC16 provides immune protection by inhibiting synapse formation between NK and ovarian tumor cells. *Mol Cancer,* 9, 11.

GUNEY, N., SOYDINC, H., DERIN, D., TAS, F., CAMLICA, H., DURANYILDIZ, D., YASASEVER, V. & TOPUZ, E. 2008. Serum levels of intercellular adhesion molecule ICAM-1 and E-selectin in advanced stage non-small cell lung cancer. *Medical Oncology,* 25, 194-200.

GUNGOR, T., KANAT-PEKTAS, M., SUCAK, A. & MOLLAMAHMUTOGLU, L. The role of thrombocytosis in prognostic evaluation of epithelial ovarian tumors. *Archives of Gynecology and Obstetrics*.

GUNGOR, T., KANAT-PEKTAS, M., SUCAK, A. & MOLLAMAHMUTOGLU, L. 2009. The role of thrombocytosis in prognostic evaluation of epithelial ovarian tumors. *Archives of Gynecology and Obstetrics,* 279, 53-56.

GUPTA, R. & EMENS, L. A. 2010. GM-CSF-secreting vaccines for solid tumors: moving forward. *Discovery medicine,* 10, 52-60.

HA, H., HAN, D. & CHOI, Y. 2001. TRAF-Mediated TNFR-Family Signaling. *Current Protocols in Immunology.* John Wiley & Sons, Inc.

HADDAD, L. B. & LAUFER, M. R. 2008. Thrombocytosis Associated with Malignant Ovarian Lesions within a Pediatric/Adolescent Population. *Journal of Pediatric and Adolescent Gynecology,* 21, 243-246.

HAIDOPOULOS, D., PARTSINEVELOS, G. A., VLACHOS, G. D., RODOLAKIS, A., MARKAKI, S., VOULGARIS, Z., DIAKOMANOLIS, E. & ANTSAKLIS, A. 2009. p16 INK4A Is a Strong

Biomarker for Cervical Intraepithelial Neoplasia and Invasive Cervical Carcinoma: A Reappraisal. *Reproductive Sciences,* 16, 685-693.

HALPERIN, R., ZEHAVI, S., LANGER, R., HADAS, E., BUKOVSKY, I. & SCHNEIDER, D. 2001. Primary peritoneal serous papillary carcinoma: A new epidemiologic trend? A matched-case comparison with ovarian serous papillary cancer. *International Journal of Gynecological Cancer,* 11, 403-408.

HAMANISHI, J., MANDAI, M., IWASAKI, M., OKAZAKI, T., TANAKA, Y., YAMAGUCHI, K., HIGUCHI, T., YAGI, H., TAKAKURA, K., MINATO, N., HONJO, T. & FUJII, S. 2007. Programmed cell death 1 ligand 1 and tumor-infiltrating CD8+ T lymphocytes are prognostic factors of human ovarian cancer. *Proceedings of the National Academy of Sciences of the United States of America,* 104, 3360-5.

HAMBURGER, S. A. & MCEVER, R. P. 1990. GMP-140 mediates adhesion of stimulated platelets to neutrophils. *Blood,* 75, 550-4.

HAN, H., YANG, Y., LU, Z., HE, Q. & LIN, Z. 2011. Decreased D2-40 and increased p16INK4A immunoreactivities correlate with higher grade of cervical intraepithelial neoplasia. *Diagnostic pathology,* 6, 59.

HANADA, K., BUDZOWSKA, M., DAVIES, S. L., VAN DRUNEN, E., ONIZAWA, H., BEVERLOO, H. B., MAAS, A., ESSERS, J., HICKSON, I. D. & KANAAR, R. 2007. The structure-specific endonuclease Mus81 contributes to replication restart by generating double-strand DNA breaks. *Nat Struct Mol Biol,* 14, 1096-1104.

HANAHAN, D. & WEINBERG, R. A. 2000. The hallmarks of cancer. *Cell,* 100, 57-70.

HANAHAN, D. & WEINBERG, R. A. 2011. Hallmarks of cancer: the next generation. *Cell,* 144, 646-74.

HARRISON, C. N., BAREFORD, D., BUTT, N., CAMPBELL, P., CONNEALLY, E., DRUMMOND, M., ERBER, W., EVERINGTON, T., GREEN, A. R., HALL, G. W., HUNT, B. J., LUDLAM, C. A., MURRIN, R., NELSON-PIERCY, C., RADIA, D. H., REILLY, J. T., VAN DER WALT, J., WILKINS, B. & MCMULLIN, M. F. 2010. Guideline for investigation and management of adults and children presenting with a thrombocytosis. *British Journal of Haematology,* 149, 352-75.

HARTKOPF, A. D., WAGNER, P., WALLWIENER, D., FEHM, T. & ROTHMUND, R. 2011. Changing Levels of Circulating Tumor Cells in Monitoring Chemotherapy Response in Patients with Metastatic Breast Cancer. *Anticancer Research,* 31, 979-984.

HASHIMOTO, K., MAN, S., XU, P., CRUZ-MUNOZ, W., TANG, T., KUMAR, R. & KERBEL, R. S. 2010. Potent preclinical impact of metronomic low-dose oral topotecan combined with the antiangiogenic drug pazopanib for the treatment of ovarian cancer. *Molecular Cancer Therapeutics,* 9, 996-1006.

HAWIGER, J., PARKINSON, S. & TIMMONS, S. 1980. Prostacyclin inhibits mobilisation of fibrinogen-binding sites on human ADP- and thrombin-treated platelets. *Nature,* 283, 195-7.

HAYAT, M. A. 2010. *General overviews, head and neck cancer, and thyroid cancer,* Dordrecht, Springer.

HAYES, D. F., CRISTOFANILLI, M., BUDD, G. T., ELLIS, M. J., STOPECK, A., MILLER, M. C., MATERA, J., ALLARD, W. J., DOYLE, G. V. & TERSTAPPEN, L. W. W. M. 2006. Circulating Tumor Cells at Each Follow-up Time Point during Therapy of Metastatic Breast Cancer Patients Predict Progression-Free and Overall Survival. *Clinical Cancer Research,* 12, 4218-4224.

HE, N., JAHCHAN, N. S., HONG, E., LI, Q., BAYFIELD, M. A., MARAIA, R. J., LUO, K. & ZHOU, Q. 2008a. A La-related protein modulates 7SK snRNP integrity to suppress P-TEFb-dependent transcriptional elongation and tumorigenesis. *Molecular cell,* 29, 588-99.

HE, W., KULARATNE, S. A., KALLI, K. R., PRENDERGAST, F. G., AMATO, R. J., KLEE, G. G., HARTMANN, L. C. & LOW, P. S. 2008b. Quantitation of circulating tumor cells in blood samples from ovarian and prostate cancer patients using tumor-specific fluorescent ligands. *International Journal of Cancer. Journal International Du Cancer,* 123, 1968-73.

HE, X., POOL, M., DARCY, K. M., LIM, S. B., AUERSPERG, N., COON, J. S. & BECK, W. T. 2007. Knockdown of polypyrimidine tract-binding protein suppresses ovarian tumor cell growth and invasiveness in vitro. *Oncogene,* 26, 4961-8.

HEINMOLLER, E., SCHROPP, T., KISKER, O., SIMON, B., SEITZ, R. & WEINEL, R. J. 1995. Tumor cell-induced platelet aggregation in vitro by human pancreatic cancer cell lines. *Scandinavian Journal of Gastroenterology,* 30, 1008-16.

HEINMOLLER, E., WEINEL, R. J., HEIDTMANN, H. H., SALGE, U., SEITZ, R., SCHMITZ, I., MULLER, K. M. & ZIRNGIBL, H. 1996. Studies on tumor-cell-induced platelet aggregation in human lung cancer cell lines. *Journal of Cancer Research and Clinical Oncology,* 122, 735-44.

HELDIN, C. H., OSTMAN, A., ERIKSSON, A., SIEGBAHN, A., CLAESSON-WELSH, L. & WESTERMARK, B. 1992. Platelet-derived growth factor: isoform-specific signalling via heterodimeric or homodimeric receptor complexes. *Kidney Int,* 41, 571-4.

HÉLIAS-RODZEWICZ, Z., PÉROT, G., CHIBON, F., FERREIRA, C., LAGARDE, P., TERRIER, P., COINDRE, J.-M. & AURIAS, A. 2010. YAP1 and VGLL3, encoding two cofactors of TEAD transcription factors, are amplified and overexpressed in a subset of soft tissue sarcomas. *Genes, Chromosomes and Cancer,* 49, 1161-1171.

HEMMINKI, K., SUNDQUIST, J. & BRANDT, A. 2011. Incidence and mortality in epithelial ovarian cancer by family history of any cancer. *Cancer*.

HENRIKSEN, R., FUNA, K., WILANDER, E., BACKSTROM, T., RIDDERHEIM, M. & OBERG, K. 1993. Expression and prognostic significance of platelet-derived growth factor and its receptors in epithelial ovarian neoplasms. *Cancer Res,* 53, 4550-4.

HERAS, P., HATZOPOULOS, A., KRITIKOS, N. & KRITIKOS, K. 2010. Platelet count and tumor progression in gastric cancer patients. *Scandinavian Journal of Gastroenterology,* 45, 1005-1006.

HESS, V., A'HERN, R., NASIRI, N., KING, D. M., BLAKE, P. R., BARTON, D. P., SHEPHERD, J. H., IND, T., BRIDGES, J., HARRINGTON, K., KAYE, S. B. & GORE, M. E. 2004. Mucinous epithelial ovarian cancer: a separate entity requiring specific treatment. *Journal of clinical oncology : official journal of the American Society of Clinical Oncology,* 22, 1040-4.

HILBERG, F., ROTH, G. J., KRSSAK, M., KAUTSCHITSCH, S., SOMMERGRUBER, W., TONTSCH-GRUNT, U., GARIN-CHESA, P., BADER, G., ZOEPHEL, A., QUANT, J., HECKEL, A. & RETTIG, W. J. 2008. BIBF 1120: Triple Angiokinase Inhibitor with Sustained Receptor Blockade and Good Antitumor Efficacy. *Cancer Research,* 68, 4774-4782.

HILDEBRAND, J. S., GAPSTUR, S. M., FEIGELSON, H. S., TERAS, L. R., THUN, M. J. & PATEL, A. V. 2010. Postmenopausal hormone use and incident ovarian cancer: Associations differ by regimen. *International Journal of Cancer,* 127, 2928-2935.

HINO, R., KABASHIMA, K., KATO, Y., YAGI, H., NAKAMURA, M., HONJO, T., OKAZAKI, T. & TOKURA, Y. 2010. Tumor cell expression of programmed cell death-1 ligand 1 is a prognostic factor for malignant melanoma. *Cancer,* 116, 1757-1766.

HIYAMA, T., KATSURA, M., YOSHIHARA, T., ISHIDA, M., KINOMURA, A., TONDA, T., ASAHARA, T. & MIYAGAWA, K. 2006. Haploinsufficiency of the Mus81-Eme1 endonuclease activates the intra-S-phase and G2/M checkpoints and promotes rereplication in human cells. *Nucleic acids research,* 34, 880-92.

HOCH, R. V. & SORIANO, P. 2003. Roles of PDGF in animal development. *Development,* 130, 4769-84.

HODGE, D. L., SUBLESKI, J. J., REYNOLDS, D. A., BUSCHMAN, M. D., SCHILL, W. B., BURKETT, M. W., MALYGUINE, A. M. & YOUNG, H. A. 2006. The Proinflammatory Cytokine Interleukin-18 Alters Multiple Signaling Pathways to Inhibit Natural Killer Cell Death. *Journal of Interferon & Cytokine Research,* 26, 706-718.

HODGKINSON, J. L. 2000. Actin and the smooth muscle regulatory proteins: a structural perspective. *Journal of muscle research and cell motility,* 21, 115-30.

HOEI-HANSEN, C. E., KRAGGERUD, S. M., ABELER, V. M., KAERN, J., RAJPERT-DE MEYTS, E. & LOTHE, R. A. 2007. Ovarian dysgerminomas are characterised by frequent KIT mutations and abundant expression of pluripotency markers. *Molecular cancer,* 6, 12.

HOFFMANN, K., KERNER, C., WILFERT, W., MUELLER, M., THIERY, J., HAUSS, J. & WITZIGMANN, H. 2007. Detection of disseminated pancreatic cells by amplification of cytokeratin-19 with quantitative RT-PCR in blood, bone marrow and peritoneal lavage of pancreatic carcinoma patients. *World journal of gastroenterology : WJG,* 13, 257-63.

HOLMES, C. E., LEVIS, J. E. & ORNSTEIN, D. L. 2009. Activated platelets enhance ovarian cancer cell invasion in a cellular model of metastasis. *Clin Exp Metastasis.*

HOSKINS, W. J. 1995. Prospective on ovarian cancer: why prevent? *J Cell Biochem Suppl,* 23, 189-99.

HOSKINS, W. J., BUNDY, B. N., THIGPEN, J. T. & OMURA, G. A. 1992. The influence of cytoreductive surgery on recurrence-free interval and survival in small-volume stage III epithelial ovarian cancer: a Gynecologic Oncology Group study. *Gynecologic Oncology,* 47, 159-66.

HOU, X., KUMAR, A., LEE, C., WANG, B., ARJUNAN, P., DONG, L., MAMINISHKIS, A., TANG, Z., LI, Y., ZHANG, F., ZHANG, S. Z., WARDEGA, P., CHAKRABARTY, S., LIU, B., WU, Z., COLOSI, P., FARISS, R. N., LENNARTSSON, J., NUSSENBLATT, R., GUTKIND, J. S., CAO, Y. & LI, X. 2010. PDGF-CC blockade inhibits pathological angiogenesis by acting on multiple cellular and molecular targets. *Proc Natl Acad Sci U S A,* 107, 12216-21.

HU, F., XU, Y., ZHOU, D., HE, X. & YU, L. 2010. Novel human pathological mutations. Gene symbol: GCH1. Disease: dystonia, dopa-responsive. *Human genetics,* 127, 482.

HU, S. & YANG, X. 2003. Cellular Inhibitor of Apoptosis 1 and 2 Are Ubiquitin Ligases for the Apoptosis Inducer Smac/DIABLO. *Journal of Biological Chemistry,* 278, 10055-10060.

HUANG DA, W., SHERMAN, B. T. & LEMPICKI, R. A. 2008. Systematic and integrative analysis of large gene lists using DAVID bioinformatics resources. *Nat. Protocols,* 4, 44-57.

HUANG DA, W., SHERMAN, B. T. & LEMPICKI, R. A. 2009. Bioinformatics enrichment tools: paths toward the comprehensive functional analysis of large gene lists. *Nucleic acids research,* 37, 1-13.

HUANG, M. E., SOUCIET, J. L., CHUAT, J. C. & GALIBERT, F. 1996. Identification of ACT4, a novel essential actin-related gene in the yeast Saccharomyces cerevisiae. *Yeast,* 12, 839-48.

HUANG, R. S., DUAN, S., BLEIBEL, W. K., KISTNER, E. O., ZHANG, W., CLARK, T. A., CHEN, T. X., SCHWEITZER, A. C., BLUME, J. E., COX, N. J. & DOLAN, M. E. 2007a. A genome-wide approach to identify genetic variants that contribute to etoposide-induced cytotoxicity. *Proceedings of the National Academy of Sciences of the United States of America,* 104**,** 9758-63.

HUANG, X., SHI, Z., WANG, W., BAI, J., CHEN, Z., XU, J., ZHANG, D. & FU, S. 2007b. Identification and characterization of a novel protein ISOC2 that interacts with p16INK4a. *Biochemical and Biophysical Research Communications,* 361**,** 287-93.

HUHTINEN, K., SUVITIE, P., HIISSA, J., JUNNILA, J., HUVILA, J., KUJARI, H., SETALA, M., HARKKI, P., JALKANEN, J., FRASER, J., MAKINEN, J., AURANEN, A., POUTANEN, M. & PERHEENTUPA, A. 2009. Serum HE4 concentration differentiates malignant ovarian tumours from ovarian endometriotic cysts. *Br J Cancer,* 100**,** 1315-1319.

HUSSEINZADEH, N. 2011. Status of tumor markers in epithelial ovarian cancer has there been any progress? A review. *Gynecol Oncol,* 120**,** 152-7.

HUYNH, N., LIU, K. H., BALDWIN, G. S. & HE, H. 2010. P21-activated kinase 1 stimulates colon cancer cell growth and migration/invasion via ERK- and AKT-dependent pathways. *Biochimica et Biophysica Acta (BBA) - Molecular Cell Research,* 1803**,** 1106-1113.

HYNES, R. O. 1992. Integrins: versatility, modulation, and signaling in cell adhesion. *Cell,* 69**,** 11-25.

ICHISE, T., ADACHI, S., OHISHI, M., IKAWA, M., OKABE, M., IWAMOTO, R. & MEKADA, E. 2010. Humanized gene replacement in mice reveals the contribution of cancer stroma-derived HB-EGF to tumor growth. *Cell structure and function,* 35**,** 3-13.

IINUMA, H., WATANABE, T., MIMORI, K., ADACHI, M., HAYASHI, N., TAMURA, J., MATSUDA, K., FUKUSHIMA, R., OKINAGA, K., SASAKO, M. & MORI, M. 2011. Clinical Significance of Circulating Tumor Cells, Including Cancer Stem-Like Cells, in Peripheral Blood for Recurrence and Prognosis in Patients With Dukes' Stage B and C Colorectal Cancer. *Journal of Clinical Oncology,* 29**,** 1547-1555.

IKEDA, M., FURUKAWA, H., IMAMURA, H., SHIMIZU, J., ISHIDA, H., MASUTANI, S., TATSUTA, M. & SATOMI, T. 2002. Poor Prognosis Associated With Thrombocytosis in Patients With Gastric Cancer. *Ann Surg Oncol,* 9**,** 287-291.

IMANAKA, T., AIHARA, K., SUZUKI, Y., YOKOTA, S. & OSUMI, T. 2000. The 70-kDa peroxisomal membrane protein (PMP70), an ATP-binding cassette transporter. *Cell biochemistry and biophysics,* 32 Spring**,** 131-8.

INAGAKI, A., SLEDDENS-LINKELS, E., WASSENAAR, E., OOMS, M., VAN CAPPELLEN, W. A., HOEIJMAKERS, J. H., SEIBLER, J., VOGT, T. F., SHIN, M. K., GROOTEGOED, J. A. &

BAARENDS, W. M. 2011. Meiotic functions of RAD18. *Journal of cell science,* 124, 2837-50.

IRIZARRY, R. A., BOLSTAD, B. M., COLLIN, F., COPE, L. M., HOBBS, B. & SPEED, T. P. 2003a. Summaries of Affymetrix GeneChip probe level data. *Nucleic acids research,* 31, e15.

IRIZARRY, R. A., HOBBS, B., COLLIN, F., BEAZER-BARCLAY, Y. D., ANTONELLIS, K. J., SCHERF, U. & SPEED, T. P. 2003b. Exploration, normalization, and summaries of high density oligonucleotide array probe level data. *Biostatistics,* 4, 249-64.

ITALIANO, J. E., JR. & SHIVDASANI, R. A. 2003. Megakaryocytes and beyond: the birth of platelets. *Journal of thrombosis and haemostasis : JTH,* 1, 1174-82.

ITALIANO, J. E., RICHARDSON, J. L., PATEL-HETT, S., BATTINELLI, E., ZASLAVSKY, A., SHORT, S., RYEOM, S., FOLKMAN, J. & KLEMENT, G. L. 2008. Angiogenesis is regulated by a novel mechanism: pro- and antiangiogenic proteins are organized into separate platelet α granules and differentially released. *Blood,* 111, 1227-1233.

IYER, V. R. & LEE, S. I. 2010. MRI, CT, and PET/CT for ovarian cancer detection and adnexal lesion characterization. *AJR. American journal of roentgenology,* 194, 311-21.

JAABACK, K. S., LUDEMAN, L., CLAYTON, N. L. & HIRSCHOWITZ, L. 2006. Primary peritoneal carcinoma in a UK cancer center: comparison with advanced ovarian carcinoma over a 5-year period. *International Journal of Gynecological Cancer,* 16, 123-128.

JAYSON, G. C., PARKER, G. J., MULLAMITHA, S., VALLE, J. W., SAUNDERS, M., BROUGHTON, L., LAWRANCE, J., CARRINGTON, B., ROBERTS, C., ISSA, B., BUCKLEY, D. L., CHEUNG, S., DAVIES, K., WATSON, Y., ZINKEWICH-PEOTTI, K., ROLFE, L. & JACKSON, A. 2005. Blockade of platelet-derived growth factor receptor-beta by CDP860, a humanized, PEGylated di-Fab', leads to fluid accumulation and is associated with increased tumor vascularized volume. *J Clin Oncol,* 23, 973-81.

JELOVAC, D. & ARMSTRONG, D. K. 2011. Recent progress in the diagnosis and treatment of ovarian cancer. *CA: A Cancer Journal for Clinicians,* 61, 183-203.

JEMAL, A., BRAY, F., CENTER, M. M., FERLAY, J., WARD, E. & FORMAN, D. 2011. Global cancer statistics. *CA: A Cancer Journal for Clinicians,* 61, 69-90.

JEYACHANDRAN, Y. L., MIELCZARSKI, J. A., MIELCZARSKI, E. & RAI, B. 2010. Efficiency of blocking of non-specific interaction of different proteins by BSA adsorbed on hydrophobic and hydrophilic surfaces. *Journal of Colloid and Interface Science,* 341, 136-142.

JOHNSON & JOHNSON INC. 2011. *Veridex, LLC Announces Collaboration to Develop Next-Generation Circulating Tumor Cell (CTC) Technology with Massachusetts General*

Hospital [Online]. Available: http://www.jnj.com/connect/news/all/veridex-llc-announces-collaboration-to-develop-next-generation-circulating-tumor-cell-technology-with-massachusetts-general-hospital [Accessed 5 January 2011].

JOHNSON, J. M., CASTLE, J., GARRETT-ENGELE, P., KAN, Z., LOERCH, P. M., ARMOUR, C. D., SANTOS, R., SCHADT, E. E., STOUGHTON, R. & SHOEMAKER, D. D. 2003. Genome-wide survey of human alternative pre-mRNA splicing with exon junction microarrays. *Science,* 302**,** 2141-4.

JUBB, A. M., HURWITZ, H. I., BAI, W., HOLMGREN, E. B., TOBIN, P., GUERRERO, A. S., KABBINAVAR, F., HOLDEN, S. N., NOVOTNY, W. F., FRANTZ, G. D., HILLAN, K. J. & KOEPPEN, H. 2006. Impact of vascular endothelial growth factor-A expression, thrombospondin-2 expression, and microvessel density on the treatment effect of bevacizumab in metastatic colorectal cancer. *J Clin Oncol,* 24**,** 217-27.

JUDSON, P. L., GELLER, M. A., BLISS, R. L., BOENTE, M. P., DOWNS, L. S., ARGENTA, P. A. & CARSON, L. F. 2003. Preoperative detection of peripherally circulating cancer cells and its prognostic significance in ovarian cancer[small star, filled]. *Gynecologic Oncology,* 91**,** 389-394.

JURASZ, P., NORTH, S., VENNER, P. & RADOMSKI, M. W. 2003. Matrix metalloproteinase-2 contributes to increased platelet reactivity in patients with metastatic prostate cancer: a preliminary study. *Thrombosis Research,* 112**,** 59-64.

JURASZ, P., SAWICKI, G., DUSZYK, M., SAWICKA, J., MIRANDA, C., MAYERS, I. & RADOMSKI, M. W. 2001a. Matrix metalloproteinase 2 in tumor cell-induced platelet aggregation: regulation by nitric oxide. *Cancer Research,* 61**,** 376-82.

JURASZ, P., STEWART, M. W., RADOMSKI, A., KHADOUR, F., DUSZYK, M. & RADOMSKI, M. W. 2001b. Role of von Willebrand factor in tumour cell-induced platelet aggregation: differential regulation by NO and prostacyclin. *British Journal of Pharmacology,* 134**,** 1104-12.

JURK, K. & KEHREL, B. E. 2005. Platelets: Physiology and Biochemistry. *Seminars in Thrombosis and Hemostasis,* 31**,** 381,392.

KAIHARA, A., IWAGAKI, H., GOUCHI, A., HIZUTA, A., ISOZAKI, H., TAKAKURA, N. & TANAKA, N. 1998. Soluble intercellular adhesion molecule-1 and natural killer cell activity in gastric cancer patients. *Research communications in molecular pathology and pharmacology,* 100**,** 283-300.

KAKKAR, A. K. 2003a. Antithrombotics and cancer: evidence for survival benefit. 33 Suppl 1**,** 67.

KAKKAR, A. K. 2003b. Low-molecular-weight heparins: beyond thrombosis in the management of the cancer patient. *Seminars in Thrombosis and Hemostasis,* 29 Suppl 1**,** 13-5.

KALOF, A. N. & COOPER, K. 2006. p16INK4a Immunoexpression: Surrogate Marker of High-risk HPV and High-grade Cervical Intraepithelial Neoplasia. *Advances in Anatomic Pathology,* 13, 190-194.

KAMYKOWSKI, J., CARLTON, P., SEHGAL, S. & STORRIE, B. 2011. Quantitative immunofluorescence mapping reveals little functional coclustering of proteins within platelet α-granules. *Blood,* 118, 1370-1373.

KANDEMIR, E. G., MAYADAGLI, A., KARAGOZ, B., BILGI, O., TURKEN, O. & YAYLACI, M. 2005. Prognostic Significance of Thrombocytosis in Node-negative Colon Cancer. *The Journal of International Medical Research,* 33, 228-235.

KANNO, T., BUCHER, E., DAXINGER, L., HUETTEL, B., BOHMDORFER, G., GREGOR, W., KREIL, D. P., MATZKE, M. & MATZKE, A. J. M. 2008. A structural-maintenance-of-chromosomes hinge domain-containing protein is required for RNA-directed DNA methylation. *Nat Genet,* 40, 670-675.

KAPLAN, D. R., CHAO, F. C., STILES, C. D., ANTONIADES, H. N. & SCHER, C. D. 1979a. Platelet alpha granules contain a growth factor for fibroblasts. *Blood,* 53, 1043-52.

KAPLAN, K. L., BROEKMAN, M. J., CHERNOFF, A., LESZNIK, G. R. & DRILLINGS, M. 1979b. Platelet alpha-granule proteins: studies on release and subcellular localization. *Blood,* 53, 604-18.

KARIM-KOS, H. E., DE VRIES, E., SOERJOMATARAM, I., LEMMENS, V., SIESLING, S. & COEBERGH, J. W. 2008. Recent trends of cancer in Europe: a combined approach of incidence, survival and mortality for 17 cancer sites since the 1990s. *Eur J Cancer,* 44, 1345-89.

KARIM, R., JORDANOVA, E. S., PIERSMA, S. J., KENTER, G. G., CHEN, L., BOER, J. M., MELIEF, C. J. M. & VAN DER BURG, S. H. 2009. Tumor-Expressed B7-H1 and B7-DC in Relation to PD-1+ T-Cell Infiltration and Survival of Patients with Cervical Carcinoma. *Clinical Cancer Research,* 15, 6341-6347.

KASER, A., BRANDACHER, G., STEURER, W., KASER, S., OFFNER, F. A., ZOLLER, H., THEURL, I., WIDDER, W., MOLNAR, C., LUDWICZEK, O., ATKINS, M. B., MIER, J. W. & TILG, H. 2001. Interleukin-6 stimulates thrombopoiesis through thrombopoietin: role in inflammatory thrombocytosis. *Blood,* 98, 2720-2725.

KASHANI-SABET, M. 2010. Tumor progression by immune evasion in melanoma. *Cancer,* 116, 1623-1625.

KATO, T., MATSUMOTO, A., OGAMI, K., TAHARA, T., MORITA, H. & MIYAZAKI, H. 1998. Native thrombopoietin: structure and function. *Stem Cells,* 16, 322-8.

KAUFMANN, W. K., NEVIS, K. R., QU, P., IBRAHIM, J. G., ZHOU, T., ZHOU, Y., SIMPSON, D. A., HELMS-DEATON, J., CORDEIRO-STONE, M., MOORE, D. T., THOMAS, N. E., HAO,

H., LIU, Z., SHIELDS, J. M., SCOTT, G. A. & SHARPLESS, N. E. 2008. Defective cell cycle checkpoint functions in melanoma are associated with altered patterns of gene expression. *J Invest Dermatol,* 128**,** 175-87.

KAUSHANSKY, K. 2003. Thrombopoietin: a tool for understanding thrombopoiesis. *J Thromb Haemost,* 1**,** 1587-92.

KAUSHANSKY, K. & WILLIAMS, W. J. 2010. *Williams hematology,* New York/London, McGraw-Hill Medical.

KAY, C. 2010. *Aspirin Cuts Death Rates From Range of Cancers, Researchers Say* [Online]. Bloomberg Businessweek. Available: http://www.businessweek.com/news/2010-12-06/aspirin-cuts-death-rates-from-range-of-cancers-researchers-say.html [Accessed 10 December 2010].

KEATING, S. E., MALONEY, G. M., MORAN, E. M. & BOWIE, A. G. 2007. IRAK-2 Participates in Multiple Toll-like Receptor Signaling Pathways to NFκB via Activation of TRAF6 Ubiquitination. *Journal of Biological Chemistry,* 282**,** 33435-33443.

KEEN, T. J., HIMS, M. M., MCKIE, A. B., MOORE, A. T., DORAN, R. M., MACKEY, D. A., MANSFIELD, D. C., MUELLER, R. F., BHATTACHARYA, S. S., BIRD, A. C., MARKHAM, A. F. & INGLEHEARN, C. F. 2002. Mutations in a protein target of the Pim-1 kinase associated with the RP9 form of autosomal dominant retinitis pigmentosa. *European journal of human genetics : EJHG,* 10**,** 245-9.

KELLAND, K. 2010. *Study finds daily aspirin cuts many cancer risks* [Online]. Thomson Reuters. Available: http://www.reuters.com/article/2010/12/07/us-cancer-aspirin-idUSTRE6B601M20101207 [Accessed 10 December 2010].

KERR, M. C., BENNETTS, J. S., SIMPSON, F., THOMAS, E. C., FLEGG, C., GLEESON, P. A., WICKING, C. & TEASDALE, R. D. 2005. A Novel Mammalian Retromer Component, Vps26B. *Traffic,* 6**,** 991-1001.

KICHINA, J. V., GOC, A., AL-HUSEIN, B., SOMANATH, P. R. & KANDEL, E. S. 2010. PAK1 as a therapeutic target. *Expert opinion on therapeutic targets,* 14**,** 703-25.

KIM, D.-H., IIJIMA, H., GOTO, K., SAKAI, J., ISHII, H., KIM, H.-J., SUZUKI, H., KONDO, H., SAEKI, S. & YAMAMOTO, T. 1996. Human Apolipoprotein E Receptor 2. *Journal of Biological Chemistry,* 271**,** 8373-8380.

KIM, D. H., LEE, S. T., WON, H. H., KIM, S., KIM, M. J., KIM, H. J., KIM, S. H., KIM, J. W., KIM, Y. K., SOHN, S. K., MOON, J. H., JUNG, C. W. & LIPTON, J. H. 2011. A genome-wide association study identifies novel loci associated with susceptibility to chronic myeloid leukemia. *Blood,* 117**,** 6906-11.

KIM, E., LEE, Y., LEE, H.-J., KIM, J. S., SONG, B.-S., HUH, J.-W., LEE, S.-R., KIM, S.-U., KIM, S.-H., HONG, Y., SHIM, I. & CHANG, K.-T. 2010a. Implication of mouse Vps26b-Vps29-

Vps35 retromer complex in sortilin trafficking. *Biochemical and Biophysical Research Communications,* 403, 167-171.

KIM, H., SCORILAS, A., KATSAROS, D., YOUSEF, G. M., MASSOBRIO, M., FRACCHIOLI, S., PICCINNO, R., GORDINI, G. & DIAMANDIS, E. P. 2001. Human kallikrein gene 5 (KLK5) expression is an indicator of poor prognosis in ovarian cancer. *Br J Cancer,* 84, 643-50.

KIM, N. & LEE, C. 2008. Bioinformatics detection of alternative splicing. *Methods Mol Biol,* 452, 179-97.

KIM, Y. G., KIM, M. J., LIM, J. S., LEE, M. S., KIM, J. S. & YOO, Y. D. 2006. ICAM-3-induced cancer cell proliferation through the PI3K/Akt pathway. *Cancer Letters,* 239, 103-110.

KIM, Y. J., BORSIG, L., VARKI, N. M. & VARKI, A. 1998. P-selectin deficiency attenuates tumor growth and metastasis. *Proceedings of the National Academy of Sciences of the United States of America,* 95, 9325-30.

KIM, Y. S., HWAN, J. D., BAE, S., BAE, D. H. & SHICK, W. A. 2010b. Identification of differentially expressed genes using an annealing control primer system in stage III serous ovarian carcinoma. *BMC Cancer,* 10, 576.

KINDELBERGER, D. W., LEE, Y., MIRON, A., HIRSCH, M. S., FELTMATE, C., MEDEIROS, F., CALLAHAN, M. J., GARNER, E. O., GORDON, R. W., BIRCH, C., BERKOWITZ, R. S., MUTO, M. G. & CRUM, C. P. 2007. Intraepithelial Carcinoma of the Fimbria and Pelvic Serous Carcinoma: Evidence for a Causal Relationship. *The American Journal of Surgical Pathology,* 31, 161-169 10.1097/01.pas.0000213335.40358.47.

KIRCHES, E., KRAUSE, G., WARICH-KIRCHES, M., WEIS, S., SCHNEIDER, T., MEYER-PUTTLITZ, B., MAWRIN, C. & DIETZMANN, K. 2001. High frequency of mitochondrial DNA mutations in glioblastoma multiforme identified by direct sequence comparison to blood samples. *International Journal of Cancer,* 93, 534-538.

KOBAYASHI, H., BOELTE, K. C. & LIN, P. C. 2007. Endothelial Cell Adhesion Molecules and Cancer Progression. *Current Medicinal Chemistry,* 14, 377-386.

KOHLER, N. & LIPTON, A. 1974. Platelets as a source of fibroblast growth-promoting activity. *Exp Cell Res,* 87, 297-301.

KOHOUTEK, J. 2009. P-TEFb- the final frontier. *Cell division,* 4, 19.

KOJIC, S., NESTOROVIC, A., RAKICEVIC, L., BELGRANO, A., STANKOVIC, M., DIVAC, A. & FAULKNER, G. 2010. A novel role for cardiac ankyrin repeat protein Ankrd1/CARP as a co-activator of the p53 tumor suppressor protein. *Archives of Biochemistry and Biophysics,* 502, 60-67.

KONSTANTOPOULOS, K. & THOMAS, S. N. 2009. Cancer cells in transit: the vascular interactions of tumor cells. *Annual review of biomedical engineering,* 11, 177-202.

KOSARY, C. L. 2007. Cancer of the Ovary. *In:* RIES, L. A., YOUNG, J., KEEL, G., EISNER, M., LIN, Y. & HORNER, M.-J. (eds.) *Cancer survival among adults : U.S. SEER program, 1988-2001 : patient and tumor characteristics.* Bethesda, MD: U.S. Dept. of Health and Human Services, National Institutes of Health, National Cancer Institute.

KOUNTOURAKIS, P., PSYRRI, A., SCORILAS, A., MARKAKIS, S., KOWALSKI, D., CAMP, R. L., DIAMANDIS, E. P. & DIMOPOULOS, M. A. 2009. Expression and prognostic significance of kallikrein-related peptidase 8 protein levels in advanced ovarian cancer by using automated quantitative analysis. *Thrombosis and Haemostasis,* 101, 541-6.

KRAUS, S. & ARBER, N. 2011. Cancer: Do aspirin and other NSAIDs protect against colorectal cancer? *Nat Rev Gastroenterol Hepatol,* 8, 125-126.

KREBS, M. G., SLOANE, R., PRIEST, L., LANCASHIRE, L., HOU, J.-M., GREYSTOKE, A., WARD, T. H., FERRALDESCHI, R., HUGHES, A., CLACK, G., RANSON, M., DIVE, C. & BLACKHALL, F. H. 2011. Evaluation and Prognostic Significance of Circulating Tumor Cells in Patients With Non–Small-Cell Lung Cancer. *Journal of Clinical Oncology,* 29, 1556-1563.

KRISHNAN, A., NAIR, S. A. & PILLAI, M. R. 2007. Biology of PPAR gamma in cancer: a critical review on existing lacunae. *Current molecular medicine,* 7, 532-40.

KROPFF, M., KIENAST, J., BISPING, G., BERDEL, W. E., GASCHLER-MARKEFSKI, B., STOPFER, P., STEFANIC, M. & MUNZERT, G. 2009. An Open-label Dose-escalation Study of BIBF 1120 in Patients with Relapsed or Refractory Multiple Myeloma. *Anticancer Research,* 29, 4233-4238.

KUHNERT, F., TAM, B. Y., SENNINO, B., GRAY, J. T., YUAN, J., JOCSON, A., NAYAK, N. R., MULLIGAN, R. C., MCDONALD, D. M. & KUO, C. J. 2008. Soluble receptor-mediated selective inhibition of VEGFR and PDGFRbeta signaling during physiologic and tumor angiogenesis. *Proc Natl Acad Sci U S A,* 105, 10185-90.

KUMARAN, G. C., JAYSON, G. C. & CLAMP, A. R. 2009. Antiangiogenic drugs in ovarian cancer. *Br J Cancer,* 100, 1-7.

KURMAN, R. J. & SHIH, I.-M. 2011. Molecular pathogenesis and extraovarian origin of epithelial ovarian cancer—Shifting the paradigm. *Human pathology,* 42, 918-931.

KURMAN, R. J. & SHIH, M. 2010. The origin and pathogenesis of epithelial ovarian cancer: a proposed unifying theory. *The American Journal of Surgical Pathology,* 34, 433-43.

KUWAHARA, H., KAMEI, J.-I., NAKAMURA, N., MATSUMOTO, M., INOUE, H. & KANAZAWA, H. 2003. The Apoptosis-Inducing Protein Kinase DRAK2 Is Inhibited in a Calcium-Dependent Manner by the Calcium-Binding Protein CHP. *Journal of biochemistry,* 134, 245-250.

KUYUMCUOGLU, U., GUZEL, A. I., CELIK, Y. & ERDEMOGLU, M. 2010. The association of preoperative thrombocytosis with prognostic factors in malign ovarian tumor. *Eur J Gynaecol Oncol,* 31, 514-6.

L. WEISS, U. N. B. R. J. U. B. 1992. Lethal deformation of cancer cells in the microcirculation: A potential rate regulator of hematogenous metastasis. *International Journal of Cancer,* 50, 103-107.

LAIOS, A., O'TOOLE, S. A., FLAVIN, R., MARTIN, C., RING, M., GLEESON, N., D'ARCY, T., MCGUINNESS, E. P., SHEILS, O., SHEPPARD, B. L. & JJ, O. L. 2008. An integrative model for recurrence in ovarian cancer. *Mol Cancer,* 7, 8.

LAKOWICZ, J. R. & MASTERS, B. R. 2008. Principles of Fluorescence Spectroscopy, Third Edition. *Journal of Biomedical Optics,* 13, 029901.

LANGLEY, R. E., BURDETT, S., TIERNEY, J. F., CAFFERTY, F., PARMAR, M. K. B. & VENNING, G. 2011. Aspirin and cancer: has aspirin been overlooked as an adjuvant therapy[quest]. *Br J Cancer.*

LARKIN, D., TREUMANN, A., MURPHY, D., DECHAUMONT, C., KIERNAN, A. & MORAN, N. 2009. Compartmentalization regulates the interaction between the platelet integrin αIIbβ3 and ICln. *British Journal of Haematology,* 144, 580-590.

LARSEN, E., CELI, A., GILBERT, G. E., FURIE, B. C., ERBAN, J. K., BONFANTI, R., WAGNER, D. D. & FURIE, B. 1989. PADGEM protein: a receptor that mediates the interaction of activated platelets with neutrophils and monocytes. *Cell,* 59, 305-12.

LATREMOLIERE, A. & COSTIGAN, M. 2011. GCH1, BH4 and Pain. *Current pharmaceutical biotechnology.*

LAVIE, O., COMERCI, G., DARAS, V., BOLGER, B. S., LOPES, A. & MONAGHAN, J. M. 1999. Thrombocytosis in women with vulvar carcinoma. *Gynecol Oncol,* 72, 82-6.

LAVORGNA, A., DE FILIPPI, R., FORMISANO, S. & LEONARDI, A. 2009. TNF receptor-associated factor 1 is a positive regulator of the NF-[kappa]B alternative pathway. *Molecular Immunology,* 46, 3278-3282.

LAW, D. A., NANNIZZI-ALAIMO, L. & PHILLIPS, D. R. 1996. Outside-in Integrin Signal Transduction. *Journal of Biological Chemistry,* 271, 10811-10815.

LAWRENCE, S. P., BRIGHT, N. A., LUZIO, J. P. & BOWERS, K. 2010. The sodium/proton exchanger NHE8 regulates late endosomal morphology and function. *Molecular biology of the cell,* 21, 3540-51.

LAWSON, C. & WOLF, S. 2009. ICAM-1 signaling in endothelial cells. *Pharmacological reports : PR,* 61, 22-32.

LEE, A. Y. & LEVINE, M. N. 2003. Venous thromboembolism and cancer: risks and outcomes. *Circulation,* 107, I17-21.

LEE, A. Y., LEVINE, M. N., BAKER, R. I., BOWDEN, C., KAKKAR, A. K., PRINS, M., RICKLES, F. R., JULIAN, J. A., HALEY, S., KOVACS, M. J., GENT, M. & 2003. Low-molecular-weight heparin versus a coumarin for the prevention of recurrent venous thromboembolism in patients with cancer. *The New England Journal of Medicine,* 349, 146-53.

LEE, C. & ROY, M. 2004. Analysis of alternative splicing with microarrays: successes and challenges. *Genome Biol,* 5, 231.

LEE, M., KIM, S. W., NAM, E. J., YIM, G. W., KIM, S. & KIM, Y. T. 2011. The impact of pretreatment thrombocytosis and persistent thrombocytosis after adjuvant chemotherapy in patients with advanced epithelial ovarian cancer. *Gynecologic Oncology,* 122, 238-241.

LEE, M. G., NORMAN, J., SHILATIFARD, A. & SHIEKHATTAR, R. 2007. Physical and functional association of a trimethyl H3K4 demethylase and Ring6a/MBLR, a polycomb-like protein. *Cell,* 128, 877-87.

LEE, M. H., MOON, Y. J., HA, C. W. & HOH, J. K. 2009. Ovarian thecoma with virilizing manifestations. *Yonsei medical journal,* 50, 169-73.

LEE, S. Y. & CHOI, Y. 2007. TRAF1 and Its Biological Functions. *In:* WU, H. (ed.) *TNF Receptor Associated Factors (TRAFs).* Springer New York.

LEEMHUIS, J., BOUCHE, E., FROTSCHER, M., HENLE, F., HEIN, L., HERZ, J., MEYER, D. K., PICHLER, M., ROTH, G., SCHWAN, C. & BOCK, H. H. 2010. Reelin signals through apolipoprotein E receptor 2 and Cdc42 to increase growth cone motility and filopodia formation. *J Neurosci,* 30, 14759-72.

LEITZMANN, M. F., KOEBNICK, C., DANFORTH, K. N., BRINTON, L. A., MOORE, S. C., HOLLENBECK, A. R., SCHATZKIN, A. & LACEY, J. V. 2009. Body mass index and risk of ovarian cancer. *Cancer,* 115, 812-822.

LERNER, D. L., WALSH, C. S., CASS, I., KARLAN, B. Y. & LI, A. J. 2007. The prognostic significance of thrombocytosis in uterine papillary serous carcinomas. *Gynecologic Oncology,* 104, 91-94.

LESNIKOVA, I., LIDANG, M., HAMILTON-DUTOIT, S. & KOCH, J. 2009. p16 as a diagnostic marker of cervical neoplasia: a tissue microarray study of 796 archival specimens. *Diagnostic pathology,* 4, 22.

LEVIN, J. & CONLEY, C. L. 1964. Thrombocytosis Associated with Malignant Disease. *Arch Intern Med,* 114, 497-500.

LEVINE, M. N. & LEE, A. Y. Y. 2001. Treatment of Venous Thrombosis in the Cancer Patient. *Acta Haematologica,* 106, 81-87.

LEVKAU, B., KOYAMA, H., RAINES, E. W., CLURMAN, B. E., HERREN, B., ORTH, K., ROBERTS, J. M. & ROSS, R. 1998. Cleavage of p21Cip1/Waf1 and p27Kip1 mediates apoptosis in endothelial cells through activation of Cdk2: role of a caspase cascade. *Molecular cell,* 1, 553-63.

LEWIS, F., MAUGHAN, N. J., SMITH, V., HILLAN, K. & QUIRKE, P. 2001. Unlocking the archive--gene expression in paraffin-embedded tissue. *J Pathol,* 195, 66-71.

LI, A. J., MADDEN, A. C., CASS, I., LEUCHTER, R. S., LAGASSE, L. D. & KARLAN, B. Y. 2004. The prognostic significance of thrombocytosis in epithelial ovarian carcinoma. *Gynecologic Oncology,* 92, 211-214.

LI, C., WANG, S., YUAN, H., LI, W., LI, Z., LI, X., GUO, X. & LI, F. 2008a. [The mutation and expression of MUS81 gene in laryngeal squamous cell carcinoma]. *Zhonghua yi xue yi chuan xue za zhi = Zhonghua yixue yichuanxue zazhi = Chinese journal of medical genetics,* 25, 560-5.

LI, J., SMYTH, P., CAHILL, S., DENNING, K., FLAVIN, R., AHERNE, S., PIROTTA, M., GUENTHER, S. M., O'LEARY, J. J. & SHEILS, O. 2008b. Improved RNA quality and TaqMan Pre-amplification method (PreAmp) to enhance expression analysis from formalin fixed paraffin embedded (FFPE) materials. *BMC Biotechnol,* 8, 10.

LI, X. & ERIKSSON, U. 2003. Novel PDGF family members: PDGF-C and PDGF-D. *Cytokine Growth Factor Rev,* 14, 91-8.

LI, X., PONTEN, A., AASE, K., KARLSSON, L., ABRAMSSON, A., UUTELA, M., BACKSTROM, G., HELLSTROM, M., BOSTROM, H., LI, H., SORIANO, P., BETSHOLTZ, C., HELDIN, C.-H., ALITALO, K., OSTMAN, A. & ERIKSSON, U. 2000. PDGF-C is a new protease-activated ligand for the PDGF [alpha]-receptor. *Nat Cell Biol,* 2, 302-309.

LI, Y., HETET, G., KILADJIAN, J. J., GARDIN, C., GRANDCHAMP, B. & BRIERE, J. 1996. Proto-oncogene c-mpl is involved in spontaneous megakaryocytopoiesis in myeloproliferative disorders. *Br J Haematol,* 92, 60-6.

LIN, P. S., MARSHALL, N. F. & DAHMUS, M. E. 2002. CTD phosphatase: role in RNA polymerase II cycling and the regulation of transcript elongation. *Progress in nucleic acid research and molecular biology,* 72, 333-65.

LINDAHL, P., JOHANSSON, B. R., LEVEEN, P. & BETSHOLTZ, C. 1997. Pericyte loss and microaneurysm formation in PDGF-B-deficient mice. *Science,* 277**,** 242-5.

LING, J., WIEDERKEHR, U., CABINESS, S., SHROYER, K. R. & ROBINSON, J. P. 2008. Application of flow cytometry for biomarker-based cervical cancer cells detection. *Diagnostic Cytopathology,* 36**,** 76-84.

LIU, M. C., SHIELDS, P. G., WARREN, R. D., COHEN, P., WILKINSON, M., OTTAVIANO, Y. L., RAO, S. B., ENG-WONG, J., SEILLIER-MOISEIWITSCH, F., NOONE, A.-M. & ISAACS, C. 2009. Circulating Tumor Cells: A Useful Predictor of Treatment Efficacy in Metastatic Breast Cancer. *Journal of Clinical Oncology,* 27**,** 5153-5159.

LIU, X.-M., PEYTON, K. J., SHEBIB, A. R., WANG, H., KORTHUIS, R. J. & DURANTE, W. 2011. Activation of AMPK stimulates heme oxygenase-1 gene expression and human endothelial cell survival. *American Journal of Physiology - Heart and Circulatory Physiology,* 300**,** H84-H93.

LIVAK, K. J. & SCHMITTGEN, T. D. 2001. Analysis of relative gene expression data using real-time quantitative PCR and the 2(-Delta Delta C(T)) Method. *Methods,* 25**,** 402-8.

LLOYD, R. V., ERICKSON, L. A., JIN, L., KULIG, E., QIAN, X., CHEVILLE, J. C. & SCHEITHAUER, B. W. 1999. p27kip1: a multifunctional cyclin-dependent kinase inhibitor with prognostic significance in human cancers. *The American Journal of Pathology,* 154**,** 313-23.

LOHELA, M., BRY, M., TAMMELA, T. & ALITALO, K. 2009. VEGFs and receptors involved in angiogenesis versus lymphangiogenesis. *Curr Opin Cell Biol,* 21**,** 154-65.

LOKMAN, N., WEEN, M., OEHLER, M. & RICCIARDELLI, C. 2011. The Role of Annexin A2 in Tumorigenesis and Cancer Progression. *Cancer Microenvironment,* 4**,** 199-208.

LONG, E. O. 2011. ICAM-1: Getting a Grip on Leukocyte Adhesion. *The Journal of Immunology,* 186**,** 5021-5023.

LORETO, M. F., DE MARTINIS, M., CORSI, M. P., MODESTI, M. & GINALDI, L. 2000. Coagulation and cancer: implications for diagnosis and management. *Pathology Oncology Research : Por,* 6**,** 301-12.

LU, C., THAKER, P. H., LIN, Y. G., SPANNUTH, W., LANDEN, C. N., MERRITT, W. M., JENNINGS, N. B., LANGLEY, R. R., GERSHENSON, D. M., YANCOPOULOS, G. D., ELLIS, L. M., JAFFE, R. B., COLEMAN, R. L. & SOOD, A. K. 2008. Impact of vessel maturation on antiangiogenic therapy in ovarian cancer. *Am J Obstet Gynecol,* 198**,** 477 e1-9; discussion 477 e9-10.

LU, C. C., CHANG, K. W., CHOU, F. C., CHENG, C. Y. & LIU, C. J. 2007. Association of pretreatment thrombocytosis with disease progression and survival in oral squamous cell carcinoma. *Oral oncology,* 43, 283-288.

LU, J., SHARMA, L. K. & BAI, Y. 2009. Implications of mitochondrial DNA mutations and mitochondrial dysfunction in tumorigenesis. *Cell Res,* 19, 802-815.

LUO, L. & KESSEL, M. 2004. Geminin coordinates cell cycle and developmental control. *Cell Cycle,* 3, 711-4.

LUO, T., YAN, H.-M., HE, P., LUO, Y., YANG, Y.-F. & ZHENG, H. Aspirin use and breast cancer risk: a meta-analysis. *Breast Cancer Research and Treatment*, 1-7.

LUTTERS, B. C. H., DERKSEN, R. H. W. M., TEKELENBURG, W. L., LENTING, P. J., ARNOUT, J. & DE GROOT, P. G. 2003. Dimers of β2-Glycoprotein I Increase Platelet Deposition to Collagen via Interaction with Phospholipids and the Apolipoprotein E Receptor 2'. *Journal of Biological Chemistry,* 278, 33831-33838.

MADHAVAN, M., SRINIVAS, P., ABRAHAM, E., AHMED, I., VIJAYALEKSHMI, N. R. & BALARAM, P. 2002. Down regulation of endothelial adhesion molecules in node positive breast cancer: possible failure of host defence mechanism. *Pathology Oncology Research : Por,* 8, 125-8.

MAEDA, K., KANG, S. M., SAWADA, T., NISHIGUCHI, Y., YASHIRO, M., OGAWA, Y., OHIRA, M., ISHIKAWA, T. & HIRAKAWA, Y. S. C. K. 2002. Expression of intercellular adhesion molecule-1 and prognosis in colorectal cancer. *Oncology reports,* 9, 511-4.

MAGKLARA, A., SCORILAS, A., KATSAROS, D., MASSOBRIO, M., YOUSEF, G. M., FRACCHIOLI, S., DANESE, S. & DIAMANDIS, E. P. 2001. The human KLK8 (neuropsin/ovasin) gene: identification of two novel splice variants and its prognostic value in ovarian cancer. *Clin Cancer Res,* 7, 806-11.

MAGOULAS, C. & FRIED, M. 1996. The Surf-6 gene of the mouse surfeit locus encodes a novel nucleolar protein. *DNA and cell biology,* 15, 305-16.

MAITA, H., KITAURA, H., KEEN, T. J., INGLEHEARN, C. F., ARIGA, H. & IGUCHI-ARIGA, S. M. M. 2004. PAP-1, the mutated gene underlying the RP9 form of dominant retinitis pigmentosa, is a splicing factor. *Experimental Cell Research,* 300, 283-296.

MALIK, A. B. 1983. Pulmonary microembolism. *Physiological Reviews,* 63, 1114-207.

MALVEZZI, M., ARFE, A., BERTUCCIO, P., LEVI, F., LA VECCHIA, C. & NEGRI, E. 2011. European cancer mortality predictions for the year 2011. *Annals of oncology : official journal of the European Society for Medical Oncology / ESMO,* 22, 947-56.

MANENTI, L., PAGANONI, P., FLORIANI, I., LANDONI, F., TORRI, V., BUDA, A., TARABOLETTI, G., LABIANCA, R., BELOTTI, D. & GIAVAZZI, R. 2003. Expression levels of vascular endothelial growth factor, matrix metalloproteinases 2 and 9 and tissue inhibitor of metalloproteinases 1 and 2 in the plasma of patients with ovarian carcinoma. *Eur J Cancer,* 39**,** 1948-56.

MANJASETTY, B. A., BUSSOW, K., FIEBER-ERDMANN, M., ROSKE, Y., GOBOM, J., SCHEICH, C., GOTZ, F., NIESEN, F. H. & HEINEMANN, U. 2006. Crystal structure of Homo sapiens PTD012 reveals a zinc-containing hydrolase fold. *Protein science : a publication of the Protein Society,* 15**,** 914-20.

MANTIA-SMALDONE, G. M., EDWARDS, R. P. & VLAD, A. M. 2011. Targeted treatment of recurrent platinum-resistant ovarian cancer: current and emerging therapies. *Cancer management and research,* 3**,** 25-38.

MARCHIONE, M. 2011. *Blood Test to Spot Cancer Gets Big Boost* [Online]. AOL News. Available: http://www.aolnews.com/2011/01/03/liquid-biopsy-a-blood-test-to-spot-cancer-gets-big-boost-fro/ [Accessed 5 January 2011].

MARKERT, A., GRIMM, M., MARTINEZ, J., WIESNER, J., MEYERHANS, A., MEYUHAS, O., SICKMANN, A. & FISCHER, U. 2008. The La-related protein LARP7 is a component of the 7SK ribonucleoprotein and affects transcription of cellular and viral polymerase II genes. *EMBO reports,* 9**,** 569-75.

MARKMAN, M. 2011. Addition of bevacizumab to weekly paclitaxel significantly improves progression-free survival in heavily pretreated recurrent epithelial ovarian cancer. *Gynecologic Oncology*.

MARSTON, S., BURTON, D., COPELAND, O., FRASER, I., GAO, Y., HODGKINSON, J., HUBER, P., LEVINE, B., EL-MEZGUELDI, M. & NOTARIANNI, G. 1998. Structural interactions between actin, tropomyosin, caldesmon and calcium binding protein and the regulation of smooth muscle thin filaments. *Acta physiologica Scandinavica,* 164**,** 401-14.

MARSTON, S. & EL-MEZGUELDI, M. 2008. Role of tropomyosin in the regulation of contraction in smooth muscle. *Advances in experimental medicine and biology,* 644**,** 110-23.

MARTIN-MARCOS, P., HINNEBUSCH, A. G. & TAMAME, M. 2007. Ribosomal protein L33 is required for ribosome biogenesis, subunit joining, and repression of GCN4 translation. *Molecular and cellular biology,* 27**,** 5968-85.

MATEI, D., EMERSON, R. E., LAI, Y. C., BALDRIDGE, L. A., RAO, J., YIANNOUTSOS, C. & DONNER, D. D. 2006. Autocrine activation of PDGFRalpha promotes the progression of ovarian cancer. *Oncogene,* 25**,** 2060-9.

MATEI, D., KELICH, S., CAO, L., MENNING, N., EMERSON, R. E., RAO, J., JENG, M. H. & SLEDGE, G. W. 2007. PDGF BB induces VEGF secretion in ovarian cancer. *Cancer Biol Ther,* 6, 1951-9.

MATEI, D., SANCHEZ, K., KELLEY, M., BALDRIDGE, L. A., WILLIAMS, S., CHANG, D. & JENG, M. H. 2003. PDGFR A is overexpressed in ovarian carcinomas and represents a potential therapeutic target *Proc Am Soc Clin Oncol,* 22.

MATEI, D., SILL, M. W., LANKES, H. A., DEGEEST, K., BRISTOW, R. E., MUTCH, D., YAMADA, S. D., COHN, D., CALVERT, V., FARLEY, J., PETRICOIN, E. F. & BIRRER, M. J. 2011. Activity of sorafenib in recurrent ovarian cancer and primary peritoneal carcinomatosis: a gynecologic oncology group trial. *Journal of clinical oncology : official journal of the American Society of Clinical Oncology,* 29, 69-75.

MATHEW, P., TANNIR, N., TU, S. M., WEN, S., GUO, C. C., MARCOTT, V., BEKELE, B. N. & PAGLIARO, L. 2011. Accelerated disease progression in prostate cancer and bone metastases with platelet-derived growth factor receptor inhibition: observations with tandutinib. *Cancer Chemother Pharmacol.*

MATSUI, T., HEIDARAN, M., MIKI, T., POPESCU, N., LA ROCHELLE, W., KRAUS, M., PIERCE, J. & AARONSON, S. 1989. Isolation of a novel receptor cDNA establishes the existence of two PDGF receptor genes. *Science,* 243, 800-4.

MATSUKAWA, T., WANG, X., LIU, R., WORTHAM, N., ONUKI, Y., KUBOTA, A., HIDA, A., KOWA, H., FUKUDA, Y., ISHIURA, H., MITSUI, J., TAKAHASHI, Y., AOKI, S., TAKIZAWA, S., SHIMIZU, J., GOTO, J., PROUD, C. & TSUJI, S. 2011. Adult-onset leukoencephalopathies with vanishing white matter with novel missense mutations in <i>EIF2B2</i>, <i>EIF2B3</i>, and <i>EIF2B5</i&gt. *neurogenetics*, 1-3.

MATTHIJS, G., SCHOLLEN, E., PARDON, E., VEIGA-DA-CUNHA, M., JAEKEN, J., CASSIMAN, J. J. & VAN SCHAFTINGEN, E. 1997. Mutations in PMM2, a phosphomannomutase gene on chromosome 16p13, in carbohydrate-deficient glycoprotein type I syndrome (Jaeken syndrome). *Nature genetics,* 16, 88-92.

MATULONIS, U. A., BERLIN, S., IVY, P., TYBURSKI, K., KRASNER, C., ZARWAN, C., BERKENBLIT, A., CAMPOS, S., HOROWITZ, N., CANNISTRA, S. A., LEE, H., LEE, J., ROCHE, M., HILL, M., WHALEN, C., SULLIVAN, L., TRAN, C., HUMPHREYS, B. D. & PENSON, R. T. 2009. Cediranib, an oral inhibitor of vascular endothelial growth factor receptor kinases, is an active drug in recurrent epithelial ovarian, fallopian tube, and peritoneal cancer. *Journal of clinical oncology : official journal of the American Society of Clinical Oncology,* 27, 5601-6.

MAUN, N. A., SPEICHER, D. W., DINUBILE, M. J. & SOUTHWICK, F. S. 1996. Purification and properties of a Ca(2+)-independent barbed-end actin filament capping protein, CapZ, from human polymorphonuclear leukocytes. *Biochemistry,* 35, 3518-24.

MAYER, M. P., HAHN, F. M., STILLMAN, D. J. & POULTER, C. D. 1992. Disruption and mapping of IDI1, the gene for isopentenyl diphosphate isomerase in Saccharomyces cerevisiae. *Yeast,* 8, 743-8.

MAYR, D., KANITZ, V., ANDEREGG, B., LUTHARDT, B., ENGEL, J., LÖHRS, U., AMANN, G. & DIEBOLD, J. 2006. Analysis of Gene Amplification and Prognostic Markers in Ovarian Cancer Using Comparative Genomic Hybridization for Microarrays and Immunohistochemical Analysis for Tissue Microarrays. *American Journal of Clinical Pathology,* 126, 101-109.

MCDONAGH, M. 2011. Improved access to genetic service could cut cancer mortality rates. *The Irish Times*, 21/06/2011.

MCGHEE, M. F. 2008. *A guide to laboratory investigations,* Oxford, Radcliffe.

MCKENZIE, M. & RYAN, M. T. 2010. Assembly factors of human mitochondrial complex I and their defects in disease. *IUBMB Life,* 62, 497-502.

MCLEMORE, M. R. & AOUIZERAT, B. 2005. Introducing the MUC16 gene: implications for prevention and early detection in epithelial ovarian cancer. *Biol Res Nurs,* 6, 262-7.

MCPHERSON, J. P., LEMMERS, B., CHAHWAN, R., PAMIDI, A., MIGON, E., MATYSIAK-ZABLOCKI, E., MOYNAHAN, M. E., ESSERS, J., HANADA, K., POONEPALLI, A., SANCHEZ-SWEATMAN, O., KHOKHA, R., KANAAR, R., JASIN, M., HANDE, M. P. & HAKEM, R. 2004. Involvement of mammalian Mus81 in genome integrity and tumor suppression. *Science,* 304, 1822-6.

MEDINA, C., JURASZ, P., SANTOS-MARTINEZ, M. J., JEONG, S. S., MITSKY, T., CHEN, R. & RADOMSKI, M. 2006. Platelet Aggregation-Induced by Caco-2 Cells: Regulation by Matrix Mealloproteinase-2 and Adenosine Diphosphate. *J Pharmacol Exp Ther,* jpet.105.098384.

MELIXETIAN, M., BALLABENI, A., MASIERO, L., GASPARINI, P., ZAMPONI, R., BARTEK, J., LUKAS, J. & HELIN, K. 2004. Loss of Geminin induces rereplication in the presence of functional p53. *J Cell Biol,* 165, 473-82.

MELIXETIAN, M. & HELIN, K. 2004. Geminin: a major DNA replication safeguard in higher eukaryotes. *Cell Cycle,* 3, 1002-4.

MENCZER, J., SCHEJTER, E., GEVA, D., GINATH, S. & ZAKUT, H. 1998. Ovarian carcinoma associated thrombocytosis. Correlation with prognostic factors and with survival. *Eur J Gynaecol Oncol,* 19, 82-4.

MENDELSOHN, M. E., O'NEILL, S., GEORGE, D. & LOSCALZO, J. 1990. Inhibition of fibrinogen binding to human platelets by S-nitroso-N-acetylcysteine. *Journal of Biological Chemistry,* 265, 19028-34.

MENDELSOHN, M. E., ZHU, Y. & O'NEILL, S. 1991. The 29-kDa proteins phosphorylated in thrombin-activated human platelets are forms of the estrogen receptor-related 27-kDa heat shock protein. *Proceedings of the National Academy of Sciences,* 88, 11212-11216.

MENON, U., GENTRY-MAHARAJ, A., HALLETT, R., RYAN, A., BURNELL, M., SHARMA, A., LEWIS, S., DAVIES, S., PHILPOTT, S., LOPES, A., GODFREY, K., ORAM, D., HEROD, J., WILLIAMSON, K., SEIF, M. W., SCOTT, I., MOULD, T., WOOLAS, R., MURDOCH, J., DOBBS, S., AMSO, N. N., LEESON, S., CRUICKSHANK, D., MCGUIRE, A., CAMPBELL, S., FALLOWFIELD, L., SINGH, N., DAWNAY, A., SKATES, S. J., PARMAR, M. & JACOBS, I. 2009. Sensitivity and specificity of multimodal and ultrasound screening for ovarian cancer, and stage distribution of detected cancers: results of the prevalence screen of the UK Collaborative Trial of Ovarian Cancer Screening (UKCTOCS). *The Lancet Oncology,* 10, 327-340.

MIESBACH, W. 2009. Malignancies and catastrophic anti-phospholipid syndrome. *Clin Rev Allergy Immunol,* 36, 91-7.

MINAMI, S. S., SUNG, Y. M., DUMANIS, S. B., CHI, S. H., BURNS, M. P., ANN, E. J., SUZUKI, T., TURNER, R. S., PARK, H. S., PAK, D. T., REBECK, G. W. & HOE, H. S. 2010. The cytoplasmic adaptor protein X11alpha and extracellular matrix protein Reelin regulate ApoE receptor 2 trafficking and cell movement. *FASEB J,* 24, 58-69.

MIYAMOTO, S., HIRATA, M., YAMAZAKI, A., KAGEYAMA, T., HASUWA, H., MIZUSHIMA, H., TANAKA, Y., YAGI, H., SONODA, K., KAI, M., KANOH, H., NAKANO, H. & MEKADA, E. 2004. Heparin-Binding EGF-Like Growth Factor Is a Promising Target for Ovarian Cancer Therapy. *Cancer Research,* 64, 5720-5727.

MOAYYEDI, P. & JANKOWSKI, J. A. 2010. Does long term aspirin prevent cancer? *BMJ,* 341.

MODAN, B., HARTGE, P., HIRSH-YECHEZKEL, G., CHETRIT, A., LUBIN, F., BELLER, U., BEN-BARUCH, G., FISHMAN, A., MENCZER, J., STRUEWING, J. P., TUCKER, M. A. & WACHOLDER, S. 2001. Parity, oral contraceptives, and the risk of ovarian cancer among carriers and noncarriers of a BRCA1 or BRCA2 mutation. *The New England Journal of Medicine,* 345, 235-40.

MODREK, B. & LEE, C. 2002. A genomic view of alternative splicing. *Nat Genet,* 30, 13-9.

MODUGNO, F. 2003. Ovarian cancer and high-risk women-implications for prevention, screening, and early detection. *Gynecologic Oncology,* 91, 15-31.

MODUGNO, F., NESS, R. B. & ALLEN, G. O. 2003. Alcohol consumption and the risk of mucinous and nonmucinous epithelial ovarian cancer. *Obstetrics and gynecology,* 102, 1336-43.

MOLLER, H., LINKLATER, K. M. & ROBINSON, D. 2009. A visual summary of the EUROCARE-4 results: a UK perspective. *Br J Cancer,* 101 Suppl 2, S110-4.

MONREAL, M., FERNANDEZ-LLAMAZARES, J., PERANDREU, J., URRUTIA, A., SAHUQUILLO, J. C. & CONTEL, E. 1997. Occult cancer in patients with venous thromboembolism: which patients, which cancers. *Thromb Haemost,* 78, 1316-8.

MOORE, R. G., MACLAUGHLAN, S. & BAST, R. C., JR. 2010. Current state of biomarker development for clinical application in epithelial ovarian cancer. *Gynecol Oncol,* 116, 240-5.

MOORE, T. 2010. *Daily Dose Of Aspirin Could Cut Cancer Risk* [Online]. Sky News/BSkyB. Available: http://news.sky.com/skynews/Article/201012115848891?chooseNews=Business [Accessed 10 December 2011].

MORI, T., LI, Y., HATA, H. & KOCHI, H. 2004. NIRF is a ubiquitin ligase that is capable of ubiquitinating PCNP, a PEST-containing nuclear protein. *FEBS Letters,* 557, 209-214.

MORI, T., LI, Y., HATA, H., ONO, K. & KOCHI, H. 2002. NIRF, a novel RING finger protein, is involved in cell-cycle regulation. *Biochemical and Biophysical Research Communications,* 296, 530-536.

MORONEY, J. W., SOOD, A. K. & COLEMAN, R. L. 2009. Aflibercept in epithelial ovarian carcinoma. *Future oncology,* 5, 591-600.

MOUSA, S. 2008. Cell Adhesion Molecules: Potential Therapeutic & Diagnostic Implications. *Molecular Biotechnology,* 38, 33-40.

MROSS, K., STEFANIC, M., GMEHLING, D., FROST, A., BAAS, F., UNGER, C., STRECKER, R., HENNING, J., GASCHLER-MARKEFSKI, B., STOPFER, P., DE ROSSI, L. & KAISER, R. 2010. Phase I Study of the Angiogenesis Inhibitor BIBF 1120 in Patients with Advanced Solid Tumors. *Clinical Cancer Research,* 16, 311-319.

MUELLER, B. M., REISFELD, R. A., EDGINGTON, T. S. & RUF, W. 1992. Expression of tissue factor by melanoma cells promotes efficient hematogenous metastasis. *Proc Natl Acad Sci U S A,* 89, 11832-6.

MUELLER, O., LIGHTFOOT, S. & SCHROEDER, A. 2004. RNA Integrity Number (RIN) – Standardization of RNA Quality Control. Available: http://www.chem.agilent.com/en-us/Search/Library/_layouts/Agilent/PrimaryDocumentViewer.ashx?whid=37507.

MULLENDERS, J., FABIUS, A. W. M., VAN DONGEN, M. M. W., KUIKEN, H. J., BEIJERSBERGEN, R. L. & BERNARDS, R. 2010. Interleukin-1R–Associated Kinase 2 Is

a Novel Modulator of the Transforming Growth Factor β Signaling Cascade. *Molecular Cancer Research,* 8, 592-603.

MUNDHENKE, C., WEIGEL, M. T., STURNER, K. H., ROESEL, F., MEINHOLD-HEERLEIN, I., BAUERSCHLAG, D. O., SCHEM, C., HILPERT, F., JONAT, W. & MAASS, N. 2008. Novel treatment of ovarian cancer cell lines with Imatinib mesylate combined with Paclitaxel and Carboplatin leads to receptor-mediated antiproliferative effects. *J Cancer Res Clin Oncol,* 134, 1397-405.

MURAKAMI, M., MIYAMOTO, T., IIDA, T., TSUKADA, H., WATANABE, M., SHIDA, M., MAEDA, H., NASU, S., YASUDA, S., YASUDA, M. & IDE, M. 2006. Whole-body positron emission tomography and tumor marker CA125 for detection of recurrence in epithelial ovarian cancer. *International journal of gynecological cancer : official journal of the International Gynecological Cancer Society,* 16 Suppl 1, 99-107.

NAKAYAMA, N., NAKAYAMA, K., YEASMIN, S., ISHIBASHI, M., KATAGIRI, A., IIDA, K., FUKUMOTO, M. & MIYAZAKI, K. 2008. KRAS or BRAF mutation status is a useful predictor of sensitivity to MEK inhibition in ovarian cancer. *Br J Cancer,* 99, 2020-2028.

NASH, G. F., TURNER, L. F., SCULLY, M. F. & KAKKAR, A. K. 2002. Platelets and cancer. *Lancet Oncol,* 3, 425-30.

NATHER, A., MAYERHOFER, K., GRIMM, C., HEFLER, L., LEODOLTER, S., OBERMAIR, A. & JOURA, E. A. 2003. Thrombocytosis and anaemia in women with recurrent ovarian cancer prior to a second-line chemotherapy. *Anticancer Res,* 23, 2991-4.

NCRI 2006. Women and Cancer in Ireland 1994-2001. National Cancer Registry (Ireland).

NCRI 2009. Cancer in Ireland 1994-2007: Annual report of the National Cancer Registry. The National Cancer Registry of Ireland.

NCRI 2011a. Cancer in Ireland 2011: Annual report of the National Cancer Registry. *In:* IRELAND, N. C. R. O. (ed.). Cork, Ireland: National Cancer Registry of Ireland.

NCRI 2011b. Cancer of the ovary (& uterine adnexa including fallopian tubes), malignant (ICD10 C56 & C57.0-C57.7): Five-year relative survival by diagnosis year and age at diagnosis. *Online Survival Statistics (Relative Survival).* 11/04/2011 ed.: National Cancer Registry, Ireland.

NEDJADI, T., KITTERINGHAM, N., CAMPBELL, F., JENKINS, R. E., PARK, B. K., NAVARRO, P., ASHCROFT, F., TEPIKIN, A., NEOPTOLEMOS, J. P. & COSTELLO, E. 2009. S100A6 binds to annexin 2 in pancreatic cancer cells and promotes pancreatic cancer cell motility. *Br J Cancer,* 101, 1145-54.

NEGUS, R. P., STAMP, G. W., RELF, M. G., BURKE, F., MALIK, S. T., BERNASCONI, S., ALLAVENA, P., SOZZANI, S., MANTOVANI, A. & BALKWILL, F. R. 1995. The detection and localization of monocyte chemoattractant protein-1 (MCP-1) in human ovarian cancer. *The Journal of Clinical Investigation,* 95**,** 2391-6.

NIESWANDT, B., HAFNER, M., ECHTENACHER, B. & MANNEL, D. N. 1999. Lysis of tumor cells by natural killer cells in mice is impeded by platelets. *Cancer Res,* 59**,** 1295-300.

NOFER, J. R., BRODDE, M. F. & KEHREL, B. E. 2010. High-density lipoproteins, platelets and the pathogenesis of atherosclerosis. *Clinical and experimental pharmacology & physiology,* 37**,** 726-35.

NOMA, T., FUJISAWA, K., YAMASHIRO, Y., SHINOHARA, M., NAKAZAWA, A., GONDO, T., ISHIHARA, T. & YOSHINOBU, K. 2001. Structure and expression of human mitochondrial adenylate kinase targeted to the mitochondrial matrix. *Biochem J,* 358**,** 225-32.

NOSSOV, V., AMNEUS, M., SU, F., LANG, J., JANCO, J. M., REDDY, S. T. & FARIAS-EISNER, R. 2008. The early detection of ovarian cancer: from traditional methods to proteomics. Can we really do better than serum CA-125? *American Journal of Obstetrics and Gynecology,* 199**,** 215-23.

NURMINEN, R., WAHLFORS, T., TAMMELA, T. L. J. & SCHLEUTKER, J. 2011. Identification of an aggressive prostate cancer predisposing variant at 11q13. *International Journal of Cancer,* 129**,** 599-606.

O'TOOLE, S. A., SHEPPARD, B. L., LAIOS, A., O'LEARY, J. J., MCGUINNESS, E. P. J., D'ARCY, T. & BONNAR, J. 2007. Potential predictors of chemotherapy response in ovarian cancer--How do we define chemosensitivity? *Gynecologic Oncology,* 104**,** 345-351.

OBIEZU, C. V., SCORILAS, A., KATSAROS, D., MASSOBRIO, M., YOUSEF, G. M., FRACCHIOLI, S., RIGAULT DE LA LONGRAIS, I. A., ARISIO, R. & DIAMANDIS, E. P. 2001. Higher human kallikrein gene 4 (KLK4) expression indicates poor prognosis of ovarian cancer patients. *Clin Cancer Res,* 7**,** 2380-6.

OHLENBUSCH, A., HENNEKE, M., BROCKMANN, K., GOERG, M., HANEFELD, F., KOHLSCHÜTTER, A. & GÄRTNER, J. 2005. Identification of ten novel mutations in patients with eIF2B-related disorders. *Human Mutation,* 25**,** 411-411.

OISHI, K., OKANO, H. & SAWA, H. 2007. RMD-1, a novel microtubule-associated protein, functions in chromosome segregation in Caenorhabditis elegans. *J Cell Biol,* 179**,** 1149-62.

OKUDAIRA, K., HOKARI, R., TSUZUKI, Y., OKADA, Y., KOMOTO, S., WATANABE, C., KURIHARA, C., KAWAGUCHI, A., NAGAO, S., AZUMA, M., YAGITA, H. & MIURA, S.

2009. Blockade of B7-H1 or B7-DC induces an anti-tumor effect in a mouse pancreatic cancer model. *Int J Oncol,* 35, 741-9.

OKUWAKI, M., KATO, K. & NAGATA, K. 2010. Functional characterization of human nucleosome assembly protein 1-like proteins as histone chaperones. *Genes to Cells,* 15, 13-27.

OLEKSOWICZ, L., BHAGWATI, N. & DELEON-FERNANDEZ, M. 1999. Deficient Activity of von Willebrand's Factor-cleaving Protease in Patients with Disseminated Malignancies. *Cancer Res,* 59, 2244-2250.

OLSEN, C. M., BAIN, C. J., JORDAN, S. J., NAGLE, C. M., GREEN, A. C., WHITEMAN, D. C. & WEBB, P. M. 2007a. Recreational Physical Activity and Epithelial Ovarian Cancer: A Case-Control Study, Systematic Review, and Meta-analysis. *Cancer Epidemiology Biomarkers & Prevention,* 16, 2321-2330.

OLSEN, C. M., GREEN, A. C., WHITEMAN, D. C., SADEGHI, S., KOLAHDOOZ, F. & WEBB, P. M. 2007b. Obesity and the risk of epithelial ovarian cancer: A systematic review and meta-analysis. *European journal of cancer (Oxford, England : 1990),* 43, 690-709.

OMA, Y. & HARATA, M. 2011. Actin-related proteins localized in the nucleus: From discovery to novel roles in nuclear organization. *Nucleus,* 2, 38-46.

ONDA, T. & YOSHIKAWA, H. 2011. Neoadjuvant chemotherapy for advanced ovarian cancer: overview of outcomes and unanswered questions. *Expert Review of Anticancer Therapy,* 11, 1055-1069.

ONGUSAHA, P. P., KWAK, J. C., ZWIBLE, A. J., MACIP, S., HIGASHIYAMA, S., TANIGUCHI, N., FANG, L. & LEE, S. W. 2004. HB-EGF Is a Potent Inducer of Tumor Growth and Angiogenesis. *Cancer Research,* 64, 5283-5290.

ORLOWSKI, J. & GRINSTEIN, S. 2004. Diversity of the mammalian sodium/proton exchanger SLC9 gene family. *Pflügers Archiv European Journal of Physiology,* 447, 549-565.

ÖSTMAN, A. & HELDIN, C. 2007. PDGF Receptors as Targets in Tumor Treatment. *In:* GEORGE, F. V. W. & GEORGE, K. (eds.) *Advances in Cancer Research.* Academic Press.

OTAHBACHI, M., SIMONI, J., SIMONI, G., MOELLER, J. F., CEVIK, C., MEYERROSE, G. E. & ROONGSRITONG, C. 2010. Gender differences in platelet aggregation in healthy individuals. *J Thromb Thrombolysis,* 30, 184-91.

OUTWATER, E. K., SIEGELMAN, E. S. & HUNT, J. L. 2001. Ovarian Teratomas: Tumor Types and Imaging Characteristics1. *Radiographics,* 21, 475-490.

PAMIDI, A., CARDOSO, R., HAKEM, A., MATYSIAK-ZABLOCKI, E., POONEPALLI, A., TAMBLYN, L., PEREZ-ORDONEZ, B., HANDE, M. P., SANCHEZ, O. & HAKEM, R. 2007. Functional Interplay of p53 and Mus81 in DNA Damage Responses and Cancer. *Cancer Research,* 67, 8527-8535.

PANIGRAHY, D., HUANG, S., KIERAN, M. W. & KAIPAINEN, A. 2005. PPARgamma as a therapeutic target for tumor angiogenesis and metastasis. *Cancer biology & therapy,* 4, 687-93.

PARCELLIER, A., TINTIGNAC, L. A., ZHURAVLEVA, E. & HEMMINGS, B. A. 2008. PKB and the mitochondria: AKTing on apoptosis. *Cellular Signalling,* 20, 21-30.

PARK, J., WOOD, M. A. & COLE, M. D. 2002. BAF53 forms distinct nuclear complexes and functions as a critical c-Myc-interacting nuclear cofactor for oncogenic transformation. *Molecular and cellular biology,* 22, 1307-16.

PARK, J. K., PARK, S. H., SO, K., BAE, I. H., YOO, Y. D. & UM, H. D. 2010. ICAM-3 enhances the migratory and invasive potential of human non-small cell lung cancer cells by inducing MMP-2 and MMP-9 via Akt and CREB. *International Journal of Oncology,* 36, 181-192.

PARK, J. S., SHARMA, L. K., LI, H., XIANG, R., HOLSTEIN, D., WU, J., LECHLEITER, J., NAYLOR, S. L., DENG, J. J., LU, J. & BAI, Y. 2009. A heteroplasmic, not homoplasmic, mitochondrial DNA mutation promotes tumorigenesis via alteration in reactive oxygen species generation and apoptosis. *Human Molecular Genetics,* 18, 1578-89.

PARKIN, D. M., BRAY, F., FERLAY, J. & PISANI, P. 2005. Global Cancer Statistics, 2002. *CA Cancer J Clin,* 55, 74-108.

PATANKAR, M. S., JING, Y., MORRISON, J. C., BELISLE, J. A., LATTANZIO, F. A., DENG, Y., WONG, N. K., MORRIS, H. R., DELL, A. & CLARK, G. F. 2005. Potent suppression of natural killer cell response mediated by the ovarian tumor marker CA125. *Gynecologic Oncology,* 99, 704-713.

PATEL, D., VÄÄNÄNEN, H., JIROUŠKOVÁ, M., HOFFMANN, T., BODIAN, C. & COLLER, B. S. 2003. Dynamics of GPIIb/IIIa-mediated platelet-platelet interactions in platelet adhesion/thrombus formation on collagen in vitro as revealed by videomicroscopy. *Blood,* 101, 929-936.

PATEL, S. R., HARTWIG, J. H. & ITALIANO, J. E. 2005. The biogenesis of platelets from megakaryocyte proplatelets. *The Journal of Clinical Investigation,* 115, 3348-3354.

PEARCE, C. L., CHUNG, K., PIKE, M. C. & WU, A. H. 2009. Increased ovarian cancer risk associated with menopausal estrogen therapy is reduced by adding a progestin. *Cancer,* 115, 531-539.

PEARLSTEIN, E., AMBROGIO, C., GASIC, G. & KARPATKIN, S. 1981. Inhibition of the platelet-aggregating activity of two human adenocarcinomas of the colon and an anaplastic murine tumor with a specific thrombin inhibitor, dansylarginine N-(3-ethyl-1,5-pentanediyl)amide. *Cancer Research,* 41, 4535-9.

PEARLSTEIN, E., AMBROGIO, C. & KARPATKIN, S. 1984. Effect of antiplatelet antibody on the development of pulmonary metastases following injection of CT26 colon adenocarcinoma, Lewis lung carcinoma, and B16 amelanotic melanoma tumor cells into mice. *Cancer Res,* 44, 3884-7.

PECTASIDES, D., PECTASIDES, E. & KASSANOS, D. 2008. Germ cell tumors of the ovary. *Cancer treatment reviews,* 34, 427-441.

PEDERSEN, L. M. & MILMAN, N. 1996. Prognostic significance of thrombocytosis in patients with primary lung cancer. *The European respiratory journal : official journal of the European Society for Clinical Respiratory Physiology,* 9, 1826-30.

PENNINGS, M. T. T., DERKSEN, R. H. W. M., VAN LUMMEL, M., ADELMEIJER, J., VANHOORELBEKE, K., URBANUS, R. T., LISMAN, T. & DE GROOT, P. G. 2007. Platelet adhesion to dimeric β2-glycoprotein I under conditions of flow is mediated by at least two receptors: glycoprotein Ibα and apolipoprotein E receptor 2'. *Journal of Thrombosis and Haemostasis,* 5, 369-377.

PERABO, F., SHARMA, S., GIERER, R., WIRGER, A., FIMMERS, R., STEINER, G., ADAM, M. & SCHULTZE-SEEMANN, W. 2001. Circulating intercellular adhesion molecule-1 (ICAM-1), vascular cell adhesion molecule-1 (VCAM-1) and E-selectin in urological malignancies. *Indian journal of cancer,* 38, 1-7.

PETERS, J. M. & GONZALEZ, F. J. 2009. Sorting out the functional role(s) of peroxisome proliferator-activated receptor-beta/delta (PPARbeta/delta) in cell proliferation and cancer. *Biochimica et biophysica acta,* 1796, 230-41.

PETERSON, J. E., ZURAKOWSKI, D., ITALIANO, J. E., JR., MICHEL, L. V., FOX, L., KLEMENT, G. L. & FOLKMAN, J. 2010. Normal ranges of angiogenesis regulatory proteins in human platelets. *American Journal of Hematology,* 85, 487-93.

PHILIPPE, C., PHILIPPE, B., FOUQUERAY, B., PEREZ, J., LEBRET, M. & BAUD, L. 1993. Protection from tumor necrosis factor-mediated cytolysis by platelets. *American Journal of Pathology,* 143, 1713-23.

PHILLIPS, D. R., CHARO, I. F., PARISE, L. V. & FITZGERALD, L. A. 1988. The platelet membrane glycoprotein IIb-IIIa complex. *Blood,* 71, 831-43.

PIDGEON, G. P., TANG, K., CAI, Y. L., PIASENTIN, E. & HONN, K. V. 2003. Overexpression of Platelet-type 12-Lipoxygenase Promotes Tumor Cell Survival by Enhancing {alpha}v{beta}3 and {alpha}v{beta}5 Integrin Expression. *Cancer Res,* 63, 4258-4267.

PIEK, J. M., VAN DIEST, P. J. & VERHEIJEN, R. H. 2008. Ovarian carcinogenesis: an alternative hypothesis. *Advances in experimental medicine and biology,* 622, 79-87.

PIEK, J. M. J., VAN DIEST, P. J., ZWEEMER, R. P., JANSEN, J. W., POORT-KEESOM, R. J. J., MENKO, F. H., GILLE, J. J. P., JONGSMA, A. P. M., PALS, G., KENEMANS, P. & VERHEIJEN, R. H. M. 2001. Dysplastic changes in prophylactically removed Fallopian tubes of women predisposed to developing ovarian cancer. *The Journal of Pathology,* 195, 451-456.

PIERSMA, S. R., BROXTERMAN, H. J., KAPCI, M., DE HAAS, R. R., HOEKMAN, K., VERHEUL, H. M. W. & JIMÉNEZ, C. R. 2009. Proteomics of the TRAP-induced platelet releasate. *Journal of Proteomics,* 72, 91-109.

PIETRAS, K., PAHLER, J., BERGERS, G. & HANAHAN, D. 2008. Functions of paracrine PDGF signaling in the proangiogenic tumor stroma revealed by pharmacological targeting. *PLoS Med,* 5, e19.

PLACKE, T., KOPP, H. G. & SALIH, H. R. 2011. Modulation of natural killer cell anti-tumor reactivity by platelets. *Journal of innate immunity,* 3, 374-82.

PLANTE, M., RUBIN, S. C., WONG, G. Y., FEDERICI, M. G., FINSTAD, C. L. & GASTL, G. A. 1994. Interleukin-6 level in serum and ascites as a prognostic factor in patients with epithelial ovarian cancer. *Cancer,* 73, 1882-8.

POLLARD, J. W. 2004. Tumour-educated macrophages promote tumour progression and metastasis. *Nat Rev Cancer,* 4, 71-78.

POVEDA, A., KAYE, S. B., MCCORMACK, R., WANG, S., PAREKH, T., RICCI, D., LEBEDINSKY, C. A., TERCERO, J. C., ZINTL, P. & MONK, B. J. 2011. Circulating tumor cells predict progression free survival and overall survival in patients with relapsed/recurrent advanced ovarian cancer. *Gynecologic Oncology,* 122, 567-572.

PRENTICE, R. L., THOMSON, C. A., CAAN, B., HUBBELL, F. A., ANDERSON, G. L., BERESFORD, S. A., PETTINGER, M., LANE, D. S., LESSIN, L., YASMEEN, S., SINGH, B., KHANDEKAR, J., SHIKANY, J. M., SATTERFIELD, S. & CHLEBOWSKI, R. T. 2007. Low-fat dietary pattern and cancer incidence in the Women's Health Initiative Dietary Modification Randomized Controlled Trial. *Journal of the National Cancer Institute,* 99, 1534-43.

PRESS ASSOCIATION. 2010. Women missing ovarian cancer signs. *The Irish Independent,* 26/02/2010.

PREZAS, P., ARLT, M. J. E., VIKTOROV, P., SOOSAIPILLAI, A., HOLZSCHEITER, L., SCHMITT, M., TALIERI, M., DIAMANDIS, E. P., KRÜGER, A. & MAGDOLEN, V. 2006. Overexpression of the human tissue kallikrein genes KLK4, 5, 6, and 7 increases

the malignant phenotype of ovarian cancer cells. *Biological Chemistry,* 387, 807-811.

PRIZMENT, A. E., FOLSOM, A. R. & ANDERSON, K. E. 2010. Nonsteroidal anti-inflammatory drugs and risk for ovarian and endometrial cancers in the Iowa Women's Health Study. *Cancer epidemiology, biomarkers & prevention : a publication of the American Association for Cancer Research, cosponsored by the American Society of Preventive Oncology,* 19, 435-42.

PRZEWLOKA, M. R., VENKEI, Z. & GLOVER, D. M. 2009. Searching for Drosophila Dsn1 kinetochore protein. *Cell Cycle,* 8, 1292-1293.

PRZYBYCIN, C. G., KURMAN, R. J., RONNETT, B. M., SHIH, I.-M. & VANG, R. 2010. Are All Pelvic (Nonuterine) Serous Carcinomas of Tubal Origin? *The American Journal of Surgical Pathology,* 34, 1407-1416 10.1097/PAS.0b013e3181ef7b16.

PRZYBYCIN, C. G. & SOSLOW, R. A. 2011. Typing of ovarian carcinomas: an update. *Diagnostic Histopathology,* 17, 165-177.

QI, Y., CHIU, J.-F., WANG, L., KWONG, D. L. W. & HE, Q.-Y. 2005. Comparative proteomic analysis of esophageal squamous cell carcinoma. *Proteomics,* 5, 2960-2971.

QIAN, H., JI, C., ZHAO, S., CHEN, J., JIANG, M., ZHANG, Y., YAN, M., ZHENG, D., SUN, Y., XIE, Y. & MAO, Y. 2007. Expression and characterization of HSPC129, a RNA polymerase II C-terminal domain phosphatase. *Molecular and cellular biochemistry,* 303, 183-8.

QUELHAS, D., QUENTAL, R., VILARINHO, L., AMORIM, A. & AZEVEDO, L. 2007. Congenital disorder of glycosylation type Ia: searching for the origin of common mutations in PMM2. *Annals of human genetics,* 71, 348-53.

RADOMSKI, M. W., JENKINS, D. C., HOLMES, L. & MONCADA, S. 1991. Human Colorectal Adenocarcinoma Cells: Differential Nitric Oxide Synthesis Determines Their Ability to Aggregate Platelets. *Cancer Research,* 51, 6073-6078.

RADOMSKI, M. W. & MONCADA, S. 1993. Regulation of vascular homeostasis by nitric oxide. *Thrombosis and Haemostasis,* 70, 36-41.

RADOMSKI, M. W., REES, D. D., DUTRA, A. & MONCADA, S. 1992. S-nitroso-glutathione inhibits platelet activation in vitro and in vivo. *Br J Pharmacol,* 107, 745-9.

RADOWITZ, J. V. 2011a. Discovery will help spot ovarian cancer early on. *The Irish Independent*, 17/08/2011.

RADOWITZ, J. V. 2011b. Survival rate for women with ovarian cancer has doubled. *The Irish Independent*, 09/03/2011.

RAICA, M. & CIMPEAN, A. M. 2010. Platelet-Derived Growth Factor (PDGF)/PDGF Receptors (PDGFR) Axis as Target for Antitumor and Antiangiogenic Therapy. *Pharmaceuticals,* 3, 572-599.

RAIT, V. K., ZHANG, Q., FABRIS, D., MASON, J. T. & O'LEARY, T. J. 2006. Conversions of formaldehyde-modified 2'-deoxyadenosine 5'-monophosphate in conditions modeling formalin-fixed tissue dehydration. *J Histochem Cytochem,* 54, 301-10.

RAJA, F. A., GRIFFIN, C. L., QIAN, W., HIRTE, H., PARMAR, M. K., SWART, A. M. & LEDERMANN, J. A. 2011. Initial toxicity assessment of ICON6: a randomised trial of cediranib plus chemotherapy in platinum-sensitive relapsed ovarian cancer. *British Journal of Cancer.*

RAMAKRISHNAN, S., SUBRAMANIAN, I. V., YOKOYAMA, Y. & GELLER, M. 2005. Angiogenesis in normal and neoplastic ovaries. *Angiogenesis,* 8, 169-82.

RAO, L. V. 1992. Tissue factor as a tumor procoagulant. *Cancer Metastasis Rev,* 11, 249-66.

RECK, M. 2010. BIBF 1120 for the treatment of non-small cell lung cancer. *Expert Opinion on Investigational Drugs,* 19, 789-794.

REIGSTAD, L. J., VARHAUG, J. E. & LILLEHAUG, J. R. 2005. Structural and functional specificities of PDGF-C and PDGF-D, the novel members of the platelet-derived growth factors family. *FEBS J,* 272, 5723-41.

RENDU, F. & BROHARD-BOHN, B. 2001. The platelet release reaction: granules' constituents, secretion and functions. *Platelets,* 12, 261-273.

REYNOLDS, E. A. & MOLLER, K. A. 2006. A review and an update on the screening of epithelial ovarian cancer. *Current Problems in Cancer,* 30, 203-32.

RIBATTI, D. & CRIVELLATO, E. 2007. Giulio Bizzozero and the discovery of platelets. *Leukemia Research,* 31, 1339-1341.

RICHARDS, J. B., WATERWORTH, D., O'RAHILLY, S., HIVERT, M. F., LOOS, R. J., PERRY, J. R., TANAKA, T., TIMPSON, N. J., SEMPLE, R. K., SORANZO, N., SONG, K., ROCHA, N., GRUNDBERG, E., DUPUIS, J., FLOREZ, J. C., LANGENBERG, C., PROKOPENKO, I., SAXENA, R., SLADEK, R., AULCHENKO, Y., EVANS, D., WAEBER, G., ERDMANN, J., BURNETT, M. S., SATTAR, N., DEVANEY, J., WILLENBORG, C., HINGORANI, A., WITTEMAN, J. C., VOLLENWEIDER, P., GLASER, B., HENGSTENBERG, C., FERRUCCI, L., MELZER, D., STARK, K., DEANFIELD, J., WINOGRADOW, J., GRASSL, M., HALL, A. S., EGAN, J. M., THOMPSON, J. R., RICKETTS, S. L., KONIG, I. R., REINHARD, W., GRUNDY, S., WICHMANN, H. E., BARTER, P., MAHLEY, R., KESANIEMI, Y. A., RADER, D. J., REILLY, M. P., EPSTEIN, S. E., STEWART, A. F., VAN DUIJN, C. M., SCHUNKERT, H., BURLING, K., DELOUKAS, P., PASTINEN, T., SAMANI, N. J., MCPHERSON, R., DAVEY SMITH, G., FRAYLING, T. M., WAREHAM, N. J., MEIGS, J. B., MOOSER, V. &

SPECTOR, T. D. 2009. A genome-wide association study reveals variants in ARL15 that influence adiponectin levels. *PLoS genetics,* 5, e1000768.

RICKLES, F. R. & FALANGA, A. 2001. Molecular Basis for the Relationship Between Thrombosis and Cancer. *Thrombosis Research,* 102, V215-V224.

RICKLES, F. R., LEVINE, M. N. & DVORAK, H. F. 2001. Abnormalities of hemostasis in malignancy. *In:* COLMAN, R. F., HIRSH, J., MARDER, V. J., CLOWES, A. W. & GEORGE, J. N. (eds.) *Hemostasis and Thrombosis Basic Principles and Clinical practice.* 4th ed. Philadelphia: Lippincott Williams & Wilkins.

RICKLES, F. R., PATIERNO, S. & FERNANDEZ, P. M. 2003a. Tissue factor, thrombin, and cancer. *Chest,* 124, 58S-68S.

RICKLES, F. R., PATIERNO, S. R. & FERNANDEZ, P. M. 2003b. Targeting the endothelium in cancer--the importance of the interaction of hemostatic mechanisms and the vascular wall for tumor growth and angiogenesis. *Pathophysiol Haemost Thromb,* 33 Suppl 1, 1-4.

RIDDELL, D. R., GRAHAM, A. & OWEN, J. S. 1997. Apolipoprotein E Inhibits Platelet Aggregation through the L-Arginine:Nitric Oxide Pathway. *Journal of Biological Chemistry,* 272, 89-95.

RIDDELL, D. R., VINOGRADOV, D. V., STANNARD, A. K., CHADWICK, N. & OWEN, J. S. 1999. Identification and characterization of LRP8 (apoER2) in human blood platelets. *Journal of lipid research,* 40, 1925-30.

RISUM, S., HOGDALL, C., LOFT, A., BERTHELSEN, A. K., HOGDALL, E., NEDERGAARD, L., LUNDVALL, L. & ENGELHOLM, S. A. 2007. The diagnostic value of PET/CT for primary ovarian cancer--a prospective study. *Gynecologic Oncology,* 105, 145-9.

RISUM, S., HOGDALL, C., MARKOVA, E., BERTHELSEN, A. K., LOFT, A., JENSEN, F., HOGDALL, E., ROED, H. & ENGELHOLM, S. A. 2009. Influence of 2-(18F) fluoro-2-deoxy-D-glucose positron emission tomography/computed tomography on recurrent ovarian cancer diagnosis and on selection of patients for secondary cytoreductive surgery. *International journal of gynecological cancer : official journal of the International Gynecological Cancer Society,* 19, 600-4.

ROBERT, C., BOLON, I., GAZZERI, S., VEYRENC, S., BRAMBILLA, C. & BRAMBILLA, E. 1999. Expression of Plasminogen Activator Inhibitors 1 and 2 in Lung Cancer and Their Role in Tumor Progression. *Clinical Cancer Research,* 5, 2094-2102.

ROBERTSON, J. O., LI, W., SILVERSTEIN, R. L., TOPOL, E. J. & SMITH, J. D. 2009. Deficiency of LRP8 in mice is associated with altered platelet function and prolonged time for in vivo thrombosis. *Thrombosis Research,* 123, 644-652.

ROCA, H., VARSOS, Z. & PIENTA, K. J. 2008a. CCL2 protects prostate cancer PC3 cells from autophagic death via phosphatidylinositol 3-kinase/AKT-dependent survivin up-regulation. *The Journal of biological chemistry,* 283, 25057-73.

ROCA, H., VARSOS, Z. S., MIZUTANI, K. & PIENTA, K. J. 2008b. CCL2, survivin and autophagy: new links with implications in human cancer. *Autophagy,* 4, 969-71.

ROCCONI, R. P., MATTHEWS, K. S., KIMBALL, K. J., CONNER, M. G., BAKER, A. C. & BARNES, M. N. 2008. Expression of c-kit and platelet-derived growth factor receptors in ovarian granulosa cell tumors. *Reprod Sci,* 15, 673-7.

RODRÍGUEZ-BURFORD, C., BARNES, M. N., OELSCHLAGER, D. K., MYERS, R. B., TALLEY, L. I., PARTRIDGE, E. E. & GRIZZLE, W. E. 2002. Effects of Nonsteroidal Anti-Inflammatory Agents (NSAIDs) on Ovarian Carcinoma Cell Lines. *Clinical Cancer Research,* 8, 202-209.

RODRIGUEZ, G. C., CLARKE-PEARSON, D. L., SOPER, J. T., BERCHUCK, A., SYNAN, I. & DODGE, R. K. 1994. The Negative Prognostic Implications of Thrombocytosis in Women With Stage IB Cervical Cancer. *Obstet Gynecol,* 83, 445-448.

ROH, M. H., KINDELBERGER, D. & CRUM, C. P. 2009. Serous Tubal Intraepithelial Carcinoma and the Dominant Ovarian Mass: Clues to Serous Tumor Origin? *The American Journal of Surgical Pathology,* 33, 376-383 10.1097/PAS.0b013e3181868904.

RONI, C. R. 2010. *Aspirin Helps in Reducing Cancer Deaths, a Study Finds* [Online]. New York Times. Available: http://www.nytimes.com/2010/12/07/us/07aspirin.html [Accessed 10 December 2010].

ROSEN, D. G., WANG, L., ATKINSON, J. N., YU, Y., LU, K. H., DIAMANDIS, E. P., HELLSTROM, I., MOK, S. C., LIU, J. & BAST JR, R. C. 2005. Potential markers that complement expression of CA125 in epithelial ovarian cancer. *Gynecologic Oncology,* 99, 267-277.

ROSS, R. 1989. Platelet-derived growth factor. *Lancet,* 1, 1179-82.

ROSS, R., GLOMSET, J., KARIYA, B. & HARKER, L. 1974. A platelet-dependent serum factor that stimulates the proliferation of arterial smooth muscle cells in vitro. *Proc Natl Acad Sci U S A,* 71, 1207-10.

ROSS, R. & GLOMSET, J. A. 1973. Atherosclerosis and the arterial smooth muscle cell: Proliferation of smooth muscle is a key event in the genesis of the lesions of atherosclerosis. *Science,* 180, 1332-9.

ROTHENBERG, M., L. , LIU, P. Y., WILCZYNSKI, S., BRALY, P., S. , WADLER, S., STUART, G., HANNIGAN, E., V. , BONEBRAKE, A., J. , ALBERTS, D., S. & MARKMAN, M. Excellent 2-year survival in women with optimally-debulked ovarian cancer treated with

intraperitoneal and intravenous chemotherapy: a SWOG-ECOG-NCIC study. Annual Meeting: American Society of Clinical Oncology 2002.

ROTHWELL, P., M. , FOWKES, F. G. R., BELCH, J., F. F. , OGAWA, H., P. WARLOW, C. & MEADE, T., W. 2011. Effect of daily aspirin on long-term risk of death due to cancer: analysis of individual patient data from randomised trials. *The Lancet,* 377, 31-41.

ROUSSIDIS, A. E., THEOCHARIS, A. D., TZANAKAKIS, G. N. & KARAMANOS, N. K. 2007. The importance of c-Kit and PDGF receptors as potential targets for molecular therapy in breast cancer. *Curr Med Chem,* 14, 735-43.

RUDOLPH, D., STEEGMAIER, M., HOFFMANN, M., GRAUERT, M., BAUM, A., QUANT, J., HASLINGER, C., GARIN-CHESA, P. & ADOLF, G. R. 2009. BI 6727, a Polo-like kinase inhibitor with improved pharmacokinetic profile and broad antitumor activity. *Clinical cancer research : an official journal of the American Association for Cancer Research,* 15, 3094-102.

RUSSO, A., CALO, V., BRUNO, L., RIZZO, S., BAZAN, V. & DI FEDE, G. 2009. Hereditary ovarian cancer. *Critical reviews in oncology/hematology,* 69, 28-44.

SAAD, E. D., KATZ, A., HOFF, P. M. & BUYSE, M. 2010. Progression-free survival as surrogate and as true end point: insights from the breast and colorectal cancer literature. *Annals of Oncology,* 21, 7-12.

SABA, L., GUERRIERO, S., SULCIS, R., VIRGILIO, B., MELIS, G. & MALLARINI, G. 2009. Mature and immature ovarian teratomas: CT, US and MR imaging characteristics. *European journal of radiology,* 72, 454-463.

SALGADO, R., VERMEULEN, P. B., BENOY, I., WEYTJENS, R., HUGET, P., MARCK, E. V. & DIRIX, L. Y. 1999. Platelet number and interleukin-6 correlate with VEGF but not with bFGF serum levels of advanced cancer patients. *Br J Cancer,* 80, 892-897.

SALINAS, S., CARAZO-SALAS, R. E., PROUKAKIS, C., SCHIAVO, G. & WARNER, T. T. 2007. Spastin and microtubules: Functions in health and disease. *Journal of neuroscience research,* 85, 2778-82.

SALVADOR, S., REMPEL, A., SOSLOW, R. A., GILKS, B., HUNTSMAN, D. & MILLER, D. 2008. Chromosomal instability in fallopian tube precursor lesions of serous carcinoma and frequent monoclonality of synchronous ovarian and fallopian tube mucosal serous carcinoma. *Gynecol Oncol,* 110, 408-17.

SANJO, H., KAWAI, T. & AKIRA, S. 1998. DRAKs, Novel Serine/Threonine Kinases Related to Death-associated Protein Kinase That Trigger Apoptosis. *Journal of Biological Chemistry,* 273, 29066-29071.

SANTOS, E., GOMEZ, J. & RAEZ, L. 2011. Targeting angiogenesis from multiple pathways simultaneously: BIBF 1120, an investigational novel triple angiokinase inhibitor. *Investigational New Drugs*, 1-9.

SARGENT, D. J., WIEAND, H. S., HALLER, D. G., GRAY, R., BENEDETTI, J. K., BUYSE, M., LABIANCA, R., SEITZ, J. F., O'CALLAGHAN, C. J., FRANCINI, G., GROTHEY, A., O'CONNELL, M., CATALANO, P. J., BLANKE, C. D., KERR, D., GREEN, E., WOLMARK, N., ANDRE, T., GOLDBERG, R. M. & DE GRAMONT, A. 2005. Disease-free survival versus overall survival as a primary end point for adjuvant colon cancer studies: individual patient data from 20,898 patients on 18 randomized trials. *J Clin Oncol,* 23, 8664-70.

SASAKI, C. Y., SLEMENDA, C. F., GHOSH, P., BARBERI, T. J. & LONGO, D. L. 2007. Traf1 Induction and Protection from Tumor Necrosis Factor by Nuclear Factor-κB p65 Is Independent of Serine 536 Phosphorylation. *Cancer Research,* 67, 11218-11225.

SATO, K., ITO, K., KOHARA, H., YAMAGUCHI, Y., ADACHI, K. & ENDO, H. 1992. Negative regulation of catalase gene expression in hepatoma cells. *Molecular and cellular biology,* 12, 2525-33.

SATO, S., TOMOMORI-SATO, C., BANKS, C. A. S., SOROKINA, I., PARMELY, T. J., KONG, S. E., JIN, J., CAI, Y., LANE, W. S., BROWER, C. S., CONAWAY, R. C. & CONAWAY, J. W. 2003. Identification of Mammalian Mediator Subunits with Similarities to Yeast Mediator Subunits Srb5, Srb6, Med11, and Rox3. *Journal of Biological Chemistry,* 278, 15123-15127.

SAWADA, T., KIMURA, K., NISHIHARA, T., ONODA, N., TERAOKA, H., YAMASHITA, Y., YAMADA, N., YASHIRO, M., OHIRA, M. & HIRAKAWA, K. 2006. TGF-beta1 down-regulates ICAM-1 expression and enhances liver metastasis of pancreatic cancer. *Adv Med Sci,* 51, 60-5.

SAWICKI, G., SANDERS, E. J., SALAS, E., WOZNIAK, M., RODRIGO, J. & RADOMSKI, M. W. 1998. Localization and translocation of MMP-2 during aggregation of human platelets. *Thromb Haemost,* 80, 836-9.

SCHAFER, A. I. 2004. Thrombocytosis. *The New England Journal of Medicine,* 350, 1211-9.

SCHER, H. I., JIA, X., DE BONO, J. S., FLEISHER, M., PIENTA, K. J., RAGHAVAN, D. & HELLER, G. 2009. Circulating tumour cells as prognostic markers in progressive, castration-resistant prostate cancer: a reanalysis of IMMC38 trial data. *The Lancet Oncology,* 10, 233-239.

SCHIAVONE, M. B., HERZOG, T. J., LEWIN, S. N., DEUTSCH, I., SUN, X., BURKE, W. M. & WRIGHT, J. D. 2011. Natural history and outcome of mucinous carcinoma of the ovary. *American Journal of Obstetrics and Gynecology,* 205, 480.e1-480.e8.

SCHILDER, R. J., SILL, M. W., LEE, R. B., SHAW, T. J., SENTERMAN, M. K., KLEIN-SZANTO, A. J., MINER, Z. & VANDERHYDEN, B. C. 2008. Phase II Evaluation of Imatinib Mesylate in the Treatment of Recurrent or Persistent Epithelial Ovarian or Primary Peritoneal Carcinoma: A Gynecologic Oncology Group Study. *J Clin Oncol,* 26, 3418-3425.

SCHLUMBRECHT, M. P., XIE, S.-S., SHIPLEY, G. L., URBAUER, D. L. & BROADDUS, R. R. 2010. Molecular clustering based on ER[alpha] and EIG121 predicts survival in high-grade serous carcinoma of the ovary/peritoneum. *Mod Pathol.*

SCHLUMBRECHT, M. P., XIE, S.-S., SHIPLEY, G. L., URBAUER, D. L. & BROADDUS, R. R. 2011. Molecular clustering based on ER[alpha] and EIG121 predicts survival in high-grade serous carcinoma of the ovary/peritoneum. *Mod Pathol,* 24, 453-462.

SCHMITT, M. & MAGDOLEN, V. 2009. Using kallikrein-related peptidases (KLK) as novel cancer biomarkers. *Thrombosis and Haemostasis,* 101, 222-4.

SCHNABL, B., HU, K., MÜHLBAUER, M., HELLERBRAND, C., STEFANOVIC, B., BRENNER, D. A. & SCHÖLMERICH, J. 2005. Zinc finger protein 267 is up-regulated during the activation process of human hepatic stellate cells and functions as a negative transcriptional regulator of MMP-10. *Biochemical and Biophysical Research Communications,* 335, 87-96.

SCHON, E. A. 2000. Mitochondrial genetics and disease. *Trends in Biochemical Sciences,* 25, 555-560.

SCHORGE, J. O., MUTO, M. G., LEE, S. J., HUANG, L. W., WELCH, W. R., BELL, D. A., KEUNG, E. Z., BERKOWITZ, R. S. & MOK, S. C. 2000. BRCA1-related papillary serous carcinoma of the peritoneum has a unique molecular pathogenesis. *Cancer Research,* 60, 1361-4.

SCHRAML, P., SCHWERDTFEGER, G., BURKHALTER, F., RAGGI, A., SCHMIDT, D., RUFFALO, T., KING, W., WILBER, K., MIHATSCH, M. J. & MOCH, H. 2003. Combined array comparative genomic hybridization and tissue microarray analysis suggest PAK1 at 11q13.5-q14 as a critical oncogene target in ovarian carcinoma. *The American Journal of Pathology,* 163, 985-92.

SCHRÖDER, J. K., KOLKENBROCK, S., TINS, J., KASIMIR-BAUER, S., SEEBER, S. & SCHÜTTE, J. 2000. Analysis of thrombopoietin receptor (c-mpl) mRNA expression in de novo acute myeloid leukemia. *Leukemia Research,* 24, 401-409.

SCHROEDER, A., MUELLER, O., STOCKER, S., SALOWSKY, R., LEIBER, M., GASSMANN, M., LIGHTFOOT, S., MENZEL, W., GRANZOW, M. & RAGG, T. 2006. The RIN: an RNA integrity number for assigning integrity values to RNA measurements. *BMC Molecular Biology,* 7, 3.

SCHULTZE, M. 1865. Ein heizbarer Objecttisch und seine Verwendung bei Untersuchungen des Blutes. *Archiv für mikroscopische Anatomie,* 1, 1-42.

SCHWAB, M. 1998. Amplification of oncogenes in human cancer cells. *BioEssays : news and reviews in molecular, cellular and developmental biology,* 20, 473-9.

SEARGENT, J. M., LOADMAN, P. M., MARTIN, S. W., NAYLOR, B., BIBBY, M. C. & GILL, J. H. 2005. Expression of matrix metalloproteinase-10 in human bladder transitional cell carcinoma. *Urology,* 65, 815-820.

SEIDMAN, J. D., HORKAYNE-SZAKALY, I., HAIBA, M., BOICE, C. R., KURMAN, R. J. & RONNETT, B. M. 2004. The histologic type and stage distribution of ovarian carcinomas of surface epithelial origin. *Int J Gynecol Pathol,* 23, 41-4.

SEIDMAN, J. D. & KURMAN, R. J. 2000. Ovarian serous borderline tumors: a critical review of the literature with emphasis on prognostic indicators. *Human pathology,* 31, 539-57.

SEIDMAN, J. D., ZHAO, P. & YEMELYANOVA, A. 2011. "Primary peritoneal" high-grade serous carcinoma is very likely metastatic from serous tubal intraepithelial carcinoma: Assessing the new paradigm of ovarian and pelvic serous carcinogenesis and its implications for screening for ovarian cancer. *Gynecologic Oncology,* 120, 470-473.

SENNINO, B., KUHNERT, F., TABRUYN, S. P., MANCUSO, M. R., HU-LOWE, D. D., KUO, C. J. & MCDONALD, D. M. 2009. Cellular source and amount of vascular endothelial growth factor and platelet-derived growth factor in tumors determine response to angiogenesis inhibitors. *Cancer Res,* 69, 4527-36.

SENTURK, A., PFENNIG, S., WEISS, A., BURK, K. & ACKER-PALMER, A. 2011. Ephrin Bs are essential components of the Reelin pathway to regulate neuronal migration. *Nature,* 472, 356-360.

SERTZNIG, P., SEIFERT, M., TILGEN, W. & REICHRATH, J. 2007. Present concepts and future outlook: function of peroxisome proliferator-activated receptors (PPARs) for pathogenesis, progression, and therapy of cancer. *Journal of Cellular Physiology,* 212, 1-12.

SHANBHOGUE, A. K., SHANBHOGUE, D. K., PRASAD, S. R., SURABHI, V. R., FASIH, N. & MENIAS, C. O. 2010. Clinical syndromes associated with ovarian neoplasms: a comprehensive review. *Radiographics : a review publication of the Radiological Society of North America, Inc,* 30, 903-19.

SHAO, M., ROSSI, S., CHELLADURAI, B., SHIMIZU, M., NTUKOGU, O., IVAN, M., CALIN, G. A. & MATEI, D. 2011. PDGF induced microRNA alterations in cancer cells. *Nucleic Acids Res.*

SHATTIL, S. J., KASHIWAGI, H. & PAMPORI, N. 1998. Integrin Signaling: The Platelet Paradigm. *Blood,* 91, 2645-2657.

SHAU, H., ROTH, M. D. & GOLUB, S. H. 1993. Regulation of natural killer function by nonlymphoid cells. *Natural Immunity,* 12, 235-49.

SHAW, P. A., ROUZBAHMAN, M., PIZER, E. S., PINTILIE, M. & BEGLEY, H. 2009. Candidate serous cancer precursors in fallopian tube epithelium of BRCA1/2 mutation carriers. *Mod Pathol,* 22, 1133-1138.

SHEFFER, M., BACOLOD, M. D., ZUK, O., GIARDINA, S. F., PINCAS, H., BARANY, F., PATY, P. B., GERALD, W. L., NOTTERMAN, D. A. & DOMANY, E. 2009. Association of survival and disease progression with chromosomal instability: A genomic exploration of colorectal cancer. *Proceedings of the National Academy of Sciences*.

SHERIDAN, K. 2011. *Blood test for cancer gets US boost* [Online]. The Sydney Morning Herald. Available: http://news.smh.com.au/breaking-news-world/blood-test-for-cancer-gets-us-boost-20110104-19e4s.html [Accessed 6 January 2011].

SHI, Q. & SARGENT, D. J. 2009. Meta-analysis for the evaluation of surrogate endpoints in cancer clinical trials. *Int J Clin Oncol,* 14, 102-11.

SHIBUYA, M. & CLAESSON-WELSH, L. 2006. Signal transduction by VEGF receptors in regulation of angiogenesis and lymphangiogenesis. *Exp Cell Res,* 312, 549-60.

SHIH, T. & LINDLEY, C. 2006. Bevacizumab: An angiogenesis inhibitor for the treatment of solid malignancies. *Clinical Therapeutics,* 28, 1779-1802.

SHIM, A. H., LIU, H., FOCIA, P. J., CHEN, X., LIN, P. C. & HE, X. 2010. Structures of a platelet-derived growth factor/propeptide complex and a platelet-derived growth factor/receptor complex. *Proc Natl Acad Sci U S A,* 107, 11307-12.

SHIMADA, M., KIGAWA, J., OHISHI, Y., YASUDA, M., SUZUKI, M., HIURA, M., NISHIMURA, R., TABATA, T., SUGIYAMA, T. & KAKU, T. 2009. Clinicopathological characteristics of mucinous adenocarcinoma of the ovary. *Gynecologic Oncology,* 113, 331-4.

SHIN, D. H., PARK, K. W., WU, L. C. & HONG, J. W. 2011. ZAS3 promotes TNFalpha-induced apoptosis by blocking NFvarkappaB-activated expression of the anti-apoptotic genes TRAF1 and TRAF2. *BMB reports,* 44, 267-72.

SHIOZAWA, Y., HAVENS, A. M., JUNG, Y., ZIEGLER, A. M., PEDERSEN, E. A., WANG, J., WANG, J., LU, G., ROODMAN, G. D., LOBERG, R. D., PIENTA, K. J. & TAICHMAN, R. S. 2008. Annexin II/Annexin II receptor axis regulates adhesion, migration, homing, and growth of prostate cancer. *Journal of Cellular Biochemistry,* 105, 370-380.

SHIOZAWA, Y., PEDERSEN, E. A., PATEL, L. R., ZIEGLER, A. M., HAVENS, A. M., JUNG, Y., WANG, J., ZALUCHA, S., LOBERG, R. D., PIENTA, K. J. & TAICHMAN, R. S. 2010. GAS6/AXL axis regulates prostate cancer invasion, proliferation, and survival in the bone marrow niche. *Neoplasia,* 12, 116-27.

SIDDIQUI, G. K., MACLEAN, A. B., ELMASRY, K., WONG TE FONG, A., MORRIS, R. W., RASHID, M., BEGENT, R. H. & BOXER, G. M. 2011. Immunohistochemical expression of VEGF predicts response to platinum based chemotherapy in patients with epithelial ovarian cancer. *Angiogenesis*.

SIEBEN, N. L. G., MACROPOULOS, P., ROEMEN, G. M. J. M., KOLKMAN-ULJEE, S. M., JAN FLEUREN, G., HOUMADI, R., DISS, T., WARREN, B., AL ADNANI, M., DE GOEIJ, A. P. M., KRAUSZ, T., THE CANCER GENOME, P. & FLANAGAN, A. M. 2004. In ovarian neoplasms, BRAF, but not KRAS, mutations are restricted to low-grade serous tumours. *The Journal of Pathology,* 202, 336-340.

SIMES, R. J. 1986. An improved Bonferroni procedure for multiple tests of significance. *Biometrika,* 73, 751-754.

SIMON, I., KATSAROS, D., RIGAULT DE LA LONGRAIS, I., MASSOBRIO, M., SCORILAS, A., KIM, N. W., SARNO, M. J., WOLFERT, R. L. & DIAMANDIS, E. P. 2007. B7-H4 is over-expressed in early-stage ovarian cancer and is independent of CA125 expression. *Gynecologic Oncology,* 106, 334-341.

SINGH, D., FEBBO, P. G., ROSS, K., JACKSON, D. G., MANOLA, J., LADD, C., TAMAYO, P., RENSHAW, A. A., D'AMICO, A. V., RICHIE, J. P., LANDER, E. S., LODA, M., KANTOFF, P. W., GOLUB, T. R. & SELLERS, W. R. 2002. Gene expression correlates of clinical prostate cancer behavior. *Cancer Cell,* 1, 203-9.

SIU, M. K., CHAN, H. Y., KONG, D. S., WONG, E. S., WONG, O. G., NGAN, H. Y., TAM, K. F., ZHANG, H., LI, Z., CHAN, Q. K., TSAO, S. W., STROMBLAD, S. & CHEUNG, A. N. 2010a. p21-activated kinase 4 regulates ovarian cancer cell proliferation, migration, and invasion and contributes to poor prognosis in patients. *Proceedings of the National Academy of Sciences of the United States of America,* 107, 18622-7.

SIU, M. K. Y., WONG, E. S. Y., CHAN, H. Y., KONG, D. S. H., WOO, N. W. S., TAM, K. F., NGAN, H. Y. S., CHAN, Q. K. Y., CHAN, D. C. W., CHAN, K. Y. K. & CHEUNG, A. N. Y. 2010b. Differential expression and phosphorylation of Pak1 and Pak2 in ovarian cancer: effects on prognosis and cell invasion. *International Journal of Cancer,* 127, 21-31.

SIVEEN, K. S. & KUTTAN, G. 2009. Role of macrophages in tumour progression. *Immunology Letters,* 123, 97-102.

SMIRNOVA, T. Y., POSPEKHOVA, N. I., LYUBCHENKO, L. N., TJULANDIN, S. A., GAR'KAVTSEVA, R. F., GINTER, E. K. & KARPUKHIN, A. V. 2007. High incidence of

mutations in BRCA1 and BRCA2 genes in ovarian cancer. *Bulletin of experimental biology and medicine,* 144, 83-5.

SMITH, R., XUE, A., GILL, A., SCARLETT, C., SAXBY, A., CLARKSON, A. & HUGH, T. 2007. High Expression of Plasminogen Activator Inhibitor-2 (PAI-2) is a Predictor of Improved Survival in Patients with Pancreatic Adenocarcinoma. *World Journal of Surgery,* 31, 493-502.

SOETH, E., GRIGOLEIT, U., MOELLMANN, B., RODER, C., SCHNIEWIND, B., KREMER, B., KALTHOFF, H. & VOGEL, I. 2005. Detection of tumor cell dissemination in pancreatic ductal carcinoma patients by CK 20 RT-PCR indicates poor survival. *Journal of Cancer Research and Clinical Oncology,* 131, 669-76.

SOLÁR, P. & SYTKOWSKI, A. J. 2011. Differentially expressed genes associated with cisplatin resistance in human ovarian adenocarcinoma cell line A2780. *Cancer Letters,* 309, 11-18.

SONG, S., EWALD, A. J., STALLCUP, W., WERB, Z. & BERGERS, G. 2005. PDGFRbeta+ perivascular progenitor cells in tumours regulate pericyte differentiation and vascular survival. *Nat Cell Biol,* 7, 870-9.

SOONTHORNTHUM, T., SURASERANEEWONG, V., KENGSAKOL, K., WIJAITHUM, K., KASEMSAN, P. & PROMMATT, S. 2007. Thrombocytosis in advanced epithelial ovarian cancer. *J Med Assoc Thai,* 90, 1495-500.

SORENSEN, H. T., MELLEMKJAER, L., OLSEN, J. H. & BARON, J. A. 2000a. Prognosis of cancers associated with venous thromboembolism. *N Engl J Med,* 343, 1846-50.

SORENSEN, H. T., MELLEMKJAER, L., STEFFENSEN, F. H., OLSEN, J. H. & NIELSEN, G. L. 2000b. [Incidence of cancer after primary deep venous thrombosis or pulmonary embolism]. *Lakartidningen,* 97, 1961-4.

SPINNER, D. M. 2001. MTT Growth Assays in Ovarian Cancer. *In:* BARTLETT, J. M. S. (ed.) *Ovarian Cancer: Methods and Protocols.* Humana Press.

STEPHENS, G., O'LUANAIGH, N., REILLY, D., HARRIOTT, P., WALKER, B., FITZGERALD, D. & MORAN, N. 1998. A Sequence within the Cytoplasmic Tail of GpIIb Independently Activates Platelet Aggregation and Thromboxane Synthesis. *Journal of Biological Chemistry,* 273, 20317-20322.

STEWART, J. J., WHITE, J. T., YAN, X., COLLINS, S., DRESCHER, C. W., URBAN, N. D., HOOD, L. & LIN, B. 2006. Proteins associated with Cisplatin resistance in ovarian cancer cells identified by quantitative proteomic technology and integrated with mRNA expression levels. *Molecular & cellular proteomics : MCP,* 5, 433-43.

STOREY, D. J., RUSH, R., STEWART, M., RYE, T., AL-NAFUSSI, A., WILLIAMS, A. R., SMYTH, J. F. & GABRA, H. 2008. Endometrioid epithelial ovarian cancer. *Cancer,* 112, 2211-2220.

SU, J. L., YEN, C. J., CHEN, P. S., CHUANG, S. E., HONG, C. C., KUO, I. H., CHEN, H. Y., HUNG, M. C. & KUO, M. L. 2007. The role of the VEGF-C/VEGFR-3 axis in cancer progression. *Br J Cancer,* 96, 541-5.

SUGHRA, K., BIRBACH, A., DE MARTIN, R. & SCHMID, J. A. 2010. Interaction of the TNFR-receptor associated factor TRAF1 with I-kappa B kinase-2 and TRAF2 indicates a regulatory function for NF-kappa B signaling. *PLoS ONE,* 5, e12683.

SUN, C. Y., ZANG, Y. C., SAN, Y. X., SUN, W. & ZHANG, L. 2010. Proteomic analysis of clear cell renal cell carcinoma. Identification of potential tumor markers. *Saudi medical journal,* 31, 525-32.

SUN, X., YASUDA, O., TAKEMURA, Y., KAWAMOTO, H., HIGUCHI, M., BABA, Y., KATSUYA, T., FUKUO, K., OGIHARA, T. & RAKUGI, H. 2008. Akt activation prevents Apop-1-induced death of cells. *Biochemical and Biophysical Research Communications,* 377, 1097-1101.

SUNG, B., PANDEY, M. K. & AGGARWAL, B. B. 2007. Fisetin, an Inhibitor of Cyclin-Dependent Kinase 6, Down-Regulates Nuclear Factor-κB-Regulated Cell Proliferation, Antiapoptotic and Metastatic Gene Products through the Suppression of TAK-1 and Receptor-Interacting Protein-Regulated IκBα Kinase Activation. *Molecular Pharmacology,* 71, 1703-1714.

SUPPIAH, R., SHAHEEN, P. E., SEEMA, P. E., MISBAH, A., WOOD, L., MOTZER, R. J., NEGRIER, S., ANDRESEN, S. W. & BUKOWSKI, R. M. 2006. Thrombocytosis as a prognostic factor for survival in patients with metastatic renal cell carcinoma. *Cancer,* 107, 1793-1800.

SUTHERLAND, D. E., WEITZ, I. C. & LIEBMAN, H. A. 2003. Thromboembolic complications of cancer: epidemiology, pathogenesis, diagnosis, and treatment. *American Journal of Hematology,* 72, 43-52.

SUZUKI-INOUE, K., KATO, Y., INOUE, O., KANEKO, M. K., MISHIMA, K., YATOMI, Y., YAMAZAKI, Y., NARIMATSU, H. & OZAKI, Y. 2007. Involvement of the snake toxin receptor CLEC-2, in podoplanin-mediated platelet activation, by cancer cells. *J Biol Chem,* 282, 25993-6001.

SUZUKI, K., AIURA, K., KITAGOU, M., HOSHIMOTO, S., TAKAHASHI, S., UEDA, M. & KITAJIMA, M. 2004. Platelets counts closely correlate with the disease-free survival interval of pancreatic cancer patients. *Hepato-gastroenterology,* 51, 847-53.

SWAIM, M. W., CHIANG, H. S. & HUANG, T. F. 1996. Characterisation of platelet aggregation induced by PC-3 human prostate adenocarcinoma cells and inhibited by venom peptides, trigramin and rhodostomin. *European journal of cancer,* 32A, 715-21.

SWAINE, J. 2011. *New 'liquid biopsy' to help with detection of cancer* [Online]. The Irish Independent. Available: http://www.independent.ie/health/latest-news/new-liquid-biopsy-to-help-with-detection-of-cancer-2482406.html [Accessed 5 January 2011].

SWICK, L. & KAPATOS, G. 2006. A yeast 2-hybrid analysis of human GTP cyclohydrolase I protein interactions. *Journal of Neurochemistry,* 97, 1447-1455.

TACHIBANA, K. E., GONZALEZ, M. A., GUARGUAGLINI, G., NIGG, E. A. & LASKEY, R. A. 2005. Depletion of licensing inhibitor geminin causes centrosome overduplication and mitotic defects. *EMBO Rep,* 6, 1052-7.

TAFE, L. J., GARG, K., CHEW, I., TORNOS, C. & SOSLOW, R. A. 2010. Endometrial and ovarian carcinomas with undifferentiated components: clinically aggressive and frequently underrecognized neoplasms. *Mod Pathol,* 23, 781-789.

TAGLIABUE, L. & PUGLIANO, M. 2011. Will aspirin rescue us from cancer? *Internal and Emergency Medicine*, 1-3.

TALUKDER, A. H., MENG, Q. & KUMAR, R. 2005. CRIPak, a novel endogenous Pak1 inhibitor. *Oncogene,* 25, 1311-1319.

TAMUSSINO, K. F., GÜCER, F., REICH, O., MOSER, F., PETRU, E. & SCHOLZ, H. S. 2001. Pretreatment hemoglobin, platelet count, and prognosis in endometrial carcinoma. *International Journal of Gynecological Cancer,* 11, 236-240.

TAN, X.-L., REID-LOMBARDO, K. M., BAMLET, W. R., OBERG, A. L., ROBINSON, D. P., ANDERSON, K. E. & PETERSEN, G. M. 2011. Aspirin, nonsteroidal anti-inflammatory drugs (NSAID), acetaminophen, and pancreatic cancer risk: A clinic-based case-control study. *Cancer Prevention Research*.

TANAKA, T., ISHIGURO, H., KUWABARA, Y., KIMURA, M., MITSUI, A., KATADA, T., SHIOZAKI, M., NAGANAWA, Y., FUJII, Y. & TAKEYAMA, H. 2010. Vascular endothelial growth factor C (VEGF-C) in esophageal cancer correlates with lymph node metastasis and poor patient prognosis. *J Exp Clin Cancer Res,* 29, 83.

TANGJITGAMOL, S., HANPRASERTPONG, J., MANUSIRIVITHAYA, S., WOOTIPOOM, V., THAVARAMARA, T. & BUHACHAT, R. 2010. Malignant ovarian germ cell tumors: clinico-pathological presentation and survival outcomes. *Acta Obstetricia et Gynecologica Scandinavica,* 89, 182-189.

TANIMOTO, A., MURATA, Y., WANG, K.-Y., TSUTSUI, M., KOHNO, K. & SASAGURI, Y. 2008. Monocyte Chemoattractant Protein-1 Expression Is Enhanced by Granulocyte-Macrophage Colony-stimulating Factor via Jak2-Stat5 Signaling and Inhibited by Atorvastatin in Human Monocytic U937 Cells. *Journal of Biological Chemistry,* 283, 4643-4651.

TAUBERT, H., BLÜMKE, K., BILKENROTH, U., MEYE, A., KUTZ, A., BARTEL, F., LAUTENSCHLÄGER, C., ULBRICH, E. J., NASS, N., HOLZHAUSEN, H.-J., KOELBL, H. & LEBRECHT, A. 2004. Detection of disseminated tumor cells in peripheral blood of patients with breast cancer: correlation to nodal status and occurrence of metastases. *Gynecologic Oncology,* 92, 256-261.

TAVASSOLI, F. A., D.P. (ed.) 2003. *Pathology and Genetics of Tumours of the Breast and Female Genital Organs,* Lyon: IARC Press.

TEW, W. P., COLOMBO, N., RAY-COQUARD, I., OZA, A., CAMPO, J. D., SCAMBIA, G. & SPRIGGS, D. VEGF-Trap for patients (pts) with recurrent platinum-resistant epithelial ovarian cancer (EOC): Preliminary results of a randomized, multicenter phase II study American Society of Clinical Oncology Annual Meeting, 2007. Journal of Clinical Oncology.

THERIAULT, C., PINARD, M., COMAMALA, M., MIGNEAULT, M., BEAUDIN, J., MATTE, I., BOIVIN, M., PICHE, A. & RANCOURT, C. 2011. MUC16 (CA125) regulates epithelial ovarian cancer cell growth, tumorigenesis and metastasis. *Gynecol Oncol.*

THERMO FISHER SCIENTIFIC INC. 2010. *Specialised Surfaces: Cell Culture Surfaces* [Online]. Thermo Fisher Scientific Inc. Available: http://www.nuncbrand.com/us/page.aspx?ID=1275#Subsection9.

THOMAS-PETER, H. 2011. *Blood Test Could Detect Cancer In One Cell* [Online]. Sky News/BSkyB. Available: http://news.sky.com/skynews/Article/201009115879000 [Accessed 5 January 2011].

THOMPSON, R. H. & KWON, E. D. 2006. Significance of B7-H1 overexpression in kidney cancer. *Clin Genitourin Cancer,* 5, 206-11.

TOMITA, M., SHIMIZU, T., HARA, M., AYABE, T. & ONITSUKA, T. 2008. Prognostic impact of thrombocytosis in resectable non-small cell lung cancer. *Interact CardioVasc Thorac Surg,* 7, 613-615.

TRINGLER, B., LIU, W., CORRAL, L., TORKKO, K. C., ENOMOTO, T., DAVIDSON, S., LUCIA, M. S., HEINZ, D. E., PAPKOFF, J. & SHROYER, K. R. 2006. B7-H4 overexpression in ovarian tumors. *Gynecologic Oncology,* 100, 44-52.

TROUSSEAU, A. 1865. Phlegmasia Alba Dolens. *Clinique Medicale de l'Hotel-Dieu de Paris,* 3.

TSILIDIS, K., ALLEN, N., KEY, T., DOSSUS, L., KAAKS, R., BAKKEN, K., LUND, E., FOURNIER, A., DAHM, C., OVERVAD, K., HANSEN, L., TJØNNELAND, A., RINALDI, S., ROMIEU, I., BOUTRON-RUAULT, M.-C., CLAVEL-CHAPELON, F., LUKANOVA, A., BOEING, H., SCHÜTZE, M., BENETOU, V., PALLI, D., BERRINO, F., GALASSO, R., TUMINO, R., SACERDOTE, C., BUENO-DE-MESQUITA, H., VAN DUIJNHOVEN, F., BRAEM, M., ONLAND-MORET, N., GRAM, I., RODRÍGUEZ, L., DUELL, E., SÁNCHEZ, M.-J., HUERTA, J., ARDANAZ, E., AMIANO, P., KHAW, K.-T., WAREHAM, N. & RIBOLI, E. 2011. Menopausal hormone therapy and risk of ovarian cancer in the European prospective investigation into cancer and nutrition. *Cancer Causes and Control,* 22, 1075-1084.

TSUKISHIRO, S., SUZUMORI, N., NISHIKAWA, H., ARAKAWA, A. & SUZUMORI, K. 2008. Preoperative serum thrombopoietin levels are higher in patients with ovarian cancer than with benign cysts. *Eur J Obstet Gynecol Reprod Biol,* 140, 67-70.

TSURUO, T. & FUJITA, N. 2008. Platelet aggregation in the formation of tumor metastasis. *Proceedings of the Japan Academy, Series B,* 84, 189-198.

TURGEON, M. L. 2005. *Clinical hematology : theory and procedures,* Philadelphia, Pa. ; London, Lippincott Williams & Wilkins.

UNITED NATIONS DEPARTMENT OF ECONOMIC AND SOCIAL AFFAIRS 2011. *United Nations Demographic Yearbook: 2009-2010,* New York, USA, United Nations.

URBANUS, R. T., PENNINGS, M. T. T., DERKSEN, R. H. W. M. & DE GROOT, P. G. 2008. Platelet activation by dimeric β2-glycoprotein I requires signaling via both glycoprotein Ibα and apolipoprotein E receptor 2'. *Journal of Thrombosis and Haemostasis,* 6, 1405-1412.

UUTELA, M., WIRZENIUS, M., PAAVONEN, K., RAJANTIE, I., HE, Y., KARPANEN, T., LOHELA, M., WIIG, H., SALVEN, P., PAJUSOLA, K., ERIKSSON, U. & ALITALO, K. 2004. PDGF-D induces macrophage recruitment, increased interstitial pressure, and blood vessel maturation during angiogenesis. *Blood,* 104, 3198-3204.

VAN ALPHEN, R. J., WIEMER, E. A. C., BURGER, H. & ESKENS, F. A. L. M. 2008. The spliceosome as target for anticancer treatment. *Br J Cancer,* 100, 228-232.

VAN DER KOLK, D. M., DE BOCK, G. H., LEEGTE, B. K., SCHAAPVELD, M., MOURITS, M. J., DE VRIES, J., VAN DER HOUT, A. H. & OOSTERWIJK, J. C. 2010. Penetrance of breast cancer, ovarian cancer and contralateral breast cancer in BRCA1 and BRCA2 families: high cancer incidence at older age. *Breast cancer research and treatment,* 124, 643-51.

VANDESOMPELE, J., DE PRETER, K., PATTYN, F., POPPE, B., VAN ROY, N., DE PAEPE, A. & SPELEMAN, F. 2002. Accurate normalization of real-time quantitative RT-PCR data by geometric averaging of multiple internal control genes. *Genome Biol,* 3, RESEARCH0034.

VANG, R., SHIH IE, M. & KURMAN, R. J. 2009. Ovarian low-grade and high-grade serous carcinoma: pathogenesis, clinicopathologic and molecular biologic features, and diagnostic problems. *Advances in Anatomic Pathology,* 16, 267-82.

VANLANGENAKKER, N., VANDEN BERGHE, T., BOGAERT, P., LAUKENS, B., ZOBEL, K., DESHAYES, K., VUCIC, D., FULDA, S., VANDENABEELE, P. & BERTRAND, M. J. M. 2011. cIAP1 and TAK1 protect cells from TNF-induced necrosis by preventing RIP1/RIP3-dependent reactive oxygen species production. *Cell Death Differ,* 18, 656-665.

VARKI, A. 2007. Trousseau's syndrome: multiple definitions and multiple mechanisms. *Blood,* 110, 1723-1729.

VARKI, N. M. & VARKI, A. 2002. Heparin Inhibition of Selectin-Mediated Interactions during the Hematogenous Phase of Carcinoma Metastasis: Rationale for Clinical Studies in Humans. *Seminars in Thrombosis and Hemostasis,* 28, 53,66.

VASEY, P. A. 2003. Resistance to chemotherapy in advanced ovarian cancer: mechanisms and current strategies. *Br J Cancer,* 89, S23-S28.

VERIDEX LLC. 2011. *An Introduction to the CellSearch™ System: Technology Overview and Analytical Validation* [Online]. Veridex LLC. Available: http://www.veridex.com/pdf%5CMKG-1767rev3CS-TechnologyAnalyticalOverview Customer PresentationFINAL.pdf [Accessed 03 September 2011].

VERSNEL, M. A., HAARBRINK, M., LANGERAK, A. W., DE LAAT, P. A., HAGEMEIJER, A., VAN DER KWAST, T. H., VAN DEN BERG-BAKKER, L. A. & SCHRIER, P. I. 1994. Human ovarian tumors of epithelial origin express PDGF in vitro and in vivo. *Cancer Genet Cytogenet,* 73, 60-4.

VICUS, D., BEINER, M. E., KLACHOOK, S., LE, L. W., LAFRAMBOISE, S. & MACKAY, H. 2010. Pure dysgerminoma of the ovary 35 years on: A single institutional experience. *Gynecologic Oncology,* 117, 23-26.

VIGNATI, S., ALBERTINI, V., RINALDI, A., KWEE, I., RIVA, C., OLDRINI, R., CAPELLA, C., BERTONI, F., CARBONE, G. M. & CATAPANO, C. V. 2006. Cellular and molecular consequences of peroxisome proliferator-activated receptor-gamma activation in ovarian cancer cells. *Neoplasia,* 8, 851-61.

VIGON, I., DREYFUS, F., MELLE, J., VIGUIE, F., RIBRAG, V., COCAULT, L., SOUYRI, M. & GISSELBRECHT, S. 1993. Expression of the c-mpl proto-oncogene in human hematologic malignancies. *Blood,* 82, 877-83.

VISUS, C., ANDRES, R., MAYORDOMO, J. I., MARTINEZ-LORENZO, M. J., MURILLO, L., SAEZ-GUTIERREZ, B., DIESTRE, C., MARCOS, I., ASTIER, P., GODINO, J., CARAPETO-MARQUEZ DE PRADO, F. J., LARRAD, L. & TRES, A. 2007. Prognostic role of

circulating melanoma cells detected by reverse transcriptase-polymerase chain reaction for tyrosinase mRNA in patients with melanoma. *Melanoma research,* 17, 83-9.

VOGEL, R. O., JANSSEN, R. J. R. J., UGALDE, C., GROVENSTEIN, M., HUIJBENS, R. J., VISCH, H.-J., VAN DEN HEUVEL, L. P., WILLEMS, P. H., ZEVIANI, M., SMEITINK, J. A. M. & NIJTMANS, L. G. J. 2005. Human mitochondrial complex I assembly is mediated by NDUFAF1. *FEBS Journal,* 272, 5317-5326.

WAHRENBROCK, M., BORSIG, L., LE, D., VARKI, N. & VARKI, A. 2003. Selectin-mucin interactions as a probable molecular explanation for the association of Trousseau syndrome with mucinous adenocarcinomas. *J. Clin. Invest.,* 112, 853-862.

WAN, M., LI, Y., XUE, H., LI, Q. & LI, J. 2006. TNF-α Induces Lnk Expression Through PI3K-Dependent Signaling Pathway in Human Umbilical Vein Endothelial Cells. *The Journal of surgical research,* 136, 53-57.

WANG, F., LIU, R., LEE, S. W., SLOSS, C. M., COUGET, J. & CUSACK, J. C. 2006. Heparin-binding EGF-like growth factor is an early response gene to chemotherapy and contributes to chemotherapy resistance. *Oncogene,* 26, 2006-2016.

WANG, J. C., CHEN, C., NOVETSKY, A. D., LICHTER, S. M., AHMED, F. & FRIEDBERG, N. M. 1998. Blood Thrombopoietin Levels in Clonal Thrombocytosis and Reactive Thrombocytosis. *The American journal of medicine,* 104, 451-455.

WANG, L., MA, Q., CHEN, X., GUO, K., LI, J. & ZHANG, M. 2010a. Clinical Significance of B7-H1 and B7-1 Expressions in Pancreatic Carcinoma. *World Journal of Surgery,* 34, 1059-1065.

WANG, Y., CHEONG, D., CHAN, S. & HOOI, S. C. 2000. Ribosomal protein L7a gene is up-regulated but not fused to the tyrosine kinase receptor as chimeric trk oncogene in human colorectal carcinoma. *International journal of oncology,* 16, 757-62.

WANG, Y., JI, M., WANG, W., MIAO, Z., HOU, P., CHEN, X., XU, F., ZHU, G., SUN, X., LI, Y., CONDOURIS, S., LIU, D., YAN, S., PAN, J. & XING, M. 2008. Association of the T1799A BRAF mutation with tumor extrathyroidal invasion, higher peripheral platelet counts, and over-expression of platelet-derived growth factor-B in papillary thyroid cancer. *Endocr Relat Cancer,* 15, 183-90.

WANG, Z., AHMAD, A., LI, Y., KONG, D., AZMI, A. S., BANERJEE, S. & SARKAR, F. H. 2010b. Emerging roles of PDGF-D signaling pathway in tumor development and progression. *Biochimica et Biophysica Acta (BBA) - Reviews on Cancer,* 1806, 122-130.

WEBPATHOLOGY.COM. 2011. *WebPathology.com: A Visual Survey of Surgical Pathology Images* [Online]. Richmond, VA, USA. Available: http://www.webpathology.com [Accessed 20 August 2011].

WECHSLER, T., NEWMAN, S. & WEST, S. C. 2011. Aberrant chromosome morphology in human cells defective for Holliday junction resolution. *Nature,* 471, 642-646.

WEEN, M. P., LOKMAN, N. A., HOFFMANN, P., RODGERS, R. J., RICCIARDELLI, C. & OEHLER, M. K. 2011. Transforming growth factor-beta-induced protein secreted by peritoneal cells increases the metastatic potential of ovarian cancer cells. *International Journal of Cancer. Journal International Du Cancer,* 128, 1570-84.

WEINER, B. E., HUANG, H., DATTILO, B. M., NILGES, M. J., FANNING, E. & CHAZIN, W. J. 2007. An Iron-Sulfur Cluster in the C-terminal Domain of the p58 Subunit of Human DNA Primase. *Journal of Biological Chemistry,* 282, 33444-33451.

WELCH, S. A., HIRTE, H. W., ELIT, L., SCHILDER, R. J., WANG, L., MACALPINE, K., WRIGHT, J. J. & OZA, A. M. 2010. Sorafenib in combination with gemcitabine in recurrent epithelial ovarian cancer: a study of the Princess Margaret Hospital Phase II Consortium. *International journal of gynecological cancer : official journal of the International Gynecological Cancer Society,* 20, 787-93.

WENDLING, F. 1999. Thrombopoietin: its role from early hematopoiesis to platelet production. *Haematologica,* 84, 158-66.

WETZLER, M., BAER, M. R., BERNSTEIN, S. H., BLUMENSON, L., STEWART, C., BARCOS, M., MROZEK, K., BLOCK, A. W., HERZIG, G. P. & BLOOMFIELD, C. D. 1997. Expression of c-mpl mRNA, the receptor for thrombopoietin, in acute myeloid leukemia blasts identifies a group of patients with poor response to intensive chemotherapy. *J Clin Oncol,* 15, 2262-2268.

WHITE-ADAMS, T. C., BERNY, M. A., TUCKER, E. I., GERTZ, J. M., GAILANI, D., URBANUS, R. T., DE GROOT, P. G., GRUBER, A. & MCCARTY, O. J. 2009. Identification of coagulation factor XI as a ligand for platelet apolipoprotein E receptor 2 (ApoER2). *Arterioscler Thromb Vasc Biol,* 29, 1602-7.

WHITE, J. G. 1988. Platelet membrane ultrastructure and its changes during platelet activation. *Progress in Clinical and Biological Research,* 283, 1-32.

WHITE, N. M., CHOW, T. F., MEJIA-GUERRERO, S., DIAMANDIS, M., ROFAEL, Y., FARAGALLA, H., MANKARUOUS, M., GABRIL, M., GIRGIS, A. & YOUSEF, G. M. 2010. Three dysregulated miRNAs control kallikrein 10 expression and cell proliferation in ovarian cancer. *British Journal of Cancer,* 102, 1244-53.

WHITE, N. M., MATHEWS, M., YOUSEF, G. M., PRIZADA, A., FONTAINE, D., GHATAGE, P., POPADIUK, C., DAWSON, L. & DORE, J. J. 2009a. Human kallikrein related peptidases 6 and 13 in combination with CA125 is a more sensitive test for ovarian cancer than CA125 alone. *Cancer Biomark,* 5, 279-87.

WHITE, N. M., MATHEWS, M., YOUSEF, G. M., PRIZADA, A., POPADIUK, C. & DORE, J. J. 2009b. KLK6 and KLK13 predict tumor recurrence in epithelial ovarian carcinoma. *Br J Cancer,* 101, 1107-13.

WHITE, R. H. 2003. The Epidemiology of Venous Thromboembolism. *Circulation,* 107, 4I--8.

WHITE, T. C., BERNY, M. A., TUCKER, E. I., URBANUS, R. T., DE GROOT, P. G., FERNÁNDEZ, J. A., GRIFFIN, J. H., GRUBER, A. & MCCARTY, O. J. T. 2008. Protein C supports platelet binding and activation under flow: role of glycoprotein Ib and apolipoprotein E receptor 2. *Journal of Thrombosis and Haemostasis,* 6, 995-1002.

WHITEHOUSE, C. & SOLOMON, E. 2003. Current Status of the Molecular Characterization of the Ovarian Cancer Antigen CA125 and Implications for Its Use in Clinical Screening. *Gynecologic Oncology,* 88, S152-S157.

WILCZYNSKI, S. P., CHEN, Y. Y., CHEN, W., HOWELL, S. B., SHIVELY, J. E. & ALBERTS, D. S. 2005. Expression and mutational analysis of tyrosine kinase receptors c-kit, PDGFRalpha, and PDGFRbeta in ovarian cancers. *Hum Pathol,* 36, 242-9.

WILLIAMS, L. T. 1989. Signal transduction by the platelet-derived growth factor receptor. *Science,* 243, 1564-70.

WILSON, P. M., FRYER, R. H., FANG, Y. & HATTEN, M. E. 2010. Astn2, A Novel Member of the Astrotactin Gene Family, Regulates the Trafficking of ASTN1 during Glial-Guided Neuronal Migration. *The Journal of Neuroscience,* 30, 8529-8540.

WOODS, L. M., RACHET, B., SHACK, L., CATNEY, D., WALSH, P. M., COOPER, N., WHITE, C., MAK, V., STEWARD, J., COMBER, H., GAVIN, A., BREWSTER, D., QUINN, M. & COLEMAN, M. P. 2010. Survival from twenty adult cancers in the UK and Republic of Ireland in the late twentieth century. *Health Statistics Quarterly: Summer 2010.* Office for National Statistics (UK).

WU, F., LIU, S.-Y., TAO, Y.-M., OU, D.-P., FANG, F. & YANG, L.-Y. 2008. Decreased expression of methyl methansulfonate and ultraviolet-sensitive gene clone 81 (Mus81) is correlated with a poor prognosis in patients with hepatocellular carcinoma. *Cancer,* 112, 2002-2010.

WU, F., SHIRAHATA, A., SAKURABA, K., KITAMURA, Y., GOTO, T., SAITO, M., ISHIBASHI, K., KIGAWA, G., NEMOTO, H., SANADA, Y. & HIBI, K. 2010. Down-regulation of Mus81 as a potential marker for the malignancy of gastric cancer. *Anticancer Research,* 30, 5011-4.

WU, F., SHIRAHATA, A., SAKURABA, K., KITAMURA, Y., GOTO, T., SAITO, M., ISHIBASHI, K., KIGAWA, G., NEMOTO, H., SANADA, Y. & HIBI, K. 2011. Downregulation of Mus81 as a novel prognostic biomarker for patients with colorectal carcinoma. *Cancer Science,* 102, 472-477.

WU, Y., PAN, Y., DU, L., WANG, J., GU, Q., GAO, Z., LI, J., LENG, X., QIN, J., WU, X. & JIANG, Y. 2009. Identification of novel EIF2B mutations in Chinese patients with vanishing white matter disease. *J Hum Genet,* 54, 74-77.

XI, Z., KAERN, J., DAVIDSON, B., KLOKK, T. I., RISBERG, B., TROPE, C. & SAATCIOGLU, F. 2004. Kallikrein 4 is associated with paclitaxel resistance in ovarian cancer. *Gynecologic Oncology,* 94, 80-5.

XU, J., YIN, Z., GAO, W., LIU, L., WANG, R., HUANG, P., YIN, Y., LIU, P., YU, R. & SHU, Y. 2011. Meta-Analysis on the Association Between Nonsteroidal Anti-Inflammatory Drug Use and Lung Cancer Risk. *Clinical lung cancer,* Article In Print.

YAGI, H., YOTSUMOTO, F. & MIYAMOTO, S. 2008. Heparin-binding epidermal growth factor–like growth factor promotes transcoelomic metastasis in ovarian cancer through epithelial-mesenchymal transition. *Molecular Cancer Therapeutics,* 7, 3441-3451.

YANG, L., FROIO, R. M., SCIUTO, T. E., DVORAK, A. M., ALON, R. & LUSCINSKAS, F. W. 2005. ICAM-1 regulates neutrophil adhesion and transcellular migration of TNF-α-activated vascular endothelium under flow. *Blood,* 106, 584-592.

YASUDA, O., FUKUO, K., SUN, X., NISHITANI, M., YOTSUI, T., HIGUCHI, M., SUZUKI, T., RAKUGI, H., SMITHIES, O., MAEDA, N. & OGIHARA, T. 2006. Apop-1, a Novel Protein Inducing Cyclophilin D-dependent but Bax/Bak-related Channel-independent Apoptosis. *Journal of Biological Chemistry,* 281, 23899-23907.

YEN, C.-Y., CHEN, C.-H., CHANG, C.-H., TSENG, H.-F., LIU, S.-Y., CHUANG, L.-Y., WEN, C.-H. & CHANG, H.-W. 2009. Matrix metalloproteinases (MMP) 1 and MMP10 but not MMP12 are potential oral cancer markers. *Biomarkers,* 14, 244-249.

YILDIRIM, Y., ERTAS, I. E., DOGAN, A., GULTEKIN, O. E. & GULTEKIN, E. 2011. The predictors of response to neoadjuvant chemotherapy in advanced epithelial ovarian cancer. *Journal of Surgical Oncology,* n/a-n/a.

YOKOYAMA, Y., TSUCHIDA, S., HATAYAMA, I., SATOH, K., NARITA, T., RAO, M. S., REDDY, J. K., YAMADA, J., SUGA, T. & SATO, K. 1992. Loss of peroxisomal enzyme expression in preneoplastic and neoplastic lesions induced by peroxisome proliferators in rat livers. *Carcinogenesis,* 13, 265-9.

YON, J., PALMER, R. W., SHEER, D. & FRIED, M. 1989. Localization of the Surfeit gene cluster containing the ribosomal protein gene L7a to chromosome bands 9q33-34. *Annals of human genetics,* 53, 149-55.

YOUSEF, G. M. & DIAMANDIS, E. P. 2009. The human kallikrein gene family: new biomarkers for ovarian cancer. *Cancer Treat Res,* 149, 165-87.

YOUSEF, G. M., KYRIAKOPOULOU, L. G., SCORILAS, A., FRACCHIOLI, S., GHIRINGHELLO, B., ZARGHOONI, M., CHANG, A., DIAMANDIS, M., GIARDINA, G., HARTWICK, W. J., RICHIARDI, G., MASSOBRIO, M., DIAMANDIS, E. P. & KATSAROS, D. 2001a. Quantitative expression of the human kallikrein gene 9 (KLK9) in ovarian cancer: a new independent and favorable prognostic marker. *Cancer Research,* 61, 7811-8.

YOUSEF, G. M., MAGKLARA, A., CHANG, A., JUNG, K., KATSAROS, D. & DIAMANDIS, E. P. 2001b. Cloning of a new member of the human kallikrein gene family, KLK14, which is down-regulated in different malignancies. *Cancer Research,* 61, 3425-31.

YOUSEF, G. M., POLYMERIS, M. E., YACOUB, G. M., SCORILAS, A., SOOSAIPILLAI, A., POPALIS, C., FRACCHIOLI, S., KATSAROS, D. & DIAMANDIS, E. P. 2003. Parallel overexpression of seven kallikrein genes in ovarian cancer. *Cancer Research,* 63, 2223-7.

YU, K., GANESAN, K., TAN, L. K., LABAN, M., WU, J., ZHAO, X. D., LI, H., LEUNG, C. H., ZHU, Y., WEI, C. L., HOOI, S. C., MILLER, L. & TAN, P. 2008. A precisely regulated gene expression cassette potently modulates metastasis and survival in multiple solid cancers. *PLoS Genet,* 4, e1000129.

YUAN, A., CHEN, J. J. & YANG, P. C. 2008. Pathophysiology of tumor-associated macrophages. *Advances in clinical chemistry,* 45, 199-223.

ZACHARSKI, L. R. 2002. Anticoagulants in cancer treatment: malignancy as a solid phase coagulopathy. *Cancer Letters,* 186, 1-9.

ZEIMET, A. G., MARTH, C., MULLER-HOLZNER, E., DAXENBICHLER, G. & DAPUNT, O. 1994. Significance of thrombocytosis in patients with epithelial ovarian cancer. *Am J Obstet Gynecol,* 170, 549-54.

ZHANG, A., MENG, L., WANG, Q., XI, L., CHEN, G., WANG, S., ZHOU, J., LU, Y. & MA, D. 2006. Enhanced in vitro invasiveness of ovarian cancer cells through up-regulation of VEGF and induction of MMP-2. *Oncol Rep,* 15, 831-6.

ZHANG, F., ZHANG, L., ZHANG, B., WEI, X., YANG, Y., QI, R. Z., YING, G., ZHANG, N. & NIU, R. 2009. Anxa2 Plays a Critical Role in Enhanced Invasiveness of the Multidrug Resistant Human Breast Cancer Cells. *Journal of Proteome Research,* 8, 5041-5047.

ZHANG, J., LU, Y. & PIENTA, K. J. 2010a. Multiple roles of chemokine (C-C motif) ligand 2 in promoting prostate cancer growth. *Journal of the National Cancer Institute,* 102, 522-8.

ZHANG, J., PATEL, L. & PIENTA, K. J. 2010b. Targeting Chemokine (C-C motif) Ligand 2 (CCL2) as an Example of Translation of Cancer Molecular Biology to the Clinic. *Prog Mol Biol Transl Sci,* 95, 31-53.

ZHANG, L., BLACKWELL, K., ALTAEVA, A., SHI, Z. & HABELHAH, H. 2010c. TRAF2 phosphorylation promotes NF-{kappa}B-dependent gene expression and inhibits oxidative stress-induced cell death. *Mol. Biol. Cell*, mbc.E10-06-0556.

ZHENG, H., JI, C., GU, S., SHI, B., WANG, J., XIE, Y. & MAO, Y. 2005. Cloning and characterization of a novel RNA polymerase II C-terminal domain phosphatase. *Biochemical and Biophysical Research Communications,* 331, 1401-7.

ZHENG, L., FOLEY, K., HUANG, L., LEUBNER, A., MO, G., OLINO, K., EDIL, B. H., MIZUMA, M., SHARMA, R., LE, D. T., ANDERS, R. A., ILLEI, P. B., VAN EYK, J. E., MAITRA, A., LAHERU, D. & JAFFEE, E. M. 2011. Tyrosine 23 phosphorylation-dependent cell-surface localization of annexin A2 is required for invasion and metastases of pancreatic cancer. *PLoS ONE,* 6, e19390.

ZHENG, S.-E., YAO, Y., DONG, Y., LIN, F., ZHAO, H., SHEN, Z., SUN, Y.-J. & TANG, L.-N. 2009a. Down-regulation of ribosomal protein L7A in human osteosarcoma. *Journal of Cancer Research and Clinical Oncology,* 135, 1025-1031.

ZHENG, S., SHEN, J., JIAO, Y., LIU, Y., ZHANG, C., WEI, M., HAO, S. & ZENG, X. 2009b. Platelets and fibrinogen facilitate each other in protecting tumor cells from natural killer cytotoxicity. *Cancer Science,* 100, 859-65.

ZHOU, L., HAYASHI, Y., ITOH, T., WANG, W., RUI, J. A. & ITOH, H. 2000. Expression of urokinase-type plasminogen activator, urokinase-type plasminogen activator receptor, and plasminogen activator inhibitor-1 and -2 in hepatocellular carcinoma. *Pathology International,* 50, 392-397.

ZHOU, L., YAN, C., GIELING, R. G., KIDA, Y., GARNER, W., LI, W. & HAN, Y. P. 2009. Tumor necrosis factor-alpha induced expression of matrix metalloproteinase-9 through p21-activated kinase-1. *BMC immunology,* 10, 15.

ZHU, W., CHEN, Y. & DUTTA, A. 2004. Rereplication by depletion of geminin is seen regardless of p53 status and activates a G2/M checkpoint. *Mol Cell Biol,* 24, 7140-50.

ZHU, Y., LIN, H., LI, Z., WANG, M. & LUO, J. 2001. Modulation of expression of ribosomal protein L7a (rpL7a) by ethanol in human breast cancer cells. *Breast cancer research and treatment,* 69, 29-38.

ZIEMIECKI, A., MUELLER, R. G., HYNES, N. E., KRIEG, J. & KOZMA, S. C. 1988. cDNA sequence of the human ribosomal large subunit protein L7a. *Nucleic acids research,* 16, 10356.

ZIEMIECKI, A., MULLER, R. G., FU, X. C., HYNES, N. E. & KOZMA, S. 1990. Oncogenic activation of the human trk proto-oncogene by recombination with the ribosomal large subunit protein L7a. *The EMBO journal,* 9, 191-6.

ZIOGAS, A. C., GAVALAS, N. G., TSIATAS, M., TSITSILONIS, O., POLITI, E., TERPOS, E., RODOLAKIS, A., VLAHOS, G., THOMAKOS, N., HAIDOPOULOS, D., ANTSAKLIS, A., DIMOPOULOS, M. A. & BAMIAS, A. 2011. VEGF directly suppresses activation of T cells from ovarian cancer patients and healthy individuals via VEGF receptor Type 2. *International Journal of Cancer*, n/a-n/a.

ZONDOR, S. D. & MEDINA, P. J. 2004. Bevacizumab: An Angiogenesis Inhibitor with Efficacy in Colorectal and Other Malignancies. *Ann Pharmacother,* 38, 1258-1264.

APPENDIX

7 Appendix

7.1 Ambion® RecoverAll™ Total Nucleic Acid Isolation Kit Protocol

Working Solution Preparation

- American Chemical Society (ACS) grade ethanol was added to Wash 1 Concentrate and Wash 2/3 Concentrate prior to use.

Deparaffinisation

- Paraffin embedded tissue sections were incubated in 1ml 100% xylene at 50°C for three minutes in 2ml microcentrifuge tubes.
- Following xylene incubation the samples were centrifuged at maximum speed (30,000 RPM) and the xylene discarded to a specific waste xylene collection vessel.
- The pelleted sample was then washed with 1ml 100% ACS grade ethanol, centrifuged at maximum speed as before and the ethanol discarded. This was then repeated once.
- The pellet was allowed to air dry for 15-45 minutes.

Protease Digestion

- 200µl digestion buffer was added to the de-paraffinised, air dried sample pellet and 4µl proprietary Ambion® protease solution added to the sample and the tube gently swirled to ensure mixing of the protease solution and immersion of the sample.
- For RNA isolation the sample was then incubated in a heat block at 50°C for 15 minutes and 80°C for 15 minutes. The sample may not clarify in the prescribed time but if left longer than 15 minutes at 80°C there is an increased risk of RNA degradation.

Nucleic Acid Isolation

- 240µl Ambion® isolation additive was added to the sample and vortexed to mix.
- 550µl of 100% ACS grade ethanol was added to the sample and the sample mixed by gentle pipetting.
- A filter cartridge was placed into one of the supplied collection tubes. 700µl of the sample/isolation additive/ethanol mixture was transferred to the filter making sure to avoid transferring large pieces of undigested tissue which would clog the filter and the lid closed.
- The filter tube was centrifuged at 10,000 RPM for thirty seconds to pass the solution through the filter. Repeat the filtration process with the remaining sample/isolation additive/ethanol mixture
- 700µl of Wash 1 buffer was transferred to the filter cartridge and centrifuged at 10,000 x *g* for 30 seconds. After centrifugation the flow-through was discarded and the filter cartridge re-inserted into the collection tube.
- 500µl of Wash 2/3 buffer was transferred to the filter cartridge and centrifuged at 10,000 x *g* to pass the mixture through the filter.
- Following centrifugation the flow-through was discarded, the filter cartridge returned to the collection tube and the assembly centrifuged at 10,000 x *g* for an additional 30 seconds to remove residual fluid from the filter.

Nuclease Digestion and Final Nucleic Acid Purification

- To isolate RNA 60µl DNAse mix, containing 6µl 10x DNAse buffer, 4µl DNAse solution and 50µl DNAse and RNAse free H_2O, was added to the centre of the filter cartridge. The cap was the cap was then closed and the filter incubated at room temperature for 30 minutes.
- After incubation 700µl of Wash 1 buffer was transferred to the filter cartridge and incubated at room temperature for 1 minute before centrifugation at 10,000 x *g* for 30 seconds.
- The flow through was discarded and the filter cartridge returned to the collection tube. 500µl of Wash 2/3 buffer was then transferred to the wash cartridge, the

cap closed and the assembly centrifuged 10,000 x *g* for 30 seconds. The flow through was discarded and one repetition of this step performed.

- Having discarded the flow through from the second Wash 2/3 centrifugation the assembly was centrifuged for 1 minute at 10,000 x *g* in order to remove any residual fluid from the filter.
- The filter cartridge was transferred to a new collection tube and 60µl of room temperature DNAse and RNAse free H_2O transferred to the centre of the filter, the cap closed and the assembly incubated at room temperature for 1 minute.
- The assembly was centrifuged at maximum speed (30,000 RPM) to pass the solution through the filter with the resultant eluate containing purified RNA.
- The RNA was analysed for yield and purity by Nanodrop spectrophotometric analysis and stored at -20°C to -80°C.

7.2 QIAGEN® RNeasy® Mini Kit Protocol

Working Solution Preparation

- Buffer RPE required the addition of four volumes of 96-100% ethanol to obtain a working solution.

- 10µl β-mercapto ethanol (β-ME) was added per 1 ml Buffer RLT to denature and inactivate intracellular RNases released during cell lysis.

- DNase I stock solution was prepared using the QIAGEN® RNase-Free DNase Set®. Lyophilized DNase I was dissolved in 550µl of the DNAse and RNase free water provided with caution shown not to lose any DNAse when opening the vial. The solution was gently mixed by inversion of the vial. Gentle inversion ensures the DNAse is not subjected to physical denaturation to which it is especially sensitive. Following mixing 100µl aliquots sufficient for ten samples were prepared and stored at -20°C for up to 9 months until required.

Cell Lysis and Homogenisation

- Cell lines were grown to 80% confluence in 75cm^2 tissue culture flasks in complete growth media and maintained in a humidified environment at 37°C, 5% CO_2 (see Section 2.5). When ready for extraction flasks containing cells were trypsinised and pelleted as described in section 2.5.
- 600µl Buffer RLT was applied to the cell pellet and gently mixed by gentle pipetting in order to lyse cells.
- The lysate was then transferred to a QIAshredder™ spin column placed in a 2ml collection tube and centrifuged for 2 minutes at maximum speed (30,000 RPM). The lysate is homogenized as it passes through the spin column and the flow through is used for subsequent RNA extraction.
- One volume of 70% ethanol was added to the homogenized lysate, and mixed well by pipetting. The volume was noted to account for volume losses ocurring during

homogenization. Also, precipitates may be visible after addition of ethanol some cell line lysates, this does not affect the procedure.

- An RNeasy® spin column was placed in a 2 ml collection tube (supplied) and 700µl of the sample, including any precipitate that may have formed, was transferred to the column. The lid was gently closed and the assembly centrifuged for 15 seconds at 10,000 RPM.
- The flow-through was discarded and the collection tube reused. If the sample volume exceeded 700µl, successive aliquots were centrifuged in the same RNeasy® spin column and the flow-through discarded as before.

On Column DNase Digestion

Although the RNeasy® silica membranes used in QIAGEN® column based RNA isolation technologies removes most contaminating DNA without DNase treatment further DNA removal is required for sensitive downstream molecular biology applications such as TaqMan® reverse transcription-polymerase chain reaction (RT-PCR) and whole transcriptome microarray analysis.

- The DNase stock solution was prepared as described earlier in this section.
- 350µl Buffer RW1 was added to the RNeasy® spin column, the lid closed and the assembly centrifuged for 15 seconds at 10,000 rpm to wash the spin column membrane. The flow-through was discarded and the collection tube reused.
- 10µl DNase I stock solution was added to 70µl Buffer RDD (supplied) and mixed by gently inverting the tube. The mixture was centrifuged briefly to collect residual liquid from the sides of the tube. To avoid denaturing the DNase enzyme mixing by vortexing was avoided.
- DNase I incubation mix (80µl) was added directly to the RNeasy® spin column membrane, and incubated at room temperature for 15 min. Note: It was important to add the DNase I incubation mix directly to the RNeasy® spin column silica-gel membrane as DNase digestion would be incomplete if part of the mix stuck to the walls or O-ring of the spin column.
- 350µl of Buffer RW1 was transferred to the RNeasy® spin column, the lid closed and the assembly centrifuged for 15 seconds at 10,000 RPM, discarding the flow

through afterwards. The flow-through contained Buffer RW1 and could not be disposed of with bleach as it contains a small amount of guanidine thiocyanate which if combined with bleach could result in the production of toxic compounds such as hydrogen chloride (HCl) and hydrogen cyanide (HCN).

- 500µl Buffer RPE was transferred to the RNeasy® spin column, the lid closed gently and the assembly centrifuged for 15s at 10,000 RPM to wash the spin column membrane.
- 500µl Buffer RPE was transferred to the RNeasy® spin column, the lid closed gently and the assembly centrifuged for 2 minutes at 10,000 RPM to wash the spin column. The extended centrifugation dries the spin column membrane, ensuring that no ethanol which might interfere with downstream reactions is carried over during RNA elution.
- The RNeasy® spin column was removed from the collection tube carefully ensuring that the column did not contact the flow-through and placed in a new 2 ml collection tube. The old collection tube and flow-through were discarded.
- The lid was gently closed and the assembly centrifuged at full speed (30,000 RPM) for 1 minute to eliminate any possible carry-over of RPE buffer or residual flow-through remaining from the previous step.
- The RNeasy® spin column was placed into a new 1.5ml collection tube and 50µl RNase-free water applied directly to the spin column membrane.
- The lid was gently closed and the assembly centrifuged for 1 minute at 10,000 RPM to elute the RNA.
- To maximise the RNA yield returned the eluate was transferred from the collection tube directly to the column membrane and reusing the collection tube, the lid gently closed and the assembly centrifuged for 1 minute at 10,000 RPM.
- Using the initial eluate for second step RNA elution, was expected to yield 15–30% less RNA than that could obtained using a second volume of RNase-free water(30–50µl) which was recommended if the expected RNA yield is >30µg, but the final RNA concentration was predicted be higher.

Eluted RNA was analysed for yield and purity and stored at -20°C to -80°C.

7.3 Ambion® *mir*Vana™ miRNA Isolation Kit Protocol

Solution Preparation

- 21ml of ACS grade ethanol must be added to Ambion® miRNA Wash Solution 1, mixed well and the bottle marked as complete with ethanol added.

- 40ml of ACS grade ethanol must be added to Wash Solution 2/3, mixed well and the bottle marked as complete with ethanol added. It was important to note that a precipitate of excess ethylenediaminetetraacetic acid (EDTA) may form in this solution but does not affect the solution and the formed crystals could be avoided when removing solution for use.

The caps of both bottles were tightly closed once ethanol was added to prevent evaporation.

Cell Lysis and Homogenisation

Cell lines were grown to 80% confluence in $75cm^2$ tissue culture flasks in complete growth media and maintained in a humidified environment at 37°C, 5% CO_2 (see section 2.5).

- When ready for extraction flasks containing cells were aspirated of full cell culture media, rinsed with 5ml room temperature PBS, placed on ice and 3ml trypsin-EDTA applied to the cells.
- Once cells detach trypsin was neutralised with 8mls Trypsin Neutralising Solution (TNS) and centrifuged at 300x g for 4 minutes.
- The supernatant was discarded, the cell pellet resuspended in 1ml PBS, transferred to a 2ml DNase and RNase free tube and centrifuged at 1200RPM/300 x *g* for 4 minutes. The supernatant was aspirated and the cell pellet placed on ice.
- 600µl Lysis/Binding Solution was added to the cell pellet and pipetted vigorously to ensure complete lysis of cells and that a homogenous lysate was formed.

Organic Extraction

- 1/10 volume (60µl) of miRNA Homogenate Additive was added to the cell lysate and mixed well by vortexing three times. The lysate/homogenate additive mixture was then left on ice for 10 minutes.
- One volume of Acid-Phenol Chloroform equal to that of the lysate (600µl) was added to the lysate/homogenate additive mixture and vortexed for 1 minute.
- The mixture was then centrifuged at maximum speed (30,000 RPM) at room temperature to separate the aqueous and organic phases. If the interphase was not compact following centrifugation a repeat centrifugation was performed.
- The aqueous (upper) phase was carefully removed without disturbing the organic and inter-phases and transferred to a fresh DNase and RNase free 2ml tube. The volume transferred was noted.

Total RNA Isolation

- 1.25 volumes of room temperature molecular grade ethanol was added to the aqueous phase solution acquired in the previous step (e.g. if 600µl was recovered then 750µl ethanol was added).
- A filter cartridge was placed into a collection tube and 700µl of the lysate/ethanol mixture applied to the filter cartridge and the cap carefully closed.
- The filter cartridge/tube assembly was centrifuged at 10,000 x *g* for 15 seconds to pass the mixture through the filter. The flow through was discarded and the remaining lysate mixture filtered. The collection tube was kept for use in subsequent steps.
- 700µl of miRNA Wash Solution 1 working solution was applied to the filter cartridge, the cap closed and the assembly centrifuged for 10 seconds at 10,000 x *g*. The flow through was discarded and the collection tube was kept for use in subsequent steps.
- The filter was washed twice with Wash Solution 2/3 requiring the application of 500µl Wash 2/3 working solution to the filter cartridge and centrifugation 10 seconds at 10,000 x *g*. The flow through was discarded following each centrifugation.

- After discarding the flow through after the last wash the filter was returned to the collection tube and the assembly centrifuged at 10,000 x *g* for one minute to remove residual fluid from the filter.
- The filter cartridge was transferred to a fresh collection tube and 100µl of preheated 95°C RNase and DNase free water applied to the centre of the filter membrane, the cap closed and the assembly centrifuged for 30 seconds at 30,000 RPM. The eluate contains isolated total RNA which is then was analysed for yield and purity and stored at -20°C to -80°C.

If required this kit will also allow the isolation of small RNA species from the aqueous phase solution acquired through the organic extraction procedure or from total RNA isolated through the described protocol.

7.4 Affymetrix® GeneChip® Human Exon 1.0 ST Array Technology

7.4.1 Day 1 Workflow Protocol

Stock Reagent and Sample Preparation

Sample Total RNA

- Total RNA extracted from experimental cells was quantified by Nanodrop as per section 2.4.1 and the quality and integrity assessed as per section Agilent Bioanalyser through Bioanalyser analysis. tRNA of a sufficiently high Δ260/Δ280 (1.7-2.1) and RIN of 7.0 or greater.
- Aliquots were taken from Total RNA samples and adjusted to a final concentration of 33ng/µl using nuclease free H_2O.

Control RNA

2µl control RNA (HeLa source, 1mg/ml) was dispensed in 38µl nuclease free H_2O resulting in 40µl of 50ng/ml RNA solution. When brought through cRNA and cDNA synthesis control RNA is expected to yield >20µg and >6µg respectively if the kit is working correctly.

Poly-A RNA Controls

Using a starting tRNA input of 100ng as recommended by Affymetrix/Ambion® a set of serial dilutions was performed on Poly-A RNA control stock solution. These are indicated in Table 7-1.

Table 7-1

tRNA Input	Serial Dilutions				Volume of Dilution 4 added to total RNA
	Dilution 1	Dilution 2	Dilution 3	Dilution 4	
100ng	1:20	1:50	1:50	1:10†	2µl

Table 7-1: Poly-A RNA Control Serial Dilution.

† Control tRNA input is 50ng and the final (fourth) dilution required as a result is 1:20.

- 2µl Poly-A Control Stock was added to 38µl Poly-A Control Dilution Buffer in a non-stick microcentrifuge tube for the first dilution. The solution was mixed thoroughly by pipette and briefly centrifuged to collect the liquid at the bottom of the tube.
- 2µl of Dilution 1 was added to 98µl Poly-A Control Dilution Buffer in a non-stick microcentrifuge tube for the second dilution. The solution was mixed thoroughly by pipette and briefly centrifuged to collect the liquid at the bottom of the tube.
- 2µl of Dilution 2 was added to 98µl Poly-A Control Dilution Buffer in a non-stick microcentrifuge tube for the third dilution. The solution was mixed thoroughly by pipette and briefly centrifuged to collect the liquid at the bottom of the tube.
- 2µl of Dilution 3 was added to 18µl Poly-A Control Dilution Buffer in a non-stick micro centrifuge tube for the fourth dilution for use with 100ng starting sample tRNA. The solution was mixed thoroughly by pipette and briefly centrifuged to collect the liquid at the bottom of the tube.
- 2µl of Dilution 3 was added to 38µl Poly-A Control Dilution Buffer in a non-stick microcentrifuge tube for the fourth dilution for use with 50ng Control tRNA. The solution was mixed thoroughly by pipette and briefly centrifuged to collect the liquid at the bottom of the tube.

Poly-A RNA dilution 1 may be stored for up to 6 weeks at -20°C in a non-frost free freezer and frozen/thawed up to eight times.

Sample total RNA/Poly-A Control Preparation

- 3µl of sample tRNA (33ng/µl) was transferred to a nuclease free, non-stick PCR tube.
- 2µl Poly-A RNA Control Dilution 4 (for use with 100ng starting RNA template) was added, mixed by gentle vortexing and briefly centrifuged.

Control tRNA/Poly-A Control Preparation

- 1µl of control tRNA (50ng/µl) was transferred to a nuclease free, non-stick PCR tube.
- 2µl of nuclease free H_2O was added to tRNA to give a final volume of 3µl.
- 2µl Poly-A RNA Control Dilution 4 (for use with 50ng starting RNA template) was added, mixed by gentle vortexing and briefly centrifuged.

7.4.1.1 First Strand cDNA Synthesis

The Ambion® WT Expression Kit is used at this step to reverse transcribe total RNA into single stranded cDNA. This reverse transcription reaction utilises engineered primers specifically designed to exclude sequences matching ribosomal RNA (rRNA) whilst priming poly-A and non-poly-A containing mRNAs. The advantage of this technique over previous protocols is it obviates the need for an initial rRNA reduction step previously requiring magnetic separation of rRNA from tRNA and negative selection of residual mRNA.

First Strand Master Mix Preparation

- The First Strand Buffer and Enzyme Mixes were removed from -20°C prior to use. The Buffer Mix was heated to 37°C for 2 minutes and briefly vortexed and centrifuged to ensure any precipitates were fully dissolved.
- The Enzyme Mix was thawed on ice until required.
- The First Strand Master Mix was prepared by combining the First Strand Buffer Mix and First Strand Enzyme Mix in a labelled nuclease free, non-stick micro

centrifuge tube as per Table 7-2. 5% excess volume was included to correct for pipetting loss. The solutions were mixed by vortexing and briefly centrifuged to collect the liquid at the bottom of the tube.

Table 7-2

First Strand Master Mix Component	Volume for 1 reaction (µl)	Volume for 10 reactions (µl)
First Strand Buffer Mix	4	42
First Strand Enzyme Mix	1	10.5
Total Volume	5	52.5

Table 7-2: First Strand cDNA Synthesis Master Mix Components and Volumes.

First Strand cDNA Synthesis

- 5µl First Strand Master Mix was transferred to supplied PCR tubes and 5µl Poly-A control spiked tRNA added, mixed gently by vortexing and the solution centrifuged briefly to collect the liquid at the bottom of the tube.
- The mixture was transferred to a GeneAmp® 7900 thermocycler (Applied Biosystems/Life Technologies Corp., Carlsbad, CA, USA) and incubated for:
    - 60 minutes at 25°C
    - 60 minutes at 42°C
    - 2-10 minutes at 4°C

Note: Keeping the reaction at 4°C for longer than 10 minutes may result in reduced cRNA yields.

- Immediately after incubation the PCR tubes were briefly centrifuged and placed on ice for 2 minutes before proceeding with second strand cDNA synthesis.

7.4.1.2 Second Strand cDNA Synthesis

Second Strand Master Mix Preparation

- The Second Strand Buffer and Enzyme Mixes were removed from -20°C prior to use. The Buffer Mix was heated to 37°C for 2 minutes and briefly vortexed and centrifuged to ensure any precipitates were fully dissolved.
- The Enzyme Mix was thawed on ice until required.
- The Second Strand Master Mix was prepared on ice by combining nuclease free H_2O, the Second Strand Buffer Mix and Second Strand Enzyme Mix in a labelled nuclease free, non-stick micro centrifuge tube as per Table 7-3. 5% excess volume was included to correct for pipetting loss. The solutions were mixed by vortexing and briefly centrifuged to collect the liquid at the bottom of the tube.

Table 7-3

Second Strand Master Mix Component	Volume for 1 reaction (µl)	Volume for 10 reactions (µl)
Nuclease Free H_2O	32.5	341.25
Second Strand Buffer Mix	12.5	131.25
Second Strand Enzyme Mix	5	52.5
Total Volume	50	525

Table 7-3: Second Strand cDNA Synthesis Master Mix Components and Volumes.

Second Strand cDNA Synthesis

- 50µl of the Second Strand Master Mix was added to each 10µl First Strand cDNA Synthesis product, mixed by gentle vortexing and briefly centrifuged to collect the liquid at the bottom of the tube.
- The mixture was transferred to a GeneAmp® 7900 thermocycler (Applied Biosystems/Life Technologies Corp., Carlsbad, CA, USA and incubated for:
    - 60 minutes at 16°C

- 10 minutes at 65°C
- minutes at 4°C

Note: The lid of the thermocycler must be disabled/off during second strand cDNA synthesis.

- Immediately after incubation the PCR tubes were briefly centrifuged and placed on ice before proceeding with IVT cRNA Synthesis.

7.4.1.3 cRNA Synthesis

IVT Master Mix Preparation

- The IVT Buffer and Enzyme Mixes were removed from -20°C prior to use and allowed to reach room temperature.

- The IVT Master Mix was prepared on ice by combining the IVT Buffer Mix and IVT Enzyme Mix in a labelled nuclease free, non-stick micro centrifuge tube as per Table 7-4.

  5% excess volume was included to correct for pipetting loss. The solutions were mixed by vortexing and briefly centrifuged to collect the liquid at the bottom of the tube.

Table 7-4

IVT Master Mix Component	Volume for 1 reaction (µl)	Volume for 10 reactions (µl)
IVT Buffer Mix	24	252
IVT Enzyme Mix	6	63
Total Volume	30	315

Table 7-4: IVT cRNA Synthesis Master Mix Components and Volumes.

IVT cRNA Synthesis

- 30µl of the IVT Master Mix was added to each 60µl Second Strand cDNA Synthesis product, mixed by gentle vortexing and briefly centrifuged to collect the liquid at the bottom of the tube.

- The mixture was transferred to a thermostatically controlled hybridisation oven and incubated for:
    - 16 hours minutes at 40°C.

- Immediately after incubation the PCR tubes were briefly centrifuged and placed on ice before proceeding with directly with cRNA purification or storage overnight at -20°C.

7.4.2 Day 2 Workflow Protocol

7.4.2.1 cRNA Purification

Stock Reagent Preparation

- Elution Solution was heated to 55°C for ≥ 10 minutes prior to use.
- 100% Ethanol (Molecular Grade, Sigma-Aldrich) was added to Nucleic Acid Wash Solution (Concentrate) prior to use.
- The Nucleic Acid Binding Buffer Concentrate was warmed to 37°C to ensure any precipitated was completely dissolved.
- Nucleic Acid Binding Beads were vigorously vortexed prior to use to ensure complete dispersal.

cRNA Purification

- cRNA Binding Mix was prepared by combining Nucleic Acid Binding Beads and Nucleic Acid Binding Buffer Concentrate in a labelled nuclease free, non-stick micro centrifuge tube as per Table 7-5. 10% excess volume was included to correct for pipetting loss. The solutions were mixed by vortexing and briefly centrifuged to collect the liquid at the bottom of the tube.

Table 7-5

cRNA Binding Mix Component	Volume for one reaction (µl)	Volume for ten reactions (µl)
Nucleic Acid Binding Beads	10	105
Nucleic Acid Binding Buffer Concentrate	50	525
Total	60	630

Table 7-5: cRNA Binding Mix Components and Volumes.

- 60µl of cRNA Binding Mix was added to each sample, the mixture pipetted up and down three times to mix and transferred to a U-bottom plate.
- 60µl of 100% isopropanol was added to each sample and pipetted up and down three times to mix.
- The plate was gently shaken for ≥2 minutes to mix allowing cRNA to bind to the Nucleic Acid Binding Beads.
- The plate was moved to a magnetic stand (Applied Biosystems) for 5 minutes to allow the beads to be captured. After 5 minutes the mixture is transparent and the magnetic beads pelleted at the point the magnetic stand touches each well.
- The supernatant was carefully aspirated ensuring the magnetic beads were not disturbed and the plate removed from the magnetic stand.
- The beads were subjected to three washes:

    - 100µl of prepared Nucleic Acid Wash Solution was added to each sample and moderately shaken for 1 minute. Note the beads may not disperse at this point, this does not affect the RNA purity/yield.
    - The plate was returned to the magnetic stand for 5 minutes as before and the supernatant carefully aspirated. This wash protocol was repeated twice more.

- After the final wash was aspirated the plate was removed from the magnetic stand and shaken vigorously for 1 minute to evaporate residual ethanol from the beads.

    - Note: it was critical at this point that the beads are dried so that there is no visible liquid but the beads still look shiny/wet. If the beads were allowed to dry out the RNA yield may be affected.

- 40µl of preheated (55°C) Elution Solution was added to each sample to elute purified cRNA from the Nucleic Acid Binding Beads and incubated at RT, without shaking for 2 minutes. After 2 minutes the plate was vigorously shaken for 3 minutes, after which any undispersed pellets were disrupted by manual pipetting.

- The plate was returned to the magnetic stand for 5 minutes after which the supernatant, containing eluted cRNA, was transferred to a new nuclease free multiwall plate.
- The samples were placed on ice before immediately proceeding with second cycle cDNA synthesis or frozen at -20°C overnight.

7.4.2.2 cRNA Yield and Size Assessment

- 1.5µl purified cRNA was assessed by Nanodrop (as per section 2.3.1).
    - The expected yield given an input of 100ng sample tRNA/50ng control tRNA is >20µg/40µl).
- 1µl purified cRNA was assessed by Bioanalyser RNA 6000 Nano assay (as per section 2.4.2).
    - The expected cRNA size distribution profile is between 50 and 4000 nucleoides (nt) with most between 200nt and 2000nt and jagged in appearance.

7.4.2.3 Second Cycle cDNA Synthesis

The Ambion® WT Expression Kit is used at this step to reverse transcribe purified antisense cRNA into sense cDNA. During this reaction dUTP is incorporated into the synthesised single standed cDNA (sscDNA).

This modification allows the cDNA to be reproducibly fragmented in subsequent steps through the application of uracil DNA glycosylase (UDG) and apurinic/apyrimidinic endonuclease 1 (APE 1) which specifically remove the uracil residue and cleave DNA at the phosphodiester backbone where the base is absent respectively.

cRNA Preparation

- On ice, purified cRNA was adjusted to 455ng/µl (10µg/22µl) using nuclease free H_2O to adjust the volume to 22µl to achieve this concentration/volume if required.

Second Cycle cDNA Synthesis: Step 1

- On ice and using the PCR tubes supplied, 22µl cRNA (10µg) was combined with 2µl random primers for each sample, mixed by vortexing and briefly centrifuged to collect the liquid at the bottom of the tube.
- The mixture was transferred to a GeneAmp® 7900 thermocycler (Applied Biosystems/Life Technologies Corp., Carlsbad, CA, USA) and incubated for:
    - 5 minutes at 70°C
    - 5 minutes at 25°C
    - minutes at 4°C
- Following incubation samples were briefly centrifuged to collect the liquid at the bottom of the tube.

Second Cycle Master Mix Preparation

- The Second Cycle Buffer and Enzyme Mixes were removed from -20°C prior to use. The Second Cycle Buffer Mix was heated to 37°C for 2 minutes and briefly vortexed and centrifuged to ensure any precipitates were fully dissolved.
- The Enzyme Mix was thawed on ice until required.
- The Second Cycle Master Mix was prepared by combining the Second Cycle Buffer Mix and Second Cycle Enzyme Mix in a labelled nuclease free, non-stick micro centrifuge tube as per Table 7-6.

  5% excess volume was included to correct for pipetting loss. The solutions were mixed by vortexing and briefly centrifuged to collect the liquid at the bottom of the tube.

Table 7-6

Second Cycle Master Mix Component	Volume for one reaction (µl)	Volume for ten reactions (µl)
Second Cycle Buffer Mix	8	84
Second Cycle Enzyme Mix	8	84
Total	16	168

Table 7-6: Second Cycle Master Mix Components and Volumes.

Second Cycle cDNA Synthesis: Step 2

- At room temperature 16µl of Second Cycle Master Mix was added to each 24µl volume of cRNA/random primer mix, the solution mixed thoroughly by vortexing and centrifuged briefly to collect the liquid at the bottom of the tube.
- The mixture was transferred to a GeneAmp® 7900 thermocycler (Applied Biosystems/Life Technologies Corp., Carlsbad, CA, USA) and incubated for:
    - 10 minutes at 25°C
    - 90 minutes at 42°C
    - 10 minutes at 70°C
    - 2-10 minutes at 4°C

Note: It is important that the lid of the thermocycler be heated, to 75°C if possible or 105°C if lid heat control is unavailable.

- Immediately after incubation samples were centrifuged briefly to collect the liquid at the bottom of the tube and placed on ice before proceeding with cDNA Hydrolysis.

7.4.2.4 cDNA Hydrolysis

- 2µl of RNAse H was added to the Second Cycle cDNA Synthesis product, pipetted up and down x3 and vortexed to mix, and centrifuged briefly to collect the liquid at the bottom of the tube.
- The samples were transferred to a GeneAmp® 7900 thermocycler (Applied Biosystems/Life Technologies Corp., Carlsbad, CA, USA) and incubated for:

    - 45 minutes at 37°C
    - 5 minutes at 90°C
    - minutes at 4°C

Note: It is important that the lid of the thermocycler be heated, to 75°C if possible or 105°C if lid heat control is unavailable.

- Immediately after incubation samples were centrifuged briefly to collect the liquid at the bottom of the tube and placed on ice before proceeding with Second Cycle cDNA Purification.

7.4.2.5 Second Cycle cDNA Purification

Stock Reagent Preparation

- Elution Solution was heated to 55°C for ≥ 10 minutes prior to use.
- 100% Ethanol (Molecular Grade, Sigma-Aldrich) was added to Nucleic Acid Wash Solution (Concentrate) prior to use.
- The Nucleic Acid Binding Buffer Concentrate was warmed to 37°C to ensure any precipitated was completely dissolved.
- Nucleic Acid Binding Beads were vigorously vortexed prior to use to ensure complete dispersal.

cDNA Purification

- cRNA Binding Mix was prepared by combining Nucleic Acid Binding Beads and Nucleic Acid Binding Buffer Concentrate in a labelled nuclease free, non-stick micro centrifuge tube as per Table 7-7.

10% excess volume was included to correct for pipetting loss. The solutions were mixed by vortexing and briefly centrifuged to collect the liquid at the bottom of the tube.

Table 7-7

cDNA Binding Mix Component	Volume for one reaction (µl)	Volume for ten reactions (µl)
Nucleic Acid Binding Beads	10	110
Nucleic Acid Binding Buffer Concentrate	50	550
Total	60	660

Table 7-7: cDNA Binding Mix Components and Volumes.

- 18µl nuclease free H_2O was added to each sample, giving a final volume of 60µl.
- 60µl cDNA Binding Mix was added to each sample, mixed by pippetting up and down x3 and each sample transferred to a well of a nuclease free U-bottom plate.
- 120µl of 100% ethanol was added to each sample and pipetted up and down three times to mix. It is critical that ethanol and NOT isopropanol is used in this step.
- The plate was gently shaken for ≥2 minutes to mix allowing cDNA to bind to the Nucleic Acid Binding Beads.
- The plate was moved to a magnetic stand (Applied Biosystems/Life Technologies Corp., Carlsbad, CA, USA) for 5 minutes to allow the beads to be captured. After 5 minutes the mixture is transparent and the magnetic beads pelleted at the point the magnetic stand touches each well.
- The supernatant was carefully aspirated ensuring the magnetic beads were not disturbed and the plate removed from the magnetic stand.
- The beads were subjected to three washes:

- 100µl of prepared Nucleic Acid Wash Solution was added to each sample and moderately shaken for 1 minute. Note the beads may not disperse at this point, this does not affect the RNA purity/yield.
- The plate was returned to the magnetic stand for 5 minutes as before and the supernatant carefully aspirated. This wash protocol was repeated twice more.

- After the final wash was aspirated the plate was removed from the magnetic stand and shaken vigorously for 1 minute to evaporate residual ethanol from the beads.
  - Note: it was critical at this point that the beads are dried so that there is no visible liquid but the beads still look shiny/wet. If the beads were allowed to dry out the RNA yield may be affected.
- 30µl of preheated (55°C) Elution Solution was added to each sample to elute purified cDNA from the Nucleic Acid Binding Beads and incubated at RT, without shaking for 2 minutes. After 2 minutes the plate was vigorously shaken for 3 minutes, after which any undispersed pellets were disrupted by manual pipetting.
- The plate was returned to the magnetic stand for 5 minutes after which the supernatant, containing eluted cDNA, was transferred to a new nuclease free multiwell plate.
- The samples were placed on ice before immediately proceeding with second cycle cDNA Fragmentation and Labelling or frozen at -20°C overnight.

7.4.2.6 cDNA Yield and Size Assessment

- 1.5µl purified cDNA was assessed by Nanodrop (as per section 2.3.1).
  - The expected yield given an input of 10µg cRNA is >6µg/30µl).

- 1µl purified cDNA was assessed by Bioanalyser RNA 6000 Nano assay (as per section 2.3.2).
  - The expected cDNA size distribution profile will not resemble the cRNA profile. The median cDNA size is expected to be ~200nt.

7.4.2.7 cDNA Fragmentation

Using the Affymetrix® GeneChip® WT Terminal Labelling Kit sense strand cDNA (with incorporated dUTP) is fragmented prior to labelling. As described in section 7.4.2.3 UDG and APE 1 mediate cutting DNA at the non-endogenous dUTP residues incorporated in place of dTTP during second cycle cDNA synthesis, allowing reproducible single stranded cDNA fragmentation.

Sample Preparation

- Single stranded cDNA samples were adjusted to 5.5µg in a final volume of 31.2µl in 0.2ml strip tubes using nuclease free H_2O.

Fragmentation Master Mix

- cRNA Binding Mix was prepared by combining Nucleic Acid Binding Beads and Nucleic Acid Binding Buffer Concentrate in a labelled nuclease free, non-stick micro centrifuge tube as per Table 7-8. 5% excess volume was included to correct for pipetting loss. The solutions were mixed by vortexing and briefly centrifuged to collect the liquid at the bottom of the tube.

Table 7-8

Fragmentation Master Mix Component	Volume for one reaction (µl)	Volume for ten reactions (µl)
RNase-free H_2O	10	105
10x cDNA Fragmentation Buffer	4.8	50.4
UDG (10u/µl)	1	10.5
APE 1 (1000u/µl)	1	10.5
Total	16.8	175.5

Table 7-8: Fragmentation Master Mix Components and Volumes.

- 16.8µl Fragmentation Master Mix was added to each of the prepared samples, the solution gently mixed by vortexing and briefly centrifuged to collect the liquid at the bottom of the tube.

- The samples were then transferred to a GeneAmp® 7900 thermocycler (Applied Biosystems/Life Technologies Corp., Carlsbad, CA, USA) and incubated for:

    - 60 minutes at 37°C
    - minutes at 93°C
    - ≥2 minutes at 4°C

- Samples where then flick mixed and briefly centrifuged before 45µl of each sample was transferred to a new 0.2ml strip tube. The remainder of the samples was used in Bioanalyser RNA Nano 6000 assays for size analysis. The typical size range anticipated for fragmented cDNA is 40-70nt.

Samples were stored overnight at -20°C if not being labelled immediately.

7.4.3 Day 3 Work Flow Protocol

7.4.3.1 Labelling of Fragmented ssDNA

The Affymetrix® GeneChip® Labelling Reaction Master Mix was prepared by combining the components required in a labelled nuclease free, non-stick micro centrifuge tube as per Table 7-9. 5% excess volume was included to correct for pipetting loss. The solutions were mixed by vortexing and briefly centrifuged to collect the liquid at the bottom of the tube.

Table 7-9

Component	Volume for one reaction (µl)	Volume for ten reactions (µl)
5X TdT Buffer	12	126
TdT	2	21
DNA Labelling Reagent (5mM)	1	10.5
Total	15	157.5

Table 7-9: Labelling Reaction Master Mix Components and Volumes.

- 15µl Labelling Reaction Master Mix was added to each of the fragmented cDNA samples ($60\mu l_{FV}$), the solution gently flick mixed and briefly centrifuged to collect the liquid at the bottom of the tube.

- The samples were then transferred to a GeneAmp® 7900 thermocycler (Applied Biosystems/Life Technologies Corp., Carlsbad, CA, USA) and incubated for:

    - 60 minutes at 37°C
    - 10 minutes at 70°C
    - ≥2 minutes at 4°C

- Samples where then flick mixed and briefly centrifuged before proceeding with hybridisation to the GeneChip® Human Exon 1.0 ST Array.

7.4.3.2 GeneChip® Human Exon 1.0 ST Array Hybridisation

Stock Reagent Preparation

- Three heating blocks were turned on at 45°C, 65°C and 99°C respectively.
- GeneChip® Eukaryotic Hybridisation Controls were heated to 65°C for 5 minutes to ensure complete cRNA suspension.

Array Hybridisation

- 60µl of each fragmented and labelled cDNA target was transferred to a new 1.5ml nuclease-free non-stick micro centrifuge tube.
- Hybridisation Cocktail was prepared in a 1.5ml nuclease-free non-stick micro centrifuge tube as per Table 7-10, flick mixed and briefly centrifuged. 10% excess volume was included to correct for pipetting loss.

Table 7-10

Component	Volume for one 64 Format Array (µl)	Volume for four 64 Format Arrays (µl)	Final Concentration
Control Oligo B2 (3 nM)	3.7	16.28	50pM
20X Eukaryotic Hybridisation Controls	11	48.4	1.5 – 100pM†
2X Hybridisation Mix	110	484	1X
DMSO	15.4	67.76	7%
Nuclease Free H_2O	19.9	87.56	N/a
Total	160	704	

Table 7-10: Hybridisation Cocktail Components and Volumes.

†Final concentrations of Hybridisation Controls bioB, bioC, bioD and cre are 1.5pM, 3pM, 25pM and 100pM respectively.

- 160µl Hybridisation Cocktail was added to each 60µl labelled, fragmented cDNA sample, the tube flick mixed and briefly centrifuged.
- The sample/hybridisation cocktail solution was heated for 5 minutes at 99°C and cooled to 45°C in heat blocks before being centrifuged at maximum speed for 1 minute.
- The Human Exon 1.0 ST Array chip to be used with each sample was labelled with the sample name and allowed to equilibrate to room temperature.
- 200µl of the specific sample was injected into the array through one of the septa as labelled in Figure 7-1.
    - Note: the alternate septa must be kept open by insertion of a p200 pipette tip to allow venting of air when filling the hybridisation chamber. It is also critical that the bubble inside the hybridisation chamber floats freely upon rotation and the hybridisation cocktail is able to contact all portions of the array.
- The septa were temporarily sealed with tough-spots® (Diversified Biotech, Dedham, MA, USA) and placed in a GeneChip® hybridisation oven 640 (Affymetrix Inc., Santa Clara, CA, USA) at 45°C, 60 rpm and incubated for 17 hours ± 1 hour.

- Prior to completion of hybridisation reagents required for subsequent wash and stain steps was prepared.

Figure 7-1

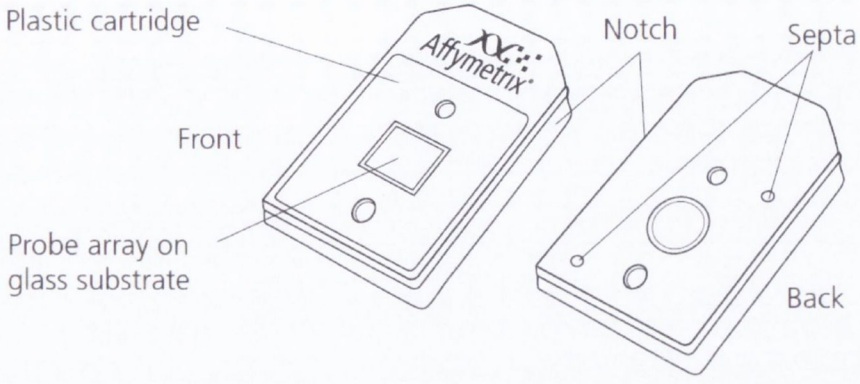

Figure 7-1: Affymetrix® GeneChip® Human Exon 1.0 ST Array.

7.4.4 Day 4 Work Flow Protocol

7.4.4.1 Entering Experiment Information

- To wash, stain and scan a GeneChip® array an experiment must first be registered using the Affymetrix® GeneChip® Command Console™ (AGCC) Portal accessed by opening the Portal icon. 
- Fields required are:
    - Experiment name
    - Probe Array Type
    - Sample Name
    - Sample Type
    - Project
- Templates for sample and experiments and array barcodes can also be used in AGCC to standardise and simplify the sample registration and experiment setup process. Comprehensive information and instructions are available in the Command Console user's guide.
- The use of necessary project, sample and experiment names establishes a user friendly GeneChip® information hierarchy in AGCC. This hierarchy has the Project at the top, followed by the Sample Name and then the Experiment Name.

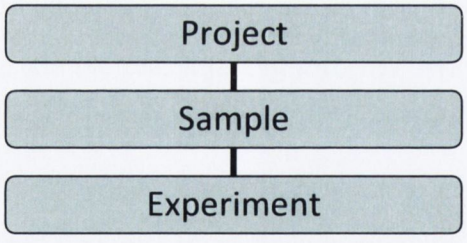

- Following the initial project set up subsequent probe assays can be added to the project through a 'Quick Registration' process where the sample is named, associated with a project and the GeneChip® barcode entered, automatically detecting the type of array being registered.

7.4.4.2 GeneChip® Wash/Stain

This procedure utilises the Affyemtrix® GeneChip® Hybridisation, Wash and Stain Kit and the GeneChip® Fluidics Station 450 controlled via the AGCC software accessed via the Fluidics portal icon . 

Stock Solution

- Wash Buffers A and B were allowed to reach room temperature prior to use and placed in the appropriate Fluidics Station Bottles at the right side of the Fluidics Station.
    - If any precipitates were visible the Buffer was briefly incubated at 37°C in a water bath until the precipitates were completely dissolved.
- The water reservoir was filled with deionised H_2O and the waste collection bottle placed in position.

Priming the Fluidics Station

Priming the fluidics station is necessary before each wash/stain run to ensure that the lines of the system are filled with the appropriate buffers and that the instrument is ready for running subsequent protocols. It is also performed if wash solutions are changed, if a shutdown has been performed before washing and if instructed by the onboard LCD window.

- The fluidics station was turned on using the toggle switch on the lower left of the instrument.
- On the operating computer the Affymetrix® GeneChip® Command Console (AGCC) program was initialised and AGCC Fluidics control selected.
- In the Fluidics Control window two dropdown lists are available for selection:
    - Probe Array type
    - Protocol
- The '**List Maintenance Protocols Only**' checkbox was selected and the **Prime_450** protocol selected from the Protocol dropdown list.

- The check boxes for the fluidics station modules to be utilised were selected. Selecting the Station ID checkbox selects all the modules available on a particular station.
- **Copy to Selected Modules** was selected applying the selected protocol to the selected modules.
- The washblock lever placed in the engaged/closed position and the needle lever pushed into the down position and the protocol selected to **Run**.

GeneChip® Array Washing and Staining

This protocol utilises the Affymetrix® GeneChip® Hybridisation, Wash and Stain Kit.

Staining Reagents Preparation

- Stain Cocktails 1 and 2 and Array Holding buffer were allowed to equilibrate to room temperature and the bottles tapped gently to ensure mixing of contents.
- For each of the Fluidics Modules to be used the following aliquots were prepared:
    - 600µl of Stain Cocktail 1 in a 1.5ml amber (non-transparent) micro centrifuge tube.
    - 600µl of Stain Cocktail 2 in a 1.5ml transparent micro centrifuge tube.
    - 800µl of Array Holding Buffer in a 1.5ml transparent micro centrifuge tube.
- The vials were briefly centrifuged to remove any air bubbles.

Note: Stain Cocktail 1 is light sensitive. Amber or other non-light transmissible micro centrifuge tubes must be used when preparing Stain Cocktail 1 aliquots.

Fluidics Station Preparation

- Table 7-11 indicates the fluidics protocols for the GeneChip® Human Exon 1.0 ST arrays. This 64 format array uses the FS450_0001 protocol.

Table 7-11

	Fluidics Station 450 FS450_0001 Protocol
Post Hyb Wash #1	10 cycles of 2 mixes/cycle with Wash Buffer A at 30°C
Post Hyb Wash #2	6 cycles of 15 mixes/cycle with Wash Buffer B at 50°C
Stain	Stain the probe array for 5 minutes in SAPE solution at 35°C
Post Stain Wash	10 cycles of 4 mixes/cycle with Wash Buffer A at 30°C
2nd Stain	Stain the probe array for 5 minutes in antibody solution at 35°C
3rd Stain	Stain the probe array for 5 minutes in SAPE solution at 35°C
Final Wash	15 cycles of 4 mixes/cycle with Wash Buffer A at 30°C
Holding Buffer	Fill probe array with Holding Buffer

Table 7-11: Fluidics Protocol for Washing/Staining GeneChip® Human Exon 1.0 ST Arrays.

Washing and Staining using the GeneChip® Fluidics Station 450

- After 17 hours ± 1hour of hybridisation the GeneChip® array was removed from the hybridisation oven.
- The array cartridge was vented by removing protective tough-spot® stickers and inserting a clean pipette tip into one of the septa and extracting the hybridisation cocktail via the remaining septum.
- The Hybridisation buffer was transferred to a nuclease free microcentrifuge tube and stored at -20°C for use on a future array if necessary.
- The array cartridge was completely filled with 250µl Wash Buffer A.
    - If necessary the probe array can be stored for up to 3 hours at 4°C, allowing the array to equilibrate to room temperature before washing and staining.
    - The wash and stain procedure takes approximately 90 minutes to complete.

- In the AGCC Fluidics Control window the correct array type () was selected from the **Probe Array Type** drop down list.
- In the **Protocol** drop down list the **FS450_0001** protocol was selected.
- The check boxes for the fluidics station modules to be utilised were selected. Selecting the Station ID checkbox selects all the modules available on a particular station.
- **Copy to Selected Modules** was selected applying the selected protocol to the selected modules.
- Three empty 1.5ml micro centrifuge tubes were placed in the stain holder positions of each of the modules to be used.
- The washblock lever placed in the engaged/closed position and the needle lever pushed into the down position and the protocol selected to **Run**.
- Following instructions on the Fluidics Station LCD screen:
    - The GeneChip® array cartridges were placed into the designated fluidics station modules after moving the cartridge lever to the down/eject position. When finished the cartridge lever was returned to the up/engage position.
    - Any microcentrifuge tubes in the sample holders were removed and the three microcentrifuge tubes containing Stain Cocktail 1, Stain Cocktail 2 and Array Holding Buffer were placed in stain holders 1 to 3 respectively.
    - The needle lever was depressed, snapping the needles into place and the wash/stain run begins.
- The AGCC Fluidics control station dialogue box on the operating PC and the LCD screen on the Fluidics Station modules display the status of the washing/staining protocol in progress.
- When the protocol is completed the Fluidics Station LCD windows display the message **EJECT and INPSECT CARTRIDGE** and the arrays removed from the Fluidics Station by pressing the cartridge lever to the eject position.
- The probe array window was inspected for bubbles or air pockets.
- If no air bubbles were present the Cartridge was immediately progressed to scanning on the GeneChip® Scanner 3000.
- If air bubbles are present the array cartridge was:

  - The returned to the wash block for refilling with Array Holding Buffer, following instructions on the LCD window. Following refilling the cartridge is ejected and inspected as before.
  - If bubbles were still present the array was manually filled with Array Holding Buffer using a micropipette.
- If the probes were not to be scanned immediately they were stored at 4°C protected from light for a maximum of 24 hours.

Fluidics Station Shutdown

If no further arrays required washing/staining the fluidics station was shut down.

- After removing the array cartridge from the fluidic module the LCD wind will display the message **ENGAGE WASHBLOCK**, and the cartridge lever raised closing the washblock.
- The unit performs an automated cleanout procedure, the LCD window indicating progress and instructing the user to **REMOVE VIALS** when complete.
- Empty 1.5ml microcentrifuge tubes were placed in the stain holders of the fluidic modules.
- Wash A and Wash B lines were placed into deionized water.
- Using the ACGG Fluidics Controll window the **SHUTDOWN_450** protocol was selected from the maintenance protocols, applied to the fluidic modules and set to **RUN.**
- Once the shutdown sequence is completed the LCD display on the Fluidics Station will indicated it is no longer primed and can be turned off using the power switch on the lower left side of the unit.

7.4.4.3 GeneChip® Scanning

The GeneChip® Scanner 3000 7G was used to image stained GeneChip® Human Exon 1.0 ST Arrays. The scanner is controlled via the AGCC software previously employed to control the Fluidics Station during priming, washing/staining and shutdown protocols, this time accessed via the Scan Control module. 

Handling the GeneChip® Array

Before a GeneChip® array is scanned the following handling directions should be followed.

- If necessary the glass surface of the array was cleaned with premium grade optical tissue paper (Peca Products Inc, Beloit, WI, USA). It is important that alcohol is not used to clean the glass.

- Tough-spots® were applied to the two septa to prevent Array Holding Buffer from leaking from the cartridge during scanning.

    - The area around the septa was dried and a tough-spot placed over it, ensuring it remained flat. If not applied flat, or if bumps, bubbles, tears or edge curling occur the tough-spot was removed and replaced.

- The cartridge was inserted into the scanner and the autofocus tested to ensure the applied tough-spots did not interfere with device operation.

Scanning the GeneChip® Array

- The GeneChip® Scanner 300 7G was turned on at the switch on the front panel. The boot up process takes a few minutes and the instrument was allowed at least 10 minutes for the laser to warm up sufficiently before scanning arrays.

- All GeneChip® arrays were allowed to warm to room temperature before scanning.
- The AGCC Scan Control software was launched from the AGCC.
- The lid of the scanner was opened GeneChip® arrays were placed in the cartridge autoloader carousel beginning at position 1 and the lid closed.
- Having attributed all samples/cartridges with the cartridge barcode during initial registration the scanner will automatically read the barcode of inserted chips and set the scanner to run the appropriate protocol for the type of cartridge used and save data to the correct experiment.
- The START button was selected and the 'Allow Rescans' checkbox deselected in the following dialogue box before selecting OK and starting the scan.
- The AutoLoader blue indicator light lights up signifying that the autoloader door is now locked and the carousel automatically homes itself and performs inventory to determine the number and position of cartridges present before the scanning run begins.
- The run will stop automatically when the last array is scanned.
- At the completion of each scan, the AGCC software will
    - Save the image data to an image file (*.dat).
    - Eject the probe array.
    - Align a grid on the image to identify the probe cells.
    - Automatically computes probe cell intensities and saves the data to the cell intensity file (*.cel).
- The progress of the scan data can be tracked using the Review Window of the AGCC Viewer accessed via this icon. 

7.4.5 Roche Mycoplasma Detection Kit Protocol

7.4.5.1 Preparation of Reagents

- Coating antibodies (vials 1a-d) were reconstituted with 30ml ddH_20, 1ml aliquots prepared and frozen at -20°C.
- Washing buffer was prepared by adding 5mls of stock 10 X concentrate to 45mls ddH20.
- Detection antibodies (vials 6a-d) were reconstituted with 25ml washing buffer, 1ml aliquots prepared and stored at -20°C until required.
- Mycoplasma positive control (vial 5) was diluted in 25ml washing buffer, 800µl aliquots prepared and stored at -20°C until required.
- Prior to starting testing 80mls 1x wash buffer was prepared fresh from concentrate using ddH_20 and all required reagents were allowed to come to room temperature.

7.4.5.2 Mycoplasma ELISA Protocol

- 2mls of media was removed from each of the cell culture flasks to be tested and transferred to a sterile 15ml tube.
- 500µl Sample Buffer was added to each media sample.
- 200ul of each primary coating antibody was pipette into 5 wells of an optically clear Nunc Maxisorp™ 96 well plate (Thermo Fisher Scientific, Roskilde, Denmark) as per Table 7-12.
- The plate was covered tightly using laboratory film and incubated at 37°C for 2 hours.

Table 7-12

SAMPLE	TEST1	TEST2	TEST3	TEST4
1	X	%	@	#
2	X	%	@	#
3	X	%	@	#
4	X	%	@	#
Positive Control	X	%	@	#

Key	
X	anti-M. *arginini* coating antibody (vial 1a)
%	anti-*M. hyorhinis* coating antibody (vial 1b)
@	anti-*A. laidlawii* coating antibody (vial 1c)
#	anti-*M. orale* coating antibody (vial 1d)

Table 7-12: Pipetting scheme for mycoplasma detection kit coating antibodies.

This pipetting scheme allows for detection of mycoplasma species in four samples and one positive control. This layout was performed in three separate plates to allow N=3 for all mycoplasma assays and one plate for negative control samples.

- Following incubation the coating antibody was aspirated by pipette, and tapping the plate on laboratory tissue paper.
- 250µl blocking solution was applied to each antibody coated well and incubated for 30 minutes at 37°C. Suction dry and tap empty on dry clean cloth.
- Following incubation the blocking solution was aspirated and each well washed 3x with 300µl washing buffer.
- Washing solution was aspirated by pipette and the plate dried by tapping on laboratory tissue.
- 200µl of samples S1-4 (previously prepared with sample buffer) and Positive Control Solution (vial 4) was added to wells as indicated in Table 7-13.
- The plate was covered tightly using laboratory film and incubated overnight at 4°C.

Table 7-13

SAMPLE	TEST1	TEST2	TEST3	TEST4
1	S1	S1	S1	S1
2	S2	S2	S2	S2
3	S3	S3	S3	S3
4	S4	S4	S4	S4
Positive Control	P.C.	P.C.	P.C.	P.C.

Key	
S1	Sample 1
S2	Sample 2
S3	Sample 3
S4	Sample 4
P.C.	Positive Control

Table 7-13: Pipetting scheme for mycoplasma detection kit samples and positive controls.

This pipetting scheme allows for detection of mycoplasma species in four samples and one positive control. This layout was performed in three separate plates to allow N=3 for all mycoplasma assays.

Note: A separate plate was prepared for negative control samples to eliminate the possibility of cross contamination from either samples or positive controls.

- Following incubation the samples/controls were aspirated by pipette, and tapping the plate on laboratory tissue paper and each well washed 3x with 300µl washing buffer.
- Washing solution was aspirated by pipette and the plate dried by tapping on laboratory tissue.
- 200µl of detection antibodies was added to the wells as indicated in Table 7-14, the plate tightly covered using laboratory film and incubated for 2 hours at 37°C.

Table 7-14

SAMPLE	TEST1	TEST2	TEST3	TEST4
1	X_1	$\%_1$	$@_1$	$\#_1$
2	X_1	$\%_1$	$@_1$	$\#_1$
3	X_1	$\%_1$	$@_1$	$\#_1$
4	X_1	$\%_1$	$@_1$	$\#_1$
Positive Control	X_1	$\%_1$	$@_1$	$\#_1$

Key	
X_1	anti-*M. arginini* detection antibody (vial 6a)
$\%_1$	anti-*M. hyorhinis* detection antibody (vial 6b)
$@_1$	anti-*A. laidlawii* detection antibody (vial 6c)
$\#_1$	anti-*M. orale* detection antibody (vial 6d)

Table 7-14: Pipetting scheme for mycoplasma detection antibodies.

- Following incubation the detection antibodies were aspirated by pipette, and tapping the plate on laboratory tissue paper and each well washed 4x with 300µl washing buffer.
- Washing solution was aspirated by pipette and the plate dried by tapping on laboratory tissue.
- 160µl of Streptavidin-AP (Strep AP) (vial 7) was applied to each well, the plate tightly covered using laboratory film and incubated for 1 hour at 37°C.
- Following incubation the Strep AP aspirated by pipette, and tapping the plate on laboratory tissue paper and each well washed 3x with 300µl washing buffer.
- Washing solution was aspirated by pipette and the plate dried by tapping on laboratory tissue.
- 200µl of freshly prepared substrate solution was applied to each well and incubated at room temperature for 30 minutes.
- Following incubation absorbance at 405nm was measured using a Wallac Victor 2 plate reader (Perkin Elmer, Waltham, MA, USA) and samples/positive controls compared against negative control samples.

7.5 Washed Platelet Preparation Stock Buffer Preparation

7.5.1 JNL Buffer Preparation

- JNL A (10x solution) – To 500ml ddH_2O add
  - 5.4g dextrose

- JNL B (10x solution) – To 500ml ddH_2O add
  - 37.99g Sodium Chloride (NaCl)
  - 3.78g Sodium Bicarbonate
  - 14.7g Sodium Citrate (tribasic, dehydrate)
  - 6.06g Tris Base
  - 74.56g Potassium Chloride (KCl)

- JNL D (10x solution) – To 500ml ddH_2O add
  - 0.55g Mono Potassium Phosphate (KH_2PO_4)

- JNL E (10x solution) – To 100ml ddH_2O add
  - 1.83g Magnesium Chloride Hexahydrate ($MgCl_26H_2O$)

All solutions were stored at 4°C until required.

To prepare a working JNL solution;

- JNL solutions A-E were allowed to return to room temperature.
- In a sterile skirted 200ml pyrex beaker 10mls of JNL solutions A, B and D were combined with 1ml of JNL solution E.
- The solution was made up to 75ml with ddH_20, the pH adjusted to 7.35 with ACD and allowed to equilibrate at RT for 5-10 minutes before adjusting to a final volume of 100ml.

7.5.2 Acid Citrate Dextrose Solution Preparation

Working stock solution of ACD was prepared by the addition of the following components of 250ml ddH_2O;

- 1.83g anhydrous citric acid.
- 5.50g sodium citrate.
- 6.13g dextrose.

ACD was then sterilised by 0.22µm filtration and stored at 4°C until required.

7.6 Bradford Protein Assay Protocol

7.6.1 Preparation of Standards and Working Reagents

Using the provided 2mg/ml bovine serum albumen (BSA) stock ampoules a set of standards was prepared by serial dilution. Two sets of dilutions were prepared to allowing measurment of both a broad range (25µg/ml – 2000µg/ml) (Table 7-15) and a narrow range (5µg/ml – 250µg/ml) (Table 7-16) of protein concentrations.

Table 7-15

Vial	Volume of Diluent	Volume and Source of BSA	Final BSA Concentration
A	0	300µl of Stock	2,000µg/ml
B	125µl	375µl of Stock	1,500µg/ml
C	325µl	325µl of Stock	1,000µg/ml
D	175µl	175µl of vial B dilution	750µg/ml
E	325µl	325µl of vial C dilution	500µg/ml
F	325µl	325µl of vial E dilution	250µg/ml
G	325µl	325µl of vial F dilution	125µg/ml
H	400µl	100µl of vial G dilution	25µg/ml
I	400µl	0	0µg/ml = Blank

Table 7-15: BSA serial dilutions for protein assay (broad range).

Using both sets of serial dilutions it is possible to investigate the protein content of an unknown sample(s) over a complete range of concentrations from 5µg/ml to 2000µg/ml. The diluent used during preparation of standards was double distilled water (ddH_2O).

Table 7-16

Vial	Volume of Diluent	Volume and Source of BSA	Final BSA Concentration
A	700µl	100µl of Stock	250µg/ml
B	400µl	400µl of vial A dilution	125µg/ml
C	450µl	300µl of vial B dilution	50µg/ml
D	400µl	400µl of vial C dilution	25µg/ml
E	400µl	100µl of vial D dilution	5µg/ml
F	400µl	0	0µg/ml = Blank

Table 7-16: BSA serial dilutions for protein assay (narrow range).

7.6.2 Preparation of the BCA Working Reagent

- Using the formula below the total volume of working reagent (WR) required was calculated:

  (# standards + # unknowns) × (# replicates) × (volume of WR per sample) = total volume WR required

- Three replicates were performed for each standard and unknown and the volume required per sample was 200µl as all quantitations were performed in microplate assays.
- WR was prepared by mixing BCA Reagent A and BCA Reagent B in a ratio of 50:1 to prepare the required final volume as calculated above. When Reagent B is initially added to Reagent A turbidity may appear on mixing that clears resulting in green WR. The WR is stable for several days when stored at RT in a closed container.

7.6.3 Microplate Procedure

- 25µl of each standard (working range = 5 - 2,000µg/ml) or unknown sample replicate was pipetted into a microplate well. If sample volume size is limited, 10µl of each unknown sample and standard can be used resulting in a sample to WR ratio of 1:20 and an assay range limited to 125-2,000µg/ml.
- 200µl of the WR was added to each well and mix plate thoroughly by shaking.
- The plate was covered and incubated at 37°C for 30 minutes.
- After incubation the plate was cooled to RT and the absorbance at (or near) 562nm measured on a plate reader. Measurement at 562nm is suggested but wavelengths between 540-590 nm have successfully been used with this method.
- The average absorbance measurement of the Blank standard replicates was subtracted from those of all other individual standard and unknown sample replicates and a standard curve prepared.
- The standard curve was then used to determine the protein concentration of each unknown sample. This was achieved using the equation of the line and applying the blank adjusted absorbance values of the unknown samples to calculate the corresponding protein concentration.

7.7 Roche Cell Proliferation Assay 1 Protocol

7.7.1 Stock Solution Preparation

- All solutions; MTT labelling solution - 5mg/ml, Solubilisation solution - 10% SDS in 0.01M HCl, were stored at -20°C until required.
- Prior to use all reagents were allowed to return to room temperature.
- MTT labelling reagent may be stored for up to four weeks protected from light at 4°C, but filtration is recommended prior to use.

7.7.2 MTT Assay Procedure

- Cells were enzymatically detached from $75cm^2$ cell culture flasks as per 2.5.3 and counted as per section 2.5.5.
- $2x10^4$ cells were seeded to tissue culture grade, 96 well, flat bottom micro-plates in a final volume of 100µl culture medium per well, according to the media needs of the cells and cultured for 24 hours at 37°C, 5% CO_2 to allow cell attachment.
- Once attached to the plates, growth media was gently aspirated and cells were briefly washed with 200µl room temperature PBS.
- Cells were then exposed to 100µl of media (full or serum free) or physiological buffer (JNL buffer) augmented by serial dilutions of a proposed modulator of cell growth.
- Cells were to grown for 24 hours at 37°C, 5% CO_2.
- 10ul MTT Labelling Reagent was added to each well (from 5ml aliquots) and incubated for 4hrs @ 37°C, 5% CO_2.
- 100ul solubilisation buffer was added to each well and the plate incubated overnight @ 37°C, 5% CO_2.
- After assessing complete solubilisation of formazan crystals absorbance was measured using a plate read at 550-600nm, taking a reference absorbance at 690nm reflective of background absorbance.

7.8 Roche *In Situ* Cell Death Detection Kit, TMR red Assay Protocol

Stock Solution Preparation

Fixation Solution – 4% Paraformaldehyde Solution

- 4g of paraformaldehyde (PAF) was dissolved in 90 ml of PBS in a pyrex container and gently heated to 58-60°C using a heat block in a fume hood. It is important not to heat over 60°C as PAF dissociates at these higher temperatures.
- 10N NaOH was added in a drop wise manner until the solution reaches pH 10 and becomes clear.

- The solution is removed from heat and the pH and carefully adjusted to pH 7.2-7.4 with 1N HCl.
- The final volume was adjusted to 100ml with PBS, 2ml aliquots prepared and stored at -20°C until required.
- Prior to use fixation solution was allowed to thawed on ice and stored at 4°C for up to a week after use.

Permeabilisation Solution – 0.1% Triton X-100 in 0.1% Sodium Citrate

- 100µg Sodium Citrate was dissolved in 90ml room temperature PBS.
- 100µl Triton X-100 was carefully dissolved in the sodium citrate solution and the volume adjusted to 100ml.

Adherent Cell Preparation

- Cells were enzymatically detached from cell culture flasks when approaching confluence as per section 2.5.3 and counted as per section 2.5.5.
- Cells were seeded to 96 well tissue culture plates at a concentration of $2x10^4$ cells per well in a volume of 200µl of appropriate full growth media and incubated in a humidified environment at 37°C, 5% CO_2 for 24 hours.
- Media was aspirated by pipette and cells gently washed 3x with room temperature PBS.
- 100µl full growth media supplemented with a proposed pro- or anti-apoptotic agent was added to each well and the tissue culture plate returned to a humidified environment at 37°C, 5% CO_2 for 24 hours.
- Media was aspirated by pipette, cells gently washed 3x with room temperature PBS and the plate dried by gentle tapping on laboratory tissue.
- 100µl Fixation Solution was applied to each well, the plate covered and incubated at room temperature for one hour.
- The Fixation solution was aspirated by pipette and wells washed 2x with 100µl PBS and the plate dried by gentle tapping on laboratory tissue.

- 100µl permeabilisation solution was applied to wells and the plate placed on ice for two minutes after which it was aspirated by pipette and wells washed once with 100µl PBS.

Sample Labelling

- Two microcentrifuge tubes were labelled 'Enzyme Solution' and 'TUNEL Reaction Mixture' respectively.
- 100µl was removed from the Label Solution (vial 2) for negative control use, and 50µl Enzyme Solution (vial 1) added to the remaining Label Solution (450µl) and mixed well. This complete TUNEL Reaction Mixture was kept on ice until used.
- Positive controls were exposed to 10µl DNase 1 Solution (Applied Biosystems/Life Technologies Corp., Carlsbad, CA, USA) for 10 minutes and washed once more with 100µl PBS.
- 50µl TUNEL Reaction Mixture was applied to experimental wells and 50µl Label Solution applied to negative control wells, the plate sealed with laboratory film and incubated in a humidified environment at 37°C for one hour.
- Following incubation TUNEL Reaction Mixture was aspirated and wells washed 3x with PBS. 10µl Hoechst nuclear stain (10mg/ml) was applied to wells and incubated for 30 minutes.
- Wells were imaged using an Olympus IX51 (Olympus Corp., Center Valley, PA, USA) inverted fluorescence microscope.
- Brightfield (white light) imaging was used to select a random field of view containing cells.
- UV laser excitation was used to image Hoechst Nuclear Stain (Ex 352nm, Em 461nm) and
- Mercury/xenon laser excitation was used to image the Tetra-Methyl-rhodamine (TMR) stain (Ex 520-560nm, Em 570-620nm) used to label DNA strand breaks.

7.8.1.1 Calculation of Apoptotic Cell Population

- Images of corresponding Hoeschst and TMR staining were analysed using Image J (National Institutes of Health, USA). Total number of cells per field of view was determined using Hoechst staining and the corresponding number of apoptotic cells in the same field of view allowing subsequent calculation of the apoptotic cell population.

7.9 BD Pharmigen™ ApoDirect™ Kit Protocol

Based on the same principle as the TMR red assay, the ApoDirect™ kit allows determination of levels of apoptosis in a cell population using TUNEL labelling of fragmented DNA. Using flow cytometry as an analysis tool allows more detailed and precise investigation of apoptosis in a large cell population.

Cell Line Preparation

- Cells were seeded at $4x10^4$ cells/well in 12 well plates and incubated overnight at 37°C, 5% CO_2 in 2ml full growth media.
- After 24 hours growth media was aspirated and cells gently washed twice with 2ml room temperature PBS.
- Cells were then exposed to 2ml full growth media supplemented with suspected proliferative/pro-apoptotic agents.

Cell Fixation

- The supernatant was removed from each well containing cells and transferred to separate labelled 15ml tubes. As adherent cells apoptose they frequently detach from their growth surface and may be present in the supernatant.
- 1ml Trypsin-EDTA was added to each well and the plates incubated at 37°C, 5% CO_2 for 5 minutes.

- Trypsin was then neutralised by addition of 2ml Trypsin Neutralising Solution and trypsinised cells added to the corresponding supernatant containing 15ml tube. **Note**: during all cell transfer and resuspension steps a Pasteur pipette is required: the narrow bore of a pipette tip may damage cells through shearing forces and result in false positive signals.
- Cells were centrifuged for 5 minutes at 300 x *g*.
- Following centrifugation the supernatant was carefully aspirated and cells gently resuspended in 1ml 1% Paraformaldehyde (PFA) and placed on ice for 45 minutes.
- Cells were centrifuged for 5 minutes at 300 x *g*.
- Following centrifugation the supernatant was carefully aspirated and cells gently resuspended in 2mls room temperature PBS and centrifuged for 5 minutes at 300 x *g*. This step was performed twice.
- Following the final wash, PBS was aspirated and cell resuspended in the residual PBS.
- 1ml ice cold 70% ethanol was added to the cell suspension and cells transferred to storage at -20°C until required. Cells can be stored under these conditions for several months prior to staining if required.

Cell Staining

- Cells were centrifuged for 5 minutes at 300 x *g*.
- The supernatant was aspirated and pellet gently resuspended in 1ml Wash Buffer. Cells were centrifuged for 5 minutes at 300 x *g*. This wash was repeated once more.
- The cell pellet was resuspended in DNA labelling solution, as prepared in Table 7-17 and incubated at 37°C for 60 minutes.

Table 7-17

DNA Labelling Solution Component	Volume for 1 Sample (µl)	Volume for 10 Samples (µl)
Reaction Buffer	10	100
TdT Enzyme	0.75	7.5
FITC dUTP	8	80
Distilled H_2O	32.25	322.5
Total Volume	51	510

Table 7-17: ApoDirect™ DNA Labelling Solution.

- Following incubation 1ml Rinse Buffer was added to each tube and cells were centrifuged for 5 minutes at 300 x *g*.
- The cell pellet was resuspended in 500µl of PR/RNase Staining Buffer and incubated in the dark at room temperature for 30 minutes.

Analysis by Flow Cytometry

- Stained, fixed cells were analysed by flow cytometry on a CyAn ADP flow cytometer (Beckman Coulter Inc., Indianapolis, IN, USA).

- Results were analysed using Summit software version 4.3 (Beckman Coulter Inc., Indianapolis, IN, USA).

- After initial gating by side- and forward scatter to determine the cell population from cell debris cells were gated into subpopulations as defined by the presence and/or absence of annexin V-FITC and PI, compensating as appropriate.

- Using this method and visualising staining by placing Annexin V-FITC on the X-axis and PI staining along the Y-axis sub-populations of the gated cells can be identified.

    - In the bottom left quadrant where annexin and PI both stain negative is the viable cell population.

- In the upper right quadrant where annexin and PI both stain positive is the late apoptotic/dead cell population.
- In the bottom right quadrant staining annexin positive but PI negative is the early apoptotic cell population.